Oil & Natural Gas Technology

DOE Award No.: DE-FC26-05NT42660

Final Scientific/Technical Report

Analysis of Critical Permeability, Capillary Pressure, and Electrical Properties for Mesaverde Tight Gas Sandstones from Western U.S. Basins

Submitted by:
University of Kansas Center for Research, Inc.
2385 Irving Hill Road
Lawrence, KS 66044

Prepared for:
United States Department of Energy
National Energy Technology Laboratory

June 30, 2009

Office of Fossil Energy

Solicitation Number: DE-PS26-04NT42072
Subtopic Area: 1-Understanding Tight Gas Resources

Contract Number: DE-FC26-05NT042660

University of Kansas Center for Research, Inc.
and the Kansas Geological Survey
2385 Irving Hill Road
Lawrence, KS 66044-7552
Technical Point of Contact - Alan P. Byrnes
voice: 785-864-3965, Fax: 785-864-5317, e-mail: apbyrnes@cox.net
Budgetary/Contractual Point of Contact- Tracie Watkins
voice: 785-864-7288, Fax: 785-864-5025, e-mail: twatkins@ku.edu

Principal Team Members:

University of Kansas-Kansas Geological Survey
Alan P. Byrnes
(Support Team Members– John Victorine, Ken Stalder, Daniel S. Osburn, Andrew Knoderer, Owen Metheny, Troy Hommertzheim, Joshua P. Byrnes)

The Discovery Group, Inc.
Robert M. Cluff, John C. Webb
(Support Team Members – Daniel A. Krygowski, Stefani Wittaker)

Title of Project:

Analysis of Critical Permeability, Capillary, and Electrical Properties for Mesaverde Tight Gas Sandstones from Western U.S. Basins

ACKNOWLEDGMENT:

This material is based upon work support by the Department of Energy (National Nuclear Security Administration) under Contract Number DE-FC26-05NT042660

DISCLAIMER:

TABLE OF CONTENTS

LIST OF TABLES

LIST OF FIGURES

LIST OF ACRONYMS

a = Archie equation constant, dimensionless
AAPG = American Association of Petroleum Geologists
C = Land equation constant
cc = cubic centimeter, cm^2
CEC = Cation exchange capacity (mequivalents/liter)
D = Fractal dimension
D = pore throat diameter (microns)
DOE = Department of Energy
D_{te} = Threshold entry pore diameter (microns)
E = Euclidean dimension

F = Fraction of total network sites where gas nucleation occurs
g = gram
GUI = graphical user interface
Hg = mercury
H_{te} = Threshold entry gas column height (ft)
K = Permeability, mD
K = thousands, x1000
KGS = Kansas Geological Survey
k_{ik} = *in situ* Klinkenberg permeability, millidarcies
k_{mk} = geometric mean of *in situ* and routine Klinkenberg permeability (md)
k_{rg} = Relative permeability to gas, fraction (v/v)
$k_{rg,Sw}$ = Relative permeability to gas at a specific water saturation S_w, fraction (v/v)
KU = University of Kansas
KUCR = University of Kansas Center for Research, Inc.
KUERC = University of Kansas Energy Research Center
L = Network size, number of nodes
ln = natural logarithm
log Rw_X = log10 of resistivity of brine at salinity X
logRw_{40K} = log10 of resistivity of 40K ppm NaCl = 0.758
m = Archie cementation (porosity) exponent, (ohm-m/ohm-m)
m_1 = matrix porosity exponent
m_2 = fracture or touching vug porosity exponent
m_{40K} = Archie porosity exponent at 40,000 ppm NaCl
md = mD = millidarcy, 1 md = $9.87x10^{-4}$ μm^2
mD = millidarcy, 1 mD = $9.87x10^{-4}$ μm^2
Mesaverde = Mesaverde Group
MICP = mercury intrusion capillary pressure
m_x = ***m*** at salinity X
n = Archie saturation exponent, dimensionless
n = number
$N_{\perp}$ = Series network
$N_{\perp d}$ = Discontinuous series network
$N_{//}$ = Parallel network
NaCl = sodium chloride
NCS = net confing stress
nD = nanodarcy, $1x10^{-6}$ mD
NETL = National Energy Technology Laboratory
N_p = Percolation network, random
^{o}F = temperature degrees Fahrenheit
P = average net effective confining pressure (psi)
Pc = capillary pressure, psia
$Pc_{Sgc,high}$ = Capillary pressure at $S_{gc,high}$
Pc_{lab} = laboratory-measured capillary pressure (psia)
Pc_{res} = capillary pressure (psia) at reservoir conditions
pdf = Adobe Acrobat protable document file
ppm = parts per million

PTTC = Petroleum Technology Transfer Council
PPTD = Principal pore throat diameter
psi = pound per square inch, 1 psi = 6.89 kPa = 0.00689 MPa
psia = pound per square inch absolute
P_{te} = Capillary pressure threshold entry pressure, psi
P_{te} = threshold entry pressure, psi
Ro = resistivity of brine saturated rock, ohm-m
Rw = resistivity of brine, ohm-m
$S_{g,Pc\text{-}Sgc,high}$ = Gas saturation at $Pc_{Sgc,high}$
S_{gc} = Critical gas saturation, expressed as a fractional (v/v) hydrocarbon saturation (1-S_w), saturation below which $k_{rg} = 0$
$S_{gc,\ low}$ = Lowest critical gas saturation in parallel network, fraction (v/v)
$S_{gc,high}$ = Highest critical gas saturation in series network, fraction (v/v)
$Slope_{m\text{-}Rw}$ = slope of m_{Rw} versus logRw for an individual sample
Snwc = critical nonwetting phase saturation
Snwi = initial nonwetting phase saturation
S_{nwi} = nonwetting saturation initial, fractional percent of pore volume
S_{nwr} = nonwetting saturation residual to imbibition, fractional percent of pore volume
SPE = Society of Petroleum Engineers
S_w = Water (or more generally wetting phase) saturation, fraction (v/v) or percent depending on context
S_{wc} = Critical water saturation, fraction (v/v), saturation below which $k_{rw} = 0$
$S_{wc,g}$ = Critical water saturation, fraction (v/v) with respect to gas drainage, saturation at which $k_{rg} = 1$ and below which $k_{rg} = 1$
Swirr = "irreducible" wetting phase saturation
S_{wirr} = "irreducible" wetting saturation, fraction of pore volume
Tcf = trillion cubic feet
TGS = tight gas sandstone(s)
USDOE = United States Department of Energy
USEIA = United States Energy Information Administration
V = System volume (v)
XML = eXensible Mark-up Language

β = pore volume compressibility (10^{-6}/psi)
ϕ = porosity, percent or fraction of bulk volume depending on context
ϕ_1 = matrix porosity
ϕ_2 = fracture or touching vug porosity
σ = interfacial tension (dyne/cm)
θ = contact angle, degrees

INTRODUCTION

I.1 Statement of Problem

Although prediction of future natural gas supply is complicated by uncertainty in such variables as demand, liquefied natural gas supply price and availability, coalbed methane and gas shale development rate, and pipeline availability, all U.S. Energy Information Administration gas supply estimates to date have predicted that Unconventional gas sources will be the dominant source of U.S. natural gas supply for at least the next two decades (Fig. 1.1). Among the Unconventional gas supply sources, Tight Gas Sandstones (TGS) will represent 50-70% of the Unconventional gas supply in this time period (Fig. 1.2). Rocky Mountain TGS are estimated to be approximately 70% of the total TGS resource base (USEIA, 2004) and the Mesaverde Group (Mesaverde) sandstones represent the principal gas productive sandstone unit in the largest Western U.S. TGS basins including the basins that are the focus of this study (Washakie, Uinta, Piceance, Upper Greater Green River, Wind River, Powder River). Industry assessment of the regional gas resource, projection of future gas supply, and exploration programs require an understanding of reservoir properties and accurate tools for formation evaluation of drilled wells. The goal of this study is to provide petrophysical formation evaluation tools related to relative permeability, capillary pressure, electrical properties, and algorithm tools for wireline log analysis. Detailed and accurate movable gas-in-place resource assessment is most critical in marginal gas plays and there is need for quantitative tools for definition of limits on gas producibility due to technology and rock physics and for defining water saturation.

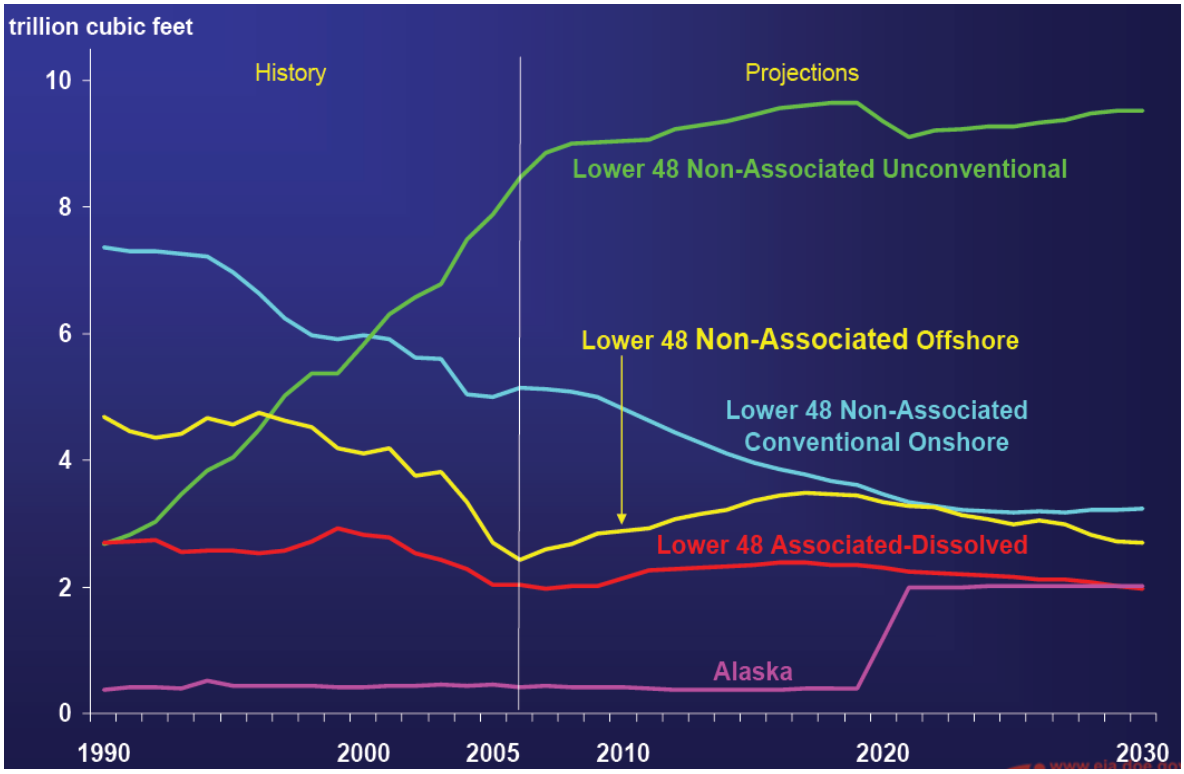

Figure 1.1 – Energy Information Administration prediction of future natural gas supply sources showing Lower 48 Unconventional sources will represent nearly 50% of consumption (Caruso, EIA, 2008).

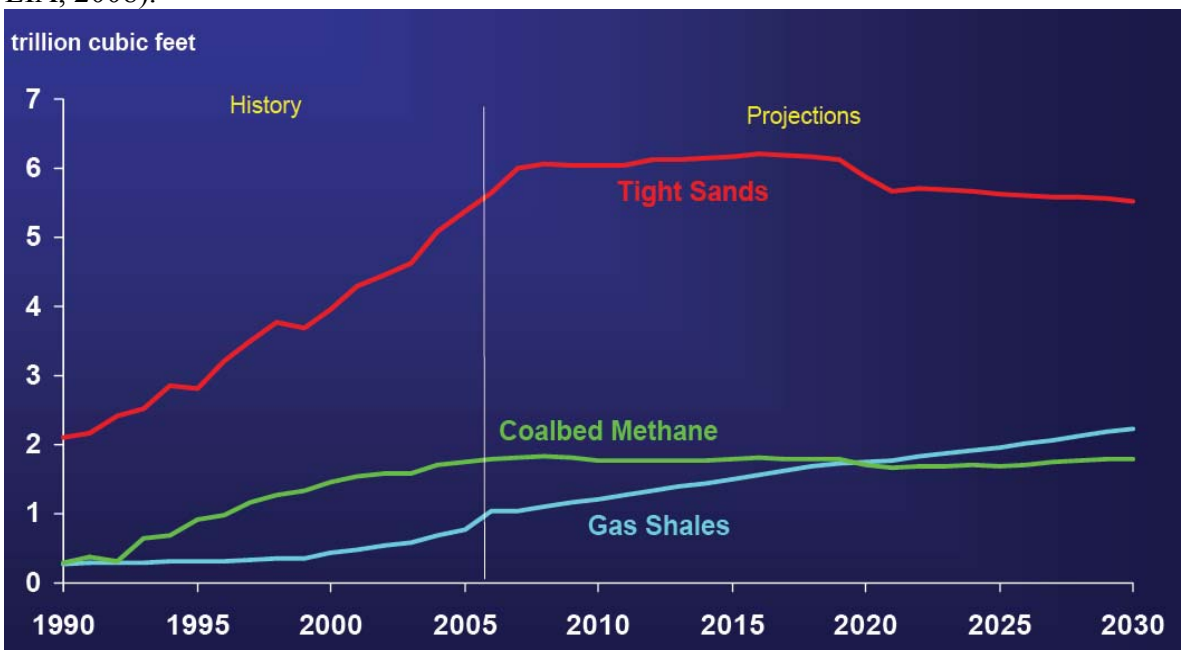

Figure 1.2 – Energy Information Administration prediction of future natural gas unconventional supply sources showing tight gas sandstones represent over half of unconventional supply (Caruso, EIA, 2008).

The results of this study address fundamental questions concerning: 1) gas storage, 2) gas flow, 3) capillary pressure, 4) electrical properties, 5) facies and upscaling issues, 6) wireline log interpretation algorithms, and 7) providing a web-accessible database of advanced rock properties. The following text briefly discusses the nature of these questions. Section 1.2 briefly discusses the objective of the study with respect to the problems reviewed.

1) Gas Storage - Issues with gas volume or storage are principally related to porosity, gas saturation, and fluid properties. Fluid properties have been well characterized in previous studies and gas saturation is defined by capillary pressure properties and wireline log response interpretation which are discussed separately. Routine (under no confining stress) porosity measurement in TGS requires careful quality control measures but is performed by commercial laboratories meeting quality standards. Although routine helium porosity is commonly measured, the influence of confining stress on porosity is not as thoroughly investigated. Further, the pore volume compressibility, or change in pore volume with change in net effective confining stress, has not been thoroughly studied for all Mesaverde rocks. This issue is important because it is necessary to know 1) how to correct higher routine porosity to reservoir (*in situ*) conditions, and 2) how *in situ* porosity changes with net effective stress increase associated with reservoir pore pressure decrease as the result of gas production.

2) Gas Flow - All assessments of gas resource are premised on assumptions concerning gas relative permeability and implicitly, the critical gas saturation (Sgc) or the minimum gas saturation at which gas flows. This saturation defines the beginning of the gas relative permeability curve. Some assessments assume that if gas is present its recovery is only a matter of price and/or technology. This premise is not valid for gas saturations less than or near critical saturation. Gas saturation less than or equal to Sgc can be achieved in nature by 1) highly local microscopic gas generation, such as from organic macerals, that have generated gas but the gas does not form a continuous phase across the pore system; 2) the rock has undergone water imbibition, either due to gas pressure decrease or water pressure increase, and the gas phase is trapped and represents a residual phase to water imbibition; 3) the gas entered the pore system under capillary pressure conditions existing during the gas entry, but the rock has since undergone further compaction or diagenetic alteration and now exhibits different capillary

pressure properties; 4) the gas is actually mobile but is near Sgc rather than at a gas saturation (Sg) significantly greater than Sgc, where it would be interpreted that the gas phase is highly mobile. If Sgc is incorrectly interpreted to be low (e.g., Sgc = 2%) when it is high (e.g., Sgc = 30%), then for a measured gas saturation of Sg = 31%, for an incorrect gas relative permeability curve with Sgc = 2%, gas at Sg = 31% is incorrectly interpreted to be significantly more mobile than if Sgc = 30%, when the gas would be incipiently mobile. Limited research has been done in this area and published data can be interpreted to indicate that Sgc increases with decreasing permeability. This would eliminate some gas from being produced and from resource base estimates. Understanding the minimum gas saturation necessary for gas flow (Sgc) is fundamental to defining the tight gas sandstone resource and is particularly critical to quantify in marginal resources.

3) Capillary Pressure - While there is a some understanding of the influence of confining stress on permeability and porosity in tight gas sandstones, little work has been done for capillary pressure. In addition, most capillary pressure studies focus on the drainage capillary pressure curve and have not investigated or reported on the imbibition capillary pressure or on capillary pressure hysteresis where saturations change under a series of drainage and imbibition cycles beginning and ending at different initial and final saturations.

4) Electrical Properties - Extensive work has been done defining regional water composition, but there is less published work characterizing the effect of cation exchange (Waxman-Smits effect) on modifying standard Archie-calculated water saturations from wireline log response for Mesaverde rocks. In Mesaverde reservoirs diagenetic clays with high cation exchange capacity can be common and water salinities can often be fresh (<25,000 ppmw total dissolved solids). These conditions can lead to low resistivity for which the standard Archie analysis of wireline electric log response must be modified (e.g. Waxman-Smits, Dual Water approaches). Mesaverde studies published to date have focused primarily on the Mesaverde in the Multiwell Experiment (MWX) in the Piceance Basin and do not analyze other Mesaverde rocks. In addition, work has presented results for rocks with porosity generally greater than 6% porosity but little has been reported for rocks with porosity less than 6%. These rocks are generally considered to not be “pay” but reservoir flow simulation shows that these rocks represent storage

for vertically adjacent beds where flow is significant. Therefore the accurate determination of water and gas saturation in these rocks is important to resource assessment. To measure this using wireline logs it is necessary to both understand the porosity exponent of these rocks and how electrical conduction changes with salinity.

5) ***Facies and Upscaling*** **-** Beyond investigating the above fundamental properties for representative lithofacies in the Mesaverde, it is necessary to know how critical gas saturation, capillary pressure, electrical properties, upscaling issues, and wireline log response and analysis change with more easily measured Mesaverde rock properties such as lithofacies, porosity, and permeability; and how flow properties, and particularly critical gas saturation, upscale with lithofacies bedding architecture. In addition, accuracy and variance of petrophysical relationships, such as permeability versus porosity, are premised on sampling, the scale of sampling, measurement methodology and accuracy and precision related to that, and the geostatistical or spatial distribution of the properties. Little published work is available that addresses how porosity or permeability change over short length scales (1-2 inches, 2.5-5 cm).

6) Wireline Log Interpretation – Petrophysical properties and relationships measured on core and at the core scale can provide critical reservoir characterization information, but core cannot reasonably, or economically, be obtained for most wells and over the entire Mesaverde interval of interest. For this reason, core are used to aid in calibration of wireline log response interpretation so that developed log algorithms can be used where core are unavailable. This requires that the wireline log response curves be correlated with core-measured petrophysical properties. These relationships can vary with such properties as rock lithology, petrophysical property, *in situ* conditions, log vendor, log vintage, log traces available in the logging suite, and the log algorithms developed and used. Algorithms can sometimes be developed that meet required accuracy and precision quality standards but that require a suite of input logs that are unavailable for historical wells and/or prohibitively expensive for new wells. Determining the number of unique lithofacies classes and the criteria for defining classes can involve four principal criteria: (1) maximum number of lithofacies recognizable using the available petrophysical wireline log curves and other variables; (2) minimum number of lithofacies needed to accurately represent lithologic and petrophysical heterogeneity; (3) maximum distinction of

core petrophysical properties among classes; and (4) the relative contribution of a lithofacies class to storage and flow.

7) Data access – The body of data concerning TGS advanced rock properties is extensive but few companies have been able to devote the time or resources to compiling the data and make the data digitally accessible. A well-designed internet-accessible database is needed to provide access to the library of data, query the data with respect to user-defined relational issues, and provide a framework for future data input through XML linkage.

I.2 Statement of Study Objectives

Major aspects of the study involved a series of tasks to measure data to reveal the nature of drainage critical gas saturation, capillary pressure, electrical properties and how these change with basic properties, such as porosity and permeability, and lithofacies for tight gas sandstones of the Mesaverde, and possibly among basins. Principal goals were to measure critical gas saturation (Sgc) and capillary pressure (Pc), using 150 rocks selected to represent the range of lithofacies, porosity, and permeability in the Mesaverde in five major TGS basins (Washakie, Uinta, Piceance, Upper Greater Green River, and Wind River). Representative samples were to be obtained from 4-5 wells in each basin and the advanced properties samples selected from a set of 300 core samples to obtain the distribution of properties needed. The investigation was to discern the relationships among the independent geologic and petrophysical variables and Sgc and Pc. As noted, in Mesaverde reservoirs diagenetic clays with high cation exchange capacity can be common and water salinities can often be fresh leading to low resistivity and necessary modification of the standard Archie analysis of wireline electric log response. An objective of the project was to evaluate this for the select samples to both determine the nature of conductive solids and to develop algorithms for wireline log analysis of water saturation. A principal goal was to compile published data and newly measured data into a publicly available database, accessible on the web.

Tasks involved with meeting the project objectives included a clarification and review of the research plan by DOE (Task 1), initial technology assessment for DOE (Task 2), collection and consolidation of published advanced rock properties data into a publicly accessible digital database, and collection of at least 300 rock samples and digital wireline logs from 4-5 wells each

from five basins that will represent the range of lithofacies present in the Mesaverde Group in these basins (Task 3). Measurement of basic properties (including routine and *in situ* porosity, permeability, and grain density) of these rocks and, based on these properties, selection of 150 samples to represent the range of porosity, permeability, and lithofacies in the wells and basins (Task 4.1). Measurements on these selected samples comprise drainage critical gas saturation (4.2); routine and *in situ* mercury intrusion capillary pressure analysis (4.3); porosity exponent and cation exchange capacity using multi-salinity method (4.4); geologic properties including core description; thin-section microscopy, including diagenetic and point-count analysis (4.5); and standard wireline log analysis (4.6). The compiled published data and data measured in the study were put in a database (5.1). Code was to be written that would provide web-based access to the data and all data were to be available as a complete database (5.2). Core and wireline log-calculated properties were to be compared and algorithms developed for improved calculation of reservoir properties from log response (Task 6). To evaluate the scale dependence of critical gas saturation, bedform-scale reservoir simulation models were to be constructed that represent the basic bedform architectures present in the Mesaverde sandstones. Simulations were to be performed that would parametrically analyze how critical gas saturation and relative permeability scale with size and bedding architecture (Task 7). An active web-based, publication, and short-course technology transfer program was to be performed (Task 8).

I.3. Report Organization

The following Results and Discussion section of the report will present the results by the tasks as defined above. The study involved the collection and organization of too much data, including core and log images, to appropriately present in a printed report format or that can be presented in Adobe Acrobat protable document file (pdf) format. In particular, core slab and rock thin section images were preserved at high-image resolution rather than reduced to lower resolution web presentation format so that future users could use the images quantitatively. Where appropriate data tables and figures are presented in the associated Task sections that follow. Where data tables or figures cannot be presented within this report due to size, the study web location for these is cited. In addition to being archived on the KGS Mesaverde Project website, all data are being archived as a Kansas Geological Survey open-file report in electronic format including both this report and the associated databases, tables, and figures.

Though technical in nature, the project administration involved tasks related to reporting and administration, such as Task 1. Details of these tasks will not be summarized in this technical final report.

RESULTS AND DISCUSSION

Task 1 - Research Management Plan

The objectives of this task were to develop a work breakdown structure and supporting narrative that concisely addresses the overall project as set forth in the agreement for the USDOE to review and accept according to the following guidelines: 1) The Recipient shall provide a concise summary of the objectives and approach for each Task and, where appropriate, for each subtask. 2) Recipient shall provide detailed schedules and planned expenditures for each Task including any necessary charts and tables, and all major milestones and decision points. This report is to be submitted within 30 days of the award. The DOE Contacting Officer's Technical Representative (COR) shall have 20 calendar days from receipt of the Research Management Plan to review and provide comments to the recipient. Within 15 calendar days after receipt of the DOE's comments, the recipient shall submit a final Research Management Plan to the DOE COR for review and approval.

A revised research management plan including Work Breakdown Structure was drafted, submitted, and approved. The approved management plan mirrored the proposal with minor modification. Based on initial contacts with gas companies that want to contribute core to the study but will not be drilling and coring wells until Spring 2006, the schedule for acquiring core material was modified from the proposal to allow time in Spring 2006 for sample acquisition. Task Statements in the Research Management Plan are presented at the beginning of each task and subtask below.

Task 2. Technology Status Assessment

The objectives of this task were to perform a Technology Status Assessment and submit a summary report describing the state of information and/or technology relevant to the proposed work. The report was to include both positive and negative aspects of each existing approach or technology. The report was to not exceed five typewritten pages in length. The report was not to contain any proprietary or confidential data, as the report was to be posted on the NETL website for public viewing.

The report contained the following:

Current state of information or technology (Note: Industry-wide, not strictly the Applicant's technology)

- Summary Background of Industry/Sector
- Technologies/Tools/Approached/Data Being Used
- Benefits and Inadequacies of Current Information or Technology

Development Strategies

- Why New Approach is Required
- Problems to Address in this Research Project

Future

- What Barriers will the Research Overcome and the Impact on the U.S. Domestic Gas Supply

2.1 Results

2.1.1. Current State of Information

2.1.1.1 Background Summary

Lower 48 unconvetional gas production became the largest natural gas source in 2001 and is projected to increase in proportion (USEIA, 2005). Rocky Mountain tight gas sandstones represent 70% of the total TGS resource base (241 Tcf; USEIA, 2003) and Mesaverde Group tight gas sandstones represent the principal gas productive unit in Western U.S. basins including the basins that are the focus of this project (Washakie, Uinta, Piceance, Upper Greater Green River, Wind River). Industry assessment of the regional gas resource, projection of future gas supply, and exploration programs require an understanding of reservoir properties and accurate tools for formation evaluation of drilled wells. The goal of this project is to provide petrophysical formation evaluation tools related to relative permeability, capillary pressure, electrical properties, and algorithm tools for wireline log analysis. Detailed and accurate moveable gas-in-

place resource assessment is most critical in marginal gas plays, and there is need for quantitative tools for definition of limits on gas producibility. Extensive work has been performed over several decades measuring TGS properties. Understanding of basic properties to date is reviewed.

2.1.1.1.1 Porosity - The stress dependence of porosity and the laboratory conditions necessary for proper measurements are now widely recognized. Walsh and Grosenbaugh (1979) developed a model for fracture compressibility, and Ostensen (1983) illustrated for low-permeability rock data from Jones and Owens (1980) and Sampath (1983) that these data conformed to the model of compressing cracks. Byrnes (1997, 2000, 2003, 2005) illustrated a relationship between routine and reservoir (*in situ*) porosity for Mesaverde/Frontier rocks.

2.1 .1.1.2 Permeability - Extensive work has shown that the difference between permeabilities measured at routine conditions (k_{air}) and those measured at confining stress increases progressively with decreasing permeability and increasing confining stress (Vairogs et al., 1971; Thomas and Ward, 1972; Byrnes et al., 1979; Jones and Owens, 1980; Sampath and Keighin, 1981; Walls et al., 1982; Ostensen, 1983; Wei et al., 1986; Luffel et al., 1991; Byrnes, 1997; Castle and Byrnes, 1998; Byrnes et al., 2001, Byrnes, 2005). Byrnes et al. (2001) presented a relationship between *in situ* Klinkenberg gas permeability (k_i) and routine air permeability (k_{air}): $\log k_{ik} = 0.059\ (\log k_{air})^3 - 0.187\ (\log k_{air})^2 + 1.154 \log k_{air} - 0.159$ (where k is in millidarcies) and illustrated the relationship between k_i and pore throat size in TGS. Mesaverde sandstones can be characterized as exhibiting either a log-linear k-ϕ relationship (Dutton et al., 1993; Byrnes 1997) or, for subpopulations may exhibit a power-law trend (Castle and Byrnes, 1998; Byrnes and Castle, 2000; Webb et al., 2005).

2.1.1.1.3 Relative Permeability and Critical Gas Saturation - Relative gas permeability (k_{rg}) data for tight gas sandstones have been reported in several studies (Thomas and Ward, 1972; Byrnes et al., 1979; Jones and Owens, 1981; Sampath and Keighin, 1981; Walls, 1981; Ward and Morrow, 1987; Byrnes, 1997; Castle and Byrnes, 1997; Byrnes and Castle, 2001; Byrnes, 2005). Byrnes et al. (1979) utilized a modified Corey (1954) equation to predict k_{rg} in low-permeability sandstones: $k_{rg} = (1 - (S_w - S_{wc,g})/(1 - S_{gc} - S_{wc,g}))^p\ (1 - ((S_w - S_{wc,g})/(1 - S_{wc,g}))^q)$; where S_w is fractional water saturation, S_{gc} is the fractional critical gas saturation, $S_{wc,g}$ is the fractional critical water saturation relevant to the gas phase, and p and q are exponents expressing pore size distribution influence. Byrnes (2005) discussed the uncertainties in the end-point properties of

TGS relative permeability curves and particularly the issues with S_{gc}. Critical gas saturation studies have primarily addressed solution gas drive gas connectivity (i.e., gas bubbles develop in pore space) and only a limited number address drainage gas displacement (Closmann, 1987; Li and Yortsos, 1993; Kamath and Boyer, 1995). Measured values of S_{gc} in the literature range from 0.2 to 38% and a function of such variables as core length, injection or pressure depletion rate, and interfacial tension. Byrnes (2005b) presented results for S_{gc} in Mesaverde TGS that ranged from 10 to 45% and varied with pore architecture.

2.1.1.1.4 Capillary Pressure - Because of small pore-throat size, low-permeability gas-producing sandstones are typically characterized by high water saturation and high capillary pressure (Thomas and Ward, 1972; Dutton et al., 1993; Byrnes, 1997, 2005). Relationships between "irreducible" water saturation and permeability (Byrnes, 1997; Byrnes and Castle, 2000) and between threshold entry pressure or principal pore throat diameter (PPTD) and permeability (Byrnes and Keighin, 1993; Keighin, 1995; Byrnes, 1997; Byrnes, 2003) have been published. The relationship between threshold entry pressure (P_{te}) and permeability and between permeability and lithofacies at any given porosity requires that capillary pressure change with lithofacies at any given porosity. With change in both the threshold entry pressure, the critical or percolating pore throat size capillary pressure (P_{pc}) and pore throat size distribution with decreasing permeability, Byrnes (2003, 2005) illustrated generalized capillary pressure shapes for western tight gas sandstones. Byrnes and Keighin (1993) and Keighin (1995) showed that the *in situ* P_{pc} values range from 15 to 84% of unconfined P_{te} values illustrating the change in capillary pressure with confining stress.

2.1.1.1.5 Water Saturation and Cation Exchange Capacity – Wireline log determination of water saturation and identification of pay in tight gas sandstones is complicated by the low porosity, argillaceousness, and, in some rocks, the high cation exchange capacity (CEC) of the clays in the sandstones and the low salinity of the formation brines (Kukal et al., 1983). The problems of wireline log analysis in shaly sands is well recognized (Fertl, 1987; Worthington, 1985), and numerous algorithms have been proposed for calculating water saturations in shaly sands including the empirical Simandoux (1963) or Indonesia and Fertl equations and the more theoretical Dual Water and Waxman-Smits models (Waxman and Smits, 1969; Waxman and Thomas, 1974; Clavier, Coats, and Dumanoir, 1984). To calculate water saturation, accurate values of formation factor, saturation exponent, and cation exchange capacity (if present) are

needed. The DOE has supported a study by Advanced Resources International to catalogue water composition data for the Greater Green River and Wind River basins. These data are critical to log-calculated water saturation, but significant saturation error can exist if CEC effects are present and are not accounted for in water saturation calculations. Isolated CEC data are available for Mesaverde (Volk et al., 1979; Gall et al., 1981), but no comprehensive study has been published.

2.1.1.1.6 Scale Dependence of Sgc and Relative Permeability - Even if relative permeability curves are known, it is important to understand how to utilize them in reservoir modeling and simulation and have an understanding of how properties upscale. Analytically rigorous solutions for upscaling of permeability and relative permeability exist only for the simplest architectural geometries such as layered beds (e.g., Weber, 1982; Craft and Hawkins, 1991; Corey and Rathjens, 1956) or for specific permeability architectures (Kortekaas, 1985; Honarpour et al., 1995; Ringrose et al., 1996). The most accurate, but most computationally intensive, method for calculation of pseudo-functions is to use flow simulations performed for representative architectures (Warren and Price, 1961; Desbarats, 1987).

2.1.1.2 Technology/Methodology Being Used

Major aspects of the proposed study involve a series of tasks to measure data to reveal the nature of drainage S_{gc}, capillary pressure, and electrical properties and how these change with basic properties, such as porosity and permeability, and among Mesaverde lithofacies in different basins. The tasks involved and the analyses to be performed are discussed briefly here.
Tasks involved with meeting the project objectives include clarification and review of the research plan (Task 1), initial technology assessment (Task 2), and collection and consolidation of published advanced rock properties data into a publicly accessible relational digital database and collection of at least 300 rock samples and digital wireline logs from 4-5 wells each from five basins that will represent the range of lithofacies present in the Mesaverde Group in these basins (Task 3). Basic properties (including routine and *in situ* porosity, permeability, and grain density) of these rocks will be measured and, based on these properties, 150 samples will be selected to represent the range of porosity, permeability, and lithofacies in the wells and basins (Task 4.1). Measurements to be performed on these selected samples comprise: 1) Drainage critical gas saturation (4.2), routine and *in situ* mercury intrusion capillary pressure analysis (4.3), porosity

exponents and cation exchange capacity using multi-salinity method (4.4), geologic properties including core description, thin-section microscopy, including diagenetic and point-count analysis (4.5), and standard wireline log analysis (4.6). The compiled published data and data measured in the study will be input in an Oracle database (5.1). XML code will be written that will provide web-based access to the data and will allow construction of rock catalog format output sheets based on user-input search and comparison criteria. The data will also be available as a complete database (5.2). Core and wireline log calculated properties will be compared and algorithms developed for improved calculation of reservoir properties from log response (Task 6). To evaluate the scale dependence of critical gas saturation, bedform-scale reservoir simulation models will be constructed that represent the basic bedform architectures present in the Mesaverde sandstones. Simulations will be performed that will parametrically analyze how critical gas saturation and relative permeability scale with size and bedding architecture (Task 7). Finally, a basic goal of the project is to provide the data compiled and measured to operators and users involved in resource evaluation. An active web-based, publication, and short-course technology transfer program will be performed. The web-based tools will provide any operator with complete access to the database and a tool for querying and analyzing data. Publications will explore important relationships in the nature and distribution of properties and the relationships between properties (Task 8).

By quantitatively measuring the geologic properties of the core plugs the study provides a defined geologic (lithofacies, petrologic) reference frame for correlation with rocks from un-sampled Mesaverde areas and other formations. Similarly, obtaining data on a complete spectrum of Mesaverde rocks increases the robustness of the empirical relationships developed and provides users of the database with a high probability of finding analog samples. Laboratory analyses will employ established methodologies.

2.1.1.3 Limitations of Present Knowledge

The significant body of literature on TGS has helped define the TGS resource base. However, fundamental aspects of the properties discussed above are not fully understood, including ***1) Gas Flow*** – All assessments of gas resource are premised on assumptions concerning gas relative permeability and implicitly, the critical gas saturation (S_{gc}), which no published studies have measured for TGS. Understanding the minimum gas saturation necessary

for gas flow (S_{gc}) is fundamental to defining the tight gas sandstone resource and is particularly critical to quantify in marginal resources; ***2) Capillary Pressure*** – Though work has been done on capillary pressure of low-permeability sandstones little work has been published on the lithofacies or pressure-dependence of capillary pressure; ***3) Electrical Properties*** – Extensive work has been done defining regional water composition, but there is little published work characterizing the effect of cation exchange (Waxman-Smits effect) on modifying standard Archie-calculated water saturations from wireline log response for Mesaverde rocks; ***4) Facies and Upscaling*** – Most published studies of TGS properties are tied to location but are not distinguished by lithofacies. This places potential, and sometimes unknown, limits on application or results. The proposed project will investigate how properties, upscaling issues, and wireline log response and analysis change with Mesaverde rock properties such as lithofacies, porosity, and permeability and how flow properties upscale with lithofacies bedding architecture; and ***5) Data Access*** – The body of data concerning TGS advanced rock properties is extensive but few companies have been able to devote the time or resources to compiling the data and make the data digitally accessible. A well-designed internet-accessible database is needed to provide access to the library of data, query the data with respect to user-defined relational issues, and provide a framework for future data input through XML linkage.

2.1.2. Development Strategies

2.1.2.1 Why New Approach is Required

The limitation of the present knowledge discussed above illustrate why this project is required. Although we know a great deal about TGS, there are fundamental properties about which we know little or nothing. The project is designed to provide data that are applicable to Mesaverde reservoirs and to similar facies in other formations. The measurement of properties on a suite of rocks that represent the range of lithofacies, porosity, and permeability in the Mesaverde is specifically designed to provide the maximum applicability of the results obtained. The construction of a web-accessible database will provide a tool that facilitates use of the data immediately. All operators in tight gas sandstones will have use for the data and the database.

2.1.2.2 Problems to Address

The experimental methodologies employed in the proposed program are well established. Measurement of *in situ* capillary pressure is a new utilization of well-known technology and has been performed previously (Byrnes and Keighin, 1995). There are no significant risks to the program. It is possible that the wells selected will not provide sufficient variance in lithofacies or porosity/permeability population. If this occurs additional wells will be sampled or alternate wells will be selected. Obtaining fresh Mesaverde core from operators will require coordinating the research program with when core are taken. This may delay obtaining some cores until later in the project than scheduled but accommodation will be made for parallel processing of multiple streams of samples. Unlike many published studies where rock geologic properties are not quantified, since these will be characterized in this study, there will be quantitative data for users to determine the similarity of their particular rocks to those in the database.

2.1.3. Future

2.1.3.1 Barriers Overcome and Impact on U.S. Domestic Gas Supply

The properties measured and deliverables provided decrease or remove several present limitations on accurate TGS formation evaluation. It is believed the properties measured and the database will have an immediate and significant impact on quantitative resource assessment of Mesaverde and other tight gas sandstones. Depending on the nature of critical gas saturation change with lithofacies and permeability, the recoverable gas resource and exploration programs in Western tight gas sandstones could change significantly. Waxman-Smits parameters for Mesaverde rocks could provide operators with tools that may indicate water saturations are 10-20% less than values calculated using standard Archie parameters. This difference could immediately change completion, stimulation, and modeling practices. The availability of a database of advanced properties compiled from the literature and the study will provide immediate evaluation tools.

Task 3. Acquire Data and Materials
Subtask 3.1. Compile Published Advanced Properties Data

3.1.1 Task Statement

Advanced rock properties data, comprising compressibility, effects of confining pressure, capillary pressure, relative permeability, and electrical properties, shall be compiled from published studies and DOE reports. These data shall be digitized and entered into a fully integrated digital data system accessible to external users.

3.1.2 Methods

Reference searches were performed in the following databases: Georef, NTIS, DAI, GPO, Compendex, USBM, WorldCat, FSProc, SPE. Of the over nearly 2,000 references that are flagged for appropriate search word criteria relevant to low-permeability sandstones and Mesaverde, over 230 geologic and engineering technical publications were identified that are relevant to Mesaverde geologic or petrophysical properties or to properties of non-Mesaverde low-permeability sandstones but appear to be geologically and petrophysically relevant. Of the 230 publications, 90 publications were interpreted to be geologically or petrophysically relevant to the issues addressed by this study (Table 3.1.2.1). Physical or electronic copies were obtained for the publications identified. Of these 90 references, more than 75% did not contain petrophysically useful tabular data. Data in the publications most relevant to Mesaverde rocks or needed for relative permeability or critical gas saturation analysis were entered into a database either from tables in the publication or interpreted from figures. Obtaining data from figures potentially introduces some error, as a function of the figure image quality and scales but was interpreted to be within acceptable quality criteria that generally ranged from an interpreted independent and dependent variable accuracy of 1%–5% of the true value used to create the figure. The significant figures reported generally reflect the accuracy of the figure interpretation process but may be one significant figure greater for some data (e.g., for a value with an error of 1% values above 10% might be reported with no decimal places whereas values less than 10% might be reported with a single decimal place). Where data were obtained directly from published tables, the number of significant figures reported were the same as in the publication,

even if the number of significant figures shown in the publication was inappropriate for the data accuracy (e.g., reporting of routine porosity to two decimal places) .

Original plans were to present data in a single database format. However, it was found that the nature of publication reporting format and the diverse nature of the data were not conducive to the use of a single database. Such a format would have resulted in the data being in what would have been subsections of a master database that would have effectively been individual tables. At two public technical presentations at technical society meetings, the audience was polled as to whether they preferred a simple Excel-style workbook format or an Oracle-style database. The response at both surveys was greater than 90% preferred the Excel-style format. An Excel format for data presentation was used.

It is important to note that the search and data capture is not comprehensive. There are publications in major journals, regional society publications, academic dissertation or theses, and government-sponsored studies that were known but were not identified in the search process or were identified but from which data were not obtained and recorded because it was not considered sufficiently relevant. Also some figures in some publications, though important, were not in a format appropriate to accurate digitization either because of the scale of presentation (e.g., relative permeability figures presented in linear format so that all values below 10% could not be accurately digitized with acceptable accuracy) or the quality of the reproduction. It is also not the purpose of this task to analyze the data, only to compile the data.

3.1.3 Results

Table 3.1.2.1 presents the 90 references that were interpreted to be relevant to Mesaverde low-permeability geologic and petrophysical properties important to this study or that addressed properties measured in this study in low-permeability sandstones. The majority of publications did not include tables of data but included figures. Figures 3.1.1-3.1.5 provide examples of compiled data presented in Appendix 3.1.3.

Figure 3.1.1 illustrates a plot of gas relative permeability measured for individual saturations compiled from sources listed in Table 3.1.1 and data presented in Supplemental Data Appendix 3.1.3.1. These gas relative permeabilities were obtained using a wide range of experimental methods involving sample preparation and permeability measurement including oven and relative-humidity oven drying; as-received saturations; water saturation achieved by

evaporation, centrifuge, porous plate; permeability measured by steady-state and pressure-pulse decay; permeability representing air permeability and Klinkenberg permeability; cores under varying net effective stress conditions; and a very wide range of lithofacies (often unspecified).

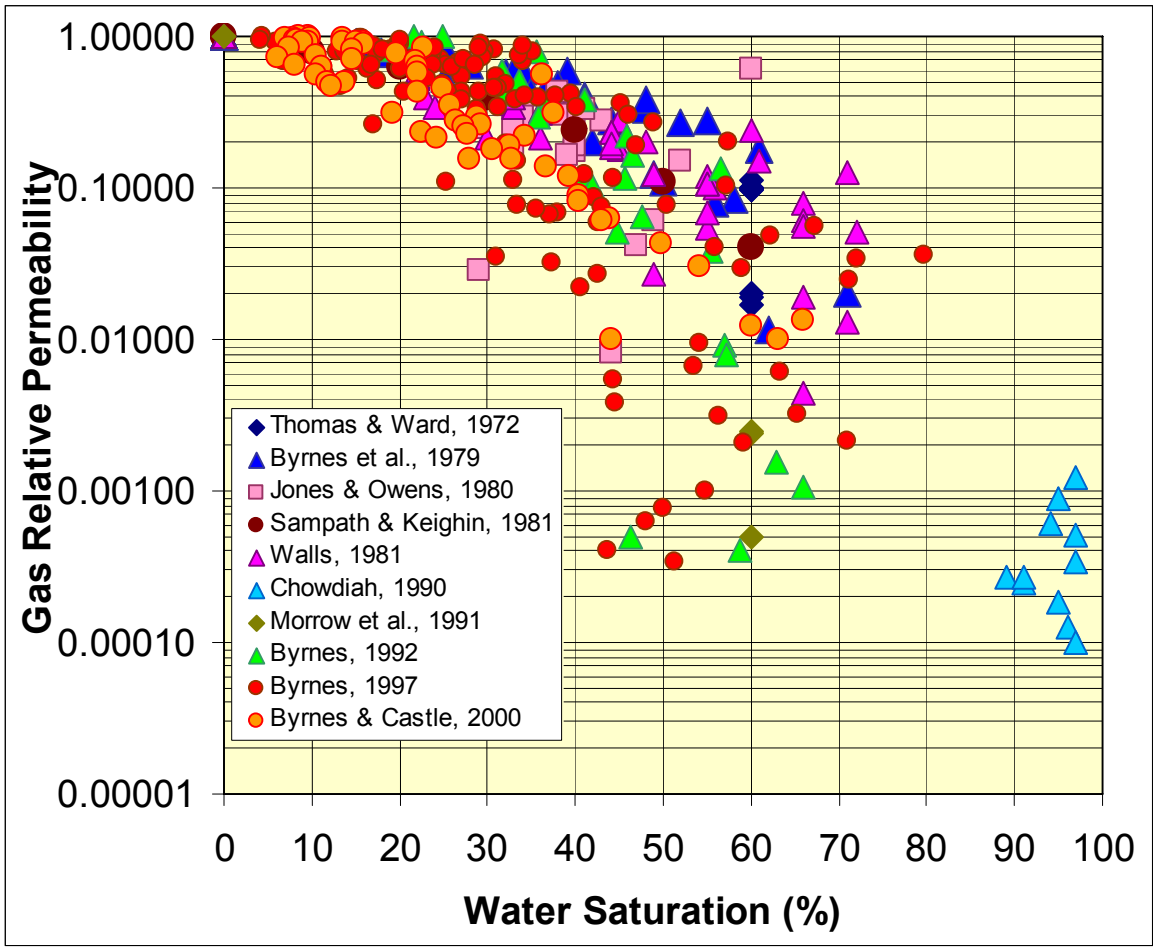

Figure 3.1.1 Gas relative permeability versus water saturation from published studies. Measurement methods and conditions including methods used to achieve saturation, measure gas relative permeability, and net effective confining stress vary among studies.

In addition to single-point data, complete gas relative permeability curves have been measured on cores in several studies using the single-phase stationary techniques where water is stationary and gas-flow measurement is performed at a low flow rate that does not change the water saturation. Figure 3.1.2 illustrates compiled curves from studies that reported complete gas relative permeability curves. As with the single-point data, these curves represent a range of experimental conditions including core drying, core desaturation method, "reference" state of absolute permeability, net effective stress, rock lithology, and notably clay type and content.

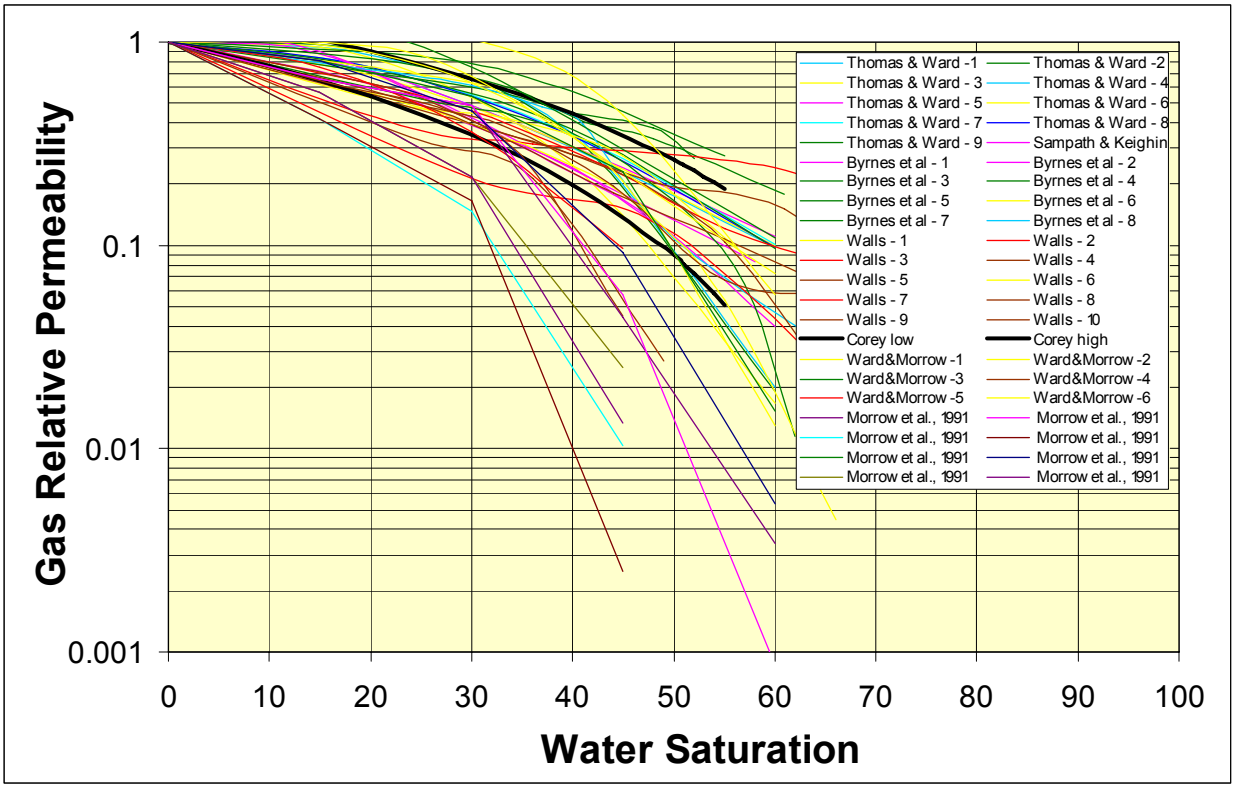

Figure 3.1.2 Gas relative permeability curves versus water saturation from published studies. Measurement methods and conditions including methods used to achieve saturation, measure gas relative permeability, and net effective confining stress vary among studies.

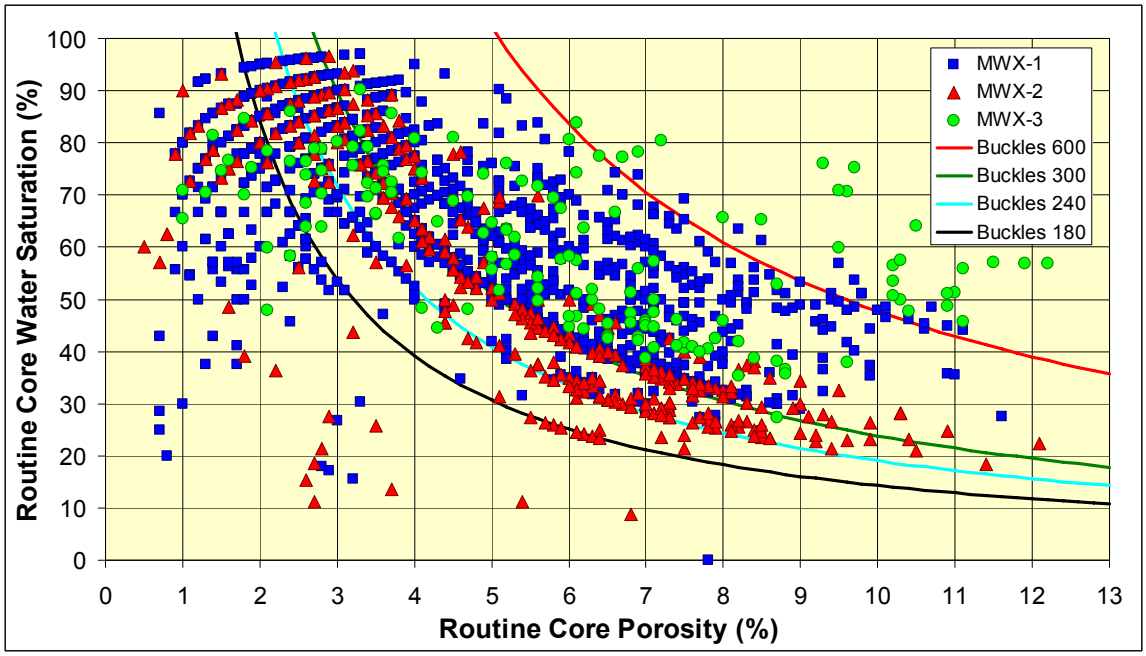

Figure 3.1.3 Routine core analysis porosity versus water saturation for the Piceance Basin MWX-1 through MWX-3 wells. Saturation versus porosity trends exhibit commonly observed Buckles power-law relationship. General trendlines shown represent $Sw = A\phi^{-1.1}$ where A = 180, 240, 300, 600. In some basins differences in trendline result from height within hydrocarbon column, but here differences are interpreted to primarily reflect lithologic differences.

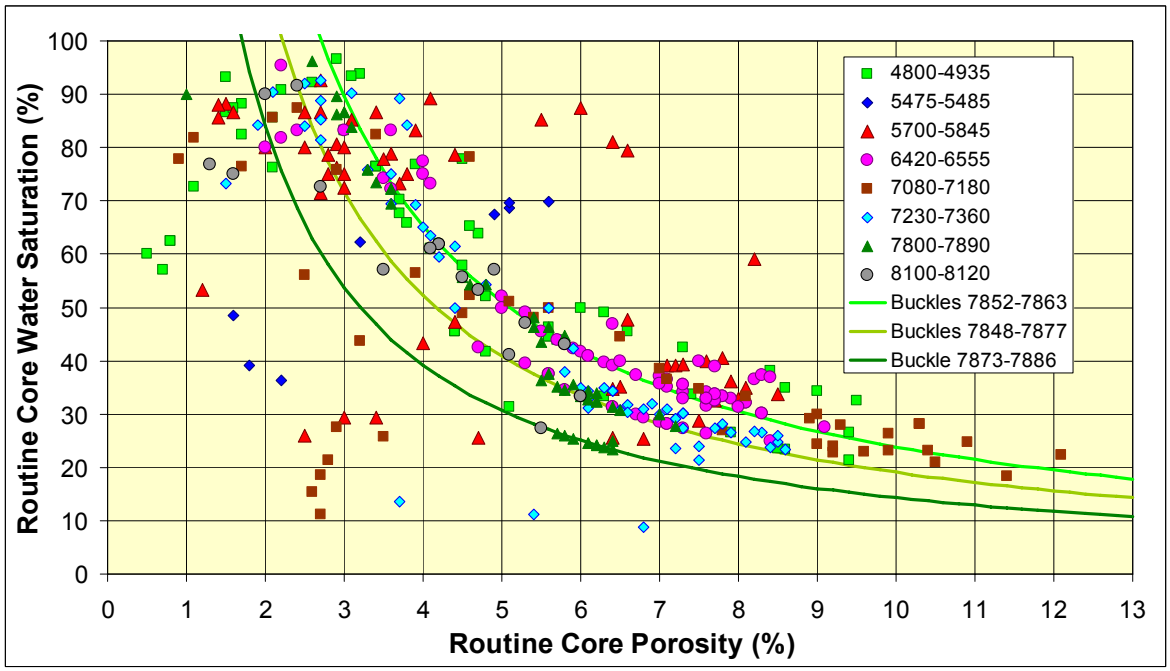

Figure 3.1.4 Routine core analysis porosity versus water saturation for the Piceance Basin MWX-2 well. Saturation versus porosity trends exhibit commonly observed Buckles power-law relationship. Trendlines for depth intervals 7852-7886 shown represent $Sw = A\phi^{-1.1}$ where A =

180, 240, and 300, respectively. Differences in trends can be postulated to be due to differences in grain size and/or clay type/content.

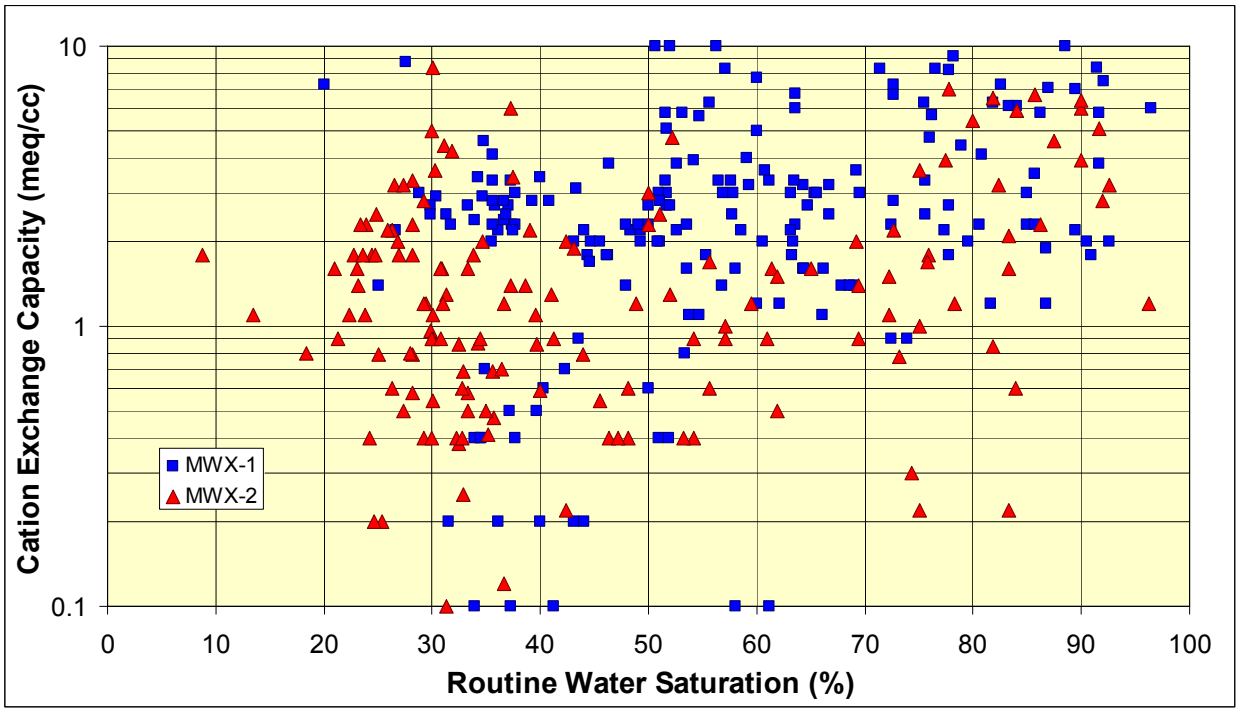

Figure 3.1.5 Routine core analysis water saturation versus cation exchange capacity for Piceance Basin MWX-1 and MWX-2 wells showing weak positive correlation.

Subtask 3.2. Compile Representative Lithofacies Core and Logs from Major Basins

3.2.1 Task Statement

Not less than a total of 300 rock samples shall be obtained from 4–5 wells in each of the five basins in the project (Washakie, Uinta, Piceance, Upper Greater Green River, and Wind River). The 4–5 wells in each basin shall be selected to provide a wide geographic distribution and shall be limited to wells that have adequate wireline log suites and core. Possible industry sponsors have been identified in each of the basins. For areas that need to be sampled but industry contribution cannot be obtained, wells shall be selected that have core available in the USGS core repository in Denver, Colorado, or other public core libraries. Cores and wells shall be selected that provide a comprehensive range in lithofacies, both reservoir and non-reservoir,

characteristic of the Mesaverde in the area and basin and that serve both the objectives of the study and assessment needs of the industry participants.

3.2.2 Methods

A principal goal of this task was to obtain a sample population of Mesaverde cores that would provide a wide range in the following properties: 1) geographic location by basin, 2) depth, 3) rock lithology, 4) porosity, 5) permeability. To achieve this goal: 1) companies were contacted to contribute core, and 2) the United States Geological Survey (USGS) Core library in Littleton, Colorado, database was searched. The drilling schedules of most of the companies did not provide core to the project until late in the first year of the project. For this reason it was decided to obtain a complete sampling of each basin from the USGS core library and supplement this with the industry cores.

Core plugs measuring approximately 2.54-cm (1-inch) in diameter and 1.9–7.6 cm (0.75–3 inches) long were cut from slabbed or full-diameter core using a diamond core drill cooled with tap water either at the United States Geological Survey (USGS) Core library in Denver, Colorado, or at service company facilities for industry-contributed core. Subsequent to coring the plugs were immediately towel dried. For two industry-contribution wells 3.8-cm (1.5-inch) diameter cores were submitted; 2.54-cm (1-inch) diameter cores were cut from these to accommodate laboratory equipment sample size constraints.

3.2.3 Results

Table 3.2.1 lists the 44 wells sampled in the six basins, comprising for each basin; Washakie – 11, Uinta – 8, Piceance – 8, Greater Green River – 7, Wind River – 4, Powder River – 6, Sand Wash – 2. Contributed cores from industry by basin included; Bill Barrett Corp. – Piceance, BP America Production – Washakie, Exxon-Mobil – Piceance, Kerr-McGee Oil & Gas Onshore – Uinta, Shell Exploration & Production – Green River, Williams Exploration & Production – Piceance. Figure 3.2.1 shows the locations of the wells sampled and Figure 3.2.2 shows the distribution of wells by basin. The addition of the Powder River and Sand Wash basins to the sampling and the geographic distribution of wells within each basin provided a comprehensive Mesaverde sampling for the size of the sampling program.

API STATE CODE	API COUNTY CODE	API WELL #	BASIN	FIELD	WELL	OPERATOR	Twn		Rng		Sec
49	035	20622	GREEN RIVER	WILDCAT	1 OLD ROAD	AMERICAN HUNTER EXPL	27	N	108	W	27
49	013	08024	GREEN RIVER	PINEDALE	5 PINEDALE	EL PASO NATURAL GAS	30	N	108	W	5
49	035	20088	GREEN RIVER	MERNA	A-1 WASP	INEXCO OIL COMPANY	36	N	112	W	28
49	035	06020	GREEN RIVER	BIG PINEY	B-54 BIG PINEY	BELCO PETROLEUM	29	N	113	W	26
49	035	05742	GREEN RIVER	TIP TOP SHALLOW	C-47 TIP TOP SHALLOW	BELCO PETROLEUM	28	N	113	W	22
49	035	06200	GREEN RIVER	MASON	K-2 MASON	BELCO PETROLEUM	31	N	113	W	13
49	035	24198	GREEN RIVER	PINEDALE	Vible 1B-11D	SHELL E&P	31	N	109	W	11
05	045		PICEANCE		1 BOOK CLIFFS-DRILL HOLE	USGS-CG	7	S	104	W	17
05	103		PICEANCE	LOWER WHITE RIVER	21011-5 MOON LAKE	WESTERN FUELS ASSOC	2	N	101	W	1
05	103	10391	PICEANCE	WILLOW RIDGE	EM T63X-2G	EXXON-MOBIL	3	S	97	W	2
05	045	11402	PICEANCE	MAMM CREEK	LAST DANCE 43C-3-792	BILL BARRETT CORP.	S	7	92	W	3
05	103	09406	PICEANCE	WHITE RIVER DOME	M-30-2-96W /D-037934	FUEL RESOURCES DEV	2	N	96	W	30
05	045	06578	PICEANCE	GRAND VALLEY	MV 24-20 CHEVRON	BARRETT ENERGY	6	S	96	W	20
05	045	06001	PICEANCE	RULISON	MWX-2 SUPERIOR	CER CORPORATION	6	S	94	W	34
05	045	10927	PICEANCE	PARACHUTE	PUCKETT/TOSCO PA 424-34	WILLIAMS E&P	6	S	95	W	34
49	005	25627	POWDER RIVER	BRIDGE DRAW	1 BARLOW 21-20	LOUISIANA LAND & EXP	48	N	75	W	20
49	009	21513	POWDER RIVER	MIKES DRAW	2 FRED STATE	DAVIS OIL COMPANY	35	N	70	W	36
49	009	06335	POWDER RIVER	FLAT TOP	2 SHAWNEE	BELCO PETROLEUM	33	N	69	W	2
49	009	05481	POWDER RIVER	FLAT TOP	3 SHAWNEE	BELCO PETROLEUM	33	N	69	W	23
05	081	06718	SAND WASH	WEST CRAIG	1-691-0513	COCKRELL OIL CORP	6	N	91	W	5
05	081	06724	SAND WASH	CRAIG DOME	1-791-2613	COCKRELL OIL CORP	7	N	91	W	26
43	047	30584	UINTA	NATURAL BUTTES	11-17F RIVER BEND UNIT	MAPCO INCOPORATED	10	S	20	E	17
43	047	30545	UINTA	BONANZA	2-7 FLAT MESA FEDERAL	ENSERCH EXPLORATION	10	S	23	E	7
43	019		UINTA		3 BOOK CLIFFS	USGS-CG	17	S	24	E	3
43	047	30860	UINTA	WILDCAT	3-24 US LAMCO	CHAMPLIN PETROLEUM	13	S	20	E	24
43	019		UINTA		4 BOOK CLIFFS	USGS-CG	17	S	24	E	31
43	047	30584	UINTA	AGENCY DRAW	4-5 US LAMCO	ENSERCH EXPLORATION	13	S	20	E	5
43	047	36565	UINTA	NATURAL BUTTES	NBU 1022-1A	KERR-MCGEE OIL&GAS ONSHORE	10	S	22	E	1
46	047	36401	UINTA	NATURAL BUTTES	NBU 920-36O	KERR-MCGEE OIL&GAS ONSHORE	9	S	22	E	36
49	037	21075	WASHAKIE		WILD ROSE 1	AMOCO PRODUCTION	17	N	94	W	5
49	037	05405	WASHAKIE	CHIMNEY ROCK	1 CHIMNEY ROCK	MOUNTAIN FUEL SUPPLY	18	N	102	W	12
49	037	21053	WASHAKIE	FIVE MILE GULCH	3 UNIT	AMOCO PRODUCTION	21	N	93	W	35
49	037	23956	WASHAKIE	SIBERIA RIDGE	5-2 SIBERIA RIDGE UNIT	AMOCO PRODUCTION	21	N	94	W	5
49	037	05683	WASHAKIE	PATRICK DRAW	65-1-7 ARCH UNIT	FOREST OIL CORP	19	N	99	W	1
49	037	05577	WASHAKIE	ARCH	ARCH UNIT UPRR #102-7-10	ANADARKO E&P CO. LP	19	N	98	W	7
49	037	05349	WASHAKIE		B-2A SPIDER CREEK	HUMBLE OIL & REF	18	N	110	W	27
49	007	21170	WASHAKIE	SAVERY	C-11 /FEE	FUEL RESOURCES DEV	12	N	90	W	11
49	037	22304	WASHAKIE	DRIPPING ROCK	DRIPPING ROCK #3	CELSIUS	14	N	94	W	8
49	037	22355	WASHAKIE	DRIPPING ROCK	DRIPPING ROCK #5	CELSIUS	14	N	94	W	19
49	037	99999	WASHAKIE		WILD ROSE	BP AMERICA PRODUCTION, INC.	18	N	94	W	33
49	013	20836	WIND RIVER	MADDEN	1-27 LOOKOUT	MONSANTO OIL	39	N	91	W	27
49	013	20786	WIND RIVER	LYSITE	1-9 LYSITE	MICH WISC PIPELINE	38	N	91	W	9
49	013	20966	WIND RIVER	MADDEN	2-1 CHEVRON	MONSANTO OIL	38	N	91	W	1
49	013	20724	WIND RIVER		31-22 TRIBAL PHILLIPS	BROWN TOM INC	4	N	3	E	31

Table 3.2.1 List of wells sampled.

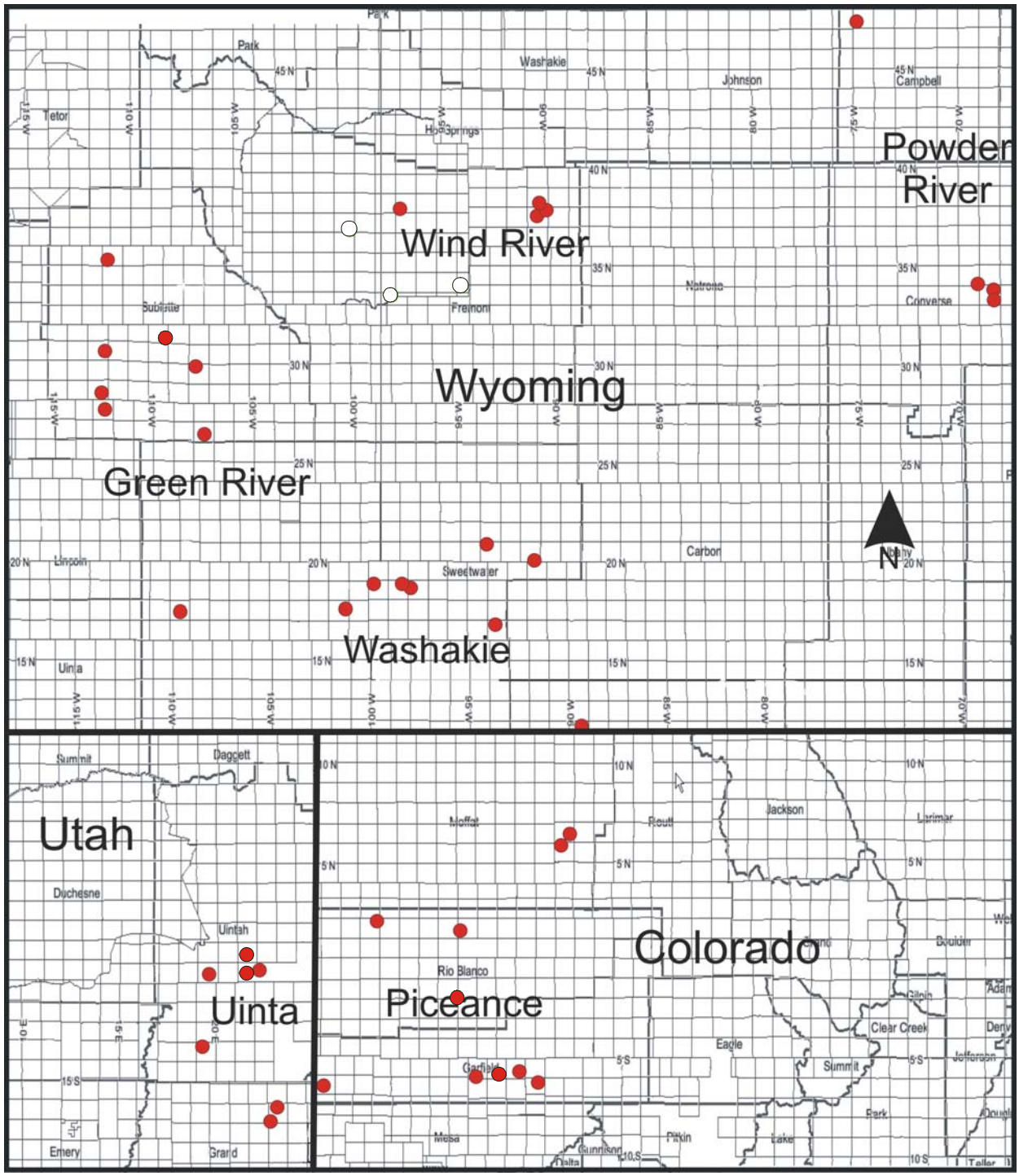

Figure 3.2.1 Location of wells sampled in study.

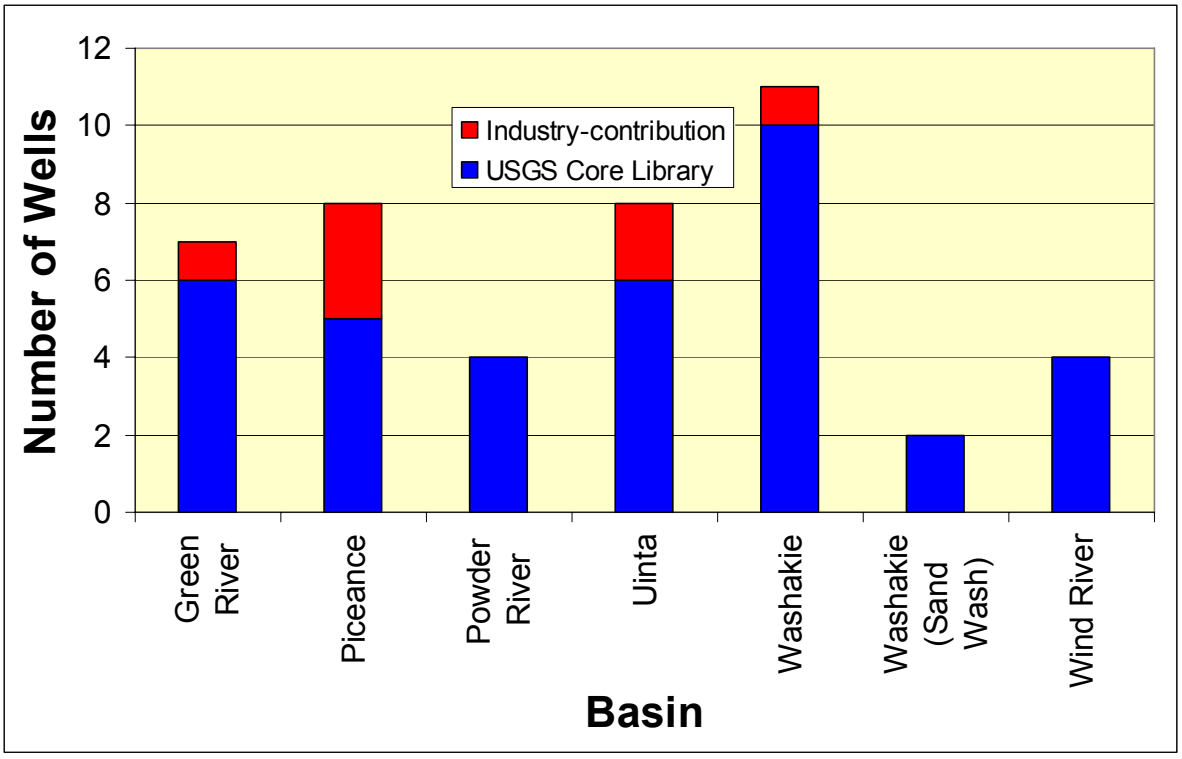

Figure 3.2.2 Number of wells sampled by basin and source.

A total of 2216 core plugs were obtained representing 1182 original plugs (A), 776 paired plugs (B), and 258 additional pair plugs (C). This sampling represents approximately four times more original plugs that the 300 core plugs proposed and six times as many paired plugs (n = 150). The decision to devote the greater effort in sampling was based on the observed variation in rock lithfacies encountered in the wells during the sampling process. To appropriately represent the lithofacies observed in core, a greater number of samples was considered necessary. Intervals sampled in wells represent the range of lithofacies and porosity exhibited by the Mesaverde in each well. Figure 3.2.3 shows the number of core plugs, original and duplicate, for each basin.

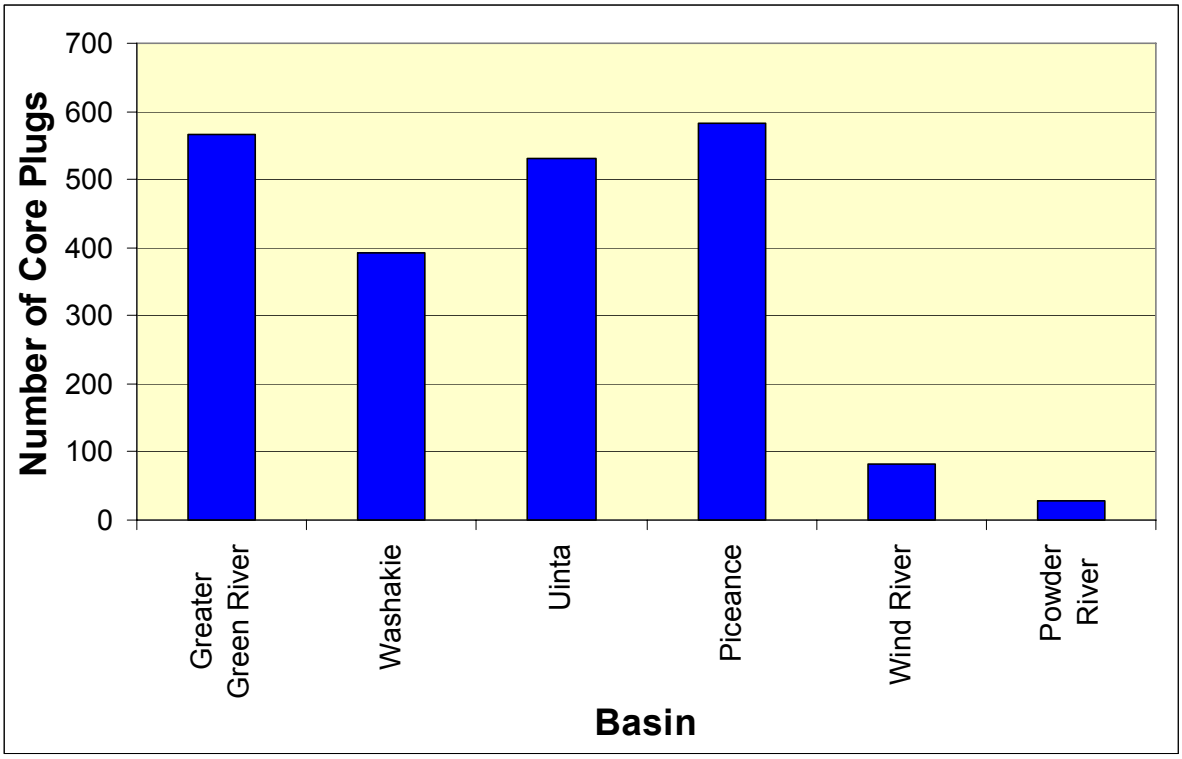

Figure 3.2.3 Number of core plugs (original and duplicate) by basin.

Core samples range in depth from 124 to 16,723 ft (Fig. 3.2.4). The distribution for the sample depths reflects the approximate complete range in depth of the Mesaverde for the basins studied.

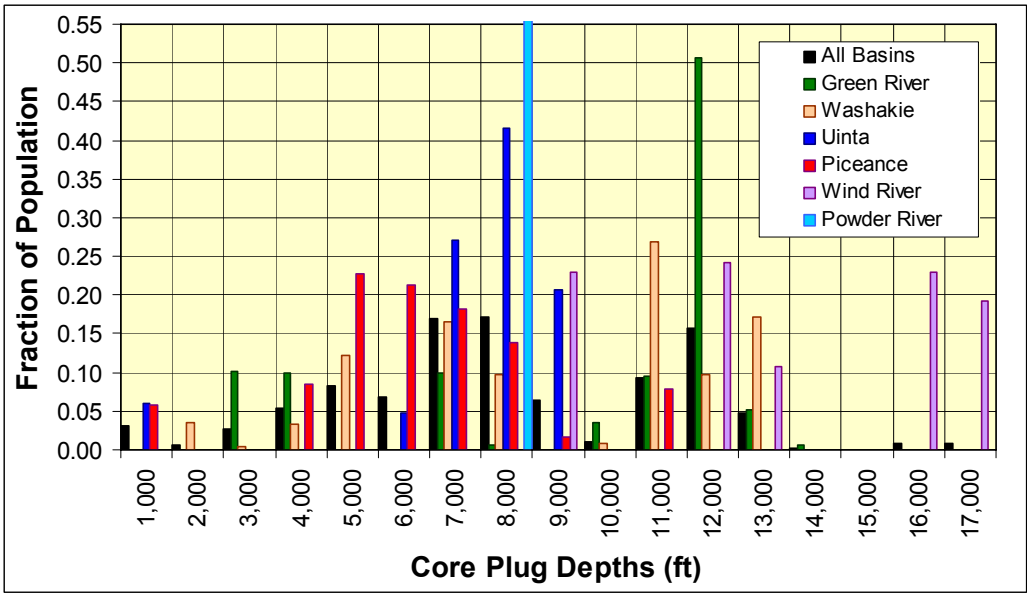

Figure 3.2.4 Distribution of core sample depths by basin.

Figure 3.2.5 illustrates that nearly the complete range in porosity exhibited by Mesaverde sandstones is present in all basins. Samples with higher porosity (ϕ>12%) were not sampled in the Wind River Basin or ϕ>16% in the Powder River Basin. Based on examination of wireline logs, this absence in the core samples reflects sampling and not absence of this range in porosity within the basins.

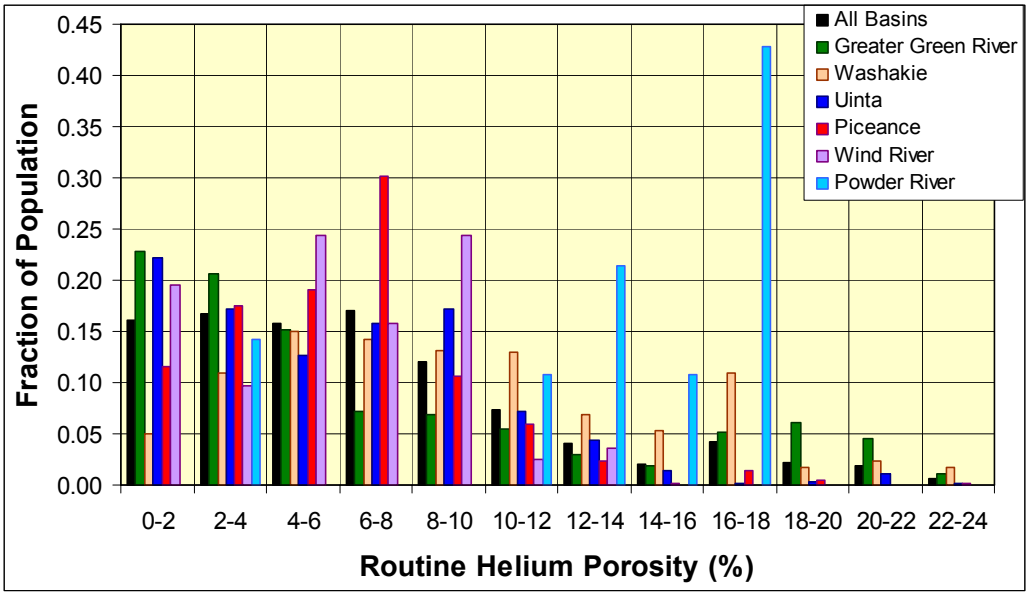

Figure 3.2.5 Routine helium porosity distribution by basin.

Subtask 3.3. Acquire logs from sample wells and digitize

3.3.1 Task Statement

A complete suite of available wireline logs shall be obtained for each of the wells from which core is obtained in Subtask 3.2. Only wells where an adequate suite of wireline logs is available shall be selected for sampling. For wells where logs are not available digitally, paper copies shall be digitized by a commercial service company.

3.3.2 Methods

Although attempts were made to select wells for which both core and a modern suite of wireline logs were available, wireline logs were not available for many of the wells for which it was important to sample for core. For industry-contributed wells, wireline logs were provided in Log ASCII Standard (LAS) format. For several of the USGS core wells LAS files were obtained from the Wyoming Oil & Gas Conservation Commission. Where digital LAS files were not available, paper copies were obtained and the log traces digitized.

3.3.3 Results

Wells shown in Table 3.3.1 were utilized for routine and advanced log analysis in Task 6. LAS files for these wells are available at **http://www.kgs.ku.edu/mesaverde/reports.html.**

BASIN	FIELD	WELL	OPERATOR	Twn		Rng		Sec
GREEN RIVER	WILDCAT	1 OLD ROAD	AMERICAN HUNTER EXPL	27	N	108	W	27
GREEN RIVER	MERNA	A-1 WASP	INEXCO OIL COMPANY	36	N	112	W	28
GREEN RIVER	PINEDALE	Vible 1B-11D	SHELL E&P	31	N	109	W	11
PICEANCE	WILLOW RIDGE	EM T63X-2G	EXXON-MOBIL	3	S	97	W	2
PICEANCE	MAMM CREEK	LAST DANCE 43C-3-792	BILL BARRETT CORP.	S	7	92	W	3
PICEANCE	GRAND VALLEY	MV 24-20 CHEVRON	BARRETT ENERGY	6	S	96	W	20
PICEANCE	RULISON	MWX-2 SUPERIOR	CER CORPORATION	6	S	94	W	34
PICEANCE	PARACHUTE	PUCKETT/TOSCO PA 424-34	WILLIAMS E&P	6	S	95	W	34
POWDER RIVER	BRIDGE DRAW	1 BARLOW 21-20	LOUISIANA LAND & EXP	48	N	75	W	20
SAND WASH	CRAIG DOME	1-791-2613	COCKRELL OIL CORP	7	N	91	W	26
UINTA	NATURAL BUTTES	11-17F RIVER BEND UNIT	MAPCO INCOPORATED	10	S	20	E	17
UINTA	BONANZA	2-7 FLAT MESA FEDERAL	ENSERCH EXPLORATION	10	S	23	E	7
UINTA	NATURAL BUTTES	NBU 1022-1A	KERR-MCGEE OIL&GAS ONSHORE	10	S	22	E	1
UINTA	NATURAL BUTTES	NBU 920-36O	KERR-MCGEE OIL&GAS ONSHORE	9	S	22	E	36
WASHAKIE	FIVE MILE GULCH	3 UNIT	AMOCO PRODUCTION	21	N	93	W	35
WASHAKIE	SIBERIA RIDGE	5-2 SIBERIA RIDGE UNIT	AMOCO PRODUCTION	21	N	94	W	5
WASHAKIE	SAVERY	C-11 /FEE	FUEL RESOURCES DEV	12	N	90	W	11
WASHAKIE	DRIPPING ROCK	DRIPPING ROCK #3	CELSIUS	14	N	94	W	8
WASHAKIE	DRIPPING ROCK	DRIPPING ROCK #5	CELSIUS	14	N	94	W	19
WASHAKIE		WILD ROSE 1	AMOCO PRODUCTION	17	N	94	W	5
WIND RIVER	MADDEN	1-27 LOOKOUT	MONSANTO OIL	39	N	91	W	27

Table 3.3.1 List of wells for which LAS files were obtained or created and are used for routine and advanced log analysis.

Task 4. Measure Rock Properties

Subtask 4.1. Measure Basic Properties (K, ϕ, Grain Density) and Select Advanced Population

4.1.1 Task Statement

Objectives of this task are to perform routine core analysis on not less than a total of 300 core samples. Data to be obtained include whole-core porosity, permeability and grain density where previously measured and publicly available, routine helium porosity, routine air and *in situ* Klinkenberg permeability, and grain density. These measurements are intended to provide a basis for selecting the representative 150 samples for more advanced testing.

4.1.2 Methods

4.1.2.1 Sample Preparation

Core plugs measuring approximately 2.54 cm (1 inch) in diameter and 1.9–7.6 cm (0.75–3 inches) long were cut from slabbed or full-diameter core using a diamond core drill cooled with tap water either at the United States Geological Survey (USGS) Core library in Denver, Colorado, or at service company facilities, for industry-contributed core. Subsequent to coring the plugs were immediately towel dried. For two industry-contribution wells, 3.8-cm (1.5-inch) diameter cores were submitted. 2.54-cm (1-inch) diameter cores were cut from these to accommodate laboratory equipment sample size constraints. Core plug ends were trimmed to make right cylinders using tap water as coolant at the Kansas Geological Survey. The core plug ends were subsequently used for geologic analysis, including rock thin sections. The first core samples obtained, from the Amoco Five Mile Gulch Unit 3 and Hunter Old Road #1 wells, were vacuum/pressure saturated with a toluene/methyl alcohol azeotrope, and then soxhlet extracted with toluene/methyl alcohol to remove any remnant oil and salts. They were dried in an oven at 60 ^{o}C to a constant weight within $\pm$ 0.003g. Subsequent to these two wells, cores from the remaining wells were vacuum saturated with methyl alcohol, maintained in the methyl alcohol bath for not less than 3 days, air dried for approximately 3 days, immersed again in methyl alcohol to rinse off any salts precipitated from surface evaporation, and then dried in a convection oven at 60 ^{o}C to a constant weight within 0.003

g. Cores were generally left in the oven for 3 to 6 days. This sample preparation procedure allowed the processing of many hundreds of core plugs.

Both low-humidity and humidity-oven drying at a relative humidity of 45% have been used for low-permeability sandstones. Experimental methodology in low-permeability sandstone core preparation is complicated by uncertainties in microscopic properties including principally water distribution, clay mineral hydration state, and salt distribution. Studies by Soeder (1988) and Morrow et al. (1991) concluded that preserved core provide more accurate effective gas permeability values. However, although porosity and saturation differences were not reported, saturation differences between the dry and hydrated can be estimated to be Sw=10$\pm$5%. For these saturation differences the observed decrease in hydrated sample gas permeability of 57–96% of dry permeability is consistent with relative permeability decreases observed in Figures 3.1.1 and 3.1.2. That is, the observed lower permeability for hydrated samples can be interpreted to have been the result of relative permeability effects and not drying.

Morrow et al. (1991) further hypothesized that the original salt content of the brine that originally occupied the pore space remained in the pores because the present lower water saturation was achieved by evaporation. Though possible, this hypothesis was not tested. To resaturate the cores Morrow et al. used freshwater and, it can be interpreted, implicitly hypothesized that 1) the remnant salt was uniformly distributed in the pore space, 2) remnant salt would dissolve in the injected freshwater in the pore and would result in a uniform brine concentration that was compatible with the clays, 3) during the process of cutting the core plug with fresh tap water no significant flushing occurred to remove the dried salts, 4) the freshwater did not damage any clays prior to dissolving the remnant salt, 5) confining stress hysteresis effects were negligible as required by comparison of stressed preserved core effective gas permeabilities to subsequently dried and stressed dried core effective gas permeabilities.

In the Morrow et al. study, comparison of the relative role of confining pressure and preservation versus drying (their Figure 7) shows that differences of +1,000 psi confining pressure result in a greater difference in effective gas permeability than differences resulting from preservation state for all saturation levels (Sw = 0%–60%). This strong influence of stress sensitivity implies that error associated stress sensitivity hysteresis has to be removed for quantitative analysis of the relative influence of preservation. Further, it is recognized that core containing swelling clays is sensitive to freshwater. If the remnant dry salts are either 1) no longer at the correct salinity, or

2) not uniformly distributed on a volumetric basis throughout the pore space such that imbibing freshwater would mix to form a brine of the correct salinity in equilibrium with the pore-lining or pore-bridging expansive clay, then imbibition of freshwater is likely to cause clay swelling and permeability decrease, consistent with the decrease observed by Morrow et al. (1991) but attributed to clay state resulting from preservation versus drying.

Soeder (1986) presents differences in preserved state and dry permeabilities but does not report porosity and saturations to provide a basis for quantitatively estimating possible relative permeability influence. Soeder (1986) also presents Scanning Electron Microscope images of dry and preserved pores noting damage in the dried samples. It is important to note that all SEM images shown were of dried samples because the SEM images presented were not obtained in an environmental SEM (commonly used for biologic SEM imaging). In fact, nearly all SEM images of tight gas sandstone clays presented in publications are from dried samples that are conventionally gold coated. The preservation of delicate clay structure in all these images can be interpreted to indicate that moderate drying does not damage clays.

The above discussion does not reject the hypothesis that gas permeabilities are most accurately measured on preserved core. To the contrary, it can be reasonably argued that the closer to native-state conditions a core remains, the more accurate the properties measured can remain. However, the above discussion illustrates that a given experimental procedure does not always guarantee that the microscopic properties of the core have been perfectly preserved nor that any change in environmental conditions results in “significant” and unacceptable change to key properties. It is also clear that gas permeabilities measured on core are always influenced by a wide range of environmental variables to which the core has been subjected and is subjected to for a given measurement, including principally 1) stress history, 2) draining and imbibing fluid composition and history, 3) testing history, and 4) pore-lining or pore-bridging mineral (e.g., clay) composition. Beyond these considerations there are considerations concerning the nature of the property for which data are needed. Preserved core may provide more accurate effective gas permeabilities but not absolute permeability, and if helium porosity is measured on the cores in this state the measured grain density and total porosity values are affected. The extent to which these are affected can only be quantitatively determined by subsequently drying the core and retesting. Further, accurate mercury-intrusion capillary-pressure analysis requires a clean dry surface for the

general mercury-mercury vapor interfacial tension and contact angle to apply. Therefore this measurement requires a dried core and initial pore volume measured at dry conditions.

The primary purpose of this research is to provide a database of basic properties and to use the observed values to select samples for mercury intrusion capillary pressure analysis, and electrical properties analysis and critical-gas permeability measurement on resaturated cores. Given; 1) the unpreserved state of 38 of the 44 cores, 2) the need for accurate total porosity, 3) the large population of cores, 4) the need for cores that do not contain significant content of remnant salt, and 5) the need for clean dry cores for MICP, it was decided to clean and dry the cores, recognizing that some modification to gas permeability might result.

4.1.2.2 Routine Helium Porosity and Grain Density

Routine helium porosities were determined using a Boyle's Law technique. Dry sample weights were measured to $\pm$0.001 g and bulk volume was determined by Archimedes's Principle method by immersion in mercury and by caliper to an accuracy of $\pm$0.02 cc. Ambient helium porosity was measured to an accuracy and precision of better than $\pm$ 0.1 porosity percent. Grain density was calculated from the helium-measured grain volume and dry weight to an accuracy and precision of better than $\pm$0.01 g/cc.

4.1.2.3 Routine Air and In Situ Klinkenberg Permeability

To measure routine air permeability each core was placed in a biaxial Hassler-type core holder and subjected to a hydrostatic confining stress of 4.14 MPa (600 psi). Permeability was measured from steady-state nitrogen-gas flow measured at a constant upstream pressure of 20 psi to 400 psi, depending on the core permeability, with the downstream pressure at atmospheric pressure. Gas flow rate was measured using a high- or ultra-low flow range electronic mass flow meter for gas flow rates down to 0.05 scc/min and a bubble tube with a stop watch for flow rates less than 0.05 scc/min.

It is well recognized that it is necessary to restore low-permeability core samples to *in situ* stress conditions to obtain permeability values that are representative of the reservoir (Vairogs et al., 1971; Thomas and Ward, 1972; Byrnes et al., 1979; Jones and Owens, 1980; Walls et al., 1982; Sampath and Keighin, 1981; Ostensen, 1983; Wei et al., 1986; Luffel et al., 1991; Byrnes, 1997; Byrnes and Castle, 2000; Byrnes, 2005). To achieve uniformly constant

approximate *in situ* conditions, subsequent to the routine air permeability measurement, the hydrostatic confining pressure was increased to 27.6 MPa (4,000 psi) greater than the mean pore pressure in the core. *In sit u* Klinkenberg permeability was determined by measurement of permeability to nitrogen at two pore pressures and extrapolation of the k vs. 1/P trend to infinite pore pressure to obtain the Klinkenberg permeability at the intercept. The Klinkenberg gas permeability, which is equivalent to single-phase inert liquid or high-pressure gas absolute permeability, increases with decreasing pore size. Equilibrium times ranged from 2 to 30 minutes with decreasing permeability.

4.1.3 Results

Table 4.1.1 summarizes all routine helium porosity, grain density, routine air permeability, in situ Klinkenberg permeability, and sample lithologic digital description data for all core plugs in the project.

Table 4.1.1

Summary of Porosity, Permeability, and Grain Density
Analysis of Critical Permeability, Capillary Pressure, and Electrical Properties for Mesaverde Tight Gas Sandstones from Western U.S. Basins
US DOE # DE-FC26-05NT42660
Alan P. Byrnes, Robert M. Cluff, John C. Webb, Daniel A. Krygowski, Stefani D. Whittaker
website: http://www.kgs.ku.edu/mesaverde

USGS Library Number	Basin	API Number	Well Name	Operator	State	Township	Range	Section	Quarter Section	Plug Depth	Plug Letter	Ambient Porosity	Grain Density	Routine Gas Permeability	*in situ* Klinkenberg Gas Permeability	*in situ* Klinkenberg *constant b*	Rock Type Code	Formations
										ft	A/B/C	%	g/cc	mD	mD	(psia)		
B029	Green River	4903520088	A-1 WASP	INEXCO OIL COMPANY	WY	36N	112W	28	NWNESW	10441.1	C	1.6	2.62	0.00427	0.000167	311	13216	MVRD
B029	Green River	4903520088	A-1 WASP	INEXCO OIL COMPANY	WY	36N	112W	28	NWNESW	10441.1	A	1.6	2.63	0.00234	0.000061	363	13216	MVRD
B029	Green River	4903520088	A-1 WASP	INEXCO OIL COMPANY	WY	36N	112W	28	NWNESW	10441.1	B	1.6	2.62	0.00226	0.000123	240	13216	MVRD
B029	Green River	4903520088	A-1 WASP	INEXCO OIL COMPANY	WY	36N	112W	28	NWNESW	10450.5	B	1.8	2.63	0.00629	0.000219	486	14276	MVRD
B029	Green River	4903520088	A-1 WASP	INEXCO OIL COMPANY	WY	36N	112W	28	NWNESW	10450.5	A	1.7	2.63	0.00172	0.000014	353	14276	MVRD
B029	Green River	4903520088	A-1 WASP	INEXCO OIL COMPANY	WY	36N	112W	28	NWNESW	10450.5	C	1.7	2.63	0.000362	0.000001	2918	14276	MVRD
B029	Green River	4903520088	A-1 WASP	INEXCO OIL COMPANY	WY	36N	112W	28	NWNESW	10455.1	B	2.2	2.62	0.0102	0.000010	737	13217	MVRD
B029	Green River	4903520088	A-1 WASP	INEXCO OIL COMPANY	WY	36N	112W	28	NWNESW	10455.1	C	1.9	2.61	0.00541	0.000131	238	13217	MVRD
B029	Green River	4903520088	A-1 WASP	INEXCO OIL COMPANY	WY	36N	112W	28	NWNESW	10455.1	A	2.2	2.63	0.00539	0.000176	283	13217	MVRD
B029	Green River	4903520088	A-1 WASP	INEXCO OIL COMPANY	WY	36N	112W	28	NWNESW	10458.8	C	3.8	2.63	0.00601	0.000019	384	13256	MVRD
B029	Green River	4903520088	A-1 WASP	INEXCO OIL COMPANY	WY	36N	112W	28	NWNESW	10458.8	A	3.7	2.64	0.00513	0.000354	169	13256	MVRD
B029	Green River	4903520088	A-1 WASP	INEXCO OIL COMPANY	WY	36N	112W	28	NWNESW	10458.8	B	3.5	2.62	0.00286	0.000169	289	13256	MVRD
B029	Green River	4903520088	A-1 WASP	INEXCO OIL COMPANY	WY	36N	112W	28	NWNESW	10462.0	B	3.5	2.64	0.00489	0.000291	260	15286	MVRD
B029	Green River	4903520088	A-1 WASP	INEXCO OIL COMPANY	WY	36N	112W	28	NWNESW	10462.0	A	3.5	2.64	0.00334	0.000223	471	15286	MVRD
B029	Green River	4903520088	A-1 WASP	INEXCO OIL COMPANY	WY	36N	112W	28	NWNESW	10462.0	C	3.1	2.63	0.00239	0.000118	242	15286	MVRD
B029	Green River	4903520088	A-1 WASP	INEXCO OIL COMPANY	WY	36N	112W	28	NWNESW	10481.9	C	1.9	2.62	0.00761	0.000021	407	14296	MVRD
B029	Green River	4903520088	A-1 WASP	INEXCO OIL COMPANY	WY	36N	112W	28	NWNESW	10481.9	B	1.8	2.62	0.00484	0.000290	109	14296	MVRD
B029	Green River	4903520088	A-1 WASP	INEXCO OIL COMPANY	WY	36N	112W	28	NWNESW	10481.9	A	2.1	2.62	0.00356	0.000045	867	14296	MVRD
B029	Green River	4903520088	A-1 WASP	INEXCO OIL COMPANY	WY	36N	112W	28	NWNESW	10493.2	C	1.0	2.63	0.0131	0.000033	189	14296	MVRD
B029	Green River	4903520088	A-1 WASP	INEXCO OIL COMPANY	WY	36N	112W	28	NWNESW	10493.2	A	1.1	2.63	0.00272	0.000022	690	14296	MVRD
B029	Green River	4903520088	A-1 WASP	INEXCO OIL COMPANY	WY	36N	112W	28	NWNESW	10493.2	B	0.8	2.63	0.00152			14296	MVRD
B029	Green River	4903520088	A-1 WASP	INEXCO OIL COMPANY	WY	36N	112W	28	NWNESW	10500.8	C	1.1	2.63	0.00846	0.000013	732	13266	MVRD
B029	Green River	4903520088	A-1 WASP	INEXCO OIL COMPANY	WY	36N	112W	28	NWNESW	10500.8	B	1.2	2.63	0.00791	0.000059	340	13266	MVRD
B029	Green River	4903520088	A-1 WASP	INEXCO OIL COMPANY	WY	36N	112W	28	NWNESW	10500.8	A	1.6	2.64	0.00160	0.000039	535	13266	MVRD
B029	Green River	4903520088	A-1 WASP	INEXCO OIL COMPANY	WY	36N	112W	28	NWNESW	10504.5	A	0.9	2.65	0.00932	0.000026	379	13266	MVRD
B029	Green River	4903520088	A-1 WASP	INEXCO OIL COMPANY	WY	36N	112W	28	NWNESW	10504.5	B	0.9	2.65	0.00470	0.000131	226	13266	MVRD
B029	Green River	4903520088	A-1 WASP	INEXCO OIL COMPANY	WY	36N	112W	28	NWNESW	10504.5	C	0.9	2.66				13266	MVRD
B029	Green River	4903520088	A-1 WASP	INEXCO OIL COMPANY	WY	36N	112W	28	NWNESW	10514.8	C	1.9	2.61	1.54	0.0642	47.6	13216	MVRD
B029	Green River	4903520088	A-1 WASP	INEXCO OIL COMPANY	WY	36N	112W	28	NWNESW	10514.8	A	1.0	2.59	0.243	0.000558	179	13216	MVRD
B029	Green River	4903520088	A-1 WASP	INEXCO OIL COMPANY	WY	36N	112W	28	NWNESW	10514.8	B	4.6	2.60	0.0336	0.000155	150	13216	MVRD
B029	Green River	4903520088	A-1 WASP	INEXCO OIL COMPANY	WY	36N	112W	28	NWNESW	10529.9	B	2.4	2.60	0.0193	0.000029	385	13296	MVRD
B029	Green River	4903520088	A-1 WASP	INEXCO OIL COMPANY	WY	36N	112W	28	NWNESW	10529.9	C	2.3	2.60	0.00344	0.000101	369	13296	MVRD
B029	Green River	4903520088	A-1 WASP	INEXCO OIL COMPANY	WY	36N	112W	28	NWNESW	10529.9	A	2.3	2.59	0.00315	0.000048	1240	13296	MVRD
B029	Green River	4903520088	A-1 WASP	INEXCO OIL COMPANY	WY	36N	112W	28	NWNESW	10537.2	A	3.5	2.65	0.0118	0.000190	195	13256	MVRD
B029	Green River	4903520088	A-1 WASP	INEXCO OIL COMPANY	WY	36N	112W	28	NWNESW	10537.2	B	3.3	2.64	0.00540	0.000337	271	13256	MVRD
B029	Green River	4903520088	A-1 WASP	INEXCO OIL COMPANY	WY	36N	112W	28	NWNESW	10537.2	C	3.4	2.63	0.00330	0.000287	121	13256	MVRD
B029	Green River	4903520088	A-1 WASP	INEXCO OIL COMPANY	WY	36N	112W	28	NWNESW	10540.5	C	1.7	2.62	0.00375	0.000120	211	13285	MVRD
B029	Green River	4903520088	A-1 WASP	INEXCO OIL COMPANY	WY	36N	112W	28	NWNESW	10540.5	B	1.6	2.62	0.00241	0.000054	391	13285	MVRD
B029	Green River	4903520088	A-1 WASP	INEXCO OIL COMPANY	WY	36N	112W	28	NWNESW	10540.5	A	1.7	2.63	0.000712	0.000006	455	13285	MVRD
B029	Green River	4903520088	A-1 WASP	INEXCO OIL COMPANY	WY	36N	112W	28	NWNESW	10544.5	B	1.0	2.67	0.00258	0.000112	206	16286	MVRD
B029	Green River	4903520088	A-1 WASP	INEXCO OIL COMPANY	WY	36N	112W	28	NWNESW	10544.5	A	1.0	2.66	0.00181	0.000057	251	16286	MVRD
B029	Green River	4903520088	A-1 WASP	INEXCO OIL COMPANY	WY	36N	112W	28	NWNESW	10544.5	C	0.6	2.66	0.000826	0.000006	426	16286	MVRD
B029	Green River	4903520088	A-1 WASP	INEXCO OIL COMPANY	WY	36N	112W	28	NWNESW	10547.9	C	0.9	2.65	0.00299	0.000242	210	15286	MVRD
B029	Green River	4903520088	A-1 WASP	INEXCO OIL COMPANY	WY	36N	112W	28	NWNESW	10547.9	A	1.2	2.65	0.000684	0.000014	464	15286	MVRD
B029	Green River	4903520088	A-1 WASP	INEXCO OIL COMPANY	WY	36N	112W	28	NWNESW	10547.9	B	0.8	2.65	0.000628	0.000024	287	15286	MVRD
B029	Green River	4903520088	A-1 WASP	INEXCO OIL COMPANY	WY	36N	112W	28	NWNESW	10557.5	C	1.1	2.63	0.00473	0.000132	214	13216	MVRD
B029	Green River	4903520088	A-1 WASP	INEXCO OIL COMPANY	WY	36N	112W	28	NWNESW	10557.5	A	0.6	2.63	0.00399	0.000185	214	13216	MVRD
B029	Green River	4903520088	A-1 WASP	INEXCO OIL COMPANY	WY	36N	112W	28	NWNESW	10557.5	B	0.8	2.63	0.00353	0.000083	247	13216	MVRD
B029	Green River	4903520088	A-1 WASP	INEXCO OIL COMPANY	WY	36N	112W	28	NWNESW	10565.3	A	1.3	2.60	0.0112	0.000020	293	13216	MVRD
B029	Green River	4903520088	A-1 WASP	INEXCO OIL COMPANY	WY	36N	112W	28	NWNESW	10565.3	B	1.1	2.60	0.00366	0.000063	454	13216	MVRD
B029	Green River	4903520088	A-1 WASP	INEXCO OIL COMPANY	WY	36N	112W	28	NWNESW	10565.3	C	0.9	2.60	0.00303	0.000047	343	13216	MVRD
B029	Green River	4903520088	A-1 WASP	INEXCO OIL COMPANY	WY	36N	112W	28	NWNESW	10573.1	B	3.1	2.66	0.00350	0.000201	152	13266	MVRD
B029	Green River	4903520088	A-1 WASP	INEXCO OIL COMPANY	WY	36N	112W	28	NWNESW	10573.1	C	3.0	2.66	0.00307	0.000160	312	13266	MVRD
B029	Green River	4903520088	A-1 WASP	INEXCO OIL COMPANY	WY	36N	112W	28	NWNESW	10573.1	A	3.3	2.67	0.00289	0.000155	465	13266	MVRD
B029	Green River	4903520088	A-1 WASP	INEXCO OIL COMPANY	WY	36N	112W	28	NWNESW	11332.9	C	3.6	2.64	0.0491	0.000832	151	16286	MVRD
B029	Green River	4903520088	A-1 WASP	INEXCO OIL COMPANY	WY	36N	112W	28	NWNESW	11332.9	A	3.5	2.64	0.0300	0.000728	136	16286	MVRD
B029	Green River	4903520088	A-1 WASP	INEXCO OIL COMPANY	WY	36N	112W	28	NWNESW	11332.9	B	7.6	2.75	0.0298	0.000609	216	16286	MVRD
B029	Green River	4903520088	A-1 WASP	INEXCO OIL COMPANY	WY	36N	112W	28	NWNESW	11338.2	B	3.7	2.64	0.0309	0.000484	135	16276	MVRD
B029	Green River	4903520088	A-1 WASP	INEXCO OIL COMPANY	WY	36N	112W	28	NWNESW	11338.2	A	3.5	2.64	0.00436	0.000402	350	16276	MVRD
B029	Green River	4903520088	A-1 WASP	INEXCO OIL COMPANY	WY	36N	112W	28	NWNESW	11338.2	C	3.6	2.66	0.00256	0.000398	178	16276	MVRD
B029	Green River	4903520088	A-1 WASP	INEXCO OIL COMPANY	WY	36N	112W	28	NWNESW	11374.9	A	0.9	2.65	0.00353	0.000098	276	14296	MVRD
B029	Green River	4903520088	A-1 WASP	INEXCO OIL COMPANY	WY	36N	112W	28	NWNESW	11374.9	C	0.9	2.65	0.00322	0.000083	226	14296	MVRD
B029	Green River	4903520088	A-1 WASP	INEXCO OIL COMPANY	WY	36N	112W	28	NWNESW	11374.9	B	0.5	2.64	0.00112	0.000018	552	14296	MVRD
B029	Green River	4903520088	A-1 WASP	INEXCO OIL COMPANY	WY	36N	112W	28	NWNESW	11388.3	C	1.4	2.62	0.00935	0.000222	276	12217	MVRD
B029	Green River	4903520088	A-1 WASP	INEXCO OIL COMPANY	WY	36N	112W	28	NWNESW	11388.3	B	1.7	2.62	0.00632	0.000096	489	12217	MVRD
B029	Green River	4903520088	A-1 WASP	INEXCO OIL COMPANY	WY	36N	112W	28	NWNESW	11388.3	A	1.1	2.61	0.00460	0.000101	743	12217	MVRD
B029	Green River	4903520088	A-1 WASP	INEXCO OIL COMPANY	WY	36N	112W	28	NWNESW	11395.5	B	0.7	2.63	0.00483	0.000105	342	13267	MVRD
B029	Green River	4903520088	A-1 WASP	INEXCO OIL COMPANY	WY	36N	112W	28	NWNESW	11395.5	C	0.8	2.64	0.00446	0.000093	350	13267	MVRD
B029	Green River	4903520088	A-1 WASP	INEXCO OIL COMPANY	WY	36N	112W	28	NWNESW	11395.5	A	1.7	2.66	0.000492	0.000001	1737	13267	MVRD
B029	Green River	4903520088	A-1 WASP	INEXCO OIL COMPANY	WY	36N	112W	28	NWNESW	11419.3	B	0.8	2.60	2.16	0.0389	43.5	11299	MVRD
B029	Green River	4903520088	A-1 WASP	INEXCO OIL COMPANY	WY	36N	112W	28	NWNESW	11419.3	A	0.6	2.61	1.18	0.0156	71.5	11299	MVRD
B029	Green River	4903520088	A-1 WASP	INEXCO OIL COMPANY	WY	36N	112W	28	NWNESW	11433.6	C	0.8	2.64	0.00340	0.000107	262	12297	MVRD
B029	Green River	4903520088	A-1 WASP	INEXCO OIL COMPANY	WY	36N	112W	28	NWNESW	11433.6	B	0.6	2.64	0.00113	0.000009	1774	12297	MVRD
B029	Green River	4903520088	A-1 WASP	INEXCO OIL COMPANY	WY	36N	112W	28	NWNESW	11433.6	A	0.4	2.64	0.000806	0.000004	728	12297	MVRD
B029	Green River	4903520088	A-1 WASP	INEXCO OIL COMPANY	WY	36N	112W	28	NWNESW	11437.3	C	1.2	2.58	0.00882	0.00128	160	14296	MVRD
B029	Green River	4903520088	A-1 WASP	INEXCO OIL COMPANY	WY	36N	112W	28	NWNESW	11437.3	A	0.9	2.57	0.00315	0.000050	402	14296	MVRD
B029	Green River	4903520088	A-1 WASP	INEXCO OIL COMPANY	WY	36N	112W	28	NWNESW	11437.3	B	0.5	2.57	0.00238	0.000039	431	14296	MVRD
B029	Green River	4903520088	A-1 WASP	INEXCO OIL COMPANY	WY	36N	112W	28	NWNESW	11443.7	B	2.7	2.64	0.00526			15276	MVRD
B029	Green River	4903520088	A-1 WASP	INEXCO OIL COMPANY	WY	36N	112W	28	NWNESW	11443.7	C	3.1	2.66	0.00495			15276	MVRD
B029	Green River	4903520088	A-1 WASP	INEXCO OIL COMPANY	WY	36N	112W	28	NWNESW	11443.7	A	2.8	2.64	0.00352	0.000322	160	15276	MVRD
B029	Green River	4903520088	A-1 WASP	INEXCO OIL COMPANY	WY	36N	112W	28	NWNESW	11443.8	B	6.6	2.75	0.0251	0.00177	30.8	15276	MVRD
B029	Green River	4903520088	A-1 WASP	INEXCO OIL COMPANY	WY	36N	112W	28	NWNESW	11443.8	A	3.1	2.64	0.0236	0.000681	45.5	15276	MVRD
B029	Green River	4903520088	A-1 WASP	INEXCO OIL COMPANY	WY	36N	112W	28	NWNESW	11443.8	C	2.8	2.64	0.00248	0.000352	50.8	15276	MVRD
B029	Green River	4903520088	A-1 WASP	INEXCO OIL COMPANY	WY	36N	112W	28	NWNESW	11447.8	C	3.1	2.60	0.132	0.00228	57.8	19276	MVRD
B029	Green River	4903520088	A-1 WASP	INEXCO OIL COMPANY	WY	36N	112W	28	NWNESW	11447.8	A	4.8	2.61	0.0143	0.00163	135	19276	MVRD
B029	Green River	4903520088	A-1 WASP	INEXCO OIL COMPANY	WY	36N	112W	28	NWNESW	11447.8	B	1.6	2.56	0.0107	0.000594	202	19276	MVRD
B029	Green River	4903520088	A-1 WASP	INEXCO OIL COMPANY	WY	36N	112W	28	NWNESW	11448.9	B	1.4	2.63	0.00469	0.000111	368	19276	MVRD
B029	Green River	4903520088	A-1 WASP	INEXCO OIL COMPANY	WY	36N	112W	28	NWNESW	11448.9	C	1.6	2.64	0.00460	0.000097	415	19276	MVRD
B029	Green River	4903520088	A-1 WASP	INEXCO OIL COMPANY	WY	36N	112W	28	NWNESW	11448.9	A	1.4	2.63	0.00341	0.000054	1085	19276	MVRD
B029	Green River	4903520088	A-1 WASP	INEXCO OIL COMPANY	WY	36N	112W	28	NWNESW	11450.2	B	4.7	2.63	0.107	0.00684	47.0	15226	MVRD
B029	Green River	4903520088	A-1 WASP	INEXCO OIL COMPANY	WY	36N	112W	28	NWNESW	11450.2	C	4.5	2.64	0.0437	0.00205	50.3	15226	MVRD
B029	Green River	4903520088	A-1 WASP	INEXCO OIL COMPANY	WY	36N	112W	28	NWNESW	11450.2	A	4.9	2.64	0.00572	0.000854	280	15226	MVRD
B029	Green River	4903520088	A-1 WASP	INEXCO OIL COMPANY	WY	36N	112W	28	NWNESW	11457.8	C	5.5	2.64	0.131	0.0116	17.0	15226	MVRD
B029	Green River	4903520088	A-1 WASP	INEXCO OIL COMPANY	WY	36N	112W	28	NWNESW	11457.8	B	5.2	2.64	0.0769	0.00596	34.4	15226	MVRD
B029	Green River	4903520088	A-1 WASP	INEXCO OIL COMPANY	WY	36N	112W	28	NWNESW	11457.8	A	4.4	2.63	0.0643	0.00271	90.3	15226	MVRD
B029	Green River	4903520088	A-1 WASP	INEXCO OIL COMPANY	WY	36N	112W	28	NWNESW	11457.9	B	5.1	2.64	0.0543	0.00218	51.5	15226	MVRD
B029	Green River	4903520088	A-1 WASP	INEXCO OIL COMPANY	WY	36N	112W	28	NWNESW	11457.9	C	5.0	2.64	0.0246	0.00519	99.3	15226	MVRD
B029	Green River	4903520088	A-1 WASP	INEXCO OIL COMPANY	WY	36N	112W	28	NWNESW	11457.9	A	5.5	2.66	0.00271	0.000110	147	15226	MVRD
B029	Green River	4903520088	A-1 WASP	INEXCO OIL COMPANY	WY	36N	112W	28	NWNESW	11459.1	C	5.6	2.63	0.0435	0.00128	78.4	15296	MVRD
B029	Green River	4903520088	A-1 WASP	INEXCO OIL COMPANY	WY	36N	112W	28	NWNESW	11459.1	A	5.4	2.64	0.0106	0.000827	105	15296	MVRD
B029	Green River	4903520088	A-1 WASP	INEXCO OIL COMPANY	WY	36N	112W	28	NWNESW	11459.1	B			0.00992	0.000933	83.5	15296	MVRD
B029	Green River	4903520088	A-1 WASP	INEXCO OIL COMPANY	WY	36N	112W	28	NWNESW	11459.2	A	4.5	2.64	0.0637	0.00184	67.5	15296	MVRD
B029	Green River	4903520088	A-1 WASP	INEXCO OIL COMPANY	WY	36N	112W	28	NWNESW	11459.2	C	5.2	2.63	0.0603	0.00369	52.8	15296	MVRD
B029	Green River	4903520088	A-1 WASP	INEXCO OIL COMPANY	WY	36N	112W	28	NWNESW	11459.2	B	5.4	2.64	0.0239	0.00549	34.3	15296	MVRD
B029	Green River	4903520088	A-1 WASP	INEXCO OIL COMPANY	WY	36N	112W	28	NWNESW	11460.5	A	4.4	2.64	0.900	0.132	30.2	15286	MVRD
B029	Green River	4903520088	A-1 WASP	INEXCO OIL COMPANY	WY	36N	112W	28	NWNESW	11460.5	C	4.1	2.63	0.0742	0.00325	57.7	15286	MVRD
B029	Green River	4903520088	A-1 WASP	INEXCO OIL COMPANY	WY	36N	112W	28	NWNESW	11460.5	B	5.1	2.65	0.0544	0.00177	104	15286	MVRD
B029	Green River	4903520088	A-1 WASP	INEXCO OIL COMPANY	WY	36N	112W	28	NWNESW	11460.6	B	4.4	2.64	0.384	0.0255	37.1	15286	MVRD
B029	Green River	4903520088	A-1 WASP	INEXCO OIL COMPANY	WY	36N	112W	28	NWNESW	11460.6	A	4.3	2.64	0.300	0.0155	83.8	15286	MVRD
B029	Green River	4903520088	A-1 WASP	INEXCO OIL COMPANY	WY	36N	112W	28	NWNESW	11460.6	C	4.7	2.65	0.144	0.00744	78.0	15286	MVRD
B029	Green River	4903520088	A-1 WASP	INEXCO OIL COMPANY	WY	36N	112W	28	NWNESW	11461.3	A	3.5	2.64	0.0105	0.000218	368	15296	MVRD
B029	Green River	4903520088	A-1 WASP	INEXCO OIL COMPANY	WY	36N	112W	28	NWNESW	11461.3	B	3.6	2.65	0.00629			15296	MVRD

Table 4.1.1. (continued)

Summary of Porosity, Permeability, and Grain Density
Analysis of Critical Permeability, Capillary Pressure, and Electrical Properties for Mesaverde Tight Gas Sandstones from Western U.S. Basins
US DOE # DE-FC26-05NT42660
Alan P. Byrnes, Robert M. Cluff, John C. Webb, Daniel A. Krygowski, Stefani D. Whittaker
website: http://www.kgs.ku.edu/mesaverde

USGS Library Number	Basin	API Number	Well Name	Operator	State	Township	Range	Section	Quarter Section	Plug Depth	Plug Letter	Ambient Porosity	Grain Density	Routine Gas Permeability	*in situ* Klinkenberg Gas Permeability	*in situ* Klinken-berg *constant b*	Rock Type Code	Formations
										ft	A/B/C	%	g/cc	mD	mD	(psia)		
B029	Green River	4903520088	A-1 WASP	INEXCO OIL COMPANY	WY	36N	112W	28	NWNESW	11461.3	C	3.4	2.66	0.000428	0.000256	155	15296	MVRD
B029	Green River	4903520088	A-1 WASP	INEXCO OIL COMPANY	WY	36N	112W	28	NWNESW	11471.5	A	3.0	2.59	49.1	1.55	21.4	13296	MVRD
B029	Green River	4903520088	A-1 WASP	INEXCO OIL COMPANY	WY	36N	112W	28	NWNESW	11471.5	C	0.7	2.59	0.0285	0.00170	147	13296	MVRD
B029	Green River	4903520088	A-1 WASP	INEXCO OIL COMPANY	WY	36N	112W	28	NWNESW	11471.5	B	1.0	2.59	0.0103	0.000026	438	13296	MVRD
B029	Green River	4903520088	A-1 WASP	INEXCO OIL COMPANY	WY	36N	112W	28	NWNESW	11474.5	C	2.8	2.64	0.0375	0.00146	43.8	13276	MVRD
B029	Green River	4903520088	A-1 WASP	INEXCO OIL COMPANY	WY	36N	112W	28	NWNESW	11474.5	A	3.2	2.64	0.0353	0.00341	133	13276	MVRD
B029	Green River	4903520088	A-1 WASP	INEXCO OIL COMPANY	WY	36N	112W	28	NWNESW	11474.5	B	2.6	2.63	0.0144	0.000407	242	13276	MVRD
B029	Green River	4903520088	A-1 WASP	INEXCO OIL COMPANY	WY	36N	112W	28	NWNESW	11477.8	B	1.0	2.66	0.00382	0.000239	224	15276	MVRD
B029	Green River	4903520088	A-1 WASP	INEXCO OIL COMPANY	WY	36N	112W	28	NWNESW	11477.8	C	1.3	2.66	0.00365	0.000121	337	15276	MVRD
B029	Green River	4903520088	A-1 WASP	INEXCO OIL COMPANY	WY	36N	112W	28	NWNESW	11477.8	A	1.2	2.66	0.00233	0.000078	370	15276	MVRD
B029	Green River	4903520088	A-1 WASP	INEXCO OIL COMPANY	WY	36N	112W	28	NWNESW	11478.1	B	0.4	2.61	0.00554	0.000105	377	13296	MVRD
B029	Green River	4903520088	A-1 WASP	INEXCO OIL COMPANY	WY	36N	112W	28	NWNESW	11478.1	A	1.3	2.63	0.00293	0.000037	675	13296	MVRD
B029	Green River	4903520088	A-1 WASP	INEXCO OIL COMPANY	WY	36N	112W	28	NWNESW	11478.1	c	1.4	2.66				13296	MVRD
B029	Green River	4903520088	A-1 WASP	INEXCO OIL COMPANY	WY	36N	112W	28	NWNESW	11487.5	B	1.2	2.63	0.00459	0.000074	485	12296	MVRD
B029	Green River	4903520088	A-1 WASP	INEXCO OIL COMPANY	WY	36N	112W	28	NWNESW	11487.5	A	1.2	2.62	0.00152	0.000010	1211	12296	MVRD
B029	Green River	4903520088	A-1 WASP	INEXCO OIL COMPANY	WY	36N	112W	28	NWNESW	11487.5	C	0.8	2.61	0.00116	0.000015	1520	12296	MVRD
B029	Green River	4903520088	A-1 WASP	INEXCO OIL COMPANY	WY	36N	112W	28	NWNESW	11488.8	A	1.0	2.62	0.00407	0.000071	496	12296	MVRD
B029	Green River	4903520088	A-1 WASP	INEXCO OIL COMPANY	WY	36N	112W	28	NWNESW	11488.8	B	0.9	2.62	0.00396	0.000052	540	12296	MVRD
B029	Green River	4903520088	A-1 WASP	INEXCO OIL COMPANY	WY	36N	112W	28	NWNESW	11488.8	C	0.9	2.60	0.00209	0.000018	262	12296	MVRD
B029	Green River	4903520088	A-1 WASP	INEXCO OIL COMPANY	WY	36N	112W	28	NWNESW	11495.5	C	0.9	2.64	0.00377	0.000107	357	15276	MVRD
B029	Green River	4903520088	A-1 WASP	INEXCO OIL COMPANY	WY	36N	112W	28	NWNESW	11495.5	A	0.7	2.63	0.00175	0.000023	409	15276	MVRD
B029	Green River	4903520088	A-1 WASP	INEXCO OIL COMPANY	WY	36N	112W	28	NWNESW	11495.5	B	1.0	2.64	0.000669	0.000013	443	15276	MVRD
B029	Green River	4903520088	A-1 WASP	INEXCO OIL COMPANY	WY	36N	112W	28	NWNESW	11504.0	B	3.5	2.64	0.0207	0.000416	190	16296	MVRD
B029	Green River	4903520088	A-1 WASP	INEXCO OIL COMPANY	WY	36N	112W	28	NWNESW	11504.0	A	3.0	2.62	0.0120	0.000194	207	16296	MVRD
B029	Green River	4903520088	A-1 WASP	INEXCO OIL COMPANY	WY	36N	112W	28	NWNESW	11504.0	A2	3.3	2.63	0.00607	0.000340	281	16296	MVRD
B029	Green River	4903520088	A-1 WASP	INEXCO OIL COMPANY	WY	36N	112W	28	NWNESW	11504.0	B2	3.2	2.63	0.00542	0.000330	187	16296	MVRD
B029	Green River	4903520088	A-1 WASP	INEXCO OIL COMPANY	WY	36N	112W	28	NWNESW	11504.0	C	3.0	2.63	0.00250	0.000235	90.6	16296	MVRD
B029	Green River	4903520088	A-1 WASP	INEXCO OIL COMPANY	WY	36N	112W	28	NWNESW	11504.0	C2	3.4	2.63	0.00240	0.000105	350	16296	MVRD
B029	Green River	4903520088	A-1 WASP	INEXCO OIL COMPANY	WY	36N	112W	28	NWNESW	11504.1	A	3.4	2.63	0.00425	0.000226	247	16296	MVRD
B029	Green River	4903520088	A-1 WASP	INEXCO OIL COMPANY	WY	36N	112W	28	NWNESW	11504.1	B	3.0	2.62	0.00422	0.000519	83.6	16296	MVRD
B029	Green River	4903520088	A-1 WASP	INEXCO OIL COMPANY	WY	36N	112W	28	NWNESW	11504.1	C	3.3	2.63	0.00230	0.000152	619	16296	MVRD
B029	Green River	4903520088	A-1 WASP	INEXCO OIL COMPANY	WY	36N	112W	28	NWNESW	11505.3	A	2.6	2.6	0.00400	0.000152	84.2	15276	MVRD
B029	Green River	4903520088	A-1 WASP	INEXCO OIL COMPANY	WY	36N	112W	28	NWNESW	11505.3	C	3.0	2.65	0.00289	0.000207	140	15276	MVRD
B029	Green River	4903520088	A-1 WASP	INEXCO OIL COMPANY	WY	36N	112W	28	NWNESW	11505.3	B	2.9	2.65	0.00275	0.000098	521	15276	MVRD
B029	Green River	4903520088	A-1 WASP	INEXCO OIL COMPANY	WY	36N	112W	28	NWNESW	11515.1	C	0.8	2.64	0.00412	0.000101	255	14296	MVRD
B029	Green River	4903520088	A-1 WASP	INEXCO OIL COMPANY	WY	36N	112W	28	NWNESW	11515.1	B1	0.5	2.64	0.00408	0.000173	250	14296	MVRD
B029	Green River	4903520088	A-1 WASP	INEXCO OIL COMPANY	WY	36N	112W	28	NWNESW	11515.1	A	0.6	2.64	0.000492			14296	MVRD
B029	Green River	4903520088	A-1 WASP	INEXCO OIL COMPANY	WY	36N	112W	28	NWNESW	11522.5	B	0.3	2.63	0.00466	0.000114	620	13266	MVRD
B029	Green River	4903520088	A-1 WASP	INEXCO OIL COMPANY	WY	36N	112W	28	NWNESW	11522.5	A	0.9	2.65	0.00199	0.000039	666	13266	MVRD
B029	Green River	4903520088	A-1 WASP	INEXCO OIL COMPANY	WY	36N	112W	28	NWNESW	11522.5	C	0.7	2.64	0.000618	0.000008	785	13266	MVRD
B029	Green River	4903520088	A-1 WASP	INEXCO OIL COMPANY	WY	36N	112W	28	NWNESW	11530.7	B	0.5	2.64	0.00423	0.000077	1169	12296	MVRD
B029	Green River	4903520088	A-1 WASP	INEXCO OIL COMPANY	WY	36N	112W	28	NWNESW	11530.7	A	0.6	2.64	0.00201	0.000023	488	12296	MVRD
B029	Green River	4903520088	A-1 WASP	INEXCO OIL COMPANY	WY	36N	112W	28	NWNESW	11530.7	C	0.7	2.65	0.00191	0.000003	1210	12296	MVRD
B029	Green River	4903520088	A-1 WASP	INEXCO OIL COMPANY	WY	36N	112W	28	NWNESW	11534.0	B	1.5	2.64	0.00631	0.000137	236	14296	MVRD
B029	Green River	4903520088	A-1 WASP	INEXCO OIL COMPANY	WY	36N	112W	28	NWNESW	11534.0	C	0.8	2.64	0.00115	0.000021	493	14296	MVRD
B029	Green River	4903520088	A-1 WASP	INEXCO OIL COMPANY	WY	36N	112W	28	NWNESW	11534.0	A	1.9	2.65	0.000901	0.000008	583	14296	MVRD
B029	Green River	4903520088	A-1 WASP	INEXCO OIL COMPANY	WY	36N	112W	28	NWNESW	11534.1	B	1.6	2.65	0.00227	0.000014	545	14296	MVRD
B029	Green River	4903520088	A-1 WASP	INEXCO OIL COMPANY	WY	36N	112W	28	NWNESW	11534.1	C	1.4	2.64	0.00151	0.000024	513	14296	MVRD
B029	Green River	4903520088	A-1 WASP	INEXCO OIL COMPANY	WY	36N	112W	28	NWNESW	11534.1	A	1.4	2.64	0.00148	0.000002	921	14296	MVRD
B029	Green River	4903520088	A-1 WASP	INEXCO OIL COMPANY	WY	36N	112W	28	NWNESW	11534.2	B	1.5	2.64	0.00603	0.000119	420	14296	MVRD
B029	Green River	4903520088	A-1 WASP	INEXCO OIL COMPANY	WY	36N	112W	28	NWNESW	11534.2	C	1.3	2.64	0.00432	0.000121	261	14296	MVRD
B029	Green River	4903520088	A-1 WASP	INEXCO OIL COMPANY	WY	36N	112W	28	NWNESW	11534.2	A	1.7	2.64	0.00263	0.000043	741	14296	MVRD
B029	Green River	4903520088	A-1 WASP	INEXCO OIL COMPANY	WY	36N	112W	28	NWNESW	11535.0	C	5.0	2.75	0.00403			14266	MVRD
B029	Green River	4903520088	A-1 WASP	INEXCO OIL COMPANY	WY	36N	112W	28	NWNESW	11535.0	B	1.1	2.64	0.00147	0.000010	368	14266	MVRD
B029	Green River	4903520088	A-1 WASP	INEXCO OIL COMPANY	WY	36N	112W	28	NWNESW	11535.0	A	1.2	2.64	0.000779	0.000037	183	14266	MVRD
B029	Green River	4903520088	A-1 WASP	INEXCO OIL COMPANY	WY	36N	112W	28	NWNESW	11539.0	A	3.1	2.64	0.00828	0.000108	126	14286	MVRD
B029	Green River	4903520088	A-1 WASP	INEXCO OIL COMPANY	WY	36N	112W	28	NWNESW	11539.0	B	2.6	2.63	0.00137	0.000029	335	14286	MVRD
B029	Green River	4903520088	A-1 WASP	INEXCO OIL COMPANY	WY	36N	112W	28	NWNESW	11539.0	C	3.3	2.65		0.000171	283	14286	MVRD
B029	Green River	4903520088	A-1 WASP	INEXCO OIL COMPANY	WY	36N	112W	28	NWNESW	11540.9	B	2.3	2.63	0.00674	0.000226	253	13266	MVRD
B029	Green River	4903520088	A-1 WASP	INEXCO OIL COMPANY	WY	36N	112W	28	NWNESW	11540.9	C	2.3	2.63	0.00608	0.000118	306	13266	MVRD
B029	Green River	4903520088	A-1 WASP	INEXCO OIL COMPANY	WY	36N	112W	28	NWNESW	11540.9	A	2.4	2.62	0.00269	0.000064	296	13266	MVRD
B029	Green River	4903520088	A-1 WASP	INEXCO OIL COMPANY	WY	36N	112W	28	NWNESW	11543.9	A	2.0	2.65	0.00284	0.000102	670	15276	MVRD
B029	Green River	4903520088	A-1 WASP	INEXCO OIL COMPANY	WY	36N	112W	28	NWNESW	11543.9	B	1.6	2.65	0.00154	0.000032	500	15276	MVRD
B029	Green River	4903520088	A-1 WASP	INEXCO OIL COMPANY	WY	36N	112W	28	NWNESW	11543.9	C	1.4	2.64	0.000461	0.000032	231	15276	MVRD
B029	Green River	4903520088	A-1 WASP	INEXCO OIL COMPANY	WY	36N	112W	28	NWNESW	11545.8	A	1.5	2.67	0.00157	0.000071	287	15276	MVRD
B029	Green River	4903520088	A-1 WASP	INEXCO OIL COMPANY	WY	36N	112W	28	NWNESW	11545.8	C	1.3	2.70	0.00104	0.000028	261	15276	MVRD
B029	Green River	4903520088	A-1 WASP	INEXCO OIL COMPANY	WY	36N	112W	28	NWNESW	11545.8	B	1.2	2.68	0.000524	0.000002	2753	15276	MVRD
B029	Green River	4903520088	A-1 WASP	INEXCO OIL COMPANY	WY	36N	112W	28	NWNESW	11548.0	A	5.1	2.64	0.0420	0.00112	36.2	13246	MVRD
B029	Green River	4903520088	A-1 WASP	INEXCO OIL COMPANY	WY	36N	112W	28	NWNESW	11548.0	C	5.8	2.63	0.0347	0.00100	57.0	13246	MVRD
B029	Green River	4903520088	A-1 WASP	INEXCO OIL COMPANY	WY	36N	112W	28	NWNESW	11548.0	B	6.2	2.66	0.0311	0.00117	29.8	13246	MVRD
B029	Green River	4903520088	A-1 WASP	INEXCO OIL COMPANY	WY	36N	112W	28	NWNESW	11550.0	C	5.1	2.63	0.0347	0.000851	161	15226	MVRD
B029	Green River	4903520088	A-1 WASP	INEXCO OIL COMPANY	WY	36N	112W	28	NWNESW	11550.0	B	5.5	2.64	0.0306	0.00106	142	15226	MVRD
B029	Green River	4903520088	A-1 WASP	INEXCO OIL COMPANY	WY	36N	112W	28	NWNESW	11550.0	A	5.3	2.63	0.0301	0.000756	74.4	15226	MVRD
B029	Green River	4903520088	A-1 WASP	INEXCO OIL COMPANY	WY	36N	112W	28	NWNESW	11550.2	A	5.1	2.64	0.0465	0.000389	170	15226	MVRD
B029	Green River	4903520088	A-1 WASP	INEXCO OIL COMPANY	WY	36N	112W	28	NWNESW	11550.2	B	5.4	2.63	0.0409	0.000369	102	15226	MVRD
B029	Green River	4903520088	A-1 WASP	INEXCO OIL COMPANY	WY	36N	112W	28	NWNESW	11550.2	C	5.3	2.64	0.0179	0.000563	43.2	15226	MVRD
B029	Green River	4903520088	A-1 WASP	INEXCO OIL COMPANY	WY	36N	112W	28	NWNESW	11551.9	B	4.1	2.62	0.0489	0.00154	69.3	13246	MVRD
B029	Green River	4903520088	A-1 WASP	INEXCO OIL COMPANY	WY	36N	112W	28	NWNESW	11551.9	C	4.4	2.63	0.0379	0.000545	181	13246	MVRD
B029	Green River	4903520088	A-1 WASP	INEXCO OIL COMPANY	WY	36N	112W	28	NWNESW	11551.9	A	3.8	2.62	0.00308	0.000313	219	13246	MVRD
B029	Green River	4903520088	A-1 WASP	INEXCO OIL COMPANY	WY	36N	112W	28	NWNESW	11552.1	B	2.2	2.65	0.00425	0.000172	474	13246	MVRD
B029	Green River	4903520088	A-1 WASP	INEXCO OIL COMPANY	WY	36N	112W	28	NWNESW	11552.1	A	2.3	2.64	0.00248	0.000123	236	13246	MVRD
B029	Green River	4903520088	A-1 WASP	INEXCO OIL COMPANY	WY	36N	112W	28	NWNESW	11552.1	C	1.7	2.64	0.00108	0.000077	191	13246	MVRD
B029	Green River	4903520088	A-1 WASP	INEXCO OIL COMPANY	WY	36N	112W	28	NWNESW	11552.3	C	4.2	2.63	0.0411	0.000280	203	15276	MVRD
B029	Green River	4903520088	A-1 WASP	INEXCO OIL COMPANY	WY	36N	112W	28	NWNESW	11552.3	A	3.9	2.64	0.0324	0.000659	125	15276	MVRD
B029	Green River	4903520088	A-1 WASP	INEXCO OIL COMPANY	WY	36N	112W	28	NWNESW	11552.3	B	4.2	2.63	0.0171	0.000383	172	15276	MVRD
B029	Green River	4903520088	A-1 WASP	INEXCO OIL COMPANY	WY	36N	112W	28	NWNESW	11554.9	C	4.3	2.64	0.0325	0.000749	53.4	15246	MVRD
B029	Green River	4903520088	A-1 WASP	INEXCO OIL COMPANY	WY	36N	112W	28	NWNESW	11554.9	A	4.5	2.65	0.00516	0.000313	113	15246	MVRD
B029	Green River	4903520088	A-1 WASP	INEXCO OIL COMPANY	WY	36N	112W	28	NWNESW	11554.9	B	4.3	2.64	0.00379			15246	MVRD
B029	Green River	4903520088	A-1 WASP	INEXCO OIL COMPANY	WY	36N	112W	28	NWNESW	11557.1	B	2.5	2.65	0.00477	0.000220	484	15296	MVRD
B029	Green River	4903520088	A-1 WASP	INEXCO OIL COMPANY	WY	36N	112W	28	NWNESW	11557.1	C	2.7	2.65	0.00206	0.000052	312	15296	MVRD
B029	Green River	4903520088	A-1 WASP	INEXCO OIL COMPANY	WY	36N	112W	28	NWNESW	11557.1	A	2.8	2.65	0.00173	0.000120	478	15296	MVRD
B029	Green River	4903520088	A-1 WASP	INEXCO OIL COMPANY	WY	36N	112W	28	NWNESW	11557.2	C	2.7	2.65	0.0150	0.000172	187	15296	MVRD
B029	Green River	4903520088	A-1 WASP	INEXCO OIL COMPANY	WY	36N	112W	28	NWNESW	11557.2	A	2.8	2.65	0.00646	0.000097	219	15296	MVRD
B029	Green River	4903520088	A-1 WASP	INEXCO OIL COMPANY	WY	36N	112W	28	NWNESW	11557.2	B	2.8	2.65	0.00480	0.000330	163	15296	MVRD
B029	Green River	4903520088	A-1 WASP	INEXCO OIL COMPANY	WY	36N	112W	28	NWNESW	11558.1	B	1.9	2.67	0.00189	0.000083	274	15276	MVRD
B029	Green River	4903520088	A-1 WASP	INEXCO OIL COMPANY	WY	36N	112W	28	NWNESW	11558.1	A	1.8	2.66	0.00156	0.000086	191	15276	MVRD
B029	Green River	4903520088	A-1 WASP	INEXCO OIL COMPANY	WY	36N	112W	28	NWNESW	11558.1	C	1.4	2.66	0.00140	0.000100	254	15276	MVRD
B029	Green River	4903520088	A-1 WASP	INEXCO OIL COMPANY	WY	36N	112W	28	NWNESW	11574.7	B	1.0	2.63	0.00593	0.000071	499	13286	MVRD
B029	Green River	4903520088	A-1 WASP	INEXCO OIL COMPANY	WY	36N	112W	28	NWNESW	11574.7	C	1.0	2.63	0.00467	0.000085	307	13286	MVRD
B029	Green River	4903520088	A-1 WASP	INEXCO OIL COMPANY	WY	36N	112W	28	NWNESW	11574.7	A	1.1	2.62	0.00291	0.000060	228	13286	MVRD
B029	Green River	4903520088	A-1 WASP	INEXCO OIL COMPANY	WY	36N	112W	28	NWNESW	11578.2	A	1.2	2.64	0.00276	0.000042	758	13266	MVRD
B029	Green River	4903520088	A-1 WASP	INEXCO OIL COMPANY	WY	36N	112W	28	NWNESW	11578.2	B	0.9	2.64	0.00165	0.000025	435	13266	MVRD
B029	Green River	4903520088	A-1 WASP	INEXCO OIL COMPANY	WY	36N	112W	28	NWNESW	11578.2	C	0.2	2.64	0.000682	0.000002	1450	13266	MVRD
B029	Green River	4903520088	A-1 WASP	INEXCO OIL COMPANY	WY	36N	112W	28	NWNESW	11584.0	C	1.8	2.64	0.00377	0.000120	405	14297	MVRD
B029	Green River	4903520088	A-1 WASP	INEXCO OIL COMPANY	WY	36N	112W	28	NWNESW	11584.0	B	1.7	2.63	0.00346	0.000111	311	14297	MVRD
B029	Green River	4903520088	A-1 WASP	INEXCO OIL COMPANY	WY	36N	112W	28	NWNESW	11584.0	A	2.2	2.64	0.00231	0.000071	329	14297	MVRD
B029	Green River	4903520088	A-1 WASP	INEXCO OIL COMPANY	WY	36N	112W	28	NWNESW	11587.2	B	4.2	2.63	0.0412	0.000394	192	13267	MVRD
B029	Green River	4903520088	A-1 WASP	INEXCO OIL COMPANY	WY	36N	112W	28	NWNESW	11587.2	A	3.5	2.63	0.0324	0.000902	45.7	13267	MVRD
B029	Green River	4903520088	A-1 WASP	INEXCO OIL COMPANY	WY	36N	112W	28	NWNESW	11587.2	C	4.4	2.64	0.0282	0.000432	101	13267	MVRD
B029	Green River	4903520088	A-1 WASP	INEXCO OIL COMPANY	WY	36N	112W	28	NWNESW	11592.7	A	4.6	2.62	0.00552	0.000233	448	13257	MVRD
B029	Green River	4903520088	A-1 WASP	INEXCO OIL COMPANY	WY	36N	112W	28	NWNESW	11592.7	C	5.4	2.65	0.00512	0.000157	834	13257	MVRD
B029	Green River	4903520088	A-1 WASP	INEXCO OIL COMPANY	WY	36N	112W	28	NWNESW	11592.7	B	4.6	2.62	0.00393	0.000227	114	13257	MVRD

Table 4.1.1. (continued)

Summary of Porosity, Permeability, and Grain Density
Analysis of Critical Permeability, Capillary Pressure, and Electrical Properties for Mesaverde Tight Gas Sandstones from Western U.S. Basins
US DOE # DE-FC26-05NT42660
Alan P. Byrnes, Robert M. Cluff, John C. Webb, Daniel A. Krygowski, Stefani D. Whittaker
website: http://www.kgs.ku.edu/mesaverde

USGS Library Number	Basin	API Number	Well Name	Operator	State	Township	Range	Section	Quarter Section	Plug Depth	Plug Letter	Ambient Porosity	Grain Density	Routine Gas Permeability	*in situ* Klinkenberg Gas Permeability	*in situ* Klinkenberg *constant b*	Rock Type Code	Formations
										ft	A/B/C	%	g/cc	mD	mD	(psia)		
B029	Green River	4903520088	A-1 WASP	INEXCO OIL COMPANY	WY	36N	112W	28	NWNESW	11605.1	A	3.0	2.64	0.00285	0.000139	683	15296	MVRD
B029	Green River	4903520088	A-1 WASP	INEXCO OIL COMPANY	WY	36N	112W	28	NWNESW	11605.1	B	3.2	2.65	0.00255	0.000228	247	15296	MVRD
B029	Green River	4903520088	A-1 WASP	INEXCO OIL COMPANY	WY	36N	112W	28	NWNESW	11605.1	C	2.9	2.64	0.00169	0.000138	368	15296	MVRD
B029	Green River	4903520088	A-1 WASP	INEXCO OIL COMPANY	WY	36N	112W	28	NWNESW	11609.1	A	5.9	2.64	0.0907	0.00772	59.4	15276	MVRD
B029	Green River	4903520088	A-1 WASP	INEXCO OIL COMPANY	WY	36N	112W	28	NWNESW	11609.2	C	6.0	2.63	0.113	0.00663	37.8	15276	MVRD
B029	Green River	4903520088	A-1 WASP	INEXCO OIL COMPANY	WY	36N	112W	28	NWNESW	11609.2	B	5.8	2.63	0.0931	0.00833	87.9	15276	MVRD
B029	Green River	4903520088	A-1 WASP	INEXCO OIL COMPANY	WY	36N	112W	28	NWNESW	11609.2	A	5.2	2.63	0.0760	0.00475	72.2	15276	MVRD
B029	Green River	4903520088	A-1 WASP	INEXCO OIL COMPANY	WY	36N	112W	28	NWNESW	11615.1	A	4.6	2.63	0.0506	0.00192	63.5	15276	MVRD
B029	Green River	4903520088	A-1 WASP	INEXCO OIL COMPANY	WY	36N	112W	28	NWNESW	11615.1	B	5.0	2.64	0.0398	0.00169	70.6	15276	MVRD
B029	Green River	4903520088	A-1 WASP	INEXCO OIL COMPANY	WY	36N	112W	28	NWNESW	11615.1	C	4.9	2.63	0.0355	0.000971	99.9	15276	MVRD
B029	Green River	4903520088	A-1 WASP	INEXCO OIL COMPANY	WY	36N	112W	28	NWNESW	11621.5	B	1.2	2.62	0.0105	0.000016	514	12286	MVRD
B029	Green River	4903520088	A-1 WASP	INEXCO OIL COMPANY	WY	36N	112W	28	NWNESW	11621.5	C	1.4	2.63	0.00393	0.000113	207	12286	MVRD
B029	Green River	4903520088	A-1 WASP	INEXCO OIL COMPANY	WY	36N	112W	28	NWNESW	11621.5	A	1.8	2.63	0.00331	0.000072	294	12286	MVRD
B029	Green River	4903520088	A-1 WASP	INEXCO OIL COMPANY	WY	36N	112W	28	NWNESW	11626.5	C	0.8	2.64	0.00483	0.000078	477	13286	MVRD
B029	Green River	4903520088	A-1 WASP	INEXCO OIL COMPANY	WY	36N	112W	28	NWNESW	11626.5	B	0.3	2.63	0.00355	0.000093	275	13286	MVRD
B029	Green River	4903520088	A-1 WASP	INEXCO OIL COMPANY	WY	36N	112W	28	NWNESW	11626.5	A	0.4	2.63	0.00195	0.000062	250	13286	MVRD
B029	Green River	4903520088	A-1 WASP	INEXCO OIL COMPANY	WY	36N	112W	28	NWNESW	11660.0	C	1.6	2.63	0.00443	0.000104	164	12216	MVRD
B029	Green River	4903520088	A-1 WASP	INEXCO OIL COMPANY	WY	36N	112W	28	NWNESW	11660.0	A	1.2	2.61	0.00288	0.000045	555	12216	MVRD
B029	Green River	4903520088	A-1 WASP	INEXCO OIL COMPANY	WY	36N	112W	28	NWNESW	11660.0	B	0.9	2.61	0.00147	0.000006	637	12216	MVRD
B029	Green River	4903520088	A-1 WASP	INEXCO OIL COMPANY	WY	36N	112W	28	NWNESW	11688.0	C	2.5	2.65	0.0201	0.000269	35.0	15296	MVRD
B029	Green River	4903520088	A-1 WASP	INEXCO OIL COMPANY	WY	36N	112W	28	NWNESW	11688.0	A	2.6	2.65	0.00461	0.000285	199	15296	MVRD
B029	Green River	4903520088	A-1 WASP	INEXCO OIL COMPANY	WY	36N	112W	28	NWNESW	11688.0	B	2.8	2.65	0.00343	0.000017	417	15296	MVRD
B029	Green River	4903520088	A-1 WASP	INEXCO OIL COMPANY	WY	36N	112W	28	NWNESW	11695.1	A	3.7	2.63	0.00378			15276	MVRD
B029	Green River	4903520088	A-1 WASP	INEXCO OIL COMPANY	WY	36N	112W	28	NWNESW	11695.1	C	3.6	2.63	0.00317	0.000202	174	15276	MVRD
B029	Green River	4903520088	A-1 WASP	INEXCO OIL COMPANY	WY	36N	112W	28	NWNESW	11695.1	B	3.6	2.63	0.00228	0.000207	153	15276	MVRD
B029	Green River	4903520088	A-1 WASP	INEXCO OIL COMPANY	WY	36N	112W	28	NWNESW	11700.0	C	2.5	2.62	0.00427	0.000237	234	13286	MVRD
B029	Green River	4903520088	A-1 WASP	INEXCO OIL COMPANY	WY	36N	112W	28	NWNESW	11700.0	A	2.8	2.62	0.00339	0.000142	239	13286	MVRD
B029	Green River	4903520088	A-1 WASP	INEXCO OIL COMPANY	WY	36N	112W	28	NWNESW	11700.0	B	2.4	2.62	0.00288	0.000117	260	13286	MVRD
B029	Green River	4903520088	A-1 WASP	INEXCO OIL COMPANY	WY	36N	112W	28	NWNESW	11705.5	A	3.2	2.64	0.0350	0.000520	107	15276	MVRD
B029	Green River	4903520088	A-1 WASP	INEXCO OIL COMPANY	WY	36N	112W	28	NWNESW	11705.5	C	3.6	2.64	0.0332	0.000551	149	15276	MVRD
B029	Green River	4903520088	A-1 WASP	INEXCO OIL COMPANY	WY	36N	112W	28	NWNESW	11705.5	B	3.6	2.64	0.0195	0.000568	109	15276	MVRD
B029	Green River	4903520088	A-1 WASP	INEXCO OIL COMPANY	WY	36N	112W	28	NWNESW	11706.7	A	4.0	2.63	0.0329	0.000524	154	16276	MVRD
B029	Green River	4903520088	A-1 WASP	INEXCO OIL COMPANY	WY	36N	112W	28	NWNESW	11706.7	C	5.1	2.63	0.0250	0.000690	155	16276	MVRD
B029	Green River	4903520088	A-1 WASP	INEXCO OIL COMPANY	WY	36N	112W	28	NWNESW	11706.8	B	3.9	2.64	0.0344	0.000810	55.4	16276	MVRD
B029	Green River	4903520088	A-1 WASP	INEXCO OIL COMPANY	WY	36N	112W	28	NWNESW	11706.8	A	3.3	2.64	0.0330	0.000572	142	16276	MVRD
B029	Green River	4903520088	A-1 WASP	INEXCO OIL COMPANY	WY	36N	112W	28	NWNESW	11706.8	C	3.7	2.64	0.0226	0.000374	116	16276	MVRD
B029	Green River	4903520088	A-1 WASP	INEXCO OIL COMPANY	WY	36N	112W	28	NWNESW	11706.9	B	3.9	2.63	0.0445	0.00103	91.1	16276	MVRD
B029	Green River	4903520088	A-1 WASP	INEXCO OIL COMPANY	WY	36N	112W	28	NWNESW	11706.9	C	4.0	2.64	0.0372	0.00110	75.7	16276	MVRD
B029	Green River	4903520088	A-1 WASP	INEXCO OIL COMPANY	WY	36N	112W	28	NWNESW	11706.9	A	3.8	2.64	0.0339	0.000405	227	16276	MVRD
B029	Green River	4903520088	A-1 WASP	INEXCO OIL COMPANY	WY	36N	112W	28	NWNESW	11716.1	C	3.4	2.63	0.0495	0.000460	200	16276	MVRD
B029	Green River	4903520088	A-1 WASP	INEXCO OIL COMPANY	WY	36N	112W	28	NWNESW	11716.1	B	4.1	2.65	0.0376	0.000431	288	16276	MVRD
B029	Green River	4903520088	A-1 WASP	INEXCO OIL COMPANY	WY	36N	112W	28	NWNESW	11716.1	A	3.8	2.65	0.0270	0.000562	155	16276	MVRD
B029	Green River	4903520088	A-1 WASP	INEXCO OIL COMPANY	WY	36N	112W	28	NWNESW	11717.9	C	3.0	2.62	0.00500	0.000112	435	13286	MVRD
B029	Green River	4903520088	A-1 WASP	INEXCO OIL COMPANY	WY	36N	112W	28	NWNESW	11717.9	A	3.3	2.63	0.00386	0.000129	440	13286	MVRD
B029	Green River	4903520088	A-1 WASP	INEXCO OIL COMPANY	WY	36N	112W	28	NWNESW	11717.9	B	3.0	2.62	0.00364	0.000233	238	13286	MVRD
B029	Green River	4903520088	A-1 WASP	INEXCO OIL COMPANY	WY	36N	112W	28	NWNESW	11721.9	C	4.6	2.64	0.0337	0.000874	104	16296	MVRD
B029	Green River	4903520088	A-1 WASP	INEXCO OIL COMPANY	WY	36N	112W	28	NWNESW	11721.9	A	4.3	2.64	0.0219	0.000320	132	16296	MVRD
B029	Green River	4903520088	A-1 WASP	INEXCO OIL COMPANY	WY	36N	112W	28	NWNESW	11721.9	B	4.5	2.64	0.00469	0.000176	343	16296	MVRD
B029	Green River	4903520088	A-1 WASP	INEXCO OIL COMPANY	WY	36N	112W	28	NWNESW	11722.0	C	4.4	2.64	0.0375	0.000503	222	16296	MVRD
B029	Green River	4903520088	A-1 WASP	INEXCO OIL COMPANY	WY	36N	112W	28	NWNESW	11722.0	B	4.3	2.65	0.0288	0.000757	64.2	16296	MVRD
B029	Green River	4903520088	A-1 WASP	INEXCO OIL COMPANY	WY	36N	112W	28	NWNESW	11722.0	A	4.3	2.64	0.0206	0.000447	236	16296	MVRD
B029	Green River	4903520088	A-1 WASP	INEXCO OIL COMPANY	WY	36N	112W	28	NWNESW	11724.2	A	3.7	2.64	0.0227	0.000863	52.8	16296	MVRD
B029	Green River	4903520088	A-1 WASP	INEXCO OIL COMPANY	WY	36N	112W	28	NWNESW	11724.2	B	4.1	2.64	0.00466	0.000545	126	16296	MVRD
B029	Green River	4903520088	A-1 WASP	INEXCO OIL COMPANY	WY	36N	112W	28	NWNESW	11724.3	A	3.5	2.64	0.00647	0.000841	42.8	16296	MVRD
B029	Green River	4903520088	A-1 WASP	INEXCO OIL COMPANY	WY	36N	112W	28	NWNESW	11724.3	B	4.1	2.63	0.00505	0.000585	82.8	16296	MVRD
B029	Green River	4903520088	A-1 WASP	INEXCO OIL COMPANY	WY	36N	112W	28	NWNESW	11727.5	A	2.6	2.65	0.00300	0.000295	111	19296	MVRD
B029	Green River	4903520088	A-1 WASP	INEXCO OIL COMPANY	WY	36N	112W	28	NWNESW	11727.5	B	2.3	2.64	0.00203	0.000154	385	19296	MVRD
B029	Green River	4903520088	A-1 WASP	INEXCO OIL COMPANY	WY	36N	112W	28	NWNESW	11728.6	B	1.0	2.64	0.00061			18296	MVRD
B029	Green River	4903520088	A-1 WASP	INEXCO OIL COMPANY	WY	36N	112W	28	NWNESW	11728.6	A	1.3	2.65	0.000710	0.000004	643	18296	MVRD
B029	Green River	4903520088	A-1 WASP	INEXCO OIL COMPANY	WY	36N	112W	28	NWNESW	11737.2	B	3.8	2.63	0.00563	0.000259	185	15266	MVRD
B029	Green River	4903520088	A-1 WASP	INEXCO OIL COMPANY	WY	36N	112W	28	NWNESW	11737.2	A	4.0	2.64	0.00517	0.000270	283	15266	MVRD
B029	Green River	4903520088	A-1 WASP	INEXCO OIL COMPANY	WY	36N	112W	28	NWNESW	11739.0	A	4.5	2.64	0.0535	0.00158	82.7	15276	MVRD
B029	Green River	4903520088	A-1 WASP	INEXCO OIL COMPANY	WY	36N	112W	28	NWNESW	11739.0	B	4.8	2.64	0.0501	0.000922	144	15276	MVRD
B029	Green River	4903520088	A-1 WASP	INEXCO OIL COMPANY	WY	36N	112W	28	NWNESW	11742.0	B	5.9	2.64	0.0224	0.000482	147	15276	MVRD
B029	Green River	4903520088	A-1 WASP	INEXCO OIL COMPANY	WY	36N	112W	28	NWNESW	11742.0	A	5.2	2.62	0.00392	0.000475	259	15276	MVRD
B029	Green River	4903520088	A-1 WASP	INEXCO OIL COMPANY	WY	36N	112W	28	NWNESW	11746.1	A	2.3	2.62	0.00227	0.000049	232	12217	MVRD
B029	Green River	4903520088	A-1 WASP	INEXCO OIL COMPANY	WY	36N	112W	28	NWNESW	11746.6	B	2.0	2.62	0.00397	0.000055	444	12217	MVRD
B029	Green River	4903520088	A-1 WASP	INEXCO OIL COMPANY	WY	36N	112W	28	NWNESW	11758.3	B	4.4	2.63	0.410	0.0336	40.8	15286	MVRD
B029	Green River	4903520088	A-1 WASP	INEXCO OIL COMPANY	WY	36N	112W	28	NWNESW	11758.3	A	4.7	2.65	0.0192	0.000470	120	15286	MVRD
B029	Green River	4903520088	A-1 WASP	INEXCO OIL COMPANY	WY	36N	112W	28	NWNESW	11758.4	B	5.0	2.64	0.147	0.0118	18.8	15296	MVRD
B029	Green River	4903520088	A-1 WASP	INEXCO OIL COMPANY	WY	36N	112W	28	NWNESW	11758.4	A	4.6	2.63	0.00725	0.00110	39.5	15296	MVRD
B029	Green River	4903520088	A-1 WASP	INEXCO OIL COMPANY	WY	36N	112W	28	NWNESW	11758.8	A			0.00266	0.000088	212	15296	MVRD
B029	Green River	4903520088	A-1 WASP	INEXCO OIL COMPANY	WY	36N	112W	28	NWNESW	11758.8	B	1.3	2.67	0.00155	0.000015	655	15296	MVRD
B029	Green River	4903520088	A-1 WASP	INEXCO OIL COMPANY	WY	36N	112W	28	NWNESW	11763.8	A	3.0	2.65	0.00376	0.000058	373	15286	MVRD
B029	Green River	4903520088	A-1 WASP	INEXCO OIL COMPANY	WY	36N	112W	28	NWNESW	11763.8	B	3.0	2.66	0.00211	0.000053	261	15286	MVRD
B029	Green River	4903520088	A-1 WASP	INEXCO OIL COMPANY	WY	36N	112W	28	NWNESW	11763.9	B	2.8	2.67	0.00326	0.000164	142	15286	MVRD
B029	Green River	4903520088	A-1 WASP	INEXCO OIL COMPANY	WY	36N	112W	28	NWNESW	11763.9	A	2.8	2.66	0.000688	0.000018	981	15286	MVRD
B029	Green River	4903520088	A-1 WASP	INEXCO OIL COMPANY	WY	36N	112W	28	NWNESW	11780.0	B	2.1	2.59	0.00670	0.000247	259	13217	MVRD
B029	Green River	4903520088	A-1 WASP	INEXCO OIL COMPANY	WY	36N	112W	28	NWNESW	11780.0	A	1.3	2.57	0.00474	0.000073	417	13217	MVRD
B029	Green River	4903520088	A-1 WASP	INEXCO OIL COMPANY	WY	36N	112W	28	NWNESW	13672.5	C	2.6	2.66	0.00255	0.000065	220	14276	MVRD
B029	Green River	4903520088	A-1 WASP	INEXCO OIL COMPANY	WY	36N	112W	28	NWNESW	13672.5	B	2.8	2.66	0.00204	0.000035	705	14276	MVRD
B029	Green River	4903520088	A-1 WASP	INEXCO OIL COMPANY	WY	36N	112W	28	NWNESW	13672.5	A	2.8	2.66	0.00181	0.000113	60.9	14276	MVRD
E712	Green River	4903506020	B-54 BIG PINEY	BELCO PETROLEUM	WY	29N	113W	26	SESENE	3396.2	B	18.5	2.66	25.3	18.0	6.8	15287	MVRD
E712	Green River	4903506020	B-54 BIG PINEY	BELCO PETROLEUM	WY	29N	113W	26	SESENE	3396.2	A	18.4	2.66	22.5	15.9	5.8	15287	MVRD
E712	Green River	4903506020	B-54 BIG PINEY	BELCO PETROLEUM	WY	29N	113W	26	SESENE	3403.9	A	16.7	2.64	4.87	1.20	20.3	13256	MVRD
E712	Green River	4903506020	B-54 BIG PINEY	BELCO PETROLEUM	WY	29N	113W	26	SESENE	3403.9	B	16.0	2.63	3.41	1.90	19.1	13256	MVRD
E712	Green River	4903506020	B-54 BIG PINEY	BELCO PETROLEUM	WY	29N	113W	26	SESENE	3413.5	B	6.3	2.59	0.0461	0.00161	77.5	11249	MVRD
E712	Green River	4903506020	B-54 BIG PINEY	BELCO PETROLEUM	WY	29N	113W	26	SESENE	3413.5	A	7.1	2.62				11249	MVRD
E712	Green River	4903506020	B-54 BIG PINEY	BELCO PETROLEUM	WY	29N	113W	26	SESENE	3419.9	B	11.5	2.62	0.273	0.0663	62.1	13277	MVRD
E712	Green River	4903506020	B-54 BIG PINEY	BELCO PETROLEUM	WY	29N	113W	26	SESENE	3419.9	A	11.8	2.57	0.197	0.0802	43.2	13277	MVRD
E712	Green River	4903506020	B-54 BIG PINEY	BELCO PETROLEUM	WY	29N	113W	26	SESENE	3431.9	B	17.5	2.64	25.2	15.7	8.7	15585	MVRD
E712	Green River	4903506020	B-54 BIG PINEY	BELCO PETROLEUM	WY	29N	113W	26	SESENE	3431.9	A	17.0	2.64	23.5	17.0	5.3	15585	MVRD
E712	Green River	4903506020	B-54 BIG PINEY	BELCO PETROLEUM	WY	29N	113W	26	SESENE	3433.8	A	17.4	2.65	32.1	22.7	5.5	15585	MVRD
E712	Green River	4903506020	B-54 BIG PINEY	BELCO PETROLEUM	WY	29N	113W	26	SESENE	3433.8	B	17.7	2.66	30.6	26.1	1.2	15585	MVRD
E712	Green River	4903506020	B-54 BIG PINEY	BELCO PETROLEUM	WY	29N	113W	26	SESENE	3433.9	B	17.5	2.65	32.6	25.1	3.0	15585	MVRD
E712	Green River	4903506020	B-54 BIG PINEY	BELCO PETROLEUM	WY	29N	113W	26	SESENE	3433.9	A	17.2	2.65	32.5	24.5	3.2	15585	MVRD
E712	Green River	4903506020	B-54 BIG PINEY	BELCO PETROLEUM	WY	29N	113W	26	SESENE	3451.8	B	18.0	2.65	30.9	12.3	24.2	15585	MVRD
E712	Green River	4903506020	B-54 BIG PINEY	BELCO PETROLEUM	WY	29N	113W	26	SESENE	3451.8	A	17.3	2.64	5.31	0.289	11.1	15585	MVRD
E712	Green River	4903506020	B-54 BIG PINEY	BELCO PETROLEUM	WY	29N	113W	26	SESENE	3461.5	B	18.7	2.65	50.0	28.1	11.2	15585	MVRD
E712	Green River	4903506020	B-54 BIG PINEY	BELCO PETROLEUM	WY	29N	113W	26	SESENE	3461.5	A	18.2	2.63	44.1	171	3.5	15585	MVRD
E712	Green River	4903506020	B-54 BIG PINEY	BELCO PETROLEUM	WY	29N	113W	26	SESENE	3461.6	B	18.7	2.65	47.5	29.5	8.1	15585	MVRD
E712	Green River	4903506020	B-54 BIG PINEY	BELCO PETROLEUM	WY	29N	113W	26	SESENE	3461.6	A	18.3	2.64	41.1	30.5	3.5	15585	MVRD
E712	Green River	4903506020	B-54 BIG PINEY	BELCO PETROLEUM	WY	29N	113W	26	SESENE	3461.6	A	18.3	2.64	41.1	27.5	6.2	15585	MVRD
E712	Green River	4903506020	B-54 BIG PINEY	BELCO PETROLEUM	WY	29N	113W	26	SESENE	3461.7	A	17.9	2.65	38.5	2.42	8.7	15585	MVRD
E712	Green River	4903506020	B-54 BIG PINEY	BELCO PETROLEUM	WY	29N	113W	26	SESENE	3461.9	A	18.1	2.65	41.4	27.9	6.9	15585	MVRD
E712	Green River	4903506020	B-54 BIG PINEY	BELCO PETROLEUM	WY	29N	113W	26	SESENE	3461.9	B	18.5	2.65	39.7	29.7	4.0	15585	MVRD
E712	Green River	4903506020	B-54 BIG PINEY	BELCO PETROLEUM	WY	29N	113W	26	SESENE	3462.0	A	18.8	2.65	43.7	26.8	9.3	15585	MVRD
E712	Green River	4903506020	B-54 BIG PINEY	BELCO PETROLEUM	WY	29N	113W	26	SESENE	3462.0	B	18.8	2.65	41.9	27.7	7.5	15585	MVRD
E712	Green River	4903506020	B-54 BIG PINEY	BELCO PETROLEUM	WY	29N	113W	26	SESENE	3471.8	A	17.9	2.63	38.2	26.1	6.5	15585	MVRD
E712	Green River	4903506020	B-54 BIG PINEY	BELCO PETROLEUM	WY	29N	113W	26	SESENE	3471.8	B	18.1	2.65	34.6	24.1	5.4	15585	MVRD
E712	Green River	4903506020	B-54 BIG PINEY	BELCO PETROLEUM	WY	29N	113W	26	SESENE	3477.8	A	16.6	2.66	15.3	10.6	8.3	15585	MVRD
E712	Green River	4903506020	B-54 BIG PINEY	BELCO PETROLEUM	WY	29N	113W	26	SESENE	3477.8	B	15.9	2.66	14.7	10.1	7.0	15585	MVRD

Table 4.1.1. (continued)

Summary of Porosity, Permeability, and Grain Density
Analysis of Critical Permeability, Capillary Pressure, and Electrical Properties for Mesaverde Tight Gas Sandstones from Western U.S. Basins
US DOE # DE-FC26-05NT42660
Alan P. Byrnes, Robert M. Cluff, John C. Webb, Daniel A. Krygowski, Stefani D. Whittaker
website: http://www.kgs.ku.edu/mesaverde

USGS Library Number	Basin	API Number	Well Name	Operator	State	Township	Range	Section	Quarter Section	Plug Depth ft	Plug Letter A/B/C	Ambient Porosity %	Grain Density g/cc	Routine Gas Permeability mD	*in situ* Klinkenberg Gas Permeability mD	*in situ* Klinkenberg *constant* b (psia)	Rock Type Code	Formations
E712	Green River	4903506020	B-54 BIG PINEY	BELCO PETROLEUM	WY	29N	113W	26	SESENE	3477.9	A	16.0	2.65	14.5	9.77	6.5	15585	MVRD
E712	Green River	4903506020	B-54 BIG PINEY	BELCO PETROLEUM	WY	29N	113W	26	SESENE	3480.8	A	8.8	2.68	0.0613	0.00580	111	13265	MVRD
E712	Green River	4903506020	B-54 BIG PINEY	BELCO PETROLEUM	WY	29N	113W	26	SESENE	3480.8	B	8.9	2.69	0.0594	0.00579	99.5	13265	MVRD
E712	Green River	4903506020	B-54 BIG PINEY	BELCO PETROLEUM	WY	29N	113W	26	SESENE	3487.9	B	16.1	2.63	9.34	6.35	4.2	16577	MVRD
E712	Green River	4903506020	B-54 BIG PINEY	BELCO PETROLEUM	WY	29N	113W	26	SESENE	3487.9	A	15.8	2.64	3.39	1.63	15.6	16577	MVRD
E712	Green River	4903506020	B-54 BIG PINEY	BELCO PETROLEUM	WY	29N	113W	26	SESENE	3489.1	B	16.5	2.66	10.2	6.49	6.4	15585	MVRD
E712	Green River	4903506020	B-54 BIG PINEY	BELCO PETROLEUM	WY	29N	113W	26	SESENE	3489.1	A	16.5	2.66	9.45	6.42	9.3	15585	MVRD
E712	Green River	4903506020	B-54 BIG PINEY	BELCO PETROLEUM	WY	29N	113W	26	SESENE	3489.3	B	16.5	2.66	9.13	5.02	12.6	15585	MVRD
E712	Green River	4903506020	B-54 BIG PINEY	BELCO PETROLEUM	WY	29N	113W	26	SESENE	3489.3	A	16.2	2.66	8.20	5.33	10.3	15585	MVRD
E712	Green River	4903506020	B-54 BIG PINEY	BELCO PETROLEUM	WY	29N	113W	26	SESENE	3497.9	A	18.4	2.65	18.5	13.9	4.3	15587	MVRD
E712	Green River	4903506020	B-54 BIG PINEY	BELCO PETROLEUM	WY	29N	113W	26	SESENE	3497.9	B	18.9	2.67	18.1	13.9	4.3	15587	MVRD
E712	Green River	4903506020	B-54 BIG PINEY	BELCO PETROLEUM	WY	29N	113W	26	SESENE	3498.1	B	18.9	2.67	18.3	11.8	8.2	15587	MVRD
E712	Green River	4903506020	B-54 BIG PINEY	BELCO PETROLEUM	WY	29N	113W	26	SESENE	3498.1	A	18.5	2.66	14.8	10.3	5.6	15587	MVRD
E712	Green River	4903506020	B-54 BIG PINEY	BELCO PETROLEUM	WY	29N	113W	26	SESENE	3503.7	B	8.8	2.66	0.0207	0.000792	130	12219	MVRD
E712	Green River	4903506020	B-54 BIG PINEY	BELCO PETROLEUM	WY	29N	113W	26	SESENE	3503.7	A	7.8	2.63	0.0201	0.000893	86.8	12219	MVRD
E712	Green River	4903506020	B-54 BIG PINEY	BELCO PETROLEUM	WY	29N	113W	26	SESENE	3503.8	B	8.4	2.65	0.160	0.0532	37.5	12219	MVRD
E712	Green River	4903506020	B-54 BIG PINEY	BELCO PETROLEUM	WY	29N	113W	26	SESENE	3503.8	A	8.4	2.66	0.0178	0.000753	108	12219	MVRD
E712	Green River	4903506020	B-54 BIG PINEY	BELCO PETROLEUM	WY	29N	113W	26	SESENE	3508.2	A	7.9	2.67	0.111	0.00371	95.2	12245	MVRD
E712	Green River	4903506020	B-54 BIG PINEY	BELCO PETROLEUM	WY	29N	113W	26	SESENE	3511.8	B	13.5	2.68	2.32	0.777	40.9	15575	MVRD
E712	Green River	4903506020	B-54 BIG PINEY	BELCO PETROLEUM	WY	29N	113W	26	SESENE	3511.8	A	13.1	2.68	1.22	0.706	20.5	15575	MVRD
E712	Green River	4903506020	B-54 BIG PINEY	BELCO PETROLEUM	WY	29N	113W	26	SESENE	3514.2	A	15.7	2.69	8.23	5.19	13.5	15575	MVRD
E712	Green River	4903506020	B-54 BIG PINEY	BELCO PETROLEUM	WY	29N	113W	26	SESENE	3514.2	B	15.5	2.69	7.86	5.05	8.4	15575	MVRD
E712	Green River	4903506020	B-54 BIG PINEY	BELCO PETROLEUM	WY	29N	113W	26	SESENE	3515.8	A	11.6	2.70	0.150	0.0205	89.5	15275	MVRD
E712	Green River	4903506020	B-54 BIG PINEY	BELCO PETROLEUM	WY	29N	113W	26	SESENE	3515.8	B	12.0	2.71	0.142	0.0199	106	15275	MVRD
E712	Green River	4903506020	B-54 BIG PINEY	BELCO PETROLEUM	WY	29N	113W	26	SESENE	3519.3	B	16.1	2.70	8.42	6.02	13.2	13235	MVRD
E712	Green River	4903506020	B-54 BIG PINEY	BELCO PETROLEUM	WY	29N	113W	26	SESENE	3519.3	A	16.3	2.70	8.29	6.81	7.3	13235	MVRD
E894	Green River	4903520622	1 OLD ROAD	AMERICAN HUNTER EXPL	WY	27N	108W	27	SENWSE	11892.8	B	7.0	2.71	0.0239	0.00431	50.8	13255	LNCE
E894	Green River	4903520622	1 OLD ROAD	AMERICAN HUNTER EXPL	WY	27N	108W	27	SENWSE	11892.8	A	7.0	2.72	0.0158	0.00283	80.7	13255	LNCE
E894	Green River	4903520622	1 OLD ROAD	AMERICAN HUNTER EXPL	WY	27N	108W	27	SENWSE	11894.1	B	6.1	2.70	0.00634	0.000648	187	15265	LNCE
E894	Green River	4903520622	1 OLD ROAD	AMERICAN HUNTER EXPL	WY	27N	108W	27	SENWSE	11894.1	A	6.3	2.70	0.00581	0.000611	158	15265	LNCE
E894	Green River	4903520622	1 OLD ROAD	AMERICAN HUNTER EXPL	WY	27N	108W	27	SENWSE	11894.2	A	7.9	2.68	0.0251	0.00364	143	15265	LNCE
E894	Green River	4903520622	1 OLD ROAD	AMERICAN HUNTER EXPL	WY	27N	108W	27	SENWSE	11894.2	B	8.1	2.68	0.0164	0.00231	148	15265	LNCE
E894	Green River	4903520622	1 OLD ROAD	AMERICAN HUNTER EXPL	WY	27N	108W	27	SENWSE	11897.3	A	5.2	2.72	0.0107	0.000995	164	12245	LNCE
E894	Green River	4903520622	1 OLD ROAD	AMERICAN HUNTER EXPL	WY	27N	108W	27	SENWSE	11897.3	B	4.6	2.72	0.00722	0.000493	223	12245	LNCE
E894	Green River	4903520622	1 OLD ROAD	AMERICAN HUNTER EXPL	WY	27N	108W	27	SENWSE	11915.2	B	8.4	2.67	0.0137	0.00372	52.6	15295	LNCE
E894	Green River	4903520622	1 OLD ROAD	AMERICAN HUNTER EXPL	WY	27N	108W	27	SENWSE	11915.2	A	9.2	2.70	0.0135	0.00256	219	15295	LNCE
E894	Green River	4903520622	1 OLD ROAD	AMERICAN HUNTER EXPL	WY	27N	108W	27	SENWSE	11921.8	A	5.0	2.67	0.00607	0.000271	188	12218	LNCE
E894	Green River	4903520622	1 OLD ROAD	AMERICAN HUNTER EXPL	WY	27N	108W	27	SENWSE	11921.8	B	5.0	2.67	0.00345	0.000232	110	12218	LNCE
E894	Green River	4903520622	1 OLD ROAD	AMERICAN HUNTER EXPL	WY	27N	108W	27	SENWSE	11923.3	A	4.1	2.58	0.0415	0.00644	151	13218	LNCE
E894	Green River	4903520622	1 OLD ROAD	AMERICAN HUNTER EXPL	WY	27N	108W	27	SENWSE	11923.3	B	3.8	2.58	0.00768	0.000189	409	13218	LNCE
E894	Green River	4903520622	1 OLD ROAD	AMERICAN HUNTER EXPL	WY	27N	108W	27	SENWSE	11927.7	A	11.5	2.66	0.0352	0.00749	43.0	15586	LNCE
E894	Green River	4903520622	1 OLD ROAD	AMERICAN HUNTER EXPL	WY	27N	108W	27	SENWSE	11927.7	B	11.4	2.66	0.0271	0.00441	234	15586	LNCE
E894	Green River	4903520622	1 OLD ROAD	AMERICAN HUNTER EXPL	WY	27N	108W	27	SENWSE	11927.8	A	11.3	2.66	0.0406	0.00925	19.1	15586	LNCE
E894	Green River	4903520622	1 OLD ROAD	AMERICAN HUNTER EXPL	WY	27N	108W	27	SENWSE	11927.8	B	11.5	2.66	0.0328	0.00686	92.1	15586	LNCE
E894	Green River	4903520622	1 OLD ROAD	AMERICAN HUNTER EXPL	WY	27N	108W	27	SENWSE	11935.2	A	10.7	2.67	0.0160	0.00296	32.2	15586	LNCE
E894	Green River	4903520622	1 OLD ROAD	AMERICAN HUNTER EXPL	WY	27N	108W	27	SENWSE	11935.2	B	10.5	2.67	0.0147	0.00148	133	15586	LNCE
E894	Green River	4903520622	1 OLD ROAD	AMERICAN HUNTER EXPL	WY	27N	108W	27	SENWSE	11936.3	B	10.3	2.66	0.0175	0.00287	122	15576	LNCE
E894	Green River	4903520622	1 OLD ROAD	AMERICAN HUNTER EXPL	WY	27N	108W	27	SENWSE	11936.3	A	9.8	2.66	0.0157	0.00238	148	15576	LNCE
E894	Green River	4903520622	1 OLD ROAD	AMERICAN HUNTER EXPL	WY	27N	108W	27	SENWSE	11956.1	B	9.1	2.70	0.0758	0.0193	58.9	15586	LNCE
E894	Green River	4903520622	1 OLD ROAD	AMERICAN HUNTER EXPL	WY	27N	108W	27	SENWSE	11956.1	A	8.5	2.69	0.0356	0.00792	75.2	15586	LNCE
E894	Green River	4903520622	1 OLD ROAD	AMERICAN HUNTER EXPL	WY	27N	108W	27	SENWSE	11966.7	A	5.9	2.74	0.00534	0.000266	278	12215	LNCE
E894	Green River	4903520622	1 OLD ROAD	AMERICAN HUNTER EXPL	WY	27N	108W	27	SENWSE	11966.7	B	5.4	2.73	0.00408	0.000209	191	12215	LNCE
E894	Green River	4903520622	1 OLD ROAD	AMERICAN HUNTER EXPL	WY	27N	108W	27	SENWSE	11971.9	B	8.9	2.71	0.0370	0.00812	110	15595	LNCE
E894	Green River	4903520622	1 OLD ROAD	AMERICAN HUNTER EXPL	WY	27N	108W	27	SENWSE	11971.9	A	8.3	2.71	0.0150	0.00270	109	15595	LNCE
E894	Green River	4903520622	1 OLD ROAD	AMERICAN HUNTER EXPL	WY	27N	108W	27	SENWSE	11980.8	B	7.5	2.71				14285	LNCE
E894	Green River	4903520622	1 OLD ROAD	AMERICAN HUNTER EXPL	WY	27N	108W	27	SENWSE	11980.9	B	7.5	2.71	0.00797	0.00142	64.5	14285	LNCE
E894	Green River	4903520622	1 OLD ROAD	AMERICAN HUNTER EXPL	WY	27N	108W	27	SENWSE	11980.9	A	7.5	2.70	0.00654	0.00171	126	14285	LNCE
E894	Green River	4903520622	1 OLD ROAD	AMERICAN HUNTER EXPL	WY	27N	108W	27	SENWSE	11981.9	A	8.3	2.69	0.0125	0.00232	112	15295	LNCE
E894	Green River	4903520622	1 OLD ROAD	AMERICAN HUNTER EXPL	WY	27N	108W	27	SENWSE	11981.9	B	8.4	2.70	0.0119	0.00255	107	15295	LNCE
E894	Green River	4903520622	1 OLD ROAD	AMERICAN HUNTER EXPL	WY	27N	108W	27	SENWSE	11986.9	A	8.2	2.70	0.0162	0.00240	137	13275	LNCE
E894	Green River	4903520622	1 OLD ROAD	AMERICAN HUNTER EXPL	WY	27N	108W	27	SENWSE	11986.9	B	7.0	2.70	0.0115	0.00132	185	13275	LNCE
E894	Green River	4903520622	1 OLD ROAD	AMERICAN HUNTER EXPL	WY	27N	108W	27	SENWSE	11991.1	B	8.7	2.71	0.0523	0.00925	112	15285	LNCE
E894	Green River	4903520622	1 OLD ROAD	AMERICAN HUNTER EXPL	WY	27N	108W	27	SENWSE	11991.1	A	8.5	2.71	0.0221	0.00496	63.7	15285	LNCE
E894	Green River	4903520622	1 OLD ROAD	AMERICAN HUNTER EXPL	WY	27N	108W	27	SENWSE	11998.2	B	6.6	2.72	0.00471	0.000526	184	15285	LNCE
E894	Green River	4903520622	1 OLD ROAD	AMERICAN HUNTER EXPL	WY	27N	108W	27	SENWSE	11998.2	A	6.6	2.71	0.00326	0.000319	326	15285	LNCE
E894	Green River	4903520622	1 OLD ROAD	AMERICAN HUNTER EXPL	WY	27N	108W	27	SENWSE	12001.9	B	6.8	2.70	0.0151	0.00114	190	15285	LNCE
E894	Green River	4903520622	1 OLD ROAD	AMERICAN HUNTER EXPL	WY	27N	108W	27	SENWSE	12001.9	A	7.2	2.71	0.0130	0.00144	153	15285	LNCE
R780	Green River	4903505742	C-47 TIP TOP SHALLOW	BELCO PETROLEUM	WY	28N	113W	22	SWNE	2699.6	A	21.4	2.65	40.7	29.9	4.1	15596	MVRD
R780	Green River	4903505742	C-47 TIP TOP SHALLOW	BELCO PETROLEUM	WY	28N	113W	22	SWNE	2699.6	B	21.2	2.66	38.1	27.6	4.3	15596	MVRD
R780	Green River	4903505742	C-47 TIP TOP SHALLOW	BELCO PETROLEUM	WY	28N	113W	22	SWNE	2699.7	A	21.7	2.66	46.7	33.8	4.2	15596	MVRD
R780	Green River	4903505742	C-47 TIP TOP SHALLOW	BELCO PETROLEUM	WY	28N	113W	22	SWNE	2699.7	B	21.7	2.66	42.2	29.0	5.2	15596	MVRD
R780	Green River	4903505742	C-47 TIP TOP SHALLOW	BELCO PETROLEUM	WY	28N	113W	22	SWNE	2699.8	B	21.1	2.66	37.6	28.2	3.4	15596	MVRD
R780	Green River	4903505742	C-47 TIP TOP SHALLOW	BELCO PETROLEUM	WY	28N	113W	22	SWNE	2699.8	A	21.3	2.66	34.9	26.4	4.3	15596	MVRD
R780	Green River	4903505742	C-47 TIP TOP SHALLOW	BELCO PETROLEUM	WY	28N	113W	22	SWNE	2717.1	A	20.0	2.67	17.3	11.3	9.3	15575	MVRD
R780	Green River	4903505742	C-47 TIP TOP SHALLOW	BELCO PETROLEUM	WY	28N	113W	22	SWNE	2717.1	B	19.9	2.67	16.3	11.5	5.0	15575	MVRD
R780	Green River	4903505742	C-47 TIP TOP SHALLOW	BELCO PETROLEUM	WY	28N	113W	22	SWNE	2717.3	A	20.4	2.67	20.2	12.9	10.6	15575	MVRD
R780	Green River	4903505742	C-47 TIP TOP SHALLOW	BELCO PETROLEUM	WY	28N	113W	22	SWNE	2717.3	B	19.9	2.66	18.4	11.7	7.6	15575	MVRD
R780	Green River	4903505742	C-47 TIP TOP SHALLOW	BELCO PETROLEUM	WY	28N	113W	22	SWNE	2729.7	B	19.4	2.67	13.1	9.24	6.0	15575	MVRD
R780	Green River	4903505742	C-47 TIP TOP SHALLOW	BELCO PETROLEUM	WY	28N	113W	22	SWNE	2729.7	A	19.4	2.67	11.4	5.52	22.1	15575	MVRD
R780	Green River	4903505742	C-47 TIP TOP SHALLOW	BELCO PETROLEUM	WY	28N	113W	22	SWNE	2729.8	A	19.5	2.67	10.7	7.34	8.4	15575	MVRD
R780	Green River	4903505742	C-47 TIP TOP SHALLOW	BELCO PETROLEUM	WY	28N	113W	22	SWNE	2729.8	B	19.4	2.67	8.51	8.02	6.9	15575	MVRD
R780	Green River	4903505742	C-47 TIP TOP SHALLOW	BELCO PETROLEUM	WY	28N	113W	22	SWNE	2729.9	B	19.2	2.66	11.5	7.96	6.7	15575	MVRD
R780	Green River	4903505742	C-47 TIP TOP SHALLOW	BELCO PETROLEUM	WY	28N	113W	22	SWNE	2729.9	A	18.7	2.64	11.2	6.14	21.5	15575	MVRD
R780	Green River	4903505742	C-47 TIP TOP SHALLOW	BELCO PETROLEUM	WY	28N	113W	22	SWNE	2754.7	A	21.3	2.62	3.67	1.90	16.5	16575	MVRD
R780	Green River	4903505742	C-47 TIP TOP SHALLOW	BELCO PETROLEUM	WY	28N	113W	22	SWNE	2754.7	B	20.7	2.62	3.26	1.29	37.2	16575	MVRD
R780	Green River	4903505742	C-47 TIP TOP SHALLOW	BELCO PETROLEUM	WY	28N	113W	22	SWNE	2754.8	B	21.0	2.62	4.90	3.08	4.8	16575	MVRD
R780	Green River	4903505742	C-47 TIP TOP SHALLOW	BELCO PETROLEUM	WY	28N	113W	22	SWNE	2754.8	A	22.0	2.65	4.63	2.43	16.2	16575	MVRD
R780	Green River	4903505742	C-47 TIP TOP SHALLOW	BELCO PETROLEUM	WY	28N	113W	22	SWNE	2754.9	B	20.3	2.62	2.55	1.46	3.7	16575	MVRD
R780	Green River	4903505742	C-47 TIP TOP SHALLOW	BELCO PETROLEUM	WY	28N	113W	22	SWNE	2754.9	A	20.6	2.62	2.18	1.15	25.1	16575	MVRD
R780	Green River	4903505742	C-47 TIP TOP SHALLOW	BELCO PETROLEUM	WY	28N	113W	22	SWNE	2759.9	A	9.1	2.68	0.0126	0.000708	120	15275	MVRD
R780	Green River	4903505742	C-47 TIP TOP SHALLOW	BELCO PETROLEUM	WY	28N	113W	22	SWNE	2759.9	B	7.2	2.66	0.00692	0.000614	106	15275	MVRD
R780	Green River	4903505742	C-47 TIP TOP SHALLOW	BELCO PETROLEUM	WY	28N	113W	22	SWNE	2771.6	B	21.3	2.63	27.4	18.5	5.3	15595	MVRD
R780	Green River	4903505742	C-47 TIP TOP SHALLOW	BELCO PETROLEUM	WY	28N	113W	22	SWNE	2771.6	A	21.4	2.64	17.5	12.2	5.2	15595	MVRD
R780	Green River	4903505742	C-47 TIP TOP SHALLOW	BELCO PETROLEUM	WY	28N	113W	22	SWNE	2771.7	A	22.4	2.65	43.5	30.4	5.0	15595	MVRD
R780	Green River	4903505742	C-47 TIP TOP SHALLOW	BELCO PETROLEUM	WY	28N	113W	22	SWNE	2771.7	B	21.4	2.64	1.99	0.498	18.4	15595	MVRD
R780	Green River	4903505742	C-47 TIP TOP SHALLOW	BELCO PETROLEUM	WY	28N	113W	22	SWNE	2783.3	B	22.1	2.64	31.3	24.0	2.8	15595	MVRD
R780	Green River	4903505742	C-47 TIP TOP SHALLOW	BELCO PETROLEUM	WY	28N	113W	22	SWNE	2783.3	A	22.3	2.64	28.9	23.3	2.7	15595	MVRD
R780	Green River	4903505742	C-47 TIP TOP SHALLOW	BELCO PETROLEUM	WY	28N	113W	22	SWNE	2783.4	A	21.9	2.63	29.6	21.7	4.3	15595	MVRD
R780	Green River	4903505742	C-47 TIP TOP SHALLOW	BELCO PETROLEUM	WY	28N	113W	22	SWNE	2783.4	B	22.3	2.65	26.0	21.5	3.9	15595	MVRD
R780	Green River	4903505742	C-47 TIP TOP SHALLOW	BELCO PETROLEUM	WY	28N	113W	22	SWNE	2800.7	A	19.9	2.63	9.85	7.13	5.8	15575	MVRD
R780	Green River	4903505742	C-47 TIP TOP SHALLOW	BELCO PETROLEUM	WY	28N	113W	22	SWNE	2800.7	B	15.6	2.67	1.42	0.810	21.7	15575	MVRD
R780	Green River	4903505742	C-47 TIP TOP SHALLOW	BELCO PETROLEUM	WY	28N	113W	22	SWNE	2800.8	B	19.7	2.65	8.18	4.17	16.1	15575	MVRD
R780	Green River	4903505742	C-47 TIP TOP SHALLOW	BELCO PETROLEUM	WY	28N	113W	22	SWNE	2800.8	A	19.9	2.65	7.74	4.24	16.1	15575	MVRD
R780	Green River	4903505742	C-47 TIP TOP SHALLOW	BELCO PETROLEUM	WY	28N	113W	22	SWNE	2811.7	B	20.0	2.66	409	204	11.7	15575	MVRD
R780	Green River	4903505742	C-47 TIP TOP SHALLOW	BELCO PETROLEUM	WY	28N	113W	22	SWNE	2811.7	A	19.1	2.63	4.50	3.08	10.4	15575	MVRD
R780	Green River	4903505742	C-47 TIP TOP SHALLOW	BELCO PETROLEUM	WY	28N	113W	22	SWNE	2811.8	A	18.9	2.63	3.81	2.51	11.1	15575	MVRD
R780	Green River	4903505742	C-47 TIP TOP SHALLOW	BELCO PETROLEUM	WY	28N	113W	22	SWNE	2811.8	B	19.7	2.66	3.01	1.88	13.1	15575	MVRD
R780	Green River	4903505742	C-47 TIP TOP SHALLOW	BELCO PETROLEUM	WY	28N	113W	22	SWNE	2817.7	A	20.1	2.69	2.90	2.12	8.9	15575	MVRD
R780	Green River	4903505742	C-47 TIP TOP SHALLOW	BELCO PETROLEUM	WY	28N	113W	22	SWNE	2817.7	B	19.8	2.69	2.46	2.07	8.2	15575	MVRD
R780	Green River	4903505742	C-47 TIP TOP SHALLOW	BELCO PETROLEUM	WY	28N	113W	22	SWNE	2817.8	B	19.6	2.69	2.80	1.19	42.4	15575	MVRD
R780	Green River	4903505742	C-47 TIP TOP SHALLOW	BELCO PETROLEUM	WY	28N	113W	22	SWNE	2817.8	A	20.1	2.69	2.61	1.61	18.7	15575	MVRD
R780	Green River	4903505742	C-47 TIP TOP SHALLOW	BELCO PETROLEUM	WY	28N	113W	22	SWNE	2829.7	A	12.2	2.69	0.0405	0.0131	130	15285	MVRD

Table 4.1.1. (continued)

Summary of Porosity, Permeability, and Grain Density
Analysis of Critical Permeability, Capillary Pressure, and Electrical Properties for Mesaverde Tight Gas Sandstones from Western U.S. Basins
US DOE # DE-FC26-05NT42660
Alan P. Byrnes, Robert M. Cluff, John C. Webb, Daniel A. Krygowski, Stefani D. Whittaker
website: http://www.kgs.ku.edu/mesaverde

USGS Library Number	Basin	API Number	Well Name	Operator	State	Township	Range	Section	Quarter Section	Plug Depth	Plug Letter	Ambient Porosity	Grain Density	Routine Gas Permeability	*in situ* Klinkenberg Gas Permeability	*in situ* Klinken-berg *constant* b	Rock Type Code	Formations
										ft	A/B/C	%	g/cc	mD	mD	(psia)		
R780	Green River	4903505742	C-47 TIP TOP SHALLOW	BELCO PETROLEUM	WY	28N	113W	22	SWNE	2829.7	B	8.4	2.68	0.0160	0.00225	124	15285	MVRD
R780	Green River	4903505742	C-47 TIP TOP SHALLOW	BELCO PETROLEUM	WY	28N	113W	22	SWNE	2829.8	A	8.6	2.70	0.0105	0.00142	111	15285	MVRD
R780	Green River	4903505742	C-47 TIP TOP SHALLOW	BELCO PETROLEUM	WY	28N	113W	22	SWNE	2829.8	B	6.1	2.69	0.00433	0.000397	169	15285	MVRD
R780	Green River	4903505742	C-47 TIP TOP SHALLOW	BELCO PETROLEUM	WY	28N	113W	22	SWNE	2829.9	A	6.6	2.67	0.00551	0.000610	185	15285	MVRD
R780	Green River	4903505742	C-47 TIP TOP SHALLOW	BELCO PETROLEUM	WY	28N	113W	22	SWNE	2829.9	B	5.3	2.70	0.00550	0.000478	201	15285	MVRD
R780	Green River	4903505742	C-47 TIP TOP SHALLOW	BELCO PETROLEUM	WY	28N	113W	22	SWNE	2831.8	B	20.9	2.68	5.38	3.18	15.2	15285	MVRD
R780	Green River	4903505742	C-47 TIP TOP SHALLOW	BELCO PETROLEUM	WY	28N	113W	22	SWNE	2831.8	A	23.6	2.68	4.68	2.73	20.3	15285	MVRD
R780	Green River	4903505742	C-47 TIP TOP SHALLOW	BELCO PETROLEUM	WY	28N	113W	22	SWNE	2831.9	B	20.4	2.68	3.93	3.22	6.8	15285	MVRD
R780	Green River	4903505742	C-47 TIP TOP SHALLOW	BELCO PETROLEUM	WY	28N	113W	22	SWNE	2831.9	A	19.2	2.67	2.80	1.86	12.1	15285	MVRD
R780	Green River	4903505742	C-47 TIP TOP SHALLOW	BELCO PETROLEUM	WY	28N	113W	22	SWNE	2845.5	B	22.0	2.67	12.6	6.34	18.2	15577	MVRD
R780	Green River	4903505742	C-47 TIP TOP SHALLOW	BELCO PETROLEUM	WY	28N	113W	22	SWNE	2845.5	A	22.6	2.67	11.8	8.69	6.2	15577	MVRD
R780	Green River	4903505742	C-47 TIP TOP SHALLOW	BELCO PETROLEUM	WY	28N	113W	22	SWNE	2850.9	A	21.1	2.69	8.50	4.51	18.1	15287	MVRD
R780	Green River	4903505742	C-47 TIP TOP SHALLOW	BELCO PETROLEUM	WY	28N	113W	22	SWNE	2850.9	B	21.0	2.69	6.91	4.93	8.5	15287	MVRD
S873	Green River	4903506200	K-2 MASON	BELCO PETROLEUM	WY	31N	113W	13	SESE	6988.1	A	10.0	2.69	0.142	0.0526	190	15275	MVRD
S873	Green River	4903506200	K-2 MASON	BELCO PETROLEUM	WY	31N	113W	13	SESE	6989.8	A	10.7	2.69	0.288	0.138	55.2	15275	MVRD
S873	Green River	4903506200	K-2 MASON	BELCO PETROLEUM	WY	31N	113W	13	SESE	6989.9	A	10.4	2.69	0.156	0.0823	44.5	15275	MVRD
S873	Green River	4903506200	K-2 MASON	BELCO PETROLEUM	WY	31N	113W	13	SESE	7703.7	A	11.9	2.69	0.393	0.228	22.6	16295	MVRD
S873	Green River	4903506200	K-2 MASON	BELCO PETROLEUM	WY	31N	113W	13	SESE	7703.7	A2	11.5	2.68	0.0210	0.0127	102	16295	MVRD
S873	Green River	4903506200	K-2 MASON	BELCO PETROLEUM	WY	31N	113W	13	SESE	7703.7	A1	11.4	2.67	0.0207	0.0115	82.0	16295	MVRD
S873	Green River	4903506200	K-2 MASON	BELCO PETROLEUM	WY	31N	113W	13	SESE	7703.8	A	12.1	2.69	0.433	0.239	25.4	16295	MVRD
S873	Green River	4903506200	K-2 MASON	BELCO PETROLEUM	WY	31N	113W	13	SESE	9370.1	A	2.9	2.67	0.00164	0.000063	352	13216	MVRD
S873	Green River	4903506200	K-2 MASON	BELCO PETROLEUM	WY	31N	113W	13	SESE	9370.2	A	2.6	2.66	0.00388	0.000143	273	13216	MVRD
S873	Green River	4903506200	K-2 MASON	BELCO PETROLEUM	WY	31N	113W	13	SESE	9379.0	A	2.7	2.70	0.000942	0.000006	2575	13215	MVRD
S873	Green River	4903506200	K-2 MASON	BELCO PETROLEUM	WY	31N	113W	13	SESE	9393.3	A	3.4	2.70	0.000745	0.000024	426	12235	MVRD
S873	Green River	4903506200	K-2 MASON	BELCO PETROLEUM	WY	31N	113W	13	SESE	9393.5	A	2.7	2.68	0.00177	0.000054	383	13265	MVRD
S873	Green River	4903506200	K-2 MASON	BELCO PETROLEUM	WY	31N	113W	13	SESE	9397.2	A	8.2	2.67	0.00594	0.000450	200	15286	MVRD
S873	Green River	4903506200	K-2 MASON	BELCO PETROLEUM	WY	31N	113W	13	SESE	9397.2	A1	8.3	2.67	0.000462	0.000041	763	15286	MVRD
S873	Green River	4903506200	K-2 MASON	BELCO PETROLEUM	WY	31N	113W	13	SESE	9397.2	A2	8.2	2.67	0.000413	0.000064	462	15286	MVRD
S873	Green River	4903506200	K-2 MASON	BELCO PETROLEUM	WY	31N	113W	13	SESE	9397.3	A	8.4	2.67	0.00476	0.000358	223	15286	MVRD
SHV	Green River	4903523799	VIBLE 1D-11D	SHELL E&P	WY	31N	109W	11	SENE	12505.7		4.7	2.69	0.00101	0.000170	197	13287	MVRD
SHV	Green River	4903523799	VIBLE 1D-11D	SHELL E&P	WY	31N	109W	11	SENE	12507.1		5.1	2.68	0.00244	0.000627	150	15287	MVRD
SHV	Green River	4903523799	VIBLE 1D-11D	SHELL E&P	WY	31N	109W	11	SENE	12508.7		3.0	2.67	0.00132	0.000219	190	15275	MVRD
SHV	Green River	4903523799	VIBLE 1D-11D	SHELL E&P	WY	31N	109W	11	SENE	12510.1		7.3	2.60	0.0694	0.0250	105	16277	MVRD
SHV	Green River	4903523799	VIBLE 1D-11D	SHELL E&P	WY	31N	109W	11	SENE	12513.0		7.4	2.65	0.0148	0.00665	150	15277	MVRD
SHV	Green River	4903523799	VIBLE 1D-11D	SHELL E&P	WY	31N	109W	11	SENE	12518.5		5.9	2.65	0.00649	0.00172	189	15217	MVRD
SHV	Green River	4903523799	VIBLE 1D-11D	SHELL E&P	WY	31N	109W	11	SENE	12520.3		4.3	2.67	0.00277	0.000212	553	16275	MVRD
SHV	Green River	4903523799	VIBLE 1D-11D	SHELL E&P	WY	31N	109W	11	SENE	12520.9		3.4	2.67	0.00389	0.000188	167	14265	MVRD
SHV	Green River	4903523799	VIBLE 1D-11D	SHELL E&P	WY	31N	109W	11	SENE	12529.0		1.4	2.67	0.000416	0.000025	372	13266	MVRD
SHV	Green River	4903523799	VIBLE 1D-11D	SHELL E&P	WY	31N	109W	11	SENE	12553.7		1.3	2.67	0.000478	0.000037	213	13265	MVRD
T195	Green River	4903508024	5 PINEDALE	EL PASO NATURAL GAS	WY	30N	108W	5	C SE	12158.5	A	11.0	2.65	0.0325	0.0167	97.2	13276	MVRD
T195	Green River	4903508024	5 PINEDALE	EL PASO NATURAL GAS	WY	30N	108W	5	C SE	12158.5	B	10.6	2.66	0.0255	0.0127	89.7	13276	MVRD
T195	Green River	4903508024	5 PINEDALE	EL PASO NATURAL GAS	WY	30N	108W	5	C SE	12159.5	B	8.9	2.66	0.0251	0.0130	75.7	16295	MVRD
T195	Green River	4903508024	5 PINEDALE	EL PASO NATURAL GAS	WY	30N	108W	5	C SE	12159.5	A	9.3	2.66	0.000295	0.000003	898	16295	MVRD
T195	Green River	4903508024	5 PINEDALE	EL PASO NATURAL GAS	WY	30N	108W	5	C SE	12159.6	A	9.0	2.66	0.0226	0.0111	65.4	16295	MVRD
T195	Green River	4903508024	5 PINEDALE	EL PASO NATURAL GAS	WY	30N	108W	5	C SE	12159.6	B	9.0	2.66	0.0222	0.0112	60.9	16295	MVRD
T195	Green River	4903508024	5 PINEDALE	EL PASO NATURAL GAS	WY	30N	108W	5	C SE	12160.5	B	9.5	2.66	0.0148	0.00492	106	15265	MVRD
T195	Green River	4903508024	5 PINEDALE	EL PASO NATURAL GAS	WY	30N	108W	5	C SE	12160.5	A	10.2	2.66	0.0144	0.00505	197	15265	MVRD
T195	Green River	4903508024	5 PINEDALE	EL PASO NATURAL GAS	WY	30N	108W	5	C SE	12160.6	A	9.7	2.66	0.0104	0.00487	69.3	15265	MVRD
T195	Green River	4903508024	5 PINEDALE	EL PASO NATURAL GAS	WY	30N	108W	5	C SE	12161.5	B	6.5	2.65	0.00546	0.000361	792	16275	MVRD
T195	Green River	4903508024	5 PINEDALE	EL PASO NATURAL GAS	WY	30N	108W	5	C SE	12161.5	A	6.5	2.66	0.00338	0.000417	189	16275	MVRD
T195	Green River	4903508024	5 PINEDALE	EL PASO NATURAL GAS	WY	30N	108W	5	C SE	12161.6	B	5.1	2.65	0.00449	0.000493	146	16275	MVRD
T195	Green River	4903508024	5 PINEDALE	EL PASO NATURAL GAS	WY	30N	108W	5	C SE	12161.6	A	5.4	2.66	0.00352	0.000582	184	16275	MVRD
T195	Green River	4903508024	5 PINEDALE	EL PASO NATURAL GAS	WY	30N	108W	5	C SE	12162.0	B	6.6	2.66	0.00518	0.000786	219	16275	MVRD
T195	Green River	4903508024	5 PINEDALE	EL PASO NATURAL GAS	WY	30N	108W	5	C SE	12162.0	A	7.2	2.67	0.00430	0.000796	151	16275	MVRD
T195	Green River	4903508024	5 PINEDALE	EL PASO NATURAL GAS	WY	30N	108W	5	C SE	12162.6	B	6.9	2.66	0.00497	0.000922	133	15275	MVRD
T195	Green River	4903508024	5 PINEDALE	EL PASO NATURAL GAS	WY	30N	108W	5	C SE	12162.6	A	6.6	2.66	0.00479	0.000545	427	15275	MVRD
T204	Green River	4903705349	B-2A SPIDER CREEK	HUMBLE OIL & REF	WY	18N	110W	27	NESW	9022.9	A	12.1	2.63	16.4	10.2	4.2	16295	MVRD
T204	Green River	4903705349	B-2A SPIDER CREEK	HUMBLE OIL & REF	WY	18N	110W	27	NESW	9038.9	A	11.5	2.64	1.89	1.08	10.2	16296	MVRD
T204	Green River	4903705349	B-2A SPIDER CREEK	HUMBLE OIL & REF	WY	18N	110W	27	NESW	9041.1	A	11.6	2.64	4.60	1.82	25.0	16296	MVRD
T204	Green River	4903705349	B-2A SPIDER CREEK	HUMBLE OIL & REF	WY	18N	110W	27	NESW	9063.0	A	15.2	2.61	317	206	2.2	17596	MVRD
T204	Green River	4903705349	B-2A SPIDER CREEK	HUMBLE OIL & REF	WY	18N	110W	27	NESW	9072.1	A	12.3	2.64	11.6	6.74	5.0	17276	MVRD
T204	Green River	4903705349	B-2A SPIDER CREEK	HUMBLE OIL & REF	WY	18N	110W	27	NESW	9072.2	A	12.4	2.64	10.8	5.89	9.3	17276	MVRD
T204	Green River	4903705349	B-2A SPIDER CREEK	HUMBLE OIL & REF	WY	18N	110W	27	NESW	9081.0	A	11.4	2.63	3.80	1.77	11.1	17276	MVRD
T204	Green River	4903705349	B-2A SPIDER CREEK	HUMBLE OIL & REF	WY	18N	110W	27	NESW	9098.0	A	6.6	2.63	0.177	0.0188	61.6	13286	MVRD
T204	Green River	4903705349	B-2A SPIDER CREEK	HUMBLE OIL & REF	WY	18N	110W	27	NESW	9103.9	A	10.0	2.63	1.45	0.564	16.3	13276	MVRD
T204	Green River	4903705349	B-2A SPIDER CREEK	HUMBLE OIL & REF	WY	18N	110W	27	NESW	9107.0	A	10.8	2.63	3.97	1.90	12.5	17576	MVRD
T204	Green River	4903705349	B-2A SPIDER CREEK	HUMBLE OIL & REF	WY	18N	110W	27	NESW	9116.9	A	2.3	2.64	0.00246	0.000138	97.1	13219	MVRD
B43C	Piceance	0504511402	LAST DANCE 43C-3-792	BILL BARRETT CORP.	CO	7S	92W	3	NESE	3544.8	C	10.5	2.64	0.798	0.392	19.6	16277	RLNS/WMFRK
B43C	Piceance	0504511402	LAST DANCE 43C-3-792	BILL BARRETT CORP.	CO	7S	92W	3	NESE	3544.8	B	11.3	2.65	0.725	0.407	11.7	16277	RLNS/WMFRK
B43C	Piceance	0504511402	LAST DANCE 43C-3-792	BILL BARRETT CORP.	CO	7S	92W	3	NESE	3544.8	A	11.1	2.65	0.621	0.395	7.8	16277	RLNS/WMFRK
B43C	Piceance	0504511402	LAST DANCE 43C-3-792	BILL BARRETT CORP.	CO	7S	92W	3	NESE	3544.9	B	11.4	2.65	0.872	0.429	22.9	16277	RLNS/WMFRK
B43C	Piceance	0504511402	LAST DANCE 43C-3-792	BILL BARRETT CORP.	CO	7S	92W	3	NESE	3544.9	C	10.8	2.64	0.851	0.447	17.0	16277	RLNS/WMFRK
B43C	Piceance	0504511402	LAST DANCE 43C-3-792	BILL BARRETT CORP.	CO	7S	92W	3	NESE	3544.9	A	11.2	2.64	0.814	0.470	16.3	16277	RLNS/WMFRK
B43C	Piceance	0504511402	LAST DANCE 43C-3-792	BILL BARRETT CORP.	CO	7S	92W	3	NESE	3555.4	B	11.4	2.63	2.05	1.06	20.6	16297	RLNS/WMFRK
B43C	Piceance	0504511402	LAST DANCE 43C-3-792	BILL BARRETT CORP.	CO	7S	92W	3	NESE	3555.4	C	12.0	2.65	2.05	1.46	6.6	16297	RLNS/WMFRK
B43C	Piceance	0504511402	LAST DANCE 43C-3-792	BILL BARRETT CORP.	CO	7S	92W	3	NESE	3555.4	A	11.8	2.64	2.04	1.20	10.0	16297	RLNS/WMFRK
B43C	Piceance	0504511402	LAST DANCE 43C-3-792	BILL BARRETT CORP.	CO	7S	92W	3	NESE	3559.9	A	6.2	2.65	0.0131	0.00173	120	13229	RLNS/WMFRK
B43C	Piceance	0504511402	LAST DANCE 43C-3-792	BILL BARRETT CORP.	CO	7S	92W	3	NESE	3559.9	B	5.5	2.65	0.00756	0.000896	146	13229	RLNS/WMFRK
B43C	Piceance	0504511402	LAST DANCE 43C-3-792	BILL BARRETT CORP.	CO	7S	92W	3	NESE	3562.6	A	6.1	2.65	0.00888	0.00155	213	15297	RLNS/WMFRK
B43C	Piceance	0504511402	LAST DANCE 43C-3-792	BILL BARRETT CORP.	CO	7S	92W	3	NESE	3566.4	B	2.9	2.66	0.00342	0.000080	348	13267	RLNS/WMFRK
B43C	Piceance	0504511402	LAST DANCE 43C-3-792	BILL BARRETT CORP.	CO	7S	92W	3	NESE	3566.4	A	2.4	2.66	0.00159	0.000018	446	13267	RLNS/WMFRK
B43C	Piceance	0504511402	LAST DANCE 43C-3-792	BILL BARRETT CORP.	CO	7S	92W	3	NESE	3573.2	B	4.7	2.67	0.00313	0.000082	492	13297	RLNS/WMFRK
B43C	Piceance	0504511402	LAST DANCE 43C-3-792	BILL BARRETT CORP.	CO	7S	92W	3	NESE	3573.2	C	4.2	2.66	0.00275	0.000095	411	13297	RLNS/WMFRK
B43C	Piceance	0504511402	LAST DANCE 43C-3-792	BILL BARRETT CORP.	CO	7S	92W	3	NESE	3573.2	A	4.3	2.66	0.00271	0.000111	323	13297	RLNS/WMFRK
B43C	Piceance	0504511402	LAST DANCE 43C-3-792	BILL BARRETT CORP.	CO	7S	92W	3	NESE	3573.3	C	4.4	2.66	0.00295	0.000083	249	13297	RLNS/WMFRK
B43C	Piceance	0504511402	LAST DANCE 43C-3-792	BILL BARRETT CORP.	CO	7S	92W	3	NESE	3573.3	A	5.0	2.67	0.00241	0.000119	308	13297	RLNS/WMFRK
B43C	Piceance	0504511402	LAST DANCE 43C-3-792	BILL BARRETT CORP.	CO	7S	92W	3	NESE	3573.3	B	4.8	2.66	0.00148	0.000092	290	13297	RLNS/WMFRK
B43C	Piceance	0504511402	LAST DANCE 43C-3-792	BILL BARRETT CORP.	CO	7S	92W	3	NESE	3577.6	C	2.0	2.69	0.00240	0.000088	152	13297	RLNS/WMFRK
B43C	Piceance	0504511402	LAST DANCE 43C-3-792	BILL BARRETT CORP.	CO	7S	92W	3	NESE	3577.6	B	2.1	2.68	0.00228	0.000059	275	13297	RLNS/WMFRK
B43C	Piceance	0504511402	LAST DANCE 43C-3-792	BILL BARRETT CORP.	CO	7S	92W	3	NESE	3577.6	A	1.8	2.69	0.00223	0.000062	419	13297	RLNS/WMFRK
B43C	Piceance	0504511402	LAST DANCE 43C-3-792	BILL BARRETT CORP.	CO	7S	92W	3	NESE	3581.5	A	3.6	2.63	1.47	0.0304	33.0	13217	RLNS/WMFRK
B43C	Piceance	0504511402	LAST DANCE 43C-3-792	BILL BARRETT CORP.	CO	7S	92W	3	NESE	3586.7	A	2.7	2.61	0.154	0.00232	106	12247	RLNS/WMFRK
B43C	Piceance	0504511402	LAST DANCE 43C-3-792	BILL BARRETT CORP.	CO	7S	92W	3	NESE	3586.7	C	2.9	2.63	0.0758	0.00241	154	12247	RLNS/WMFRK
B43C	Piceance	0504511402	LAST DANCE 43C-3-792	BILL BARRETT CORP.	CO	7S	92W	3	NESE	3586.7	B	3.1	2.64	0.0228	0.00105	83.3	12247	RLNS/WMFRK
B43C	Piceance	0504511402	LAST DANCE 43C-3-792	BILL BARRETT CORP.	CO	7S	92W	3	NESE	3591.1	B			0.00218	0.000049	232	13267	RLNS/WMFRK
B43C	Piceance	0504511402	LAST DANCE 43C-3-792	BILL BARRETT CORP.	CO	7S	92W	3	NESE	3591.5	B	2.9	2.67	0.00313	0.000131	270	13267	RLNS/WMFRK
B43C	Piceance	0504511402	LAST DANCE 43C-3-792	BILL BARRETT CORP.	CO	7S	92W	3	NESE	3591.5	A	2.4	2.66	0.00292	0.000045	467	13267	RLNS/WMFRK
B43C	Piceance	0504511402	LAST DANCE 43C-3-792	BILL BARRETT CORP.	CO	7S	92W	3	NESE	3593.6	A	3.3	2.63	0.0115	0.000342	410	13267	RLNS/WMFRK
B43C	Piceance	0504511402	LAST DANCE 43C-3-792	BILL BARRETT CORP.	CO	7S	92W	3	NESE	3593.6	B	3.3	2.63	0.00586	0.000262	477	13267	RLNS/WMFRK
B43C	Piceance	0504511402	LAST DANCE 43C-3-792	BILL BARRETT CORP.	CO	7S	92W	3	NESE	3593.6	C	3.4	2.63	0.00480	0.000174	290	13267	RLNS/WMFRK
B43C	Piceance	0504511402	LAST DANCE 43C-3-792	BILL BARRETT CORP.	CO	7S	92W	3	NESE	3593.8	A	3.1	2.62	0.155	0.00577	379	13267	RLNS/WMFRK
B43C	Piceance	0504511402	LAST DANCE 43C-3-792	BILL BARRETT CORP.	CO	7S	92W	3	NESE	3593.8	B	2.9	2.60	0.0154	0.00122	166	13267	RLNS/WMFRK
B43C	Piceance	0504511402	LAST DANCE 43C-3-792	BILL BARRETT CORP.	CO	7S	92W	3	NESE	3598.1	A	2.0	2.66	0.00443	0.000064	404	12215	RLNS/WMFRK
B43C	Piceance	0504511402	LAST DANCE 43C-3-792	BILL BARRETT CORP.	CO	7S	92W	3	NESE	3598.1	B	2.5	2.67	0.00340	0.000038	893	12215	RLNS/WMFRK
B43C	Piceance	0504511402	LAST DANCE 43C-3-792	BILL BARRETT CORP.	CO	7S	92W	3	NESE	3970.0	A	1.1	2.67	0.00344	0.000097	167	12215	RLNS/WMFRK
B43C	Piceance	0504511402	LAST DANCE 43C-3-792	BILL BARRETT CORP.	CO	7S	92W	3	NESE	3970.0	C	1.2	2.69	0.00258	0.000054	387	12215	RLNS/WMFRK
B43C	Piceance	0504511402	LAST DANCE 43C-3-792	BILL BARRETT CORP.	CO	7S	92W	3	NESE	3970.0	B	0.9	2.69	0.00224	0.000088	172	12215	RLNS/WMFRK
B43C	Piceance	0504511402	LAST DANCE 43C-3-792	BILL BARRETT CORP.	CO	7S	92W	3	NESE	3974.4	A	1.9	2.65	0.00445	0.000085	187	13267	RLNS/WMFRK
B43C	Piceance	0504511402	LAST DANCE 43C-3-792	BILL BARRETT CORP.	CO	7S	92W	3	NESE	3974.4	C	1.9	2.64	0.00394	0.000038	466	13267	RLNS/WMFRK
B43C	Piceance	0504511402	LAST DANCE 43C-3-792	BILL BARRETT CORP.	CO	7S	92W	3	NESE	3974.4	B	1.8	2.64	0.00237	0.000031	429	13267	RLNS/WMFRK
B43C	Piceance	0504511402	LAST DANCE 43C-3-792	BILL BARRETT CORP.	CO	7S	92W	3	NESE	3992.4	A	2.8	2.64	0.00528	0.000419	254	13257	RLNS/WMFRK
B43C	Piceance	0504511402	LAST DANCE 43C-3-792	BILL BARRETT CORP.	CO	7S	92W	3	NESE	3992.4	C	2.8	2.63	0.00498	0.000360	225	13257	RLNS/WMFRK

Table 4.1.1. (continued)

Summary of Porosity, Permeability, and Grain Density
Analysis of Critical Permeability, Capillary Pressure, and Electrical Properties for Mesaverde Tight Gas Sandstones from Western U.S. Basins
US DOE # DE-FC26-05NT42660
Alan P. Byrnes, Robert M. Cluff, John C. Webb, Daniel A. Krygowski, Stefani D. Whittaker
website: http://www.kgs.ku.edu/mesaverde

USGS Library Number	Basin	API Number	Well Name	Operator	State	Township	Range	Section	Quarter Section	Plug Depth	Plug Letter	Ambient Porosity	Grain Density	Routine Gas Permeability	*in situ* Klinkenberg Gas Permeability	*in situ* Klinken-berg *constant* b	Rock Type Code	Formations
										ft	A/B/C	%	g/cc	mD	mD	(psia)		
B43C	Piceance	0504511402	LAST DANCE 43C-3-792	BILL BARRETT CORP.	CO	7S	92W	3	NESE	3992.4	B	2.9	2.63	0.00493	0.000387	301	13257	RLNS/WMFRK
B43C	Piceance	0504511402	LAST DANCE 43C-3-792	BILL BARRETT CORP.	CO	7S	92W	3	NESE	3992.5	B	3.2	2.61	0.291	0.00798	62.3	13257	RLNS/WMFRK
B43C	Piceance	0504511402	LAST DANCE 43C-3-792	BILL BARRETT CORP.	CO	7S	92W	3	NESE	3992.5	A	3.5	2.60	0.0170	0.000830	139	13257	RLNS/WMFRK
B43C	Piceance	0504511402	LAST DANCE 43C-3-792	BILL BARRETT CORP.	CO	7S	92W	3	NESE	3992.5	C	2.9	2.62	0.0125	0.000576	334	13257	RLNS/WMFRK
B43C	Piceance	0504511402	LAST DANCE 43C-3-792	BILL BARRETT CORP.	CO	7S	92W	3	NESE	3997.1	A	1.0	2.62	0.000979	0.000025	755	13297	RLNS/WMFRK
B43C	Piceance	0504511402	LAST DANCE 43C-3-792	BILL BARRETT CORP.	CO	7S	92W	3	NESE	4001.2	A	3.6	2.62	0.00739	0.00106	110	16287	RLNS/WMFRK
B43C	Piceance	0504511402	LAST DANCE 43C-3-792	BILL BARRETT CORP.	CO	7S	92W	3	NESE	4004.2	C	8.8	2.67				16287	RLNS/WMFRK
B43C	Piceance	0504511402	LAST DANCE 43C-3-792	BILL BARRETT CORP.	CO	7S	92W	3	NESE	4004.3	B	10.2	2.63	0.127	0.0288	51.2	16287	RLNS/WMFRK
B43C	Piceance	0504511402	LAST DANCE 43C-3-792	BILL BARRETT CORP.	CO	7S	92W	3	NESE	4004.3	A	10.7	2.63	0.122	0.0341	42.1	16287	RLNS/WMFRK
B43C	Piceance	0504511402	LAST DANCE 43C-3-792	BILL BARRETT CORP.	CO	7S	92W	3	NESE	4004.3	C	10.5	2.63	0.109	0.0262	65.2	16287	RLNS/WMFRK
B43C	Piceance	0504511402	LAST DANCE 43C-3-792	BILL BARRETT CORP.	CO	7S	92W	3	NESE	4006.2	A	5.8	2.64	0.0259	0.00782	37.8	16227	RLNS/WMFRK
B43C	Piceance	0504511402	LAST DANCE 43C-3-792	BILL BARRETT CORP.	CO	7S	92W	3	NESE	4009.2	A	7.7	2.54	0.701	0.346	13.9	16287	RLNS/WMFRK
B43C	Piceance	0504511402	LAST DANCE 43C-3-792	BILL BARRETT CORP.	CO	7S	92W	3	NESE	4012.2	A	8.7	2.54	0.474	0.239	30.7	16227	RLNS/WMFRK
B43C	Piceance	0504511402	LAST DANCE 43C-3-792	BILL BARRETT CORP.	CO	7S	92W	3	NESE	4013.2	C	6.7	2.53	4.43	0.220	40.3	16297	RLNS/WMFRK
B43C	Piceance	0504511402	LAST DANCE 43C-3-792	BILL BARRETT CORP.	CO	7S	92W	3	NESE	4013.3	C	12.7	2.64	0.702	0.320	9.6	16297	RLNS/WMFRK
B43C	Piceance	0504511402	LAST DANCE 43C-3-792	BILL BARRETT CORP.	CO	7S	92W	3	NESE	4013.3	B	12.9	2.64	0.491	0.190	19.5	16297	RLNS/WMFRK
B43C	Piceance	0504511402	LAST DANCE 43C-3-792	BILL BARRETT CORP.	CO	7S	92W	3	NESE	4013.3	A	11.9	2.62	0.460	0.163	15.6	16297	RLNS/WMFRK
B43C	Piceance	0504511402	LAST DANCE 43C-3-792	BILL BARRETT CORP.	CO	7S	92W	3	NESE	4015.2	A	7.8	2.62	0.0338	0.00568	317	16287	RLNS/WMFRK
B43C	Piceance	0504511402	LAST DANCE 43C-3-792	BILL BARRETT CORP.	CO	7S	92W	3	NESE	4017.2	A	8.9	2.64	0.0186	0.00699	118	16287	RLNS/WMFRK
B43C	Piceance	0504511402	LAST DANCE 43C-3-792	BILL BARRETT CORP.	CO	7S	92W	3	NESE	4019.2	A	9.5	2.67				16287	RLNS/WMFRK
B43C	Piceance	0504511402	LAST DANCE 43C-3-792	BILL BARRETT CORP.	CO	7S	92W	3	NESE	4019.3	A	10.0	2.63	0.0636	0.0132	76.1	16287	RLNS/WMFRK
B43C	Piceance	0504511402	LAST DANCE 43C-3-792	BILL BARRETT CORP.	CO	7S	92W	3	NESE	4019.3	B	9.8	2.64	0.0574	0.00872	164	16287	RLNS/WMFRK
B43C	Piceance	0504511402	LAST DANCE 43C-3-792	BILL BARRETT CORP.	CO	7S	92W	3	NESE	4019.3	C	8.2	2.64	0.0267	0.00506	225	16287	RLNS/WMFRK
B43C	Piceance	0504511402	LAST DANCE 43C-3-792	BILL BARRETT CORP.	CO	7S	92W	3	NESE	4021.5	B	4.9	2.66	0.00693	0.000214	161	13297	RLNS/WMFRK
B43C	Piceance	0504511402	LAST DANCE 43C-3-792	BILL BARRETT CORP.	CO	7S	92W	3	NESE	4021.5	C	5.2	2.60	0.00403	0.000137	282	13297	RLNS/WMFRK
B43C	Piceance	0504511402	LAST DANCE 43C-3-792	BILL BARRETT CORP.	CO	7S	92W	3	NESE	4021.5	A	4.9	2.66	0.00256	0.000120	418	13297	RLNS/WMFRK
B43C	Piceance	0504511402	LAST DANCE 43C-3-792	BILL BARRETT CORP.	CO	7S	92W	3	NESE	4356.3	A	1.1	2.65	0.462	0.0348	27.8	13227	RLNS/WMFRK
B43C	Piceance	0504511402	LAST DANCE 43C-3-792	BILL BARRETT CORP.	CO	7S	92W	3	NESE	4356.3	B		2.58	0.00965	0.00181	114	13227	RLNS/WMFRK
B43C	Piceance	0504511402	LAST DANCE 43C-3-792	BILL BARRETT CORP.	CO	7S	92W	3	NESE	4356.3	C	0.8	2.65	0.00372	0.000079	216	13227	RLNS/WMFRK
B43C	Piceance	0504511402	LAST DANCE 43C-3-792	BILL BARRETT CORP.	CO	7S	92W	3	NESE	4358.6	A			0.0212	0.00175	142	13217	RLNS/WMFRK
B43C	Piceance	0504511402	LAST DANCE 43C-3-792	BILL BARRETT CORP.	CO	7S	92W	3	NESE	4358.6	B	1.6	2.64	0.00417	0.000073	318	13217	RLNS/WMFRK
B43C	Piceance	0504511402	LAST DANCE 43C-3-792	BILL BARRETT CORP.	CO	7S	92W	3	NESE	4367.3	A	2.4	2.67	0.00191	0.000516	77.8	13217	RLNS/WMFRK
B43C	Piceance	0504511402	LAST DANCE 43C-3-792	BILL BARRETT CORP.	CO	7S	92W	3	NESE	4372.0	B	2.5	2.63	0.0183	0.000604	192	14297	RLNS/WMFRK
B43C	Piceance	0504511402	LAST DANCE 43C-3-792	BILL BARRETT CORP.	CO	7S	92W	3	NESE	4372.0	C	3.0	2.64	0.0116	0.000708	148	14297	RLNS/WMFRK
B43C	Piceance	0504511402	LAST DANCE 43C-3-792	BILL BARRETT CORP.	CO	7S	92W	3	NESE	4372.0	A	3.3	2.64	0.00667	0.000631	165	14297	RLNS/WMFRK
B43C	Piceance	0504511402	LAST DANCE 43C-3-792	BILL BARRETT CORP.	CO	7S	92W	3	NESE	4372.4	A	2.1	2.63	0.00172	0.000239	75.2	14297	RLNS/WMFRK
B43C	Piceance	0504511402	LAST DANCE 43C-3-792	BILL BARRETT CORP.	CO	7S	92W	3	NESE	4378.2	A	2.8	2.63	0.00292	0.000387	278	13217	RLNS/WMFRK
B43C	Piceance	0504511402	LAST DANCE 43C-3-792	BILL BARRETT CORP.	CO	7S	92W	3	NESE	4382.6	A	4.6	2.63	0.00827	0.000709	41.9	13267	RLNS/WMFRK
B43C	Piceance	0504511402	LAST DANCE 43C-3-792	BILL BARRETT CORP.	CO	7S	92W	3	NESE	4382.6	B	5.1	2.64	0.00652	0.000498	342	13267	RLNS/WMFRK
B43C	Piceance	0504511402	LAST DANCE 43C-3-792	BILL BARRETT CORP.	CO	7S	92W	3	NESE	4388.2	A	9.0	2.62				16287	RLNS/WMFRK
B43C	Piceance	0504511402	LAST DANCE 43C-3-792	BILL BARRETT CORP.	CO	7S	92W	3	NESE	4388.4	C	10.9	2.63	0.106	0.0139	44.0	16287	RLNS/WMFRK
B43C	Piceance	0504511402	LAST DANCE 43C-3-792	BILL BARRETT CORP.	CO	7S	92W	3	NESE	4388.4	A	11.0	2.63	0.101	0.0159	66.9	16287	RLNS/WMFRK
B43C	Piceance	0504511402	LAST DANCE 43C-3-792	BILL BARRETT CORP.	CO	7S	92W	3	NESE	4388.4	B	10.9	2.64	0.0850	0.0135	47.3	16287	RLNS/WMFRK
B43C	Piceance	0504511402	LAST DANCE 43C-3-792	BILL BARRETT CORP.	CO	7S	92W	3	NESE	4388.6	A	10.4	2.63	0.834	0.201	26.0	16287	RLNS/WMFRK
B43C	Piceance	0504511402	LAST DANCE 43C-3-792	BILL BARRETT CORP.	CO	7S	92W	3	NESE	4388.6	C	10.9	2.63	0.0905	0.0132	80.6	16287	RLNS/WMFRK
B43C	Piceance	0504511402	LAST DANCE 43C-3-792	BILL BARRETT CORP.	CO	7S	92W	3	NESE	4388.6	B	10.5	2.63	0.0673	0.00996	148	16287	RLNS/WMFRK
B43C	Piceance	0504511402	LAST DANCE 43C-3-792	BILL BARRETT CORP.	CO	7S	92W	3	NESE	4392.2	A	6.6	2.63	0.0355	0.00889	80.8	16277	RLNS/WMFRK
B43C	Piceance	0504511402	LAST DANCE 43C-3-792	BILL BARRETT CORP.	CO	7S	92W	3	NESE	4393.6	C	8.6	2.63	0.0357	0.00582	116	16277	RLNS/WMFRK
B43C	Piceance	0504511402	LAST DANCE 43C-3-792	BILL BARRETT CORP.	CO	7S	92W	3	NESE	4393.6	B	8.7	2.63	0.0344	0.00583	60.4	16277	RLNS/WMFRK
B43C	Piceance	0504511402	LAST DANCE 43C-3-792	BILL BARRETT CORP.	CO	7S	92W	3	NESE	4393.6	A	8.7	2.63	0.0315	0.00652	75.6	16277	RLNS/WMFRK
B43C	Piceance	0504511402	LAST DANCE 43C-3-792	BILL BARRETT CORP.	CO	7S	92W	3	NESE	4393.7	B	9.2	2.63	0.0667	0.0112	73.9	16277	RLNS/WMFRK
B43C	Piceance	0504511402	LAST DANCE 43C-3-792	BILL BARRETT CORP.	CO	7S	92W	3	NESE	4393.7	C	9.4	2.63	0.0660	0.00871	76.7	16277	RLNS/WMFRK
B43C	Piceance	0504511402	LAST DANCE 43C-3-792	BILL BARRETT CORP.	CO	7S	92W	3	NESE	4393.7	A	9.5	2.63	0.0631	0.00945	146	16277	RLNS/WMFRK
B43C	Piceance	0504511402	LAST DANCE 43C-3-792	BILL BARRETT CORP.	CO	7S	92W	3	NESE	4395.2	A	7.2	2.64	0.0182	0.00413	94.2	17297	RLNS/WMFRK
B43C	Piceance	0504511402	LAST DANCE 43C-3-792	BILL BARRETT CORP.	CO	7S	92W	3	NESE	4398.4	A	8.5	2.65	0.0330	0.00698	110	16277	RLNS/WMFRK
B43C	Piceance	0504511402	LAST DANCE 43C-3-792	BILL BARRETT CORP.	CO	7S	92W	3	NESE	4404.2	A	10.4	2.67	0.0373	0.00934	90.5	16297	RLNS/WMFRK
B43C	Piceance	0504511402	LAST DANCE 43C-3-792	BILL BARRETT CORP.	CO	7S	92W	3	NESE	4404.4	A	10.3	2.64	0.0782	0.00843	89.6	16297	RLNS/WMFRK
B43C	Piceance	0504511402	LAST DANCE 43C-3-792	BILL BARRETT CORP.	CO	7S	92W	3	NESE	4404.4	B	9.9	2.63	0.0780	0.00585	127	16297	RLNS/WMFRK
B43C	Piceance	0504511402	LAST DANCE 43C-3-792	BILL BARRETT CORP.	CO	7S	92W	3	NESE	4406.3	A	8.3	2.69	0.00750	0.00170	66.7	15297	RLNS/WMFRK
B43C	Piceance	0504511402	LAST DANCE 43C-3-792	BILL BARRETT CORP.	CO	7S	92W	3	NESE	4411.2	A	5.5	2.66	0.00334	0.000427	245	16287	RLNS/WMFRK
B43C	Piceance	0504511402	LAST DANCE 43C-3-792	BILL BARRETT CORP.	CO	7S	92W	3	NESE	4414.1	A	6.5	2.68	0.00204	0.000204	290	13287	RLNS/WMFRK
B43C	Piceance	0504511402	LAST DANCE 43C-3-792	BILL BARRETT CORP.	CO	7S	92W	3	NESE	4416.5	A	13.1	2.64	0.0443	0.0139	37.0	16297	RLNS/WMFRK
B43C	Piceance	0504511402	LAST DANCE 43C-3-792	BILL BARRETT CORP.	CO	7S	92W	3	NESE	4416.5	B	12.9	2.63				16297	RLNS/WMFRK
B43C	Piceance	0504511402	LAST DANCE 43C-3-792	BILL BARRETT CORP.	CO	7S	92W	3	NESE	4416.6	B	13.4	2.64	0.0685	0.0138	98.5	16297	RLNS/WMFRK
B43C	Piceance	0504511402	LAST DANCE 43C-3-792	BILL BARRETT CORP.	CO	7S	92W	3	NESE	4416.6	A	13.6	2.64	0.0632	0.0176	22.7	16297	RLNS/WMFRK
B43C	Piceance	0504511402	LAST DANCE 43C-3-792	BILL BARRETT CORP.	CO	7S	92W	3	NESE	4853.8	A	2.5	2.67	0.00376	0.000245	272	13267	RLNS/WMFRK
B43C	Piceance	0504511402	LAST DANCE 43C-3-792	BILL BARRETT CORP.	CO	7S	92W	3	NESE	4856.2	A	2.9	2.66	0.00775	0.000639	181	13297	RLNS/WMFRK
B43C	Piceance	0504511402	LAST DANCE 43C-3-792	BILL BARRETT CORP.	CO	7S	92W	3	NESE	4856.2	C	3.6	2.67	0.00668	0.000605	197	13297	RLNS/WMFRK
B43C	Piceance	0504511402	LAST DANCE 43C-3-792	BILL BARRETT CORP.	CO	7S	92W	3	NESE	4856.2	B	3.0	2.67	0.00534	0.000429	452	13297	RLNS/WMFRK
B43C	Piceance	0504511402	LAST DANCE 43C-3-792	BILL BARRETT CORP.	CO	7S	92W	3	NESE	5329.8	B	2.4	2.66	0.00310	0.000132	372	13266	RLNS/WMFRK
B43C	Piceance	0504511402	LAST DANCE 43C-3-792	BILL BARRETT CORP.	CO	7S	92W	3	NESE	5329.8	A	2.8	2.67	0.00232	0.000088	723	13266	RLNS/WMFRK
B43C	Piceance	0504511402	LAST DANCE 43C-3-792	BILL BARRETT CORP.	CO	7S	92W	3	NESE	5713.1	C	6.8	2.70	0.0114	0.00108	541	15287	RLNS/WMFRK
B43C	Piceance	0504511402	LAST DANCE 43C-3-792	BILL BARRETT CORP.	CO	7S	92W	3	NESE	5715.3	C	7.1	2.67	0.0159	0.00276	123	15297	RLNS/WMFRK
B43C	Piceance	0504511402	LAST DANCE 43C-3-792	BILL BARRETT CORP.	CO	7S	92W	3	NESE	5715.3	A	7.1	2.67	0.0150	0.00270	79.4	15297	RLNS/WMFRK
B43C	Piceance	0504511402	LAST DANCE 43C-3-792	BILL BARRETT CORP.	CO	7S	92W	3	NESE	5715.3	B	7.3	2.68	0.0140	0.00231	169	15297	RLNS/WMFRK
B43C	Piceance	0504511402	LAST DANCE 43C-3-792	BILL BARRETT CORP.	CO	7S	92W	3	NESE	5715.4	A	7.7	2.67	0.0184	0.00319	102	15297	RLNS/WMFRK
B43C	Piceance	0504511402	LAST DANCE 43C-3-792	BILL BARRETT CORP.	CO	7S	92W	3	NESE	5715.4	C	7.8	2.67	0.0170	0.00340	24.9	15297	RLNS/WMFRK
B43C	Piceance	0504511402	LAST DANCE 43C-3-792	BILL BARRETT CORP.	CO	7S	92W	3	NESE	5715.4	B	7.6	2.71	0.0169	0.00334	53.5	15297	RLNS/WMFRK
B43C	Piceance	0504511402	LAST DANCE 43C-3-792	BILL BARRETT CORP.	CO	7S	92W	3	NESE	5720.1	C	6.2	2.68	0.00622	0.000834	355	15277	RLNS/WMFRK
B43C	Piceance	0504511402	LAST DANCE 43C-3-792	BILL BARRETT CORP.	CO	7S	92W	3	NESE	5720.3	C	6.6	2.67	0.0142	0.00182	95.1	15277	RLNS/WMFRK
B43C	Piceance	0504511402	LAST DANCE 43C-3-792	BILL BARRETT CORP.	CO	7S	92W	3	NESE	5720.3	A	6.4	2.67	0.0128	0.00189	95.6	15277	RLNS/WMFRK
B43C	Piceance	0504511402	LAST DANCE 43C-3-792	BILL BARRETT CORP.	CO	7S	92W	3	NESE	5720.3	B			0.0116	0.00165	151	15277	RLNS/WMFRK
B43C	Piceance	0504511402	LAST DANCE 43C-3-792	BILL BARRETT CORP.	CO	7S	92W	3	NESE	5720.4	B	7.0	2.64	0.0103	0.00140	130	15277	RLNS/WMFRK
B43C	Piceance	0504511402	LAST DANCE 43C-3-792	BILL BARRETT CORP.	CO	7S	92W	3	NESE	5720.4	C	6.9	2.68	0.00959	0.000935	98.8	15277	RLNS/WMFRK
B43C	Piceance	0504511402	LAST DANCE 43C-3-792	BILL BARRETT CORP.	CO	7S	92W	3	NESE	5720.4	A	6.3	2.67	0.00894	0.00124	151	15277	RLNS/WMFRK
B43C	Piceance	0504511402	LAST DANCE 43C-3-792	BILL BARRETT CORP.	CO	7S	92W	3	NESE	5723.3	C	4.7	2.68	0.00471	0.000573	128	15277	RLNS/WMFRK
B43C	Piceance	0504511402	LAST DANCE 43C-3-792	BILL BARRETT CORP.	CO	7S	92W	3	NESE	5726.1	C	4.8	2.65	0.00561	0.000668	284	15287	RLNS/WMFRK
B43C	Piceance	0504511402	LAST DANCE 43C-3-792	BILL BARRETT CORP.	CO	7S	92W	3	NESE	5727.1	C	5.9	2.65	0.0167	0.00246	117	15277	RLNS/WMFRK
B43C	Piceance	0504511402	LAST DANCE 43C-3-792	BILL BARRETT CORP.	CO	7S	92W	3	NESE	5727.1	A	6.2	2.66	0.0154	0.00182	240	15277	RLNS/WMFRK
B43C	Piceance	0504511402	LAST DANCE 43C-3-792	BILL BARRETT CORP.	CO	7S	92W	3	NESE	5727.1	B	6.1	2.66	0.0153	0.00255	75.8	15277	RLNS/WMFRK
B43C	Piceance	0504511402	LAST DANCE 43C-3-792	BILL BARRETT CORP.	CO	7S	92W	3	NESE	5727.2	A	5.5	2.66	0.00900	0.00104	135	15277	RLNS/WMFRK
B43C	Piceance	0504511402	LAST DANCE 43C-3-792	BILL BARRETT CORP.	CO	7S	92W	3	NESE	5727.2	B	5.5	2.66	0.00884	0.00120	128	15277	RLNS/WMFRK
B43C	Piceance	0504511402	LAST DANCE 43C-3-792	BILL BARRETT CORP.	CO	7S	92W	3	NESE	5727.2	C	5.2	2.66	0.00821	0.000743	240	15277	RLNS/WMFRK
B43C	Piceance	0504511402	LAST DANCE 43C-3-792	BILL BARRETT CORP.	CO	7S	92W	3	NESE	5730.1	C	5.4	2.68	0.00408	0.000635	201	15397	RLNS/WMFRK
B43C	Piceance	0504511402	LAST DANCE 43C-3-792	BILL BARRETT CORP.	CO	7S	92W	3	NESE	5730.4	A	7.9	2.67	0.0154	0.00218	223	15397	RLNS/WMFRK
B43C	Piceance	0504511402	LAST DANCE 43C-3-792	BILL BARRETT CORP.	CO	7S	92W	3	NESE	5730.4	C	7.6	2.67	0.0146	0.00151	246	15397	RLNS/WMFRK
B43C	Piceance	0504511402	LAST DANCE 43C-3-792	BILL BARRETT CORP.	CO	7S	92W	3	NESE	5730.4	B	7.9	2.67	0.0125	0.00201	103	15397	RLNS/WMFRK
B43C	Piceance	0504511402	LAST DANCE 43C-3-792	BILL BARRETT CORP.	CO	7S	92W	3	NESE	5734.4	C	6.5	2.67	0.00524	0.00118	173	15387	RLNS/WMFRK
B43C	Piceance	0504511402	LAST DANCE 43C-3-792	BILL BARRETT CORP.	CO	7S	92W	3	NESE	5737.1	C	6.0	2.68	0.00810	0.00178	107	13317	RLNS/WMFRK
B43C	Piceance	0504511402	LAST DANCE 43C-3-792	BILL BARRETT CORP.	CO	7S	92W	3	NESE	5737.3	C	6.3	2.67	0.0143	0.00143	251	13317	RLNS/WMFRK
B43C	Piceance	0504511402	LAST DANCE 43C-3-792	BILL BARRETT CORP.	CO	7S	92W	3	NESE	5737.3	A	6.9	2.65	0.0124	0.00157	238	13317	RLNS/WMFRK
B43C	Piceance	0504511402	LAST DANCE 43C-3-792	BILL BARRETT CORP.	CO	7S	92W	3	NESE	5737.3	B	6.6	2.67	0.00999	0.00123	159	13317	RLNS/WMFRK
B43C	Piceance	0504511402	LAST DANCE 43C-3-792	BILL BARRETT CORP.	CO	7S	92W	3	NESE	5740.1	C	4.4	2.68	0.00265	0.000492	186	13317	RLNS/WMFRK
B43C	Piceance	0504511402	LAST DANCE 43C-3-792	BILL BARRETT CORP.	CO	7S	92W	3	NESE	5743.0	A	6.7	2.67	0.0101	0.000731	141	13397	RLNS/WMFRK
B43C	Piceance	0504511402	LAST DANCE 43C-3-792	BILL BARRETT CORP.	CO	7S	92W	3	NESE	5743.0	C	5.8	2.67	0.00738	0.000523	196	13397	RLNS/WMFRK
B43C	Piceance	0504511402	LAST DANCE 43C-3-792	BILL BARRETT CORP.	CO	7S	92W	3	NESE	5743.0	B	6.6	2.68	0.00651	0.000591	201	13397	RLNS/WMFRK
B43C	Piceance	0504511402	LAST DANCE 43C-3-792	BILL BARRETT CORP.	CO	7S	92W	3	NESE	5743.6	C	4.9	2.68	0.00296	0.000585	176	13287	RLNS/WMFRK
B43C	Piceance	0504511402	LAST DANCE 43C-3-792	BILL BARRETT CORP.	CO	7S	92W	3	NESE	5747.3	C	5.0	2.67	0.00381	0.000610	223	15287	RLNS/WMFRK
B43C	Piceance	0504511402	LAST DANCE 43C-3-792	BILL BARRETT CORP.	CO	7S	92W	3	NESE	5750.6	C	7.1	2.73	0.00471	0.000746	182	15397	RLNS/WMFRK
B43C	Piceance	0504511402	LAST DANCE 43C-3-792	BILL BARRETT CORP.	CO	7S	92W	3	NESE	5753.5	C	4.4	2.65	0.00359	0.000671	215	15387	RLNS/WMFRK
B43C	Piceance	0504511402	LAST DANCE 43C-3-792	BILL BARRETT CORP.	CO	7S	92W	3	NESE	5755.6	B	6.1	2.67	0.0104	0.000736	557	15277	RLNS/WMFRK
B43C	Piceance	0504511402	LAST DANCE 43C-3-792	BILL BARRETT CORP.	CO	7S	92W	3	NESE	5755.6	C	6.1	2.67	0.00890	0.00130	146	15277	RLNS/WMFRK

Table 4.1.1. (continued)

Summary of Porosity, Permeability, and Grain Density
Analysis of Critical Permeability, Capillary Pressure, and Electrical Properties for Mesaverde Tight Gas Sandstones from Western U.S. Basins
US DOE # DE-FC26-05NT42660
Alan P. Byrnes, Robert M. Cluff, John C. Webb, Daniel A. Krygowski, Stefani D. Whittaker
website: http://www.kgs.ku.edu/mesaverde

USGS Library Number	Basin	API Number	Well Name	Operator	State	Township	Range	Section	Quarter Section	Plug Depth	Plug Letter	Ambient Porosity	Grain Density	Routine Gas Permeability	*in situ* Klinkenberg Gas Permeability	*in situ* Klinkenberg *constant b*	Rock Type Code	Formations
										ft	A/B/C	%	g/cc	mD	mD	(psia)		
B43C	Piceance	0504511402	LAST DANCE 43C-3-792	BILL BARRETT CORP.	CO	7S	92W	3	NESE	5755.6	A	6.8	2.67	0.00820	0.00105	175	15277	RLNS/WMFRK
B43C	Piceance	0504511402	LAST DANCE 43C-3-792	BILL BARRETT CORP.	CO	7S	92W	3	NESE	5757.3	B	5.1	2.67	0.00749	0.000866	134	15277	RLNS/WMFRK
B43C	Piceance	0504511402	LAST DANCE 43C-3-792	BILL BARRETT CORP.	CO	7S	92W	3	NESE	5757.3	C	5.3	2.68	0.00724	0.000573	218	15277	RLNS/WMFRK
B43C	Piceance	0504511402	LAST DANCE 43C-3-792	BILL BARRETT CORP.	CO	7S	92W	3	NESE	5757.3	A	5.2	2.68	0.00580	0.000560	178	15277	RLNS/WMFRK
B43C	Piceance	0504511402	LAST DANCE 43C-3-792	BILL BARRETT CORP.	CO	7S	92W	3	NESE	5757.7	C	5.0	2.72	0.00209	0.000287	219	15277	RLNS/WMFRK
B43C	Piceance	0504511402	LAST DANCE 43C-3-792	BILL BARRETT CORP.	CO	7S	92W	3	NESE	5760.5	C	3.6	2.64	0.00579	0.00113	143	13228	RLNS/WMFRK
B43C	Piceance	0504511402	LAST DANCE 43C-3-792	BILL BARRETT CORP.	CO	7S	92W	3	NESE	6042.2	C	4.1	2.64				15387	RLNS/WMFRK
B43C	Piceance	0504511402	LAST DANCE 43C-3-792	BILL BARRETT CORP.	CO	7S	92W	3	NESE	6042.4	B	6.1	2.66	0.0106	0.000677	403	15387	RLNS/WMFRK
B43C	Piceance	0504511402	LAST DANCE 43C-3-792	BILL BARRETT CORP.	CO	7S	92W	3	NESE	6042.4	C	5.8	2.66	0.00991	0.00129	93.9	15387	RLNS/WMFRK
B43C	Piceance	0504511402	LAST DANCE 43C-3-792	BILL BARRETT CORP.	CO	7S	92W	3	NESE	6042.4	A	5.4	2.65	0.00945	0.000854	279	15387	RLNS/WMFRK
B43C	Piceance	0504511402	LAST DANCE 43C-3-792	BILL BARRETT CORP.	CO	7S	92W	3	NESE	6053.1	C	6.1	2.72	0.00403	0.000540	428	13287	RLNS/WMFRK
B43C	Piceance	0504511402	LAST DANCE 43C-3-792	BILL BARRETT CORP.	CO	7S	92W	3	NESE	6056.0	C	7.0	2.69	0.00826	0.000945	178	13287	RLNS/WMFRK
B43C	Piceance	0504511402	LAST DANCE 43C-3-792	BILL BARRETT CORP.	CO	7S	92W	3	NESE	6058.5	B	6.1	2.68	0.0172	0.00238	142	13287	RLNS/WMFRK
B43C	Piceance	0504511402	LAST DANCE 43C-3-792	BILL BARRETT CORP.	CO	7S	92W	3	NESE	6058.5	C	6.9	2.69	0.0157	0.00207	156	13287	RLNS/WMFRK
B43C	Piceance	0504511402	LAST DANCE 43C-3-792	BILL BARRETT CORP.	CO	7S	92W	3	NESE	6058.5	A	6.2	2.70	0.0149	0.00243	81.3	13287	RLNS/WMFRK
B43C	Piceance	0504511402	LAST DANCE 43C-3-792	BILL BARRETT CORP.	CO	7S	92W	3	NESE	6058.6	A	4.9	2.70	2.53	0.109	22.9	13287	RLNS/WMFRK
B43C	Piceance	0504511402	LAST DANCE 43C-3-792	BILL BARRETT CORP.	CO	7S	92W	3	NESE	6058.6	B	5.1	2.69	0.0411	0.00333	131	13287	RLNS/WMFRK
B43C	Piceance	0504511402	LAST DANCE 43C-3-792	BILL BARRETT CORP.	CO	7S	92W	3	NESE	6058.6	C	6.0	2.69	0.0139	0.00176	132	13287	RLNS/WMFRK
B43C	Piceance	0504511402	LAST DANCE 43C-3-792	BILL BARRETT CORP.	CO	7S	92W	3	NESE	6060.7	C	6.3	2.75	0.00733	0.00235	205	13218	RLNS/WMFRK
B43C	Piceance	0504511402	LAST DANCE 43C-3-792	BILL BARRETT CORP.	CO	7S	92W	3	NESE	6291.9	A	1.0	2.75	0.000756	0.000024	600	13256	RLNS/WMFRK
B43C	Piceance	0504511402	LAST DANCE 43C-3-792	BILL BARRETT CORP.	CO	7S	92W	3	NESE	6297.6	A	0.5	2.69	0.00110	0.000017	299	12219	RLNS/WMFRK
B43C	Piceance	0504511402	LAST DANCE 43C-3-792	BILL BARRETT CORP.	CO	7S	92W	3	NESE	6299.4	A	0.4	2.64	0.00169	0.000034	943	11289	RLNS/WMFRK
B43C	Piceance	0504511402	LAST DANCE 43C-3-792	BILL BARRETT CORP.	CO	7S	92W	3	NESE	6305.5	A	0.5	2.66	0.00148	0.000449	238	12219	RLNS/WMFRK
B43C	Piceance	0504511402	LAST DANCE 43C-3-792	BILL BARRETT CORP.	CO	7S	92W	3	NESE	6305.9	A	0.4	2.70	0.000406	0.000010	775	12219	RLNS/WMFRK
B43C	Piceance	0504511402	LAST DANCE 43C-3-792	BILL BARRETT CORP.	CO	7S	92W	3	NESE	6309.1	A	0.8	2.63	0.00132	0.000037	261	11219	RLNS/WMFRK
B43C	Piceance	0504511402	LAST DANCE 43C-3-792	BILL BARRETT CORP.	CO	7S	92W	3	NESE	6314.8	A	0.4	2.70	0.000261	0.000012	350	12289	RLNS/WMFRK
B43C	Piceance	0504511402	LAST DANCE 43C-3-792	BILL BARRETT CORP.	CO	7S	92W	3	NESE	6327.8	B	0.5	2.71	0.00434	0.000094	214	11229	RLNS/WMFRK
B43C	Piceance	0504511402	LAST DANCE 43C-3-792	BILL BARRETT CORP.	CO	7S	92W	3	NESE	6327.8	A	0.6	2.70	0.00287	0.000044	475	11229	RLNS/WMFRK
B43C	Piceance	0504511402	LAST DANCE 43C-3-792	BILL BARRETT CORP.	CO	7S	92W	3	NESE	6327.8	C	0.4	2.70	0.000711	0.000012	465	11229	RLNS/WMFRK
B43C	Piceance	0504511402	LAST DANCE 43C-3-792	BILL BARRETT CORP.	CO	7S	92W	3	NESE	6336.1	C	3.7	2.75	0.00160	0.000091	451	13265	RLNS/WMFRK
B43C	Piceance	0504511402	LAST DANCE 43C-3-792	BILL BARRETT CORP.	CO	7S	92W	3	NESE	6337.1	B	4.3	2.64	0.0105	0.000182	284	13245	RLNS/WMFRK
B43C	Piceance	0504511402	LAST DANCE 43C-3-792	BILL BARRETT CORP.	CO	7S	92W	3	NESE	6337.1	C	3.8	2.64	0.0103	0.000212	361	13245	RLNS/WMFRK
B43C	Piceance	0504511402	LAST DANCE 43C-3-792	BILL BARRETT CORP.	CO	7S	92W	3	NESE	6337.1	A	4.2	2.64	0.00784	0.000221	335	13245	RLNS/WMFRK
B43C	Piceance	0504511402	LAST DANCE 43C-3-792	BILL BARRETT CORP.	CO	7S	92W	3	NESE	6340.1	C	3.3	2.80	0.000816	0.000028	1044	14285	RLNS/WMFRK
B43C	Piceance	0504511402	LAST DANCE 43C-3-792	BILL BARRETT CORP.	CO	7S	92W	3	NESE	6343.1	C	1.6	2.67	0.000776	0.000045	404	12215	RLNS/WMFRK
E436	Piceance	0504506571	MV 33-34	BARRETT ENERGY	CO	6S	96W	34	NENW	6574.6	B	0.7	2.61	0.0105	0.000534	290	11298	CMEO
E436	Piceance	0504506571	MV 33-34	BARRETT ENERGY	CO	6S	96W	34	NENW	6577.2	A	0.7	2.63		0.000104	107	11298	CMEO
E436	Piceance	0504506571	MV 33-34	BARRETT ENERGY	CO	6S	96W	34	NENW	6577.3	A	1.7	2.65	0.00404	0.000032	800	11298	CMEO
E436	Piceance	0504506571	MV 33-34	BARRETT ENERGY	CO	6S	96W	34	NENW	6577.3	B	0.7	2.66	0.00195	0.000018	991	11298	CMEO
E436	Piceance	0504506571	MV 33-34	BARRETT ENERGY	CO	6S	96W	34	NENW	6579.2	B	3.4	2.66	0.0988	0.0101	112	11228	CMEO
E436	Piceance	0504506571	MV 33-34	BARRETT ENERGY	CO	6S	96W	34	NENW	6579.2	A	2.2	2.56		0.000050	107	11228	CMEO
E436	Piceance	0504506571	MV 33-34	BARRETT ENERGY	CO	6S	96W	34	NENW	6579.5	A	7.5	2.74	0.00705	0.000441	224	13226	CMEO
E436	Piceance	0504506571	MV 33-34	BARRETT ENERGY	CO	6S	96W	34	NENW	6579.5	B	5.8	2.68	0.00280	0.000363	51.0	13226	CMEO
E436	Piceance	0504506571	MV 33-34	BARRETT ENERGY	CO	6S	96W	34	NENW	6579.7	A	5.6	2.70	0.00593	0.000396	525	13268	CMEO
E436	Piceance	0504506571	MV 33-34	BARRETT ENERGY	CO	6S	96W	34	NENW	6579.7	B	5.5	2.69	0.00367	0.000578	174	13268	CMEO
E436	Piceance	0504506571	MV 33-34	BARRETT ENERGY	CO	6S	96W	34	NENW	6579.8	A	5.3	2.68	0.00637	0.000247	872	13268	CMEO
E436	Piceance	0504506571	MV 33-34	BARRETT ENERGY	CO	6S	96W	34	NENW	6579.8	B	5.6	2.69	0.00516	0.000742	61.5	13268	CMEO
E436	Piceance	0504506571	MV 33-34	BARRETT ENERGY	CO	6S	96W	34	NENW	6580.1	A	5.3	2.68	0.00772	0.000579	166	13268	CMEO
E436	Piceance	0504506571	MV 33-34	BARRETT ENERGY	CO	6S	96W	34	NENW	6580.1	B	5.6	2.69	0.00380	0.000470	201	13268	CMEO
E436	Piceance	0504506571	MV 33-34	BARRETT ENERGY	CO	6S	96W	34	NENW	6581.1	B	3.8	2.67	0.0450	0.00841	78.4	12228	CMEO
E436	Piceance	0504506571	MV 33-34	BARRETT ENERGY	CO	6S	96W	34	NENW	6581.1	A	13.1	2.68	0.00385	0.000219	299	12228	CMEO
E436	Piceance	0504506571	MV 33-34	BARRETT ENERGY	CO	6S	96W	34	NENW	6582.0	A	3.8	2.68	0.00454	0.000479	67.5	14266	CMEO
E436	Piceance	0504506571	MV 33-34	BARRETT ENERGY	CO	6S	96W	34	NENW	6582.0	B	5.8	2.70	0.00415	0.000286	198	14266	CMEO
E436	Piceance	0504506571	MV 33-34	BARRETT ENERGY	CO	6S	96W	34	NENW	6582.3	A	5.2	2.69	0.00487	0.000377	237	14266	CMEO
E436	Piceance	0504506571	MV 33-34	BARRETT ENERGY	CO	6S	96W	34	NENW	6582.3	B	5.7	2.69	0.00375	0.000344	191	14266	CMEO
E436	Piceance	0504506571	MV 33-34	BARRETT ENERGY	CO	6S	96W	34	NENW	6582.8	B	4.2	2.67	0.00530	0.000177	225	12246	CMEO
E436	Piceance	0504506571	MV 33-34	BARRETT ENERGY	CO	6S	96W	34	NENW	6582.8	A	3.8	2.66	0.00352	0.000109	240	12246	CMEO
E436	Piceance	0504506571	MV 33-34	BARRETT ENERGY	CO	6S	96W	34	NENW	6583.2	A	4.5	2.70	0.00630	0.000401	135	13265	CMEO
E436	Piceance	0504506571	MV 33-34	BARRETT ENERGY	CO	6S	96W	34	NENW	6583.5	A	5.1	2.69	0.00383	0.000267	122	13265	CMEO
E436	Piceance	0504506571	MV 33-34	BARRETT ENERGY	CO	6S	96W	34	NENW	6583.5	B	5.3	2.69	0.00357	0.000284	181	13265	CMEO
E436	Piceance	0504506571	MV 33-34	BARRETT ENERGY	CO	6S	96W	34	NENW	6591.3	A	2.5	2.73	0.00320	0.000096	531	13266	CMEO
E436	Piceance	0504506571	MV 33-34	BARRETT ENERGY	CO	6S	96W	34	NENW	6591.7	B	3.1	2.73	0.00854	0.000304	246	13266	CMEO
E436	Piceance	0504506571	MV 33-34	BARRETT ENERGY	CO	6S	96W	34	NENW	6591.9	B	3.4	2.65	0.00374	0.000148	450	13266	CMEO
E436	Piceance	0504506571	MV 33-34	BARRETT ENERGY	CO	6S	96W	34	NENW	6591.9	A	2.4	2.65	0.00222	0.000711	239	13266	CMEO
E436	Piceance	0504506571	MV 33-34	BARRETT ENERGY	CO	6S	96W	34	NENW	6592.2	A	1.0	2.62	0.00308	0.000050	308	12246	CMEO
E436	Piceance	0504506571	MV 33-34	BARRETT ENERGY	CO	6S	96W	34	NENW	6592.5	A	2.6	2.63	0.00729	0.000163	390	12246	CMEO
E436	Piceance	0504506571	MV 33-34	BARRETT ENERGY	CO	6S	96W	34	NENW	6592.5	B	3.1	2.63	0.00435	0.000126	303	12246	CMEO
E436	Piceance	0504506571	MV 33-34	BARRETT ENERGY	CO	6S	96W	34	NENW	6594.8	A	0.6	2.62	0.0558	0.00778	86.2	11218	CMEO
E458	Piceance	0510309406	M-30-2-96W /D-037934	FUEL RESOURCES DEV	CO	2N	96W	30	SWSW	6372.5	A	3.9	2.59	0.522	0.000073	317	12229	WMFK
E458	Piceance	0510309406	M-30-2-96W /D-037934	FUEL RESOURCES DEV	CO	2N	96W	30	SWSW	6374.1	A	5.2	2.64	0.00417	0.000154	187	13216	WMFK
E458	Piceance	0510309406	M-30-2-96W /D-037934	FUEL RESOURCES DEV	CO	2N	96W	30	SWSW	6374.4	A	3.3	2.64	0.00230	0.000176	412	13216	WMFK
E458	Piceance	0510309406	M-30-2-96W /D-037934	FUEL RESOURCES DEV	CO	2N	96W	30	SWSW	6375.4	A	3.4	2.64	0.00189	0.000080	348	13226	WMFK
E458	Piceance	0510309406	M-30-2-96W /D-037934	FUEL RESOURCES DEV	CO	2N	96W	30	SWSW	6375.6	A	3.3	2.63	0.00228	0.000101	237	13226	WMFK
E458	Piceance	0510309406	M-30-2-96W /D-037934	FUEL RESOURCES DEV	CO	2N	96W	30	SWSW	6379.2	A	4.1	2.61	0.00769	0.000250	221	12246	WMFK
E458	Piceance	0510309406	M-30-2-96W /D-037934	FUEL RESOURCES DEV	CO	2N	96W	30	SWSW	6379.5	A	3.8	2.63	0.00328	0.000303	115	13246	WMFK
E458	Piceance	0510309406	M-30-2-96W /D-037934	FUEL RESOURCES DEV	CO	2N	96W	30	SWSW	6379.9	A	3.1	2.68	0.00155	0.000036	652	12226	WMFK
E458	Piceance	0510309406	M-30-2-96W /D-037934	FUEL RESOURCES DEV	CO	2N	96W	30	SWSW	6380.5	A	4.9	2.72		0.000055	107	11236	WMFK
E458	Piceance	0510309406	M-30-2-96W /D-037934	FUEL RESOURCES DEV	CO	2N	96W	30	SWSW	6380.6	A	13.5	2.70	0.559	0.436	5.7	12246	WMFK
E458	Piceance	0510309406	M-30-2-96W /D-037934	FUEL RESOURCES DEV	CO	2N	96W	30	SWSW	6402.2	A	0.5	2.51	0.00203	0.000021	599	11229	WMFK
E458	Piceance	0510309406	M-30-2-96W /D-037934	FUEL RESOURCES DEV	CO	2N	96W	30	SWSW	6404.7	A	9.1	2.65	0.0254	0.00309	142	14296	WMFK
E458	Piceance	0510309406	M-30-2-96W /D-037934	FUEL RESOURCES DEV	CO	2N	96W	30	SWSW	6404.8	A	9.5	2.66	0.0112	0.00186	157	14296	WMFK
E458	Piceance	0510309406	M-30-2-96W /D-037934	FUEL RESOURCES DEV	CO	2N	96W	30	SWSW	6407.1	A	6.7	2.70	0.00529	0.000641	180	15276	WMFK
E458	Piceance	0510309406	M-30-2-96W /D-037934	FUEL RESOURCES DEV	CO	2N	96W	30	SWSW	6407.3	A	5.4	2.71	0.00317	0.000284	360	15276	WMFK
E458	Piceance	0510309406	M-30-2-96W /D-037934	FUEL RESOURCES DEV	CO	2N	96W	30	SWSW	6508.1	A	10.6	2.65	0.0393	0.0189	151	13286	WMFK
E458	Piceance	0510309406	M-30-2-96W /D-037934	FUEL RESOURCES DEV	CO	2N	96W	30	SWSW	6508.3	A	9.1	2.66	0.0365	0.0180	146	13286	WMFK
E458	Piceance	0510309406	M-30-2-96W /D-037934	FUEL RESOURCES DEV	CO	2N	96W	30	SWSW	6509.4	A	10.7	2.66	0.0484	0.0269	46.6	14286	WMFK
PA424	Piceance	0504510927	Williams PA-424-34	WILLIAMS E&P	CO	6S	95W	34	NWSWSE	4569.5	A	3.1	2.68	0.00323	0.000505	176	13217	WMFK
PA424	Piceance	0504510927	Williams PA-424-34	WILLIAMS E&P	CO	6S	95W	34	NWSWSE	4572.2	A	6.3	2.64	0.00747	0.00468	191	15277	WMFK
PA424	Piceance	0504510927	Williams PA-424-34	WILLIAMS E&P	CO	6S	95W	34	NWSWSE	4574.6	A	4.7	2.66	0.0136	0.00279	144	13277	WMFK
PA424	Piceance	0504510927	Williams PA-424-34	WILLIAMS E&P	CO	6S	95W	34	NWSWSE	4578.8	A	3.9	2.65	0.0162	0.00216	158	16225	WMFK
PA424	Piceance	0504510927	Williams PA-424-34	WILLIAMS E&P	CO	6S	95W	34	NWSWSE	4578.8	A1	4.5	2.65	0.00124	0.000252	133	16225	WMFK
PA424	Piceance	0504510927	Williams PA-424-34	WILLIAMS E&P	CO	6S	95W	34	NWSWSE	4578.8	A2	4.5	2.65	0.00116	0.000173	413	16225	WMFK
PA424	Piceance	0504510927	Williams PA-424-34	WILLIAMS E&P	CO	6S	95W	34	NWSWSE	4582.5	A	6.1	2.66	0.0232	0.00649	40.3	17226	WMFK
PA424	Piceance	0504510927	Williams PA-424-34	WILLIAMS E&P	CO	6S	95W	34	NWSWSE	4585.2	A	7.5	2.65	0.109	0.0170	259	16296	WMFK
PA424	Piceance	0504510927	Williams PA-424-34	WILLIAMS E&P	CO	6S	95W	34	NWSWSE	4587.3	A	7.5	2.66	0.551	0.0996	66.4	16296	WMFK
PA424	Piceance	0504510927	Williams PA-424-34	WILLIAMS E&P	CO	6S	95W	34	NWSWSE	4592.3	A	2.5	2.67	0.00288	0.000325	142	13246	WMFK
PA424	Piceance	0504510927	Williams PA-424-34	WILLIAMS E&P	CO	6S	95W	34	NWSWSE	4593.4	A	4.9	2.64	0.00577	0.000847	113	13226	WMFK
PA424	Piceance	0504510927	Williams PA-424-34	WILLIAMS E&P	CO	6S	95W	34	NWSWSE	4596.5	A	5.2	2.64	0.00711	0.000583	209	15286	WMFK
PA424	Piceance	0504510927	Williams PA-424-34	WILLIAMS E&P	CO	6S	95W	34	NWSWSE	4598.2	A	6.8	2.65	0.0100	0.000531	177	15226	WMFK
PA424	Piceance	0504510927	Williams PA-424-34	WILLIAMS E&P	CO	6S	95W	34	NWSWSE	4600.3	A	12.2	2.65	0.0178	0.00188	150	15297	WMFK
PA424	Piceance	0504510927	Williams PA-424-34	WILLIAMS E&P	CO	6S	95W	34	NWSWSE	4603.2	A	4.5	2.65	0.00809	0.000721	100	15277	WMFK
PA424	Piceance	0504510927	Williams PA-424-34	WILLIAMS E&P	CO	6S	95W	34	NWSWSE	4604.8	A	8.3	2.66	0.0122	0.00119	113	13227	WMFK
PA424	Piceance	0504510927	Williams PA-424-34	WILLIAMS E&P	CO	6S	95W	34	NWSWSE	4606.5	A	12.6	2.66	0.0244	0.00313	348	16227	WMFK
PA424	Piceance	0504510927	Williams PA-424-34	WILLIAMS E&P	CO	6S	95W	34	NWSWSE	4606.5	A1	12.7	2.65	0.00243	0.000431	190	16227	WMFK
PA424	Piceance	0504510927	Williams PA-424-34	WILLIAMS E&P	CO	6S	95W	34	NWSWSE	4606.5	A2	12.8	2.65	0.00217	0.000473	203	16227	WMFK
PA424	Piceance	0504510927	Williams PA-424-34	WILLIAMS E&P	CO	6S	95W	34	NWSWSE	4609.2	A	4.3	2.66	0.0138	0.00146	94.8	16277	WMFK
PA424	Piceance	0504510927	Williams PA-424-34	WILLIAMS E&P	CO	6S	95W	34	NWSWSE	4615.6	A	2.1	2.69	0.00486	0.000638	184	13266	WMFK
PA424	Piceance	0504510927	Williams PA-424-34	WILLIAMS E&P	CO	6S	95W	34	NWSWSE	4623.3	A	5.3	2.69	0.00209	0.000051	738	13246	WMFK
PA424	Piceance	0504510927	Williams PA-424-34	WILLIAMS E&P	CO	6S	95W	34	NWSWSE	4626.5	A	6.9	2.66	0.00985	0.000889	156	15276	WMFK
PA424	Piceance	0504510927	Williams PA-424-34	WILLIAMS E&P	CO	6S	95W	34	NWSWSE	4630.4	A	5.0	2.65	0.0146	0.00140	214	13228	WMFK
PA424	Piceance	0504510927	Williams PA-424-34	WILLIAMS E&P	CO	6S	95W	34	NWSWSE	4635.4	A	2.4	2.65	0.0123	0.000771	245	13245	WMFK
PA424	Piceance	0504510927	Williams PA-424-34	WILLIAMS E&P	CO	6S	95W	34	NWSWSE	4637.5	A	6.7	2.65	0.00856	0.000812	148	15226	WMFK

Table 4.1.1. (continued)

Summary of Porosity, Permeability, and Grain Density
Analysis of Critical Permeability, Capillary Pressure, and Electrical Properties for Mesaverde Tight Gas Sandstones from Western U.S. Basins
US DOE # DE-FC26-05NT42660
Alan P. Byrnes, Robert M. Cluff, John C. Webb, Daniel A. Krygowski, Stefani D. Whittaker
website: http://www.kgs.ku.edu/mesaverde

USGS Library Number	Basin	API Number	Well Name	Operator	State	Township	Range	Section	Quarter Section	Plug Depth	Plug Letter	Ambient Porosity	Grain Density	Routine Gas Permeability	*in situ* Klinkenberg Gas Permeability	*in situ* Klinkenberg *constant b*	Rock Type Code	Formations
										ft	A/B/C	%	g/cc	mD	mD	(psia)		
PA424	Piceance	0504510927	Williams PA-424-34	WILLIAMS E&P	CO	6S	95W	34	NWSWSE	4638.8	A	5.5	2.65	0.00992	0.000698	200	13276	WMFK
PA424	Piceance	0504510927	Williams PA-424-34	WILLIAMS E&P	CO	6S	95W	34	NWSWSE	4640.7	A	6.1	2.65	0.0130	0.00144	97.7	16276	WMFK
PA424	Piceance	0504510927	Williams PA-424-34	WILLIAMS E&P	CO	6S	95W	34	NWSWSE	4645.8	A	7.2	2.64	0.0230	0.00318	108	13276	WMFK
PA424	Piceance	0504510927	Williams PA-424-34	WILLIAMS E&P	CO	6S	95W	34	NWSWSE	4651.6	A	6.7	2.64	0.104	0.0134	61.8	17276	WMFK
PA424	Piceance	0504510927	Williams PA-424-34	WILLIAMS E&P	CO	6S	95W	34	NWSWSE	4654.5	A	4.5	2.64	0.0275	0.00247	114	13276	WMFK
PA424	Piceance	0504510927	Williams PA-424-34	WILLIAMS E&P	CO	6S	95W	34	NWSWSE	4656.7	A	5.8	2.64	0.0330	0.00182	471	16296	WMFK
PA424	Piceance	0504510927	Williams PA-424-34	WILLIAMS E&P	CO	6S	95W	34	NWSWSE	4660.4	A	7.0	2.64	0.0307	0.00357	82.9	16286	WMFK
PA424	Piceance	0504510927	Williams PA-424-34	WILLIAMS E&P	CO	6S	95W	34	NWSWSE	4666.2	A	5.1	2.65	0.0238	0.00242	87.6	16226	WMFK
PA424	Piceance	0504510927	Williams PA-424-34	WILLIAMS E&P	CO	6S	95W	34	NWSWSE	4671.5	A	5.8	2.64	0.0347	0.00280	333	16276	WMFK
PA424	Piceance	0504510927	Williams PA-424-34	WILLIAMS E&P	CO	6S	95W	34	NWSWSE	4674.7	A	5.7	2.65	0.685	0.0527	65.6	13276	WMFK
PA424	Piceance	0504510927	Williams PA-424-34	WILLIAMS E&P	CO	6S	95W	34	NWSWSE	4677.7	A	4.6	2.66	0.0168	0.000814	312	19296	WMFK
PA424	Piceance	0504510927	Williams PA-424-34	WILLIAMS E&P	CO	6S	95W	34	NWSWSE	4679.4	A	7.1	2.65	0.0164	0.00162	129	15296	WMFK
PA424	Piceance	0504510927	Williams PA-424-34	WILLIAMS E&P	CO	6S	95W	34	NWSWSE	4681.5	A	7.1	2.64	0.0146	0.00102	169	15286	WMFK
PA424	Piceance	0504510927	Williams PA-424-34	WILLIAMS E&P	CO	6S	95W	34	NWSWSE	4683.5	A	6.9	2.64	0.0270	0.00254	143	15285	WMFK
PA424	Piceance	0504510927	Williams PA-424-34	WILLIAMS E&P	CO	6S	95W	34	NWSWSE	4686.4	A	7.9	2.65	0.0211	0.00311	85.9	15286	WMFK
PA424	Piceance	0504510927	Williams PA-424-34	WILLIAMS E&P	CO	6S	95W	34	NWSWSE	4691.5	A	13.3	2.65	0.0565	0.00687	234	16296	WMFK
PA424	Piceance	0504510927	Williams PA-424-34	WILLIAMS E&P	CO	6S	95W	34	NWSWSE	4696.5	A	10.8	2.65	0.0223	0.00306	94.4	16296	WMFK
PA424	Piceance	0504510927	Williams PA-424-34	WILLIAMS E&P	CO	6S	95W	34	NWSWSE	4698.5	A	7.3	2.64	0.0288	0.00385	29.8	16276	WMFK
PA424	Piceance	0504510927	Williams PA-424-34	WILLIAMS E&P	CO	6S	95W	34	NWSWSE	4699.4	A	4.9	2.64	0.0140	0.00102	171	15276	WMFK
PA424	Piceance	0504510927	Williams PA-424-34	WILLIAMS E&P	CO	6S	95W	34	NWSWSE	4704.2	A	7.9	2.64	0.0266	0.00168	137	13226	WMFK
PA424	Piceance	0504510927	Williams PA-424-34	WILLIAMS E&P	CO	6S	95W	34	NWSWSE	4707.8	A	7.7	2.64	0.0330	0.00509	148	16276	WMFK
PA424	Piceance	0504510927	Williams PA-424-34	WILLIAMS E&P	CO	6S	95W	34	NWSWSE	4712.5	A	5.2	2.66	0.00468	0.000530	183	13246	WMFK
PA424	Piceance	0504510927	Williams PA-424-34	WILLIAMS E&P	CO	6S	95W	34	NWSWSE	4714.2	A	5.3	2.66	0.0127	0.000792	294	16276	WMFK
PA424	Piceance	0504510927	Williams PA-424-34	WILLIAMS E&P	CO	6S	95W	34	NWSWSE	4718.2	A	0.6	2.68	0.00125	0.000028	531	12225	WMFK
PA424	Piceance	0504510927	Williams PA-424-34	WILLIAMS E&P	CO	6S	95W	34	NWSWSE	4725.5	A	7.2	2.66	0.0278	0.00396	187	16276	WMFK
PA424	Piceance	0504510927	Williams PA-424-34	WILLIAMS E&P	CO	6S	95W	34	NWSWSE	4728.6	A	8.7	2.66	0.0115	0.00146	127	13286	WMFK
PA424	Piceance	0504510927	Williams PA-424-34	WILLIAMS E&P	CO	6S	95W	34	NWSWSE	4731.6	A	8.1	2.65	0.0534	0.00697	90.6	16276	WMFK
PA424	Piceance	0504510927	Williams PA-424-34	WILLIAMS E&P	CO	6S	95W	34	NWSWSE	4733.1	A	6.7	2.66	0.00948	0.00103	186	15276	WMFK
PA424	Piceance	0504510927	Williams PA-424-34	WILLIAMS E&P	CO	6S	95W	34	NWSWSE	4735.2	A	7.5	2.65	0.0224	0.00275	91.9	16286	WMFK
PA424	Piceance	0504510927	Williams PA-424-34	WILLIAMS E&P	CO	6S	95W	34	NWSWSE	5109.5	A	3.0	2.67	0.00245	0.000327	295	13255	WMFK
PA424	Piceance	0504510927	Williams PA-424-34	WILLIAMS E&P	CO	6S	95W	34	NWSWSE	5113.5	A	0.7	2.68	0.0113	0.000782	290	11299	WMFK
PA424	Piceance	0504510927	Williams PA-424-34	WILLIAMS E&P	CO	6S	95W	34	NWSWSE	5118.5	A	1.1	2.67	0.00164	0.000059	428	13275	WMFK
PA424	Piceance	0504510927	Williams PA-424-34	WILLIAMS E&P	CO	6S	95W	34	NWSWSE	5123.5	A	6.0	2.66	0.0213	0.00363	94.8	15296	WMFK
PA424	Piceance	0504510927	Williams PA-424-34	WILLIAMS E&P	CO	6S	95W	34	NWSWSE	5128.5	A	7.7	2.65	0.0761	0.0139	68.5	15296	WMFK
PA424	Piceance	0504510927	Williams PA-424-34	WILLIAMS E&P	CO	6S	95W	34	NWSWSE	5129.7	A	6.6	2.65	0.0205	0.00310	61.7	16226	WMFK
PA424	Piceance	0504510927	Williams PA-424-34	WILLIAMS E&P	CO	6S	95W	34	NWSWSE	5131.5	A	7.3	2.65	0.0249	0.00408	105	16296	WMFK
PA424	Piceance	0504510927	Williams PA-424-34	WILLIAMS E&P	CO	6S	95W	34	NWSWSE	5135.8	A	6.6	2.64	0.0267	0.00360	115	16276	WMFK
PA424	Piceance	0504510927	Williams PA-424-34	WILLIAMS E&P	CO	6S	95W	34	NWSWSE	5138.8	A	7.8	2.65	0.0279	0.00464	80.7	16286	WMFK
PA424	Piceance	0504510927	Williams PA-424-34	WILLIAMS E&P	CO	6S	95W	34	NWSWSE	5140.5	A	11.6	2.65	0.145	0.0251	53.6	16296	WMFK
PA424	Piceance	0504510927	Williams PA-424-34	WILLIAMS E&P	CO	6S	95W	34	NWSWSE	5142.5	A	8.3	2.65	0.0454	0.00844	140	16286	WMFK
PA424	Piceance	0504510927	Williams PA-424-34	WILLIAMS E&P	CO	6S	95W	34	NWSWSE	5143.5	A	6.8	2.67	0.0191	0.00180	152	16276	WMFK
PA424	Piceance	0504510927	Williams PA-424-34	WILLIAMS E&P	CO	6S	95W	34	NWSWSE	5144.5	A	8.4	2.65	0.0497	0.00923	126	16296	WMFK
PA424	Piceance	0504510927	Williams PA-424-34	WILLIAMS E&P	CO	6S	95W	34	NWSWSE	5148.2	A	6.0	2.66	0.0206	0.00235	131	16276	WMFK
PA424	Piceance	0504510927	Williams PA-424-34	WILLIAMS E&P	CO	6S	95W	34	NWSWSE	5154.5	A	0.3	2.62	0.00168	0.000047	407	12299	WMFK
PA424	Piceance	0504510927	Williams PA-424-34	WILLIAMS E&P	CO	6S	95W	34	NWSWSE	5162.5	A	5.3	2.67	0.00970	0.00181	111	13266	WMFK
PA424	Piceance	0504510927	Williams PA-424-34	WILLIAMS E&P	CO	6S	95W	34	NWSWSE	5171.6	A	2.6	2.68	0.00289	0.000302	312	13265	WMFK
PA424	Piceance	0504510927	Williams PA-424-34	WILLIAMS E&P	CO	6S	95W	34	NWSWSE	5175.7	A	5.5	2.68	0.00507	0.000669	169	13265	WMFK
PA424	Piceance	0504510927	Williams PA-424-34	WILLIAMS E&P	CO	6S	95W	34	NWSWSE	5178.3	A	3.9	2.68	0.00193	0.000157	238	13255	WMFK
PA424	Piceance	0504510927	Williams PA-424-34	WILLIAMS E&P	CO	6S	95W	34	NWSWSE	5179.5	A	2.2	2.66	0.00456	0.000188	366	19246	WMFK
PA424	Piceance	0504510927	Williams PA-424-34	WILLIAMS E&P	CO	6S	95W	34	NWSWSE	5182.7	A	6.7	2.66	0.0692	0.00869	110	16296	WMFK
PA424	Piceance	0504510927	Williams PA-424-34	WILLIAMS E&P	CO	6S	95W	34	NWSWSE	5185.6	A	6.6	2.64				15286	WMFK
PA424	Piceance	0504510927	Williams PA-424-34	WILLIAMS E&P	CO	6S	95W	34	NWSWSE	5189.5	A	7.2	2.65	0.0497	0.00620	87.6	16286	WMFK
PA424	Piceance	0504510927	Williams PA-424-34	WILLIAMS E&P	CO	6S	95W	34	NWSWSE	5192.7	A	7.9	2.65	0.0423	0.00936	55.1	16296	WMFK
PA424	Piceance	0504510927	Williams PA-424-34	WILLIAMS E&P	CO	6S	95W	34	NWSWSE	5193.5	A	7.1	2.65	0.0302	0.00625	164	16286	WMFK
PA424	Piceance	0504510927	Williams PA-424-34	WILLIAMS E&P	CO	6S	95W	34	NWSWSE	5193.5	A1	7.8	2.66	0.00252	0.000617	160	16286	WMFK
PA424	Piceance	0504510927	Williams PA-424-34	WILLIAMS E&P	CO	6S	95W	34	NWSWSE	5193.5	A2	7.3	2.64	0.00234	0.000664	164	16286	WMFK
PA424	Piceance	0504510927	Williams PA-424-34	WILLIAMS E&P	CO	6S	95W	34	NWSWSE	5195.7	A	7.7	2.65	0.0312	0.00419	189	16276	WMFK
PA424	Piceance	0504510927	Williams PA-424-34	WILLIAMS E&P	CO	6S	95W	34	NWSWSE	6071.5	A	3.0	2.67	0.00207	0.000175	349	11291	WMFK
PA424	Piceance	0504510927	Williams PA-424-34	WILLIAMS E&P	CO	6S	95W	34	NWSWSE	6073.5	A	4.4	2.68	0.00304	0.000399	153	14266	WMFK
PA424	Piceance	0504510927	Williams PA-424-34	WILLIAMS E&P	CO	6S	95W	34	NWSWSE	6073.6	A	4.6	2.67	0.00319	0.000490	220	14266	WMFK
PA424	Piceance	0504510927	Williams PA-424-34	WILLIAMS E&P	CO	6S	95W	34	NWSWSE	6077.5	A	4.9	2.68	0.00418	0.000535	286	13265	WMFK
PA424	Piceance	0504510927	Williams PA-424-34	WILLIAMS E&P	CO	6S	95W	34	NWSWSE	6077.7	A	4.6	2.68	0.00492	0.000885	92.2	13265	WMFK
PA424	Piceance	0504510927	Williams PA-424-34	WILLIAMS E&P	CO	6S	95W	34	NWSWSE	6079.5	A	3.1	2.71	0.0119	0.000598	181	12216	WMFK
PA424	Piceance	0504510927	Williams PA-424-34	WILLIAMS E&P	CO	6S	95W	34	NWSWSE	6082.5	A	4.6	2.68	0.00505	0.000880	189	16275	WMFK
PA424	Piceance	0504510927	Williams PA-424-34	WILLIAMS E&P	CO	6S	95W	34	NWSWSE	6085.5	A	6.0	2.70	0.00496	0.000570	191	13265	WMFK
PA424	Piceance	0504510927	Williams PA-424-34	WILLIAMS E&P	CO	6S	95W	34	NWSWSE	6085.6	A	6.1	2.71	0.0233	0.00263	84.6	13265	WMFK
PA424	Piceance	0504510927	Williams PA-424-34	WILLIAMS E&P	CO	6S	95W	34	NWSWSE	6090.7	A	7.1	2.66	0.0134	0.00229	138	16276	WMFK
PA424	Piceance	0504510927	Williams PA-424-34	WILLIAMS E&P	CO	6S	95W	34	NWSWSE	6098.5	A	0.6	2.41	0.00542	0.000319	309	11229	WMFK
PA424	Piceance	0504510927	Williams PA-424-34	WILLIAMS E&P	CO	6S	95W	34	NWSWSE	6102.3	A	1.2	2.69	0.00183	0.000061	418	14295	WMFK
PA424	Piceance	0504510927	Williams PA-424-34	WILLIAMS E&P	CO	6S	95W	34	NWSWSE	6115.5	A	1.7	2.74	0.00776	0.000761	123	12221	WMFK
PA424	Piceance	0504510927	Williams PA-424-34	WILLIAMS E&P	CO	6S	95W	34	NWSWSE	6130.3	A	6.0	2.68	0.00745			13255	WMFK
PA424	Piceance	0504510927	Williams PA-424-34	WILLIAMS E&P	CO	6S	95W	34	NWSWSE	6135.5	A	8.1	2.69	0.00660	0.000876	242	13256	WMFK
PA424	Piceance	0504510927	Williams PA-424-34	WILLIAMS E&P	CO	6S	95W	34	NWSWSE	6138.8	A	8.4	2.67	0.0196	0.00442	113	15271	WMFK
PA424	Piceance	0504510927	Williams PA-424-34	WILLIAMS E&P	CO	6S	95W	34	NWSWSE	6140.1	A	6.3	2.66	0.00365	0.000502	182	13226	WMFK
PA424	Piceance	0504510927	Williams PA-424-34	WILLIAMS E&P	CO	6S	95W	34	NWSWSE	6144.5	A	7.9	2.66	0.0228	0.00674	166	15286	WMFK
PA424	Piceance	0504510927	Williams PA-424-34	WILLIAMS E&P	CO	6S	95W	34	NWSWSE	6146.5	A	9.4	2.66	0.0204	0.00580	55.6	16276	WMFK
PA424	Piceance	0504510927	Williams PA-424-34	WILLIAMS E&P	CO	6S	95W	34	NWSWSE	6148.6	A	9.9	2.66	0.0237	0.00761	82.3	15276	WMFK
PA424	Piceance	0504510927	Williams PA-424-34	WILLIAMS E&P	CO	6S	95W	34	NWSWSE	6152.5	A	9.5	2.65	0.0281	0.00567	59.1	13278	WMFK
PA424	Piceance	0504510927	Williams PA-424-34	WILLIAMS E&P	CO	6S	95W	34	NWSWSE	6155.5	A	6.6	2.73	0.00519	0.000693	247	15276	WMFK
PA424	Piceance	0504510927	Williams PA-424-34	WILLIAMS E&P	CO	6S	95W	34	NWSWSE	6584.5	A	1.7	2.65	0.00163	0.000031	551	11219	WMFK
PA424	Piceance	0504510927	Williams PA-424-34	WILLIAMS E&P	CO	6S	95W	34	NWSWSE	6586.8	A	4.5	2.70	0.00480	0.000537	138	13265	WMFK
PA424	Piceance	0504510927	Williams PA-424-34	WILLIAMS E&P	CO	6S	95W	34	NWSWSE	6590.4	A	1.7	2.65	0.00488	0.000325	259	11249	WMFK
PA424	Piceance	0504510927	Williams PA-424-34	WILLIAMS E&P	CO	6S	95W	34	NWSWSE	6593.8	A	4.4	2.68	0.00275	0.000294	314	14265	WMFK
PA424	Piceance	0504510927	Williams PA-424-34	WILLIAMS E&P	CO	6S	95W	34	NWSWSE	6597.3	A	6.9	2.65	0.0154	0.00109	126	13266	WMFK
PA424	Piceance	0504510927	Williams PA-424-34	WILLIAMS E&P	CO	6S	95W	34	NWSWSE	6599.5	A	7.8	2.68	0.0113	0.00155	231	13266	WMFK
PA424	Piceance	0504510927	Williams PA-424-34	WILLIAMS E&P	CO	6S	95W	34	NWSWSE	6603.8	A	0.4	2.64				11229	WMFK
PA424	Piceance	0504510927	Williams PA-424-34	WILLIAMS E&P	CO	6S	95W	34	NWSWSE	6604.0	A	5.9	2.62				11229	WMFK
PA424	Piceance	0504510927	Williams PA-424-34	WILLIAMS E&P	CO	6S	95W	34	NWSWSE	6620.2	A	0.4	2.67	0.00118	0.000035	300	12295	WMFK
PA424	Piceance	0504510927	Williams PA-424-34	WILLIAMS E&P	CO	6S	95W	34	NWSWSE	6626.5	A	1.0	2.65	0.00918	0.00163	131	13225	WMFK
PA424	Piceance	0504510927	Williams PA-424-34	WILLIAMS E&P	CO	6S	95W	34	NWSWSE	6632.8	A	3.5	2.68	0.0654	0.00507	88.0	13245	WMFK
PA424	Piceance	0504510927	Williams PA-424-34	WILLIAMS E&P	CO	6S	95W	34	NWSWSE	6635.1	A	3.8	2.67	0.00339	0.000362	191	13265	WMFK
PA424	Piceance	0504510927	Williams PA-424-34	WILLIAMS E&P	CO	6S	95W	34	NWSWSE	6639.4	A	8.3	2.66	0.0131	0.00231	150	14295	WMFK
PA424	Piceance	0504510927	Williams PA-424-34	WILLIAMS E&P	CO	6S	95W	34	NWSWSE	6640.5	A	8.9	2.67	0.0132	0.00374	39.6	13248	WMFK
PA424	Piceance	0504510927	Williams PA-424-34	WILLIAMS E&P	CO	6S	95W	34	NWSWSE	6641.5	A	10.3	2.67	0.0204	0.00265	227	14295	WMFK
PA424	Piceance	0504510927	Williams PA-424-34	WILLIAMS E&P	CO	6S	95W	34	NWSWSE	6643.5	A	9.4	2.66	0.0182	0.00463	56.7	14295	WMFK
PA424	Piceance	0504510927	Williams PA-424-34	WILLIAMS E&P	CO	6S	95W	34	NWSWSE	6645.5	A	9.1	2.66	0.0139	0.00344	60.4	13225	WMFK
PA424	Piceance	0504510927	Williams PA-424-34	WILLIAMS E&P	CO	6S	95W	34	NWSWSE	6645.5	A2	10.0	2.67	0.00108	0.000261	321	13225	WMFK
PA424	Piceance	0504510927	Williams PA-424-34	WILLIAMS E&P	CO	6S	95W	34	NWSWSE	6645.5	A1	10.2	2.67	0.00108	0.000359	122	13225	WMFK
PA424	Piceance	0504510927	Williams PA-424-34	WILLIAMS E&P	CO	6S	95W	34	NWSWSE	6647.1	A	8.8	2.70	0.00998	0.00276	95.3	14295	WMFK
PA424	Piceance	0504510927	Williams PA-424-34	WILLIAMS E&P	CO	6S	95W	34	NWSWSE	6649.5	A	6.1	2.72	0.00358	0.000644	175	13265	WMFK
R091	Piceance	05045XXXX4	BOOK CLIFFS 1	USGS-CG	CO	7S	104W	17	NESW	213.0	A	6.4	2.64	0.00617	0.000225	156	12293	MVRD
R091	Piceance	05045XXXX4	BOOK CLIFFS 1	USGS-CG	CO	7S	104W	17	NESW	242.4	A	6.7	2.56	0.00626	0.000164	163	13219	MVRD
R091	Piceance	05045XXXX4	BOOK CLIFFS 1	USGS-CG	CO	7S	104W	17	NESW	247.0	A	14.9	2.66	0.0973	0.0542	51.7	13217	MVRD
R091	Piceance	05045XXXX4	BOOK CLIFFS 1	USGS-CG	CO	7S	104W	17	NESW	255.8	A	24.9	2.64	141	112	1.6	15567	MVRD
R091	Piceance	05045XXXX4	BOOK CLIFFS 1	USGS-CG	CO	7S	104W	17	NESW	255.9	A	24.8	2.64	138	95.9	4.5	15567	MVRD
R091	Piceance	05045XXXX4	BOOK CLIFFS 1	USGS-CG	CO	7S	104W	17	NESW	255.9	A1	24.5	2.63	28.5	12.9	23.4	15567	MVRD
R091	Piceance	05045XXXX4	BOOK CLIFFS 1	USGS-CG	CO	7S	104W	17	NESW	255.9	A2	24.3	2.63	26.3	19.6	6.5	15567	MVRD
R091	Piceance	05045XXXX4	BOOK CLIFFS 1	USGS-CG	CO	7S	104W	17	NESW	256.5	A	11.0	2.69	0.242	0.000082	322	13258	MVRD
R091	Piceance	05045XXXX4	BOOK CLIFFS 1	USGS-CG	CO	7S	104W	17	NESW	257.3	A	6.9	2.63	0.00460	0.000167	336	11219	MVRD
R091	Piceance	05045XXXX4	BOOK CLIFFS 1	USGS-CG	CO	7S	104W	17	NESW	264.0	A	23.4	2.59				13247	MVRD
R091	Piceance	05045XXXX4	BOOK CLIFFS 1	USGS-CG	CO	7S	104W	17	NESW	296.9	A	4.9	2.71	0.00258	0.000168	272	13225	MVRD
R091	Piceance	05045XXXX4	BOOK CLIFFS 1	USGS-CG	CO	7S	104W	17	NESW	387.3	A	9.6	2.59	0.00742	0.000985	163	12219	MVRD
R091	Piceance	05045XXXX4	BOOK CLIFFS 1	USGS-CG	CO	7S	104W	17	NESW	512.2	A	10.6	2.61	0.0376	0.00904	79.7	12236	MVRD
R091	Piceance	05045XXXX4	BOOK CLIFFS 1	USGS-CG	CO	7S	104W	17	NESW	523.5	A	12.2	2.64	0.0107	0.00321	145	13227	MVRD

Table 4.1.1. (continued)

Summary of Porosity, Permeability, and Grain Density
Analysis of Critical Permeability, Capillary Pressure, and Electrical Properties for Mesaverde Tight Gas Sandstones from Western U.S. Basins
US DOE # DE-FC26-05NT42660
Alan P. Byrnes, Robert M. Cluff, John C. Webb, Daniel A. Krygowski, Stefani D. Whittaker
website: http://www.kgs.ku.edu/mesaverde

USGS Library Number	Basin	API Number	Well Name	Operator	State	Township	Range	Section	Quarter Section	Plug Depth	Plug Letter	Ambient Porosity	Grain Density	Routine Gas Permeability	*in situ* Klinkenberg Gas Permeability	*in situ* Klinkenberg *constant* b	Rock Type Code	Formations
										ft	A/B/C	%	g/cc	mD	mD	(psia)		
S905	Piceance	05103XXXX3	21011-5 MOON LAKE	WESTERN FUELS ASSOC	CO	2N	101W	1	NESW	788.0	A	1.9	2.62	0.00222	0.000067	213	13225	MVRD
S905	Piceance	05103XXXX3	21011-5 MOON LAKE	WESTERN FUELS ASSOC	CO	2N	101W	1	NESW	790.3	A	5.0	2.65	0.00775	0.000209	263	12239	MVRD
S905	Piceance	05103XXXX3	21011-5 MOON LAKE	WESTERN FUELS ASSOC	CO	2N	101W	1	NESW	790.3	B	5.0	2.64	0.00198	0.000132	76.5	12239	MVRD
S905	Piceance	05103XXXX3	21011-5 MOON LAKE	WESTERN FUELS ASSOC	CO	2N	101W	1	NESW	812.2	B	17.7	2.64	11.1	6.80	13.6	13216	MVRD
S905	Piceance	05103XXXX3	21011-5 MOON LAKE	WESTERN FUELS ASSOC	CO	2N	101W	1	NESW	812.2	A	17.4	2.63	9.24	5.89	10.5	13216	MVRD
S905	Piceance	05103XXXX3	21011-5 MOON LAKE	WESTERN FUELS ASSOC	CO	2N	101W	1	NESW	812.3	B	17.9	2.65	54.1	42.1	3.7	14296	MVRD
S905	Piceance	05103XXXX3	21011-5 MOON LAKE	WESTERN FUELS ASSOC	CO	2N	101W	1	NESW	812.3	A	17.6	2.64	54.1	37.9	5.3	14296	MVRD
S905	Piceance	05103XXXX3	21011-5 MOON LAKE	WESTERN FUELS ASSOC	CO	2N	101W	1	NESW	812.6	B	18.4	2.63	20.4	17.2	1.6	13236	MVRD
S905	Piceance	05103XXXX3	21011-5 MOON LAKE	WESTERN FUELS ASSOC	CO	2N	101W	1	NESW	812.6	A	18.3	2.63	20.3	16.2	2.5	13236	MVRD
S905	Piceance	05103XXXX3	21011-5 MOON LAKE	WESTERN FUELS ASSOC	CO	2N	101W	1	NESW	812.7	B	17.8	2.65	33.3	26.3	3.7	13276	MVRD
S905	Piceance	05103XXXX3	21011-5 MOON LAKE	WESTERN FUELS ASSOC	CO	2N	101W	1	NESW	812.7	A	18.1	2.65	32.6	22.0	6.9	13276	MVRD
S905	Piceance	05103XXXX3	21011-5 MOON LAKE	WESTERN FUELS ASSOC	CO	2N	101W	1	NESW	812.9	B	17.9	2.65	33.8	24.6	4.7	14577	MVRD
S905	Piceance	05103XXXX3	21011-5 MOON LAKE	WESTERN FUELS ASSOC	CO	2N	101W	1	NESW	812.9	A	17.0	2.64	32.5	20.9	7.7	14577	MVRD
S905	Piceance	05103XXXX3	21011-5 MOON LAKE	WESTERN FUELS ASSOC	CO	2N	101W	1	NESW	815.5	B	16.7	2.61				13256	MVRD
S905	Piceance	05103XXXX3	21011-5 MOON LAKE	WESTERN FUELS ASSOC	CO	2N	101W	1	NESW	815.5	A	7.4	2.35				13256	MVRD
S905	Piceance	05103XXXX3	21011-5 MOON LAKE	WESTERN FUELS ASSOC	CO	2N	101W	1	NESW	816.5	B	11.1	2.66	0.0730	0.0241	29.4	12239	MVRD
S905	Piceance	05103XXXX3	21011-5 MOON LAKE	WESTERN FUELS ASSOC	CO	2N	101W	1	NESW	816.5	A	10.6	2.63	0.0408	0.0205	62.7	12239	MVRD
S905	Piceance	05103XXXX3	21011-5 MOON LAKE	WESTERN FUELS ASSOC	CO	2N	101W	1	NESW	817.6	B	2.7	2.53	0.0119	0.000441	148	11239	MVRD
S905	Piceance	05103XXXX3	21011-5 MOON LAKE	WESTERN FUELS ASSOC	CO	2N	101W	1	NESW	817.6	A	5.6	2.53	0.00315	0.000126	247	11239	MVRD
S905	Piceance	05103XXXX3	21011-5 MOON LAKE	WESTERN FUELS ASSOC	CO	2N	101W	1	NESW	817.8	B	8.4	2.55	0.0516	0.00739	49.8	11239	MVRD
S905	Piceance	05103XXXX3	21011-5 MOON LAKE	WESTERN FUELS ASSOC	CO	2N	101W	1	NESW	817.8	A	8.7	2.56	0.00692	0.00118	277	11239	MVRD
T63X-2G	Piceance	0510310391	T63X-2G	EXXON-MOBIL	CO	3S	97W	2	NESWNE	10547.5	B	5.5	2.65	0.00245	0.000343	84.1	15286	MVRD
T63X-2G	Piceance	0510310391	T63X-2G	EXXON-MOBIL	CO	3S	97W	2	NESWNE	10547.5	A	5.3	2.65	0.00223	0.000373	214	15286	MVRD
T63X-2G	Piceance	0510310391	T63X-2G	EXXON-MOBIL	CO	3S	97W	2	NESWNE	10551.0	A	5.1	2.65	0.00907	0.00124	78.1	15285	MVRD
T63X-2G	Piceance	0510310391	T63X-2G	EXXON-MOBIL	CO	3S	97W	2	NESWNE	10551.0	B	4.9	2.64	0.00730	0.00111	155	15285	MVRD
T63X-2G	Piceance	0510310391	T63X-2G	EXXON-MOBIL	CO	3S	97W	2	NESWNE	10555.6	B	7.0	2.63	0.0131	0.00155	185	15286	MVRD
T63X-2G	Piceance	0510310391	T63X-2G	EXXON-MOBIL	CO	3S	97W	2	NESWNE	10555.6	A	7.2	2.64	0.0125	0.00230	108	15286	MVRD
T63X-2G	Piceance	0510310391	T63X-2G	EXXON-MOBIL	CO	3S	97W	2	NESWNE	10555.7	B	7.2	2.64	0.0122	0.00213	86.5	15286	MVRD
T63X-2G	Piceance	0510310391	T63X-2G	EXXON-MOBIL	CO	3S	97W	2	NESWNE	10555.7	A	7.1	2.64	0.0120	0.00226	102	15286	MVRD
T63X-2G	Piceance	0510310391	T63X-2G	EXXON-MOBIL	CO	3S	97W	2	NESWNE	10561.0	B	6.4	2.65	0.00734	0.000666	271	15285	MVRD
T63X-2G	Piceance	0510310391	T63X-2G	EXXON-MOBIL	CO	3S	97W	2	NESWNE	10561.0	A	6.4	2.62	0.00732	0.00104	223	15285	MVRD
T63X-2G	Piceance	0510310391	T63X-2G	EXXON-MOBIL	CO	3S	97W	2	NESWNE	10563.1	A	3.7	2.68	0.0233	0.00180	84.8	15296	MVRD
T63X-2G	Piceance	0510310391	T63X-2G	EXXON-MOBIL	CO	3S	97W	2	NESWNE	10568.7	B	0.9	2.66	0.00131	0.000048	412	13215	MVRD
T63X-2G	Piceance	0510310391	T63X-2G	EXXON-MOBIL	CO	3S	97W	2	NESWNE	10568.7	A	0.8	2.66	0.00119	0.000012	668	13215	MVRD
T63X-2G	Piceance	0510310391	T63X-2G	EXXON-MOBIL	CO	3S	97W	2	NESWNE	10572.9	B	4.3	2.67	0.00215	0.000214	218	15265	MVRD
T63X-2G	Piceance	0510310391	T63X-2G	EXXON-MOBIL	CO	3S	97W	2	NESWNE	10572.9	A	4.6	2.68	0.00209	0.000341	209	15265	MVRD
T63X-2G	Piceance	0510310391	T63X-2G	EXXON-MOBIL	CO	3S	97W	2	NESWNE	10574.5	A	6.5	2.66	0.00791	0.00145	173	15276	MVRD
T63X-2G	Piceance	0510310391	T63X-2G	EXXON-MOBIL	CO	3S	97W	2	NESWNE	10574.5	B	6.2	2.65	0.00790	0.00135	159	15276	MVRD
T63X-2G	Piceance	0510310391	T63X-2G	EXXON-MOBIL	CO	3S	97W	2	NESWNE	10578.5	B	1.4	2.66	0.00233	0.000206	268	13266	MVRD
T63X-2G	Piceance	0510310391	T63X-2G	EXXON-MOBIL	CO	3S	97W	2	NESWNE	10578.5	A	1.4	2.68	0.00152	0.000127	244	13266	MVRD
T63X-2G	Piceance	0510310391	T63X-2G	EXXON-MOBIL	CO	3S	97W	2	NESWNE	10588.3	A	0.6	2.66	0.0295	0.000163	237	13229	MVRD
T63X-2G	Piceance	0510310391	T63X-2G	EXXON-MOBIL	CO	3S	97W	2	NESWNE	10602.8	B	1.8	2.67	0.00101	0.000052	169	13217	MVRD
T63X-2G	Piceance	0510310391	T63X-2G	EXXON-MOBIL	CO	3S	97W	2	NESWNE	10602.8	A	2.0	2.67	0.000563	0.000027	495	13217	MVRD
T63X-2G	Piceance	0510310391	T63X-2G	EXXON-MOBIL	CO	3S	97W	2	NESWNE	10604.5	A	3.4	2.68	0.00154	0.000215	395	15225	MVRD
T63X-2G	Piceance	0510310391	T63X-2G	EXXON-MOBIL	CO	3S	97W	2	NESWNE	10606.5	B	7.5	2.67	0.00457	0.000891	304	15225	MVRD
T63X-2G	Piceance	0510310391	T63X-2G	EXXON-MOBIL	CO	3S	97W	2	NESWNE	10606.5	A	7.2	2.67	0.00422	0.00118	101	15225	MVRD
T63X-2G	Piceance	0510310391	T63X-2G	EXXON-MOBIL	CO	3S	97W	2	NESWNE	10609.7	B	7.3	2.64	0.00835	0.00178	139	15296	MVRD
T63X-2G	Piceance	0510310391	T63X-2G	EXXON-MOBIL	CO	3S	97W	2	NESWNE	10609.7	A	7.5	2.65	0.00821	0.00174	117	15296	MVRD
T63X-2G	Piceance	0510310391	T63X-2G	EXXON-MOBIL	CO	3S	97W	2	NESWNE	10612.6	B	6.8	2.65	0.00644	0.00122	158	16276	MVRD
T63X-2G	Piceance	0510310391	T63X-2G	EXXON-MOBIL	CO	3S	97W	2	NESWNE	10612.6	A	6.7	2.66	0.00612	0.00127	169	16276	MVRD
T63X-2G	Piceance	0510310391	T63X-2G	EXXON-MOBIL	CO	3S	97W	2	NESWNE	10615.6	B	6.3	2.65	0.00994	0.00178	73.9	15225	MVRD
T63X-2G	Piceance	0510310391	T63X-2G	EXXON-MOBIL	CO	3S	97W	2	NESWNE	10615.6	A	6.1	2.64	0.00894	0.00175	124	15225	MVRD
T63X-2G	Piceance	0510310391	T63X-2G	EXXON-MOBIL	CO	3S	97W	2	NESWNE	10615.7	A	6.3	2.65	0.0101	0.00251	55.6	15225	MVRD
T63X-2G	Piceance	0510310391	T63X-2G	EXXON-MOBIL	CO	3S	97W	2	NESWNE	10615.7	B	6.5	2.64	0.00903	0.00187	198	15225	MVRD
T63X-2G	Piceance	0510310391	T63X-2G	EXXON-MOBIL	CO	3S	97W	2	NESWNE	10619.7	B	7.4	2.64	0.00884	0.00245	101	15276	MVRD
T63X-2G	Piceance	0510310391	T63X-2G	EXXON-MOBIL	CO	3S	97W	2	NESWNE	10619.7	A	7.3	2.64	0.00774	0.00247	126	15276	MVRD
T63X-2G	Piceance	0510310391	T63X-2G	EXXON-MOBIL	CO	3S	97W	2	NESWNE	10623.6	B	7.0	2.66	0.00463	0.000535	323	15265	MVRD
T63X-2G	Piceance	0510310391	T63X-2G	EXXON-MOBIL	CO	3S	97W	2	NESWNE	10623.6	A	6.9	2.67	0.00332	0.000839	101	15265	MVRD
T63X-2G	Piceance	0510310391	T63X-2G	EXXON-MOBIL	CO	3S	97W	2	NESWNE	10625.0	B	7.7	2.65	0.00546	0.00129	216	15276	MVRD
T63X-2G	Piceance	0510310391	T63X-2G	EXXON-MOBIL	CO	3S	97W	2	NESWNE	10625.0	A	7.1	2.65	0.00478	0.00162	93.6	15276	MVRD
T63X-2G	Piceance	0510310391	T63X-2G	EXXON-MOBIL	CO	3S	97W	2	NESWNE	10633.6	B	3.0	2.66	0.00127	0.000088	317	13265	MVRD
T63X-2G	Piceance	0510310391	T63X-2G	EXXON-MOBIL	CO	3S	97W	2	NESWNE	10633.6	A	3.0	2.68	0.000829	0.000084	316	13265	MVRD
T63X-2G	Piceance	0510310391	T63X-2G	EXXON-MOBIL	CO	3S	97W	2	NESWNE	10636.3	B	2.5	2.68	0.0272	0.000874	145	13265	MVRD
T63X-2G	Piceance	0510310391	T63X-2G	EXXON-MOBIL	CO	3S	97W	2	NESWNE	10636.3	A	2.5	2.69	0.000584	0.000038	602	13265	MVRD
T63X-2G	Piceance	0510310391	T63X-2G	EXXON-MOBIL	CO	3S	97W	2	NESWNE	10643.9	A	0.4	2.68	0.000703	0.000014	516	13267	MVRD
T63X-2G	Piceance	0510310391	T63X-2G	EXXON-MOBIL	CO	3S	97W	2	NESWNE	10643.9	B	0.4	2.68	0.000525	0.000006	920	13267	MVRD
T63X-2G	Piceance	0510310391	T63X-2G	EXXON-MOBIL	CO	3S	97W	2	NESWNE	10653.8	A	1.1	2.65	0.00149	0.000050	412	13265	MVRD
T63X-2G	Piceance	0510310391	T63X-2G	EXXON-MOBIL	CO	3S	97W	2	NESWNE	10653.8	B	1.1	2.65	0.000834	0.000020	835	13265	MVRD
T649	Piceance	0504560011	MWX-2	CER CORPORATION	CO	6S	94W	34	SESWNW	4885.4	A	4.1	2.65	0.00400	0.000372	285	15215	MVRD
T649	Piceance	0504560011	MWX-2	CER CORPORATION	CO	6S	94W	34	SESWNW	4885.4	B	4.3	2.65	0.00382	0.000427	251	15215	MVRD
T649	Piceance	0504560011	MWX-2	CER CORPORATION	CO	6S	94W	34	SESWNW	4905.1	B	3.2	2.64	0.00405	0.000517	159	15276	MVRD
T649	Piceance	0504560011	MWX-2	CER CORPORATION	CO	6S	94W	34	SESWNW	4905.1	A	2.8	2.64	0.00301	0.000377	258	15276	MVRD
T649	Piceance	0504560011	MWX-2	CER CORPORATION	CO	6S	94W	34	SESWNW	4909.1	A	7.7	2.64	0.0220	0.00485	44.5	16276	MVRD
T649	Piceance	0504560011	MWX-2	CER CORPORATION	CO	6S	94W	34	SESWNW	4909.1	B	7.5	2.64	0.0211	0.00330	180	16276	MVRD
T649	Piceance	0504560011	MWX-2	CER CORPORATION	CO	6S	94W	34	SESWNW	4918.2	A	7.4	2.63	0.0939	0.0108	87.4	17276	MVRD
T649	Piceance	0504560011	MWX-2	CER CORPORATION	CO	6S	94W	34	SESWNW	4918.2	B	7.1	2.64	0.0890	0.0141	113	17276	MVRD
T649	Piceance	0504560011	MWX-2	CER CORPORATION	CO	6S	94W	34	SESWNW	4930.4	A	3.5	2.65	0.0163	0.00193	104	15266	MVRD
T649	Piceance	0504560011	MWX-2	CER CORPORATION	CO	6S	94W	34	SESWNW	4930.4	B	3.4	2.65	0.0139	0.00231	36.7	15266	MVRD
T649	Piceance	0504560011	MWX-2	CER CORPORATION	CO	6S	94W	34	SESWNW	4935.5	B	6.7	2.63	0.0465	0.00646	91.0	13276	MVRD
T649	Piceance	0504560011	MWX-2	CER CORPORATION	CO	6S	94W	34	SESWNW	4935.5	A	6.4	2.63	0.0210	0.00331	72.9	13276	MVRD
T649	Piceance	0504560011	MWX-2	CER CORPORATION	CO	6S	94W	34	SESWNW	4939.8	B	9.0	2.63	0.0283	0.00340	105	16275	MVRD
T649	Piceance	0504560011	MWX-2	CER CORPORATION	CO	6S	94W	34	SESWNW	4939.8	A	9.0	2.63	0.0260	0.00426	86.9	16275	MVRD
T649	Piceance	0504560011	MWX-2	CER CORPORATION	CO	6S	94W	34	SESWNW	4945.1	A	9.9	2.63	0.0415	0.00627	128	16275	MVRD
T649	Piceance	0504560011	MWX-2	CER CORPORATION	CO	6S	94W	34	SESWNW	4945.1	B	10.1	2.63	0.0409	0.00750	86.6	16275	MVRD
T649	Piceance	0504560011	MWX-2	CER CORPORATION	CO	6S	94W	34	SESWNW	5714.8	B	1.3		0.00298	0.000056	200	13215	MVRD
T649	Piceance	0504560011	MWX-2	CER CORPORATION	CO	6S	94W	34	SESWNW	5714.8	A	3.1	2.71	0.00232	0.000040	588	13215	MVRD
T649	Piceance	0504560011	MWX-2	CER CORPORATION	CO	6S	94W	34	SESWNW	5719.4	A	3.1	2.68	0.00125	0.000035	526	13355	MVRD
T649	Piceance	0504560011	MWX-2	CER CORPORATION	CO	6S	94W	34	SESWNW	5719.4	B	0.7	2.68				13355	MVRD
T649	Piceance	0504560011	MWX-2	CER CORPORATION	CO	6S	94W	34	SESWNW	5720.7	A	4.7	2.69	0.00765	0.000058	250	13226	MVRD
T649	Piceance	0504560011	MWX-2	CER CORPORATION	CO	6S	94W	34	SESWNW	5720.7	B	0.3	2.68				13226	MVRD
T649	Piceance	0504560011	MWX-2	CER CORPORATION	CO	6S	94W	34	SESWNW	5725.0	A	3.8	2.66	0.00217	0.000117	279	16295	MVRD
T649	Piceance	0504560011	MWX-2	CER CORPORATION	CO	6S	94W	34	SESWNW	5727.7	B	8.8	2.65	0.0284	0.00356	133	16276	MVRD
T649	Piceance	0504560011	MWX-2	CER CORPORATION	CO	6S	94W	34	SESWNW	5727.7	A	9.0	2.65	0.0235	0.00181	423	16276	MVRD
T649	Piceance	0504560011	MWX-2	CER CORPORATION	CO	6S	94W	34	SESWNW	5734.1	B	8.7		0.0324	0.00514	91.1	16276	MVRD
T649	Piceance	0504560011	MWX-2	CER CORPORATION	CO	6S	94W	34	SESWNW	5734.1	A	8.7	2.66	0.0259	0.00471	64.1	16276	MVRD
T649	Piceance	0504560011	MWX-2	CER CORPORATION	CO	6S	94W	34	SESWNW	5737.3	B	9.7		0.0282	0.00419	39.2	16276	MVRD
T649	Piceance	0504560011	MWX-2	CER CORPORATION	CO	6S	94W	34	SESWNW	5737.3	A	9.4	2.66	0.0180	0.00220	112	16276	MVRD
T649	Piceance	0504560011	MWX-2	CER CORPORATION	CO	6S	94W	34	SESWNW	5744.2	B	5.3	2.67	0.00579	0.000107	490	12226	MVRD
T649	Piceance	0504560011	MWX-2	CER CORPORATION	CO	6S	94W	34	SESWNW	5744.2	A	4.3	2.67	0.00278	0.000042	549	12226	MVRD
T649	Piceance	0504560011	MWX-2	CER CORPORATION	CO	6S	94W	34	SESWNW	5745.5	A	5.7	2.65	0.0210	0.00294	72.0	13265	MVRD
T649	Piceance	0504560011	MWX-2	CER CORPORATION	CO	6S	94W	34	SESWNW	5746.6	B	4.4	2.69	0.00834	0.000315	242	13286	MVRD
T649	Piceance	0504560011	MWX-2	CER CORPORATION	CO	6S	94W	34	SESWNW	5746.6	A	4.1	2.69	0.00338	0.000169	320	13286	MVRD
T649	Piceance	0504560011	MWX-2	CER CORPORATION	CO	6S	94W	34	SESWNW	5757.0	B	1.0	2.80	0.00355	0.000103	554	13225	MVRD
T649	Piceance	0504560011	MWX-2	CER CORPORATION	CO	6S	94W	34	SESWNW	5757.0	A	0.8	2.71	0.000922	0.000014	674	13225	MVRD
T649	Piceance	0504560011	MWX-2	CER CORPORATION	CO	6S	94W	34	SESWNW	5760.4	B	5.3	2.68	0.00568	0.000288	207	14265	MVRD
T649	Piceance	0504560011	MWX-2	CER CORPORATION	CO	6S	94W	34	SESWNW	5760.4	A	5.1	2.69	0.00175	0.000223	224	14265	MVRD
T649	Piceance	0504560011	MWX-2	CER CORPORATION	CO	6S	94W	34	SESWNW	5771.2	A	1.3	2.61	0.00552	0.000027	283	12229	MVRD
T649	Piceance	0504560011	MWX-2	CER CORPORATION	CO	6S	94W	34	SESWNW	5771.2	B	2.4	2.62				12229	MVRD
T649	Piceance	0504560011	MWX-2	CER CORPORATION	CO	6S	94W	34	SESWNW	5772.9	B	0.6	2.67	0.000902	0.000022	525	14216	MVRD
T649	Piceance	0504560011	MWX-2	CER CORPORATION	CO	6S	94W	34	SESWNW	5772.9	A	1.2	2.67	0.000853	0.000024	398	14216	MVRD
T649	Piceance	0504560011	MWX-2	CER CORPORATION	CO	6S	94W	34	SESWNW	5776.1	A	1.2	2.68	0.00182	0.000052	295	13255	MVRD
T649	Piceance	0504560011	MWX-2	CER CORPORATION	CO	6S	94W	34	SESWNW	5776.1	B	1.3	2.68	0.00140	0.000015	555	13255	MVRD

Table 4.1.1. (continued)

Summary of Porosity, Permeability, and Grain Density
Analysis of Critical Permeability, Capillary Pressure, and Electrical Properties for Mesaverde Tight Gas Sandstones from Western U.S. Basins
US DOE # DE-FC26-05NT42660
Alan P. Byrnes, Robert M. Cluff, John C. Webb, Daniel A. Krygowski, Stefani D. Whittaker
website: http://www.kgs.ku.edu/mesaverde

USGS Library Number	Basin	API Number	Well Name	Operator	State	Township	Range	Section	Quarter Section	Plug Depth	Plug Letter	Ambient Porosity	Grain Density	Routine Gas Permeability	*in situ* Klinkenberg Gas Permeability	*in situ* Klinken-berg *constant* b	Rock Type Code	Formations
										ft	A/B/C	%	g/cc	mD	mD	(psia)		
T649	Piceance	0504560011	MWX-2	CER CORPORATION	CO	6S	94W	34	SESWNW	5786.4	B	5.2	2.69	0.00476	0.000176	567	14295	MVRD
T649	Piceance	0504560011	MWX-2	CER CORPORATION	CO	6S	94W	34	SESWNW	5786.4	A	5.7	2.69	0.00309	0.000109	225	14295	MVRD
T649	Piceance	0504560011	MWX-2	CER CORPORATION	CO	6S	94W	34	SESWNW	5786.5	B	5.4	2.68	0.00541	0.000252	192	14295	MVRD
T649	Piceance	0504560011	MWX-2	CER CORPORATION	CO	6S	94W	34	SESWNW	5786.5	A	5.7	2.68	0.00196	0.000120	158	14295	MVRD
T649	Piceance	0504560011	MWX-2	CER CORPORATION	CO	6S	94W	34	SESWNW	5786.7	B	5.6	2.68	0.00509	0.000443	69.1	14295	MVRD
T649	Piceance	0504560011	MWX-2	CER CORPORATION	CO	6S	94W	34	SESWNW	5786.7	A			0.00368	0.000167	305	14295	MVRD
T649	Piceance	0504560011	MWX-2	CER CORPORATION	CO	6S	94W	34	SESWNW	5795.9	B	1.1	2.66	0.00452	0.000081	280	13249	MVRD
T649	Piceance	0504560011	MWX-2	CER CORPORATION	CO	6S	94W	34	SESWNW	5812.0	A2	1.9	2.67	0.00521	0.000109	315	13296	MVRD
T649	Piceance	0504560011	MWX-2	CER CORPORATION	CO	6S	94W	34	SESWNW	5812.0	A		2.58	0.00498	0.000059	434	13296	MVRD
T649	Piceance	0504560011	MWX-2	CER CORPORATION	CO	6S	94W	34	SESWNW	5819.0	B	4.0	2.67	0.00375	0.000102	398	13255	MVRD
T649	Piceance	0504560011	MWX-2	CER CORPORATION	CO	6S	94W	34	SESWNW	5819.0	A	5.6	2.68	0.00298	0.000140	259	13255	MVRD
T649	Piceance	0504560011	MWX-2	CER CORPORATION	CO	6S	94W	34	SESWNW	5826.0	B	3.1	2.68	0.00566	0.000049	491	13216	MVRD
T649	Piceance	0504560011	MWX-2	CER CORPORATION	CO	6S	94W	34	SESWNW	5826.0	A	3.2	2.69	0.00221	0.000030	120	13216	MVRD
T649	Piceance	0504560011	MWX-2	CER CORPORATION	CO	6S	94W	34	SESWNW	5838.6	B	7.1	2.66	0.0147	0.00160	281	16275	MVRD
T649	Piceance	0504560011	MWX-2	CER CORPORATION	CO	6S	94W	34	SESWNW	5838.6	A	7.1	2.66	0.0110	0.00138	107	16275	MVRD
T649	Piceance	0504560011	MWX-2	CER CORPORATION	CO	6S	94W	34	SESWNW	5838.7	B	6.9	2.66	0.0146	0.00127	206	16275	MVRD
T649	Piceance	0504560011	MWX-2	CER CORPORATION	CO	6S	94W	34	SESWNW	5838.7	A	6.6	2.66	0.0110	0.00146	110	16275	MVRD
T649	Piceance	0504560011	MWX-2	CER CORPORATION	CO	6S	94W	34	SESWNW	5844.6	B	7.9		0.0209	0.00329	94.9	16276	MVRD
T649	Piceance	0504560011	MWX-2	CER CORPORATION	CO	6S	94W	34	SESWNW	5844.6	A	7.9	2.66	0.0185	0.00232	137	16276	MVRD
T649	Piceance	0504560011	MWX-2	CER CORPORATION	CO	6S	94W	34	SESWNW	5845.5	A	6.0	2.66	0.0281	0.00311	185	16276	MVRD
T649	Piceance	0504560011	MWX-2	CER CORPORATION	CO	6S	94W	34	SESWNW	5846.0	A	6.9	2.66	0.0118	0.00117	69.9	16276	MVRD
T649	Piceance	0504560011	MWX-2	CER CORPORATION	CO	6S	94W	34	SESWNW	5852.3	A	2.8	2.72	0.00172	0.000047	235	13216	MVRD
T649	Piceance	0504560011	MWX-2	CER CORPORATION	CO	6S	94W	34	SESWNW	6536.3	B	8.7	2.67	0.0285	0.00420	34.6	15295	MVRD
T649	Piceance	0504560011	MWX-2	CER CORPORATION	CO	6S	94W	34	SESWNW	6536.3	A	8.2	2.66	0.0192	0.00318	91.4	15295	MVRD
T649	Piceance	0504560011	MWX-2	CER CORPORATION	CO	6S	94W	34	SESWNW	6536.4	A	7.2	2.67	0.0448	0.00206	126	15295	MVRD
T649	Piceance	0504560011	MWX-2	CER CORPORATION	CO	6S	94W	34	SESWNW	6536.4	B	9.6	2.66				15295	MVRD
T649	Piceance	0504560011	MWX-2	CER CORPORATION	CO	6S	94W	34	SESWNW	6541.9	B	6.5	2.72	0.00834	0.000300	237	13265	MVRD
T649	Piceance	0504560011	MWX-2	CER CORPORATION	CO	6S	94W	34	SESWNW	6541.9	A	6.5	2.72	0.00250	0.000128	356	13265	MVRD
T649	Piceance	0504560011	MWX-2	CER CORPORATION	CO	6S	94W	34	SESWNW	6542.2	A	5.8	2.70	0.00429	0.000249	159	13255	MVRD
T649	Piceance	0504560011	MWX-2	CER CORPORATION	CO	6S	94W	34	SESWNW	6550.3	B	7.4	2.69	0.0144	0.00102	123	15286	MVRD
T649	Piceance	0504560011	MWX-2	CER CORPORATION	CO	6S	94W	34	SESWNW	6550.3	A	7.2	2.69	0.00848	0.000870	224	15286	MVRD
T649	Piceance	0504560011	MWX-2	CER CORPORATION	CO	6S	94W	34	SESWNW	6550.5	B	7.4	2.69	0.0150	0.000925	163	15286	MVRD
T649	Piceance	0504560011	MWX-2	CER CORPORATION	CO	6S	94W	34	SESWNW	6550.5	A	7.8	2.69	0.0118	0.000738	528	15286	MVRD
T649	Piceance	0504560011	MWX-2	CER CORPORATION	CO	6S	94W	34	SESWNW	6554.3	B2	6.4	2.67	0.0233	0.00301	50.2	15276	MVRD
T649	Piceance	0504560011	MWX-2	CER CORPORATION	CO	6S	94W	34	SESWNW	6554.3	B	6.3	2.66	0.0229	0.00227	83.5	15276	MVRD
T649	Piceance	0504560011	MWX-2	CER CORPORATION	CO	6S	94W	34	SESWNW	6554.3	A	6.5	2.67	0.0210	0.00214	96.2	15276	MVRD
T649	Piceance	0504560011	MWX-2	CER CORPORATION	CO	6S	94W	34	SESWNW	6554.3	A2	6.1	2.66	0.0203	0.00114	128	15276	MVRD
T649	Piceance	0504560011	MWX-2	CER CORPORATION	CO	6S	94W	34	SESWNW	6557.8	B	6.9	2.68	0.0335	0.00587	54.1	15276	MVRD
T649	Piceance	0504560011	MWX-2	CER CORPORATION	CO	6S	94W	34	SESWNW	6557.8	A	6.6	2.67	0.0226	0.00355	70.7	15276	MVRD
T649	Piceance	0504560011	MWX-2	CER CORPORATION	CO	6S	94W	34	SESWNW	6557.9	B	6.6	2.67	0.0313	0.00432	203	15276	MVRD
T649	Piceance	0504560011	MWX-2	CER CORPORATION	CO	6S	94W	34	SESWNW	6557.9	A	6.3	2.68	0.0246	0.00453	32.5	15276	MVRD
T649	Piceance	0504560011	MWX-2	CER CORPORATION	CO	6S	94W	34	SESWNW	7082.5	B	1.0	2.65	0.00208	0.000132	270	11299	MVRD
T649	Piceance	0504560011	MWX-2	CER CORPORATION	CO	6S	94W	34	SESWNW	7082.5	A	0.9	2.66	0.00117	0.000024	502	11299	MVRD
T649	Piceance	0504560011	MWX-2	CER CORPORATION	CO	6S	94W	34	SESWNW	7085.5	B	1.9	2.68	0.00423	0.000162	364	11299	MVRD
T649	Piceance	0504560011	MWX-2	CER CORPORATION	CO	6S	94W	34	SESWNW	7085.5	A	2.4	2.70	0.00204	0.000041	440	11299	MVRD
T649	Piceance	0504560011	MWX-2	CER CORPORATION	CO	6S	94W	34	SESWNW	7088.3	B	2.7	2.70	0.00299	0.000042	371	12215	MVRD
T649	Piceance	0504560011	MWX-2	CER CORPORATION	CO	6S	94W	34	SESWNW	7088.3	A	2.5	2.70	0.00199	0.000073	429	12215	MVRD
T649	Piceance	0504560011	MWX-2	CER CORPORATION	CO	6S	94W	34	SESWNW	7096.3	A	3.0	2.62	0.00576	0.000080	485	12219	MVRD
T649	Piceance	0504560011	MWX-2	CER CORPORATION	CO	6S	94W	34	SESWNW	7113.4	A	5.8	2.76	0.00379	0.000110	262	13216	MVRD
T649	Piceance	0504560011	MWX-2	CER CORPORATION	CO	6S	94W	34	SESWNW	7113.4	B	3.7	2.70	0.00204	0.000027	427	13216	MVRD
T649	Piceance	0504560011	MWX-2	CER CORPORATION	CO	6S	94W	34	SESWNW	7124.7	B	10.9	2.68	0.160	0.0496	66.2	15266	MVRD
T649	Piceance	0504560011	MWX-2	CER CORPORATION	CO	6S	94W	34	SESWNW	7124.7	A	11.1	2.68	0.0145	0.00345	237	15266	MVRD
T649	Piceance	0504560011	MWX-2	CER CORPORATION	CO	6S	94W	34	SESWNW	7133.5	A	10.2	2.73	0.0163	0.00670	91.3	15266	MVRD
T649	Piceance	0504560011	MWX-2	CER CORPORATION	CO	6S	94W	34	SESWNW	7136.8	B	10.6	2.68	0.0192	0.00342	104	13266	MVRD
T649	Piceance	0504560011	MWX-2	CER CORPORATION	CO	6S	94W	34	SESWNW	7136.8	A	6.9	2.58	0.0104	0.00219	182	13266	MVRD
T649	Piceance	0504560011	MWX-2	CER CORPORATION	CO	6S	94W	34	SESWNW	7140.2	B	7.6	2.68	0.0117	0.000709	195	13216	MVRD
T649	Piceance	0504560011	MWX-2	CER CORPORATION	CO	6S	94W	34	SESWNW	7140.2	A	8.4	2.69	0.00768	0.00101	87.3	13216	MVRD
T649	Piceance	0504560011	MWX-2	CER CORPORATION	CO	6S	94W	34	SESWNW	7140.7	B	8.6	2.68	0.0163	0.00129	157	13226	MVRD
T649	Piceance	0504560011	MWX-2	CER CORPORATION	CO	6S	94W	34	SESWNW	7140.7	A	6.5	2.62	0.00936	0.00127	87.3	13226	MVRD
T649	Piceance	0504560011	MWX-2	CER CORPORATION	CO	6S	94W	34	SESWNW	7141.9	A	3.9	2.67	0.00459	0.000065	562	13246	MVRD
T649	Piceance	0504560011	MWX-2	CER CORPORATION	CO	6S	94W	34	SESWNW	7145.5	B	8.0	2.68	0.00754	0.000502	182	15296	MVRD
T649	Piceance	0504560011	MWX-2	CER CORPORATION	CO	6S	94W	34	SESWNW	7145.5	A	6.6	2.66	0.00368	0.000258	115	15296	MVRD
T649	Piceance	0504560011	MWX-2	CER CORPORATION	CO	6S	94W	34	SESWNW	7204.0	B	2.2	2.68	0.00422	0.000180	357	30000	MVRD
T649	Piceance	0504560011	MWX-2	CER CORPORATION	CO	6S	94W	34	SESWNW	7204.0	A	7.1	2.84	0.00292	0.000078	396	30000	MVRD
T649	Piceance	0504560011	MWX-2	CER CORPORATION	CO	6S	94W	34	SESWNW	7217.8	B	2.7	2.66	0.00858	0.000085	506	13229	MVRD
T649	Piceance	0504560011	MWX-2	CER CORPORATION	CO	6S	94W	34	SESWNW	7217.8	A	3.1	2.67				13229	MVRD
T649	Piceance	0504560011	MWX-2	CER CORPORATION	CO	6S	94W	34	SESWNW	7218.7	B	3.6	2.75	0.00587	0.000385	96.8	13266	MVRD
T649	Piceance	0504560011	MWX-2	CER CORPORATION	CO	6S	94W	34	SESWNW	7218.7	A	6.1	2.84	0.000898	0.000056	402	13266	MVRD
T649	Piceance	0504560011	MWX-2	CER CORPORATION	CO	6S	94W	34	SESWNW	7223.0	B	6.7	2.69	0.00870	0.000547	125	15266	MVRD
T649	Piceance	0504560011	MWX-2	CER CORPORATION	CO	6S	94W	34	SESWNW	7223.0	A	5.7	2.66	0.00299	0.000439	180	15266	MVRD
T649	Piceance	0504560011	MWX-2	CER CORPORATION	CO	6S	94W	34	SESWNW	7249.7	B	2.9	2.68	0.00145	0.000019	569	12219	MVRD
T649	Piceance	0504560011	MWX-2	CER CORPORATION	CO	6S	94W	34	SESWNW	7249.9	A	3.4	2.69	0.00310	0.000047	310	12219	MVRD
T649	Piceance	0504560011	MWX-2	CER CORPORATION	CO	6S	94W	34	SESWNW	7264.4	A	4.1	2.59	0.00744	0.000346	240	13265	MVRD
T649	Piceance	0504560011	MWX-2	CER CORPORATION	CO	6S	94W	34	SESWNW	7264.4	B	6.3	2.64	0.00729	0.000255	159	13265	MVRD
T649	Piceance	0504560011	MWX-2	CER CORPORATION	CO	6S	94W	34	SESWNW	7264.5	A	6.1	2.63	0.00360	0.000221	277	13265	MVRD
T649	Piceance	0504560011	MWX-2	CER CORPORATION	CO	6S	94W	34	SESWNW	7270.7	B	4.1	2.67	0.00474	0.000097	339	13256	MVRD
T649	Piceance	0504560011	MWX-2	CER CORPORATION	CO	6S	94W	34	SESWNW	7270.7	A	4.7	2.68	0.00382	0.000123	147	13256	MVRD
T649	Piceance	0504560011	MWX-2	CER CORPORATION	CO	6S	94W	34	SESWNW	7272.8	B	9.0	2.68	0.0115	0.00148	154	13285	MVRD
T649	Piceance	0504560011	MWX-2	CER CORPORATION	CO	6S	94W	34	SESWNW	7272.8	A	8.9	2.68	0.00873	0.00234	38.9	13285	MVRD
T649	Piceance	0504560011	MWX-2	CER CORPORATION	CO	6S	94W	34	SESWNW	7276.2	B	8.2	2.68	0.00898	0.00202	159	15295	MVRD
T649	Piceance	0504560011	MWX-2	CER CORPORATION	CO	6S	94W	34	SESWNW	7276.2	A	8.4	2.69	0.00669	0.00173	134	15295	MVRD
T649	Piceance	0504560011	MWX-2	CER CORPORATION	CO	6S	94W	34	SESWNW	7319.7	B	5.2		0.00553	0.000550	120	13257	MVRD
T649	Piceance	0504560011	MWX-2	CER CORPORATION	CO	6S	94W	34	SESWNW	7319.7	A	5.6	2.68	0.00448	0.000183	394	13257	MVRD
T649	Piceance	0504560011	MWX-2	CER CORPORATION	CO	6S	94W	34	SESWNW	7331.6	B	8.3		0.180	0.0115	51.0	15276	MVRD
T649	Piceance	0504560011	MWX-2	CER CORPORATION	CO	6S	94W	34	SESWNW	7331.6	A	7.9	2.72	0.00573	0.000836	235	15276	MVRD
T649	Piceance	0504560011	MWX-2	CER CORPORATION	CO	6S	94W	34	SESWNW	7334.8	B	8.6		0.00818	0.00134	118	15276	MVRD
T649	Piceance	0504560011	MWX-2	CER CORPORATION	CO	6S	94W	34	SESWNW	7334.8	A	8.7	2.69	0.00460	0.000911	240	15276	MVRD
T649	Piceance	0504560011	MWX-2	CER CORPORATION	CO	6S	94W	34	SESWNW	7337.3	B	6.6	2.71	0.00605	0.000434	179	13265	MVRD
T649	Piceance	0504560011	MWX-2	CER CORPORATION	CO	6S	94W	34	SESWNW	7337.3	A	6.4	2.70	0.00217	0.000212	444	13265	MVRD
T649	Piceance	0504560011	MWX-2	CER CORPORATION	CO	6S	94W	34	SESWNW	7340.4	A	2.1	2.78	0.00279	0.000106	265	15275	MVRD
T649	Piceance	0504560011	MWX-2	CER CORPORATION	CO	6S	94W	34	SESWNW	7340.4	B	2.3	2.78	0.00254	0.000160	388	15275	MVRD
T649	Piceance	0504560011	MWX-2	CER CORPORATION	CO	6S	94W	34	SESWNW	7347.8	B	3.1		0.00905	0.000344	66.1	12235	MVRD
T649	Piceance	0504560011	MWX-2	CER CORPORATION	CO	6S	94W	34	SESWNW	7347.8	A	4.1	2.71	0.00279	0.000058	260	12235	MVRD
T649	Piceance	0504560011	MWX-2	CER CORPORATION	CO	6S	94W	34	SESWNW	7350.4	B			0.00455	0.000386	146	15265	MVRD
T649	Piceance	0504560011	MWX-2	CER CORPORATION	CO	6S	94W	34	SESWNW	7350.4	A	4.5	2.71	0.00331	0.000372	67.7	15265	MVRD
T649	Piceance	0504560011	MWX-2	CER CORPORATION	CO	6S	94W	34	SESWNW	7832.9	B	3.5	2.65	0.0135	0.000308	289	13266	MVRD
T649	Piceance	0504560011	MWX-2	CER CORPORATION	CO	6S	94W	34	SESWNW	7832.9	B	4.1	2.66	0.00892	0.000437	192	13266	MVRD
T649	Piceance	0504560011	MWX-2	CER CORPORATION	CO	6S	94W	34	SESWNW	7832.9	A	3.9	2.65				13266	MVRD
T649	Piceance	0504560011	MWX-2	CER CORPORATION	CO	6S	94W	34	SESWNW	7841.4	A	2.9	2.66	0.00349	0.000074	533	13316	MVRD
T649	Piceance	0504560011	MWX-2	CER CORPORATION	CO	6S	94W	34	SESWNW	7841.4	B	2.4	2.64				13316	MVRD
T649	Piceance	0504560011	MWX-2	CER CORPORATION	CO	6S	94W	34	SESWNW	7841.5	B	3.7	2.66	0.893	0.0101	73.8	13316	MVRD
T649	Piceance	0504560011	MWX-2	CER CORPORATION	CO	6S	94W	34	SESWNW	7841.5	A	4.0	2.67	0.00704	0.000171	180	13316	MVRD
T649	Piceance	0504560011	MWX-2	CER CORPORATION	CO	6S	94W	34	SESWNW	7851.3	A	3.8	2.66	0.00412	0.000244	291	13276	MVRD
T649	Piceance	0504560011	MWX-2	CER CORPORATION	CO	6S	94W	34	SESWNW	7857.6	B	7.4	2.67	0.0100	0.000628	159	14286	MVRD
T649	Piceance	0504560011	MWX-2	CER CORPORATION	CO	6S	94W	34	SESWNW	7857.6	A	7.7	2.68	0.00853	0.000538	278	14286	MVRD
T649	Piceance	0504560011	MWX-2	CER CORPORATION	CO	6S	94W	34	SESWNW	7865.5	B	7.7	2.66	0.0117	0.000929	180	15286	MVRD
T649	Piceance	0504560011	MWX-2	CER CORPORATION	CO	6S	94W	34	SESWNW	7865.5	A	7.6	2.66	0.00598	0.000721	167	15286	MVRD
T649	Piceance	0504560011	MWX-2	CER CORPORATION	CO	6S	94W	34	SESWNW	7865.6	B	7.6	2.67	0.0124	0.000505	91.4	15286	MVRD
T649	Piceance	0504560011	MWX-2	CER CORPORATION	CO	6S	94W	34	SESWNW	7877.3	B	8.1	2.68	0.0113	0.00152	214	14286	MVRD
T649	Piceance	0504560011	MWX-2	CER CORPORATION	CO	6S	94W	34	SESWNW	7877.3	A	7.9	2.68	0.00760	0.00137	114	14286	MVRD
T649	Piceance	0504560011	MWX-2	CER CORPORATION	CO	6S	94W	34	SESWNW	7877.4	B	7.8	2.68	0.0112	0.00185	146	14286	MVRD
T649	Piceance	0504560011	MWX-2	CER CORPORATION	CO	6S	94W	34	SESWNW	7877.4	A	7.9	2.68	0.00627	0.00143	124	14286	MVRD

Table 4.1.1. (continued)

Summary of Porosity, Permeability, and Grain Density
Analysis of Critical Permeability, Capillary Pressure, and Electrical Properties for Mesaverde Tight Gas Sandstones from Western U.S. Basins
US DOE # DE-FC26-05NT42660
Alan P. Byrnes, Robert M. Cluff, John C. Webb, Daniel A. Krygowski, Stefani D. Whittaker
website: http://www.kgs.ku.edu/mesaverde

USGS Library Number	Basin	API Number	Well Name	Operator	State	Township	Range	Section	Quarter Section	Plug Depth	Plug Letter	Ambient Porosity	Grain Density	Routine Gas Permeability	*in situ* Klinkenberg Gas Permeability	*in situ* Klinkenberg *constant* b	Rock Type Code	Formations
										ft	A/B/C	%	g/cc	mD	mD	(psia)		
T649	Piceance	0504560011	MWX-2	CER CORPORATION	CO	6S	94W	34	SESWNW	7877.5	A	7.6	2.67	0.00564	0.000910	264	14286	MVRD
T649	Piceance	0504560011	MWX-2	CER CORPORATION	CO	6S	94W	34	SESWNW	7877.6	B	7.7	2.68	0.0100	0.00165	139	14286	MVRD
T649	Piceance	0504560011	MWX-2	CER CORPORATION	CO	6S	94W	34	SESWNW	7877.6	A	7.6	2.68	0.00860	0.00152	74.7	14286	MVRD
T649	Piceance	0504560011	MWX-2	CER CORPORATION	CO	6S	94W	34	SESWNW	7880.1	A	7.6	2.68	0.00859	0.00179	145	14286	MVRD
T649	Piceance	0504560011	MWX-2	CER CORPORATION	CO	6S	94W	34	SESWNW	7880.2	B	8.2	2.69	0.0141	0.00374	92.3	14286	MVRD
T649	Piceance	0504560011	MWX-2	CER CORPORATION	CO	6S	94W	34	SESWNW	7880.2	A	7.9	2.69	0.00904	0.00237	214	14286	MVRD
T649	Piceance	0504560011	MWX-2	CER CORPORATION	CO	6S	94W	34	SESWNW	7891.1	B	7.5	2.68	0.0144	0.00261	244	14286	MVRD
T649	Piceance	0504560011	MWX-2	CER CORPORATION	CO	6S	94W	34	SESWNW	7891.1	A	7.4	2.68	0.0113	0.00254	176	14286	MVRD
T649	Piceance	0504560011	MWX-2	CER CORPORATION	CO	6S	94W	34	SESWNW	7895.0	B	7.2	2.69	0.0112	0.00175	55.1	15296	MVRD
T649	Piceance	0504560011	MWX-2	CER CORPORATION	CO	6S	94W	34	SESWNW	7895.0	A	7.0	2.69	0.00803	0.00206	61.0	15296	MVRD
T649	Piceance	0504560011	MWX-2	CER CORPORATION	CO	6S	94W	34	SESWNW	7903.6	A	3.0	2.69	0.0184	0.000232	560	12226	MVRD
T649	Piceance	0504560011	MWX-2	CER CORPORATION	CO	6S	94W	34	SESWNW	7903.6	B	3.6	2.71	0.00645	0.000172	307	12226	MVRD
T649	Piceance	0504560011	MWX-2	CER CORPORATION	CO	6S	94W	34	SESWNW	8106.2	A	3.8	2.72	0.00558	0.000076	263	13229	MVRD
T649	Piceance	0504560011	MWX-2	CER CORPORATION	CO	6S	94W	34	SESWNW	8106.2	B	3.3	2.70	0.00476	0.000074	668	13229	MVRD
T649	Piceance	0504560011	MWX-2	CER CORPORATION	CO	6S	94W	34	SESWNW	8106.9	A	3.4	2.70	0.00548	0.000695	189	13276	MVRD
T649	Piceance	0504560011	MWX-2	CER CORPORATION	CO	6S	94W	34	SESWNW	8111.2	B	6.5	2.68	0.00977	0.000639	65.8	15296	MVRD
T649	Piceance	0504560011	MWX-2	CER CORPORATION	CO	6S	94W	34	SESWNW	8111.2	A	7.2	2.68	0.00167	0.000156	326	15296	MVRD
T649	Piceance	0504560011	MWX-2	CER CORPORATION	CO	6S	94W	34	SESWNW	8117.9	B	6.2	2.58	0.101	0.0102	84.6	13246	MVRD
T649	Piceance	0504560011	MWX-2	CER CORPORATION	CO	6S	94W	34	SESWNW	8117.9	A	6.5	2.61	0.0183	0.00227	146	13246	MVRD
T649	Piceance	0504560011	MWX-2	CER CORPORATION	CO	6S	94W	34	SESWNW	8118.5	B	5.6	2.70	0.293	0.0256	49.4	14296	MVRD
T649	Piceance	0504560011	MWX-2	CER CORPORATION	CO	6S	94W	34	SESWNW	8118.5	A	5.7	2.69	0.0176	0.00189	140	14296	MVRD
T649	Piceance	0504560011	MWX-2	CER CORPORATION	CO	6S	94W	34	SESWNW	8138.5	A	2.5	2.67	0.0107	0.000294	177	12219	MVRD
E393	Powder River	4900525627	1 BARLOW 21-20	LOUISIANA LAND & EXP	WY	48N	75W	20	NENW	6969.7	B	20.7	2.70	2.35	1.18	25.3	15287	PRKM
E393	Powder River	4900525627	1 BARLOW 21-20	LOUISIANA LAND & EXP	WY	48N	75W	20	NENW	6969.7	A	20.2	2.69	2.21	1.29	17.0	15287	PRKM
E393	Powder River	4900525627	1 BARLOW 21-20	LOUISIANA LAND & EXP	WY	48N	75W	20	NENW	6969.9	B	20.4	2.70	2.08	1.25	14.8	15287	PRKM
E393	Powder River	4900525627	1 BARLOW 21-20	LOUISIANA LAND & EXP	WY	48N	75W	20	NENW	6969.9	A	20.2	2.70	2.02	1.20	29.3	15287	PRKM
E393	Powder River	4900525627	1 BARLOW 21-20	LOUISIANA LAND & EXP	WY	48N	75W	20	NENW	6973.2	B	17.0	2.67	88.4	63.0	4.0	16557	PRKM
E393	Powder River	4900525627	1 BARLOW 21-20	LOUISIANA LAND & EXP	WY	48N	75W	20	NENW	6973.2	A	16.5	2.66	57.9	39.6	4.4	16557	PRKM
E393	Powder River	4900525627	1 BARLOW 21-20	LOUISIANA LAND & EXP	WY	48N	75W	20	NENW	6973.4	B	17.0	2.66	64.9	42.4	5.5	16557	PRKM
E393	Powder River	4900525627	1 BARLOW 21-20	LOUISIANA LAND & EXP	WY	48N	75W	20	NENW	6973.4	A	17.1	2.66	59.9	38.7	5.8	16557	PRKM
E393	Powder River	4900525627	1 BARLOW 21-20	LOUISIANA LAND & EXP	WY	48N	75W	20	NENW	6974.9	A	8.4	2.66	1.52	0.0931	17.0	13517	PRKM
E393	Powder River	4900525627	1 BARLOW 21-20	LOUISIANA LAND & EXP	WY	48N	75W	20	NENW	6974.9	B	9.8	2.67	0.285	0.0329	91.4	13517	PRKM
E393	Powder River	4900525627	1 BARLOW 21-20	LOUISIANA LAND & EXP	WY	48N	75W	20	NENW	6975.1	A	10.1	2.64	2.14	0.0699	43.5	13517	PRKM
E393	Powder River	4900525627	1 BARLOW 21-20	LOUISIANA LAND & EXP	WY	48N	75W	20	NENW	6975.1	B	10.4	2.65	1.84	0.262	24.8	13517	PRKM
E393	Powder River	4900525627	1 BARLOW 21-20	LOUISIANA LAND & EXP	WY	48N	75W	20	NENW	6976.9	B	10.9	2.65	0.364	0.0259	80.6	13517	PRKM
E393	Powder River	4900525627	1 BARLOW 21-20	LOUISIANA LAND & EXP	WY	48N	75W	20	NENW	6976.9	A	9.1	2.64	0.233	0.0211	131	13517	PRKM
E393	Powder River	4900525627	1 BARLOW 21-20	LOUISIANA LAND & EXP	WY	48N	75W	20	NENW	6984.8	B	8.6	2.65	0.221	0.00618	364	13517	PRKM
E393	Powder River	4900525627	1 BARLOW 21-20	LOUISIANA LAND & EXP	WY	48N	75W	20	NENW	6984.8	A	7.2	2.64	0.107	0.00796	63.4	13517	PRKM
E393	Powder River	4900525627	1 BARLOW 21-20	LOUISIANA LAND & EXP	WY	48N	75W	20	NENW	6985.0	A	7.3	2.63	4.18	0.191	15.9	13517	PRKM
E393	Powder River	4900525627	1 BARLOW 21-20	LOUISIANA LAND & EXP	WY	48N	75W	20	NENW	6985.0	B	8.7	2.64	0.419	0.0325	25.6	13517	PRKM
E393	Powder River	4900525627	1 BARLOW 21-20	LOUISIANA LAND & EXP	WY	48N	75W	20	NENW	6989.2	A	4.0	2.62	0.607	0.0248	54.1	12219	PRKM
E393	Powder River	4900525627	1 BARLOW 21-20	LOUISIANA LAND & EXP	WY	48N	75W	20	NENW	6989.2	B	5.0	2.65	0.00346	0.000058	425	12219	PRKM
E393	Powder River	4900525627	1 BARLOW 21-20	LOUISIANA LAND & EXP	WY	48N	75W	20	NENW	6994.1	A	18.1	2.67	50.8	36.5	3.8	15587	PRKM
E393	Powder River	4900525627	1 BARLOW 21-20	LOUISIANA LAND & EXP	WY	48N	75W	20	NENW	6994.1	B	18.0	2.66	50.2	30.0	9.0	15587	PRKM
E393	Powder River	4900525627	1 BARLOW 21-20	LOUISIANA LAND & EXP	WY	48N	75W	20	NENW	6995.8	A	5.1	2.69	0.0131	0.00115	50.2	15295	PRKM
E393	Powder River	4900525627	1 BARLOW 21-20	LOUISIANA LAND & EXP	WY	48N	75W	20	NENW	6995.8	B	5.4	2.70	0.00934	0.00111	130	15295	PRKM
E393	Powder River	4900525627	1 BARLOW 21-20	LOUISIANA LAND & EXP	WY	48N	75W	20	NENW	6996.0	A	5.9	2.69	0.0121	0.00143	172	15295	PRKM
E393	Powder River	4900525627	1 BARLOW 21-20	LOUISIANA LAND & EXP	WY	48N	75W	20	NENW	6996.0	B	6.2	2.70	0.00963	0.00108	176	15295	PRKM
E393	Powder River	4900525627	1 BARLOW 21-20	LOUISIANA LAND & EXP	WY	48N	75W	20	NENW	6996.2	A	7.1	2.69	0.0245	0.00473	121	15295	PRKM
E393	Powder River	4900525627	1 BARLOW 21-20	LOUISIANA LAND & EXP	WY	48N	75W	20	NENW	6996.2	B	6.3	2.69	0.0156	0.00207	213	15295	PRKM
E393	Powder River	4900525627	1 BARLOW 21-20	LOUISIANA LAND & EXP	WY	48N	75W	20	NENW	7000.9	B	17.3	2.67	46.0	31.0	5.9	15587	PRKM
E393	Powder River	4900525627	1 BARLOW 21-20	LOUISIANA LAND & EXP	WY	48N	75W	20	NENW	7000.9	A	17.1	2.66	44.5	29.1	7.4	15587	PRKM
E393	Powder River	4900525627	1 BARLOW 21-20	LOUISIANA LAND & EXP	WY	48N	75W	20	NENW	7001.1	A	17.0	2.67	41.9	34.6	1.7	15587	PRKM
E393	Powder River	4900525627	1 BARLOW 21-20	LOUISIANA LAND & EXP	WY	48N	75W	20	NENW	7001.1	B	17.4	2.68	41.6	28.9	5.3	15587	PRKM
E393	Powder River	4900525627	1 BARLOW 21-20	LOUISIANA LAND & EXP	WY	48N	75W	20	NENW	7008.1	A	16.6	2.66	32.5	23.6	5.8	15577	PRKM
E393	Powder River	4900525627	1 BARLOW 21-20	LOUISIANA LAND & EXP	WY	48N	75W	20	NENW	7008.1	B	16.6	2.65	30.5	21.0	4.8	15577	PRKM
E393	Powder River	4900525627	1 BARLOW 21-20	LOUISIANA LAND & EXP	WY	48N	75W	20	NENW	7012.0	B	6.2	2.72	0.00155			14276	PRKM
E393	Powder River	4900525627	1 BARLOW 21-20	LOUISIANA LAND & EXP	WY	48N	75W	20	NENW	7012.0	A	6.2	2.70	0.00140	0.000068	291	14276	PRKM
E393	Powder River	4900525627	1 BARLOW 21-20	LOUISIANA LAND & EXP	WY	48N	75W	20	NENW	7012.2	B	6.1	2.66	0.00256	0.000090	75.9	14276	PRKM
E393	Powder River	4900525627	1 BARLOW 21-20	LOUISIANA LAND & EXP	WY	48N	75W	20	NENW	7012.2	A	5.9	2.71	0.000959	0.000019	481	14276	PRKM
E393	Powder River	4900525627	1 BARLOW 21-20	LOUISIANA LAND & EXP	WY	48N	75W	20	NENW	7013.9	A	16.6	2.65	25.4	20.2	2.7	15587	PRKM
E393	Powder River	4900525627	1 BARLOW 21-20	LOUISIANA LAND & EXP	WY	48N	75W	20	NENW	7013.9	B	17.0	2.66	23.2	16.3	5.9	15587	PRKM
E393	Powder River	4900525627	1 BARLOW 21-20	LOUISIANA LAND & EXP	WY	48N	75W	20	NENW	7014.1	A	17.2	2.66	21.8	16.8	3.3	15587	PRKM
E393	Powder River	4900525627	1 BARLOW 21-20	LOUISIANA LAND & EXP	WY	48N	75W	20	NENW	7014.1	B	17.3	2.66	20.6	12.9	9.3	15587	PRKM
E393	Powder River	4900525627	1 BARLOW 21-20	LOUISIANA LAND & EXP	WY	48N	75W	20	NENW	7019.9	B	9.9	2.69	0.149	0.0745	26.9	15285	PRKM
E393	Powder River	4900525627	1 BARLOW 21-20	LOUISIANA LAND & EXP	WY	48N	75W	20	NENW	7019.9	A	9.0	2.68	0.127	0.0577	65.1	15285	PRKM
E393	Powder River	4900525627	1 BARLOW 21-20	LOUISIANA LAND & EXP	WY	48N	75W	20	NENW	7027.0	B	15.0	2.68	4.00	2.65	11.4	14286	PRKM
E393	Powder River	4900525627	1 BARLOW 21-20	LOUISIANA LAND & EXP	WY	48N	75W	20	NENW	7027.0	A	15.3	2.69	3.95	2.45	19.2	14286	PRKM
E393	Powder River	4900525627	1 BARLOW 21-20	LOUISIANA LAND & EXP	WY	48N	75W	20	NENW	7027.2	A	14.7	2.68	4.07	2.53	11.8	14286	PRKM
E393	Powder River	4900525627	1 BARLOW 21-20	LOUISIANA LAND & EXP	WY	48N	75W	20	NENW	7027.2	B	15.0	2.70	3.24	1.93	17.1	14286	PRKM
E393	Powder River	4900525627	1 BARLOW 21-20	LOUISIANA LAND & EXP	WY	48N	75W	20	NENW	7039.2	B	17.1	2.70	8.59	6.21	5.6	14286	PRKM
E393	Powder River	4900525627	1 BARLOW 21-20	LOUISIANA LAND & EXP	WY	48N	75W	20	NENW	7039.2	A	16.6	2.68	8.32	6.28	6.3	14286	PRKM
E393	Powder River	4900525627	1 BARLOW 21-20	LOUISIANA LAND & EXP	WY	48N	75W	20	NENW	7039.4	A	16.6	2.69	9.03	6.29	8.2	14286	PRKM
E393	Powder River	4900525627	1 BARLOW 21-20	LOUISIANA LAND & EXP	WY	48N	75W	20	NENW	7039.4	B	16.6	2.69	8.92	7.50	1.7	14286	PRKM
E393	Powder River	4900525627	1 BARLOW 21-20	LOUISIANA LAND & EXP	WY	48N	75W	20	NENW	7052.9	B	23.8	2.71	11.1	7.67	5.4	14597	PRKM
E393	Powder River	4900525627	1 BARLOW 21-20	LOUISIANA LAND & EXP	WY	48N	75W	20	NENW	7052.9	A	23.6	2.70	9.88	6.90	6.3	14597	PRKM
E393	Powder River	4900525627	1 BARLOW 21-20	LOUISIANA LAND & EXP	WY	48N	75W	20	NENW	7053.0	A	23.7	2.70	9.72	7.37	3.5	14597	PRKM
E393	Powder River	4900525627	1 BARLOW 21-20	LOUISIANA LAND & EXP	WY	48N	75W	20	NENW	7053.0	B	23.8	2.70	9.71	5.98	9.6	14597	PRKM
E393	Powder River	4900525627	1 BARLOW 21-20	LOUISIANA LAND & EXP	WY	48N	75W	20	NENW	7060.1	A	6.4	2.67	0.00430	0.000281	489	12285	PRKM
E393	Powder River	4900525627	1 BARLOW 21-20	LOUISIANA LAND & EXP	WY	48N	75W	20	NENW	7060.1	B	7.0	2.68	0.00255	0.000230	201	12285	PRKM
E393	Powder River	4900525627	1 BARLOW 21-20	LOUISIANA LAND & EXP	WY	48N	75W	20	NENW	7060.4	B	15.4	2.68	0.128	0.0669	16.2	13285	PRKM
E393	Powder River	4900525627	1 BARLOW 21-20	LOUISIANA LAND & EXP	WY	48N	75W	20	NENW	7060.4	A	14.5	2.66	0.110	0.0564	30.0	13285	PRKM
E393	Powder River	4900525627	1 BARLOW 21-20	LOUISIANA LAND & EXP	WY	48N	75W	20	NENW	7060.6	A	16.1	2.67	4.19	2.74	9.4	13285	PRKM
E393	Powder River	4900525627	1 BARLOW 21-20	LOUISIANA LAND & EXP	WY	48N	75W	20	NENW	7060.6	B	15.9	2.67	0.253	0.126	51.8	13285	PRKM
E393	Powder River	4900525627	1 BARLOW 21-20	LOUISIANA LAND & EXP	WY	48N	75W	20	NENW	7076.6	B	15.0	2.69	2.77	1.88	9.5	14297	PRKM
E393	Powder River	4900525627	1 BARLOW 21-20	LOUISIANA LAND & EXP	WY	48N	75W	20	NENW	7076.6	A	22.4	2.69	1.50	1.03	16.8	14297	PRKM
E393	Powder River	4900525627	1 BARLOW 21-20	LOUISIANA LAND & EXP	WY	48N	75W	20	NENW	7076.7	B	21.8	2.70	2.85	1.77	15.3	14297	PRKM
E393	Powder River	4900525627	1 BARLOW 21-20	LOUISIANA LAND & EXP	WY	48N	75W	20	NENW	7076.7	A	22.6	2.70	1.88	1.28	6.1	14297	PRKM
E932	Powder River	4900921513	2 FRED STATE	DAVIS OIL COMPANY	WY	35N	70W	36	NESESW	7538.0	B	16.7	2.65	3.15	2.02	10.8	13517	TPOT
E932	Powder River	4900921513	2 FRED STATE	DAVIS OIL COMPANY	WY	35N	70W	36	NESESW	7538.0	A	15.9	2.66	1.64	0.940	15.9	13517	TPOT
E932	Powder River	4900921513	2 FRED STATE	DAVIS OIL COMPANY	WY	35N	70W	36	NESESW	7544.1	A	16.6	2.67	5.30	3.53	9.2	15597	TPOT
E932	Powder River	4900921513	2 FRED STATE	DAVIS OIL COMPANY	WY	35N	70W	36	NESESW	7544.1	B	16.7	2.67	4.93	3.35	9.7	15597	TPOT
E932	Powder River	4900921513	2 FRED STATE	DAVIS OIL COMPANY	WY	35N	70W	36	NESESW	7544.3	A	16.4	2.66	4.80	3.13	11.5	15597	TPOT
E932	Powder River	4900921513	2 FRED STATE	DAVIS OIL COMPANY	WY	35N	70W	36	NESESW	7544.3	B	16.6	2.68	4.36	2.98	6.2	15597	TPOT
E932	Powder River	4900921513	2 FRED STATE	DAVIS OIL COMPANY	WY	35N	70W	36	NESESW	7546.7	B	13.4	2.69	0.118	0.0559	33.0	13217	TPOT
E932	Powder River	4900921513	2 FRED STATE	DAVIS OIL COMPANY	WY	35N	70W	36	NESESW	7546.7	A	13.1	2.67	0.0944	0.0407	53.9	13217	TPOT
E932	Powder River	4900921513	2 FRED STATE	DAVIS OIL COMPANY	WY	35N	70W	36	NESESW	7546.9	A	10.5	2.69	0.0583	0.0192	264	13217	TPOT
E932	Powder River	4900921513	2 FRED STATE	DAVIS OIL COMPANY	WY	35N	70W	36	NESESW	7546.9	B	10.3	2.75	0.0256	0.00809	72.2	13217	TPOT
E932	Powder River	4900921513	2 FRED STATE	DAVIS OIL COMPANY	WY	35N	70W	36	NESESW	7549.9	B	3.3	2.71	0.00213	0.000051	784	15295	TPOT
E932	Powder River	4900921513	2 FRED STATE	DAVIS OIL COMPANY	WY	35N	70W	36	NESESW	7549.9	A	2.6	2.70	0.00192	0.000152	285	15295	TPOT
E932	Powder River	4900921513	2 FRED STATE	DAVIS OIL COMPANY	WY	35N	70W	36	NESESW	7550.1	B	4.0	2.71	0.00287	0.000191	206	15295	TPOT
E932	Powder River	4900921513	2 FRED STATE	DAVIS OIL COMPANY	WY	35N	70W	36	NESESW	7550.1	A	3.4	2.71	0.00194	0.000146	185	15295	TPOT
E932	Powder River	4900921513	2 FRED STATE	DAVIS OIL COMPANY	WY	35N	70W	36	NESESW	7557.1	A	12.4	2.67	0.0195	0.00259	213	13217	TPOT
E932	Powder River	4900921513	2 FRED STATE	DAVIS OIL COMPANY	WY	35N	70W	36	NESESW	7557.1	B	13.2	2.70	0.0131	0.00217	139	13217	TPOT
E932	Powder River	4900921513	2 FRED STATE	DAVIS OIL COMPANY	WY	35N	70W	36	NESESW	7557.4	B	12.8	2.68	0.0280	0.00647	103	13217	TPOT
E932	Powder River	4900921513	2 FRED STATE	DAVIS OIL COMPANY	WY	35N	70W	36	NESESW	7557.4	A	12.0	2.67	0.0143	0.00217	182	13217	TPOT
E932	Powder River	4900921513	2 FRED STATE	DAVIS OIL COMPANY	WY	35N	70W	36	NESESW	7560.0	A	16.0	2.67	0.0205	0.00416	79.1	15297	TPOT
E932	Powder River	4900921513	2 FRED STATE	DAVIS OIL COMPANY	WY	35N	70W	36	NESESW	7560.0	B	16.3	2.68	0.0201	0.00251	116	15297	TPOT
E932	Powder River	4900921513	2 FRED STATE	DAVIS OIL COMPANY	WY	35N	70W	36	NESESW	7568.1	B	16.7	2.66	0.0478	0.00635	78.4	15587	TPOT
E932	Powder River	4900921513	2 FRED STATE	DAVIS OIL COMPANY	WY	35N	70W	36	NESESW	7568.1	A	16.2	2.66	0.0244	0.00609	56.6	15587	TPOT
E932	Powder River	4900921513	2 FRED STATE	DAVIS OIL COMPANY	WY	35N	70W	36	NESESW	7568.3	A	13.8	2.60	0.0705	0.0120	70.0	13587	TPOT
E932	Powder River	4900921513	2 FRED STATE	DAVIS OIL COMPANY	WY	35N	70W	36	NESESW	7568.3	B	15.1	2.67	0.0461	0.00472	136	13587	TPOT

Table 4.1.1. (continued)

Summary of Porosity, Permeability, and Grain Density
Analysis of Critical Permeability, Capillary Pressure, and Electrical Properties for Mesaverde Tight Gas Sandstones from Western U.S. Basins
US DOE # DE-FC26-05NT42660
Alan P. Byrnes, Robert M. Cluff, John C. Webb, Daniel A. Krygowski, Stefani D. Whittaker
website: http://www.kgs.ku.edu/mesaverde

USGS Library Number	Basin	API Number	Well Name	Operator	State	Township	Range	Section	Quarter Section	Plug Depth	Plug Letter	Ambient Porosity	Grain Density	Routine Gas Permeability	*in situ* Klinkenberg Gas Permeability	*in situ* Klinken-berg *constant* b	Rock Type Code	Formations
										ft	A/B/C	%	g/cc	mD	mD	(psia)		
E932	Powder River	4900921513	2 FRED STATE	DAVIS OIL COMPANY	WY	35N	70W	36	NESESW	7568.5	A	15.2	2.71	0.0291	0.00660	120	15597	TPOT
E932	Powder River	4900921513	2 FRED STATE	DAVIS OIL COMPANY	WY	35N	70W	36	NESESW	7568.5	B	16.0	2.67	0.0257	0.00539	96.4	15597	TPOT
E932	Powder River	4900921513	2 FRED STATE	DAVIS OIL COMPANY	WY	35N	70W	36	NESESW	7579.1	B	16.9	2.67	0.0291	0.00563	81.1	15597	TPOT
E932	Powder River	4900921513	2 FRED STATE	DAVIS OIL COMPANY	WY	35N	70W	36	NESESW	7579.1	A	16.5	2.66	0.0255	0.00529	117	15597	TPOT
S835	Powder River	4900906335	2 SHAWNEE	BELCO PETROLEUM	WY	33N	69W	2	NENW	6946.1	A	15.6	2.65	5.81	2.59	8.3	14286	TPOT
S835	Powder River	4900906335	2 SHAWNEE	BELCO PETROLEUM	WY	33N	69W	2	NENW	6946.1	B	16.5	2.66	7.14	5.33	6.2	14286	TPOT
S835	Powder River	4900906335	2 SHAWNEE	BELCO PETROLEUM	WY	33N	69W	2	NENW	6946.2	A	14.3	2.65	2.96	2.17	11.5	14286	TPOT
S835	Powder River	4900906335	2 SHAWNEE	BELCO PETROLEUM	WY	33N	69W	2	NENW	6946.2	B	13.7	2.66	1.83	1.08	21.6	14286	TPOT
S835	Powder River	4900906335	2 SHAWNEE	BELCO PETROLEUM	WY	33N	69W	2	NENW	6956.1	A	15.2	2.65	2.34	1.62	11.6	13216	TPOT
S835	Powder River	4900906335	2 SHAWNEE	BELCO PETROLEUM	WY	33N	69W	2	NENW	6956.1	B	16.2	2.66	3.36	1.33	15.8	13216	TPOT
S835	Powder River	4900906335	2 SHAWNEE	BELCO PETROLEUM	WY	33N	69W	2	NENW	6956.2	A	13.8	2.64	0.371	0.235	9.9	13216	TPOT
S835	Powder River	4900906335	2 SHAWNEE	BELCO PETROLEUM	WY	33N	69W	2	NENW	6956.2	B	15.3	2.66	0.875	0.558	16.1	13216	TPOT
S835	Powder River	4900906335	2 SHAWNEE	BELCO PETROLEUM	WY	33N	69W	2	NENW	6957.8	A	16.9	2.66	0.0262	0.00564	124	15297	TPOT
S835	Powder River	4900906335	2 SHAWNEE	BELCO PETROLEUM	WY	33N	69W	2	NENW	6957.8	B	17.0	2.67	0.0240	0.00507	122	15297	TPOT
S835	Powder River	4900906335	2 SHAWNEE	BELCO PETROLEUM	WY	33N	69W	2	NENW	6957.9	A	16.7	2.66	0.0230	0.00509	86.2	15297	TPOT
S835	Powder River	4900906335	2 SHAWNEE	BELCO PETROLEUM	WY	33N	69W	2	NENW	6957.9	B	16.9	2.68	0.0268	0.00535	71.6	15297	TPOT
S835	Powder River	4900906335	2 SHAWNEE	BELCO PETROLEUM	WY	33N	69W	2	NENW	6966.1	A	10.0	2.65	0.0283	0.00878	82.5	13216	TPOT
S835	Powder River	4900906335	2 SHAWNEE	BELCO PETROLEUM	WY	33N	69W	2	NENW	6966.1	B	11.7	2.67	0.0428	0.0185	44.7	13216	TPOT
S835	Powder River	4900906335	2 SHAWNEE	BELCO PETROLEUM	WY	33N	69W	2	NENW	6968.1	A	8.9	2.64	0.0449	0.0140	40.4	13215	TPOT
S835	Powder River	4900906335	2 SHAWNEE	BELCO PETROLEUM	WY	33N	69W	2	NENW	6968.1	B	9.0	2.65	0.0312	0.0110	77.2	13215	TPOT
S835	Powder River	4900906335	2 SHAWNEE	BELCO PETROLEUM	WY	33N	69W	2	NENW	6975.1	A	9.8	2.66	0.0620	0.0338	40.0	15277	TPOT
S835	Powder River	4900906335	2 SHAWNEE	BELCO PETROLEUM	WY	33N	69W	2	NENW	6975.1	B	9.4	2.68	0.0406	0.0160	164	15277	TPOT
S835	Powder River	4900906335	2 SHAWNEE	BELCO PETROLEUM	WY	33N	69W	2	NENW	6978.8	A	7.6	2.68	0.0319	0.0117	75.6	15585	TPOT
S835	Powder River	4900906335	2 SHAWNEE	BELCO PETROLEUM	WY	33N	69W	2	NENW	6978.8	B	1.2	2.50	0.138	0.0147	79.8	15585	TPOT
S835	Powder River	4900906335	2 SHAWNEE	BELCO PETROLEUM	WY	33N	69W	2	NENW	6978.9	A	13.0	2.67	0.507	0.294	35.5	15585	TPOT
S835	Powder River	4900906335	2 SHAWNEE	BELCO PETROLEUM	WY	33N	69W	2	NENW	6978.9	B	11.5	2.65	0.701	0.415	19.2	15585	TPOT
S835	Powder River	4900906335	2 SHAWNEE	BELCO PETROLEUM	WY	33N	69W	2	NENW	6979.0	A	16.6	2.64	1.56	0.958	18.4	13287	TPOT
S835	Powder River	4900906335	2 SHAWNEE	BELCO PETROLEUM	WY	33N	69W	2	NENW	6979.0	B	17.5	2.66	1.86	1.11	14.5	13287	TPOT
S835	Powder River	4900906335	2 SHAWNEE	BELCO PETROLEUM	WY	33N	69W	2	NENW	6982.8	A	13.5	2.65	1.95	1.32	13.3	15287	TPOT
S835	Powder River	4900906335	2 SHAWNEE	BELCO PETROLEUM	WY	33N	69W	2	NENW	6982.8	B	13.2	2.67	1.31	0.911	5.4	15287	TPOT
S835	Powder River	4900906335	2 SHAWNEE	BELCO PETROLEUM	WY	33N	69W	2	NENW	6982.9	A	11.6	2.66	0.760	0.547	8.8	15285	TPOT
S835	Powder River	4900906335	2 SHAWNEE	BELCO PETROLEUM	WY	33N	69W	2	NENW	6982.9	B	12.8	2.67	1.34	0.812	19.6	15285	TPOT
S835	Powder River	4900906335	2 SHAWNEE	BELCO PETROLEUM	WY	33N	69W	2	NENW	6990.1	A	6.4	2.66	0.00307	0.000076	1211	13287	TPOT
S835	Powder River	4900906335	2 SHAWNEE	BELCO PETROLEUM	WY	33N	69W	2	NENW	6990.1	B	6.1	2.65	0.00401	0.000264	229	13287	TPOT
S835	Powder River	4900906335	2 SHAWNEE	BELCO PETROLEUM	WY	33N	69W	2	NENW	6991.2	A	9.0	2.65	0.0406	0.00763	140	13217	TPOT
S835	Powder River	4900906335	2 SHAWNEE	BELCO PETROLEUM	WY	33N	69W	2	NENW	6991.2	B	8.6	2.64	0.0339	0.00633	134	13217	TPOT
S835	Powder River	4900906335	2 SHAWNEE	BELCO PETROLEUM	WY	33N	69W	2	NENW	6992.0	A	1.9	2.55	0.00321	0.000037	752	12217	TPOT
S838	Powder River	4900905481	3 SHAWNEE	BELCO PETROLEUM	WY	33N	69W	23	C SENE	6977.9	A	4.1	2.72	0.00124	0.000068	393	15275	TPOT
S838	Powder River	4900905481	3 SHAWNEE	BELCO PETROLEUM	WY	33N	69W	23	C SENE	6977.9	B	4.3	2.72	0.00116	0.000131	250	15275	TPOT
S838	Powder River	4900905481	3 SHAWNEE	BELCO PETROLEUM	WY	33N	69W	23	C SENE	6979.9	B	15.7	2.77	0.0598	0.0170	45.8	13216	TPOT
S838	Powder River	4900905481	3 SHAWNEE	BELCO PETROLEUM	WY	33N	69W	23	C SENE	6979.9	A	11.2	2.65	0.0461	0.0153	134	13216	TPOT
S838	Powder River	4900905481	3 SHAWNEE	BELCO PETROLEUM	WY	33N	69W	23	C SENE	6982.1	A	7.1	2.67	0.0200	0.00451	275	15285	TPOT
S838	Powder River	4900905481	3 SHAWNEE	BELCO PETROLEUM	WY	33N	69W	23	C SENE	6982.1	B	7.6	2.68	0.0150	0.00406	293	15285	TPOT
S838	Powder River	4900905481	3 SHAWNEE	BELCO PETROLEUM	WY	33N	69W	23	C SENE	6985.7	A	7.8	2.67	0.0103	0.000798	243	13286	TPOT
S838	Powder River	4900905481	3 SHAWNEE	BELCO PETROLEUM	WY	33N	69W	23	C SENE	6985.7	B	8.0	2.67	0.00882	0.00123	51.9	13286	TPOT
S838	Powder River	4900905481	3 SHAWNEE	BELCO PETROLEUM	WY	33N	69W	23	C SENE	6985.8	B	6.5	2.68	0.00743	0.000925	168	13286	TPOT
S838	Powder River	4900905481	3 SHAWNEE	BELCO PETROLEUM	WY	33N	69W	23	C SENE	6985.8	A	5.5	2.68	0.00735	0.000378	223	13286	TPOT
S838	Powder River	4900905481	3 SHAWNEE	BELCO PETROLEUM	WY	33N	69W	23	C SENE	6988.0	B	18.3	2.66	9.91	5.61	15.8	15296	TPOT
S838	Powder River	4900905481	3 SHAWNEE	BELCO PETROLEUM	WY	33N	69W	23	C SENE	6988.0	A	17.3	2.65	8.24	5.15	16.1	15296	TPOT
S838	Powder River	4900905481	3 SHAWNEE	BELCO PETROLEUM	WY	33N	69W	23	C SENE	6995.9	A	11.8	2.64	0.0739	0.0377	50.7	13216	TPOT
S838	Powder River	4900905481	3 SHAWNEE	BELCO PETROLEUM	WY	33N	69W	23	C SENE	6995.9	B	13.5	2.66	0.0693	0.0340	61.0	13216	TPOT
S838	Powder River	4900905481	3 SHAWNEE	BELCO PETROLEUM	WY	33N	69W	23	C SENE	6996.0	A	12.8	2.65	0.991	0.639	17.7	15216	TPOT
S838	Powder River	4900905481	3 SHAWNEE	BELCO PETROLEUM	WY	33N	69W	23	C SENE	6996.0	B	13.7	2.66	0.452	0.295	17.8	15216	TPOT
S838	Powder River	4900905481	3 SHAWNEE	BELCO PETROLEUM	WY	33N	69W	23	C SENE	6996.9	A	11.1	2.64	0.0220	0.00584	40.3	13216	TPOT
S838	Powder River	4900905481	3 SHAWNEE	BELCO PETROLEUM	WY	33N	69W	23	C SENE	6996.9	B	11.7	2.66	0.0141	0.00315	136	13216	TPOT
S838	Powder River	4900905481	3 SHAWNEE	BELCO PETROLEUM	WY	33N	69W	23	C SENE	6998.5	B	6.3	2.64	0.0200	0.00159	48.3	12216	TPOT
S838	Powder River	4900905481	3 SHAWNEE	BELCO PETROLEUM	WY	33N	69W	23	C SENE	6998.5	A	5.8	2.63	0.0138	0.00121	207	12216	TPOT
T715	Sand Wash	0508106724	1-791-2613 Craig Dome	COCKRELL OIL CORP	CO	7N	91W	26	NESWSW	3465.9	B	16.9	2.64	22.4	9.67	10.5	13266	WMFK
T715	Sand Wash	0508106724	1-791-2613 Craig Dome	COCKRELL OIL CORP	CO	7N	91W	26	NESWSW	3465.9	A	16.7	2.64	17.4	12.1	8.5	13266	WMFK
T715	Sand Wash	0508106724	1-791-2613 Craig Dome	COCKRELL OIL CORP	CO	7N	91W	26	NESWSW	3467.1	A	17.3	2.64	15.3	8.04	28.3	15557	WMFK
T715	Sand Wash	0508106724	1-791-2613 Craig Dome	COCKRELL OIL CORP	CO	7N	91W	26	NESWSW	3467.2	A	17.1	2.64				15557	WMFK
T715	Sand Wash	0508106724	1-791-2613 Craig Dome	COCKRELL OIL CORP	CO	7N	91W	26	NESWSW	3467.3	A	17.0	2.64	18.8	12.7	6.4	15557	WMFK
T715	Sand Wash	0508106724	1-791-2613 Craig Dome	COCKRELL OIL CORP	CO	7N	91W	26	NESWSW	3467.4	A	17.5	2.64	30.4	23.4	5.0	15577	WMFK
T715	Sand Wash	0508106724	1-791-2613 Craig Dome	COCKRELL OIL CORP	CO	7N	91W	26	NESWSW	3467.6	A	17.3	2.64	39.4	30.1	5.5	15577	WMFK
T715	Sand Wash	0508106724	1-791-2613 Craig Dome	COCKRELL OIL CORP	CO	7N	91W	26	NESWSW	3467.8	A	16.4	2.64	4.40	2.89	5.3	13277	WMFK
T715	Sand Wash	0508106724	1-791-2613 Craig Dome	COCKRELL OIL CORP	CO	7N	91W	26	NESWSW	3467.9	A	16.4	2.64	4.62	2.97	7.4	13277	WMFK
T715	Sand Wash	0508106724	1-791-2613 Craig Dome	COCKRELL OIL CORP	CO	7N	91W	26	NESWSW	3469.2	A	17.8	2.64	37.2	30.2	1.8	15577	WMFK
T715	Sand Wash	0508106724	1-791-2613 Craig Dome	COCKRELL OIL CORP	CO	7N	91W	26	NESWSW	3469.2	B	17.9	2.64	33.6	27.2	2.6	15577	WMFK
T715	Sand Wash	0508106724	1-791-2613 Craig Dome	COCKRELL OIL CORP	CO	7N	91W	26	NESWSW	3470.8	A	16.5	2.66	21.3	16.7	6.5	13577	WMFK
T715	Sand Wash	0508106724	1-791-2613 Craig Dome	COCKRELL OIL CORP	CO	7N	91W	26	NESWSW	3470.9	A	17.1	2.67	26.9	17.7	13.1	13577	WMFK
T717	Sand Wash	0508106718	1-691-0513 West Craig	COCKRELL OIL CORP	CO	6N	91W	5	SESWSW	1732.9	A	3.5	2.59	0.0861	0.00390	55.4	11219	WMFK
T717	Sand Wash	0508106718	1-691-0513 West Craig	COCKRELL OIL CORP	CO	6N	91W	5	SESWSW	1732.9	B	4.1	2.59	0.0137	0.000304	299	11219	WMFK
T717	Sand Wash	0508106718	1-691-0513 West Craig	COCKRELL OIL CORP	CO	6N	91W	5	SESWSW	1733.0	A	5.8	2.65	0.0693	0.0247	42.8	12226	WMFK
T717	Sand Wash	0508106718	1-691-0513 West Craig	COCKRELL OIL CORP	CO	6N	91W	5	SESWSW	1733.0	B	17.9	2.63	0.00591	0.00102	269	12226	WMFK
T717	Sand Wash	0508106718	1-691-0513 West Craig	COCKRELL OIL CORP	CO	6N	91W	5	SESWSW	1733.8	A	3.9	2.61	0.00617	0.000172	281	12216	WMFK
T717	Sand Wash	0508106718	1-691-0513 West Craig	COCKRELL OIL CORP	CO	6N	91W	5	SESWSW	1733.8	B	4.7	2.62	0.00415	0.000303	214	12216	WMFK
T717	Sand Wash	0508106718	1-691-0513 West Craig	COCKRELL OIL CORP	CO	6N	91W	5	SESWSW	1734.0	A	4.2	2.62	0.00490	0.000277	283	12216	WMFK
T717	Sand Wash	0508106718	1-691-0513 West Craig	COCKRELL OIL CORP	CO	6N	91W	5	SESWSW	1734.0	B	4.8	2.63	0.00338	0.000300	248	12216	WMFK
T717	Sand Wash	0508106718	1-691-0513 West Craig	COCKRELL OIL CORP	CO	6N	91W	5	SESWSW	1747.9	A	6.0	2.59	0.0124	0.00126	171	13225	WMFK
T717	Sand Wash	0508106718	1-691-0513 West Craig	COCKRELL OIL CORP	CO	6N	91W	5	SESWSW	1747.9	B	5.1	2.65	0.00317	0.000168	527	13225	WMFK
T717	Sand Wash	0508106718	1-691-0513 West Craig	COCKRELL OIL CORP	CO	6N	91W	5	SESWSW	1749.9	A	5.8	2.61				12229	WMFK
T717	Sand Wash	0508106718	1-691-0513 West Craig	COCKRELL OIL CORP	CO	6N	91W	5	SESWSW	1750.1	A	6.3	2.63	0.00777	0.00131	133	13226	WMFK
T717	Sand Wash	0508106718	1-691-0513 West Craig	COCKRELL OIL CORP	CO	6N	91W	5	SESWSW	1750.1	B	6.9	2.65	0.00592	0.00118	114	13226	WMFK
T717	Sand Wash	0508106718	1-691-0513 West Craig	COCKRELL OIL CORP	CO	6N	91W	5	SESWSW	1750.7	A	4.6	2.62	0.365	0.0121	113	13226	WMFK
B646	Uinta	4304730584	11-17F RIVER BEND UNIT	MAPCO INCOPORATED	UT	10S	20E	17	SENENW	7287.7	A	6.5	2.65	0.114	0.0148	68.1	17286	MVRD
B646	Uinta	4304730584	11-17F RIVER BEND UNIT	MAPCO INCOPORATED	UT	10S	20E	17	SENENW	7287.7	B	4.7	2.61	0.0859	0.0151	87.7	17286	MVRD
B646	Uinta	4304730584	11-17F RIVER BEND UNIT	MAPCO INCOPORATED	UT	10S	20E	17	SENENW	8229.7	B	7.9	2.65	0.0422	0.00629	124	16286	MVRD
B646	Uinta	4304730584	11-17F RIVER BEND UNIT	MAPCO INCOPORATED	UT	10S	20E	17	SENENW	8229.7	A	7.4	2.64	0.0380	0.00406	32.5	16286	MVRD
B646	Uinta	4304730584	11-17F RIVER BEND UNIT	MAPCO INCOPORATED	UT	10S	20E	17	SENENW	8233.0	A	5.7	2.65	0.0415	0.00466	92.1	16296	MVRD
B646	Uinta	4304730584	11-17F RIVER BEND UNIT	MAPCO INCOPORATED	UT	10S	20E	17	SENENW	8233.0	B	5.8	2.65	0.0344	0.00464	125	16296	MVRD
B646	Uinta	4304730584	11-17F RIVER BEND UNIT	MAPCO INCOPORATED	UT	10S	20E	17	SENENW	8233.7	A	5.6	2.65	0.0416	0.00399	112	16296	MVRD
B646	Uinta	4304730584	11-17F RIVER BEND UNIT	MAPCO INCOPORATED	UT	10S	20E	17	SENENW	8233.7	B	5.5	2.65	0.0365	0.00464	131	16296	MVRD
B646	Uinta	4304730584	11-17F RIVER BEND UNIT	MAPCO INCOPORATED	UT	10S	20E	17	SENENW	8236.9	B	5.5	2.67	0.0246	0.00163	237	15276	MVRD
B646	Uinta	4304730584	11-17F RIVER BEND UNIT	MAPCO INCOPORATED	UT	10S	20E	17	SENENW	8236.9	A	5.3	2.66	0.0197	0.00170	385	15276	MVRD
B646	Uinta	4304730584	11-17F RIVER BEND UNIT	MAPCO INCOPORATED	UT	10S	20E	17	SENENW	8245.1	A	2.6	2.68	0.00786	0.000781	109	13296	MVRD
B646	Uinta	4304730584	11-17F RIVER BEND UNIT	MAPCO INCOPORATED	UT	10S	20E	17	SENENW	8245.1	B	3.0	2.69	0.00676	0.000580	490	13296	MVRD
B646	Uinta	4304730584	11-17F RIVER BEND UNIT	MAPCO INCOPORATED	UT	10S	20E	17	SENENW	8282.8	B	2.5	2.67	0.00682	0.000165	264	12219	MVRD
B646	Uinta	4304730584	11-17F RIVER BEND UNIT	MAPCO INCOPORATED	UT	10S	20E	17	SENENW	8282.8	A	1.7	2.65	0.00534	0.000091	205	12219	MVRD
B646	Uinta	4304730584	11-17F RIVER BEND UNIT	MAPCO INCOPORATED	UT	10S	20E	17	SENENW	8287.4	A	8.2	2.66	0.134	0.0187	83.7	16277	MVRD
B646	Uinta	4304730584	11-17F RIVER BEND UNIT	MAPCO INCOPORATED	UT	10S	20E	17	SENENW	8287.4	B	7.5	2.64	0.131	0.0217	74.8	16277	MVRD
B646	Uinta	4304730584	11-17F RIVER BEND UNIT	MAPCO INCOPORATED	UT	10S	20E	17	SENENW	8287.8	A	6.4	2.65	0.0943	0.0112	143	16276	MVRD
B646	Uinta	4304730584	11-17F RIVER BEND UNIT	MAPCO INCOPORATED	UT	10S	20E	17	SENENW	8287.8	B	6.3	2.65	0.0702	0.0124	85.0	16276	MVRD
B646	Uinta	4304730584	11-17F RIVER BEND UNIT	MAPCO INCOPORATED	UT	10S	20E	17	SENENW	8294.2	B	7.6	2.65	0.288	0.0344	73.9	16277	MVRD
B646	Uinta	4304730584	11-17F RIVER BEND UNIT	MAPCO INCOPORATED	UT	10S	20E	17	SENENW	8294.2	A	7.8	2.65	0.229	0.0283	62.0	16277	MVRD
B646	Uinta	4304730584	11-17F RIVER BEND UNIT	MAPCO INCOPORATED	UT	10S	20E	17	SENENW	8294.4	A	7.7	2.65	0.188	0.0252	89.6	16277	MVRD
B646	Uinta	4304730584	11-17F RIVER BEND UNIT	MAPCO INCOPORATED	UT	10S	20E	17	SENENW	8294.4	B	7.6	2.65	0.169	0.0220	52.2	16277	MVRD
B646	Uinta	4304730584	11-17F RIVER BEND UNIT	MAPCO INCOPORATED	UT	10S	20E	17	SENENW	8302.5	A	1.0	2.67	0.00361	0.000112	142	13265	MVRD
B646	Uinta	4304730584	11-17F RIVER BEND UNIT	MAPCO INCOPORATED	UT	10S	20E	17	SENENW	8302.5	B	1.8	2.69	0.00274	0.000056	309	13265	MVRD
B646	Uinta	4304730584	11-17F RIVER BEND UNIT	MAPCO INCOPORATED	UT	10S	20E	17	SENENW	8305.8	B	6.9	2.69	0.0233	0.00292	139	15266	MVRD
B646	Uinta	4304730584	11-17F RIVER BEND UNIT	MAPCO INCOPORATED	UT	10S	20E	17	SENENW	8305.8	A	6.4	2.68	0.0212	0.00255	151	15266	MVRD
B646	Uinta	4304730584	11-17F RIVER BEND UNIT	MAPCO INCOPORATED	UT	10S	20E	17	SENENW	8362.3	B	8.9	2.66	0.112	0.0143	80.1	16296	MVRD
B646	Uinta	4304730584	11-17F RIVER BEND UNIT	MAPCO INCOPORATED	UT	10S	20E	17	SENENW	8362.3	A	8.5	2.65	0.0833	0.0127	104	16296	MVRD

Table 4.1.1. (continued)

Summary of Porosity, Permeability, and Grain Density
Analysis of Critical Permeability, Capillary Pressure, and Electrical Properties for Mesaverde Tight Gas Sandstones from Western U.S. Basins
US DOE # DE-FC26-05NT42660
Alan P. Byrnes, Robert M. Cluff, John C. Webb, Daniel A. Krygowski, Stefani D. Whittaker
website: http://www.kgs.ku.edu/mesaverde

USGS Library Number	Basin	API Number	Well Name	Operator	State	Township	Range	Section	Quarter Section	Plug Depth	Plug Letter	Ambient Porosity	Grain Density	Routine Gas Permeability	*in situ* Klinkenberg Gas Permeability	*in situ* Klinkenberg *constant* b	Rock Type Code	Formations
										ft	A/B/C	%	g/cc	mD	mD	(psia)		
B646	Uinta	4304730584	11-17F RIVER BEND UNIT	MAPCO INCOPORATED	UT	10S	20E	17	SENENW	8362.5	A	8.7	2.65	0.129	0.0131	212	16296	MVRD
B646	Uinta	4304730584	11-17F RIVER BEND UNIT	MAPCO INCOPORATED	UT	10S	20E	17	SENENW	8362.5	B	8.3	2.67	0.123	0.0133	92.1	16296	MVRD
B646	Uinta	4304730584	11-17F RIVER BEND UNIT	MAPCO INCOPORATED	UT	10S	20E	17	SENENW	8448.3	B	5.6	2.68	0.0152	0.00129	121	15266	MVRD
B646	Uinta	4304730584	11-17F RIVER BEND UNIT	MAPCO INCOPORATED	UT	10S	20E	17	SENENW	8448.3	A	5.6	2.68	0.0128	0.00159	121	15266	MVRD
B646	Uinta	4304730584	11-17F RIVER BEND UNIT	MAPCO INCOPORATED	UT	10S	20E	17	SENENW	8450.2	A	5.7	2.66	0.0408	0.00481	91.0	15266	MVRD
B646	Uinta	4304730584	11-17F RIVER BEND UNIT	MAPCO INCOPORATED	UT	10S	20E	17	SENENW	8450.2	B	6.0	2.67	0.0402	0.00602	85.1	15266	MVRD
E946	Uinta	4304730545	2-7 FLAT MESA	ENSERCH EXPLORATION	UT	10S	23E	7	NESENW	6344.9	B	2.4	2.58	0.255	0.00802	56.2	13216	MVRD
E946	Uinta	4304730545	2-7 FLAT MESA	ENSERCH EXPLORATION	UT	10S	23E	7	NESENW	6344.9	A	3.8	2.57	0.0699	0.000312	164	13216	MVRD
E946	Uinta	4304730545	2-7 FLAT MESA	ENSERCH EXPLORATION	UT	10S	23E	7	NESENW	6344.9	C	2.5	2.61	0.0106	0.000664	144	13216	MVRD
E946	Uinta	4304730545	2-7 FLAT MESA	ENSERCH EXPLORATION	UT	10S	23E	7	NESENW	6348.9	C	1.8	2.59	0.00820	0.000643	174	13216	MVRD
E946	Uinta	4304730545	2-7 FLAT MESA	ENSERCH EXPLORATION	UT	10S	23E	7	NESENW	6348.9	B	1.9	2.61				13216	MVRD
E946	Uinta	4304730545	2-7 FLAT MESA	ENSERCH EXPLORATION	UT	10S	23E	7	NESENW	6351.5	A	9.5	2.65	0.0931	0.00649	33.4	14266	MVRD
E946	Uinta	4304730545	2-7 FLAT MESA	ENSERCH EXPLORATION	UT	10S	23E	7	NESENW	6351.5	C	10.1	2.65	0.0782	0.00923	55.9	14266	MVRD
E946	Uinta	4304730545	2-7 FLAT MESA	ENSERCH EXPLORATION	UT	10S	23E	7	NESENW	6351.5	B	10.0	2.65	0.0761	0.00845	54.0	14266	MVRD
E946	Uinta	4304730545	2-7 FLAT MESA	ENSERCH EXPLORATION	UT	10S	23E	7	NESENW	6351.7	B	8.1	2.61	0.0725	0.00124	143	13266	MVRD
E946	Uinta	4304730545	2-7 FLAT MESA	ENSERCH EXPLORATION	UT	10S	23E	7	NESENW	6351.7	C	8.3	2.63	0.0572	0.000778	165	13266	MVRD
E946	Uinta	4304730545	2-7 FLAT MESA	ENSERCH EXPLORATION	UT	10S	23E	7	NESENW	6351.7	A	8.3	2.62	0.0552	0.00164	65.7	13266	MVRD
E946	Uinta	4304730545	2-7 FLAT MESA	ENSERCH EXPLORATION	UT	10S	23E	7	NESENW	6352.1	B	8.1	2.66	0.0314	0.000793	109	13276	MVRD
E946	Uinta	4304730545	2-7 FLAT MESA	ENSERCH EXPLORATION	UT	10S	23E	7	NESENW	6352.1	A	7.3	2.66	0.0287	0.00110	74.0	13276	MVRD
E946	Uinta	4304730545	2-7 FLAT MESA	ENSERCH EXPLORATION	UT	10S	23E	7	NESENW	6352.1	c	8.1	2.67	0.0246	0.000310	219	13276	MVRD
E946	Uinta	4304730545	2-7 FLAT MESA	ENSERCH EXPLORATION	UT	10S	23E	7	NESENW	6357.5	B	0.6	2.67	0.0126	0.00127	141	13266	MVRD
E946	Uinta	4304730545	2-7 FLAT MESA	ENSERCH EXPLORATION	UT	10S	23E	7	NESENW	6357.5	A	0.9	2.67	0.00348	0.000141	328	13266	MVRD
E946	Uinta	4304730545	2-7 FLAT MESA	ENSERCH EXPLORATION	UT	10S	23E	7	NESENW	6362.5	C	4.0	2.64	0.0248	0.000384	104	13246	MVRD
E946	Uinta	4304730545	2-7 FLAT MESA	ENSERCH EXPLORATION	UT	10S	23E	7	NESENW	6362.5	A	2.8	2.63	0.0217	0.000170	135	13246	MVRD
E946	Uinta	4304730545	2-7 FLAT MESA	ENSERCH EXPLORATION	UT	10S	23E	7	NESENW	6362.5	B	3.5	2.63	0.00509	0.000412	122	13246	MVRD
E946	Uinta	4304730545	2-7 FLAT MESA	ENSERCH EXPLORATION	UT	10S	23E	7	NESENW	6363.7	B	2.2	2.63	0.00547	0.000234	226	13276	MVRD
E946	Uinta	4304730545	2-7 FLAT MESA	ENSERCH EXPLORATION	UT	10S	23E	7	NESENW	6363.7	A	1.9	2.63	0.00214	0.000080	330	13276	MVRD
E946	Uinta	4304730545	2-7 FLAT MESA	ENSERCH EXPLORATION	UT	10S	23E	7	NESENW	6467.7	C	8.3	2.63	0.150	0.0282	47.1	13276	MVRD
E946	Uinta	4304730545	2-7 FLAT MESA	ENSERCH EXPLORATION	UT	10S	23E	7	NESENW	6468.4	C	12.0	2.64	0.900	0.390	18.0	16576	MVRD
E946	Uinta	4304730545	2-7 FLAT MESA	ENSERCH EXPLORATION	UT	10S	23E	7	NESENW	6468.4	A	12.1	2.63	0.884	0.434	9.6	16576	MVRD
E946	Uinta	4304730545	2-7 FLAT MESA	ENSERCH EXPLORATION	UT	10S	23E	7	NESENW	6468.4	B	12.1	2.64	0.835	0.387	10.5	16576	MVRD
E946	Uinta	4304730545	2-7 FLAT MESA	ENSERCH EXPLORATION	UT	10S	23E	7	NESENW	6468.5	B	12.7	2.63	1.45	0.587	18.7	16576	MVRD
E946	Uinta	4304730545	2-7 FLAT MESA	ENSERCH EXPLORATION	UT	10S	23E	7	NESENW	6468.5	A	11.9	2.63	0.911	0.382	14.7	16576	MVRD
E946	Uinta	4304730545	2-7 FLAT MESA	ENSERCH EXPLORATION	UT	10S	23E	7	NESENW	6468.5	C	12.2	2.63	0.877	0.431	12.3	16576	MVRD
E946	Uinta	4304730545	2-7 FLAT MESA	ENSERCH EXPLORATION	UT	10S	23E	7	NESENW	6468.6	A	12.1	2.64	0.838	0.257	39.1	16576	MVRD
E946	Uinta	4304730545	2-7 FLAT MESA	ENSERCH EXPLORATION	UT	10S	23E	7	NESENW	6468.6	C	12.1	2.63	0.740	0.297	20.6	16576	MVRD
E946	Uinta	4304730545	2-7 FLAT MESA	ENSERCH EXPLORATION	UT	10S	23E	7	NESENW	6468.6	B	12.3	2.63	0.715	0.319	6.5	16576	MVRD
E946	Uinta	4304730545	2-7 FLAT MESA	ENSERCH EXPLORATION	UT	10S	23E	7	NESENW	6472.7	A	9.0	2.64	0.303	0.0454	26.9	16276	MVRD
E946	Uinta	4304730545	2-7 FLAT MESA	ENSERCH EXPLORATION	UT	10S	23E	7	NESENW	6472.7	B	8.5	2.64	0.163	0.0262	60.5	16276	MVRD
E946	Uinta	4304730545	2-7 FLAT MESA	ENSERCH EXPLORATION	UT	10S	23E	7	NESENW	6475.2	C	12.5	2.63	1.21	0.532	16.6	16576	MVRD
E946	Uinta	4304730545	2-7 FLAT MESA	ENSERCH EXPLORATION	UT	10S	23E	7	NESENW	6475.2	A	13.0	2.64	1.13	0.390	30.7	16576	MVRD
E946	Uinta	4304730545	2-7 FLAT MESA	ENSERCH EXPLORATION	UT	10S	23E	7	NESENW	6475.2	B	12.4	2.63	1.11	0.444	18.5	16576	MVRD
E946	Uinta	4304730545	2-7 FLAT MESA	ENSERCH EXPLORATION	UT	10S	23E	7	NESENW	6475.3	A	12.4	2.63	1.29	0.583	10.3	16576	MVRD
E946	Uinta	4304730545	2-7 FLAT MESA	ENSERCH EXPLORATION	UT	10S	23E	7	NESENW	6475.3	B	12.1	2.63	1.14	0.479	17.7	16576	MVRD
E946	Uinta	4304730545	2-7 FLAT MESA	ENSERCH EXPLORATION	UT	10S	23E	7	NESENW	6475.3	C	12.5	2.63	0.922	0.266	22.5	16576	MVRD
E946	Uinta	4304730545	2-7 FLAT MESA	ENSERCH EXPLORATION	UT	10S	23E	7	NESENW	6475.4	C	11.9	2.63	0.884	0.293	18.6	16576	MVRD
E946	Uinta	4304730545	2-7 FLAT MESA	ENSERCH EXPLORATION	UT	10S	23E	7	NESENW	6475.4	B	11.8	2.63	0.779	0.313	16.6	16576	MVRD
E946	Uinta	4304730545	2-7 FLAT MESA	ENSERCH EXPLORATION	UT	10S	23E	7	NESENW	6475.4	A	11.9	2.64	0.736	0.307	15.5	16576	MVRD
E946	Uinta	4304730545	2-7 FLAT MESA	ENSERCH EXPLORATION	UT	10S	23E	7	NESENW	6482.0	B	3.7	2.67	0.0224	0.000092	210	16286	MVRD
E946	Uinta	4304730545	2-7 FLAT MESA	ENSERCH EXPLORATION	UT	10S	23E	7	NESENW	6482.0	A	2.6	2.65	0.0181	0.000095	272	16286	MVRD
E946	Uinta	4304730545	2-7 FLAT MESA	ENSERCH EXPLORATION	UT	10S	23E	7	NESENW	6482.0	C	2.9	2.66	0.0149	0.000027	782	16286	MVRD
E946	Uinta	4304730545	2-7 FLAT MESA	ENSERCH EXPLORATION	UT	10S	23E	7	NESENW	6486.4	A	12.5	2.64	2.28	0.658	20.1	16576	MVRD
E946	Uinta	4304730545	2-7 FLAT MESA	ENSERCH EXPLORATION	UT	10S	23E	7	NESENW	6486.4	C	12.1	2.64	2.26	0.633	27.8	16576	MVRD
E946	Uinta	4304730545	2-7 FLAT MESA	ENSERCH EXPLORATION	UT	10S	23E	7	NESENW	6486.4	B	12.2	2.64	2.06	0.637	23.7	16576	MVRD
E946	Uinta	4304730545	2-7 FLAT MESA	ENSERCH EXPLORATION	UT	10S	23E	7	NESENW	6486.5	B	11.3	2.63	1.44	0.286	36.7	16576	MVRD
E946	Uinta	4304730545	2-7 FLAT MESA	ENSERCH EXPLORATION	UT	10S	23E	7	NESENW	6486.5	C	11.3	2.63	1.29	0.391	24.7	16576	MVRD
E946	Uinta	4304730545	2-7 FLAT MESA	ENSERCH EXPLORATION	UT	10S	23E	7	NESENW	6486.5	A	10.9	2.63	1.05	0.246	17.9	16576	MVRD
E946	Uinta	4304730545	2-7 FLAT MESA	ENSERCH EXPLORATION	UT	10S	23E	7	NESENW	6486.6	C	9.3	2.63	0.467	0.0724	37.9	16576	MVRD
E946	Uinta	4304730545	2-7 FLAT MESA	ENSERCH EXPLORATION	UT	10S	23E	7	NESENW	6486.6	B	9.3	2.63	0.365	0.0476	26.9	16576	MVRD
E946	Uinta	4304730545	2-7 FLAT MESA	ENSERCH EXPLORATION	UT	10S	23E	7	NESENW	6486.6	A	8.7	2.63	0.344	0.0532	50.5	16576	MVRD
E946	Uinta	4304730545	2-7 FLAT MESA	ENSERCH EXPLORATION	UT	10S	23E	7	NESENW	6486.7	B	9.6	2.63	0.780	0.254	10.2	16576	MVRD
E946	Uinta	4304730545	2-7 FLAT MESA	ENSERCH EXPLORATION	UT	10S	23E	7	NESENW	6486.7	C	9.6	2.63	0.686	0.182	32.3	16576	MVRD
E946	Uinta	4304730545	2-7 FLAT MESA	ENSERCH EXPLORATION	UT	10S	23E	7	NESENW	6486.7	A	9.9	2.63	0.629	0.146	16.4	16576	MVRD
E946	Uinta	4304730545	2-7 FLAT MESA	ENSERCH EXPLORATION	UT	10S	23E	7	NESENW	6489.6	A	11.3	2.63	0.792	0.186	54.9	16576	MVRD
E946	Uinta	4304730545	2-7 FLAT MESA	ENSERCH EXPLORATION	UT	10S	23E	7	NESENW	6489.6	C	11.2	2.63	0.756	0.216	21.9	16576	MVRD
E946	Uinta	4304730545	2-7 FLAT MESA	ENSERCH EXPLORATION	UT	10S	23E	7	NESENW	6489.6	B	11.3	2.64	0.700	0.172	35.9	16576	MVRD
E946	Uinta	4304730545	2-7 FLAT MESA	ENSERCH EXPLORATION	UT	10S	23E	7	NESENW	6489.7	A	11.8	2.63	0.827	0.269	18.1	16576	MVRD
E946	Uinta	4304730545	2-7 FLAT MESA	ENSERCH EXPLORATION	UT	10S	23E	7	NESENW	6489.7	B	11.4	2.63	0.533	0.139	58.4	16576	MVRD
E946	Uinta	4304730545	2-7 FLAT MESA	ENSERCH EXPLORATION	UT	10S	23E	7	NESENW	6489.7	C	11.1	2.63	0.512	0.178	25.0	16576	MVRD
E946	Uinta	4304730545	2-7 FLAT MESA	ENSERCH EXPLORATION	UT	10S	23E	7	NESENW	6492.5	B	9.9	2.66	0.260	0.0629	26.8	15286	MVRD
E946	Uinta	4304730545	2-7 FLAT MESA	ENSERCH EXPLORATION	UT	10S	23E	7	NESENW	6492.5	A	9.8	2.66	0.166	0.0314	36.3	15286	MVRD
E946	Uinta	4304730545	2-7 FLAT MESA	ENSERCH EXPLORATION	UT	10S	23E	7	NESENW	6492.5	C	9.7	2.66	0.0896	0.0126	45.4	15286	MVRD
E946	Uinta	4304730545	2-7 FLAT MESA	ENSERCH EXPLORATION	UT	10S	23E	7	NESENW	6492.6	C	9.8	2.66	0.190	0.0193	86.8	15286	MVRD
E946	Uinta	4304730545	2-7 FLAT MESA	ENSERCH EXPLORATION	UT	10S	23E	7	NESENW	6492.6	A	10.2	2.66	0.182	0.0166	122	15286	MVRD
E946	Uinta	4304730545	2-7 FLAT MESA	ENSERCH EXPLORATION	UT	10S	23E	7	NESENW	6492.6	B	9.9	2.66	0.156	0.0282	44.1	15286	MVRD
E946	Uinta	4304730545	2-7 FLAT MESA	ENSERCH EXPLORATION	UT	10S	23E	7	NESENW	6507.5	B	2.5	2.65	0.00479	0.000308	243	13266	MVRD
E946	Uinta	4304730545	2-7 FLAT MESA	ENSERCH EXPLORATION	UT	10S	23E	7	NESENW	6507.5	A	3.0	2.66	0.00385	0.000339	237	13266	MVRD
E946	Uinta	4304730545	2-7 FLAT MESA	ENSERCH EXPLORATION	UT	10S	23E	7	NESENW	6507.5	C	2.5	2.65	0.00312	0.000200	820	13266	MVRD
E946	Uinta	4304730545	2-7 FLAT MESA	ENSERCH EXPLORATION	UT	10S	23E	7	NESENW	6508.2	A	3.1	2.65	0.0319	0.000484	125	13266	MVRD
E946	Uinta	4304730545	2-7 FLAT MESA	ENSERCH EXPLORATION	UT	10S	23E	7	NESENW	6508.3	C	2.9	2.63	0.520	0.0736	67.3	13266	MVRD
E946	Uinta	4304730545	2-7 FLAT MESA	ENSERCH EXPLORATION	UT	10S	23E	7	NESENW	6508.3	B	3.4	2.64	0.345	1.94	12.5	13266	MVRD
E946	Uinta	4304730545	2-7 FLAT MESA	ENSERCH EXPLORATION	UT	10S	23E	7	NESENW	6511.4	C	9.3	2.65	0.264	0.0369	38.5	15276	MVRD
E946	Uinta	4304730545	2-7 FLAT MESA	ENSERCH EXPLORATION	UT	10S	23E	7	NESENW	6511.4	B	9.2	2.65	0.162	0.0314	47.6	15276	MVRD
E946	Uinta	4304730545	2-7 FLAT MESA	ENSERCH EXPLORATION	UT	10S	23E	7	NESENW	6511.4	A	8.4	2.65	0.125	0.0244	58.8	15276	MVRD
E946	Uinta	4304730545	2-7 FLAT MESA	ENSERCH EXPLORATION	UT	10S	23E	7	NESENW	6511.5	A	8.7	2.65	0.181	0.0367	29.2	15276	MVRD
E946	Uinta	4304730545	2-7 FLAT MESA	ENSERCH EXPLORATION	UT	10S	23E	7	NESENW	6511.5	C	9.5	2.65	0.148	0.0290	51.5	15276	MVRD
E946	Uinta	4304730545	2-7 FLAT MESA	ENSERCH EXPLORATION	UT	10S	23E	7	NESENW	6511.5	B	9.0	2.65	0.119	0.0198	41.5	15276	MVRD
E946	Uinta	4304730545	2-7 FLAT MESA	ENSERCH EXPLORATION	UT	10S	23E	7	NESENW	6515.5	B	14.5	2.64	4.35	1.86	14.6	16586	MVRD
E946	Uinta	4304730545	2-7 FLAT MESA	ENSERCH EXPLORATION	UT	10S	23E	7	NESENW	6515.5	A	16.3	2.64	4.27	2.00	13.9	16586	MVRD
E946	Uinta	4304730545	2-7 FLAT MESA	ENSERCH EXPLORATION	UT	10S	23E	7	NESENW	6515.5	C	13.3	2.72	4.06	1.31	21.1	16586	MVRD
E946	Uinta	4304730545	2-7 FLAT MESA	ENSERCH EXPLORATION	UT	10S	23E	7	NESENW	6515.6	A	15.1	2.63	4.79	1.94	14.5	16586	MVRD
E946	Uinta	4304730545	2-7 FLAT MESA	ENSERCH EXPLORATION	UT	10S	23E	7	NESENW	6515.6	B	15.4	2.64	4.70	1.61	26.3	16586	MVRD
E946	Uinta	4304730545	2-7 FLAT MESA	ENSERCH EXPLORATION	UT	10S	23E	7	NESENW	6515.6	C	13.8	2.63	3.79	1.67	9.9	16586	MVRD
E946	Uinta	4304730545	2-7 FLAT MESA	ENSERCH EXPLORATION	UT	10S	23E	7	NESENW	6518.1	A	5.2	2.63	0.0459	0.00125	155	13266	MVRD
E946	Uinta	4304730545	2-7 FLAT MESA	ENSERCH EXPLORATION	UT	10S	23E	7	NESENW	6518.1	C	4.8	2.63	0.0292	0.00117	42.5	13266	MVRD
E946	Uinta	4304730545	2-7 FLAT MESA	ENSERCH EXPLORATION	UT	10S	23E	7	NESENW	6518.1	B	5.1	2.63	0.0284	0.00125	75.2	13266	MVRD
E946	Uinta	4304730545	2-7 FLAT MESA	ENSERCH EXPLORATION	UT	10S	23E	7	NESENW	6527.6	B	9.8	2.64	0.378	0.0512	34.8	16596	MVRD
E946	Uinta	4304730545	2-7 FLAT MESA	ENSERCH EXPLORATION	UT	10S	23E	7	NESENW	6527.6	A	10.4	2.64	0.361	0.0643	34.2	16596	MVRD
E946	Uinta	4304730545	2-7 FLAT MESA	ENSERCH EXPLORATION	UT	10S	23E	7	NESENW	6527.6	C	9.8	2.64	0.350	0.0978	12.8	16596	MVRD
E946	Uinta	4304730545	2-7 FLAT MESA	ENSERCH EXPLORATION	UT	10S	23E	7	NESENW	6527.7	B	8.6	2.61	0.357	0.0566	32.6	16596	MVRD
E946	Uinta	4304730545	2-7 FLAT MESA	ENSERCH EXPLORATION	UT	10S	23E	7	NESENW	6527.7	A	9.6	2.64	0.347	0.0567	46.7	16596	MVRD
E946	Uinta	4304730545	2-7 FLAT MESA	ENSERCH EXPLORATION	UT	10S	23E	7	NESENW	6527.7	C	9.6	2.64	0.334	0.0530	40.4	16596	MVRD
E946	Uinta	4304730545	2-7 FLAT MESA	ENSERCH EXPLORATION	UT	10S	23E	7	NESENW	6530.2	A	9.8	2.63	0.300	0.0235	139	16586	MVRD
E946	Uinta	4304730545	2-7 FLAT MESA	ENSERCH EXPLORATION	UT	10S	23E	7	NESENW	6530.2	C	9.5	2.63	0.284	0.0609	28.4	16586	MVRD
E946	Uinta	4304730545	2-7 FLAT MESA	ENSERCH EXPLORATION	UT	10S	23E	7	NESENW	6530.2	B	9.6	2.63	0.239	0.0405	37.2	16586	MVRD
E946	Uinta	4304730545	2-7 FLAT MESA	ENSERCH EXPLORATION	UT	10S	23E	7	NESENW	6530.3	A	8.9	2.63	0.777	0.0701	32.6	16586	MVRD
E946	Uinta	4304730545	2-7 FLAT MESA	ENSERCH EXPLORATION	UT	10S	23E	7	NESENW	6530.3	C	9.0	2.63	0.260	0.0364	29.7	16586	MVRD
E946	Uinta	4304730545	2-7 FLAT MESA	ENSERCH EXPLORATION	UT	10S	23E	7	NESENW	6530.3	B	9.4	2.63	0.257	0.0416	22.5	16586	MVRD
E946	Uinta	4304730545	2-7 FLAT MESA	ENSERCH EXPLORATION	UT	10S	23E	7	NESENW	6530.4	A	9.9	2.63	0.315	0.0639	26.9	16586	MVRD
E946	Uinta	4304730545	2-7 FLAT MESA	ENSERCH EXPLORATION	UT	10S	23E	7	NESENW	6530.4	C	9.9	2.63	0.287	0.0454	51.2	16586	MVRD
E946	Uinta	4304730545	2-7 FLAT MESA	ENSERCH EXPLORATION	UT	10S	23E	7	NESENW	6530.4	B	10.2	2.64	0.282	0.0293	25.4	16586	MVRD
E946	Uinta	4304730545	2-7 FLAT MESA	ENSERCH EXPLORATION	UT	10S	23E	7	NESENW	6537.5	C	0.9	2.67	0.00216	0.000073	184	16586	MVRD

Table 4.1.1. (continued)

Summary of Porosity, Permeability, and Grain Density
Analysis of Critical Permeability, Capillary Pressure, and Electrical Properties for Mesaverde Tight Gas Sandstones from Western U.S. Basins
US DOE # DE-FC26-05NT42660
Alan P. Byrnes, Robert M. Cluff, John C. Webb, Daniel A. Krygowski, Stefani D. Whittaker
website: http://www.kgs.ku.edu/mesaverde

USGS Library Number	Basin	API Number	Well Name	Operator	State	Township	Range	Section	Quarter Section	Plug Depth	Plug Letter	Ambient Porosity	Grain Density	Routine Gas Permeability	*in situ* Klinkenberg Gas Permeability	*in situ* Klinkenberg *constant b*	Rock Type Code	Formations
										ft	A/B/C	%	g/cc	mD	mD	(psia)		
E946	Uinta	4304730545	2-7 FLAT MESA	ENSERCH EXPLORATION	UT	10S	23E	7	NESENW	6546.1	A	1.6	2.65	0.00181	0.000048	233	13296	MVRD
E946	Uinta	4304730545	2-7 FLAT MESA	ENSERCH EXPLORATION	UT	10S	23E	7	NESENW	6546.1	B	1.2	2.62				13296	MVRD
E946	Uinta	4304730545	2-7 FLAT MESA	ENSERCH EXPLORATION	UT	10S	23E	7	NESENW	6546.1	C	10.1	2.61				13296	MVRD
E946	Uinta	4304730545	2-7 FLAT MESA	ENSERCH EXPLORATION	UT	10S	23E	7	NESENW	6550.5	B	1.5	2.66	0.00299	0.000111	326	13216	MVRD
E946	Uinta	4304730545	2-7 FLAT MESA	ENSERCH EXPLORATION	UT	10S	23E	7	NESENW	6550.5	A	1.3	2.66	0.00270	0.000109	187	13216	MVRD
E946	Uinta	4304730545	2-7 FLAT MESA	ENSERCH EXPLORATION	UT	10S	23E	7	NESENW	6550.5	C	1.4	2.68	0.00225	0.000069	360	13216	MVRD
E946	Uinta	4304730545	2-7 FLAT MESA	ENSERCH EXPLORATION	UT	10S	23E	7	NESENW	6559.4	B	1.9	2.64	0.00393	0.000098	450	13266	MVRD
E946	Uinta	4304730545	2-7 FLAT MESA	ENSERCH EXPLORATION	UT	10S	23E	7	NESENW	6559.4	A	2.0	2.65	0.00273	0.000073	298	13266	MVRD
E946	Uinta	4304730545	2-7 FLAT MESA	ENSERCH EXPLORATION	UT	10S	23E	7	NESENW	6559.4	C	1.9	2.65	0.00236	0.000076	194	13266	MVRD
E946	Uinta	4304730545	2-7 FLAT MESA	ENSERCH EXPLORATION	UT	10S	23E	7	NESENW	6683.9	C	1.1	2.68	0.00281	0.000140	119	13246	MVRD
E946	Uinta	4304730545	2-7 FLAT MESA	ENSERCH EXPLORATION	UT	10S	23E	7	NESENW	6683.9	A	1.9	2.69	0.00237	0.000158	108	13246	MVRD
E946	Uinta	4304730545	2-7 FLAT MESA	ENSERCH EXPLORATION	UT	10S	23E	7	NESENW	6683.9	B	1.1	2.68	0.00218	0.000056	610	13246	MVRD
E946	Uinta	4304730545	2-7 FLAT MESA	ENSERCH EXPLORATION	UT	10S	23E	7	NESENW	6686.8	C	7.8	2.67	0.0736	0.00747	99.4	14276	MVRD
E946	Uinta	4304730545	2-7 FLAT MESA	ENSERCH EXPLORATION	UT	10S	23E	7	NESENW	6686.8	B	7.7	2.67	0.0613	0.00751	21.6	14276	MVRD
E946	Uinta	4304730545	2-7 FLAT MESA	ENSERCH EXPLORATION	UT	10S	23E	7	NESENW	6686.8	A	8.1	2.68	0.0353	0.00236	155	14276	MVRD
E946	Uinta	4304730545	2-7 FLAT MESA	ENSERCH EXPLORATION	UT	10S	23E	7	NESENW	6688.2	C	6.8	2.67	0.0968	0.00546	59.8	15276	MVRD
E946	Uinta	4304730545	2-7 FLAT MESA	ENSERCH EXPLORATION	UT	10S	23E	7	NESENW	6688.2	B	7.2	2.67	0.0681	0.00137	217	15276	MVRD
E946	Uinta	4304730545	2-7 FLAT MESA	ENSERCH EXPLORATION	UT	10S	23E	7	NESENW	6688.2	A	7.0	2.66	0.0655	0.00474	91.4	15276	MVRD
E946	Uinta	4304730545	2-7 FLAT MESA	ENSERCH EXPLORATION	UT	10S	23E	7	NESENW	6688.3	C	7.1	2.67	0.0596	0.00317	118	15276	MVRD
E946	Uinta	4304730545	2-7 FLAT MESA	ENSERCH EXPLORATION	UT	10S	23E	7	NESENW	6688.3	A	7.2	2.67	0.0518	0.00389	82.9	15276	MVRD
E946	Uinta	4304730545	2-7 FLAT MESA	ENSERCH EXPLORATION	UT	10S	23E	7	NESENW	6688.3	B	7.1	2.67	0.0284	0.00207	82.5	15276	MVRD
E946	Uinta	4304730545	2-7 FLAT MESA	ENSERCH EXPLORATION	UT	10S	23E	7	NESENW	6695.8	A	4.0	2.65	0.0444	0.000606	203	13276	MVRD
E946	Uinta	4304730545	2-7 FLAT MESA	ENSERCH EXPLORATION	UT	10S	23E	7	NESENW	6695.8	B	5.0	2.66	0.0398	0.00115	74.7	13276	MVRD
E946	Uinta	4304730545	2-7 FLAT MESA	ENSERCH EXPLORATION	UT	10S	23E	7	NESENW	6695.8	C	8.2	2.66	0.0290	0.00112	70.9	13276	MVRD
E946	Uinta	4304730545	2-7 FLAT MESA	ENSERCH EXPLORATION	UT	10S	23E	7	NESENW	6698.0	C	2.8	2.67	0.00363	0.000047	1097	12266	MVRD
E946	Uinta	4304730545	2-7 FLAT MESA	ENSERCH EXPLORATION	UT	10S	23E	7	NESENW	6698.0	B	2.6	2.65	0.00265	0.000049	481	12266	MVRD
E946	Uinta	4304730545	2-7 FLAT MESA	ENSERCH EXPLORATION	UT	10S	23E	7	NESENW	6698.0	A	2.0	2.63	0.00133	0.000034	436	12266	MVRD
E946	Uinta	4304730545	2-7 FLAT MESA	ENSERCH EXPLORATION	UT	10S	23E	7	NESENW	6700.1	B	2.2	2.62	0.00329	0.000072	483	12216	MVRD
E946	Uinta	4304730545	2-7 FLAT MESA	ENSERCH EXPLORATION	UT	10S	23E	7	NESENW	6700.1	A	2.1	2.63	0.00275	0.000068	370	12216	MVRD
E946	Uinta	4304730545	2-7 FLAT MESA	ENSERCH EXPLORATION	UT	10S	23E	7	NESENW	6700.1	C	1.7	2.65	0.00264	0.000055	314	12216	MVRD
E946	Uinta	4304730545	2-7 FLAT MESA	ENSERCH EXPLORATION	UT	10S	23E	7	NESENW	6702.8	C	8.2	2.67	0.0615	0.00355	56.0	13266	MVRD
E946	Uinta	4304730545	2-7 FLAT MESA	ENSERCH EXPLORATION	UT	10S	23E	7	NESENW	6702.8	A	7.8	2.68	0.0532	0.00250	90.6	13266	MVRD
E946	Uinta	4304730545	2-7 FLAT MESA	ENSERCH EXPLORATION	UT	10S	23E	7	NESENW	6702.8	B	8.4	2.68	0.0385	0.00280	83.3	13266	MVRD
E946	Uinta	4304730545	2-7 FLAT MESA	ENSERCH EXPLORATION	UT	10S	23E	7	NESENW	6709.8	B	1.7	2.67	0.00364	0.000170	293	13216	MVRD
E946	Uinta	4304730545	2-7 FLAT MESA	ENSERCH EXPLORATION	UT	10S	23E	7	NESENW	6709.8	C	1.8	2.67	0.00347	0.000154	378	13216	MVRD
E946	Uinta	4304730545	2-7 FLAT MESA	ENSERCH EXPLORATION	UT	10S	23E	7	NESENW	6709.8	A	2.2	2.68	0.00179	0.000117	231	13216	MVRD
E946	Uinta	4304730545	2-7 FLAT MESA	ENSERCH EXPLORATION	UT	10S	23E	7	NESENW	7272.3	C	8.9	2.65	0.128	0.00751	57.6	13276	MVRD
E946	Uinta	4304730545	2-7 FLAT MESA	ENSERCH EXPLORATION	UT	10S	23E	7	NESENW	7272.3	A	9.0	2.66	0.125	0.00638	94.7	13276	MVRD
E946	Uinta	4304730545	2-7 FLAT MESA	ENSERCH EXPLORATION	UT	10S	23E	7	NESENW	7272.3	B	9.4	2.66	0.0836	0.00442	94.0	13276	MVRD
E946	Uinta	4304730545	2-7 FLAT MESA	ENSERCH EXPLORATION	UT	10S	23E	7	NESENW	7276.2	A	7.3	2.67	0.0600	0.00653	60.5	14266	MVRD
E946	Uinta	4304730545	2-7 FLAT MESA	ENSERCH EXPLORATION	UT	10S	23E	7	NESENW	7276.2	B	7.3	2.68	0.0563	0.00230	84.9	14266	MVRD
E946	Uinta	4304730545	2-7 FLAT MESA	ENSERCH EXPLORATION	UT	10S	23E	7	NESENW	7276.2	C	8.1	2.68	0.0467	0.00189	81.2	14266	MVRD
E946	Uinta	4304730545	2-7 FLAT MESA	ENSERCH EXPLORATION	UT	10S	23E	7	NESENW	7278.8	A	7.0	2.66	0.0592	0.00133	75.3	13266	MVRD
E946	Uinta	4304730545	2-7 FLAT MESA	ENSERCH EXPLORATION	UT	10S	23E	7	NESENW	7278.8	C	7.8	2.66	0.0413	0.000556	172	13266	MVRD
E946	Uinta	4304730545	2-7 FLAT MESA	ENSERCH EXPLORATION	UT	10S	23E	7	NESENW	7278.8	B	7.5	2.65	0.0404	0.00133	62.8	13266	MVRD
E946	Uinta	4304730545	2-7 FLAT MESA	ENSERCH EXPLORATION	UT	10S	23E	7	NESENW	7279.2	C	6.1	2.64	0.0515	0.00168	41.0	13286	MVRD
E946	Uinta	4304730545	2-7 FLAT MESA	ENSERCH EXPLORATION	UT	10S	23E	7	NESENW	7279.2	A	6.1	2.64	0.0284	0.000356	142	13286	MVRD
E946	Uinta	4304730545	2-7 FLAT MESA	ENSERCH EXPLORATION	UT	10S	23E	7	NESENW	7279.2	B	6.6	2.64	0.0246	0.000781	86.0	13286	MVRD
E946	Uinta	4304730545	2-7 FLAT MESA	ENSERCH EXPLORATION	UT	10S	23E	7	NESENW	7279.4	A	7.0	2.65	0.0489	0.00146	89.9	13286	MVRD
E946	Uinta	4304730545	2-7 FLAT MESA	ENSERCH EXPLORATION	UT	10S	23E	7	NESENW	7279.4	C	7.3	2.65	0.0393	0.00105	116	13286	MVRD
E946	Uinta	4304730545	2-7 FLAT MESA	ENSERCH EXPLORATION	UT	10S	23E	7	NESENW	7279.4	B	7.4	2.65	0.0340	0.00120	112	13286	MVRD
E946	Uinta	4304730545	2-7 FLAT MESA	ENSERCH EXPLORATION	UT	10S	23E	7	NESENW	7279.9	B	6.6	2.63	0.0332	0.000490	293	13296	MVRD
E946	Uinta	4304730545	2-7 FLAT MESA	ENSERCH EXPLORATION	UT	10S	23E	7	NESENW	7279.9	A	6.3	2.63	0.0318	0.000735	110	13296	MVRD
E946	Uinta	4304730545	2-7 FLAT MESA	ENSERCH EXPLORATION	UT	10S	23E	7	NESENW	7279.9	C	6.9	2.64	0.0241	0.00235	43.2	13296	MVRD
E946	Uinta	4304730545	2-7 FLAT MESA	ENSERCH EXPLORATION	UT	10S	23E	7	NESENW	7284.3	B	7.8	2.65	0.0627	0.00310	63.9	14296	MVRD
E946	Uinta	4304730545	2-7 FLAT MESA	ENSERCH EXPLORATION	UT	10S	23E	7	NESENW	7284.3	A	7.7	2.65	0.0499	0.00323	56.7	14296	MVRD
E946	Uinta	4304730545	2-7 FLAT MESA	ENSERCH EXPLORATION	UT	10S	23E	7	NESENW	7284.3	C	7.9	2.65	0.0261	0.00206	55.2	14296	MVRD
E946	Uinta	4304730545	2-7 FLAT MESA	ENSERCH EXPLORATION	UT	10S	23E	7	NESENW	7284.4	A	8.0	2.65	0.0451	0.00266	96.7	14296	MVRD
E946	Uinta	4304730545	2-7 FLAT MESA	ENSERCH EXPLORATION	UT	10S	23E	7	NESENW	7284.4	B	8.0	2.65	0.0373	0.00248	66.5	14296	MVRD
E946	Uinta	4304730545	2-7 FLAT MESA	ENSERCH EXPLORATION	UT	10S	23E	7	NESENW	7284.4	C	8.2	2.66	0.0303	0.00191	103	14296	MVRD
E946	Uinta	4304730545	2-7 FLAT MESA	ENSERCH EXPLORATION	UT	10S	23E	7	NESENW	7284.5	C	7.9	2.65	0.0491	0.00261	94.6	14296	MVRD
E946	Uinta	4304730545	2-7 FLAT MESA	ENSERCH EXPLORATION	UT	10S	23E	7	NESENW	7284.5	B	8.2	2.65	0.0404	0.00115	239	14296	MVRD
E946	Uinta	4304730545	2-7 FLAT MESA	ENSERCH EXPLORATION	UT	10S	23E	7	NESENW	7284.5	A	7.8	2.65	0.0359	0.00505	61.0	14296	MVRD
E946	Uinta	4304730545	2-7 FLAT MESA	ENSERCH EXPLORATION	UT	10S	23E	7	NESENW	7287.1	C	5.6	2.64	0.0498	0.00115	90.6	13286	MVRD
E946	Uinta	4304730545	2-7 FLAT MESA	ENSERCH EXPLORATION	UT	10S	23E	7	NESENW	7287.1	A	5.6	2.64	0.0426	0.00147	25.7	13286	MVRD
E946	Uinta	4304730545	2-7 FLAT MESA	ENSERCH EXPLORATION	UT	10S	23E	7	NESENW	7287.1	B	5.7	2.64	0.0311	0.000610	139	13286	MVRD
E946	Uinta	4304730545	2-7 FLAT MESA	ENSERCH EXPLORATION	UT	10S	23E	7	NESENW	7289.9	A	4.9	2.65	0.0503	0.00139	129	13266	MVRD
E946	Uinta	4304730545	2-7 FLAT MESA	ENSERCH EXPLORATION	UT	10S	23E	7	NESENW	7289.9	B	5.1	2.65	0.0351	0.000616	189	13266	MVRD
E946	Uinta	4304730545	2-7 FLAT MESA	ENSERCH EXPLORATION	UT	10S	23E	7	NESENW	7289.9	C	5.5	2.66	0.0298	0.00150	68.1	13266	MVRD
E946	Uinta	4304730545	2-7 FLAT MESA	ENSERCH EXPLORATION	UT	10S	23E	7	NESENW	7290.9	C	2.3	2.63	0.00591	0.000308	227	12266	MVRD
E946	Uinta	4304730545	2-7 FLAT MESA	ENSERCH EXPLORATION	UT	10S	23E	7	NESENW	7290.9	B	1.8	2.62	0.00445	0.000334	180	12266	MVRD
E946	Uinta	4304730545	2-7 FLAT MESA	ENSERCH EXPLORATION	UT	10S	23E	7	NESENW	7290.9	A	3.2	2.66	0.00422	0.000124	400	12266	MVRD
E946	Uinta	4304730545	2-7 FLAT MESA	ENSERCH EXPLORATION	UT	10S	23E	7	NESENW	7293.4	C	3.7	2.67	0.0270	0.000584	78.1	13206	MVRD
E946	Uinta	4304730545	2-7 FLAT MESA	ENSERCH EXPLORATION	UT	10S	23E	7	NESENW	7293.4	B	3.1	2.66	0.00455	0.000435	180	13206	MVRD
E946	Uinta	4304730545	2-7 FLAT MESA	ENSERCH EXPLORATION	UT	10S	23E	7	NESENW	7293.4	A	3.5	2.68	0.00372	0.000053	306	13206	MVRD
E946	Uinta	4304730545	2-7 FLAT MESA	ENSERCH EXPLORATION	UT	10S	23E	7	NESENW	7293.5	C	3.3	2.66	0.0304	0.000487	94.8	13206	MVRD
E946	Uinta	4304730545	2-7 FLAT MESA	ENSERCH EXPLORATION	UT	10S	23E	7	NESENW	7293.5	A	3.8	2.68	0.0294	0.000490	145	13206	MVRD
E946	Uinta	4304730545	2-7 FLAT MESA	ENSERCH EXPLORATION	UT	10S	23E	7	NESENW	7293.5	B	3.1	2.66	0.00401	0.000579	194	13206	MVRD
E946	Uinta	4304730545	2-7 FLAT MESA	ENSERCH EXPLORATION	UT	10S	23E	7	NESENW	7294.4	A			0.00434	0.000216	92.3	13206	MVRD
E946	Uinta	4304730545	2-7 FLAT MESA	ENSERCH EXPLORATION	UT	10S	23E	7	NESENW	7297.1	C	1.1	2.61	0.00800	0.000344	167	13216	MVRD
E946	Uinta	4304730545	2-7 FLAT MESA	ENSERCH EXPLORATION	UT	10S	23E	7	NESENW	7297.1	B	1.9	2.63	0.00411	0.000144	232	13216	MVRD
E946	Uinta	4304730545	2-7 FLAT MESA	ENSERCH EXPLORATION	UT	10S	23E	7	NESENW	7297.1	A	1.9	2.62	0.00358	0.000137	226	13216	MVRD
E946	Uinta	4304730545	2-7 FLAT MESA	ENSERCH EXPLORATION	UT	10S	23E	7	NESENW	7299.3	A	6.9	2.68	0.0704	0.00170	172	13256	MVRD
E946	Uinta	4304730545	2-7 FLAT MESA	ENSERCH EXPLORATION	UT	10S	23E	7	NESENW	7299.3	B	6.4	2.68	0.0691	0.00251	86.6	13256	MVRD
E946	Uinta	4304730545	2-7 FLAT MESA	ENSERCH EXPLORATION	UT	10S	23E	7	NESENW	7299.3	C	6.8	2.68	0.0536	0.00186	70.0	13256	MVRD
E946	Uinta	4304730545	2-7 FLAT MESA	ENSERCH EXPLORATION	UT	10S	23E	7	NESENW	7300.1	C	5.5	2.67	0.0646	0.00268	71.5	13256	MVRD
E946	Uinta	4304730545	2-7 FLAT MESA	ENSERCH EXPLORATION	UT	10S	23E	7	NESENW	7300.1	A	5.5	2.68	0.0643	0.00244	90.5	13256	MVRD
E946	Uinta	4304730545	2-7 FLAT MESA	ENSERCH EXPLORATION	UT	10S	23E	7	NESENW	7300.1	B	5.7	2.68	0.0585	0.00231	90.0	13256	MVRD
E946	Uinta	4304730545	2-7 FLAT MESA	ENSERCH EXPLORATION	UT	10S	23E	7	NESENW	7300.6	B	5.9	2.68	0.0922	0.00202	100	13256	MVRD
E946	Uinta	4304730545	2-7 FLAT MESA	ENSERCH EXPLORATION	UT	10S	23E	7	NESENW	7300.6	A	5.8	2.68	0.0524	0.00156	82.5	13256	MVRD
E946	Uinta	4304730545	2-7 FLAT MESA	ENSERCH EXPLORATION	UT	10S	23E	7	NESENW	7300.6	C	5.9	2.68	0.0431	0.00163	73.2	13256	MVRD
E946	Uinta	4304730545	2-7 FLAT MESA	ENSERCH EXPLORATION	UT	10S	23E	7	NESENW	7301.4	C	2.5	2.60	0.00721	0.000536	116	13266	MVRD
E946	Uinta	4304730545	2-7 FLAT MESA	ENSERCH EXPLORATION	UT	10S	23E	7	NESENW	7301.4	A	2.5	2.57	0.00641	0.000209	588	13266	MVRD
E946	Uinta	4304730545	2-7 FLAT MESA	ENSERCH EXPLORATION	UT	10S	23E	7	NESENW	7301.4	B	2.6	2.58	0.00609	0.000282	296	13266	MVRD
E946	Uinta	4304730545	2-7 FLAT MESA	ENSERCH EXPLORATION	UT	10S	23E	7	NESENW	7311.7	C	2.0	2.62	0.0351			12216	MVRD
E946	Uinta	4304730545	2-7 FLAT MESA	ENSERCH EXPLORATION	UT	10S	23E	7	NESENW	7311.7	A	1.9	2.61	0.0172	0.00102	35.6	12216	MVRD
E946	Uinta	4304730545	2-7 FLAT MESA	ENSERCH EXPLORATION	UT	10S	23E	7	NESENW	7311.7	B	1.4	2.61	0.00363	0.000117	312	12216	MVRD
E946	Uinta	4304730545	2-7 FLAT MESA	ENSERCH EXPLORATION	UT	10S	23E	7	NESENW	7311.9	C	5.9	2.66	0.0536	0.00153	65.9	13266	MVRD
E946	Uinta	4304730545	2-7 FLAT MESA	ENSERCH EXPLORATION	UT	10S	23E	7	NESENW	7311.9	A	5.3	2.67	0.0508	0.000665	162	13266	MVRD
E946	Uinta	4304730545	2-7 FLAT MESA	ENSERCH EXPLORATION	UT	10S	23E	7	NESENW	7311.9	B	5.9	2.67	0.0348	0.000894	149	13266	MVRD
E946	Uinta	4304730545	2-7 FLAT MESA	ENSERCH EXPLORATION	UT	10S	23E	7	NESENW	7312.7	B	8.3	2.66	0.0728	0.00252	110	14296	MVRD
E946	Uinta	4304730545	2-7 FLAT MESA	ENSERCH EXPLORATION	UT	10S	23E	7	NESENW	7312.7	A	7.8	2.66	0.0708	0.00303	60.6	14296	MVRD
E946	Uinta	4304730545	2-7 FLAT MESA	ENSERCH EXPLORATION	UT	10S	23E	7	NESENW	7312.7	C	8.4	2.67	0.0569	0.00373	59.4	14296	MVRD
E946	Uinta	4304730545	2-7 FLAT MESA	ENSERCH EXPLORATION	UT	10S	23E	7	NESENW	7313.4	A	5.7	2.65	0.614	0.0748	15.3	13256	MVRD
E946	Uinta	4304730545	2-7 FLAT MESA	ENSERCH EXPLORATION	UT	10S	23E	7	NESENW	7313.4	C	6.4	2.65	0.280	0.0192	54.7	13256	MVRD
E946	Uinta	4304730545	2-7 FLAT MESA	ENSERCH EXPLORATION	UT	10S	23E	7	NESENW	7313.4	B	6.3	2.65	0.128	0.00761	35.3	13256	MVRD
E946	Uinta	4304730545	2-7 FLAT MESA	ENSERCH EXPLORATION	UT	10S	23E	7	NESENW	7313.8	C	6.7	2.66	0.132	0.0151	15.9	13266	MVRD
E946	Uinta	4304730545	2-7 FLAT MESA	ENSERCH EXPLORATION	UT	10S	23E	7	NESENW	7313.8	A	5.9	2.65	0.102	0.00386	89.9	13266	MVRD
E946	Uinta	4304730545	2-7 FLAT MESA	ENSERCH EXPLORATION	UT	10S	23E	7	NESENW	7313.8	B	6.1	2.65	0.0670	0.00375	60.0	13266	MVRD
E946	Uinta	4304730545	2-7 FLAT MESA	ENSERCH EXPLORATION	UT	10S	23E	7	NESENW	7314.3	B	5.7	2.65	0.125	0.00451	53.2	13266	MVRD
E946	Uinta	4304730545	2-7 FLAT MESA	ENSERCH EXPLORATION	UT	10S	23E	7	NESENW	7314.3	C	6.3	2.66	0.122	0.00470	88.0	13266	MVRD
E946	Uinta	4304730545	2-7 FLAT MESA	ENSERCH EXPLORATION	UT	10S	23E	7	NESENW	7314.3	A	5.8	2.65	0.0838	0.00412	80.1	13266	MVRD

Table 4.1.1. (continued)

Summary of Porosity, Permeability, and Grain Density
Analysis of Critical Permeability, Capillary Pressure, and Electrical Properties for Mesaverde Tight Gas Sandstones from Western U.S. Basins
US DOE # DE-FC26-05NT42660
Alan P. Byrnes, Robert M. Cluff, John C. Webb, Daniel A. Krygowski, Stefani D. Whittaker
website: http://www.kgs.ku.edu/mesaverde

USGS Library Number	Basin	API Number	Well Name	Operator	State	Township	Range	Section	Quarter Section	Plug Depth	Plug Letter	Ambient Porosity	Grain Density	Routine Gas Permeability	*in situ* Klinkenberg Gas Permeability	*in situ* Klinkenberg *constant b*	Rock Type Code	Formations
										ft	A/B/C	%	g/cc	mD	mD	(psia)		
E946	Uinta	4304730545	2-7 FLAT MESA	ENSERCH EXPLORATION	UT	10S	23E	7	NESENW	7587.1	B	11.9	2.64	0.115	0.0298	34.0	13266	MVRD
E946	Uinta	4304730545	2-7 FLAT MESA	ENSERCH EXPLORATION	UT	10S	23E	7	NESENW	7668.7	A	3.0	2.63	0.0114	0.000833	177	13226	MVRD
E946	Uinta	4304730545	2-7 FLAT MESA	ENSERCH EXPLORATION	UT	10S	23E	7	NESENW	7668.7	B	3.6	2.64	0.00611	0.000315	205	13226	MVRD
E946	Uinta	4304730545	2-7 FLAT MESA	ENSERCH EXPLORATION	UT	10S	23E	7	NESENW	7668.7	C	3.0	2.62	0.00593	0.000216	509	13226	MVRD
E946	Uinta	4304730545	2-7 FLAT MESA	ENSERCH EXPLORATION	UT	10S	23E	7	NESENW	7671.1	B	4.3	2.65	1.55	0.0658	32.5	13256	MVRD
E946	Uinta	4304730545	2-7 FLAT MESA	ENSERCH EXPLORATION	UT	10S	23E	7	NESENW	7671.1	A	4.8	2.67	0.685	0.0973	25.6	13256	MVRD
E946	Uinta	4304730545	2-7 FLAT MESA	ENSERCH EXPLORATION	UT	10S	23E	7	NESENW	7676.4	B	1.1	2.61	0.00404	0.000058	688	12216	MVRD
E946	Uinta	4304730545	2-7 FLAT MESA	ENSERCH EXPLORATION	UT	10S	23E	7	NESENW	7676.4	A	1.8	2.64	0.00342	0.000120	160	12216	MVRD
E946	Uinta	4304730545	2-7 FLAT MESA	ENSERCH EXPLORATION	UT	10S	23E	7	NESENW	7676.4	C	1.4	2.62	0.00307	0.000088	155	12216	MVRD
E946	Uinta	4304730545	2-7 FLAT MESA	ENSERCH EXPLORATION	UT	10S	23E	7	NESENW	7678.8	B	2.0	2.63	0.0476	0.00346	75.0	12266	MVRD
E946	Uinta	4304730545	2-7 FLAT MESA	ENSERCH EXPLORATION	UT	10S	23E	7	NESENW	7678.8	C	1.5	2.62	0.0152	0.00117	80.5	12266	MVRD
E946	Uinta	4304730545	2-7 FLAT MESA	ENSERCH EXPLORATION	UT	10S	23E	7	NESENW	7678.8	A	1.6	2.63	0.00877	0.000355	295	12266	MVRD
E946	Uinta	4304730545	2-7 FLAT MESA	ENSERCH EXPLORATION	UT	10S	23E	7	NESENW	7686.4	A	3.8	2.65	8.36	0.315	22.8	13266	MVRD
E946	Uinta	4304730545	2-7 FLAT MESA	ENSERCH EXPLORATION	UT	10S	23E	7	NESENW	7686.4	B	3.5	2.65	0.106	0.0236	50.1	13266	MVRD
E946	Uinta	4304730545	2-7 FLAT MESA	ENSERCH EXPLORATION	UT	10S	23E	7	NESENW	7686.4	C	3.7	2.67	0.0901	0.00323	91.5	13266	MVRD
E946	Uinta	4304730545	2-7 FLAT MESA	ENSERCH EXPLORATION	UT	10S	23E	7	NESENW	7689.7	B	7.6	2.68	0.0744	0.00452	90.0	14276	MVRD
E946	Uinta	4304730545	2-7 FLAT MESA	ENSERCH EXPLORATION	UT	10S	23E	7	NESENW	7689.7	A	7.4	2.67	0.0741	0.00374	105	14276	MVRD
E946	Uinta	4304730545	2-7 FLAT MESA	ENSERCH EXPLORATION	UT	10S	23E	7	NESENW	7689.7	C	7.8	2.68	0.0589	0.00618	44.2	14276	MVRD
E946	Uinta	4304730545	2-7 FLAT MESA	ENSERCH EXPLORATION	UT	10S	23E	7	NESENW	7701.1	C	1.0	2.59	0.00821	0.000155	220	13216	MVRD
E946	Uinta	4304730545	2-7 FLAT MESA	ENSERCH EXPLORATION	UT	10S	23E	7	NESENW	7701.1	B	0.7	2.60	0.00382	0.000099	817	13216	MVRD
E946	Uinta	4304730545	2-7 FLAT MESA	ENSERCH EXPLORATION	UT	10S	23E	7	NESENW	7701.1	A	0.9	2.61	0.00263	0.000097	172	13216	MVRD
E946	Uinta	4304730545	2-7 FLAT MESA	ENSERCH EXPLORATION	UT	10S	23E	7	NESENW	7704.4	A	3.5	2.62	0.00991	0.000414	58.8	12226	MVRD
E946	Uinta	4304730545	2-7 FLAT MESA	ENSERCH EXPLORATION	UT	10S	23E	7	NESENW	7704.4	C	2.6	2.61	0.00527	0.000213	152	12226	MVRD
E946	Uinta	4304730545	2-7 FLAT MESA	ENSERCH EXPLORATION	UT	10S	23E	7	NESENW	7704.4	B	3.2	2.62				12226	MVRD
E946	Uinta	4304730545	2-7 FLAT MESA	ENSERCH EXPLORATION	UT	10S	23E	7	NESENW	7707.5	A	2.9	2.66	0.216	0.0364	32.6	13256	MVRD
E946	Uinta	4304730545	2-7 FLAT MESA	ENSERCH EXPLORATION	UT	10S	23E	7	NESENW	7707.5	B	3.4	2.67	0.0630	0.00364	58.7	13256	MVRD
E946	Uinta	4304730545	2-7 FLAT MESA	ENSERCH EXPLORATION	UT	10S	23E	7	NESENW	7707.5	C	3.0	2.65	0.0629	0.00335	83.4	13256	MVRD
E946	Uinta	4304730545	2-7 FLAT MESA	ENSERCH EXPLORATION	UT	10S	23E	7	NESENW	7712.7	B	3.2	2.69	0.0343	0.000383	134	13266	MVRD
E946	Uinta	4304730545	2-7 FLAT MESA	ENSERCH EXPLORATION	UT	10S	23E	7	NESENW	7712.7	C	3.5	2.71	0.0222	0.000449	91.9	13266	MVRD
E946	Uinta	4304730545	2-7 FLAT MESA	ENSERCH EXPLORATION	UT	10S	23E	7	NESENW	7712.7	A	3.0	2.69	0.0100	0.000528	234	13266	MVRD
E946	Uinta	4304730545	2-7 FLAT MESA	ENSERCH EXPLORATION	UT	10S	23E	7	NESENW	7856.3	A	2.0	2.57	0.00895	0.000065	714	12296	MVRD
E946	Uinta	4304730545	2-7 FLAT MESA	ENSERCH EXPLORATION	UT	10S	23E	7	NESENW	7856.3	B	1.2	2.56	0.00338	0.000129	221	12296	MVRD
E946	Uinta	4304730545	2-7 FLAT MESA	ENSERCH EXPLORATION	UT	10S	23E	7	NESENW	7856.3	C	0.6	2.54	0.00303	0.000066	325	12296	MVRD
E946	Uinta	4304730545	2-7 FLAT MESA	ENSERCH EXPLORATION	UT	10S	23E	7	NESENW	7885.4	C	10.2	2.65	0.121	0.0222	61.6	14266	MVRD
E946	Uinta	4304730545	2-7 FLAT MESA	ENSERCH EXPLORATION	UT	10S	23E	7	NESENW	7885.4	A	9.8	2.65	0.117	0.0258	44.2	14266	MVRD
E946	Uinta	4304730545	2-7 FLAT MESA	ENSERCH EXPLORATION	UT	10S	23E	7	NESENW	7885.4	B	10.2	2.65	0.115	0.0189	89.9	14266	MVRD
E946	Uinta	4304730545	2-7 FLAT MESA	ENSERCH EXPLORATION	UT	10S	23E	7	NESENW	7887.1	A	11.9	2.65	0.130	0.0284	45.9	14266	MVRD
E946	Uinta	4304730545	2-7 FLAT MESA	ENSERCH EXPLORATION	UT	10S	23E	7	NESENW	7887.8	C	7.0	2.61	0.133	0.00462	99.4	13266	MVRD
E946	Uinta	4304730545	2-7 FLAT MESA	ENSERCH EXPLORATION	UT	10S	23E	7	NESENW	7887.8	A	6.9	2.61	0.0972	0.00423	44.7	13266	MVRD
E946	Uinta	4304730545	2-7 FLAT MESA	ENSERCH EXPLORATION	UT	10S	23E	7	NESENW	7887.8	B	7.0	2.61				13266	MVRD
E946	Uinta	4304730545	2-7 FLAT MESA	ENSERCH EXPLORATION	UT	10S	23E	7	NESENW	7889.1	B	1.1	2.53	0.00378	0.000079	255	12296	MVRD
E946	Uinta	4304730545	2-7 FLAT MESA	ENSERCH EXPLORATION	UT	10S	23E	7	NESENW	7889.1	C	1.9	2.55	0.00246	0.000040	424	12296	MVRD
E946	Uinta	4304730545	2-7 FLAT MESA	ENSERCH EXPLORATION	UT	10S	23E	7	NESENW	7889.1	A	1.8	2.54	0.00166	0.000030	362	12296	MVRD
E946	Uinta	4304730545	2-7 FLAT MESA	ENSERCH EXPLORATION	UT	10S	23E	7	NESENW	7892.7	C	0.8	2.68	0.00145	0.000014	1349	12216	MVRD
E946	Uinta	4304730545	2-7 FLAT MESA	ENSERCH EXPLORATION	UT	10S	23E	7	NESENW	7892.7	A	1.0	2.68	0.00134	0.000042	443	12216	MVRD
E946	Uinta	4304730545	2-7 FLAT MESA	ENSERCH EXPLORATION	UT	10S	23E	7	NESENW	7892.7	B	0.7	2.67	0.00130	0.000032	442	12216	MVRD
E946	Uinta	4304730545	2-7 FLAT MESA	ENSERCH EXPLORATION	UT	10S	23E	7	NESENW	7896.2	A	1.3	2.53	0.00517	0.000107	274	12296	MVRD
E946	Uinta	4304730545	2-7 FLAT MESA	ENSERCH EXPLORATION	UT	10S	23E	7	NESENW	7896.2	C	0.8	2.54	0.00328	0.000090	206	12296	MVRD
E946	Uinta	4304730545	2-7 FLAT MESA	ENSERCH EXPLORATION	UT	10S	23E	7	NESENW	7896.2	B	1.8	2.53	0.00247	0.000056	175	12296	MVRD
E946	Uinta	4304730545	2-7 FLAT MESA	ENSERCH EXPLORATION	UT	10S	23E	7	NESENW	7898.5	B	2.7	2.60	0.0112	0.00107	139	13226	MVRD
E946	Uinta	4304730545	2-7 FLAT MESA	ENSERCH EXPLORATION	UT	10S	23E	7	NESENW	7898.5	A	2.6	2.61	0.00938	0.000631	180	13226	MVRD
E946	Uinta	4304730545	2-7 FLAT MESA	ENSERCH EXPLORATION	UT	10S	23E	7	NESENW	7898.5	C	2.2	2.60	0.00717	0.000557	88.3	13226	MVRD
KM1022	Uinta	4304736565	NBU 1022-1A Natural Butte	KERR-MCGEE OIL&GAS ONSHORE	UT	10S	22E	1	SWSE	7803.5	A	2.0	2.61	0.00469	0.000077	196	12290	MVRD
KM1022	Uinta	4304736565	NBU 1022-1A Natural Butte	KERR-MCGEE OIL&GAS ONSHORE	UT	10S	22E	1	SWSE	7803.5	B			0.00135	0.000020	363	12290	MVRD
KM1022	Uinta	4304736565	NBU 1022-1A Natural Butte	KERR-MCGEE OIL&GAS ONSHORE	UT	10S	22E	1	SWSE	7803.8	A	2.1	2.60	0.00256	0.000039	193	12290	MVRD
KM1022	Uinta	4304736565	NBU 1022-1A Natural Butte	KERR-MCGEE OIL&GAS ONSHORE	UT	10S	22E	1	SWSE	7806.5	B	8.1	2.66	0.0412	0.00175	160	13260	MVRD
KM1022	Uinta	4304736565	NBU 1022-1A Natural Butte	KERR-MCGEE OIL&GAS ONSHORE	UT	10S	22E	1	SWSE	7806.5	A	8.1	2.66	0.00795	0.00110	193	13260	MVRD
KM1022	Uinta	4304736565	NBU 1022-1A Natural Butte	KERR-MCGEE OIL&GAS ONSHORE	UT	10S	22E	1	SWSE	7808.7	A	9.8	2.65	0.0382	0.00573	56.0	13260	MVRD
KM1022	Uinta	4304736565	NBU 1022-1A Natural Butte	KERR-MCGEE OIL&GAS ONSHORE	UT	10S	22E	1	SWSE	7808.7	B	10.0	2.65	0.0358	0.00380	173	13260	MVRD
KM1022	Uinta	4304736565	NBU 1022-1A Natural Butte	KERR-MCGEE OIL&GAS ONSHORE	UT	10S	22E	1	SWSE	7810.4	B	9.1	2.68	0.0419	0.00147	226	13260	MVRD
KM1022	Uinta	4304736565	NBU 1022-1A Natural Butte	KERR-MCGEE OIL&GAS ONSHORE	UT	10S	22E	1	SWSE	7810.4	A	9.8	2.69	0.0114	0.00178	139	13260	MVRD
KM1022	Uinta	4304736565	NBU 1022-1A Natural Butte	KERR-MCGEE OIL&GAS ONSHORE	UT	10S	22E	1	SWSE	7815.8	B	1.2	2.32	0.0390	0.000145	338	13220	MVRD
KM1022	Uinta	4304736565	NBU 1022-1A Natural Butte	KERR-MCGEE OIL&GAS ONSHORE	UT	10S	22E	1	SWSE	7815.8	A	1.5	2.34	0.0174	0.000507	90.9	13260	MVRD
KM1022	Uinta	4304736565	NBU 1022-1A Natural Butte	KERR-MCGEE OIL&GAS ONSHORE	UT	10S	22E	1	SWSE	7818.4	B	1.7	2.65	0.0230	0.000326	283	13220	MVRD
KM1022	Uinta	4304736565	NBU 1022-1A Natural Butte	KERR-MCGEE OIL&GAS ONSHORE	UT	10S	22E	1	SWSE	7818.4	A	1.8	2.65	0.00480	0.000057	422	13260	MVRD
KM1022	Uinta	4304736565	NBU 1022-1A Natural Butte	KERR-MCGEE OIL&GAS ONSHORE	UT	10S	22E	1	SWSE	7823.5	A	2.0	2.60	0.00445	0.000037	601	12220	MVRD
KM1022	Uinta	4304736565	NBU 1022-1A Natural Butte	KERR-MCGEE OIL&GAS ONSHORE	UT	10S	22E	1	SWSE	7823.5	B	1.3	2.59	0.00301	0.000012	1587	13240	MVRD
KM1022	Uinta	4304736565	NBU 1022-1A Natural Butte	KERR-MCGEE OIL&GAS ONSHORE	UT	10S	22E	1	SWSE	7825.5	B	4.7	2.73	0.00536	0.000299	363	13260	MVRD
KM1022	Uinta	4304736565	NBU 1022-1A Natural Butte	KERR-MCGEE OIL&GAS ONSHORE	UT	10S	22E	1	SWSE	7825.5	A			0.00517	0.000244	184	13260	MVRD
KM1022	Uinta	4304736565	NBU 1022-1A Natural Butte	KERR-MCGEE OIL&GAS ONSHORE	UT	10S	22E	1	SWSE	7827.7	A	5.8	2.75	0.00242	0.000225	378	13260	MVRD
KM1022	Uinta	4304736565	NBU 1022-1A Natural Butte	KERR-MCGEE OIL&GAS ONSHORE	UT	10S	22E	1	SWSE	7827.7	A	0.8	2.51	0.0243	0.000195	262	13260	MVRD
KM1022	Uinta	4304736565	NBU 1022-1A Natural Butte	KERR-MCGEE OIL&GAS ONSHORE	UT	10S	22E	1	SWSE	7830.7	B	1.2	2.49	0.141	0.00462	60.7	13240	MVRD
KM1022	Uinta	4304736565	NBU 1022-1A Natural Butte	KERR-MCGEE OIL&GAS ONSHORE	UT	10S	22E	1	SWSE	7830.7	A	9.9	2.73	0.00292	0.000028	673	13240	MVRD
KM1022	Uinta	4304736565	NBU 1022-1A Natural Butte	KERR-MCGEE OIL&GAS ONSHORE	UT	10S	22E	1	SWSE	7836.5	B	1.1	2.44	0.0323	0.000187	86.4	13240	MVRD
KM1022	Uinta	4304736565	NBU 1022-1A Natural Butte	KERR-MCGEE OIL&GAS ONSHORE	UT	10S	22E	1	SWSE	7836.5	A	1.1	2.47	0.00818	0.000137	234	13240	MVRD
KM1022	Uinta	4304736565	NBU 1022-1A Natural Butte	KERR-MCGEE OIL&GAS ONSHORE	UT	10S	22E	1	SWSE	7840.5	B	1.0	2.48	0.0517	0.000390	88.2	13260	MVRD
KM1022	Uinta	4304736565	NBU 1022-1A Natural Butte	KERR-MCGEE OIL&GAS ONSHORE	UT	10S	22E	1	SWSE	7840.5	A	1.6	2.51	0.00113	0.000013	699	13260	MVRD
KM1022	Uinta	4304736565	NBU 1022-1A Natural Butte	KERR-MCGEE OIL&GAS ONSHORE	UT	10S	22E	1	SWSE	7840.5	A	0.7	2.49	0.000184	0.000005	161	13260	MVRD
KM1022	Uinta	4304736565	NBU 1022-1A Natural Butte	KERR-MCGEE OIL&GAS ONSHORE	UT	10S	22E	1	SWSE	7841.5	B	0.9	2.80	0.00898	0.000085	513	13260	MVRD
KM1022	Uinta	4304736565	NBU 1022-1A Natural Butte	KERR-MCGEE OIL&GAS ONSHORE	UT	10S	22E	1	SWSE	7841.5	A			0.00251	0.000040	416	13260	MVRD
KM1022	Uinta	4304736565	NBU 1022-1A Natural Butte	KERR-MCGEE OIL&GAS ONSHORE	UT	10S	22E	1	SWSE	7848.8	B	2.2	2.30	0.0210	0.000750	127	13290	MVRD
KM1022	Uinta	4304736565	NBU 1022-1A Natural Butte	KERR-MCGEE OIL&GAS ONSHORE	UT	10S	22E	1	SWSE	7848.8	A	1.3	2.36	0.00255	0.000061	152	12290	MVRD
KM1022	Uinta	4304736565	NBU 1022-1A Natural Butte	KERR-MCGEE OIL&GAS ONSHORE	UT	10S	22E	1	SWSE	7849.4	A	1.5	2.60	0.00351	0.000015	488	13260	MVRD
KM1022	Uinta	4304736565	NBU 1022-1A Natural Butte	KERR-MCGEE OIL&GAS ONSHORE	UT	10S	22E	1	SWSE	7849.4	B	1.1	2.59	0.00132	0.000041	133	13290	MVRD
KM1022	Uinta	4304736565	NBU 1022-1A Natural Butte	KERR-MCGEE OIL&GAS ONSHORE	UT	10S	22E	1	SWSE	7851.5	A	4.4	2.68	0.0105	0.000781	153	13210	MVRD
KM1022	Uinta	4304736565	NBU 1022-1A Natural Butte	KERR-MCGEE OIL&GAS ONSHORE	UT	10S	22E	1	SWSE	7851.5	B	4.4	2.64				13210	MVRD
KM1022	Uinta	4304736565	NBU 1022-1A Natural Butte	KERR-MCGEE OIL&GAS ONSHORE	UT	10S	22E	1	SWSE	7853.5	A	3.8	2.68	0.00739	0.000921	161	13220	MVRD
KM1022	Uinta	4304736565	NBU 1022-1A Natural Butte	KERR-MCGEE OIL&GAS ONSHORE	UT	10S	22E	1	SWSE	7853.5	B	4.0	2.67	0.00592	0.000754	148	13240	MVRD
KM1022	Uinta	4304736565	NBU 1022-1A Natural Butte	KERR-MCGEE OIL&GAS ONSHORE	UT	10S	22E	1	SWSE	7857.5	A	4.6	2.65	0.00187	0.000031	710	13290	MVRD
KM1022	Uinta	4304736565	NBU 1022-1A Natural Butte	KERR-MCGEE OIL&GAS ONSHORE	UT	10S	22E	1	SWSE	7857.5	B			0.00170	0.000041	458	13240	MVRD
KM1022	Uinta	4304736565	NBU 1022-1A Natural Butte	KERR-MCGEE OIL&GAS ONSHORE	UT	10S	22E	1	SWSE	7858.5	A	2.8	2.63	0.00312	0.000009	797	13290	MVRD
KM1022	Uinta	4304736565	NBU 1022-1A Natural Butte	KERR-MCGEE OIL&GAS ONSHORE	UT	10S	22E	1	SWSE	7862.6	A	6.3	2.66	1.45	0.0296	58.1	13260	MVRD
KM1022	Uinta	4304736565	NBU 1022-1A Natural Butte	KERR-MCGEE OIL&GAS ONSHORE	UT	10S	22E	1	SWSE	7862.6	B	6.1	2.65	0.0109	0.00140	125	14240	MVRD
KM1022	Uinta	4304736565	NBU 1022-1A Natural Butte	KERR-MCGEE OIL&GAS ONSHORE	UT	10S	22E	1	SWSE	7865.6	A	1.3	2.74	0.0310	0.00424	66.4	13240	MVRD
KM1022	Uinta	4304736565	NBU 1022-1A Natural Butte	KERR-MCGEE OIL&GAS ONSHORE	UT	10S	22E	1	SWSE	7865.6	B	0.8	2.72	0.0280	0.000352	180	13240	MVRD
KM1022	Uinta	4304736565	NBU 1022-1A Natural Butte	KERR-MCGEE OIL&GAS ONSHORE	UT	10S	22E	1	SWSE	7867.8	B	5.5	2.67	0.0213	0.000201	672	13240	MVRD
KM1022	Uinta	4304736565	NBU 1022-1A Natural Butte	KERR-MCGEE OIL&GAS ONSHORE	UT	10S	22E	1	SWSE	7867.8	A	8.2	2.69	0.00526	0.000791	138	13240	MVRD
KM1022	Uinta	4304736565	NBU 1022-1A Natural Butte	KERR-MCGEE OIL&GAS ONSHORE	UT	10S	22E	1	SWSE	7869.5	B	7.5	2.67	0.0113	0.00232	215	13240	MVRD
KM1022	Uinta	4304736565	NBU 1022-1A Natural Butte	KERR-MCGEE OIL&GAS ONSHORE	UT	10S	22E	1	SWSE	7870.5	A	9.0	2.71	0.0367	0.00639	235	14290	MVRD
KM1022	Uinta	4304736565	NBU 1022-1A Natural Butte	KERR-MCGEE OIL&GAS ONSHORE	UT	10S	22E	1	SWSE	7872.5	B	1.9	2.60	0.0129	0.000192	218	13290	MVRD
KM1022	Uinta	4304736565	NBU 1022-1A Natural Butte	KERR-MCGEE OIL&GAS ONSHORE	UT	10S	22E	1	SWSE	7872.5	A	2.9	2.63	0.00328	0.000056	281	13290	MVRD
KM1022	Uinta	4304736565	NBU 1022-1A Natural Butte	KERR-MCGEE OIL&GAS ONSHORE	UT	10S	22E	1	SWSE	7882.7	A	2.0	2.57	4.05	0.251	41.2	13260	MVRD
KM1022	Uinta	4304736565	NBU 1022-1A Natural Butte	KERR-MCGEE OIL&GAS ONSHORE	UT	10S	22E	1	SWSE	7886.5	A	0.7	2.57		0.00169	154	13210	MVRD
KM1022	Uinta	4304736565	NBU 1022-1A Natural Butte	KERR-MCGEE OIL&GAS ONSHORE	UT	10S	22E	1	SWSE	7888.5	B	1.2	2.58	0.00910	0.000027	863	13260	MVRD
KM1022	Uinta	4304736565	NBU 1022-1A Natural Butte	KERR-MCGEE OIL&GAS ONSHORE	UT	10S	22E	1	SWSE	7888.5	A			0.00228	0.000022	571	13260	MVRD
KM1022	Uinta	4304736565	NBU 1022-1A Natural Butte	KERR-MCGEE OIL&GAS ONSHORE	UT	10S	22E	1	SWSE	7891.8	A	1.2	2.53	0.00733	0.000061	105	13260	MVRD
KM1022	Uinta	4304736565	NBU 1022-1A Natural Butte	KERR-MCGEE OIL&GAS ONSHORE	UT	10S	22E	1	SWSE	7899.6	B	0.6	2.58	0.0554	0.000190	344	12210	MVRD
KM1022	Uinta	4304736565	NBU 1022-1A Natural Butte	KERR-MCGEE OIL&GAS ONSHORE	UT	10S	22E	1	SWSE	7899.6	A	0.7	2.56	0.00134	0.000038	216	13260	MVRD
KM1022	Uinta	4304736565	NBU 1022-1A Natural Butte	KERR-MCGEE OIL&GAS ONSHORE	UT	10S	22E	1	SWSE	7904.5	B	1.5	2.53	0.00314	0.000060	348	13270	MVRD
KM1022	Uinta	4304736565	NBU 1022-1A Natural Butte	KERR-MCGEE OIL&GAS ONSHORE	UT	10S	22E	1	SWSE	7904.5	A	1.2	2.51	0.00208	0.000028	608	13270	MVRD
KM1022	Uinta	4304736565	NBU 1022-1A Natural Butte	KERR-MCGEE OIL&GAS ONSHORE	UT	10S	22E	1	SWSE	7906.5	A	0.9	2.52	0.00358	0.000107	356	13290	MVRD
KM1022	Uinta	4304736565	NBU 1022-1A Natural Butte	KERR-MCGEE OIL&GAS ONSHORE	UT	10S	22E	1	SWSE	7906.5	B	0.8	2.53	0.00305	0.000128	160	13290	MVRD

Table 4.1.1. (continued)

Summary of Porosity, Permeability, and Grain Density
Analysis of Critical Permeability, Capillary Pressure, and Electrical Properties for Mesaverde Tight Gas Sandstones from Western U.S. Basins
US DOE # DE-FC26-05NT42660
Alan P. Byrnes, Robert M. Cluff, John C. Webb, Daniel A. Krygowski, Stefani D. Whittaker
website: http://www.kgs.ku.edu/mesaverde

USGS Library Number	Basin	API Number	Well Name	Operator	State	Township	Range	Section	Quarter Section	Plug Depth ft	Plug Letter A/B/C	Ambient Porosity %	Grain Density g/cc	Routine Gas Permeability mD	*in situ* Klinkenberg Gas Permeability mD	*in situ* Klinken-berg *constant* b (psia)	Rock Type Code	Formations
KM1022	Uinta	4304736565	NBU 1022-1A Natural Butte	KERR-MCGEE OIL&GAS ONSHORE	UT	10S	22E	1	SWSE	7909.5	B	2.2	2.60	0.00860	0.000131	259	13290	MVRD
KM1022	Uinta	4304736565	NBU 1022-1A Natural Butte	KERR-MCGEE OIL&GAS ONSHORE	UT	10S	22E	1	SWSE	7909.5	A	2.7	2.63	0.00430	0.000521	106	13290	MVRD
KM1022	Uinta	4304736565	NBU 1022-1A Natural Butte	KERR-MCGEE OIL&GAS ONSHORE	UT	10S	22E	1	SWSE	7912.5	A	2.8	2.59	0.0213	0.00108	198	13260	MVRD
KM1022	Uinta	4304736565	NBU 1022-1A Natural Butte	KERR-MCGEE OIL&GAS ONSHORE	UT	10S	22E	1	SWSE	7912.5	B	2.5	2.55	0.0133	0.000066	111	13260	MVRD
KM1022	Uinta	4304736565	NBU 1022-1A Natural Butte	KERR-MCGEE OIL&GAS ONSHORE	UT	10S	22E	1	SWSE	7914.5	B	1.3	2.60	0.0688	0.000384	136	13260	MVRD
KM1022	Uinta	4304736565	NBU 1022-1A Natural Butte	KERR-MCGEE OIL&GAS ONSHORE	UT	10S	22E	1	SWSE	7914.5	A	2.0	2.61	0.00589	0.000063	442	13260	MVRD
KM1022	Uinta	4304736565	NBU 1022-1A Natural Butte	KERR-MCGEE OIL&GAS ONSHORE	UT	10S	22E	1	SWSE	7920.5	A	2.0	2.55	0.0111	0.000204	295	13290	MVRD
KM1022	Uinta	4304736565	NBU 1022-1A Natural Butte	KERR-MCGEE OIL&GAS ONSHORE	UT	10S	22E	1	SWSE	7920.5	B	1.8	2.54	0.00721	0.000029	306	13290	MVRD
KM1022	Uinta	4304736565	NBU 1022-1A Natural Butte	KERR-MCGEE OIL&GAS ONSHORE	UT	10S	22E	1	SWSE	7922.5	A	1.8	2.45	0.00543	0.000112	243	13290	MVRD
KM1022	Uinta	4304736565	NBU 1022-1A Natural Butte	KERR-MCGEE OIL&GAS ONSHORE	UT	10S	22E	1	SWSE	7922.5	B	1.0	2.43	0.00318	0.000096	334	13290	MVRD
KM1022	Uinta	4304736565	NBU 1022-1A Natural Butte	KERR-MCGEE OIL&GAS ONSHORE	UT	10S	22E	1	SWSE	7924.5	A	0.9	2.58	0.00298	0.000033	390	13290	MVRD
KM1022	Uinta	4304736565	NBU 1022-1A Natural Butte	KERR-MCGEE OIL&GAS ONSHORE	UT	10S	22E	1	SWSE	7924.5	B	0.8	2.57	0.00132	0.000014	578	13290	MVRD
KM1022	Uinta	4304736565	NBU 1022-1A Natural Butte	KERR-MCGEE OIL&GAS ONSHORE	UT	10S	22E	1	SWSE	7926.5	A	1.5	2.61	0.00123	0.000007	978	13290	MVRD
KM1022	Uinta	4304736565	NBU 1022-1A Natural Butte	KERR-MCGEE OIL&GAS ONSHORE	UT	10S	22E	1	SWSE	7934.5	A			0.0119	0.000618	99.6	13290	MVRD
KM1022	Uinta	4304736565	NBU 1022-1A Natural Butte	KERR-MCGEE OIL&GAS ONSHORE	UT	10S	22E	1	SWSE	7934.5	B2	1.1	2.64	0.00750	0.000045	424	13290	MVRD
KM1022	Uinta	4304736565	NBU 1022-1A Natural Butte	KERR-MCGEE OIL&GAS ONSHORE	UT	10S	22E	1	SWSE	7934.5	B	1.1	2.52	0.00393	0.000049	282	13290	MVRD
KM1022	Uinta	4304736565	NBU 1022-1A Natural Butte	KERR-MCGEE OIL&GAS ONSHORE	UT	10S	22E	1	SWSE	7934.5	A2	1.0	2.56	0.00127	0.000011	921	13260	MVRD
KM1022	Uinta	4304736565	NBU 1022-1A Natural Butte	KERR-MCGEE OIL&GAS ONSHORE	UT	10S	22E	1	SWSE	7943.5	A	1.4	2.60	0.00811	0.000267	254	13290	MVRD
KM1022	Uinta	4304736565	NBU 1022-1A Natural Butte	KERR-MCGEE OIL&GAS ONSHORE	UT	10S	22E	1	SWSE	7945.5	B	1.9	2.32	0.0528	0.000934	82.4	13220	MVRD
KM1022	Uinta	4304736565	NBU 1022-1A Natural Butte	KERR-MCGEE OIL&GAS ONSHORE	UT	10S	22E	1	SWSE	7952.5	A	1.0	2.64	0.0319	0.00138	277	12290	MVRD
KM1022	Uinta	4304736565	NBU 1022-1A Natural Butte	KERR-MCGEE OIL&GAS ONSHORE	UT	10S	22E	1	SWSE	7955.5	A	6.2	2.66	0.00486	0.000054	198	13260	MVRD
KM1022	Uinta	4304736565	NBU 1022-1A Natural Butte	KERR-MCGEE OIL&GAS ONSHORE	UT	10S	22E	1	SWSE	7955.5	B	6.2	2.65	0.00474	0.000067	605	13240	MVRD
KM1022	Uinta	4304736565	NBU 1022-1A Natural Butte	KERR-MCGEE OIL&GAS ONSHORE	UT	10S	22E	1	SWSE	7957.5	A	2.5	2.61	0.00547	0.000044	496	13260	MVRD
KM1022	Uinta	4304736565	NBU 1022-1A Natural Butte	KERR-MCGEE OIL&GAS ONSHORE	UT	10S	22E	1	SWSE	7957.5	B	1.1	2.56	0.00348	0.000060	235	13260	MVRD
KM1022	Uinta	4304736565	NBU 1022-1A Natural Butte	KERR-MCGEE OIL&GAS ONSHORE	UT	10S	22E	1	SWSE	7961.5	A	1.4	2.66	0.00258	0.000054	428	13260	MVRD
KM36O	Uinta	4304735788	NBU 9-20-360 State	KERR-MCGEE OIL&GAS ONSHORE	UT	9S	20E	36	SESE	8175.5	B	6.6	2.64	0.0320	0.00134	89.6	15225	MVRD
KM36O	Uinta	4304735788	NBU 9-20-360 State	KERR-MCGEE OIL&GAS ONSHORE	UT	9S	20E	36	SESE	8175.5	A	6.9	2.66	0.0293	0.00129	87.4	15225	MVRD
KM36O	Uinta	4304735788	NBU 9-20-360 State	KERR-MCGEE OIL&GAS ONSHORE	UT	9S	20E	36	SESE	8178.9	A	7.7	2.66	0.0233	0.00295	81.1	15295	MVRD
KM36O	Uinta	4304735788	NBU 9-20-360 State	KERR-MCGEE OIL&GAS ONSHORE	UT	9S	20E	36	SESE	8181.8	B	1.6	2.66	0.00972	0.000322	411	15285	MVRD
KM36O	Uinta	4304735788	NBU 9-20-360 State	KERR-MCGEE OIL&GAS ONSHORE	UT	9S	20E	36	SESE	8181.8	A	1.5	2.66	0.00583	0.000284	232	15285	MVRD
KM36O	Uinta	4304735788	NBU 9-20-360 State	KERR-MCGEE OIL&GAS ONSHORE	UT	9S	20E	36	SESE	8184.5	A	7.0	2.65	0.0520	0.00228	79.1	13286	MVRD
KM36O	Uinta	4304735788	NBU 9-20-360 State	KERR-MCGEE OIL&GAS ONSHORE	UT	9S	20E	36	SESE	8184.5	B	7.1	2.65	0.0233	0.00240	159	13286	MVRD
KM36O	Uinta	4304735788	NBU 9-20-360 State	KERR-MCGEE OIL&GAS ONSHORE	UT	9S	20E	36	SESE	8184.6	A	6.9	2.66	0.0589	0.00170	71.5	13286	MVRD
KM36O	Uinta	4304735788	NBU 9-20-360 State	KERR-MCGEE OIL&GAS ONSHORE	UT	9S	20E	36	SESE	8184.6	B	6.7	2.65	0.0128	0.00231	39.6	13286	MVRD
KM36O	Uinta	4304735788	NBU 9-20-360 State	KERR-MCGEE OIL&GAS ONSHORE	UT	9S	20E	36	SESE	8185.7	A	5.7	2.65	0.0551	0.000809	131	13286	MVRD
KM36O	Uinta	4304735788	NBU 9-20-360 State	KERR-MCGEE OIL&GAS ONSHORE	UT	9S	20E	36	SESE	8185.7	B	5.9	2.65	0.0145	0.000696	153	13286	MVRD
KM36O	Uinta	4304735788	NBU 9-20-360 State	KERR-MCGEE OIL&GAS ONSHORE	UT	9S	20E	36	SESE	8187.2	A	4.5	2.67	0.0519	0.00136	97.5	15296	MVRD
KM36O	Uinta	4304735788	NBU 9-20-360 State	KERR-MCGEE OIL&GAS ONSHORE	UT	9S	20E	36	SESE	8187.2	B	4.7	2.68	0.0149	0.000530	394	15296	MVRD
KM36O	Uinta	4304735788	NBU 9-20-360 State	KERR-MCGEE OIL&GAS ONSHORE	UT	9S	20E	36	SESE	8193.6	B	2.1	2.64	0.00619	0.000205	195	13226	MVRD
KM36O	Uinta	4304735788	NBU 9-20-360 State	KERR-MCGEE OIL&GAS ONSHORE	UT	9S	20E	36	SESE	8193.6	A	2.2	2.64	0.00368	0.000051	357	13226	MVRD
KM36O	Uinta	4304735788	NBU 9-20-360 State	KERR-MCGEE OIL&GAS ONSHORE	UT	9S	20E	36	SESE	8195.6	B	3.0	2.67	0.00558	0.000133	405	14275	MVRD
KM36O	Uinta	4304735788	NBU 9-20-360 State	KERR-MCGEE OIL&GAS ONSHORE	UT	9S	20E	36	SESE	8195.6	A	3.0	2.68	0.00265	0.000075	496	14275	MVRD
KM36O	Uinta	4304735788	NBU 9-20-360 State	KERR-MCGEE OIL&GAS ONSHORE	UT	9S	20E	36	SESE	8198.1	A	6.8	2.67	0.0554	0.000855	100	12219	MVRD
KM36O	Uinta	4304735788	NBU 9-20-360 State	KERR-MCGEE OIL&GAS ONSHORE	UT	9S	20E	36	SESE	8198.1	B	7.3	2.67	0.00406	0.000361	235	12219	MVRD
KM36O	Uinta	4304735788	NBU 9-20-360 State	KERR-MCGEE OIL&GAS ONSHORE	UT	9S	20E	36	SESE	8209.2	B	1.2	2.69				13255	MVRD
KM36O	Uinta	4304735788	NBU 9-20-360 State	KERR-MCGEE OIL&GAS ONSHORE	UT	9S	20E	36	SESE	8209.5	B	1.5	2.69	0.00315	0.000074	403	13255	MVRD
KM36O	Uinta	4304735788	NBU 9-20-360 State	KERR-MCGEE OIL&GAS ONSHORE	UT	9S	20E	36	SESE	8209.5	A	0.8	2.69	0.00275	0.000053	466	13255	MVRD
KM36O	Uinta	4304735788	NBU 9-20-360 State	KERR-MCGEE OIL&GAS ONSHORE	UT	9S	20E	36	SESE	8216.5	A	2.1	2.65	0.0150	0.000415	114	11219	MVRD
KM36O	Uinta	4304735788	NBU 9-20-360 State	KERR-MCGEE OIL&GAS ONSHORE	UT	9S	20E	36	SESE	8218.5	A	5.8	2.66	0.0436	0.00117	109	15795	MVRD
KM36O	Uinta	4304735788	NBU 9-20-360 State	KERR-MCGEE OIL&GAS ONSHORE	UT	9S	20E	36	SESE	8218.6	B	6.0	2.66	0.0111	0.00111	132	15795	MVRD
KM36O	Uinta	4304735788	NBU 9-20-360 State	KERR-MCGEE OIL&GAS ONSHORE	UT	9S	20E	36	SESE	8218.6	A	5.9	2.66	0.0111	0.000638	262	15795	MVRD
KM36O	Uinta	4304735788	NBU 9-20-360 State	KERR-MCGEE OIL&GAS ONSHORE	UT	9S	20E	36	SESE	8223.5	B	6.7	2.65	0.0178	0.00148	162	15395	MVRD
KM36O	Uinta	4304735788	NBU 9-20-360 State	KERR-MCGEE OIL&GAS ONSHORE	UT	9S	20E	36	SESE	8223.5	A	6.3	2.65	0.0159	0.000936	192	15395	MVRD
KM36O	Uinta	4304735788	NBU 9-20-360 State	KERR-MCGEE OIL&GAS ONSHORE	UT	9S	20E	36	SESE	8225.6	B	1.6	2.67	0.00696	0.000133	962	16295	MVRD
KM36O	Uinta	4304735788	NBU 9-20-360 State	KERR-MCGEE OIL&GAS ONSHORE	UT	9S	20E	36	SESE	8225.6	A	1.4	2.67	0.00312	0.000100	400	16295	MVRD
KM36O	Uinta	4304735788	NBU 9-20-360 State	KERR-MCGEE OIL&GAS ONSHORE	UT	9S	20E	36	SESE	8227.3	A		2.54	0.00337	0.000081	1185	16295	MVRD
KM36O	Uinta	4304735788	NBU 9-20-360 State	KERR-MCGEE OIL&GAS ONSHORE	UT	9S	20E	36	SESE	8228.3	A	4.9	2.65	0.0504	0.000887	312	16295	MVRD
KM36O	Uinta	4304735788	NBU 9-20-360 State	KERR-MCGEE OIL&GAS ONSHORE	UT	9S	20E	36	SESE	8228.3	B	5.2	2.64	0.0371	0.00151	197	16295	MVRD
KM36O	Uinta	4304735788	NBU 9-20-360 State	KERR-MCGEE OIL&GAS ONSHORE	UT	9S	20E	36	SESE	8229.5	A	5.4	2.66	0.0489	0.000695	93.6	13225	MVRD
KM36O	Uinta	4304735788	NBU 9-20-360 State	KERR-MCGEE OIL&GAS ONSHORE	UT	9S	20E	36	SESE	8229.5	B	4.4	2.66	0.0134	0.000623	94.2	13225	MVRD
KM36O	Uinta	4304735788	NBU 9-20-360 State	KERR-MCGEE OIL&GAS ONSHORE	UT	9S	20E	36	SESE	8230.6	A	6.0	2.65	0.0441	0.00115	145	15225	MVRD
KM36O	Uinta	4304735788	NBU 9-20-360 State	KERR-MCGEE OIL&GAS ONSHORE	UT	9S	20E	36	SESE	8230.6	B	5.8	2.64	0.0188	0.00112	144	15225	MVRD
KM36O	Uinta	4304735788	NBU 9-20-360 State	KERR-MCGEE OIL&GAS ONSHORE	UT	9S	20E	36	SESE	8233.5	B	9.0	2.64	0.0774	0.00612	116	17225	MVRD
KM36O	Uinta	4304735788	NBU 9-20-360 State	KERR-MCGEE OIL&GAS ONSHORE	UT	9S	20E	36	SESE	8233.5	A	8.8	2.65	0.0612	0.00474	79.3	17225	MVRD
KM36O	Uinta	4304735788	NBU 9-20-360 State	KERR-MCGEE OIL&GAS ONSHORE	UT	9S	20E	36	SESE	8234.4	A	8.7	2.64	0.0740	0.00340	106	16275	MVRD
KM36O	Uinta	4304735788	NBU 9-20-360 State	KERR-MCGEE OIL&GAS ONSHORE	UT	9S	20E	36	SESE	8234.6	A	9.1	2.65	0.0947	0.00688	103	16275	MVRD
KM36O	Uinta	4304735788	NBU 9-20-360 State	KERR-MCGEE OIL&GAS ONSHORE	UT	9S	20E	36	SESE	8234.6	B	9.1	2.64	0.0880	0.00825	91.6	16275	MVRD
KM36O	Uinta	4304735788	NBU 9-20-360 State	KERR-MCGEE OIL&GAS ONSHORE	UT	9S	20E	36	SESE	8237.5	A	7.7	2.65	0.0621	0.00411	92.8	16295	MVRD
KM36O	Uinta	4304735788	NBU 9-20-360 State	KERR-MCGEE OIL&GAS ONSHORE	UT	9S	20E	36	SESE	8237.5	B	8.0	2.64	0.0302	0.00455	57.2	16295	MVRD
KM36O	Uinta	4304735788	NBU 9-20-360 State	KERR-MCGEE OIL&GAS ONSHORE	UT	9S	20E	36	SESE	8251.4	B	2.8	2.64	0.0886	0.00407	110	12219	MVRD
KM36O	Uinta	4304735788	NBU 9-20-360 State	KERR-MCGEE OIL&GAS ONSHORE	UT	9S	20E	36	SESE	8251.4	A	3.1	2.65				12219	MVRD
KM36O	Uinta	4304735788	NBU 9-20-360 State	KERR-MCGEE OIL&GAS ONSHORE	UT	9S	20E	36	SESE	8257.4	B	2.0	2.67	0.0102	0.000252	231	13265	MVRD
KM36O	Uinta	4304735788	NBU 9-20-360 State	KERR-MCGEE OIL&GAS ONSHORE	UT	9S	20E	36	SESE	8257.4	A	2.4	2.69	0.00342	0.000042	687	13265	MVRD
KM36O	Uinta	4304735788	NBU 9-20-360 State	KERR-MCGEE OIL&GAS ONSHORE	UT	9S	20E	36	SESE	8260.6	B	0.9	2.68	0.00755	0.000301	197	14285	MVRD
KM36O	Uinta	4304735788	NBU 9-20-360 State	KERR-MCGEE OIL&GAS ONSHORE	UT	9S	20E	36	SESE	8260.6	A	1.3	2.67	0.00380	0.000158	192	14285	MVRD
KM36O	Uinta	4304735788	NBU 9-20-360 State	KERR-MCGEE OIL&GAS ONSHORE	UT	9S	20E	36	SESE	8262.3	A	7.0	2.65	0.0246	0.00140	101	13276	MVRD
KM36O	Uinta	4304735788	NBU 9-20-360 State	KERR-MCGEE OIL&GAS ONSHORE	UT	9S	20E	36	SESE	8262.3	B	7.1	2.65	0.0217	0.00178	127	13276	MVRD
KM36O	Uinta	4304735788	NBU 9-20-360 State	KERR-MCGEE OIL&GAS ONSHORE	UT	9S	20E	36	SESE	8264.8	A	9.0	2.65	0.0608	0.00354	328	16276	MVRD
KM36O	Uinta	4304735788	NBU 9-20-360 State	KERR-MCGEE OIL&GAS ONSHORE	UT	9S	20E	36	SESE	8264.8	B	8.8	2.63	0.0374	0.00428	430	16276	MVRD
KM36O	Uinta	4304735788	NBU 9-20-360 State	KERR-MCGEE OIL&GAS ONSHORE	UT	9S	20E	36	SESE	8267.7	A	8.1	2.65	0.0539	0.00258	107	16276	MVRD
KM36O	Uinta	4304735788	NBU 9-20-360 State	KERR-MCGEE OIL&GAS ONSHORE	UT	9S	20E	36	SESE	8267.7	B	8.2	2.64	0.0424	0.00302	147	16276	MVRD
KM36O	Uinta	4304735788	NBU 9-20-360 State	KERR-MCGEE OIL&GAS ONSHORE	UT	9S	20E	36	SESE	8267.8	A	7.9	2.64	0.0330	0.00404	84.6	16276	MVRD
KM36O	Uinta	4304735788	NBU 9-20-360 State	KERR-MCGEE OIL&GAS ONSHORE	UT	9S	20E	36	SESE	8267.8	B	8.0	2.65	0.0226	0.00374	85.1	16276	MVRD
KM36O	Uinta	4304735788	NBU 9-20-360 State	KERR-MCGEE OIL&GAS ONSHORE	UT	9S	20E	36	SESE	8269.2	A	8.9	2.66	0.0575	0.00236	196	16276	MVRD
KM36O	Uinta	4304735788	NBU 9-20-360 State	KERR-MCGEE OIL&GAS ONSHORE	UT	9S	20E	36	SESE	8271.8	A	8.2	2.66	0.0277	0.000958	159	15386	MVRD
KM36O	Uinta	4304735788	NBU 9-20-360 State	KERR-MCGEE OIL&GAS ONSHORE	UT	9S	20E	36	SESE	8272.7	A	9.1	2.65	0.0406	0.00188	95.3	16376	MVRD
KM36O	Uinta	4304735788	NBU 9-20-360 State	KERR-MCGEE OIL&GAS ONSHORE	UT	9S	20E	36	SESE	8277.4	A	4.2	2.62	0.0516	0.00335	189	13246	MVRD
KM36O	Uinta	4304735788	NBU 9-20-360 State	KERR-MCGEE OIL&GAS ONSHORE	UT	9S	20E	36	SESE	8277.7	B	4.7	2.64	0.0553	0.00146	158	13246	MVRD
KM36O	Uinta	4304735788	NBU 9-20-360 State	KERR-MCGEE OIL&GAS ONSHORE	UT	9S	20E	36	SESE	8279.5	A	7.6	2.68	0.00466	0.000260	191	13256	MVRD
KM36O	Uinta	4304735788	NBU 9-20-360 State	KERR-MCGEE OIL&GAS ONSHORE	UT	9S	20E	36	SESE	8279.5	B	7.8	2.68	0.00390	0.000252	232	13256	MVRD
KM36O	Uinta	4304735788	NBU 9-20-360 State	KERR-MCGEE OIL&GAS ONSHORE	UT	9S	20E	36	SESE	8286.2	B	2.8	2.67	0.00886	0.000156	738	13255	MVRD
KM36O	Uinta	4304735788	NBU 9-20-360 State	KERR-MCGEE OIL&GAS ONSHORE	UT	9S	20E	36	SESE	8286.2	A	2.5	2.67	0.00337	0.000123	328	13255	MVRD
KM36O	Uinta	4304735788	NBU 9-20-360 State	KERR-MCGEE OIL&GAS ONSHORE	UT	9S	20E	36	SESE	8287.8	B	3.0	2.65	0.00668	0.000080	393	13216	MVRD
KM36O	Uinta	4304735788	NBU 9-20-360 State	KERR-MCGEE OIL&GAS ONSHORE	UT	9S	20E	36	SESE	8287.8	A	3.1	2.66	0.00550	0.000083	308	13216	MVRD
KM36O	Uinta	4304735788	NBU 9-20-360 State	KERR-MCGEE OIL&GAS ONSHORE	UT	9S	20E	36	SESE	8290.4	A	5.7	2.67	0.0193	0.000402	239	14286	MVRD
KM36O	Uinta	4304735788	NBU 9-20-360 State	KERR-MCGEE OIL&GAS ONSHORE	UT	9S	20E	36	SESE	8290.4	B	5.8	2.66	0.0104	0.000617	40.0	14286	MVRD
KM36O	Uinta	4304735788	NBU 9-20-360 State	KERR-MCGEE OIL&GAS ONSHORE	UT	9S	20E	36	SESE	8300.5	B	1.4	2.64	0.00530	0.000105	156	13216	MVRD
KM36O	Uinta	4304735788	NBU 9-20-360 State	KERR-MCGEE OIL&GAS ONSHORE	UT	9S	20E	36	SESE	8300.5	A	1.7	2.64	0.00363	0.000047	342	13216	MVRD
KM36O	Uinta	4304735788	NBU 9-20-360 State	KERR-MCGEE OIL&GAS ONSHORE	UT	9S	20E	36	SESE	8312.8	B	4.2	2.67	0.00447	0.000223	218	13356	MVRD
KM36O	Uinta	4304735788	NBU 9-20-360 State	KERR-MCGEE OIL&GAS ONSHORE	UT	9S	20E	36	SESE	8312.8	A	4.4	2.68	0.00213	0.000051	348	13356	MVRD
KM36O	Uinta	4304735788	NBU 9-20-360 State	KERR-MCGEE OIL&GAS ONSHORE	UT	9S	20E	36	SESE	8317.5	B	8.6	2.68	0.00928	0.000403	177	12249	MVRD
KM36O	Uinta	4304735788	NBU 9-20-360 State	KERR-MCGEE OIL&GAS ONSHORE	UT	9S	20E	36	SESE	8317.5	A	7.7	2.66	0.00330	0.000149	260	12249	MVRD
KM36O	Uinta	4304735788	NBU 9-20-360 State	KERR-MCGEE OIL&GAS ONSHORE	UT	9S	20E	36	SESE	8319.6	A	7.6	2.65	0.0475	0.000766	167	13366	MVRD
KM36O	Uinta	4304735788	NBU 9-20-360 State	KERR-MCGEE OIL&GAS ONSHORE	UT	9S	20E	36	SESE	8319.6	B	8.2	2.65	0.0141	0.00111	103	13366	MVRD

Table 4.1.1. (continued)

Summary of Porosity, Permeability, and Grain Density
Analysis of Critical Permeability, Capillary Pressure, and Electrical Properties for Mesaverde Tight Gas Sandstones from Western U.S. Basins
US DOE # DE-FC26-05NT42660
Alan P. Byrnes, Robert M. Cluff, John C. Webb, Daniel A. Krygowski, Stefani D. Whittaker
website: http://www.kgs.ku.edu/mesaverde

USGS Library Number	Basin	API Number	Well Name	Operator	State	Township	Range	Section	Quarter Section	Plug Depth	Plug Letter	Ambient Porosity	Grain Density	Routine Gas Permeability	*in situ* Klinkenberg Gas Permeability	*in situ* Klinkenberg *constant b*	Rock Type Code	Formations
										ft	A/B/C	%	g/cc	mD	mD	(psia)		
R829	Uinta	4304730852	4-5 US LAMCO	ENSERCH EXPLORATION	UT	13S	20E	5	C SW	5612.9	A	8.2	2.67	0.375	0.0973	61.0	16276	MVRD
R829	Uinta	4304730852	4-5 US LAMCO	ENSERCH EXPLORATION	UT	13S	20E	5	C SW	5612.9	B	7.2	2.69	0.233	0.0495	33.2	16276	MVRD
R829	Uinta	4304730852	4-5 US LAMCO	ENSERCH EXPLORATION	UT	13S	20E	5	C SW	5613.7	B	10.8	2.66	106	76.2	1.4	16225	MVRD
R829	Uinta	4304730852	4-5 US LAMCO	ENSERCH EXPLORATION	UT	13S	20E	5	C SW	5613.7	A	10.2	2.66	0.710	0.374	21.3	16225	MVRD
R829	Uinta	4304730852	4-5 US LAMCO	ENSERCH EXPLORATION	UT	13S	20E	5	C SW	5618.3	B	9.2	2.68	0.541	0.287	18.6	16286	MVRD
R829	Uinta	4304730852	4-5 US LAMCO	ENSERCH EXPLORATION	UT	13S	20E	5	C SW	5618.3	A	9.0	2.67	0.535	0.274	18.7	16286	MVRD
R829	Uinta	4304730852	4-5 US LAMCO	ENSERCH EXPLORATION	UT	13S	20E	5	C SW	5621.2	A	10.4	2.66	0.783	0.394	28.9	16276	MVRD
R829	Uinta	4304730852	4-5 US LAMCO	ENSERCH EXPLORATION	UT	13S	20E	5	C SW	5621.2	B	10.1	2.66	0.664	0.368	5.2	16276	MVRD
R829	Uinta	4304730852	4-5 US LAMCO	ENSERCH EXPLORATION	UT	13S	20E	5	C SW	5626.2	B	12.8	2.65	14.1	8.66	8.2	16275	MVRD
R829	Uinta	4304730852	4-5 US LAMCO	ENSERCH EXPLORATION	UT	13S	20E	5	C SW	5626.2	A	12.5	2.65	12.6	7.19	10.1	16275	MVRD
R829	Uinta	4304730852	4-5 US LAMCO	ENSERCH EXPLORATION	UT	13S	20E	5	C SW	5626.4	B	12.3	2.65	10.3	7.30	4.2	16275	MVRD
R829	Uinta	4304730852	4-5 US LAMCO	ENSERCH EXPLORATION	UT	13S	20E	5	C SW	5626.4	A	12.4	2.65	10.2	6.89	3.5	16275	MVRD
R829	Uinta	4304730852	4-5 US LAMCO	ENSERCH EXPLORATION	UT	13S	20E	5	C SW	5633.1	B	11.8	2.66	14.5	6.11	20.9	16296	MVRD
R829	Uinta	4304730852	4-5 US LAMCO	ENSERCH EXPLORATION	UT	13S	20E	5	C SW	5633.1	A	11.7	2.65	12.7	8.47	6.5	16296	MVRD
R829	Uinta	4304730852	4-5 US LAMCO	ENSERCH EXPLORATION	UT	13S	20E	5	C SW	5638.8	A	5.0	2.69	0.0332	0.00333	134	15296	MVRD
R829	Uinta	4304730852	4-5 US LAMCO	ENSERCH EXPLORATION	UT	13S	20E	5	C SW	5638.8	B	5.0	2.68	0.0141	0.00379	97.1	15296	MVRD
R829	Uinta	4304730852	4-5 US LAMCO	ENSERCH EXPLORATION	UT	13S	20E	5	C SW	5702.2	A	2.3	2.67	0.00185	0.000035	231	12245	MVRD
R829	Uinta	4304730852	4-5 US LAMCO	ENSERCH EXPLORATION	UT	13S	20E	5	C SW	5702.2	B	0.9	2.63	0.00179	0.000024	303	12245	MVRD
R829	Uinta	4304730852	4-5 US LAMCO	ENSERCH EXPLORATION	UT	13S	20E	5	C SW	5792.9	B	8.3	2.67	0.00429	0.000538	45.4	13266	MVRD
R829	Uinta	4304730852	4-5 US LAMCO	ENSERCH EXPLORATION	UT	13S	20E	5	C SW	5792.9	A	8.1	2.67	0.00155	0.000275	272	13266	MVRD
R829	Uinta	4304730852	4-5 US LAMCO	ENSERCH EXPLORATION	UT	13S	20E	5	C SW	5802.9	B	4.6	2.67	0.00405	0.000191	213	13256	MVRD
R829	Uinta	4304730852	4-5 US LAMCO	ENSERCH EXPLORATION	UT	13S	20E	5	C SW	5802.9	A	4.6	2.67	0.00387	0.000145	279	13256	MVRD
R829	Uinta	4304730852	4-5 US LAMCO	ENSERCH EXPLORATION	UT	13S	20E	5	C SW	5812.1	B	3.8	2.71	0.00212	0.000101	202	13266	MVRD
R829	Uinta	4304730852	4-5 US LAMCO	ENSERCH EXPLORATION	UT	13S	20E	5	C SW	5812.1	A	3.1	2.69	0.000904	0.000038	669	13266	MVRD
R829	Uinta	4304730852	4-5 US LAMCO	ENSERCH EXPLORATION	UT	13S	20E	5	C SW	5818.0	B	13.2	2.66	0.124	0.0543	30.1	15276	MVRD
R829	Uinta	4304730852	4-5 US LAMCO	ENSERCH EXPLORATION	UT	13S	20E	5	C SW	5818.0	A	10.6	2.65	0.0323	0.0134	103	15276	MVRD
R999	Uinta	4304730860	3-24 US LAMCO	CHAMPLIN PETROLEUM	UT	13S	20E	24	NESE	6809.8	B	3.7	2.64	0.00688	0.000159	333	13216	CSLG
R999	Uinta	4304730860	3-24 US LAMCO	CHAMPLIN PETROLEUM	UT	13S	20E	24	NESE	6809.8	A	3.3	2.64	0.00287	0.000133	124	13216	CSLG
R999	Uinta	4304730860	3-24 US LAMCO	CHAMPLIN PETROLEUM	UT	13S	20E	24	NESE	6812.2	B	6.0	2.65	0.0503	0.0122	70.9	14266	CSLG
R999	Uinta	4304730860	3-24 US LAMCO	CHAMPLIN PETROLEUM	UT	13S	20E	24	NESE	6812.2	A	5.1	2.65	0.0175	0.00513	60.6	14266	CSLG
R999	Uinta	4304730860	3-24 US LAMCO	CHAMPLIN PETROLEUM	UT	13S	20E	24	NESE	7137.1	A	0.6	2.63	0.00368	0.000064	246	12219	CSLG
R999	Uinta	4304730860	3-24 US LAMCO	CHAMPLIN PETROLEUM	UT	13S	20E	24	NESE	7148.1	A	0.8	2.63	0.00277	0.000045	512	11219	CSLG
R999	Uinta	4304730860	3-24 US LAMCO	CHAMPLIN PETROLEUM	UT	13S	20E	24	NESE	7148.1	B	0.7	2.63	0.00133	0.000025	164	11219	CSLG
R999	Uinta	4304730860	3-24 US LAMCO	CHAMPLIN PETROLEUM	UT	13S	20E	24	NESE	7156.0	A	2.7	2.65	0.00493	0.000105	176	11219	CSLG
R999	Uinta	4304730860	3-24 US LAMCO	CHAMPLIN PETROLEUM	UT	13S	20E	24	NESE	7156.0	B	2.8	2.65	0.00317			11219	CSLG
R999	Uinta	4304730860	3-24 US LAMCO	CHAMPLIN PETROLEUM	UT	13S	20E	24	NESE	7158.9	B	2.7	2.68	0.00491	0.000149	145	13215	CSLG
R999	Uinta	4304730860	3-24 US LAMCO	CHAMPLIN PETROLEUM	UT	13S	20E	24	NESE	7158.9	A	2.3	2.67	0.00444	0.000171	109	13215	CSLG
R999	Uinta	4304730860	3-24 US LAMCO	CHAMPLIN PETROLEUM	UT	13S	20E	24	NESE	7169.6	A	1.9	2.68	0.00459	0.000110	370	14295	CSLG
R999	Uinta	4304730860	3-24 US LAMCO	CHAMPLIN PETROLEUM	UT	13S	20E	24	NESE	7169.6	B	2.0	2.69	0.00409	0.000082	287	14295	CSLG
S172	Uinta	43019XXXX1	3 BOOK CLIFFS	USGS-CG	UT	17S	24E	3	SE	124.1	A	15.2	2.63	0.144	0.103	16.4	13219	NSLN
S172	Uinta	43019XXXX1	3 BOOK CLIFFS	USGS-CG	UT	17S	24E	3	SE	124.3	A	11.1	2.63	0.0393	0.00460	149	13219	NSLN
S172	Uinta	43019XXXX1	3 BOOK CLIFFS	USGS-CG	UT	17S	24E	3	SE	124.7	A	18.9	2.64	0.725	0.496	11.0	13217	NSLN
S172	Uinta	43019XXXX1	3 BOOK CLIFFS	USGS-CG	UT	17S	24E	3	SE	174.0	A	7.0	2.61	0.00594	0.000416	177	12217	NSLN
S172	Uinta	43019XXXX1	3 BOOK CLIFFS	USGS-CG	UT	17S	24E	3	SE	175.2	A	19.9	2.62	15.8	34.0	5.3	13257	NSLN
S172	Uinta	43019XXXX1	3 BOOK CLIFFS	USGS-CG	UT	17S	24E	3	SE	175.3	A	21.5	2.64	41.2	29.7	6.2	13257	NSLN
S172	Uinta	43019XXXX1	3 BOOK CLIFFS	USGS-CG	UT	17S	24E	3	SE	175.3	A2	21.5	2.64	24.6	18.6	6.8	13257	NSLN
S172	Uinta	43019XXXX1	3 BOOK CLIFFS	USGS-CG	UT	17S	24E	3	SE	175.3	A1	21.2	2.64	23.6	17.7	6.0	13257	NSLN
S172	Uinta	43019XXXX1	3 BOOK CLIFFS	USGS-CG	UT	17S	24E	3	SE	206.0	A	10.6	2.56	0.0294	0.00486	102	11219	NSLN
S172	Uinta	43019XXXX1	3 BOOK CLIFFS	USGS-CG	UT	17S	24E	3	SE	252.0	A	14.2	2.61	0.154	0.0922	40.8	12217	NSLN
S172	Uinta	43019XXXX1	3 BOOK CLIFFS	USGS-CG	UT	17S	24E	3	SE	252.1	A	14.9	2.61	0.175	0.133	31.8	12217	NSLN
S172	Uinta	43019XXXX1	3 BOOK CLIFFS	USGS-CG	UT	17S	24E	3	SE	334.5	A	3.6	2.54	0.00579	0.000142	236	11219	NSLN
S172	Uinta	43019XXXX1	3 BOOK CLIFFS	USGS-CG	UT	17S	24E	3	SE	384.0	A	7.8	2.59	0.00550	0.000289	263	11219	NSLN
S172	Uinta	43019XXXX1	3 BOOK CLIFFS	USGS-CG	UT	17S	24E	3	SE	389.8	A	9.9	2.65	0.0133	0.00545	93.1	12219	NSLN
S172	Uinta	43019XXXX1	3 BOOK CLIFFS	USGS-CG	UT	17S	24E	3	SE	389.9	A	11.5	2.66	0.0290	0.0145	54.1	12219	NSLN
S172	Uinta	43019XXXX1	3 BOOK CLIFFS	USGS-CG	UT	17S	24E	3	SE	392.5	A	11.0	2.64	0.0134	0.00569	122	12239	NSLN
S172	Uinta	43019XXXX1	3 BOOK CLIFFS	USGS-CG	UT	17S	24E	3	SE	392.5	A2	11.7	2.66	0.00155	0.000920	142	12239	NSLN
S172	Uinta	43019XXXX1	3 BOOK CLIFFS	USGS-CG	UT	17S	24E	3	SE	392.5	A1	11.6	2.65	0.00142	0.000769	148	12239	NSLN
S172	Uinta	43019XXXX1	3 BOOK CLIFFS	USGS-CG	UT	17S	24E	3	SE	392.7	A	9.3	2.63	0.0167	0.00465	53.0	12239	NSLN
S172	Uinta	43019XXXX1	3 BOOK CLIFFS	USGS-CG	UT	17S	24E	3	SE	398.8	A	10.8	2.65	0.0737	0.0463	29.5	12239	NSLN
S174	Uinta	43019XXXX2	4 BOOK CLIFFS	USGS-CG	UT	17S	24E	31	NWSW	161.7	B	11.6	2.69	0.110	0.0348	13.5	13249	NSLN
S174	Uinta	43019XXXX2	4 BOOK CLIFFS	USGS-CG	UT	17S	24E	31	NWSW	161.7	A	12.1	2.66	0.107	0.0313	32.7	13249	NSLN
S174	Uinta	43019XXXX2	4 BOOK CLIFFS	USGS-CG	UT	17S	24E	31	NWSW	183.2	B	8.8	2.73	0.128	0.0287	83.3	15276	NSLN
S174	Uinta	43019XXXX2	4 BOOK CLIFFS	USGS-CG	UT	17S	24E	31	NWSW	183.2	A	8.7	2.73	0.105	0.0453	38.9	15276	NSLN
S174	Uinta	43019XXXX2	4 BOOK CLIFFS	USGS-CG	UT	17S	24E	31	NWSW	183.4	B	10.1	2.72	0.242	0.146	20.6	15276	NSLN
S174	Uinta	43019XXXX2	4 BOOK CLIFFS	USGS-CG	UT	17S	24E	31	NWSW	183.4	A	9.8	2.72	0.238	0.112	36.6	15276	NSLN
S174	Uinta	43019XXXX2	4 BOOK CLIFFS	USGS-CG	UT	17S	24E	31	NWSW	184.5	A	14.2	2.70	0.371	0.210	22.4	15526	NSLN
S174	Uinta	43019XXXX2	4 BOOK CLIFFS	USGS-CG	UT	17S	24E	31	NWSW	184.5	B	14.6	2.69	0.272	0.149	24.3	15526	NSLN
S174	Uinta	43019XXXX2	4 BOOK CLIFFS	USGS-CG	UT	17S	24E	31	NWSW	189.2	A	21.0	2.67	19.7	5.65	8.1	15596	NSLN
S174	Uinta	43019XXXX2	4 BOOK CLIFFS	USGS-CG	UT	17S	24E	31	NWSW	189.2	B	22.2	2.67	15.2	9.31	11.3	15596	NSLN
S174	Uinta	43019XXXX2	4 BOOK CLIFFS	USGS-CG	UT	17S	24E	31	NWSW	189.3	A	21.9	2.67	17.2	6.12	29.3	15596	NSLN
S174	Uinta	43019XXXX2	4 BOOK CLIFFS	USGS-CG	UT	17S	24E	31	NWSW	189.3	B	21.5	2.67	13.9	6.50	7.9	15596	NSLN
DR3	Washakie	4903722304	3 DRIPPING ROCK	CELSIUS	WY	14N	94W	8	SESWNW	12415.1	A	14.1	2.68	0.0468	0.0276	70.8	15586	MVRD
DR3	Washakie	4903722304	3 DRIPPING ROCK	CELSIUS	WY	14N	94W	8	SESWNW	12416.8	A	13.7	2.68	0.0464	0.0271	87.5	15516	MVRD
DR3	Washakie	4903722304	3 DRIPPING ROCK	CELSIUS	WY	14N	94W	8	SESWNW	12416.9	A	13.2	2.68	0.0486	0.0284	81.0	15516	MVRD
DR3	Washakie	4903722304	3 DRIPPING ROCK	CELSIUS	WY	14N	94W	8	SESWNW	12419.3	A	12.9	2.70	0.0294	0.0144	124	15586	MVRD
DR3	Washakie	4903722304	3 DRIPPING ROCK	CELSIUS	WY	14N	94W	8	SESWNW	12420.2	A	7.5	2.69	0.00427	0.000418	212	13546	MVRD
DR3	Washakie	4903722304	3 DRIPPING ROCK	CELSIUS	WY	14N	94W	8	SESWNW	12422.8	A	11.6	2.69	0.0112	0.00281	116	10286	MVRD
DR3	Washakie	4903722304	3 DRIPPING ROCK	CELSIUS	WY	14N	94W	8	SESWNW	12426.0	A	11.8	2.67	0.0124	0.00278	339	15576	MVRD
DR3	Washakie	4903722304	3 DRIPPING ROCK	CELSIUS	WY	14N	94W	8	SESWNW	12428.1	A	12.0	2.69	0.0131	0.00500	93.7	15286	MVRD
DR3	Washakie	4903722304	3 DRIPPING ROCK	CELSIUS	WY	14N	94W	8	SESWNW	12430.0	A	12.5	2.68	0.0239	0.00733	107	15576	MVRD
DR3	Washakie	4903722304	3 DRIPPING ROCK	CELSIUS	WY	14N	94W	8	SESWNW	12434.5	A	11.7	2.67	0.0188	0.00635	151	15576	MVRD
DR3	Washakie	4903722304	3 DRIPPING ROCK	CELSIUS	WY	14N	94W	8	SESWNW	12434.6	A	11.8	2.68	0.0194	0.00668	26.7	15576	MVRD
DR3	Washakie	4903722304	3 DRIPPING ROCK	CELSIUS	WY	14N	94W	8	SESWNW	12439.1	A	10.8	2.68	0.0102	0.00386	110	15584	MVRD
DR3	Washakie	4903722304	3 DRIPPING ROCK	CELSIUS	WY	14N	94W	8	SESWNW	12439.2	A	9.8	2.67	0.0104	0.00246	135	15584	MVRD
DR3	Washakie	4903722304	3 DRIPPING ROCK	CELSIUS	WY	14N	94W	8	SESWNW	12441.8	A	10.3	2.71	0.0163	0.00791	55.8	15285	MVRD
DR3	Washakie	4903722304	3 DRIPPING ROCK	CELSIUS	WY	14N	94W	8	SESWNW	12441.9	A	10.2	2.69	0.0181	0.00957	68.9	15285	MVRD
DR3	Washakie	4903722304	3 DRIPPING ROCK	CELSIUS	WY	14N	94W	8	SESWNW	12447.5	A	10.4	2.66	0.0117	0.00369	84.9	13214	MVRD
DR3	Washakie	4903722304	3 DRIPPING ROCK	CELSIUS	WY	14N	94W	8	SESWNW	12448.3	A	9.4	2.68	0.00840	0.00107	153	13216	MVRD
DR3	Washakie	4903722304	3 DRIPPING ROCK	CELSIUS	WY	14N	94W	8	SESWNW	12452.8	A	7.6	2.67	0.00434			15285	MVRD
DR3	Washakie	4903722304	3 DRIPPING ROCK	CELSIUS	WY	14N	94W	8	SESWNW	12453.7	A	5.5	2.65	0.00478	0.000107	970	13245	MVRD
DR3	Washakie	4903722304	3 DRIPPING ROCK	CELSIUS	WY	14N	94W	8	SESWNW	12455.4	A	6.5	2.68	0.00327	0.000310	264	13245	MVRD
DR3	Washakie	4903722304	3 DRIPPING ROCK	CELSIUS	WY	14N	94W	8	SESWNW	12469.5	A	1.4	2.69	0.00115	0.000022	435	13225	MVRD
DR3	Washakie	4903722304	3 DRIPPING ROCK	CELSIUS	WY	14N	94W	8	SESWNW	12474.2	A	2.9	2.70	0.00121	0.000027	574	11295	MVRD
DR5	Washakie	4903722355	5 DRIPPING ROCK	CELSIUS	WY	14N	94W	19	SESWNE	12466.9	A	1.9	2.72	0.00221	0.000069	359	13265	MVRD
DR5	Washakie	4903722355	5 DRIPPING ROCK	CELSIUS	WY	14N	94W	19	SESWNE	12671.9	B	10.9	2.67	0.0176	0.00275	226	13586	MVRD
DR5	Washakie	4903722355	5 DRIPPING ROCK	CELSIUS	WY	14N	94W	19	SESWNE	12671.9	A	10.7	2.67	0.0143	0.00319	110	13586	MVRD
DR5	Washakie	4903722355	5 DRIPPING ROCK	CELSIUS	WY	14N	94W	19	SESWNE	12673.3	A	13.3	2.70	0.0346	0.0155	54.1	15586	MVRD
DR5	Washakie	4903722355	5 DRIPPING ROCK	CELSIUS	WY	14N	94W	19	SESWNE	12673.6	B	12.7	2.66	0.0355	0.00750	51.1	15586	MVRD
DR5	Washakie	4903722355	5 DRIPPING ROCK	CELSIUS	WY	14N	94W	19	SESWNE	12673.6	A	11.8	2.64	0.0254	0.00858	73.2	15586	MVRD
DR5	Washakie	4903722355	5 DRIPPING ROCK	CELSIUS	WY	14N	94W	19	SESWNE	12675.8	A	12.6	2.69	0.0326	0.0158	39.4	13586	MVRD
DR5	Washakie	4903722355	5 DRIPPING ROCK	CELSIUS	WY	14N	94W	19	SESWNE	12675.8	B	12.7	2.69	0.0326	0.0121	129	13586	MVRD
DR5	Washakie	4903722355	5 DRIPPING ROCK	CELSIUS	WY	14N	94W	19	SESWNE	12677.1	A	11.9	2.67	0.0269	0.00725	114	13516	MVRD
DR5	Washakie	4903722355	5 DRIPPING ROCK	CELSIUS	WY	14N	94W	19	SESWNE	12677.2	A	11.4	2.66	0.0181	0.00617	89.2	13516	MVRD
DR5	Washakie	4903722355	5 DRIPPING ROCK	CELSIUS	WY	14N	94W	19	SESWNE	12678.9	A	11.4	2.65	0.0261	0.00737	91.3	13586	MVRD
DR5	Washakie	4903722355	5 DRIPPING ROCK	CELSIUS	WY	14N	94W	19	SESWNE	12678.9	B	12.2	2.67	0.0101	0.00348	92.5	13586	MVRD
DR5	Washakie	4903722355	5 DRIPPING ROCK	CELSIUS	WY	14N	94W	19	SESWNE	12680.7	A	12.3	2.67	0.0275	0.00983	109	15586	MVRD
DR5	Washakie	4903722355	5 DRIPPING ROCK	CELSIUS	WY	14N	94W	19	SESWNE	12680.7	B	12.2	2.67	0.0260	0.0102	72.1	15586	MVRD
DR5	Washakie	4903722355	5 DRIPPING ROCK	CELSIUS	WY	14N	94W	19	SESWNE	12686.4	B	12.5	2.68	0.0286	0.0132	82.0	13586	MVRD
DR5	Washakie	4903722355	5 DRIPPING ROCK	CELSIUS	WY	14N	94W	19	SESWNE	12686.5	A	11.7	2.65	0.0265	0.0119	74.2	13586	MVRD
DR5	Washakie	4903722355	5 DRIPPING ROCK	CELSIUS	WY	14N	94W	19	SESWNE	12686.5	B	12.5	2.67	0.0262	0.0121	40.3	13586	MVRD
DR5	Washakie	4903722355	5 DRIPPING ROCK	CELSIUS	WY	14N	94W	19	SESWNE	12686.7	A	12.8	2.68	0.0289	0.0120	100	13586	MVRD
DR5	Washakie	4903722355	5 DRIPPING ROCK	CELSIUS	WY	14N	94W	19	SESWNE	12688.8	B			0.0350	0.0163	63.4	15596	MVRD

Table 4.1.1. (continued)

Summary of Porosity, Permeability, and Grain Density
Analysis of Critical Permeability, Capillary Pressure, and Electrical Properties for Mesaverde Tight Gas Sandstones from Western U.S. Basins
US DOE # DE-FC26-05NT42660
Alan P. Byrnes, Robert M. Cluff, John C. Webb, Daniel A. Krygowski, Stefani D. Whittaker
website: http://www.kgs.ku.edu/mesaverde

USGS Library Number	Basin	API Number	Well Name	Operator	State	Township	Range	Section	Quarter Section	Plug Depth	Plug Letter	Ambient Porosity	Grain Density	Routine Gas Permeability	*in situ* Klinkenberg Gas Permeability	*in situ* Klinkenberg *constant* b	Rock Type Code	Formations
										ft	A/B/C	%	g/cc	mD	mD	(psia)		
DR5	Washakie	4903722355	5 DRIPPING ROCK	CELSIUS	WY	14N	94W	19	SESWNE	12688.8	A	12.7	2.67	0.0314	0.0166	36.4	15596	MVRD
DR5	Washakie	4903722355	5 DRIPPING ROCK	CELSIUS	WY	14N	94W	19	SESWNE	12690.0	A	11.5	2.68	0.0202	0.00564	143	15586	MVRD
DR5	Washakie	4903722355	5 DRIPPING ROCK	CELSIUS	WY	14N	94W	19	SESWNE	12690.1	A	11.7	2.66	0.0245	0.00605	145	15586	MVRD
DR5	Washakie	4903722355	5 DRIPPING ROCK	CELSIUS	WY	14N	94W	19	SESWNE	12693.3	B	13.2	2.70	0.0195	0.0151	56.5	15586	MVRD
DR5	Washakie	4903722355	5 DRIPPING ROCK	CELSIUS	WY	14N	94W	19	SESWNE	12695.9	B	13.0	2.69	0.835	0.265	22.5	15576	MVRD
DR5	Washakie	4903722355	5 DRIPPING ROCK	CELSIUS	WY	14N	94W	19	SESWNE	12695.9	A	12.7	2.60	0.0292	0.0136	56.1	15576	MVRD
DR5	Washakie	4903722355	5 DRIPPING ROCK	CELSIUS	WY	14N	94W	19	SESWNE	12698.5	A	12.0	2.70	0.0264	0.00885	97.5	15686	MVRD
DR5	Washakie	4903722355	5 DRIPPING ROCK	CELSIUS	WY	14N	94W	19	SESWNE	12698.6	A	12.5	2.70	0.0255	0.0111	47.3	15686	MVRD
DR5	Washakie	4903722355	5 DRIPPING ROCK	CELSIUS	WY	14N	94W	19	SESWNE	12700.8	A	11.4	2.69	0.0315	0.00974	36.5	15696	MVRD
DR5	Washakie	4903722355	5 DRIPPING ROCK	CELSIUS	WY	14N	94W	19	SESWNE	12703.0	B	12.0	2.68	0.0241	0.00712	90.2	15576	MVRD
DR5	Washakie	4903722355	5 DRIPPING ROCK	CELSIUS	WY	14N	94W	19	SESWNE	12703.0	A	11.4	2.67	0.0234	0.00601	113	15576	MVRD
DR5	Washakie	4903722355	5 DRIPPING ROCK	CELSIUS	WY	14N	94W	19	SESWNE	12703.2	A	11.6	2.67	0.0195	0.00644	53.5	15576	MVRD
DR5	Washakie	4903722355	5 DRIPPING ROCK	CELSIUS	WY	14N	94W	19	SESWNE	12703.2	B	15.4	2.47	0.0185	0.00648	46.5	15576	MVRD
DR5	Washakie	4903722355	5 DRIPPING ROCK	CELSIUS	WY	14N	94W	19	SESWNE	12704.2	A	11.4	2.68	0.0190	0.00348	109	13586	MVRD
DR5	Washakie	4903722355	5 DRIPPING ROCK	CELSIUS	WY	14N	94W	19	SESWNE	12704.2	B	10.6	2.67	0.0141	0.00282	156	13586	MVRD
DR5	Washakie	4903722355	5 DRIPPING ROCK	CELSIUS	WY	14N	94W	19	SESWNE	12704.3	B	11.4	2.67	0.0115	0.00175	123	13586	MVRD
DR5	Washakie	4903722355	5 DRIPPING ROCK	CELSIUS	WY	14N	94W	19	SESWNE	12704.3	A	10.8	2.67	0.0113	0.00220	209	13586	MVRD
DR5	Washakie	4903722355	5 DRIPPING ROCK	CELSIUS	WY	14N	94W	19	SESWNE	12709.8	B	9.9	2.67	0.0186	0.00283	147	15276	MVRD
DR5	Washakie	4903722355	5 DRIPPING ROCK	CELSIUS	WY	14N	94W	19	SESWNE	12709.8	A	16.0	2.77	0.0140	0.00353	100	15276	MVRD
DR5	Washakie	4903722355	5 DRIPPING ROCK	CELSIUS	WY	14N	94W	19	SESWNE	12713.7	B	17.3	2.70	0.00814	0.00180	129	15295	MVRD
DR5	Washakie	4903722355	5 DRIPPING ROCK	CELSIUS	WY	14N	94W	19	SESWNE	12713.7	A	8.6	2.68	0.00766	0.00191	95.6	15295	MVRD
DR5	Washakie	4903722355	5 DRIPPING ROCK	CELSIUS	WY	14N	94W	19	SESWNE	12718.3	A	3.6	2.69	0.00206	0.000136	169	15285	MVRD
DR5	Washakie	4903722355	5 DRIPPING ROCK	CELSIUS	WY	14N	94W	19	SESWNE	12718.3	B	3.5	2.69	0.00189	0.000008	449	15285	MVRD
DR5	Washakie	4903722355	5 DRIPPING ROCK	CELSIUS	WY	14N	94W	19	SESWNE	12721.2	A	1.9	2.69	0.00164	0.000044	212	13225	MVRD
DR5	Washakie	4903722355	5 DRIPPING ROCK	CELSIUS	WY	14N	94W	19	SESWNE	12721.2	B	2.3	2.71	0.000652	0.000003	1851	13225	MVRD
DR5	Washakie	4903722355	5 DRIPPING ROCK	CELSIUS	WY	14N	94W	19	SESWNE	12723.0	A	4.8	2.78	0.00172	0.000046	356	13265	MVRD
DR5	Washakie	4903722355	5 DRIPPING ROCK	CELSIUS	WY	14N	94W	19	SESWNE	12723.0	B	1.7	2.69	0.00133	0.000007	512	13265	MVRD
E489	Washakie	4903721053	3 UNIT FIVE MILE GULCH	AMOCO PRODUCTION	WY	21N	93W	35	C SW	10608.7	B	4.1	2.67	0.00108			11239	ALMD
E489	Washakie	4903721053	3 UNIT FIVE MILE GULCH	AMOCO PRODUCTION	WY	21N	93W	35	C SW	10608.7	A	4.3	2.67		0.000079	107	11239	ALMD
E489	Washakie	4903721053	3 UNIT FIVE MILE GULCH	AMOCO PRODUCTION	WY	21N	93W	35	C SW	10612.0	B	6.2	2.67	0.00786	0.000719	182	14266	ALMD
E489	Washakie	4903721053	3 UNIT FIVE MILE GULCH	AMOCO PRODUCTION	WY	21N	93W	35	C SW	10612.0	A	6.5	2.68	0.00226			14266	ALMD
E489	Washakie	4903721053	3 UNIT FIVE MILE GULCH	AMOCO PRODUCTION	WY	21N	93W	35	C SW	10612.1	A	6.0	2.68	0.00453	0.000382	267	14266	ALMD
E489	Washakie	4903721053	3 UNIT FIVE MILE GULCH	AMOCO PRODUCTION	WY	21N	93W	35	C SW	10612.3	A	5.6	2.67	0.00437			13236	ALMD
E489	Washakie	4903721053	3 UNIT FIVE MILE GULCH	AMOCO PRODUCTION	WY	21N	93W	35	C SW	10612.3	B	5.8	2.68	0.00299	0.000185	264	13236	ALMD
E489	Washakie	4903721053	3 UNIT FIVE MILE GULCH	AMOCO PRODUCTION	WY	21N	93W	35	C SW	10613.8	B	9.1	2.68	0.0112	0.00284	126	13256	ALMD
E489	Washakie	4903721053	3 UNIT FIVE MILE GULCH	AMOCO PRODUCTION	WY	21N	93W	35	C SW	10613.8	A	9.5	2.68	0.00607	0.00140	107	13256	ALMD
E489	Washakie	4903721053	3 UNIT FIVE MILE GULCH	AMOCO PRODUCTION	WY	21N	93W	35	C SW	10615.6	A	11.0	2.65	0.0532	0.00814	108	13226	ALMD
E489	Washakie	4903721053	3 UNIT FIVE MILE GULCH	AMOCO PRODUCTION	WY	21N	93W	35	C SW	10615.6	B	10.1	2.65	0.0375	0.0117	152	13226	ALMD
E489	Washakie	4903721053	3 UNIT FIVE MILE GULCH	AMOCO PRODUCTION	WY	21N	93W	35	C SW	10615.8	B	10.6	2.65	0.0560	0.0134	40.5	14216	ALMD
E489	Washakie	4903721053	3 UNIT FIVE MILE GULCH	AMOCO PRODUCTION	WY	21N	93W	35	C SW	10615.8	A	10.4	2.65	0.0512	0.0159	21.0	14216	ALMD
E489	Washakie	4903721053	3 UNIT FIVE MILE GULCH	AMOCO PRODUCTION	WY	21N	93W	35	C SW	10618.1	A	5.8	2.67	0.00823	0.000545	193	15266	ALMD
E489	Washakie	4903721053	3 UNIT FIVE MILE GULCH	AMOCO PRODUCTION	WY	21N	93W	35	C SW	10619.0	B	8.8	2.67	0.0234	0.00132	102	13266	ALMD
E489	Washakie	4903721053	3 UNIT FIVE MILE GULCH	AMOCO PRODUCTION	WY	21N	93W	35	C SW	10619.0	A	7.9	2.66	0.00994	0.00205	81.7	13266	ALMD
E489	Washakie	4903721053	3 UNIT FIVE MILE GULCH	AMOCO PRODUCTION	WY	21N	93W	35	C SW	10623.0	A	2.8	2.64	0.00357	0.000106	205	12246	ALMD
E489	Washakie	4903721053	3 UNIT FIVE MILE GULCH	AMOCO PRODUCTION	WY	21N	93W	35	C SW	10627.0	A	2.3	2.65	0.00463			11289	ALMD
E489	Washakie	4903721053	3 UNIT FIVE MILE GULCH	AMOCO PRODUCTION	WY	21N	93W	35	C SW	10627.0	B	8.4	2.66	0.00282	0.000083	155	11289	ALMD
E489	Washakie	4903721053	3 UNIT FIVE MILE GULCH	AMOCO PRODUCTION	WY	21N	93W	35	C SW	10629.0	A	5.8	2.65		0.000826	67.5	13296	ALMD
E489	Washakie	4903721053	3 UNIT FIVE MILE GULCH	AMOCO PRODUCTION	WY	21N	93W	35	C SW	10634.0	A	3.3	2.65	0.00501	0.000139	89.7	11229	ALMD
E489	Washakie	4903721053	3 UNIT FIVE MILE GULCH	AMOCO PRODUCTION	WY	21N	93W	35	C SW	10634.0	B	2.2	2.64	0.00417	0.000184	276	11229	ALMD
E489	Washakie	4903721053	3 UNIT FIVE MILE GULCH	AMOCO PRODUCTION	WY	21N	93W	35	C SW	10636.2	A	5.4	2.65	0.0125	0.00145	122	11299	ALMD
E489	Washakie	4903721053	3 UNIT FIVE MILE GULCH	AMOCO PRODUCTION	WY	21N	93W	35	C SW	10636.2	B	5.3	2.66	0.00636	0.000836	78.0	11299	ALMD
E489	Washakie	4903721053	3 UNIT FIVE MILE GULCH	AMOCO PRODUCTION	WY	21N	93W	35	C SW	10641.2	A	1.6	2.71	0.000291			13216	ALMD
E489	Washakie	4903721053	3 UNIT FIVE MILE GULCH	AMOCO PRODUCTION	WY	21N	93W	35	C SW	10641.2	B	1.7	2.71	0.000090	0.000144	227	13216	ALMD
E489	Washakie	4903721053	3 UNIT FIVE MILE GULCH	AMOCO PRODUCTION	WY	21N	93W	35	C SW	10645.0	B	4.0	2.65	0.00933	0.000293	171	30000	ALMD
E489	Washakie	4903721053	3 UNIT FIVE MILE GULCH	AMOCO PRODUCTION	WY	21N	93W	35	C SW	10645.0	A	4.3	2.64	0.00493	0.000349	180	30000	ALMD
E489	Washakie	4903721053	3 UNIT FIVE MILE GULCH	AMOCO PRODUCTION	WY	21N	93W	35	C SW	10650.0	B	5.8	2.76	0.00693	0.000512	248	13216	ALMD
E489	Washakie	4903721053	3 UNIT FIVE MILE GULCH	AMOCO PRODUCTION	WY	21N	93W	35	C SW	10650.0	A	6.2	2.76	0.00238	0.000309	120	13216	ALMD
E489	Washakie	4903721053	3 UNIT FIVE MILE GULCH	AMOCO PRODUCTION	WY	21N	93W	35	C SW	10651.0	A	4.3	2.65	0.0103			13216	ALMD
E489	Washakie	4903721053	3 UNIT FIVE MILE GULCH	AMOCO PRODUCTION	WY	21N	93W	35	C SW	10651.0	B	4.2	2.64	0.00754	0.000190	870	13216	ALMD
E489	Washakie	4903721053	3 UNIT FIVE MILE GULCH	AMOCO PRODUCTION	WY	21N	93W	35	C SW	10654.5	B	9.3	2.64	0.0132	0.00236	87.8	30000	ALMD
E489	Washakie	4903721053	3 UNIT FIVE MILE GULCH	AMOCO PRODUCTION	WY	21N	93W	35	C SW	10654.5	A	9.1	2.63	0.00943	0.00197	56.6	30000	ALMD
E489	Washakie	4903721053	3 UNIT FIVE MILE GULCH	AMOCO PRODUCTION	WY	21N	93W	35	C SW	10658.1	A	8.4	2.64	0.0367	0.00541	43.5	14256	ALMD
E489	Washakie	4903721053	3 UNIT FIVE MILE GULCH	AMOCO PRODUCTION	WY	21N	93W	35	C SW	10658.1	B	8.1	2.65	0.0187	0.00519	99.1	14256	ALMD
E489	Washakie	4903721053	3 UNIT FIVE MILE GULCH	AMOCO PRODUCTION	WY	21N	93W	35	C SW	10662.1	A	6.2	2.65	0.0169	0.00147	37.3	13256	ALMD
E489	Washakie	4903721053	3 UNIT FIVE MILE GULCH	AMOCO PRODUCTION	WY	21N	93W	35	C SW	10662.1	B	5.4	2.65	0.00790	0.000940	322	13256	ALMD
E489	Washakie	4903721053	3 UNIT FIVE MILE GULCH	AMOCO PRODUCTION	WY	21N	93W	35	C SW	10662.5	A	4.7	2.60	0.0137	0.000234	90.2	13236	ALMD
E489	Washakie	4903721053	3 UNIT FIVE MILE GULCH	AMOCO PRODUCTION	WY	21N	93W	35	C SW	10662.5	B	4.0	2.59	0.00449	0.000107	386	13236	ALMD
E489	Washakie	4903721053	3 UNIT FIVE MILE GULCH	AMOCO PRODUCTION	WY	21N	93W	35	C SW	10666.3	B	8.4	2.65	0.0210	0.00117	60.2	13256	ALMD
E489	Washakie	4903721053	3 UNIT FIVE MILE GULCH	AMOCO PRODUCTION	WY	21N	93W	35	C SW	10666.3	A	8.4	2.66	0.0170	0.000785	151	13256	ALMD
E489	Washakie	4903721053	3 UNIT FIVE MILE GULCH	AMOCO PRODUCTION	WY	21N	93W	35	C SW	10668.2	A	7.9	2.64	0.0226	0.00215	65.3	14276	ALMD
E489	Washakie	4903721053	3 UNIT FIVE MILE GULCH	AMOCO PRODUCTION	WY	21N	93W	35	C SW	10668.2	B	7.9	2.65	0.0111	0.00232	60.7	14276	ALMD
E489	Washakie	4903721053	3 UNIT FIVE MILE GULCH	AMOCO PRODUCTION	WY	21N	93W	35	C SW	10668.9	A	6.7	2.65	0.0244	0.00203	73.2	14276	ALMD
E489	Washakie	4903721053	3 UNIT FIVE MILE GULCH	AMOCO PRODUCTION	WY	21N	93W	35	C SW	10668.9	B	6.0	2.65	0.0128	0.00201	168	14276	ALMD
E489	Washakie	4903721053	3 UNIT FIVE MILE GULCH	AMOCO PRODUCTION	WY	21N	93W	35	C SW	10669.0	B	6.5	2.65	0.0320	0.00290	65.5	14276	ALMD
E489	Washakie	4903721053	3 UNIT FIVE MILE GULCH	AMOCO PRODUCTION	WY	21N	93W	35	C SW	10669.0	A	6.7	2.65	0.0287	0.00261	83.8	14276	ALMD
E489	Washakie	4903721053	3 UNIT FIVE MILE GULCH	AMOCO PRODUCTION	WY	21N	93W	35	C SW	10670.0	A	9.4	2.65	0.0971	0.0199	50.9	14286	ALMD
E489	Washakie	4903721053	3 UNIT FIVE MILE GULCH	AMOCO PRODUCTION	WY	21N	93W	35	C SW	10670.9	A	8.7	2.62	0.106	0.0309	32.2	15286	ALMD
E489	Washakie	4903721053	3 UNIT FIVE MILE GULCH	AMOCO PRODUCTION	WY	21N	93W	35	C SW	10670.9	B	8.9	2.65	0.0517	0.0208	77.0	15286	ALMD
E489	Washakie	4903721053	3 UNIT FIVE MILE GULCH	AMOCO PRODUCTION	WY	21N	93W	35	C SW	10675.2	B	10.0	2.65	0.0520	0.0280	18.3	15296	ALMD
E489	Washakie	4903721053	3 UNIT FIVE MILE GULCH	AMOCO PRODUCTION	WY	21N	93W	35	C SW	10675.2	A	7.6	2.58	0.0506	0.0245	106	15296	ALMD
E489	Washakie	4903721053	3 UNIT FIVE MILE GULCH	AMOCO PRODUCTION	WY	21N	93W	35	C SW	10675.3	A	10.4	2.65	0.0923	0.0299	28.5	15286	ALMD
E489	Washakie	4903721053	3 UNIT FIVE MILE GULCH	AMOCO PRODUCTION	WY	21N	93W	35	C SW	10675.3	B	9.7	2.65	0.0530	0.0271	59.9	15286	ALMD
E489	Washakie	4903721053	3 UNIT FIVE MILE GULCH	AMOCO PRODUCTION	WY	21N	93W	35	C SW	10675.4	B	10.4	2.65	0.104	0.0235	58.9	15286	ALMD
E489	Washakie	4903721053	3 UNIT FIVE MILE GULCH	AMOCO PRODUCTION	WY	21N	93W	35	C SW	10675.4	A	10.1	2.65	0.0988	0.0327	27.4	15286	ALMD
E489	Washakie	4903721053	3 UNIT FIVE MILE GULCH	AMOCO PRODUCTION	WY	21N	93W	35	C SW	10675.7	A	10.2	2.65	0.0741	0.0208	32.0	15286	ALMD
E489	Washakie	4903721053	3 UNIT FIVE MILE GULCH	AMOCO PRODUCTION	WY	21N	93W	35	C SW	10675.7	B		2.65	0.0482	0.0227	72.1	15286	ALMD
E489	Washakie	4903721053	3 UNIT FIVE MILE GULCH	AMOCO PRODUCTION	WY	21N	93W	35	C SW	10675.8	A	10.1	2.65	0.0700	0.0255	17.2	15286	ALMD
E489	Washakie	4903721053	3 UNIT FIVE MILE GULCH	AMOCO PRODUCTION	WY	21N	93W	35	C SW	10675.8	B	9.8	2.66	0.0392	0.0198	48.9	15286	ALMD
E489	Washakie	4903721053	3 UNIT FIVE MILE GULCH	AMOCO PRODUCTION	WY	21N	93W	35	C SW	10678.7	B	8.6	2.61	0.0439	0.0197	22.0	15286	ALMD
E489	Washakie	4903721053	3 UNIT FIVE MILE GULCH	AMOCO PRODUCTION	WY	21N	93W	35	C SW	10678.7	A	10.2	2.65	0.0413	0.0174	81.9	15286	ALMD
E489	Washakie	4903721053	3 UNIT FIVE MILE GULCH	AMOCO PRODUCTION	WY	21N	93W	35	C SW	10681.2	B	10.4	2.66	0.0538	0.00804	52.9	15286	ALMD
E489	Washakie	4903721053	3 UNIT FIVE MILE GULCH	AMOCO PRODUCTION	WY	21N	93W	35	C SW	10681.2	A	10.4	2.66	0.0201	0.00617	149	15286	ALMD
E489	Washakie	4903721053	3 UNIT FIVE MILE GULCH	AMOCO PRODUCTION	WY	21N	93W	35	C SW	10682.0	A	10.2	2.67	0.0211	0.00243	87.8	15286	ALMD
E489	Washakie	4903721053	3 UNIT FIVE MILE GULCH	AMOCO PRODUCTION	WY	21N	93W	35	C SW	10682.0	B	9.8	2.67	0.00715	0.00262	118	15286	ALMD
E489	Washakie	4903721053	3 UNIT FIVE MILE GULCH	AMOCO PRODUCTION	WY	21N	93W	35	C SW	10682.3	B	9.9	2.67	0.0141	0.00419	128	15286	ALMD
E489	Washakie	4903721053	3 UNIT FIVE MILE GULCH	AMOCO PRODUCTION	WY	21N	93W	35	C SW	10682.3	A	9.2	2.67				15286	ALMD
E489	Washakie	4903721053	3 UNIT FIVE MILE GULCH	AMOCO PRODUCTION	WY	21N	93W	35	C SW	10693.4	B	2.3	2.60	0.00370	0.000139	126	12228	ALMD
E489	Washakie	4903721053	3 UNIT FIVE MILE GULCH	AMOCO PRODUCTION	WY	21N	93W	35	C SW	10693.4	A	2.6	2.59				12228	ALMD
E489	Washakie	4903721053	3 UNIT FIVE MILE GULCH	AMOCO PRODUCTION	WY	21N	93W	35	C SW	10701.0	A	3.9	2.62				12218	ALMD
E489	Washakie	4903721053	3 UNIT FIVE MILE GULCH	AMOCO PRODUCTION	WY	21N	93W	35	C SW	10701.2	A	8.8	2.79	0.00557	0.000207	318	12218	ALMD
E489	Washakie	4903721053	3 UNIT FIVE MILE GULCH	AMOCO PRODUCTION	WY	21N	93W	35	C SW	10701.8	A	3.1	2.63	0.00782	0.000403	159	13229	ALMD
E489	Washakie	4903721053	3 UNIT FIVE MILE GULCH	AMOCO PRODUCTION	WY	21N	93W	35	C SW	10701.8	B		2.63	0.00710	0.000226	370	13229	ALMD
E489	Washakie	4903721053	3 UNIT FIVE MILE GULCH	AMOCO PRODUCTION	WY	21N	93W	35	C SW	10703.5	A	3.5	2.62				13248	ALMD
E489	Washakie	4903721053	3 UNIT FIVE MILE GULCH	AMOCO PRODUCTION	WY	21N	93W	35	C SW	10705.3	B	3.1	2.62	0.00835	0.000417	240	12219	ALMD
E489	Washakie	4903721053	3 UNIT FIVE MILE GULCH	AMOCO PRODUCTION	WY	21N	93W	35	C SW	10705.3	A	3.6	2.65	0.00693	0.000129	339	12219	ALMD
E489	Washakie	4903721053	3 UNIT FIVE MILE GULCH	AMOCO PRODUCTION	WY	21N	93W	35	C SW	10706.9	B		2.65	0.00845	0.000828	155	15266	ALMD
E489	Washakie	4903721053	3 UNIT FIVE MILE GULCH	AMOCO PRODUCTION	WY	21N	93W	35	C SW	10706.9	A	5.0	2.65				15266	ALMD
E489	Washakie	4903721053	3 UNIT FIVE MILE GULCH	AMOCO PRODUCTION	WY	21N	93W	35	C SW	10708.9	B	3.9	2.60	1.86	0.0410	67.1	13246	ALMD
E489	Washakie	4903721053	3 UNIT FIVE MILE GULCH	AMOCO PRODUCTION	WY	21N	93W	35	C SW	10708.9	A	4.0	2.60	0.0271	0.000656	149	13246	ALMD
E489	Washakie	4903721053	3 UNIT FIVE MILE GULCH	AMOCO PRODUCTION	WY	21N	93W	35	C SW	10709.7	B	6.0	2.64	0.00834	0.000376	324	13246	ALMD
E489	Washakie	4903721053	3 UNIT FIVE MILE GULCH	AMOCO PRODUCTION	WY	21N	93W	35	C SW	10709.7	A	6.1	2.63				13246	ALMD
E489	Washakie	4903721053	3 UNIT FIVE MILE GULCH	AMOCO PRODUCTION	WY	21N	93W	35	C SW	10710.3	B	6.4	2.65	0.0325	0.00309	31.1	14266	ALMD

Table 4.1.1. (continued)

Summary of Porosity, Permeability, and Grain Density
Analysis of Critical Permeability, Capillary Pressure, and Electrical Properties for Mesaverde Tight Gas Sandstones from Western U.S. Basins
US DOE # DE-FC26-05NT42660
Alan P. Byrnes, Robert M. Cluff, John C. Webb, Daniel A. Krygowski, Stefani D. Whittaker
website: http://www.kgs.ku.edu/mesaverde

USGS Library Number	Basin	API Number	Well Name	Operator	State	Township	Range	Section	Quarter Section	Plug Depth	Plug Letter	Ambient Porosity	Grain Density	Routine Gas Permeability	*in situ* Klinkenberg Gas Permeability	*In situ* Klinkenberg *constant* b (psia)	Rock Type Code	Formations
										ft	A/B/C	%	g/cc	mD	mD			
E489	Washakie	4903721053	3 UNIT FIVE MILE GULCH	AMOCO PRODUCTION	WY	21N	93W	35	C SW	10710.3	A	6.2	2.65				14266	ALMD
E489	Washakie	4903721053	3 UNIT FIVE MILE GULCH	AMOCO PRODUCTION	WY	21N	93W	35	C SW	10715.8	B	5.1	2.66	0.00765	0.000916	169	14276	ALMD
E489	Washakie	4903721053	3 UNIT FIVE MILE GULCH	AMOCO PRODUCTION	WY	21N	93W	35	C SW	10715.8	A	5.3	2.65				14276	ALMD
E489	Washakie	4903721053	3 UNIT FIVE MILE GULCH	AMOCO PRODUCTION	WY	21N	93W	35	C SW	10717.0	B	6.3	2.64	0.0127	0.00118	133	13246	ALMD
E489	Washakie	4903721053	3 UNIT FIVE MILE GULCH	AMOCO PRODUCTION	WY	21N	93W	35	C SW	10717.0	A	11.9	2.63				13246	ALMD
E489	Washakie	4903721053	3 UNIT FIVE MILE GULCH	AMOCO PRODUCTION	WY	21N	93W	35	C SW	10723.7	B	0.8	2.62	0.00212	0.000081	266	12219	ALMD
E489	Washakie	4903721053	3 UNIT FIVE MILE GULCH	AMOCO PRODUCTION	WY	21N	93W	35	C SW	10723.7	A	1.6	2.63				12219	ALMD
N/A	Washakie	9999999999	WILD ROSE 1	N/A	WY	N/A	N/A	N/A	N/A	9762.5	A	14.4	2.68	0.0761	0.0320	63.1	15597	MVRD
N/A	Washakie	9999999999	WILD ROSE 1	N/A	WY	N/A	N/A	N/A	N/A	9837.7	A	6.7	2.64				12219	MVRD
N/A	Washakie	9999999999	WILD ROSE 1	N/A	WY	N/A	N/A	N/A	N/A	9839.4	A	6.4	2.69	0.00278	0.000445	166	12219	MVRD
N/A	Washakie	9999999999	WILD ROSE 1	N/A	WY	N/A	N/A	N/A	N/A	10015.6	A	5.3	2.66	0.00516	0.000779	47.9	14267	MVRD
N/A	Washakie	9999999999	WILD ROSE 1	N/A	WY	N/A	N/A	N/A	N/A	10132.7	A	7.2	2.68	0.0105	0.00287	112	14266	MVRD
N/A	Washakie	9999999999	WILD ROSE 1	N/A	WY	N/A	N/A	N/A	N/A	10133.5	A	6.1	2.68	0.00889	0.00243	101	14267	MVRD
N/A	Washakie	9999999999	WILD ROSE 1	N/A	WY	N/A	N/A	N/A	N/A	10204.8	A	8.8	2.68	0.0401	0.0231	28.2	14266	MVRD
N/A	Washakie	9999999999	WILD ROSE 1	N/A	WY	N/A	N/A	N/A	N/A	10207.8	A	11.1	2.67	0.254	0.192	25.8	14326	MVRD
S265	Washakie	4903720033	102-7-10 ARCH UNIT	ANADARKO E&P CO. LP	WY	19N	98W	7	SWSW	4868.0	A	18.9	2.62	1.19	44.2	4.6	16696	ALMD
S265	Washakie	4903720033	102-7-10 ARCH UNIT	ANADARKO E&P CO. LP	WY	19N	98W	7	SWSW	4878.0	A	18.9	2.62	34.2	26.3	2.3	16576	ALMD
S265	Washakie	4903720033	102-7-10 ARCH UNIT	ANADARKO E&P CO. LP	WY	19N	98W	7	SWSW	4878.0	B	18.7	2.61	32.7	23.2	2.9	16576	ALMD
S265	Washakie	4903720033	102-7-10 ARCH UNIT	ANADARKO E&P CO. LP	WY	19N	98W	7	SWSW	4885.0	B	19.8	2.65	35.6	24.2	4.3	16576	ALMD
S265	Washakie	4903720033	102-7-10 ARCH UNIT	ANADARKO E&P CO. LP	WY	19N	98W	7	SWSW	4885.0	A	19.3	2.63	34.8	23.7	3.6	16576	ALMD
S265	Washakie	4903720033	102-7-10 ARCH UNIT	ANADARKO E&P CO. LP	WY	19N	98W	7	SWSW	4889.0	A	17.9	2.62	29.5	19.6	3.5	16576	ALMD
S265	Washakie	4903720033	102-7-10 ARCH UNIT	ANADARKO E&P CO. LP	WY	19N	98W	7	SWSW	4889.0	c			17.6	10.4	6.6	16576	ALMD
S265	Washakie	4903720033	102-7-10 ARCH UNIT	ANADARKO E&P CO. LP	WY	19N	98W	7	SWSW	4889.0	B	17.5	2.63	16.6	10.2	7.1	16576	ALMD
S265	Washakie	4903720033	102-7-10 ARCH UNIT	ANADARKO E&P CO. LP	WY	19N	98W	7	SWSW	4890.0	A	8.4	2.67	0.0356	0.00949	85.4	13265	ALMD
S265	Washakie	4903720033	102-7-10 ARCH UNIT	ANADARKO E&P CO. LP	WY	19N	98W	7	SWSW	4890.0	B	8.9	2.69	0.0236	0.00814	60.9	13265	ALMD
S265	Washakie	4903720033	102-7-10 ARCH UNIT	ANADARKO E&P CO. LP	WY	19N	98W	7	SWSW	4891.0	A	21.1	2.63	138	84.7	7.3	16576	ALMD
S265	Washakie	4903720033	102-7-10 ARCH UNIT	ANADARKO E&P CO. LP	WY	19N	98W	7	SWSW	4895.0	A	20.6	2.63	96.8	75.2	1.9	16576	ALMD
S265	Washakie	4903720033	102-7-10 ARCH UNIT	ANADARKO E&P CO. LP	WY	19N	98W	7	SWSW	4898.0	B	11.7	2.66	0.136	0.0156	41.1	13245	ALMD
S265	Washakie	4903720033	102-7-10 ARCH UNIT	ANADARKO E&P CO. LP	WY	19N	98W	7	SWSW	4898.0	A	10.1	2.65	0.0147	0.00422	177	13245	ALMD
S265	Washakie	4903720033	102-7-10 ARCH UNIT	ANADARKO E&P CO. LP	WY	19N	98W	7	SWSW	4899.0	C	22.4	2.65	161	121	2.8	13245	ALMD
S265	Washakie	4903720033	102-7-10 ARCH UNIT	ANADARKO E&P CO. LP	WY	19N	98W	7	SWSW	4899.0	D	21.6	2.65	140	57.3	17.4	13245	ALMD
S265	Washakie	4903720033	102-7-10 ARCH UNIT	ANADARKO E&P CO. LP	WY	19N	98W	7	SWSW	4899.0	B	18.1	2.57	56.8	32.1	8.6	13245	ALMD
S265	Washakie	4903720033	102-7-10 ARCH UNIT	ANADARKO E&P CO. LP	WY	19N	98W	7	SWSW	4899.0	A	20.1	2.62	41.2	28.5	3.8	13245	ALMD
S276	Washakie	4903705683	65-1-7 ARCH UNIT	FOREST OIL CORP	WY	19N	99W	1	NWSE	4728.0	A	7.4	2.62	0.00639	0.000322	241	12219	ALMD
S276	Washakie	4903705683	65-1-7 ARCH UNIT	FOREST OIL CORP	WY	19N	99W	1	NWSE	4728.0	B	6.8	2.62	0.00510	0.000262	409	12219	ALMD
S276	Washakie	4903705683	65-1-7 ARCH UNIT	FOREST OIL CORP	WY	19N	99W	1	NWSE	4729.0	B	13.0	2.64	0.0829	0.0278	36.3	12219	ALMD
S276	Washakie	4903705683	65-1-7 ARCH UNIT	FOREST OIL CORP	WY	19N	99W	1	NWSE	4729.0	A	12.2	2.62	0.0691	0.0261	81.8	12219	ALMD
S276	Washakie	4903705683	65-1-7 ARCH UNIT	FOREST OIL CORP	WY	19N	99W	1	NWSE	4731.0	A	9.4	2.60	0.0681	0.00691	76.9	12236	ALMD
S276	Washakie	4903705683	65-1-7 ARCH UNIT	FOREST OIL CORP	WY	19N	99W	1	NWSE	4731.0	B	10.0	2.61	0.0143	0.00406	98.2	12236	ALMD
S276	Washakie	4903705683	65-1-7 ARCH UNIT	FOREST OIL CORP	WY	19N	99W	1	NWSE	4733.0	A	16.1	2.64	1.15	0.644	22.1	13215	ALMD
S276	Washakie	4903705683	65-1-7 ARCH UNIT	FOREST OIL CORP	WY	19N	99W	1	NWSE	4733.0	B	15.2	2.64	0.734	0.437	14.8	13215	ALMD
S276	Washakie	4903705683	65-1-7 ARCH UNIT	FOREST OIL CORP	WY	19N	99W	1	NWSE	4736.1	A	17.6	2.65	17.2	11.3	6.2	15275	ALMD
S276	Washakie	4903705683	65-1-7 ARCH UNIT	FOREST OIL CORP	WY	19N	99W	1	NWSE	4736.1	B	17.7	2.65	14.9	8.81	11.7	15275	ALMD
S276	Washakie	4903705683	65-1-7 ARCH UNIT	FOREST OIL CORP	WY	19N	99W	1	NWSE	4736.2	B	18.0	2.66	14.1	8.84	9.1	15275	ALMD
S276	Washakie	4903705683	65-1-7 ARCH UNIT	FOREST OIL CORP	WY	19N	99W	1	NWSE	4736.2	A	17.3	2.65	8.84	4.87	16.6	15275	ALMD
S276	Washakie	4903705683	65-1-7 ARCH UNIT	FOREST OIL CORP	WY	19N	99W	1	NWSE	4738.0	A	17.4	2.64	2.83	1.91	11.5	13275	ALMD
S276	Washakie	4903705683	65-1-7 ARCH UNIT	FOREST OIL CORP	WY	19N	99W	1	NWSE	4738.0	B	15.5	2.64	0.401	0.250	16.2	13275	ALMD
S276	Washakie	4903705683	65-1-7 ARCH UNIT	FOREST OIL CORP	WY	19N	99W	1	NWSE	4743.0	B	14.7	2.66	0.821	0.585	5.2	13255	ALMD
S276	Washakie	4903705683	65-1-7 ARCH UNIT	FOREST OIL CORP	WY	19N	99W	1	NWSE	4743.0	A	14.1	2.66	0.733	0.487	18.8	13255	ALMD
S276	Washakie	4903705683	65-1-7 ARCH UNIT	FOREST OIL CORP	WY	19N	99W	1	NWSE	4745.0	B	14.6	2.64	0.669	0.393	17.2	13255	ALMD
S276	Washakie	4903705683	65-1-7 ARCH UNIT	FOREST OIL CORP	WY	19N	99W	1	NWSE	4745.0	A	14.8	2.66	0.454	0.288	13.3	13255	ALMD
S276	Washakie	4903705683	65-1-7 ARCH UNIT	FOREST OIL CORP	WY	19N	99W	1	NWSE	4746.0	A	8.1	2.63	0.00526	0.000611	193	12235	ALMD
S276	Washakie	4903705683	65-1-7 ARCH UNIT	FOREST OIL CORP	WY	19N	99W	1	NWSE	4746.0	B	8.3	2.65	0.00380	0.000451	228	12235	ALMD
S276	Washakie	4903705683	65-1-7 ARCH UNIT	FOREST OIL CORP	WY	19N	99W	1	NWSE	4746.2	A	10.1	2.66	0.0118	0.00292	156	12235	ALMD
S276	Washakie	4903705683	65-1-7 ARCH UNIT	FOREST OIL CORP	WY	19N	99W	1	NWSE	4746.2	B	9.6	2.66	0.00858	0.00145	210	12235	ALMD
S276	Washakie	4903705683	65-1-7 ARCH UNIT	FOREST OIL CORP	WY	19N	99W	1	NWSE	4747.0	A	8.4	2.62	0.00728	0.00209	73.6	12235	ALMD
S276	Washakie	4903705683	65-1-7 ARCH UNIT	FOREST OIL CORP	WY	19N	99W	1	NWSE	4747.0	B	8.0	2.62	0.00513	0.00106	160	12235	ALMD
S276	Washakie	4903705683	65-1-7 ARCH UNIT	FOREST OIL CORP	WY	19N	99W	1	NWSE	4756.9	A	8.5	2.60	0.0629	0.00308	111	12239	ALMD
S276	Washakie	4903705683	65-1-7 ARCH UNIT	FOREST OIL CORP	WY	19N	99W	1	NWSE	4756.9	B	8.7	2.60				12239	ALMD
S276	Washakie	4903705683	65-1-7 ARCH UNIT	FOREST OIL CORP	WY	19N	99W	1	NWSE	4757.9	B	11.1	2.67	0.145	0.0368	49.6	12235	ALMD
S276	Washakie	4903705683	65-1-7 ARCH UNIT	FOREST OIL CORP	WY	19N	99W	1	NWSE	4757.9	A	10.6	2.68	0.124	0.0369	69.6	12235	ALMD
S276	Washakie	4903705683	65-1-7 ARCH UNIT	FOREST OIL CORP	WY	19N	99W	1	NWSE	4761.0	A	7.6	2.75	0.00336	0.000260	121	11235	ALMD
S276	Washakie	4903705683	65-1-7 ARCH UNIT	FOREST OIL CORP	WY	19N	99W	1	NWSE	4761.0	B	8.4	2.77	0.00205	0.000118	365	11235	ALMD
T592	Washakie	4900721170	C-11 /FEE	FUEL RESOURCES DEV	WY	12N	90W	11	NENW	2340.7	B	14.1	2.60	0.296	0.0728	41.7	11239	ALMD
T592	Washakie	4900721170	C-11 /FEE	FUEL RESOURCES DEV	WY	12N	90W	11	NENW	2340.7	A	13.5	2.57	0.218	0.0305	62.6	11239	ALMD
T695	Washakie	4903723956	5-2 SIBERIA RIDGE	AMOCO PRODUCTION	WY	21N	94W	5	SW	10646.2	A	3.0	2.64	0.0115	0.000296	179	13218	ALMD
T695	Washakie	4903723956	5-2 SIBERIA RIDGE	AMOCO PRODUCTION	WY	21N	94W	5	SW	10648.3	A	9.4	2.64	0.0191	0.00475	96.8	13216	ALMD
T695	Washakie	4903723956	5-2 SIBERIA RIDGE	AMOCO PRODUCTION	WY	21N	94W	5	SW	10651.9	A	10.1	2.64	0.0298	0.00677	126	15286	ALMD
T695	Washakie	4903723956	5-2 SIBERIA RIDGE	AMOCO PRODUCTION	WY	21N	94W	5	SW	10657.1	A	10.1	2.63	0.0207	0.00373	26.1	15286	ALMD
T695	Washakie	4903723956	5-2 SIBERIA RIDGE	AMOCO PRODUCTION	WY	21N	94W	5	SW	10660.3	A	9.4	2.65	0.0145	0.00232	152	15296	ALMD
T695	Washakie	4903723956	5-2 SIBERIA RIDGE	AMOCO PRODUCTION	WY	21N	94W	5	SW	10661.7	A	8.8	2.67	0.00710	0.00161	141	15296	ALMD
T695	Washakie	4903723956	5-2 SIBERIA RIDGE	AMOCO PRODUCTION	WY	21N	94W	5	SW	10664.9	A	8.8	2.69	0.00604	0.000922	280	15286	ALMD
T695	Washakie	4903723956	5-2 SIBERIA RIDGE	AMOCO PRODUCTION	WY	21N	94W	5	SW	10669.4	B	1.9	2.60	0.0219	0.000937	162	12217	ALMD
T695	Washakie	4903723956	5-2 SIBERIA RIDGE	AMOCO PRODUCTION	WY	21N	94W	5	SW	10669.4	A	3.0	2.60	0.00588	0.000070	176	12217	ALMD
B049	Wind River	4901320724	31-22 TRIBAL PHILLIPS	BROWN TOM INC	WY	4N	3E	31	NWSENW	11685.0	A	0.7	2.69	0.00439	0.000087	337	13255	MVRD
B049	Wind River	4901320724	31-22 TRIBAL PHILLIPS	BROWN TOM INC	WY	4N	3E	31	NWSENW	11698.9	A	1.0	2.72	0.00489	0.000133	224	13226	MVRD
B049	Wind River	4901320724	31-22 TRIBAL PHILLIPS	BROWN TOM INC	WY	4N	3E	31	NWSENW	11770.2	A	2.8	2.64	0.00402	0.000211	130	15276	MVRD
B049	Wind River	4901320724	31-22 TRIBAL PHILLIPS	BROWN TOM INC	WY	4N	3E	31	NWSENW	11801.8	A	1.4	2.63	0.00852	0.000163	354	13246	MVRD
B049	Wind River	4901320724	31-22 TRIBAL PHILLIPS	BROWN TOM INC	WY	4N	3E	31	NWSENW	11807.5	A	1.8	2.70	0.00206	0.000066	464	14266	MVRD
B049	Wind River	4901320724	31-22 TRIBAL PHILLIPS	BROWN TOM INC	WY	4N	3E	31	NWSENW	11807.6	A	1.6	2.71	0.00190	0.000039	773	14266	MVRD
B049	Wind River	4901320724	31-22 TRIBAL PHILLIPS	BROWN TOM INC	WY	4N	3E	31	NWSENW	11812.9	A	4.0	2.68	0.00510	0.000514	42.5	14267	MVRD
C899	Wind River	4901320836	1-27 LOOKOUT	MONSANTO OIL	WY	39N	91W	27	CSWNE	16565.1	A	2.8	2.68	0.00669	0.000224	206	15286	MVRD
C899	Wind River	4901320836	1-27 LOOKOUT	MONSANTO OIL	WY	39N	91W	27	CSWNE	16569.6	A	1.8	2.68	0.00586	0.000120	332	15296	MVRD
C899	Wind River	4901320836	1-27 LOOKOUT	MONSANTO OIL	WY	39N	91W	27	CSWNE	16580.0	A	1.0	2.61	0.00639	0.000057	681	11299	MVRD
C899	Wind River	4901320836	1-27 LOOKOUT	MONSANTO OIL	WY	39N	91W	27	CSWNE	16580.0	A			0.00315	0.000051	290	11299	MVRD
C899	Wind River	4901320836	1-27 LOOKOUT	MONSANTO OIL	WY	39N	91W	27	CSWNE	16591.9	A	1.6	2.66	0.000526	0.000100	298	12219	MVRD
C899	Wind River	4901320836	1-27 LOOKOUT	MONSANTO OIL	WY	39N	91W	27	CSWNE	16616.5	A	0.9	2.70	0.00425	0.000014	421	12249	MVRD
C899	Wind River	4901320836	1-27 LOOKOUT	MONSANTO OIL	WY	39N	91W	27	CSWNE	16625.1	A	1.0	2.71	0.00275	0.000032	735	13259	MVRD
C899	Wind River	4901320836	1-27 LOOKOUT	MONSANTO OIL	WY	39N	91W	27	CSWNE	16626.0	A	1.9	2.71	0.00300	0.000077	282	11299	MVRD
C899	Wind River	4901320836	1-27 LOOKOUT	MONSANTO OIL	WY	39N	91W	27	CSWNE	16653.8	A	1.4	2.69	0.00732	0.000158	199	12246	MVRD
C899	Wind River	4901320836	1-27 LOOKOUT	MONSANTO OIL	WY	39N	91W	27	CSWNE	16665.9	A	5.5	2.66	0.00591	0.000439	186	15286	MVRD
C899	Wind River	4901320836	1-27 LOOKOUT	MONSANTO OIL	WY	39N	91W	27	CSWNE	16678.9	A	5.5	2.66	0.00474	0.000621	260	15286	MVRD
C899	Wind River	4901320836	1-27 LOOKOUT	MONSANTO OIL	WY	39N	91W	27	CSWNE	16686.8	A	4.6	2.66	0.0136	0.000779	74.5	16286	MVRD
C899	Wind River	4901320836	1-27 LOOKOUT	MONSANTO OIL	WY	39N	91W	27	CSWNE	16698.9	A	5.1	2.66	0.0105	0.000623	176	16286	MVRD
C899	Wind River	4901320836	1-27 LOOKOUT	MONSANTO OIL	WY	39N	91W	27	CSWNE	16706.8	A	5.6	2.68	0.00579	0.000518	323	15286	MVRD
C899	Wind River	4901320836	1-27 LOOKOUT	MONSANTO OIL	WY	39N	91W	27	CSWNE	16709.9	A	5.6	2.68	0.00578	0.000616	160	15216	MVRD
C899	Wind River	4901320836	1-27 LOOKOUT	MONSANTO OIL	WY	39N	91W	27	CSWNE	16723.9	A	5.2	2.66	0.00770	0.000702	138	15286	MVRD
D031	Wind River	4901320966	CHEVRON 2-1	MONSANTO OIL	WY	38N	91W	1	SWNENW	15647.1	A	0.9	2.65	0.00207	0.000024	478	11239	MVRD
D031	Wind River	4901320966	CHEVRON 2-1	MONSANTO OIL	WY	38N	91W	1	SWNENW	15656.0	A	4.1	2.68	0.0144	0.000321	321	15276	MVRD
D031	Wind River	4901320966	CHEVRON 2-1	MONSANTO OIL	WY	38N	91W	1	SWNENW	15663.2	A	7.3	2.66	0.0110	0.000768	175	15276	MVRD
D031	Wind River	4901320966	CHEVRON 2-1	MONSANTO OIL	WY	38N	91W	1	SWNENW	15666.1	A	8.6	2.66	0.0146	0.00183	145	16276	MVRD
D031	Wind River	4901320966	CHEVRON 2-1	MONSANTO OIL	WY	38N	91W	1	SWNENW	15668.8	A	8.4	2.66	0.00913	0.00147	109	15286	MVRD
D031	Wind River	4901320966	CHEVRON 2-1	MONSANTO OIL	WY	38N	91W	1	SWNENW	15676.1	A	9.4	2.68	0.0123	0.00166	146	15276	MVRD
D031	Wind River	4901320966	CHEVRON 2-1	MONSANTO OIL	WY	38N	91W	1	SWNENW	15681.1	A	9.9	2.68	0.0170	0.00212	141	15276	MVRD
D031	Wind River	4901320966	CHEVRON 2-1	MONSANTO OIL	WY	38N	91W	1	SWNENW	15682.8	A	9.7	2.67	0.0161	0.00247	80.7	15296	MVRD
D031	Wind River	4901320966	CHEVRON 2-1	MONSANTO OIL	WY	38N	91W	1	SWNENW	15697.4	A	7.8	2.68	0.00994	0.000685	230	15296	MVRD
D031	Wind River	4901320966	CHEVRON 2-1	MONSANTO OIL	WY	38N	91W	1	SWNENW	15702.1	A	6.9	2.68	0.0134	0.000669	144	13216	MVRD
D031	Wind River	4901320966	CHEVRON 2-1	MONSANTO OIL	WY	38N	91W	1	SWNENW	15705.8	A	5.4	2.68	0.00980	0.000439	113	13216	MVRD
D031	Wind River	4901320966	CHEVRON 2-1	MONSANTO OIL	WY	38N	91W	1	SWNENW	15708.0	A	4.5	2.67	0.00888	0.000302	127	13216	MVRD
D031	Wind River	4901320966	CHEVRON 2-1	MONSANTO OIL	WY	38N	91W	1	SWNENW	15711.9	A		2.51	0.00620	0.000096	491	13269	MVRD
D031	Wind River	4901320966	CHEVRON 2-1	MONSANTO OIL	WY	38N	91W	1	SWNENW	15716.9	A	1.8	2.68	0.00138	0.000008	1310	12239	MVRD
D031	Wind River	4901320966	CHEVRON 2-1	MONSANTO OIL	WY	38N	91W	1	SWNENW	15726.9	A	8.4	2.69	0.0115	0.00145	86.0	15266	MVRD
D031	Wind River	4901320966	CHEVRON 2-1	MONSANTO OIL	WY	38N	91W	1	SWNENW	15736.0	A	5.5	2.70	0.00463	0.000197	959	15286	MVRD
D031	Wind River	4901320966	CHEVRON 2-1	MONSANTO OIL	WY	38N	91W	1	SWNENW	15750.1	A	4.1	2.71	0.00691	0.000218	245	14286	MVRD
D031	Wind River	4901320966	CHEVRON 2-1	MONSANTO OIL	WY	38N	91W	1	SWNENW	15751.9	A	0.9	2.73	0.00568	0.000114	286	14286	MVRD
D031	Wind River	4901320966	CHEVRON 2-1	MONSANTO OIL	WY	38N	91W	1	SWNENW	15754.1	A	3.6	2.71	0.00674	0.000215	184	14286	MVRD

4.1.3.1 Grain Density

Grain density distribution averages 2.653±0.04 g/cc (error bar is 1 standard deviation; Fig. 4.1.1). Grain density distribution is skewed slightly to high density reflecting variable concentration of calcite, dolomite, and rare pyrite cement. Grain densities for the wells sampled exhibit a slight difference in distribution among basins (Fig 4.1.2, Table 4.1.2). It is important to note the small sample population of the Powder and Wind River Basin samples and these may be biased for conditions in the few wells and intervals sampled.

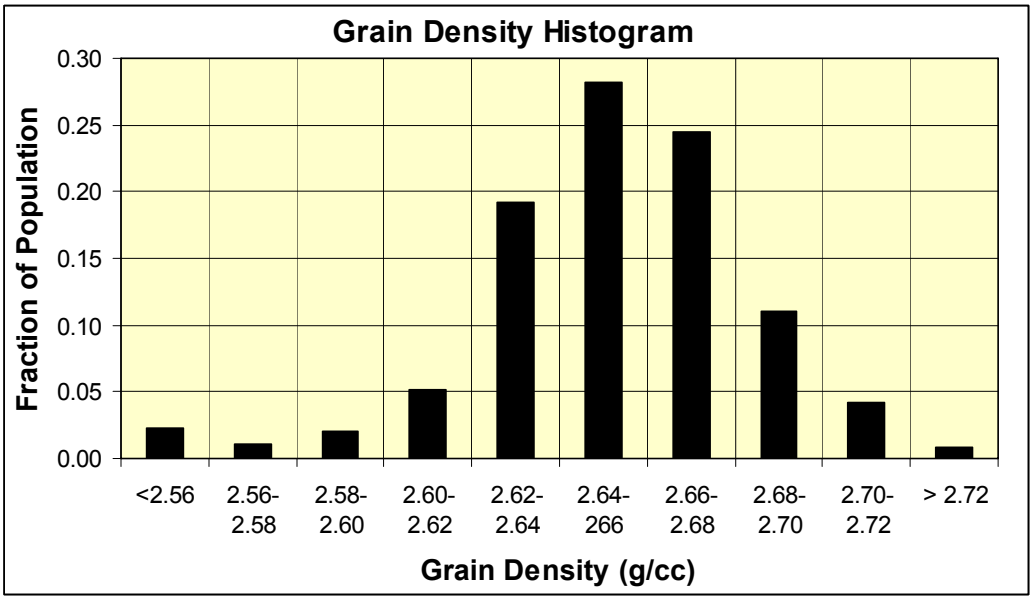

Figure 4.1.1. Grain density distribution for all basins and all samples (n = 2200). Distribution is near normal with mean = 2.653±0.04 g/cc. Slight skewness to higher values primarily reflects variable concentration of carbonate cement (n = 2184).

	All Basins	Greater Green River	Washakie	Uinta	Piceance	Wind River	Powder River
Mean	2.653	2.648	2.660	2.639	2.660	2.673	2.679
Median	2.654	2.645	2.662	2.649	2.661	2.673	2.674
St Dev	0.040	0.029	0.034	0.052	0.038	0.029	0.026
Minimum	2.30	2.50	2.47	2.30	2.35	2.51	2.60
Maximum	2.84	2.77	2.79	2.80	2.84	2.73	2.75
Kurtosis	15.1	2.6	3.7	13.2	14.0	10.2	3.9
Skewness	-2.00	0.28	-0.18	-2.82	-1.19	-1.87	-0.28
Count	2184	566	393	532	583	82	28

Table 4.1.2. Summary statistics for grain density for all original and duplicate cores by basin.

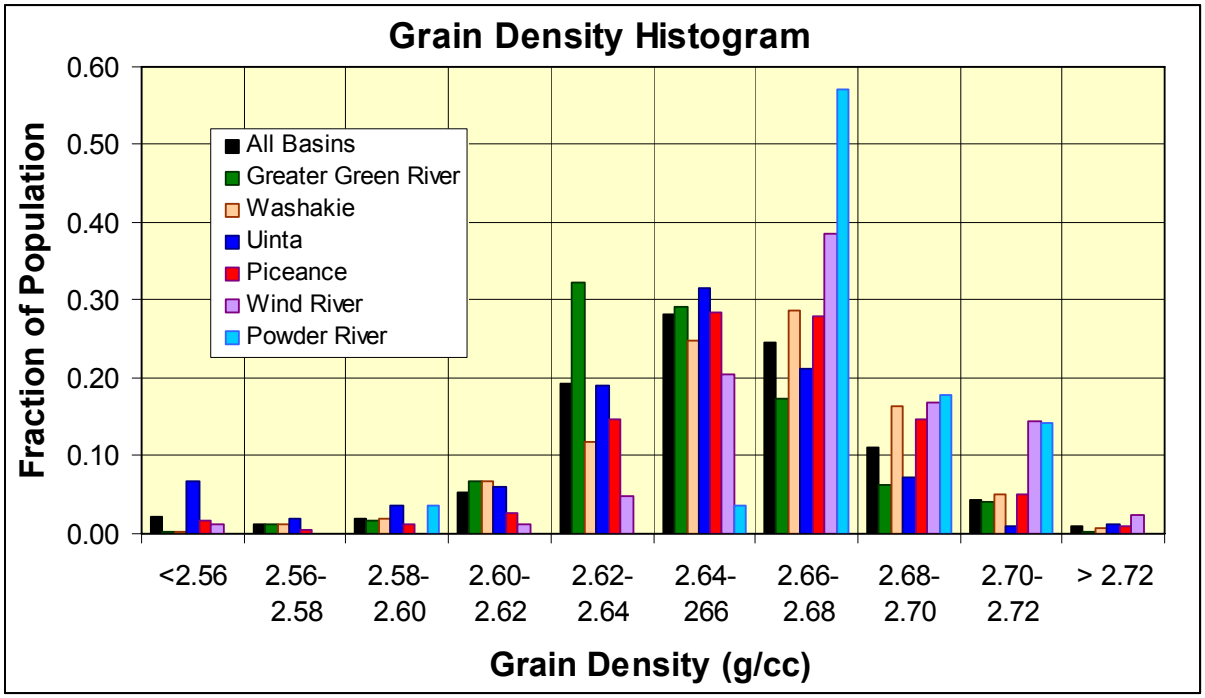

Figure 4.1.2. Grain density distribution by basin showing differences among basins as in Table 4.1.1 (n = 2184).

4.1.3.2 Porosity

The porosity distribution is skewed to lower porosity (Fig. 4.1.3) consistent with general porosity distribution in the Mesaverde sandstone (Table 4.1.3). The large population of cores with porosity of ϕ = 0–2% partially reflects a heavy sampling of low porosity intervals in two Green River Basin wells (Fig. 4.1.5).

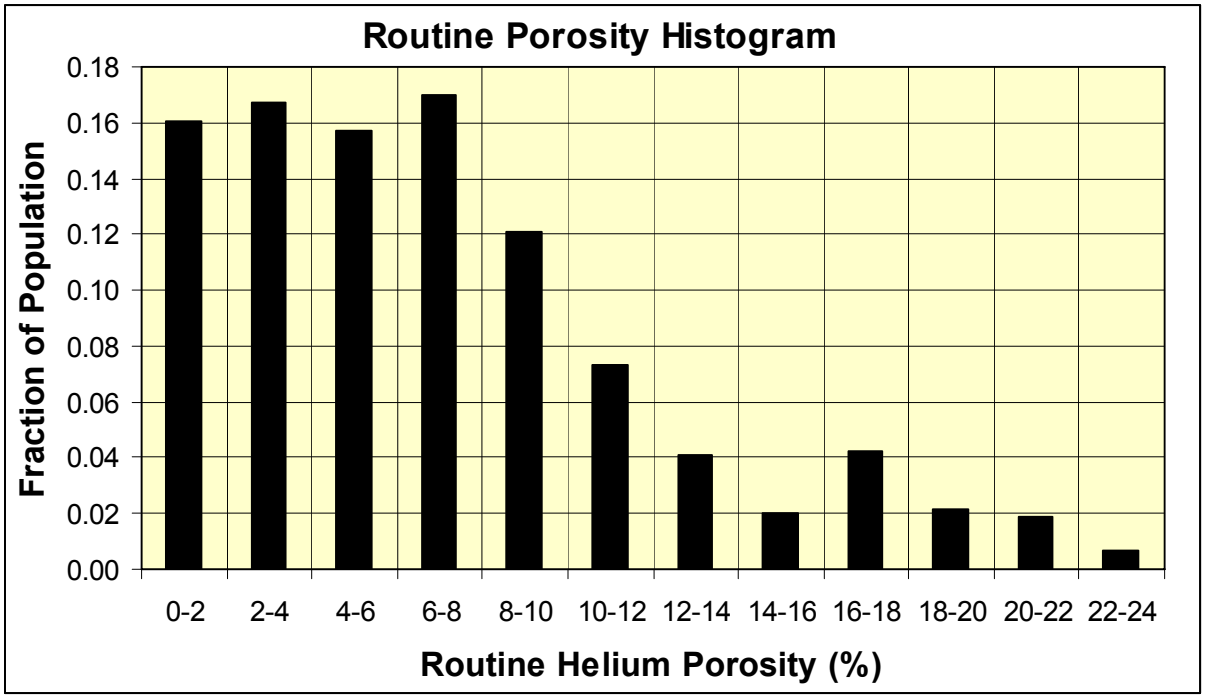

Figure 4.1.3. Porosity distribution for all samples (n = 2200).

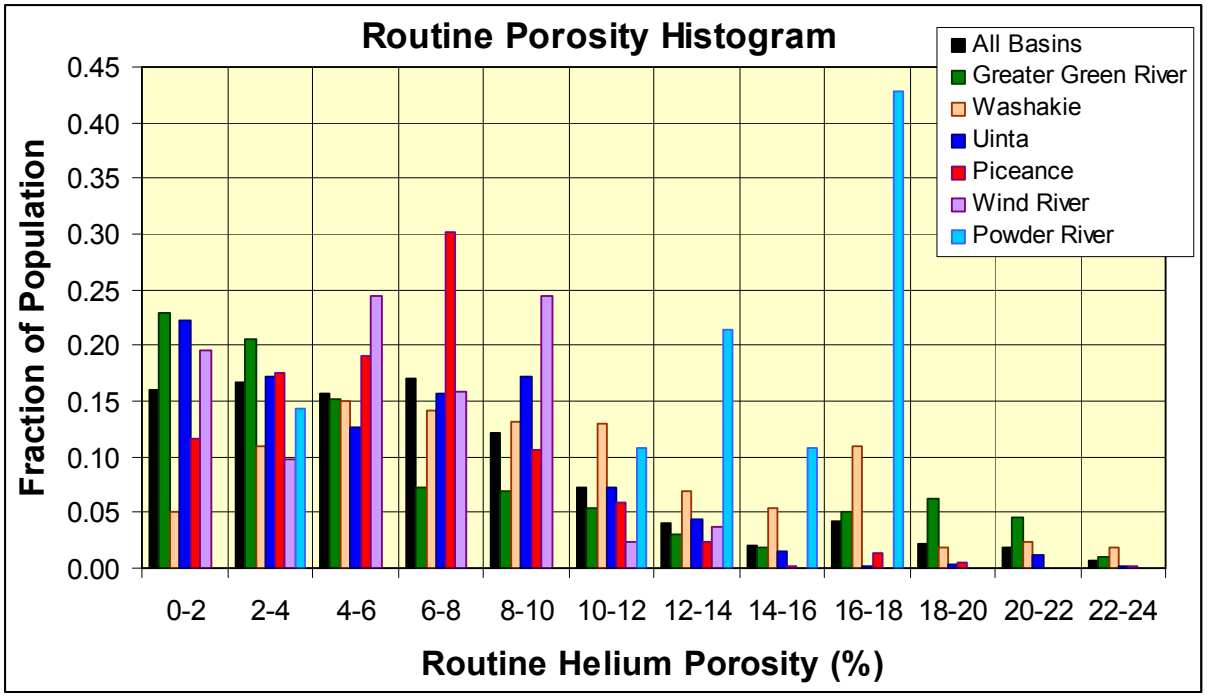

Figure 4.1.4. Porosity distribution by basin.

	All Basins	Greater Green River	Washakie	Uinta	Piceance	Wind River	Powder River
Mean	7.1	7.3	9.5	6.1	6.1	5.8	13.2
Median	6.2	4.6	8.7	5.9	6.1	5.5	15.1
St Dev	5.1	6.4	5.4	4.2	3.8	3.3	4.5
Minimum	0.0	0.0	0.0	0.0	0.0	0.0	2.6
Maximum	24.9	23.6	23.8	22.2	24.9	13.2	16.9
Kurtosis	0.7	-0.4	-0.4	1.1	4.5	-0.8	1.0
Skewness	1.0	1.0	0.5	0.9	1.4	0.1	-1.5
Count	2209	568	395	539	596	83	28

Table 4.1.3. Summary statistics for routine helium porosity for all samples by basin.

For 776 core plugs greater than 7.5 cm (3 inches) in length, the cores were cut in half to provide two paired core plugs for advanced properties measurements. Figure 4.1.5 illustrates the ratio of helium porosities of samples to the mean porosity of the sample pair. Over 75% of all samples exhibit porosity within 10% of the mean porosity of the porosity pair, and 88% exhibit porosities within 20%. For a rock with 10% porosity this distribution translates to 75% of adjacent cores would exhibit a porosity of 9–11% and an additional 13% of the population would exhibit porosities of 8–9% or 11–12%.

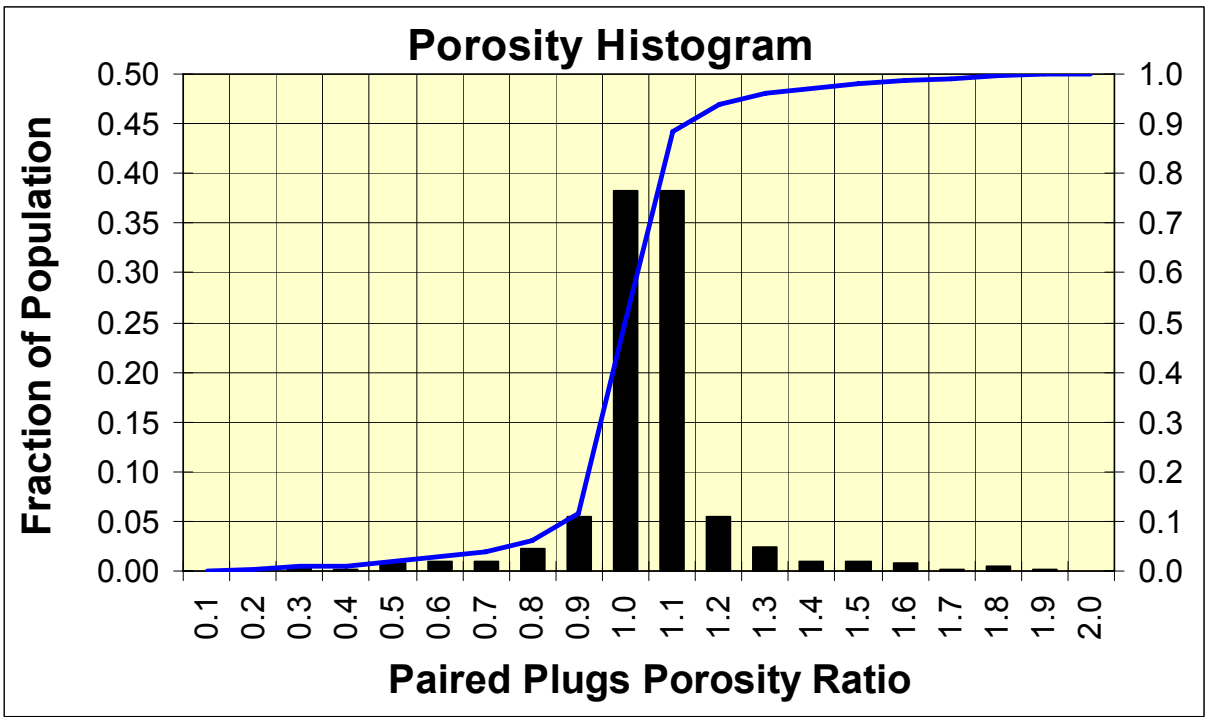

Figure 4.1.5. Histogram of ratio of paired plug porosities to mean porosity of plug pair. n = 652 pairs (n = 1304).

4.1.3.2.1 In situ Porosity and Pore Volume Compressibility – Although pore volume compressibility was not a stated objective of this study, it is necessary to understand how pore volume changes with increasing confining pressure because the *in situ* permeability, electrical properties, critical gas saturation, and MICP measurements are all measured with the core under confining pressure. To better understand how pore volume changes with confining stress, pore volume compressibility measurements were performed on 113 representative samples. To measure *in situ* porosity the cores were evacuated for a period of eight (8) hours and then saturated with a deaerated 200,000 parts per million by weight sodium chloride (ppmw NaCl) brine solution. After vacuum saturation, complete saturation was obtained by applying a pressure of 7 MPa (1,000 psi) for a period of 24 hours to the saturating brine and samples. Complete saturation was confirmed by agreement between helium-measured porosity and gravimetric-saturation porosity values within 0.1 porosity percent. The cores were left immersed in deaerated brine for a period of 1 week.

After the cores had reached equilibrium with the brine, each was placed in a biaxial Hassler-type core holder and subjected to a series of increasing hydrostatic confining stresses of 1.38, 2.76, 6.9, 13.8, and 27.6 MPa (200, 400, 1000, 2000, and 4000 psi) approximating a range of reservoir stress conditions. For the Hassler cell used, the porosity change from unconfined conditions to the first confining pressure of 1.38 MPa (200 psi) could not be measured because the rubber confining sleeve had to be "set " to make full contact with the outer surface of the sample to prevent expulsion of brine in open gaps between the core and sleeve from being incorrectly interpreted as expelled pore water. This pressure varies with the core diameter and surface roughness. Calibration measurements indicate that the sleeve is set for most regular core samples with diameter of 2.50–2.54 cm (0.98–1.00 inches) at 0.35+0.17 MPa (50 $\pm$ 25 psi). Based on this sleeve response to stress, the hydrostatic confining pressures were estimated to induce the following net effective confining pressure on the core 1.0, 2.4, 6.7, 13.4, and 27.2 MPa (150, 350 950, 1950, 3950 psi).

Pore volume decrease was determined by measuring the brine displaced from the core by compression using a micropipette, correcting for system compressibility changes. Pore pressure was at atmospheric pressure. Porosity calculations were performed assuming that the grains of the rock were incompressible and hence the bulk volume decreased by the same amount as the pore volume. Porosity was referenced to an assumed condition that at 0.35 MPa (50 psi) the pore volume equaled the routine helium pore volume. Pore volume change from 0.35 MPa (50 psi) to 1.38 MPa (200 psi) confining pressure was estimated by extrapolation of the pore volume

compressibility trend from 1.39 to 27.6 MPa (200–4,000 psi). Equilibrium at pressure was assumed if pore volume change was less than 0.001 cc for a 10-minute period.

In addition to the compressibility measurements, *in situ* porosity measurement was obtained on 310 core samples during the electrical resistivity measurements. The complete experimental method for the electrical properties measurement is described under Task 4.4. For the *in situ* porosity aspect of the resistivity measurement, the core pore volume change was measured as described above for compressibility except that only a zero reading at 1.38 MPa (200 psi) and the expelled brine at 27.2 MPa (3950 psi) were recorded. The total porosity change was calculated as described above. A key difference in this measurement is that equilibrium was established when the electrical resistance was stable and not necessarily when pore volume change met compressibility equilibrium conditions. Electrical equilibrium was generally established within 10±5 minutes which represented only 10%–15% of the time for compressibility analysis.

Previous studies have investigated the effect of confining pressure on porosity and pore volume compressibility in sandstones, carbonates, and siltstones (Carpenter and Spencer, 1940; Hall, 1953; Fatt, 1958; McLatchie et al., 1958; Mann and Fatt, 1960; Dobrynin; 1962; Knutson and Bohor, 1962; Somerton, 1967; Newman, 1973; Mattax et al., 1975; Newman and Martin, 1977; Somerton and Matherson, 1978; Greenwald and Somerton, 1981). The nature of pore volume change to confining stress has been shown to be a function of a range of variables, most notably including stress history (Mattax et al., 1975), two- and three-dimensional stress distribution (Keelan, 1984; Andersen, 1985; Worthington et al., 1997), degree of consolidation (Newman, 1975; Yale et al., 1993), water saturation (Mann and Fatt, 1960), temperature (Somerton and Mather, 1980), and pore geometry (Toksoz et al., 1976; Cheng and Toksoz, 1979; Walsh and Grosenbaugh, 1979; Ostensen, 1983; Katsube et al., 1992). The modeling of Cheng and Toksoz (1979) shows that the pressure dependence of pores is highly sensitive to pore aspect ratio (α). Based on this, Katsube et al. (1992) divided pores into three types: elastically rigid ($\alpha > 0.1$), elastically flexible ($\alpha = 0.001–0.1$), and highly stress sensitive sheet-like or crack-like pores ($\alpha < 0.001$). The work of Walsh and Grosenbaugh (1979) and Ostensen (1983) defined the nature of stress dependence of cracks, and Jones and Owens (1980) showed that low-permeability sandstones had thin, sheet-like tabular pores based on their response to stress. The crack-compression model of Walsh and Grosenbaugh (1979) expresses the relationship between porosity and stress as

$$\phi_i/\phi_o = A \log Pe + B \qquad [4.1.1]$$

Where ϕ_i = porosity at defined effective *in situ* stress Pe, ϕ_o = reference initial porosity, Pe = effective confining stress, and A and B are empirical constants that vary with rock properties.

The work of Jones and Owens (1980) and Sampath (1982) on the pore volume compressibility of low-permeability sandstones demonstrated that pore-volume compressibility values are generally low ($\beta < 6 \times 10^{-6}$ psi^{-1}). A population of 113 core samples representing a range of lithofacies and porosity was selected to measure pore volume compressibility (Table 4.1.4). Figure 4.1.6 illustrates the measured pore volume change from 1.0 to 27.2 MPa (150–3,950 psi) net effective confining pressure and estimated from 1.0 MPa down to a confining pressure predicted by the log-linear trend where the pore volume equals the routine helium porosity. In general this pressure was at a net effective stress of approximately 69 kPa (10 psi). Every sample exhibits a log-linear relationship between the fraction of initial pore volume (unconfined pore volume) at confining stress and the confining stress. The average correlation coefficient of the log-linear relationships is 0.99±0.031 (error range is 2 standard deviations).

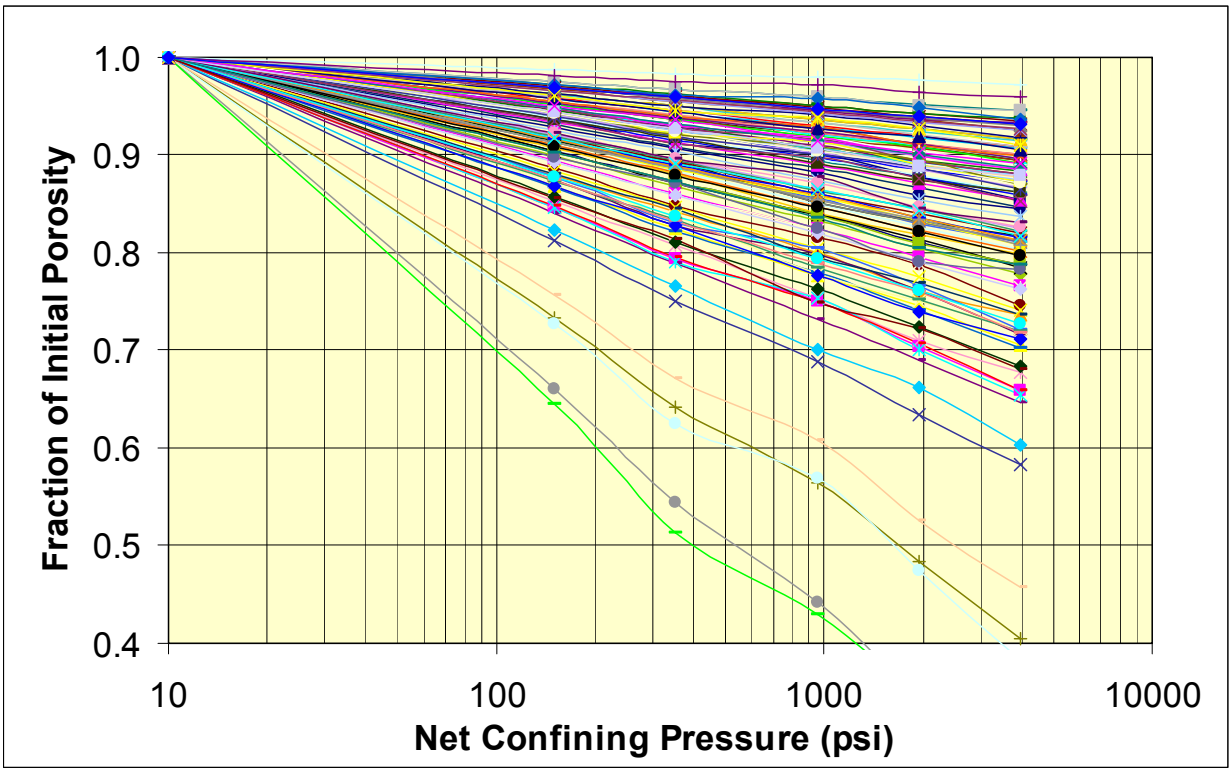

Figure 4.1.6. Crossplot of fraction of initial pore volume versus net confining stress for 113 Mesaverde samples. Every sample exhibits a log-linear relationship though slopes and intercepts differ.

Table 4.1.4.

Summary of Pore Volume Compressibility Results
Analysis of Critical Permeability, Capillary Pressure, and Electrical Properties for Mesaverde Tight Gas Sandstones from Western U.S. Basins
US DOE # DE-FC26-05NT42660
Alan P. Byrnes, Robert M. Cluff, John C. Webb, Daniel A. Krygowski, Stefani D. Whittaker
website: http://www.kgs.ku.edu/mesaverde

USGS Library Number	Basin	API Number	Well Name	Operator	State	Township	Range	Sec	Quarter Section	Plug Depth ft	Plug Letter A/B/C	Ambient Porosity %	*in situ* Klinkenberg Gas Permeability mD	Ratio (In situ Pore Volume)/(Ambient Pore Volume) at Stress: Approximate Net Effective Confining Pressure 10 psi	Approximate Net Effective Confining Pressure 150 psi	Approx. Net Effective Confining Pressure 250 psi	Approximate Net Effective Confining Pressure 950 psi	Approximate Net Effective Confining Pressure 1,950 psi	Approximate Net Effective Confining Pressure 3,950 psi	PVi/ PVa vs log Pe intercept 1/psi	PVi/ PVa vs log Pe Slope 1/psi	Correlation Coefficient of PVi/PVa vs logPe
B029	Green River	4903520088	A-1 WASP	INEXCO OIL COMPANY	WY	36N	112W	28	NWNESW	11332.9	A	3.5	0.000728	1.000	0.873	0.833	0.784	0.752	0.719	1.1084	-0.1084	0.9999
B029	Green River	4903520088	A-1 WASP	INEXCO OIL COMPANY	WY	36N	112W	28	NWNESW	11443.8	A	3.1	0.000681	1.000	0.857	0.811	0.763	0.723	0.683	1.1213	-0.1213	0.9998
B029	Green River	4903520088	A-1 WASP	INEXCO OIL COMPANY	WY	36N	112W	28	NWNESW	11457.9	A	5.5	0.000110	1.000	0.884	0.846	0.805	0.775	0.742	1.0990	-0.0990	0.9999
B029	Green River	4903520088	A-1 WASP	INEXCO OIL COMPANY	WY	36N	112W	28	NWNESW	11459.1	A	5.4	0.000827	1.000	0.914	0.886	0.855	0.834	0.808	1.0734	-0.0734	0.9998
B029	Green River	4903520088	A-1 WASP	INEXCO OIL COMPANY	WY	36N	112W	28	NWNESW	11460.6	A	4.3	0.0155	1.000	0.872	0.838	0.778	0.750	0.722	1.1085	-0.1085	0.9979
B029	Green River	4903520088	A-1 WASP	INEXCO OIL COMPANY	WY	36N	112W	28	NWNESW	11552.3	A	3.9	0.000659	1.000	0.846	0.791	0.753	0.701	0.655	1.1309	-0.1309	0.9970
B029	Green River	4903520088	A-1 WASP	INEXCO OIL COMPANY	WY	36N	112W	28	NWNESW	11609.1	A	5.9	0.00772	1.000	0.916	0.888	0.860	0.836	0.812	1.0718	-0.0718	0.9997
B029	Green River	4903520088	A-1 WASP	INEXCO OIL COMPANY	WY	36N	112W	28	NWNESW	11609.2	A	5.2	0.00475	1.000	0.903	0.872	0.839	0.809	0.787	1.0824	-0.0824	0.9996
B029	Green River	4903520088	A-1 WASP	INEXCO OIL COMPANY	WY	36N	112W	28	NWNESW	11615.1	A	4.6	0.00192	1.000	0.898	0.871	0.825	0.791	0.783	1.0868	-0.0868	0.9939
B029	Green River	4903520088	A-1 WASP	INEXCO OIL COMPANY	WY	36N	112W	28	NWNESW	11706.7	A	4.0	0.000524	1.000	0.881	0.845	0.796	0.769	0.737	1.1016	-0.1016	0.9997
B029	Green River	4903520088	A-1 WASP	INEXCO OIL COMPANY	WY	36N	112W	28	NWNESW	11706.9	A	3.8	0.000405	1.000	0.942	0.923	0.904	0.888	0.871	1.0492	-0.0492	0.9997
B029	Green River	4903520088	A-1 WASP	INEXCO OIL COMPANY	WY	36N	112W	28	NWNESW	11721.9	A	4.3	0.000320	1.000	0.877	0.831	0.804	0.766	0.720	1.1045	-0.1045	0.9941
B029	Green River	4903520088	A-1 WASP	INEXCO OIL COMPANY	WY	36N	112W	28	NWNESW	11758.3	A	4.7	0.000470	1.000	0.840	0.790	0.731	0.690	0.646	1.1359	-0.1359	1.0000
B029	Green River	4903520088	A-1 WASP	INEXCO OIL COMPANY	WY	36N	112W	28	NWNESW	11758.4	A	4.6	0.00110	1.000	0.908	0.879	0.847	0.822	0.797	1.0779	-0.0779	0.9999
E712	Green River	4903506020	B-54 BIG PINEY	BELCO PETROLEUM	WY	29N	113W	26	SESENE	3461.7	A	17.9	2.42	1.000	0.937	0.918	0.894	0.878	0.862	1.0533	-0.0533	1.0000
E712	Green River	4903506020	B-54 BIG PINEY	BELCO PETROLEUM	WY	29N	113W	26	SESENE	3462.0	A	18.8	26.8	1.000	0.942	0.925	0.900	0.886	0.873	1.0494	-0.0494	0.9992
E712	Green River	4903506020	B-54 BIG PINEY	BELCO PETROLEUM	WY	29N	113W	26	SESENE	3503.7	B	8.8	0.000792	1.000	0.903	0.871	0.839	0.814	0.784	1.0823	-0.0823	0.9994
E712	Green River	4903506020	B-54 BIG PINEY	BELCO PETROLEUM	WY	29N	113W	26	SESENE	3519.3	B	16.1	6.02	1.000	0.944	0.928	0.905	0.891	0.878	1.0474	-0.0474	0.9997
E894	Green River	4903520622	1 OLD ROAD	AMERICAN HUNTER EXPL	WY	27N	108W	27	SENWSE	11921.8	A	5.0	0.000271	1.000	0.950	0.934	0.918	0.904	0.889	1.0422	-0.0422	0.9995
E894	Green River	4903520622	1 OLD ROAD	AMERICAN HUNTER EXPL	WY	27N	108W	27	SENWSE	11923.3	A	4.1	0.00644	1.000	0.940	0.920	0.901	0.886	0.865	1.0509	-0.0509	0.9984
E894	Green River	4903520622	1 OLD ROAD	AMERICAN HUNTER EXPL	WY	27N	108W	27	SENWSE	11956.1	A	8.5	0.00792	1.000	0.967	0.955	0.946	0.936	0.926	1.0282	-0.0282	0.9982
R780	Green River	4903505742	C-47 TIP TOP SHALLOW	BELCO PETROLEUM	WY	28N	113W	22	SWNE	2754.7	A	21.3	1.90	1.000	0.946	0.929	0.909	0.894	0.881	1.0461	-0.0461	0.9999
R780	Green River	4903505742	C-47 TIP TOP SHALLOW	BELCO PETROLEUM	WY	28N	113W	22	SWNE	2783.3	A	22.3	23.1	1.000	0.945	0.928	0.907	0.893	0.879	1.0467	-0.0467	1.0000
R780	Green River	4903505742	C-47 TIP TOP SHALLOW	BELCO PETROLEUM	WY	28N	113W	22	SWNE	2817.7	A	20.1	2.12	1.000	0.954	0.940	0.923	0.907	0.900	1.0393	-0.0393	0.9981
R780	Green River	4903505742	C-47 TIP TOP SHALLOW	BELCO PETROLEUM	WY	28N	113W	22	SWNE	2831.8		23.6	2.73	1.000	0.958	0.945	0.928	0.918	0.906	1.0361	-0.0361	0.9998
R780	Green River	4903505742	C-47 TIP TOP SHALLOW	BELCO PETROLEUM	WY	28N	113W	22	SWNE	2831.9	B	20.4	3.22	1.000	0.952	0.937	0.920	0.908	0.894	1.0406	-0.0406	0.9999
R780	Green River	4903505742	C-47 TIP TOP SHALLOW	BELCO PETROLEUM	WY	28N	113W	22	SWNE	2845.5	A	22.6	8.69	1.000	0.961	0.950	0.934	0.924	0.915	1.0329	-0.0329	0.9993
S873	Green River	4903506200	K-2 MASON	BELCO PETROLEUM	WY	31N	113W	13	SESE	9393.3	A	3.4	0.000024	1.000	0.973	0.962	0.958	0.949	0.937	1.0231	-0.0231	0.9874
T195	Green River	4903508024	5 PINEDALE	EL PASO NATURAL GAS	WY	30N	108W	5	C SE	12158.5	A	11.0	0.0167	1.000	0.962	0.950	0.937	0.927	0.917	1.0320	-0.0320	0.9999
T195	Green River	4903508024	5 PINEDALE	EL PASO NATURAL GAS	WY	30N	108W	5	C SE	12159.5	A	9.3	0.000003	1.000	0.929	0.907	0.882	0.859	0.847	1.0602	-0.0602	0.9990
T195	Green River	4903508024	5 PINEDALE	EL PASO NATURAL GAS	WY	30N	108W	5	C SE	12162.0	A	7.2	0.000796	1.000	0.938	0.918	0.896	0.879	0.862	1.0530	-0.0530	0.9999
T203	Green River	4903705405	1 CHIMNEY ROCK	MOUNTAIN FUEL SUPPLY	WY	18N	102W	12	SESW	6741.0	A	14.3	81.9	1.000	0.969	0.960	0.947	0.939	0.932	1.0264	-0.0264	0.9995
T204	Green River	4903705349	B-2A SPIDER CREEK	HUMBLE OIL & REF	WY	18N	110W	27	NESW	9041.1	A	11.6	1.82	1.000	0.920	0.894	0.864	0.846	0.821	1.0684	-0.0684	0.9997
T204	Green River	4903705349	B-2A SPIDER CREEK	HUMBLE OIL & REF	WY	18N	110W	27	NESW	9116.9	A	2.3	0.000138	1.000	0.660	0.544	0.442	0.343	0.240	1.2892	-0.2892	0.9989
R091	Piceance	05045XXXX4	BOOK CLIFFS 1	USGS-CG	CO	7S	104W	17	NESW	242.4	A	6.7	0.000164	1.000	0.914	0.885	0.857	0.833	0.808	1.0734	-0.0734	0.9996
R091	Piceance	05045XXXX4	BOOK CLIFFS 1	USGS-CG	CO	7S	104W	17	NESW	257.3	A	6.9	0.000167	1.000	0.914	0.887	0.856	0.830	0.810	1.0734	-0.0734	0.9997
R091	Piceance	05045XXXX4	BOOK CLIFFS 1	USGS-CG	CO	7S	104W	17	NESW	296.9	A	4.9	0.000168	1.000	0.955	0.939	0.928	0.911	0.900	1.0383	-0.0383	0.9962
R091	Piceance	05045XXXX4	BOOK CLIFFS 1	USGS-CG	CO	7S	104W	17	NESW	387.3	A	9.6	0.000985	1.000	0.903	0.873	0.839	0.811	0.787	1.0821	-0.0821	0.9999
S905	Piceance	05103XXXX3	21011-5 MOON LAKE	WESTERN FUELS ASSOC	CO	2N	101W	1	NESW	790.3	A	5.0	0.000209	1.000	0.949	0.932	0.915	0.900	0.886	1.0436	-0.0436	0.9998
S905	Piceance	05103XXXX3	21011-5 MOON LAKE	WESTERN FUELS ASSOC	CO	2N	101W	1	NESW	812.7	A	18.1	22.0	1.000	0.959	0.946	0.930	0.919	0.909	1.0352	-0.0352	1.0000
S905	Piceance	05103XXXX3	21011-5 MOON LAKE	WESTERN FUELS ASSOC	CO	2N	101W	1	NESW	812.9	A	17.0	20.9	1.000	0.953	0.939	0.921	0.910	0.897	1.0397	-0.0397	0.9998
S905	Piceance	05103XXXX3	21011-5 MOON LAKE	WESTERN FUELS ASSOC	CO	2N	101W	1	NESW	816.5	A	10.6	0.0205	1.000	0.915	0.892	0.852	0.833	0.816	1.0721	-0.0721	0.9973
S905	Piceance	05103XXXX3	21011-5 MOON LAKE	WESTERN FUELS ASSOC	CO	2N	101W	1	NESW	817.8	A	8.7	0.00118	1.000	0.847	0.794	0.750	0.704	0.658	1.1300	-0.1300	0.9986
T649	Piceance	0504560011	MWX-2	CER CORPORATION	CO	6S	94W	34	SESWNW	5737.3	A	9.4	0.00220	1.000	0.952	0.936	0.919	0.908	0.892	1.0411	-0.0411	0.9992
T649	Piceance	0504560011	MWX-2	CER CORPORATION	CO	6S	94W	34	SESWNW	5744.2	A	4.3	0.000042	1.000	0.968	0.958	0.947	0.939	0.930	1.0269	-0.0269	0.9996
T649	Piceance	0504560011	MWX-2	CER CORPORATION	CO	6S	94W	34	SESWNW	5838.7	A	6.6	0.00146	1.000	0.954	0.938	0.925	0.911	0.897	1.0392	-0.0392	0.9985
T649	Piceance	0504560011	MWX-2	CER CORPORATION	CO	6S	94W	34	SESWNW	5852.3	A	2.8	0.000047	1.000	0.943	0.921	0.908	0.894	0.869	1.0484	-0.0484	0.9921
T649	Piceance	0504560011	MWX-2	CER CORPORATION	CO	6S	94W	34	SESWNW	6542.2	B	5.8	0.000249	1.000	0.969	0.960	0.948	0.939	0.933	1.0262	-0.0262	0.9994
T649	Piceance	0504560011	MWX-2	CER CORPORATION	CO	6S	94W	34	SESWNW	7136.8	A	6.9	0.00219	1.000	0.948	0.932	0.913	0.900	0.885	1.0441	-0.0441	0.9998
T649	Piceance	0504560011	MWX-2	CER CORPORATION	CO	6S	94W	34	SESWNW	7264.5	B	6.1	0.000221	1.000	0.971	0.964	0.951	0.943	0.938	1.0243	-0.0243	0.9976
T649	Piceance	0504560011	MWX-2	CER CORPORATION	CO	6S	94W	34	SESWNW	7272.8	A	8.9	0.00234	1.000	0.967	0.955	0.945	0.937	0.926	1.0282	-0.0282	0.9984
T649	Piceance	0504560011	MWX-2	CER CORPORATION	CO	6S	94W	34	SESWNW	7340.4	A	2.1	0.000106	1.000	0.918	0.891	0.864	0.843	0.817	1.0695	-0.0695	0.9992
T649	Piceance	0504560011	MWX-2	CER CORPORATION	CO	6S	94W	34	SESWNW	7350.4	A	4.5	0.000372	1.000	0.963	0.950	0.940	0.930	0.917	1.0311	-0.0311	0.9970
T649	Piceance	0504560011	MWX-2	CER CORPORATION	CO	6S	94W	34	SESWNW	7851.3	B	3.8	0.000244	1.000	0.967	0.956	0.944	0.935	0.927	1.0283	-0.0283	0.9999
T649	Piceance	0504560011	MWX-2	CER CORPORATION	CO	6S	94W	34	SESWNW	7880.1	B	7.6	0.00179	1.000	0.955	0.941	0.922	0.912	0.901	1.0385	-0.0385	0.9994
T649	Piceance	0504560011	MWX-2	CER CORPORATION	CO	6S	94W	34	SESWNW	8106.9	B	3.4	0.000695	1.000	0.949	0.930	0.917	0.899	0.885	1.0437	-0.0437	0.9976
S835	Powder River	4900906335	2 SHAWNEE	BELCO PETROLEUM	WY	33N	69W	2	NENW	6946.1	A	15.6	2.59	1.000	0.943	0.925	0.904	0.889	0.874	1.0485	-0.0485	1.0000
S835	Powder River	4900906335	2 SHAWNEE	BELCO PETROLEUM	WY	33N	69W	2	NENW	6946.2	A	14.3	2.17	1.000	0.955	0.940	0.927	0.911	0.901	1.0383	-0.0383	0.9983
S835	Powder River	4900906335	2 SHAWNEE	BELCO PETROLEUM	WY	33N	69W	2	NENW	6956.2		13.8	0.235	1.000	0.953	0.936	0.922	0.908	0.894	1.0404	-0.0404	0.9991
S838	Powder River	4900905481	3 SHAWNEE	BELCO PETROLEUM	WY	33N	69W	23	C SENE	6985.7		7.8	0.000798	1.000	0.975	0.967	0.960	0.950	0.946	1.0212	-0.0212	0.9973
S838	Powder River	4900905481	3 SHAWNEE	BELCO PETROLEUM	WY	33N	69W	23	C SENE	6998.5	A	6.3	0.00159	1.000	0.853	0.807	0.753	0.710	0.677	1.1252	-0.1252	0.9997
B646	Uinta	4304730584	11-17F RIVER BEND UNIT	MAPCO INCOPORATED	UT	10S	20E	17	SENENW	8233.0	B	5.7	0.00466	1.000	0.880	0.842	0.799	0.762	0.737	1.1023	-0.1023	0.9994
B646	Uinta	4304730584	11-17F RIVER BEND UNIT	MAPCO INCOPORATED	UT	10S	20E	17	SENENW	8282.8	A	1.7	0.000091	1.000	0.868	0.828	0.777	0.739	0.711	1.1123	-0.1123	0.9995
B646	Uinta	4304730584	11-17F RIVER BEND UNIT	MAPCO INCOPORATED	UT	10S	20E	17	SENENW	8287.4	B	7.5	0.0217	1.000	0.900	0.868	0.832	0.805	0.778	1.0852	-0.0852	0.9999
B646	Uinta	4304730584	11-17F RIVER BEND UNIT	MAPCO INCOPORATED	UT	10S	20E	17	SENENW	8302.5	A	1.0	0.000112	1.000	0.874	0.833	0.789	0.760	0.718	1.1072	-0.1072	0.9991
E946	Uinta	4304730545	2-7 FLAT MESA	ENSERCH EXPLORATION	UT	10S	23E	7	NESENW	6357.5	A	0.9	0.000141	1.000	0.646	0.513	0.429	0.336	0.189	1.3013	-0.3013	0.9935
E946	Uinta	4304730545	2-7 FLAT MESA	ENSERCH EXPLORATION	UT	10S	23E	7	NESENW	6362.5	A	2.8	0.000170	1.000	0.733	0.642	0.564	0.484	0.404	1.2266	-0.2266	0.9988
E946	Uinta	4304730545	2-7 FLAT MESA	ENSERCH EXPLORATION	UT	10S	23E	7	NESENW	6468.4	A	12.1	0.434	1.000	0.910	0.882	0.847	0.824	0.802	1.0767	-0.0767	0.9999
E946	Uinta	4304730545	2-7 FLAT MESA	ENSERCH EXPLORATION	UT	10S	23E	7	NESENW	6475.2	A	13.0	0.390	1.000	0.914	0.888	0.854	0.833	0.811	1.0729	-0.0729	0.9998
E946	Uinta	4304730545	2-7 FLAT MESA	ENSERCH EXPLORATION	UT	10S	23E	7	NESENW	6475.3	C	12.4	0.583	1.000	0.907	0.881	0.841	0.818	0.798	1.0788	-0.0788	0.9991
E946	Uinta	4304730545	2-7 FLAT MESA	ENSERCH EXPLORATION	UT	10S	23E	7	NESENW	6482.0	C	2.6	0.000095	1.000	0.923	0.896	0.877	0.846	0.831	1.0654	-0.0654	0.9961
E946	Uinta	4304730545	2-7 FLAT MESA	ENSERCH EXPLORATION	UT	10S	23E	7	NESENW	6515.6	A	15.1	1.94	1.000	0.911	0.883	0.850	0.826	0.803	1.0758	-0.0758	1.0000
E946	Uinta	4304730545	2-7 FLAT MESA	ENSERCH EXPLORATION	UT	10S	23E	7	NESENW	6530.2	A	9.8	0.0235	1.000	0.918	0.894	0.860	0.841	0.820	1.0697	-0.0697	0.9996
E946	Uinta	4304730545	2-7 FLAT MESA	ENSERCH EXPLORATION	UT	10S	23E	7	NESENW	6709.8	A	2.2	0.000117	1.000	0.727	0.625	0.568	0.475	0.383	1.2318	-0.2318	0.9946
E946	Uinta	4304730545	2-7 FLAT MESA	ENSERCH EXPLORATION	UT	10S	23E	7	NESENW	7284.3	A	7.7	0.00323	1.000	0.894	0.860	0.825	0.795	0.766	1.0897	-0.0897	0.9998
E946	Uinta	4304730545	2-7 FLAT MESA	ENSERCH EXPLORATION	UT	10S	23E	7	NESENW	7289.9	A	4.9	0.00139	1.000	0.812	0.750	0.689	0.634	0.582	1.1600	-0.1600	0.9996
E946	Uinta	4304730545	2-7 FLAT MESA	ENSERCH EXPLORATION	UT	10S	23E	7	NESENW	7301.4	A	2.5	0.000209	1.000	0.848	0.796	0.749	0.707	0.659	1.1295	-0.1295	0.9988
E946	Uinta	4304730545	2-7 FLAT MESA	ENSERCH EXPLORATION	UT	10S	23E	7	NESENW	7311.7	C	2.0	0.000100	1.000	0.757	0.671	0.608	0.526	0.457	1.2067	-0.2067	0.9978
E946	Uinta	4304730545	2-7 FLAT MESA	ENSERCH EXPLORATION	UT	10S	23E	7	NESENW	7313.8	A	5.9	0.00386	1.000	0.893	0.859	0.820	0.791	0.763	1.0913	-0.0913	1.0000
E946	Uinta	4304730545	2-7 FLAT MESA	ENSERCH EXPLORATION	UT	10S	23E	7	NESENW	7671.1	A	4.8	0.0973	1.000	0.866	0.821	0.781	0.741	0.702	1.1136	-0.1136	0.9992
E946	Uinta	4304730545	2-7 FLAT MESA	ENSERCH EXPLORATION	UT	10S	23E	7	NESENW	7701.1	A	0.9	0.000097	1.000	0.902	0.873	0.835	0.804	0.787	1.0834	-0.0834	0.9987
E946	Uinta	4304730545	2-7 FLAT MESA	ENSERCH EXPLORATION	UT	10S	23E	7	NESENW	7704.4	B	3.2	0.000200	1.000	0.823	0.765	0.701	0.662	0.603	1.1509	-0.1509	0.9992
E946	Uinta	4304730545	2-7 FLAT MESA	ENSERCH EXPLORATION	UT	10S	23E	7	NESENW	7885.4	A	9.8	0.0258	1.000	0.934	0.913	0.889	0.872	0.854	1.0562	-0.0562	0.9999
R999	Uinta	4304730860	3-24 US LAMCO	CHAMPLIN PETROLEUM	UT	13S	20E	24	NESE	7156.0		2.7	0.000105	1.000	0.961	0.946	0.938	0.928	0.910	1.0331	-0.0331	0.9894
R999	Uinta	4304730860	3-24 US LAMCO	CHAMPLIN PETROLEUM	UT	13S	20E	24	NESE	7158.9	B	2.7	0.000149	1.000	0.957	0.944	0.927	0.920	0.905	1.0362	-0.0362	0.9979
S172	Uinta	43019XXXX1	3 BOOK CLIFFS	USGS-CG	UT	17S	24E	3	SE	174.0	A	7.0	0.000416	1.000	0.931	0.908	0.886	0.866	0.846	1.0586	-0.0586	0.9993
S172	Uinta	43019XXXX1	3 BOOK CLIFFS	USGS-CG	UT	17S	24E	3	SE	398.8	A	10.9	0.0463	1.000	0.959	0.946	0.931	0.920	0.909	1.0349	-0.0349	1.0000
S174	Uinta	43019XXXX2	4 BOOK CLIFFS	USGS-CG	UT	17S	24E	31	NWSW	189.2	A	21.0	5.65	1.000	0.952	0.937	0.919	0.907	0.894	1.0408	-0.0408	0.9999
E489	Washakie	4903721053	3 UNIT FIVE MILE GULCH	AMOCO PRODUCTION	WY	21N	93W	35	C SW	10608.7	A	4.3	0.000079	1.000	0.982	0.975	0.972	0.964	0.959	1.0154	-0.0154	0.9900
E489	Washakie	4903721053	3 UNIT FIVE MILE GULCH	AMOCO PRODUCTION	WY	21N	93W	35	C SW	10612.0	A	6.5	0.000011	1.000	0.942	0.922	0.906	0.889	0.871	1.0489	-0.0489	0.9981
E489	Washakie	4903721053	3 UNIT FIVE MILE GULCH	AMOCO PRODUCTION	WY	21N	93W	35	C SW	10615.6	A	11.0	0.00814	1.000	0.959	0.945	0.933	0.921	0.909	1.0348	-0.0348	0.9991
E489	Washakie	4903721053	3 UNIT FIVE MILE GULCH	AMOCO PRODUCTION	WY	21N	93W	35	C SW	10651.0	A	4.3	0.000187	1.000	0.935	0.911	0.898	0.876	0.853	1.0549	-0.0549	0.9939
E489	Washakie	4903721053	3 UNIT FIVE MILE GULCH	AMOCO PRODUCTION	WY	21N	93W	35	C SW	10668.9	A	6.7	0.00203	1.000	0.968	0.960	0.946	0.936	0.933	1.0269	-0.0269	0.9947
E489	Washakie	4903721053	3 UNIT FIVE MILE GULCH	AMOCO PRODUCTION	WY	21N	93W	35	C SW	10670.9	A	8.7	0.0309	1.000	0.947	0.927	0.916	0.895	0.881	1.0454	-0.0454	0.9953
E489	Washakie	4903721053	3 UNIT FIVE MILE GULCH	AMOCO PRODUCTION	WY	21N	93W	35	C SW	10675.8	A	10.1	0.0255	1.000	0.946	0.932	0.905	0.895	0.884	1.0457	-0.0457	0.9962
E489	Washakie	4903721053	3 UNIT FIVE MILE GULCH	AMOCO PRODUCTION	WY	21N	93W	35	C SW	10682.3	A	9.2	0.00420	1.000	0.937	0.915	0.898	0.878	0.859	1.0535	-0.0535	0.9984
E489	Washakie	4903721053	3 UNIT FIVE MILE GULCH	AMOCO PRODUCTION	WY	21N	93W	35	C SW	10693.4	A	2.6	0.000140	1.000	0.950	0.936	0.915	0.903	0.892	1.0422	-0.0422	0.9993
E489	Washakie	4903721053	3 UNIT FIVE MILE GULCH	AMOCO PRODUCTION	WY	21N	93W	35	C SW	10706.9	A	5.0	0.000830	1.000	0.922	0.895	0.872	0.846	0.827	1.0665	-0.0665	0.9990
E489	Washakie	4903721053	3 UNIT FIVE MILE GULCH	AMOCO PRODUCTION	WY	21N	93W	35	C SW	10709.7	A	6.1	0.000376	1.000	0.916	0.889	0.860	0.835	0.815	1.0715	-0.0715	0.9998
E489	Washakie	4903721053	3 UNIT FIVE MILE GULCH	AMOCO PRODUCTION	WY	21N	93W	35	C SW	10710.3	A	6.2	0.00310	1.000	0.941	0.889	0.851	0.831	0.812	1.0735	-0.0735	0.9987
E489	Washakie	4903721053	3 UNIT FIVE MILE GULCH	AMOCO PRODUCTION	WY	21N	93W	35	C SW	10715.8	A	5.3	0.000920	1.000	0.944	0.922	0.913	0.891	0.874	1.0476	-0.0476	0.9919
E489	Washakie	4903721053	3 UNIT FIVE MILE GULCH	AMOCO PRODUCTION	WY	21N	93W	35	C SW	10717.0	A	11.9	0.00120	1.000	0.988	0.983	0.980	0.977	0.972	1.0104	-0.0104	0.9911
S231	Washakie	4903721075	1 CHAMPLIN 237 AMOCO C	AMOCO PRODUCTION	WY	17N	94W	5	SWNESW	11110.1	A	4.3	0.000170	1.000	0.893	0.858	0.824	0.789	0.765	1.0909	-0.0909	0.9994
S231	Washakie	4903721075	1 CHAMPLIN 237 AMOCO C	AMOCO PRODUCTION	WY	17N	94W	5	SWNESW	11132.3	B	5.6	0.000168	1.000	0.966	0.955	0.943	0.934	0.925	1.0289	-0.0289	1.0000
S231	Washakie	4903721075	1 CHAMPLIN 237 AMOCO C	AMOCO PRODUCTION	WY	17N	94W	5	SWNESW	11174.7		7.1	0.000745	1.000	0.941	0.920	0.903	0.885	0.867	1.0505	-0.0505	0.9987
S231	Washakie	4903721075	1 CHAMPLIN 237 AMOCO C	AMOCO PRODUCTION	WY	17N	94W	5	SWNESW	11202.6		4.0	0.000846	1.000	0.875	0.828	0.799	0.761	0.716	1.1066	-0.1066	0.9952
S276	Washakie	4903705683	65-1-7 ARCH UNIT	FOREST OIL CORP	WY	19N	99W	1	NWSE	4731.0	B	10.0	0.00406	1.000	0.888	0.848	0.815	0.787	0.746	1.0956	-0.0956	0.9972
S276	Washakie	4903705683	65-1-7 ARCH UNIT	FOREST OIL CORP	WY	19N	99W	1	NWSE	4756.9		8.5	0.00308	1.000	0.868	0.825	0.777	0.746	0.705	1.1125	-0.1125	0.9996
S276	Washakie	4903705683	65-1-7 ARCH UNIT	FOREST OIL CORP	WY	19N	99W	1	NWSE	4

To develop an approximate predictive model of pore volume and pore volume compressibility change, the slopes and intercepts of the curves in Figure 4.1.6 were correlated with porosity (Figs. 4.1.7 and 4.1.8). The slope and intercept of the curves shown in Figure 4.1.6 can be predicted using

$$\phi_i/\phi_{o\ Slope} = A = -0.00549 - 0.155/\phi^{0.5} \quad [4.1.2]$$

$$\phi_i/\phi_{o\ Intercept} = B = 1.045 + 0.128/\phi \quad [4.1.3]$$

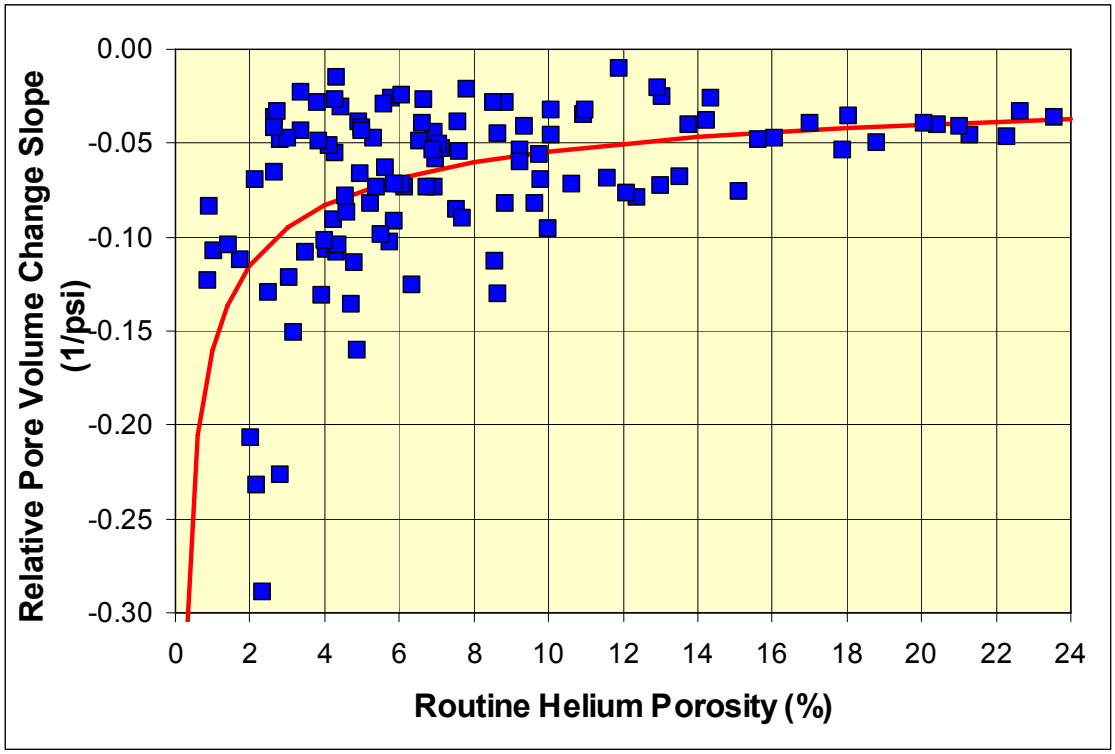

Figure 4.1.7. Crossplot of slope of log-linear curves in Figure 4.1.6 with porosity. The relationship between the slope and porosity can be expressed: Slope = -0.00549 -0.155/$\phi^{0.5}$.

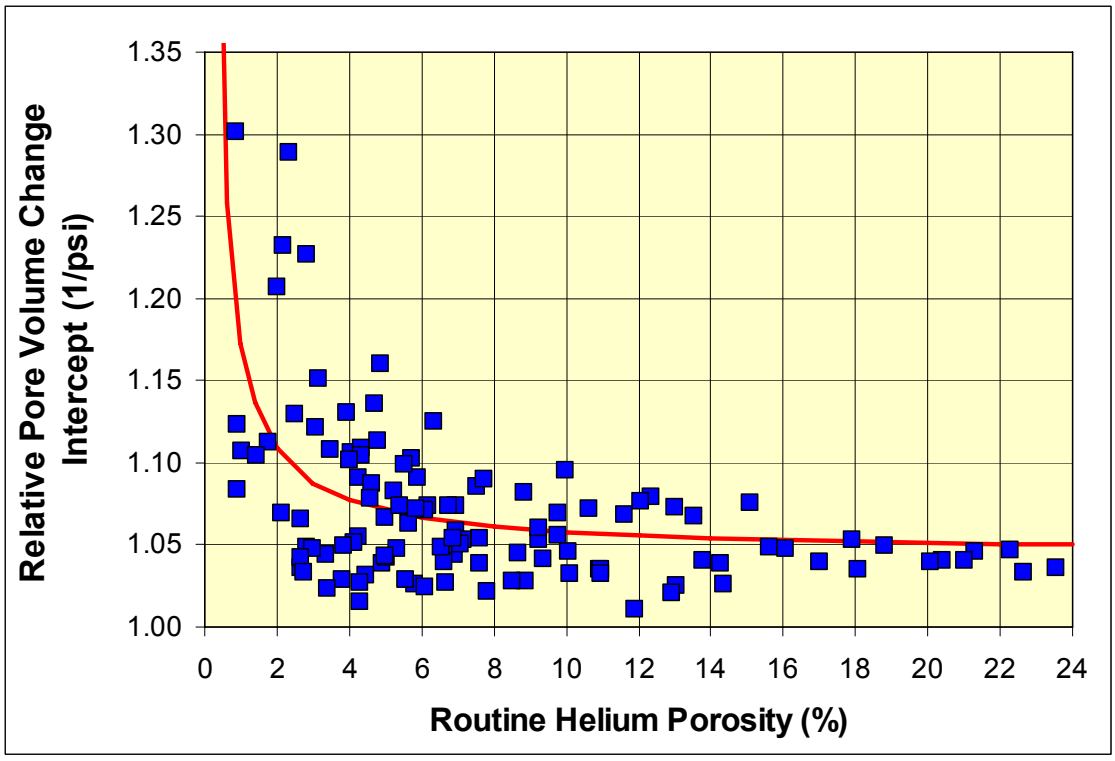

Figure 4.1.8. Crossplot of intercept of log-linear curves in Figure 4.1.6 with porosity. The relationship between the intercept and porosity can be expressed: Intercept = 0.013 ϕ + 1.08.

Utilizing equations 4.1.2 and 4.1.3 to calculate slopes and intercepts for rocks of different porosity, the fraction of initial pore volume relationship can be transformed to pore volume compressibility (change in volume/unit volume/change in pressure; β, 1/psi or 1/MPa). The above equations result in a power-law relationship between pore volume compressibility and net effective confining pressure of a form:

$$\log_{10} \beta = C \log_{10} P_e + D \qquad [4.1.4]$$

Figures 4.1.9 and 4.1.10 show the slope and intercept relationships for prediction of pore volume compressibility of low-permeability sandstones that conform to equations 4.1.2 and 4.1.3. The slope and intercept of the pore volume compressibility relations can be predicted using:

$$C = -1.035 + 0.106/\phi^{0.5} \qquad [4.1.4]$$

$$D = 4.857\ \phi^{-0.038} \qquad [4.1.5]$$

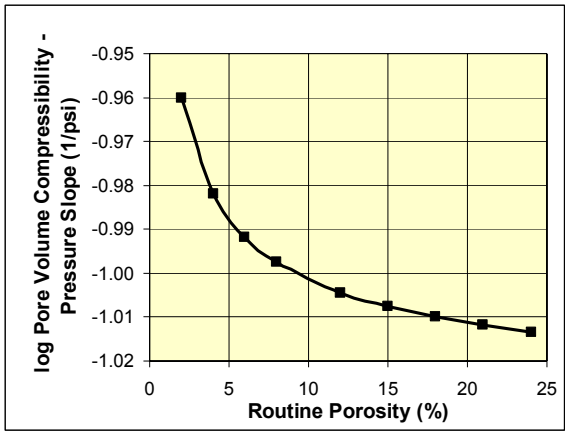

Figure 4.1.9. Crossplot of pore volume compressibility slope function versus porosity.

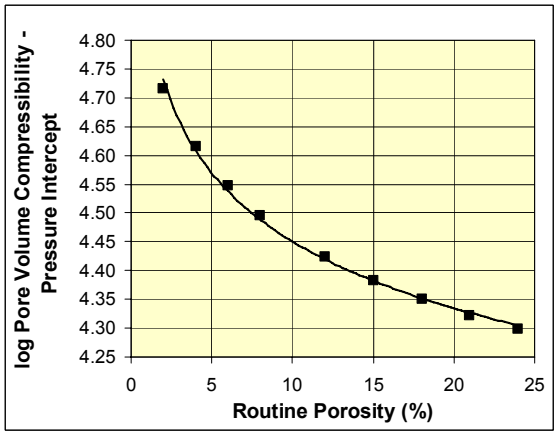

Figure 4.1.10. Crossplot of pore volume compressibility intercept function versus porosity.

Inserting equations 4.1.4 and 4.15 into equation 4.13 and taking the antilog of both sides:

$$\beta = 10\text{^}[(-1.035+0.106/\phi^{0.5})*\log_{10} P_e+(4.857\phi^{-0.038})] \qquad [4.1.6]$$

where β is the pore volume compressibility (10^{-6}/psi), P_e is the average net effective confining pressure at which β applies, and ϕ is the unconfined routine porosity (%). From equation 4.1.6, it is evident that compressibility changes with sandstone porosity and the net effective stress. Figure 4.1.11 illustrates general compressibility curves for different porosity Mesaverde sandstones and siltstones.

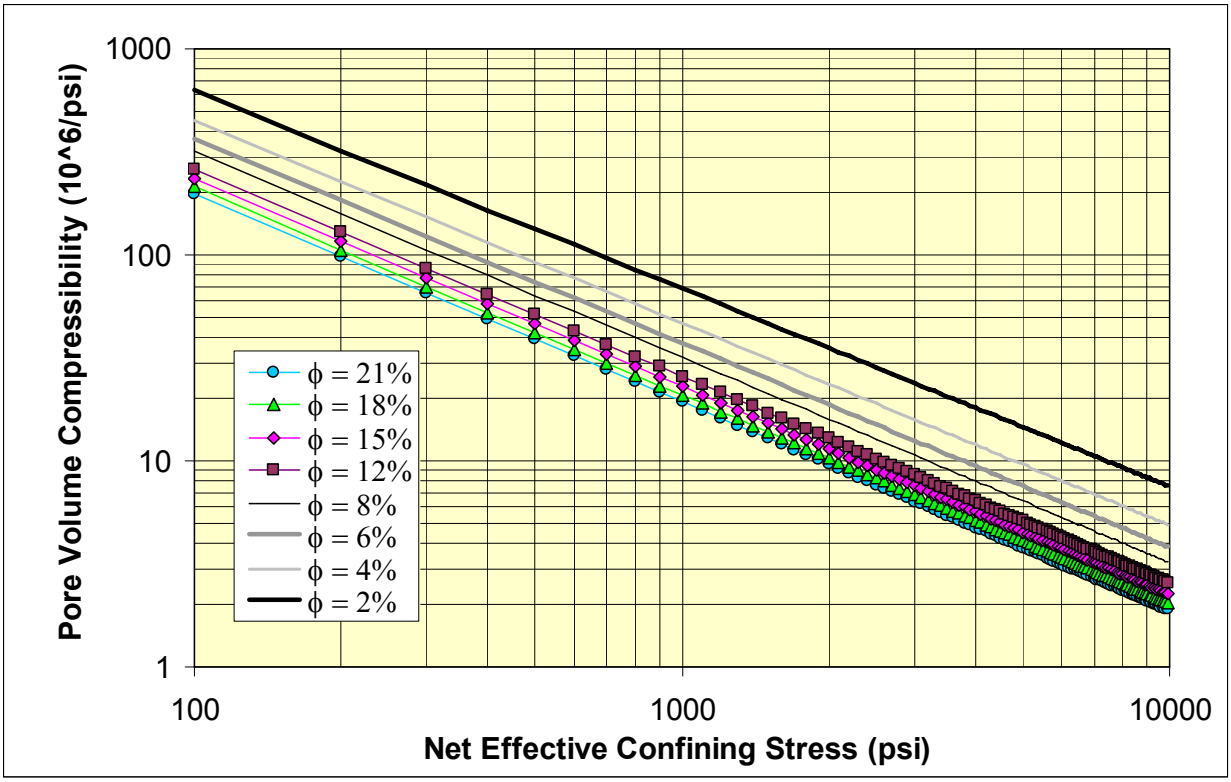

Figure 4.1.11. Pore volume compressibility versus net effective stress for Mesaverde sandstones and siltstones of various porosity as predicted using equation 4.1.6.

Pore volume compressibilities predicted using equation 4.1.6 are generally consistent with values published in the literature (e.g., Jones and Owens, 1981) for individual samples, usually reported at a single net effective stress. It is important to note that compressibility increases with decreasing confining stress and with decreasing porosity.

To compare *in situ* and routine porosity, it is necessary to correct the bulk volume of the sample for the pore volume change, assuming that grain compressibility is negligible. In this study both the compressibility and the pore volume change during electrical properties measurement provided a basis for comparison of routine and *in situ* porosity. Figure 4.1.12 illustrates the relationship between the measured *in situ* porosity (at 26.7 MPa (4,000 psi) net effective stress) and the routine porosity. Reduced major axis analysis of this relationship can be expressed

$$\phi_i = 0.943\ \phi_{routine} - 0.23 \qquad [4.1.7]$$

where ϕ_i = *in situ* porosity at 26.7 MPa (4,000 psi) net effective stress and $\phi_{routine}$ = unconfined routine porosity.

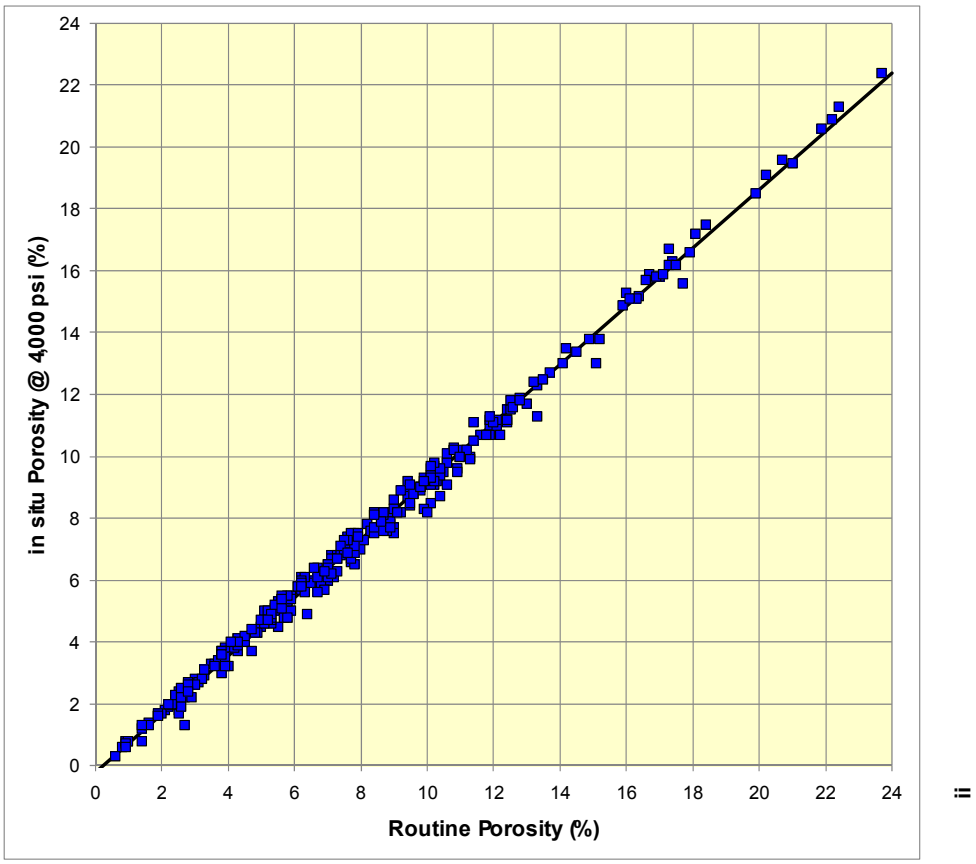

Figure 4.1.12. Crossplot of routine porosity and *in situ* porosity measured at 26.7 MPa (4,000 psi) net effective hydrostatic confining stress for 310 cores during electrical resistivity measurement. Correlation line represents equation 4.1.7.

Applying equation 4.1.6 at Pe = 26.7 MPa (4,000 psi) we can estimate the pore volume change and calculate the corresponding *in situ* porosity for any given initial porosity. Figure 4.1.13 illustrates a comparison of the estimated porosity at Pe = 26.7 MPa (4,000 psi) compared to the initial "routine" porosity. Equation 4.1.8 illustrates the general form of an *in situ* versus routine porosity trend and equations 4.1.9 through 4.1.113 show models from this study (Mesaverde Study) for the compressibility measurements, for porosity change measured in conjunction with electrical properties measurement, and from other previously published low-permeability sandstone studies including the Travis Peak (Luffel et al., 1991), Mesaverde/Frontier (Byrnes, 1997), and Clinton/Medina (Byrnes and Castle, 2000):

All Studies:	$\phi_i = A\ \phi_{routine} + B$	[4.1.8]
Mesaverde Study Compressibility:	$\phi_i = 0.96\ \phi_{routine} - 0.73$	[4.1.9]
Mesaverde Study Electrical Properties:	$\phi_i = 0.943\ \phi_{routine} - 0.23$	[4.1.10]
Travis Peak:	$\phi_i = 0.95\ \phi_{routine} - 0.3$	[4.1.11]
Mesaverde/Frontier:	$\phi_i = 0.998\ \phi_{routine} - 0.8$	[4.1.12]
Clinton/Medina:	$\phi_i = 0.966\ \phi_{routine} + 0.02$	[4.1.13]

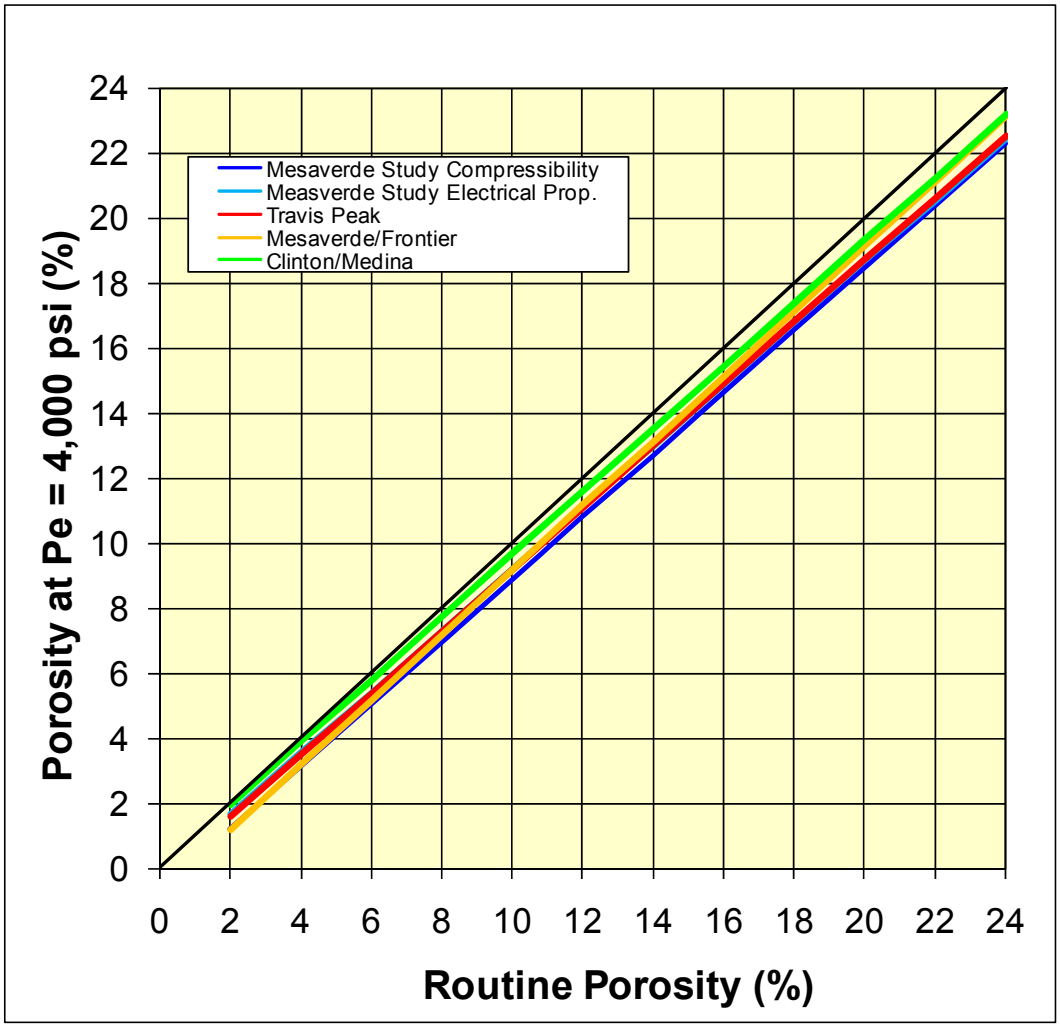

Figure 4.1.13. Crossplot of estimated *in situ* porosity (at Pe = 4,000 psi) versus routine porosity, based on equation 4.1.6 assuming that pore volume change also represents bulk volume change, versus unconfined (e.g., routine) porosity. The slope and intercept are similar to values reported from low-permeability sandstones.

Predicted values can be compared for high and low porosity (Table 4.1.5) illustrating differences between the rocks and models.

	Travis Peak	Mesaverde/ Frontier	Clinton/ Medina	Mesaverde Study-Comp	Mesaverde Study-Elec
A >	0.950	0.998	0.966	0.960	0.943
B >	-0.300	-0.800	0.020	-0.73	-0.226
Routine Porosity	*In situ* Porosity (%)				
2	1.6	1.2	2.0	1.2	1.7
4	3.5	3.2	3.9	3.1	3.5
6	5.4	5.2	5.8	5.0	5.4
8	7.3	7.2	7.7	6.9	7.3
10	9.2	9.2	9.7	8.9	9.2
12	11.1	11.2	11.6	10.8	11.1
14	13.0	13.2	13.5	12.7	13.0
16	14.9	15.2	15.5	14.6	14.9
18	16.8	17.2	17.4	16.5	16.7
20	18.7	19.2	19.3	18.5	18.6
22	20.6	21.2	21.3	20.4	20.5
24	22.5	23.2	23.2	22.3	22.4

Table 4.1.5. Comparison of predicted porosity for present study (Mesaverde Study) from both the compressibility measurements and measurements performed in conjunction with electrical properties and previously published low-permeability sandstone studies cited in text.

Comparing predicted *in situ* porosity values for the different studies and measurements illustrates that the Clinton/Medina quartzose tight gas sandstones are the least compressible. Porosity changes for the Travis Peak and as measured with electrical properties for the Mesaverde are statistically identical. The greatest porosity decrease from routine conditions is exhibited by the Mesaverde samples measured in the compressibility analysis. The greater compressibility for these samples may be attributed to several causes including: 1) lithologic differences, 2) correction for sleeve effects, 3) wet versus dry, and 4) equilibration time under stress. For the samples measured in this study, because the compressibilities were measured in the same apparatus, it is interpreted that the two variables influencing the differences between the compressibility and electrical properties porosity changes are 1) equilibration time, and to a small degree, 2) correction for sleeve effects. Given that the porosity changes observed during the compressibility measurements conformed to equilibrium criteria that would produce data for pore volume change that are more accurate, the compressibility data are interpreted to be most

accurate. The increasing difference between the compressibility and electrical properties *in situ* porosities with deceasing porosity can be interpreted to indicate that pore volume compression equilibration time increases with decreasing porosity.

It is important to note that pore volume compressibility represents the elastic response to stress-field changes and does not necessarily exhibit the same pressure-dependence exhibited by porosity versus depth trends or compaction curve models (Athy, 1930; Dickinson, 1953):

$$\phi_i/\phi_o = \exp[-\beta(Pe-Po)] \qquad [4.1.14]$$

Where ϕ_i = porosity at defined effective *in situ* stress Pe, ϕ_o = reference initial porosity, Pe = effective confining stress, Po = effective confining stress for ϕ_o, and β is an empirical constant that varies with rock properties.

4.1.3.3 Permeability

Permeability for the core samples from all basins is approximately log-normally distributed (Fig. 4.1.14) with 52% of the samples exhibiting *in situ* Klinkenberg permeability in the range 0.0001–0.01 mD ($1x10^{-7}$–$1x10^{-5}\mu m^2$) and 18% of the samples exhibiting $k_{ik} < 0.0001$ mD ($1x10^{-7}\mu m^2$) and 30% exhibiting $k_{ik} > 0.01$ mD ($1x10^{-5}\mu m^2$). The distribution of permeability for samples from different basins is generally similar (Fig. 4.1.15; Table 4.1.6) though slight differences in the mean and standard deviation exist. It is important to note that these distributions are for the sample set and may not reflect actually distributions within the basins.

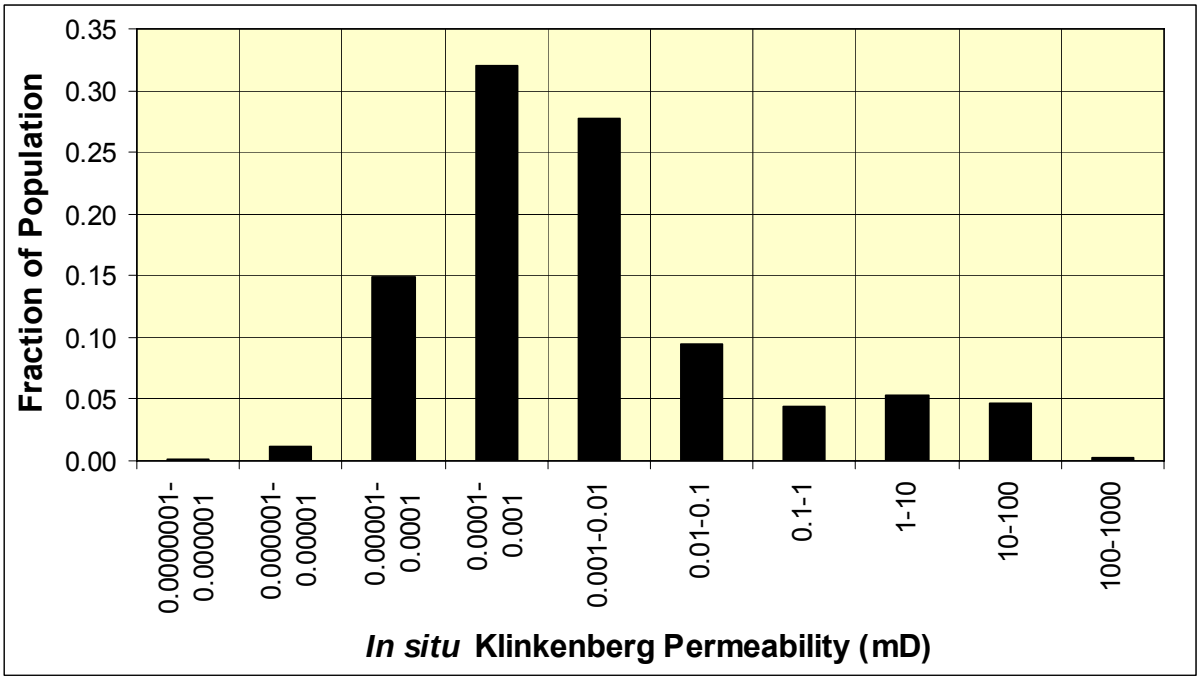

Figure 4.1.14. Distribution of *in situ* Klinkenberg permeability measured at 26.7 MPa (4,000 psi) net effective stress for all samples.

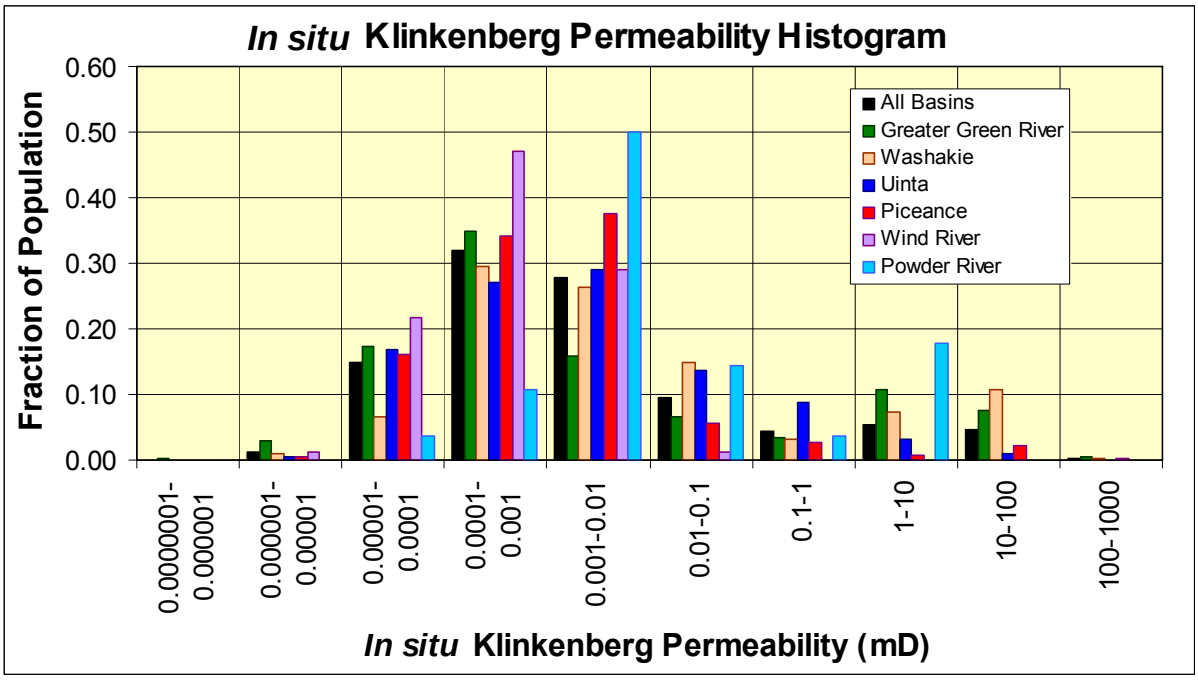

Figure 4.1.15. Distribution of *in situ* Klinkenberg permeability measured at 26.7 MPa (4,000 psi) net effective stress by basin.

	All Basins	Greater Green River	Washakie	Uinta	Piceance	Wind River	Powder River
Mean logk	-2.60	-2.49	-2.03	-2.66	-2.95	-3.44	-1.88
Median logk	-2.93	-3.15	-2.46	-2.86	-3.03	-3.36	-2.21
St Dev log	1.58	1.94	1.78	1.36	1.13	0.69	1.39
Minimum logk	-6.19	-6.19	-5.66	-5.33	-5.23	-5.11	-4.29
Maximum logk	2.31	2.31	2.08	1.88	2.05	-1.98	0.55
Kurtosis	0.62	-0.54	-0.39	0.17	4.02	-0.49	-0.38
Skewness	1.05	0.79	0.76	0.74	1.48	-0.01	0.50
Count	2143	555	373	529	577	81	28
Mean	0.0025	0.0032	0.0094	0.0022	0.0011	0.0004	0.0133
Median	0.0012	0.0007	0.0035	0.0014	0.0009	0.0004	0.0062
St Dev	37.9	87.4	59.9	23.0	13.4	4.9	24.5
Minimum	0.000001	0.000001	0.000002	0.000005	0.000006	0.000008	0.000051
Maximum	206.0	206.0	121.0	76.2	112.2	0.010	3.53
Kurtosis	0.62	-0.54	-0.39	0.17	4.02	-0.49	-0.38
Skewness	1.05	0.79	0.76	0.74	1.48	-0.01	0.50
Count	2143	555	373	529	577	81	28

Table 4.1.6. Summary statistics for *in situ* Klinkenberg permeability for all samples by basin.

To provide a common stress reference frame, *in situ* Klinkenberg permeability was measured at 4,000 psi net overburden. *In situ* Klinkenberg permeability was determined by measurement of permeability to nitrogen at two pore pressures and extrapolation of the k vs. 1/P trend to infinite pore pressure to obtain the Klinkenberg permeability at the intercept. The Klinkenberg gas permeability, which is equivalent to single-phase inert liquid or high pressure gas absolute permeability, increases with decreasing pore size.

The influence of Klinkenberg gas slippage, which results from greater gas movement due to decreased molecule-molecule interactions at lower pressure, was characterized by Klinkenberg (1954) as

$$k_{gas} = k_{liquid} (1 + 4cL/r) = k_{liquid} (1 + b/P) \quad [4.1.15]$$

where k_{gas} = gas permeability at pore pressure, k_{liquid} is liquid permeability and is equal to the Klinkenberg permeability k_{klink}, c = proportionality constant ($\simeq$ 1), L = mean free path of gas molecule at pore pressure, r = pore radius, *b* = proportionality constant (= f(c, L, r)), and P = pore pressure (atm).

Because *b* is a function of pore radius distribution, it can vary between rock samples. However, general values for *b* can be estimated from the relation presented by (Heid et al., 1950):

$$b = 0.777\ k_{klink}^{-0.39} \quad [4.1.16]$$

and Jones and Owens (1980):

$$b = 0.867\ k_{klink}^{-0.33} \quad [4.1.17]$$

Figure 4.1.16 shows the Klinkenberg proportionality constant *b* values measured on core in this study. Reduced major axis analysis predicts a slope and coefficient intermediate between values reported by Jones and Owens (1980) and Heid et al. (1950):

$$b = 0.851\ k_{klink}^{-0.341} \quad [4.1.18]$$

The *b* term is expressed in atmospheres to be consistent with previous studies. This figure extends the published trend to permeabilities below 0.001 mD and supplements the public data for the trend for permeabilities less than 0.01 mD. The variance in *b* at any given permeability is interpreted to result from several possible conditions including: 1) variance in lithology and corresponding pore throat size and size distribution for the same permeability, 2) heterogeneity of samples resulting in variable *b* within a sample and resulting averaging of the measured *b* during measurement, 3) variable *b* from one end of the sample to the other due to pressure drop across sample, and 4) error in one or both gas permeability measurements.

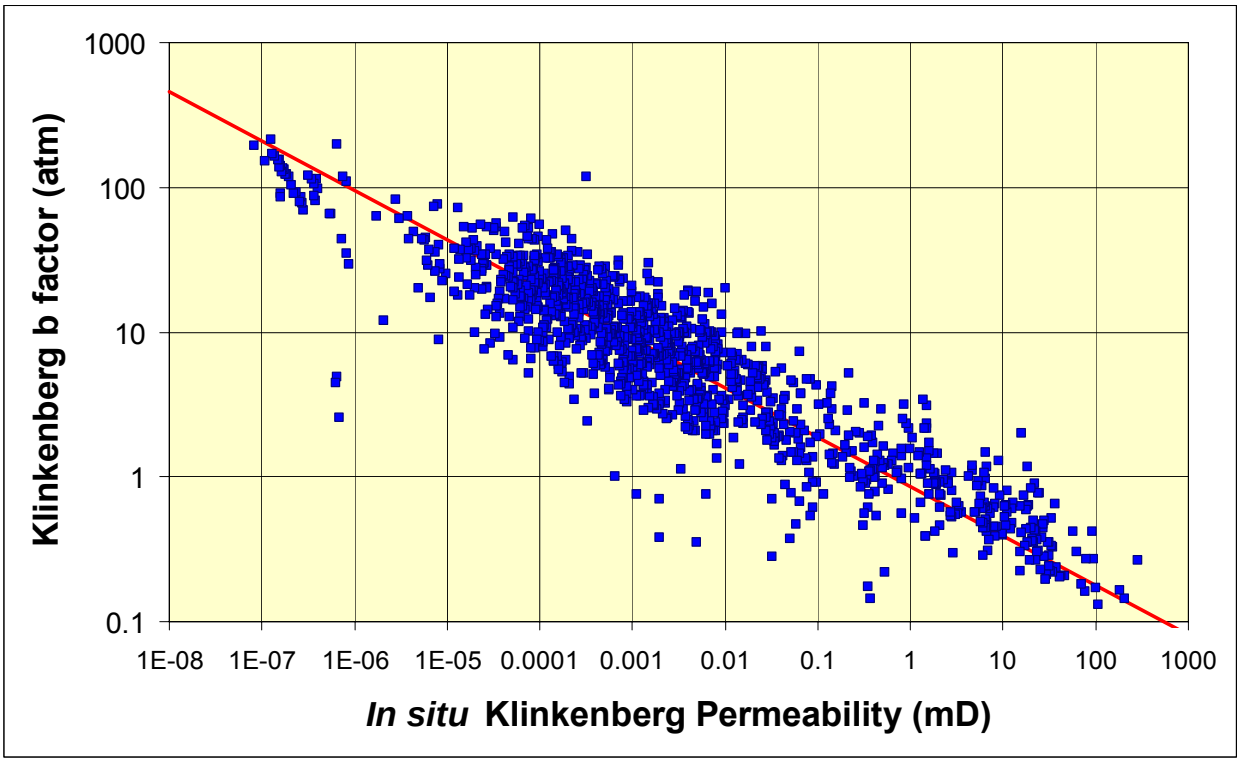

Figure 4.1.16. Crossplot of Klinkenberg proportionality constant, *b*, versus *in situ* Klinkenberg permeability measured at 26.7 MPa (4,000 psi) net effective stress using nitrogen gas. Reduced major axis analysis indicates the correlation can be expressed as $b(\text{atm}) = 0.851\ k_{ik}^{-0.341}$, n = 1264.

As described previously, 776 core plugs greater than 7.6 cm (3-inch) in length were cut in half to provide two paired core plugs for advanced properties measurements. Figure 4.1.17 illustrates the ratio of *in situ* Klinkenberg permeabilities of samples to the geometric mean permeability of the sample pair. Approximately 35% of all samples exhibit permeabilities within 10% of the mean, 55% within 20%, 70% within 30%, and 80% within 40%.

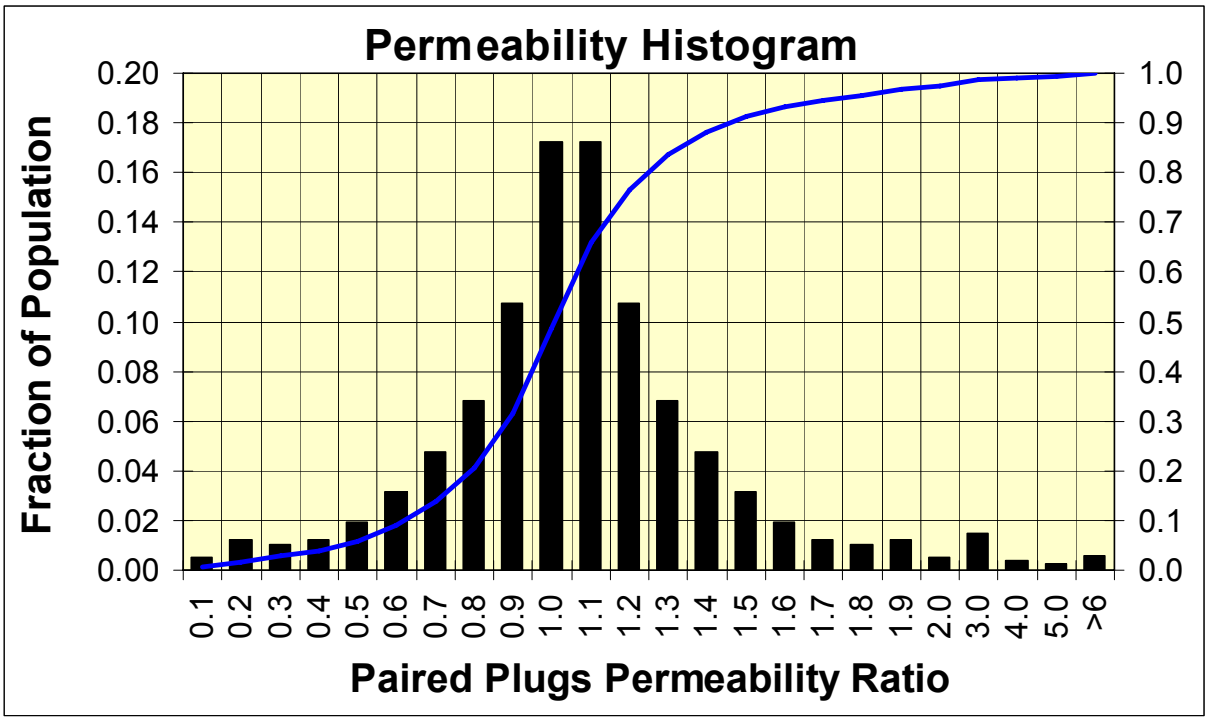

Figure 4.1.17. Histogram of ratio of paired plug *in situ* Klinkenberg permeabilities to mean permeability of plug pair. n = 634 x 2 = 1268.

4.1.3.4 Porosity-Permeability Relationship

Comparison of measured *in situ* Klinkenberg permeability versus an estimated approximate *in situ* porosity (routine porosity – 0.6%) for 2200 Mesaverde sandstones (Figure 4.1.18) shows that the present sample population exhibits higher permeability than previously published Mesaverde/Frontier studies (e.g., Byrnes, 1997). This is interpreted as due in part to the absence of argillaceous Frontier samples and to the high fraction of less argillaceous sandstones in the analyzed sample set.

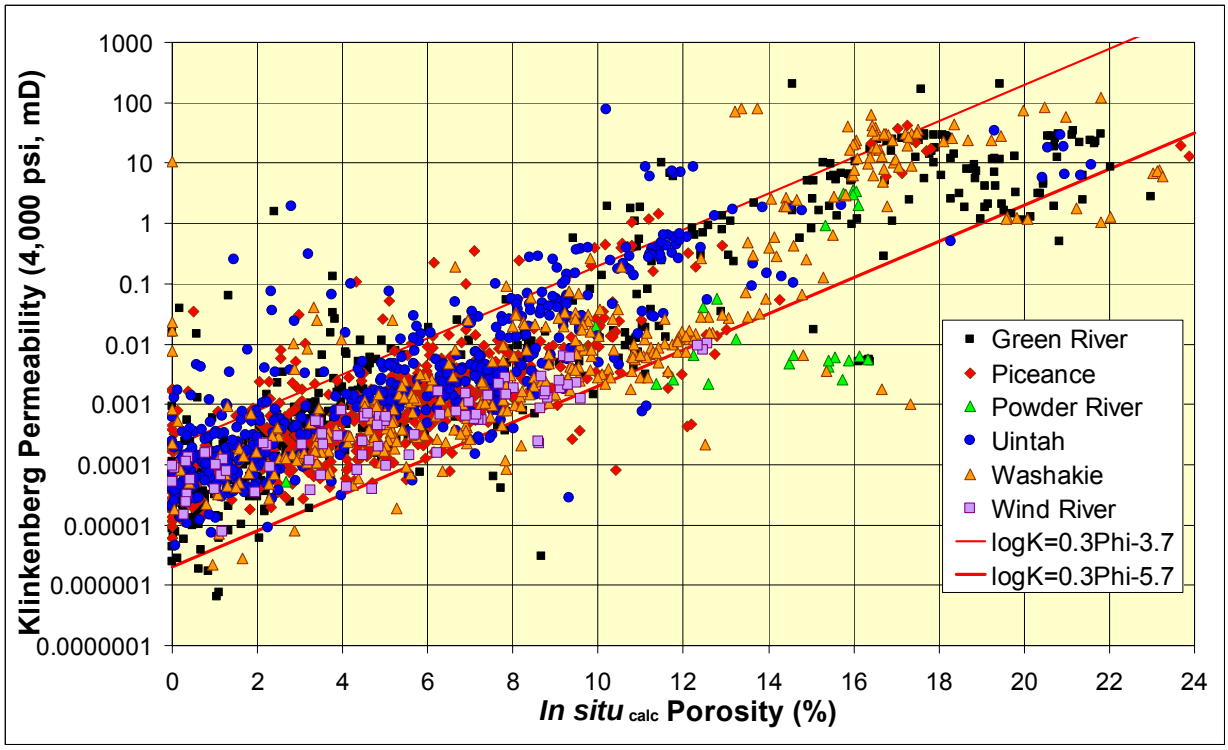

Figure 4.1.18. *In situ* Klinkenberg permeability versus calculated *in situ* porosity for all core samples by basin. Range of porosity and permeability of Mesaverde sandstones is generally exhibited by all basins.

Predictive equations for porosity-permeability

Figure 4.1.19 illustrates the relationship between permeability and porosity parametric with the second rock classification digit which represents size-sorting (see Subtask 4.5). Characteristic of most sandstones, permeability at any given porosity increases with increasing grain size and increasing sorting though this relationship is further influenced by sedimentary structure (rock digit 4) and the nature of cementation (rock digit 5). Samples exhibiting permeability greater than the empirically defined high limit generally exhibit an anomalous lithologic property that influences core plug permeability such as microfracturing along fine shale lamination, microfracture, and lithologic heterogeneity parallel to bedding with the presence of a high permeability lamina in a core plug dominantly composed of a lower permeability-porosity rock. Conversely, cores exhibiting permeability below the lower limit can exhibit such lithologic properties as churned-bioturbated texture, crossbedding with fine-grained or shaly bed boundaries that are sub-parallel or perpendicular to flow and act as restrictions to flow, or high clay content. Permeability in low porosity samples and particularly below approximately 1%

(vertical red line) is generally a complex function of final pore architecture after cementation and is only weakly correlated with original grain size.

The estimated range in permeability at any given porosity increases with porosity and can be as great as four orders of magnitude for $\phi > 12\%$ but decreases to approximately 20X near $\phi=0\%$. Though in unconsolidated grain packs the influence of size and sorting can be quantified, in consolidated porous media the influence of these variables and particularly the influence of sedimentary structure can be nonlinear and noncontinuous. For example coarse grain size results in high permeability, but if the sand was deposited in a trough crossbedded structure and there is some orientation of bedding in the core that is not parallel to flow then the permeability can be significantly reduced. The rock classification system used works to both quantify and make continuous these parameters but has limits.

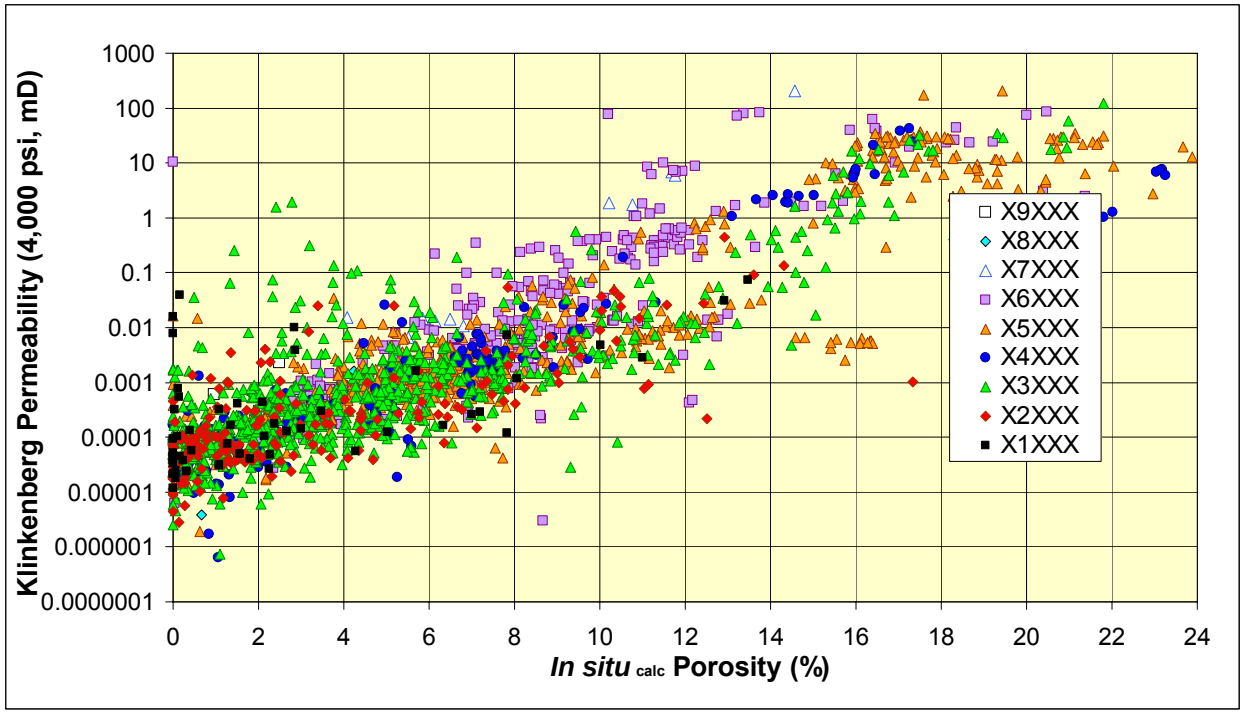

Figure 4.1.19. Crossplot of *in situ* Klinkenberg permeability (k_{ik}, mD, measured at 27.6 MPa (4,000 psi) net effective stress versus calculated *in situ* porosity ($\phi_{routine}$-0.6) by second rock type digit 2 representing size-sorting. The high limit generally defines the upper range for medium-coarse grained rocks. The lower limit generally represents the limit for siltstone rocks.

Excluding samples exhibiting permeability outside the limits shown in Figure 4.1.11 the relationship between the porosity and lithologic variables and permeability was explored. Multivariate linear regression analysis provides a predictive relationship:

$$\log k_{ik} = 0.282\ \phi_i + 0.18\ RC2 - 5.13 \qquad [4.1.19]$$

where k_{ik} is the *in situ* Klinkenberg permeability at 4,000 psi net confining stress (mD), ϕ_i is the approximate *in situ* porosity (%), and RC2 is the second digit of the rock classification representing size-sorting. Standard error of prediction for this equation is a factor of 4.5X (1 standard deviation). The simplest nonlinear relation is

$$\log k_{ik} = 0.034\ \phi_i^2 - 0.00109\ \hat{\phi}_i + 0.0032\ RC2 - 4.13 \qquad [4.1.20]$$

which exhibits a standard error of prediction of 4.1X (1 std dev).

Because of the nonlinear nature of the influence of the independent variable, an Artificial Neural Network (ANN) approach was also examined. A single hidden layer, 10-node network was used where the output from the hidden layer was a sigmoidal function (1/1 + exp(-x)) of the hidden-layer output. Table 4.1.7 shows the ANN parameters. The ANN, using *in situ* porosity (Phii), RC2 and RC4 provides prediction of k_{ik} with a standard error of prediction of 3.3X (1 std dev, Fig. 4.1.20). Although Artificial Neural Network (ANN) methods are capable of predicting permeability within a factor of 3.3X, the ease of sharing and applying an ANN model is not as great as simpler algebraic equations.

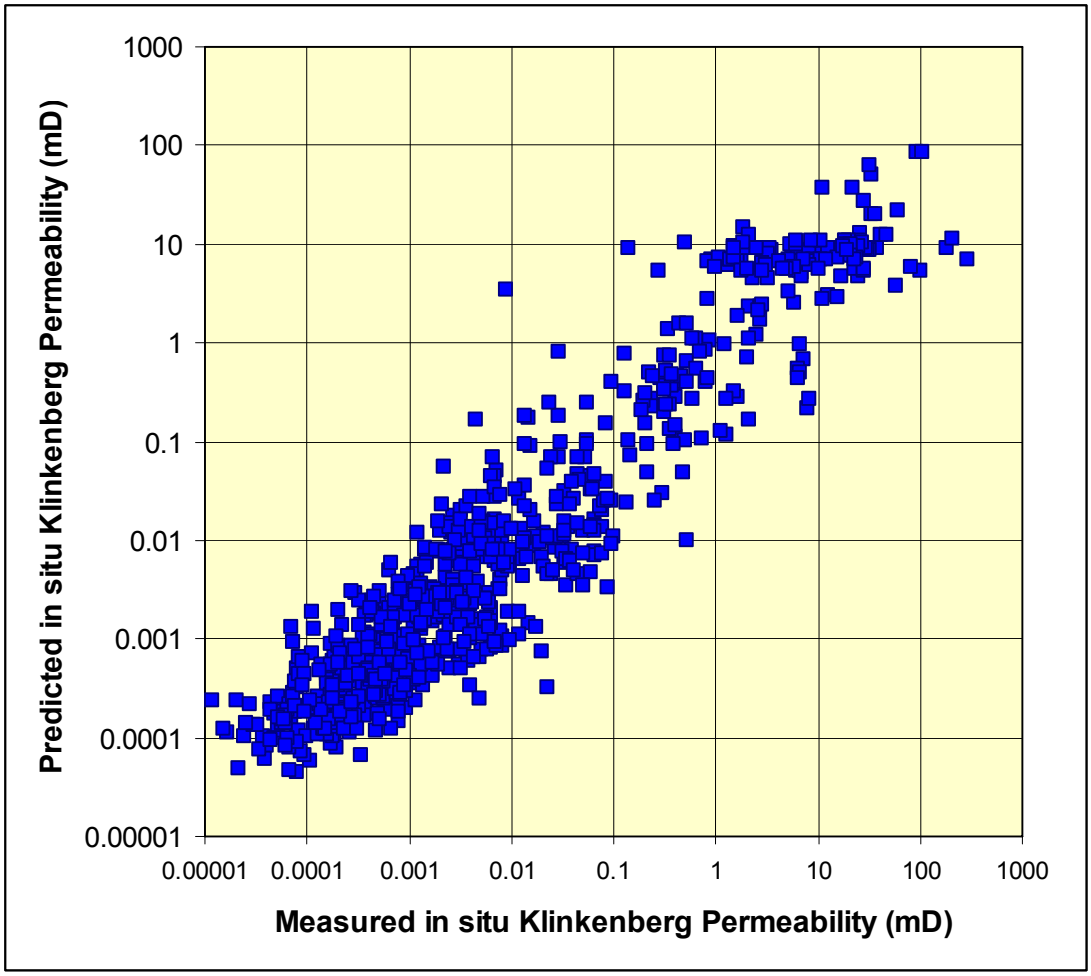

Figure 4.1.20. Crossplot of measured versus predicted *in situ* Klinkenberg permeability using artificial neural network with parameters shown in Table 4.1.2. Correlation standard error is 3.5X.

Although inclusion of a term for size/sorting significantly improves permeability prediction, a unique wireline log signature for predicting the size/sorting rock digit 2 was not identified that could be applied universally. The difficulty in identifying the unique log signature is interpreted to be the result of lack of log normalization. Within a given well, wireline response can predict Rock Digit 2 with appropriate accuracy but the nature of the relationship changes from one to another. It was, however, found that three classes of size/sorting could be reliably identified from all wireline log response. These three classes comprise 1) shales/mudstones, silty shales, siltstones, and very shaly sandstones with digit X(0-2)XXX, 2) moderately shaly sandstones X3XXX, and 3) very fine to coarse grained sandstones X(4-9)XXX. The relationship between permeability and porosity for the three classes of rock is shown in Figure 4.1.21.

Hidden layer: 1					
Hidden layer nodes: 10					
	Mean>	8.239	4.280	6.294	hidden layer-
	Std Dev>	5.260	1.335	2.527	to-output
	Input-to-hidden layer weights				weights
Node	Constant	Phii	RC2	RC4	
Constant					-0.388
1	-0.760	2.946	-2.027	-6.438	-0.885
2	-2.155	4.637	1.279	0.895	2.323
3	-4.999	7.901	0.957	3.167	-2.583
4	-1.484	-0.307	-1.695	6.175	-0.154
5	-4.597	4.582	1.568	0.730	4.022
6	-2.609	0.320	-2.201	-2.257	-2.495
7	-1.765	-1.843	-1.122	0.145	-3.859
8	2.839	-3.146	-9.237	0.264	0.789
9	-1.566	1.029	-1.588	-3.390	2.400
10	2.951	0.778	3.316	0.179	-2.136

Table 4.1.7. Artificial neural network parameters for k_{ik} prediction using ϕ_i, RC2, and RC4 as input variables. ANN utilized was a single hidden layer with 10 nodes and sigmoidal base function.

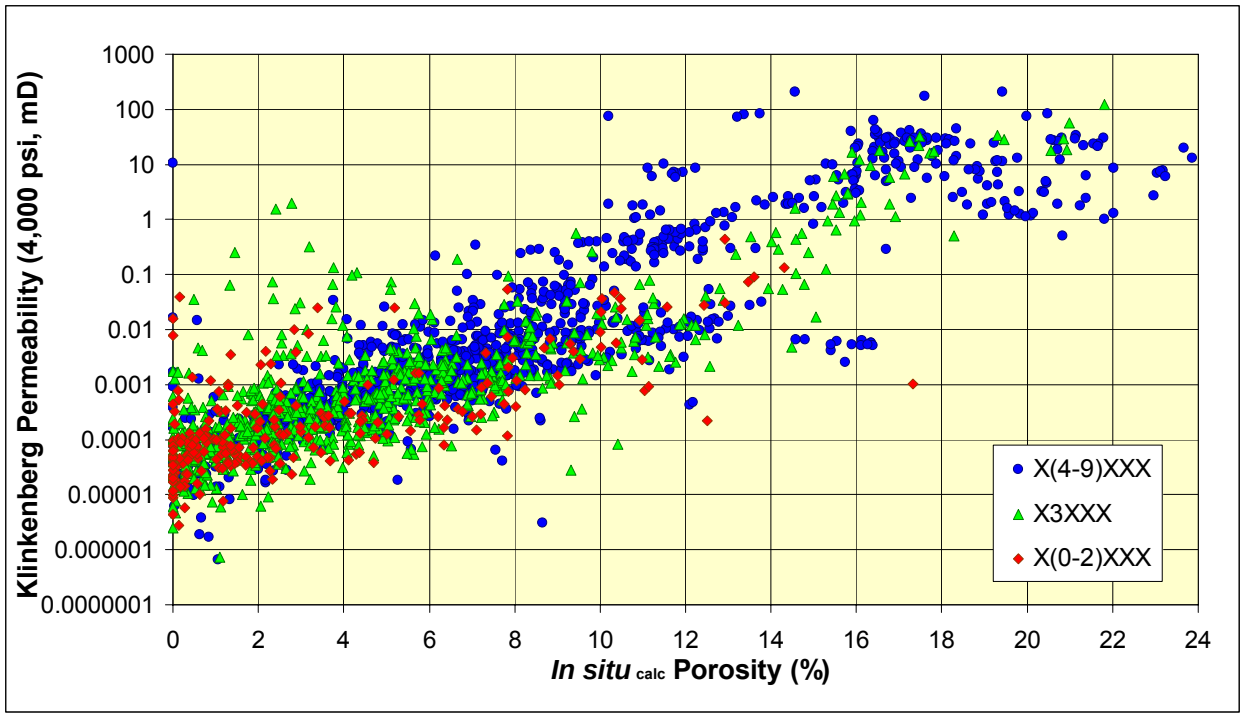

Figure 4.1.21. Crossplot of *in situ* Klinkenberg permeability (k_{ik}, mD, measured at 4,000 psi net effective stress) versus calculated *in situ* porosity ($f_{routine}$-0.8) by clustered second rock type digit representing size-sorting classes that are identifiable by wireline gamma ray log response.

Utilizing a multivariate linear equation similar to Eq. 4.1.4, regression analysis provides a predictive relationship:

$$\log k_{ik} = C_1 \phi_i + C_2 RC2_{log} + C_3 \quad [4.1.21]$$

where k_{ik} is the *in situ* Klinkenberg permeability at 4,000 psi net confining stress (mD), ϕ_i is the approximate *in situ* porosity (%), $RC2_{log}$ is the log-predicted 3-class second digit of the rock classification representing size-sorting, and C_1 is the porosity coefficient, C_2 is the RC2 coefficient, and C_3 is the intercept. Examination of Figure 4.1.21 shows that the permeability-porosity trend exhibits different relationships for the porosity ranges; 0–12%, 12–18%, and > 18%. Multivariate equations using 1) porosity, 2) rock class (1–3), and for each of these three porosity classes separately (0–12%, 12–18%, >18%), and also performed separately for each basin provided equations that exhibit an average standard error of prediction of 0–12%: 3.8±1X; 12–18%: 3.8±1X; >18%: 3.1X (for all basins undifferentiated; Table 4.1.8).

	All Mesaverde	Green River	Piceance	Powder River	Uinta	Washakie	Wind River
Porosity < 24%							
Porosity Coefficient	0.266	0.278	0.252	0.210	0.255	0.298	0.159
RC2 Coefficient	0.148	0.085	0.108	0.000	0.357	0.078	0.249
Intercept	-4.713	-4.612	-4.615	-4.515	-4.891	-4.950	-4.863
Count	1983	536	553	28	504	283	79
Std Error of Prediction	5.4	5.3	4.2	10.8	4.8	7.4	2.1
Porosity ≤ 12%							
Porosity Coefficient	0.241	0.273	0.215	0.193	0.247	0.221	0.152
RC2 Coefficient	0.174	0.069	0.206	0.000	0.365	0.039	0.260
Intercept	-4.678	-4.573	-4.669	-4.382	-4.877	-4.546	-4.860
Count	1691	418	528	8	486	175	76
Std Error of Prediction	4.6	4.7	3.8	3	4.8	3.5	2.1
12% < Porosity < 18%							
Porosity Coefficient	0.464	0.282	0.555	0.547	0.108	0.638	
RC2 Coefficient	0.681	0.548	0.013	0.689	0.584	0.229	
Intercept	-8.614	-5.366	-8.382	-10.282	-3.178	-10.082	
Count	184	56	18	12	13	74	
Std Error of Prediction	5.4	2.4	4.3	4.3	3.6	2.9	
Porosity ≥ 18%							
Porosity Coefficient	0.264						
RC2 Coefficient	0.000						
Intercept	-4.596						
Count	35						
Std Error of Prediction	3.1						

Table 4.1.8. Summary of *in situ* Klinkenberg permeability equations for each basin separated by porosity class. The standard error of prediction is expressed as a factor (e.g. 5.4 = ±5.4X).

Subtask 4.2. Measure Critical Gas Saturation

4.2.1 Task Statement

The objective of this task was to measure critical nonwetting phase and gas saturation using air-mercury capillary pressure analysis and air-brine displacement.

4.2.2 Methods

Both air-mercury critical nonwetting phase saturation measurements and air-brine critical gas were performed. All mercury capillary pressure data are posted on the Project Website.

4.2.2.1 Air-Mercury Critical Nonwetting Phase Saturation

Both unconfined mercury intrusion capillary pressure (MICP) analysis and confined MICP analysis were performed. Samples ranged widely in lithology with samples representing arkose to sub-litharenite composition, grain sizes ranging from siltstone to upper medium-grained, argillaceousness ranging from clean to shaly, and sedimentary structures comprising massive, laminar, low-angle cross, ripple-laminated, and convolute or bioturbated bedding. The low-permeability sandstones analyzed exhibited a range in porosity and permeability characteristic of the sampled population of Mesaverde sandstones (Figure 4.2.1).

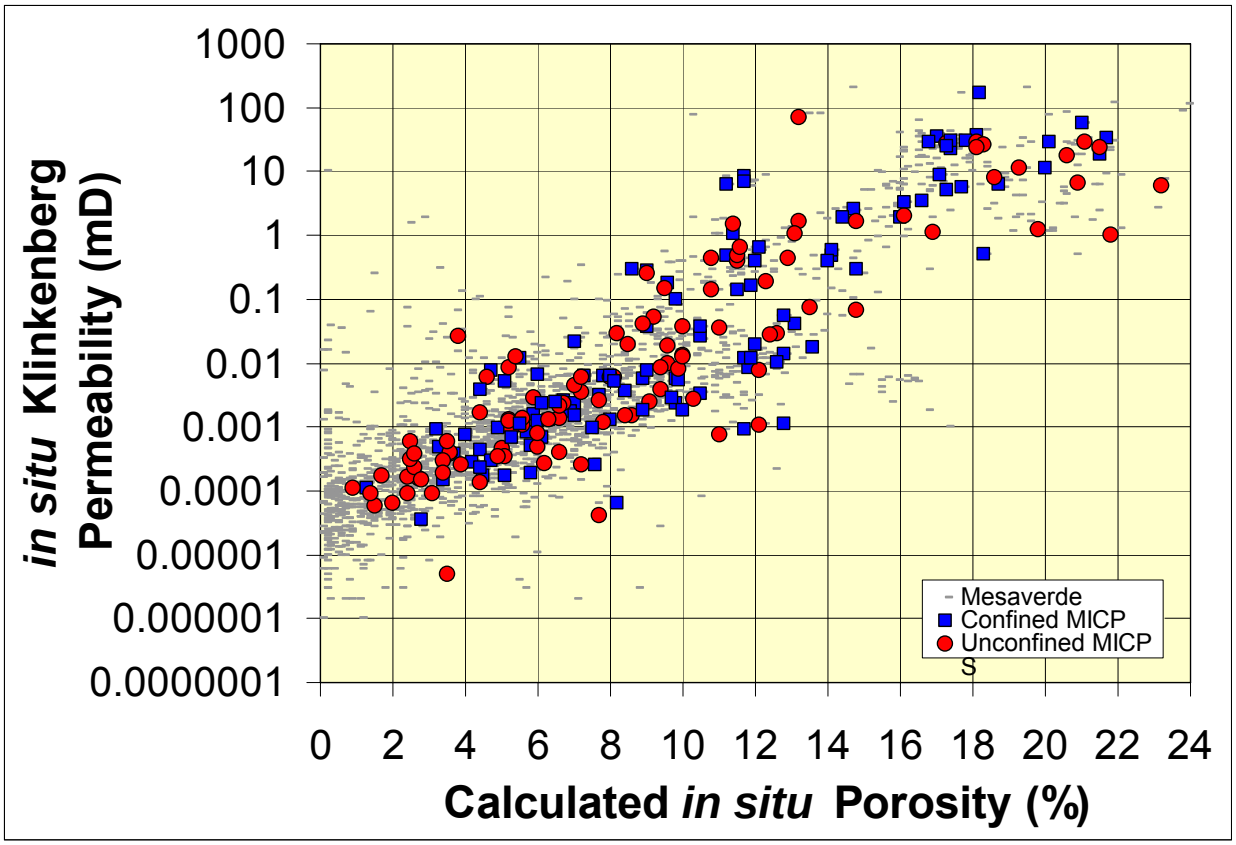

Figure 4.2.1. Crossplot of *in situ* Klinkenberg permeability versus *in situ* porosity for low-permeability sandstones for which unconfined (red circles) and confined (blue squares) mercury intrusion capillary pressure analysis was performed to determine the critical mercury (non-wetting phase) saturation. Samples range widely in lithology from siltstone to lower- and medium-grained sandstone with varying clay content and different sedimentary structures.

The mercury intrusion method was selected both to approximately reproduce the methodology of Thompson et al. (1987) and Schowalter (1979). Because mercury allows examination of empty pores, volumes can be measured with accuracy, and equilibration times are brief because there is no wetting phase displacement, it is possible to investigate properties of the porous network at saturations greater than the percolation threshold, it allows electrical conductance of the nonwetting phase to be measured, and it allows establishment of capillary equilibrium in association with percolation threshold measurements. Though useful, this method does present the significant limitation that a water wetting-phase is not present, which can influence results compared to MICP. To measure *in situ* porosity and permeability, the cores were subjected to

a hydrostatic confining stress of 0.0113 MPa/m depth (0.5 psi/foot depth) to simulate *in situ* stress. Helium porosities were measured using a Boyle's Law method and Klinkenberg permeabilities were determined using a pressure pulse decay method.

For unconfined mercury intrusion analysis each sample was subjected to step-wise, increasing, mercury-injection pressures ranging from 0.014 to 69 MPa (2–10,000 psia). Unconfined mercury porosimetry allows mercury to enter a sample from all sides. To measure percolation threshold or critical saturation, it is necessary to test for continuity from one side of a network to another. To determine the nonwetting phase, critical saturation, S_{nwc}, mercury intrusion analysis was performed on 2.54-cm diameter by 5-cm to 7-cm long cores hydrostatically confined. The first 20 analyses were performed at a confining pressure of 33.4 MPa (5,000 psi) greater than the mercury injection pressure, maintaining a net effective stress of 33.4 MPa (5,000 psi). All subsequent samples were measured at a confining pressure of 26.7 MPa (4,000 psi) greater than the mercury injection pressure, maintaining a net effective stress of 26.7 MPa (4,000 psi). Resistance across the core was measured using stainless steel electrodes on each end of the core (Figure 4.2.2).

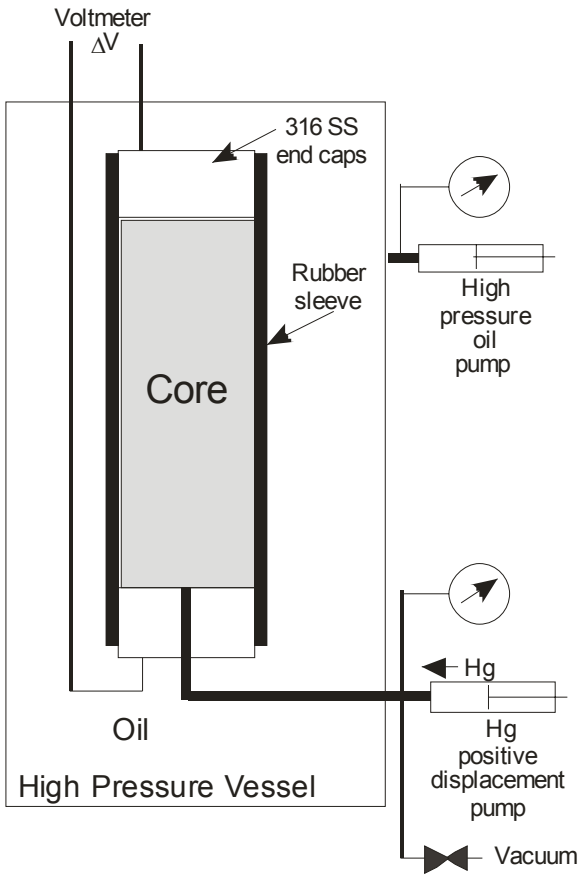

Figure 4.2.2. Schematic of high-pressure, mercury-intrusion, and electrical-resistance instrument. Samples were confined at a pressure of 26.7 MPa (4,000 psi) greater than the mercury-injection pressure for all pressures.

Sandstone matrix and evacuated pore space are both highly resistive and the clean, dry, evacuated sandstone samples investigated all exhibited resistance ranging from 0.15 to 4 x 10^6 ohms (ohms). At the critical saturation of the percolation threshold, with formation of a continuous mercury tendril across the sample, resistance across the core decreases abruptly by one to five orders of magnitude. From each sample's capillary pressure curve the saturation associated with the characteristic length, l_c, as defined by Thompson et al. (1987), was measured at the first inflection point. Figure 4.2.3 illustrates the determination of the inflection point saturation for two samples of different permeability. Curvature at wetting phase saturations above the inflection is zero or positive and below the inflection is negative. Uncertainty in the determination of the mercury saturation associated with the inflection point is estimated to be S_{nwc} $\pm$0.01 to $\pm$0.005 depending on the injection curve profile.

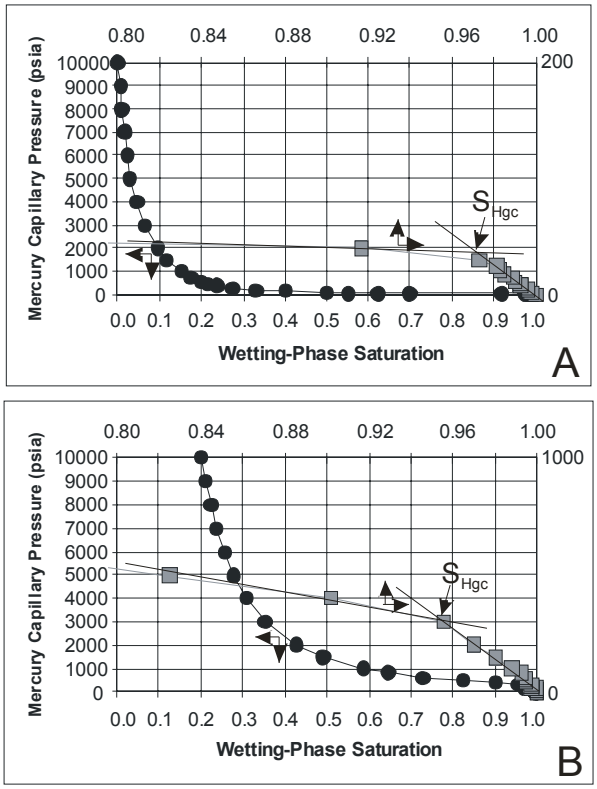

Figure 4.2.3. Illustration of the estimation of the critical-mercury saturation at which mercury forms a sample-spanning cluster using the method of Thompson et al. (1987) for sandstone samples of k = 1.16 mD (A) and k = 0.0035 mD (B). Prior to forming the sample-spanning cluster, mercury saturation increases approximately linearly or has positive curvature with pressure. Note black curves show entire capillary-pressure curve and gray curves show only low-pressure portion of curve to magnify the region of the critical-saturation inflection.

4.2.2.2 Air-Brine Critical Gas Saturation Measurement

Sample preparation for air-brine critical gas saturation, S_{gc}, measurements involved vacuum/pressure saturation of the cores with brine as described in Section 4.1.3.2.1 for compressibility measurements. For most of the samples the critical gas saturation measurement was performed subsequent to electrical properties measurements with the core saturated and in equilibrium with brines of either 80,000 ppmw NaCl or 200,000 ppmw NaCl. Measurement of S_{gc} by gravimetric methods involved the following steps:

1. Place the core in a Hassler cell (Figure 4.2.4) with one end sealed by a solid stainless steel billet

2. hydrostatically confine the sample with a confining stress of P = 26.7 MPa (4,000 psi)
3. allow the core to expel water due to pore volume compressibility for a period of 2 days
4. record total brine expelled
5. remove core from Hassler cell and weigh
6. immediately after weighing place the core with excess brine back in a Hassler cell (Figure 4.2.4)
7. hydrostatically confine the sample with a confining stress of P = 26.7 MPa (4,000 psi)
8. allow the core to equilibrate with confining pressure for 1 day
9. displace brine from inlet tube by inserting wire in tube
10. attach partially water-filled micropipette to effluent tube with water meniscus marked on tube
11. attach high-pressure gas line to inlet tube
12. apply first gas pressure to inlet tube
13. twice a day inspect effluent tube for meniscus movement and/or presence of gas bubbles
14. if no bubbles are observed after a period of 2 days record any meniscus movement and incrementally increase inlet gas pressure and apply new gas pressure to inlet tube
15. repeat steps 13-14 until gas bubble(s) are observed in the effluent micropipette
16. when gas bubble(s) are observed, remove micropipette
17. remove core from Hassler cell and weigh
18. calculate *in situ* porosity, pore volume, and saturated weight from change in weight resulting from steps 1-5 and any meniscus movement in pressure steps prior to breakthrough pressure
19. calculate critical gas saturation from change in weight between steps 17 and 18 correcting for brine density.

It should be noted that gas effective permeability and gas saturation were not estimated from the volume of brine displaced prior to gas bubble breakthrough. Because it was not known at what applied gas pressure breakthrough would occur, the rate of brine expulsion for a given applied gas pressure could only be known if the precise time from gas pressure application to gas bubble breakthrough was known. With 15 cells running simultaneously over a period of

months it was not feasible to make meniscus observations on the time scale required for accurate rate values, and many cells exhibited breakthrough during the night.

Steps 1-5 were designed to remove most of the pore volume compression effects but small volumes of brine were expelled in the period prior to the pressure step resulting in breakthrough. The in situ porosity, pore volume, and weight of the core were corrected for this compression in step 18. Correction for the additional compression that occurred during the period associated with the breakthrough pressure step was not done because these values were less than the error in the weight measurement.

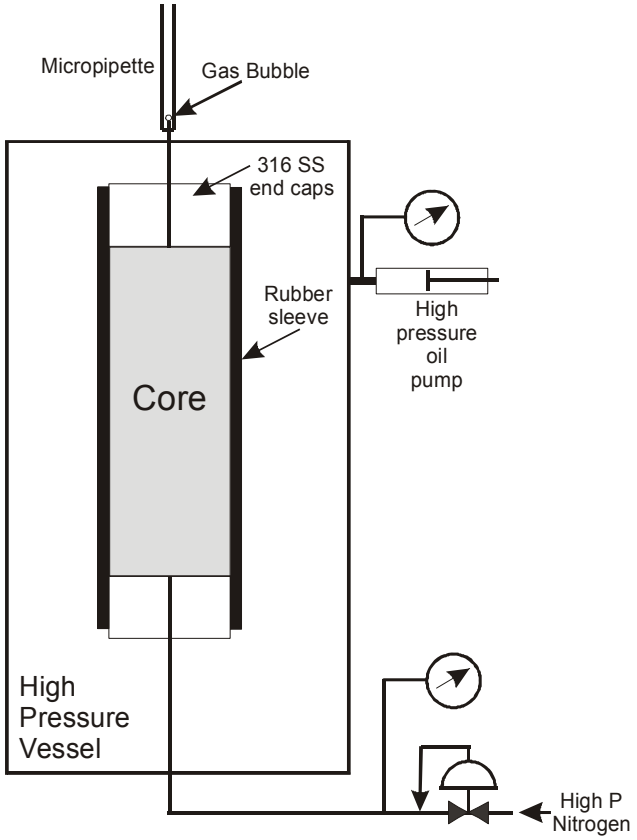

Figure 4.2.4. Schematic of high-pressure, air-brine critical gas saturation measurement apparatus. Samples were confined at a pressure of 26.7 MPa (4,000 psi) greater than the mean gas injection pressure.

The cores were analyzed in sequence sorted from the highest to lowest permeability and beginning analysis with the highest permeability core that required the lowest inlet gas pressure to achieve breakthrough. Fifteen (15) Hassler cells, plumbed in parallel for overburden and inlet pressure, were in operation for this measurement allowing the simultaneous analysis of 15 cores.

When a core measurement was complete for a sample, the next core in the series was placed in the available Hassler cell and the first gas pressure applied was equal to the gas pressure being applied for the other cores. Using this procedure, the first gas pressure for the lowest-permeability cores, analyzed near the end of the series, was significantly greater than the first gas pressure for the early, high-permeability cores. Only four cores exhibited breakthrough on the first gas pressure application, indicating breakthrough might have been achieved at a lower pressure and gas saturation might have been less than observed.

4.2.3 Results

4.2.3.1 Abstract

Review of gas relative permeability (k_{rg}) studies of low-permeability sandstones indicates they can be modeled using the Corey equation, but scarce data near the critical-gas saturation (S_{gc}) limit k_{rg} modeling at high water saturations. Confined mercury-injection capillary pressure and coupled electrical resistance measurements on Mesaverde sandstones of varied lithology were used to measure critical nonwetting saturation. Most of these data support the commonly applied assumption that $S_{gc} < 0.05$. However, a few heterolithic samples exhibiting higher S_{gc} indicate the dependence of S_{gc} on pore network architecture. Concepts from percolation theory and upscaling indicate that S_{gc} varies among four pore network architecture models: 1) percolation (N_p), 2) parallel ($N_{//}$), 3) series ($N_{\perp}$), and 4) discontinuous series ($N_{\perp d}$). Analysis suggests that S_{gc} is scale- and bedding-architecture dependent in cores and in the field.

The models suggest that S_{gc} is likely to be very low in cores with laminae and laminated reservoirs and low (e.g., $S_{gc} < 0.03$–0.07 at core scale and $S_{gc} < 0.02$ at reservoir scale) in massive-bedded sandstones of any permeability. In crossbedded lithologies exhibiting series network properties, S_{gc} approaches a constant reflecting the capillary pressure property differences and relative pore volumes among the beds in series. For these networks S_{gc} can range widely but can reach high values (e.g., $S_{gc} < 0.6$). Discontinuous series networks, representing lithologies exhibiting series network properties but for which the restrictive beds are not sample-spanning, exhibit S_{gc} intermediate between N_p and $N_{\perp}$ networks.

Consideration of the four network architectures lends insight into the complications of heterogeneous lithologies at differing spatial scales and underscores the difficulty of upscaling laboratory-derived relative permeabilities for reservoir simulation. Analysis also indicates that

for some architectures capillary pressure and relative permeability anisotropy may need to be considered.

4.2.3.2 Introduction

Industry assessment of the regional low-permeability gas resource, projection of future gas supply, and exploration programs require an understanding of reservoir properties and accurate tools for formation evaluation. Numerous studies have investigated absolute permeability in low-permeability sandstones. Studies of gas relative permeability (k_{rg}) have appropriately focused first on the gas relative permeability curve at low water saturations but fewer studies have investigated the end-point of the relative permeabilty curve, the critical-gas saturation (S_{gc}). The critical-gas saturation can be defined as the minimum gas saturation at which the gas phase has sufficient connectivity to form a system-spanning cluster and can consequently flow freely across the system. Compared to higher permeability sandstones, low-permeability sandstones commonly produce gas with little water at high water saturations. Experimental complexity makes it difficult to obtain k_{rg} data at high water saturations due to the extremely low gas permeabilities of the rocks and questions of the uniform distribution of saturation. High water saturation rocks are abundant and may predominate in resource plays. Therefore, understanding gas relative permeability at high water saturations is important to defining reservoir performance and the recoverable resource.

Although low-permeability sandstone petrophysical properties exhibit a continuum with higher permeability rocks, their properties can be significantly more sensitive to pressure-volume-temperature-composition-time (PVTXt) conditions and can change with PVTXt changes that for higher permeability rocks might be unimportant. This often requires that petrophysical properties, and the PVTXt conditions under which they apply, be carefully defined and measured. It also often leads to miscommunication where property definitions that are robust for a wide PVTXt range in high-permeability rocks must be modified to account for PVTXt influences in low-permeability rocks. Definitions for petrophysical terms used in this paper are presented in Table 4.2.1.

This paper examines some, but certainly not all, of the issues concerning gas relative permeability in low-permeability sandstone with a focus on critical-gas saturation that represents the end-point of the gas relative permeability curve. The

paper briefly summarizes previous work. It attempts to add to the data on critical-gas saturation by presenting mercury injection and resistance analyses directed at measuring the critical nonwetting phase saturation, which is analogous to the critical-gas saturation. To understand the observed critical saturations and the theoretical scale-dependence and bedding-architecture dependence of S_{gc}, models of pore architecture and percolation theory analysis are examined and applied.

Table 4.2.1 List of Abbreviations and Symbols in Critical Gas Analysis

Abbreviation	Definition
D	Fractal dimension
E	Euclidean dimension
f	Fraction of total network sites where gas nucleation occurs
k	Permeability, mD
kik	*In situ* Klinkenberg-corrected gas permeability, mD
krg	Relative permeability to gas, fractional (v/v)
L	Network size
MICP	Mercury injection capillary pressure, MPa
Mpa	Megapascals, 10^6 pascals
Nii	Parallel network
Np	Percolation network, random
Ns	Series network
Ns2	Discontinuous series network
p	Modified Corey equation gas exponent
Pc	Capillary pressure, Pa
Pc Sgc,high	Capillary pressure at Sgc,high
phi	Porosity, fraction (v/v)
psi	Pounds per square inch
PVTXt	Pressure-Volume-Temperature-Composition-time
q	Modified Corey equation gas exponent
Sg,Pc-Sgc-high	Gas saturation at PcSgc, high
Sgc	Critical gas saturation, expressed as a fractional (v/v) hydrocarbon saturation (1-Sw), saturation below which krg = 0
Sgc, low	Lowest critical gas saturation in parallel network, fraction (v/v)
Sgc,high	Highest critical gas saturation in series network, fraction (v/v)
Shg	Mercury (nonwetting phase) saturation, fraction (v/v)
Snwc	Critical nonwetting phase saturation, fraction (v/v), saturation below which nonwetting phase does not form a sample-spanning cluster
Sw	Water saturation, fraction (v/v)
Swc	Critical water saturation, fraction (v/v), saturation below which krw = 0
Swc,g	Critical water saturation, fraction (v/v) with respect to gas drainage, saturation at which krg = 1 and below which krg = 1
V	System volume (v)

4.2.3.3 Previous Work

4.2.3.3.1 Gas Relative Permeability

Relative gas permeability (k_{rg}) data for low-permeability sandstones have been reported in numerous studies (Thomas and Ward, 1972; Byrnes et al., 1979; Jones and Owens, 1980; Sampath and Keighin, 1981; Walls, 1981; Walls et al., 1982; Randolph, 1983; Ward and Morrow, 1987; Chowdiah, 1987; Byrnes, 1997; Kamath and Boyer, 1995; Castle and Byrnes, 1997, 2005; Byrnes and Castle, 2000; Byrnes, 2003, 2005; Shanley et al., 2004). Some k_{rg} measurements have been performed at water saturations (S_w) less than the saturation at which water may be immobile under a pressure gradient, and by definition, water relative permeability is zero. In the laboratory these sub-S_{wc} saturations were usually achieved by evaporation. Such saturations may or may not also exist in nature where PVTX changes to the fluids and rock or sufficiently long times are available for ultra-low flow rates that can potentially reduce water saturations below S_{wc}. The k_{rg} data in the $S_w < S_{wc}$ region exhibit continuity with data in the $S_w \geq S_{wc}$ region. To model these data in Corey-type equations, and avoid the apparent contradiction of water saturations below the saturation at which water is immobile, the term $S_{wc,g}$ that is used here defines water saturations specific for gas only. Alternately, Boolean expressions could be used to model these conditions but this approach was considered simpler. Byrnes et al. (1979) utilized a modified-Corey (1954) equation to predict gas relative permeability in low-permeability sandstones:

$$k_{rg} = (1 - (S_w\text{-}S_{wc,g})/(1\text{-}S_{gc}\text{-}S_{wc,g}))^p \, (1\text{-}((S_w\text{-}S_{wc,g})/(1\text{-}S_{wc,g}))^q) \qquad [4.2.1]$$

where all terms are defined in Table 4.2.1. Assigning $p = 2$ and $q = 2$ to generally model theoretical and observed data, Corey noted that p and q can change with pore structure. Brooks and Corey (1966) more thoroughly investigated the nature of pore-size distribution influence on relative permeability. They also noted that the Corey- or Brooks-Corey type equations are not defined at water saturations greater than S_{gc} and less than $S_{wc,g}$ even though "minor" flow may exist in these saturation regions. Issues related to operational, experimental, and theoretical definitions of critical saturations underlie many debates about these properties.

Byrnes et al. (1979) modeled k_{rg} data of Mesaverde cores using Equation 1 with S_{gc} = 0.2–0.3, $S_{wc,g}$ = 0, p = 1.1–1.3, and q = 2. For Mesaverde cores studied by Sampath and Keighin (1981) and Ward and Morrow (1987), reformatted to Equation 1, their equations utilized S_{gc} = 0.3, $S_{wc,g}$ = 0, p = 1.5, and q = 2. Chowdiah (1987) utilized a Corey-type equation formulated differently than Equation 4.2.1 that included a S_{gc} term in the parenthetic portion of the numerator of the first term in Equation 4.2.1. For this formulation, Chowdiah reported S_{gc} values of 0.096–0.47 and p values of 1.40–4.13 for data where water saturation was obtained by evaporation. The k_{rg} formulation of Chowdiah implicitly assumed $S_{wc,g}$ = 0. For the other studies cited above k_{rg} data and curves are reported but model equations are not presented. Byrnes (2003, 2005) compiled published k_{rg} curves for 43 samples from various western low-permeability sandstone formations (Figure 4.2.5) and individual k_{rg} values obtained at single S_w conditions (Figure 4.2.6). These data are shown parametrically with respect to the absolute permeability of the samples. For most of the studies, water saturations were achieved by drainage gas displacement of water (i.e., water saturation decreasing) using centrifuge, porous-plate, or evaporation. Chowdiah (1987) hypothesized that saturations obtained by evaporation represented imbibition conditions and that k_{rg} values measured for these conditions are lower than those obtained by drainage displacement. Many of the data in Figure 4.2.6 were obtained using centrifuge, though samples were briefly reversed to remove water retained at the end-face, and some were obtained using porous-plate method. The difference among methods is not immediately evident but needs to be investigated further. For all data shown in Figures 4.2.5 and 4.2.6, the relative permeabilities were measured under a confining pressure generally greater than 10.3 MPa (megapascals = 10^6 pascals; 1,500 pounds per square inch, psi) and the relative permeability values represent Klinkenberg-corrected values that are referenced to the Klinkenberg absolute-gas permeability measured on a dry sample (k_{ik} at S_w = 0) and not to water permeability. Chowdiah (1987) also hypothesizes that stress hysteresis resulting from sample removal from pressure for desaturation might result in a decrease in relative permeability. The reproducibility of k_{rg} curves in studies such as Thomas and Ward (1972) argues that this effect is not universal.

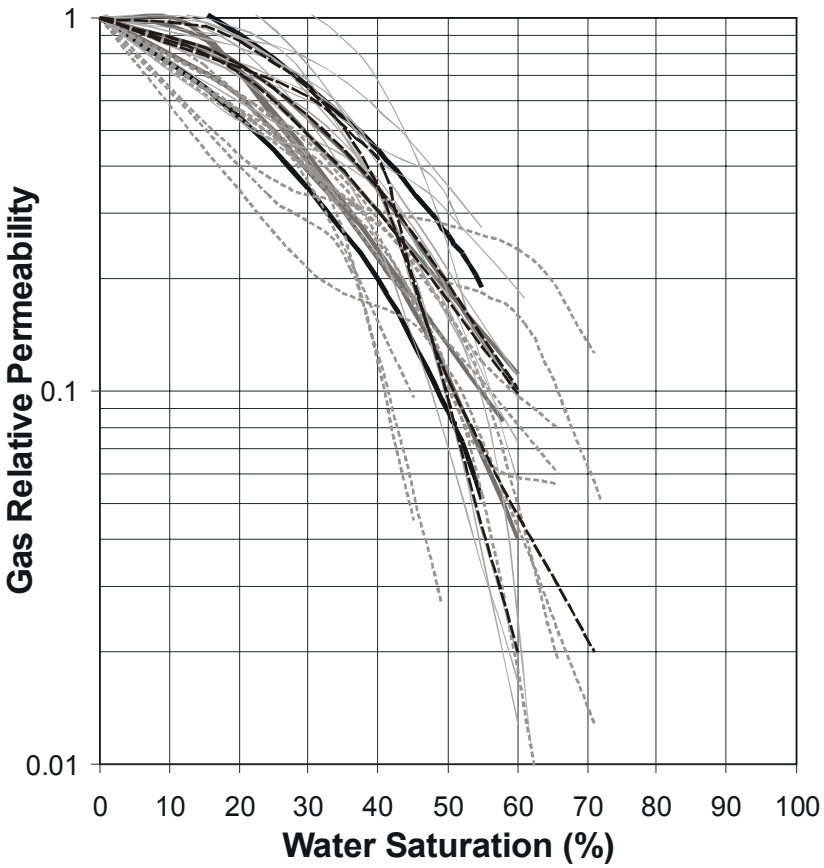

Figure 4.2.5. Relative gas permeability curves for 43 samples shown parametrically with permeability compiled from seven studies. Curves are separated into $k_{ik} < 0.01$ mD (dashed gray), $0.01 < k_{ik} < 0.03$ mD (thin light gray), $0.03 < k_{ik} < 0.1$ mD (heavy dark gray), $0.1 < k_{ik}$ mD (dashed black). Bounding heavy black curves are derived from the Corey equation model using parameters discussed in the text for $k_{ik} = 0.001$ mD (lower curve) and $k_{ik} = 1$ mD (upper curve).

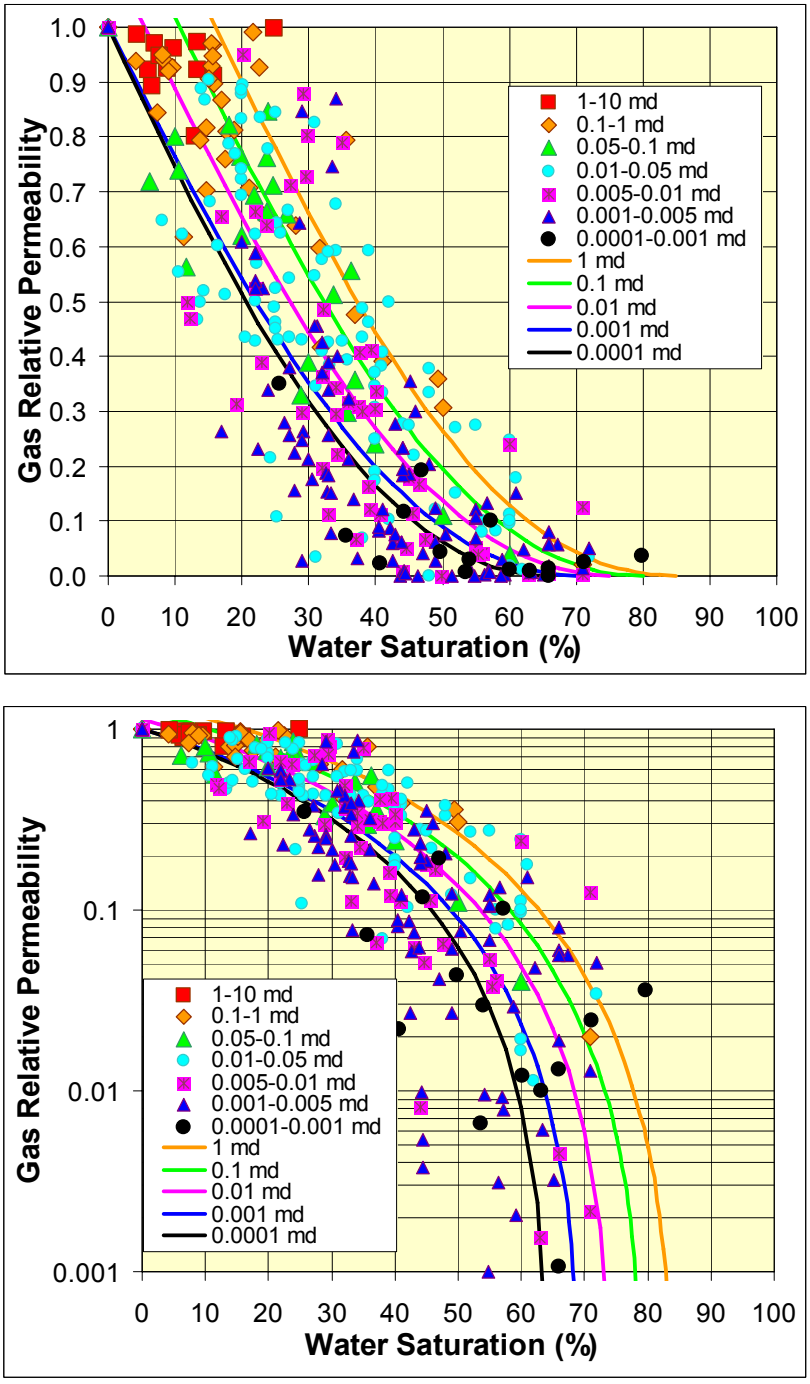

Figure 4.2.6. Gas relative permeabilities measured at single water saturations shown parametrically with sample k_{ik}. Curves show Corey-predicted $k_{rg,Sw}$ values for samples with k_{ik} = 0.0001 mD to k_{ik} = 1 mD using Equations 1–6. Linear format (A) illustrates the decrease in critical-water saturation from ~0.16 for 1 mD rocks to zero for 0.001 mD rocks. The logarithmic format (B) illustrates the abrupt decrease in relative permeability as water saturations increase above 0.5 and how critical-gas saturation appears to increase with decreasing permeability.

Though there is scatter, interpreted to primarily represent pore architecture variation in rocks of different lithofacies, for both the complete k_{rg} curves and the composite individual $k_{rg,Sw}$ measurements there is a general trend that at any given water saturation the gas relative permeability of lower permeability samples is less than that of higher permeability samples. Byrnes (2003) empirically fit the data in Figures 4.2.5 and 4.2.6 to Equation 4.2.1 using:

$$S_{wc,g} \approx 0.16 + 0.053*\log_{10}k_{ik} \quad \text{(for } k_{ik} \geq 0.001 \text{ mD)} \quad [4.2.2]$$

$$S_{wc,g} = 0 \quad \text{(for } k_{ik} < 0.001 \text{ mD)} \quad [4.2.3]$$

$$S_{gc} \approx 0.15 - 0.05*\log_{10}k_{ik} \quad [4.2.4]$$

$$p = 1.7 \quad [4.2.5]$$

$$q = 2 \quad [4.2.6]$$

These empirical equations were interpreted to be consistent with previously published parameters and to bracket existing data and approximately model the parametric relationship with absolute permeability. Figure 4.2.7 shows the same bounding k_{rg} curves as Figures 4.2.5 and 4.2.6 but extended to high S_w and low k_{rg} values. The bounding black curves were constructed using the equations for rocks of 0.001 millidarcies (mD; 1 mD = 0.000987 μm^2) and 1 mD, where $S_{gc} = 0.3$ for $k_{ik} = 0.001$ mD and $S_{gc} = 0.15$ for 1 mD, and $p = 1.7$, $q = 2$. The bounding dark gray curves illustrate a match for the data but with a constant $S_{gc} = 0.01$ and with the exponent p varying with absolute permeability and $q = 2$; e.g., $p = 2.9$ for $k_{ik} = 0.001$ mD and $p = 2$ for $k_{ik} = 1$ mD, respectively. Within the relative permeability range of most of the measured data (S_w<0.6), k_{rg} can be modeled equally well by holding S_{gc} constant and expressing $p(k)$ or setting p constant and expressing $S_{gc}(k)$. However, at $S_w > 0.6$ the variable p/constant low-S_{gc} model ($p(k)$; S_{gc}<0.05) exhibits significantly higher k_{rg} values than the constant p/variable S_{gc} model ($p \approx$ C; $S_{gc}(k)$).

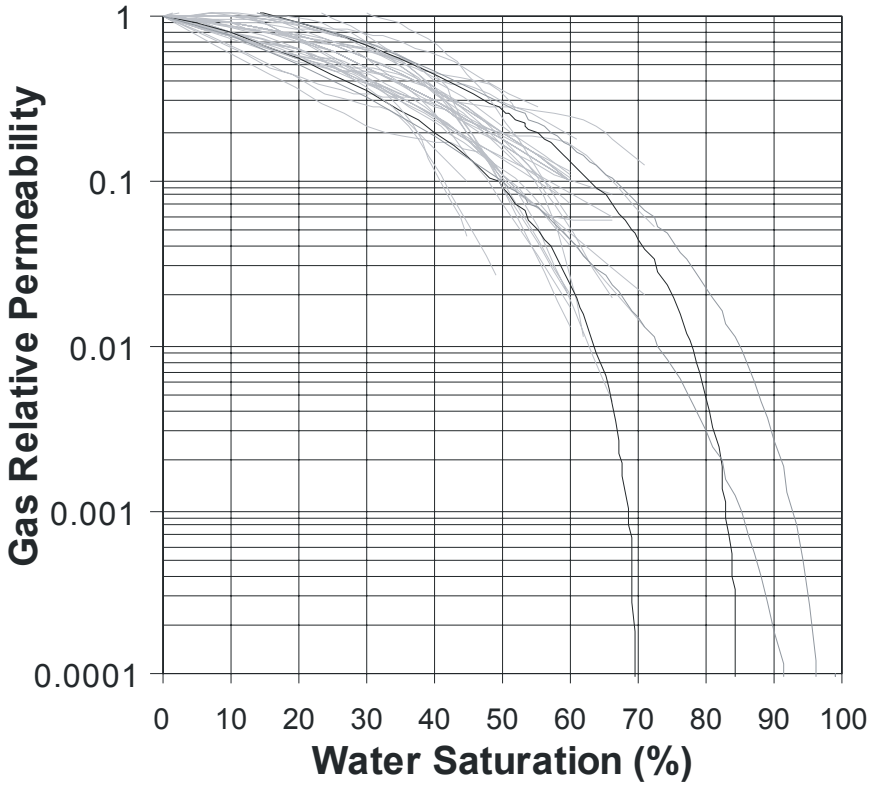

Figure 4.2.7. Relative-, gas-permeability curves (light gray) for 43 samples compiled from seven studies shown in Figure 4.2.5. The bounding black curves are the same as shown in Figure 4.2.5 and were constructed using the Equations 4.2.1–4.2.6 for rocks of 0.001 mD and 1 mD, where S_{gc} = 0.3 and 0.15 for k_{ik} = 0.001 mD and 1 mD, respectively, and p = 1.7, q = 2. The bounding dark gray curves illustrate a match for the data but with a constant S_{gc} = 0.01 and p = 2.9 for k_{ik} = 0.001mD and p = 2 for k_{ik} = 1 mD, respectively.

4.2.3.3.2 Critical-Gas Saturation

Critical-gas saturation has been defined variously as the minimum gas saturation at which the gas phase flows freely (Firoozabadi et al., 1989), the maximum gas saturation before any gas flow occurs (Moulo and Longeron, 1989), the gas saturation at which gas freely flows to the top of a reservoir (Kortekaas and Poelgeest, 1989), and the gas saturation at which gas is produced at the outlet of a core (Li and Yortsos, 1991). Li and Yortsos (1993) appropriately clarified a robust definition as the gas saturation at which the gas forms a system-spanning cluster (and consequently flows freely). This definition is consistent with the critical percolation threshold at which the gas is connected to all parts of the system and not just flowing in a subset

of the system. Using this definition, S_{gc} denotes the critical value of the pore volume fraction occupied by the gas for the formation of a system-spanning cluster.

The majority of critical-gas saturation studies have focused on modeling S_{gc} in solution gas drive oil reservoirs where gas saturation is achieved by gas nucleation resulting from pressure decline and gas bubble growth within a network of variable pore size and connectivity. Solution-gas laboratory-measured S_{gc} values have ranged from 0.006 to 0.38 (Hunt and Berry, 1956; Handy, 1958; Moulu and Longeron, 1989; Kortekaas and Poelgeest, 1989; Firoozabadi et al., 1989; Kamath and Boyer, 1993). The majority of studies report that S_{gc} increases with increasing pressure decline rate, interpreted to be due to the formation of a greater number of nucleation sites (Li and Yortsos, 1993). Sampling the Mesaverde in two closely spaced Piceance Basin wells, Chowdiah (1987) performed drainage experiments on 11 Mesaverde cores with 0.0008 mD < k_{ik} < 0.031 mD and reported 0.03 < S_{gc} < 0.11. For a low-permeability (k = 0.10 mD) Colton sandstone sample, Kamath and Boyer (1993) reported S_{gc} = 0.01 for external gas drive and S_{gc} = 0.10 for solution gas drive. In gas injection studies on a long Torpedo sandstone core with k = 413 mD, Closmann (1987) found a saturation gradient from the inlet S_g = 0.08 to the outlet (S_g = 0.02) of the core. They interpreted the low S_g = 0.02 value at the outlet end of the core as representing the critical-gas saturation. Schowalter (1979) reported results from nitrogen-water and mercury intrusion displacement tests on 10 samples of various sandstone and carbonate lithologies, ranging in permeability from 0.01 mD < k < 30.09 mD that exhibited a range of critical saturations ranging from 0.045 to 0.17.

4.2.3.3.4 Percolation Theory

Introduced by Broadbent and Hammersley (1957), the application of percolation theory has provided significant insight to the problem of critical-gas saturation and relative permeability. Using this approach, the pore system can be considered to comprise a network of pore bodies (sites) connected by pore throats (bonds) with specified size distribution for each, random distribution of the sizes in the network, and with a specified connectivity. The properties of an invading phase can be modeled either by random occupation of bonds or sites (site or bond ordinary percolation (OP), or occupation from the boundaries of the network or within the network at one or more nucleation sites by an invading phase that grows while maintaining connectivity following specified rules of occupation for how the invader-defender interface is

allowed to move (invasion percolation, IP; first introduced by Wilkinsen and Willemsen, 1983). For any network the probability that a site is occupied must equal or exceed a critical threshold value, the percolation threshold, before sufficient sites are occupied and connected to form an infinitely spanning, or system-spanning, cluster. This condition can be considered to correspond to the critical-gas saturation. Occupation fractions less than the percolation threshold do not allow gas flow across the system. It is important to note that percolation theory applies to networks with randomly distributed properties (i.e. no spatial correlation for site or bond sizes). Spatial correlations can modify the percolation threshold and consequently the critical-gas saturation. Possible implications of this are discussed below.

The physics and petroleum literature exploring percolation theory and application to porous media is extensive. Sahimi (1993, 1994) provides a comprehensive review. Berkowitz and Ewing (1998) review application to soils, and Du and Yortsos (1999) summarize work on gas bubble growth and percolation. Beyond the experimental, critical-gas saturation work cited above, studies have investigated various aspects of two-phase percolation including issues with mathematics of percolation in networks (Larson et al., 1977; Larson et al., 1981; Wall and Brown, 1981; Chandler et al., 1982; Koplik and Lasseter, 1982; Lenormand et al., 1983, 1985; Feder, 1988); invasion percolation (Wilkinsen and Willemsen, 1983), invasion under buoyant force (Wilkinson, 1984, 1986); invasion with trapping (Yanuka and Balberg, 1991); surface effects (Yortsos and Parlar, 1989; Cafiero et al., 1997); gas bubble formation, growth, and percolation as a function of fraction of nucleation sites and capillary number (Li and Yortsos, 1995a, 1995b; Du and Yortsos, 1999; Ferer et al., 2003). Using a variety of methods Lin and Cohenm (1982), Koplik et al. (1984), and Yanuka et al. (1986) estimated that average coordination numbers, Z, for sandstones range between approximately 4 and 8, indicating that a simple cubic lattice with $Z = 6$ is appropriate for representing rock pore network topology.

Gas invasion of a reservoir can be envisioned to be sufficiently slow that concentration profiles should be quasi-static similar to the stepwise increase associated with the measurement of a drainage capillary pressure curve. In this process, the invasion of gas into the water-saturated reservoir is represented by growth of a cluster(s) where gas–liquid interfaces in any gas-occupied pore advance one-at-a-time by invading perimeter pore throats in order of increasing capillary resistance (or corresponding decreasing radius). This process has been termed invasion percolation (Wilkinson and Willemsen, 1983; Feder, 1988) for invasion from

one side or point on the perimeter of a network, and is a simpler form of invasion percolation where growth occurs from multiple clusters (Yortsos and Parler, 1989).

Wilkinson and Willemsen (1983) showed that the volume fraction of the percolation threshold, equivalent to S_{gc}, scales with network dimension, L, as:

$$S_{\mathrm{gc}}(L) = \mathrm{A}\, L^{D-E} \qquad [4.2.7]$$

where A is a numerical constant, D is the mass fractal dimension of the percolation cluster (D = 1.89 for 2-D, D = 2.52 for 3-D), E is the Euclidean dimension (E = 2 for 2-D, E = 3 for 3-D). For a simple 3-D cubic network A ≈ 0.65. This relation indicates that as $L \rightarrow \infty$ $S_{gc} \rightarrow 0$ (e.g., S_{gc} = 0.215 for L = 10; S_{gc} = 0.024 for L = 1,000; S_{gc} = 0.008 for L = 10,000).

Li and Yortsos (1993, 1995a) and Du and Yortsos (1999) extended the invasion percolation work to include gas nucleation at one or more sites showing that S_{gc} scales with network size, L, and the fraction of total network sites where gas nucleation occurs, f, as

$$S_{gc}(L; fq) = \mathrm{A}\, L^{D-E} + \mathrm{B}\, f^{1-D/E} \qquad [4.2.8]$$

where A and B are numerical constants, D is the mass fractal dimension of the percolation cluster (D = 1.89 for 2-D OP, D = 1.82 for 2-D IP with trapping, D = 2.52 for 3-D OP or IP, with or without trapping), E is the Euclidean dimension (E = 2 for 2-D and E = 3 for 3-D), and f is the fraction of total network sites where gas nucleation occurs. In the limit of very small f (e.g., one nucleation site only or external drive) the second term is approximately zero and S_{gc} corresponds to the volume fraction of the percolation cluster only, as presented in Equation 4.2.7. When the nucleation fraction increases, the main contribution to S_{gc} results from clusters growing around nucleation sites and not from the percolation cluster (Du and Yortsos, 1999). For large networks the first term in Equation 8 vanishes and S_{gc} becomes primarily a function of the fraction of nucleation sites.

4.2.3.4 Critical Nonwetting Phase Saturation

Figure 4.2.8 illustrates the relationship between S_{nwc} and permeability, as measured by the inflection point on the 71 unconfined MICP curves and 54 confined MICP curves. Average unconfined $S_{nwc} = 0.026 \pm 0.028$ for rocks with $k_{ik} > 0.01$ mD and average $S_{nwc} = 0.050 \pm 0.050$ for rocks with $k_{ik} \leq 0.01$ mD (error bars represent two standard deviations). Ignoring the six confined samples with $S_{nwc} > 0.010$, confined S_{nwc} values range from 4% to 22% less than unconfined with average $S_{nwc} = 0.025 \pm 0.052$ for $k_{ik} \geq 0.01$ mD, and average $S_{nwc} = 0.039 \pm 0.050$ for $k_{ik} < 0.01$ mD. Both the unconfined and confined S_{nwc} data sets exhibit a weak increase in S_{nwc} with decreasing permeability.

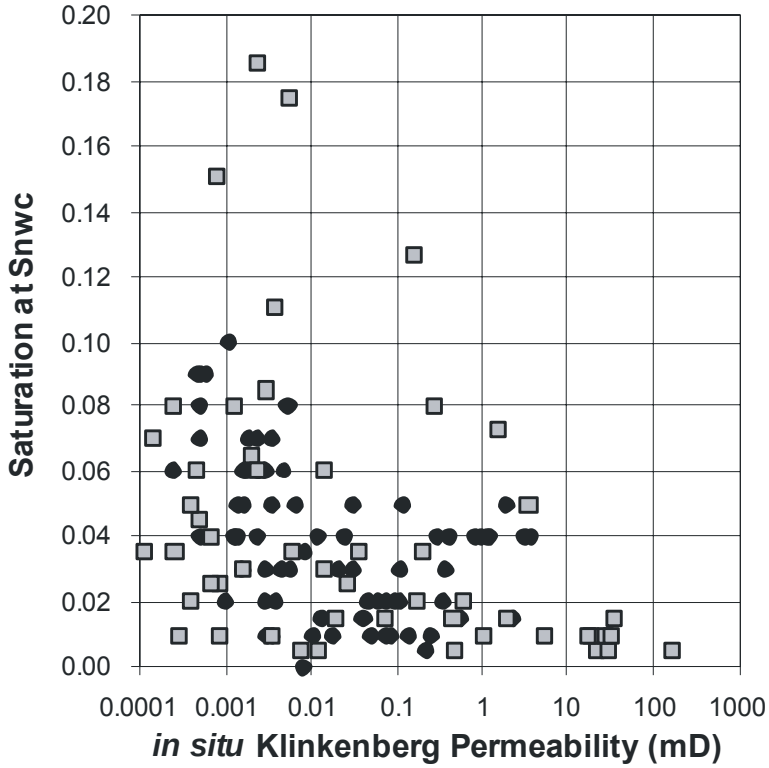

Figure 4.2.8. Critical-, mercury (nonwetting phase) saturation (S_{nwc}) versus *in situ* Klinkenberg permeability, interpreted from the inflection in the capillary-pressure curve shown in Figure 4.2.3, for unconfined (black circles) and confined (gray squares) samples. Average unconfined $S_{nwc} = 0.026 \pm 0.028$ for rocks with $k_{ik} > 0.01$ mD and average $S_{nwc} = 0.050 \pm 0.050$ for rocks with $k_{ik} \leq 0.01$ mD (error bars represent two standard deviations). Ignoring the six confined samples with $S_{nwc} > 0.010$, average confined $S_{nwc} = 0.025 \pm 0.052$ for $k_{ik} \geq 0.01$ mD, and average $S_{nwc} = 0.039 \pm 0.050$ for $k_{ik} < 0.01$ mD).

The majority of the cores that exhibit low S_{nwc} also exhibit massive, laminar, low-angle cross- and ripple-laminated bedding that provides a continuous sandstone path across the core. Six cores exhibit anomalously higher S_{nwc}. Five of these six cores are moderately shaly sandstones with convolute, discontinuous-wavy, or flaser-bedded sedimentary structures. The sixth core exhibited low-angle crossbedding.

Figure 4.2.9 compares the mercury saturations associated with resistance decreases and the inflection-interpreted S_{nwc}. For 52% of the samples, the inflection-interpreted S_{nwc} corresponds to the mercury saturation (S_{Hg}) above which electrical resistance across the core exhibits values greater than 0.15–4 x 10^6 ohms and below which resistance values are less than 5–50 ohm, a decrease of more than four to six orders of magnitude. This is interpreted to result from formation of a highly conductive continuous path of mercury through the sample. For an additional 19% of the samples, the interpreted S_{nwc} corresponded to a decrease in resistance of greater than 20%, interpreted to result from formation of a continuous mercury path of limited volume and high tortuosity. From these results it can be interpreted that for 71% of the samples, the inflection and the resistance measurements agree on the interpreted critical saturation. Within this population, average S_{nwc} = 0.042 with a maximum value of S_{nwc} = 0.175. The remaining 29% of samples did not exhibit a resistance decrease until mercury saturation increased an additional S_{Hg} = 0.03–0.29 (average S_{Hg} = 0.13), corresponding to mercury saturations of S_{Hg} = 0.04–0.44 (average S_{Hg} = 0.18). For these 29% of samples the inflection S_{nwc} is interpreted to represent "pretender" clusters in a series network and the resistance-interpreted S_{nwc} provides a measure of the sample-spanning S_{nwc}.

Within a given capillary pressure step increase, it is worthwhile to note that for almost 33% of samples the decrease in resistance did not occur at the final equilibrium saturation for a given applied capillary pressure. Rather, the resistance decrease occurred at a lower mercury saturation intermediate between the previous, lower, equilibrium saturation and the final, higher, equilibrium saturation associated with the applied capillary pressure. This implies that a backbone cluster formed at a lower saturation than the final equilibrium saturation for the applied pressure, and that subsequent saturation increase was associated with either filling of adjacent sample-spanning clusters or sites peripheral to the backbone cluster. For some samples the saturation increase between resistance decrease and capillary equilibrium was as high as S_{Hg} =

0.15. This saturation difference can also result from the application of capillary pressure steps that result in large saturation changes due to a narrow pore size distribution.

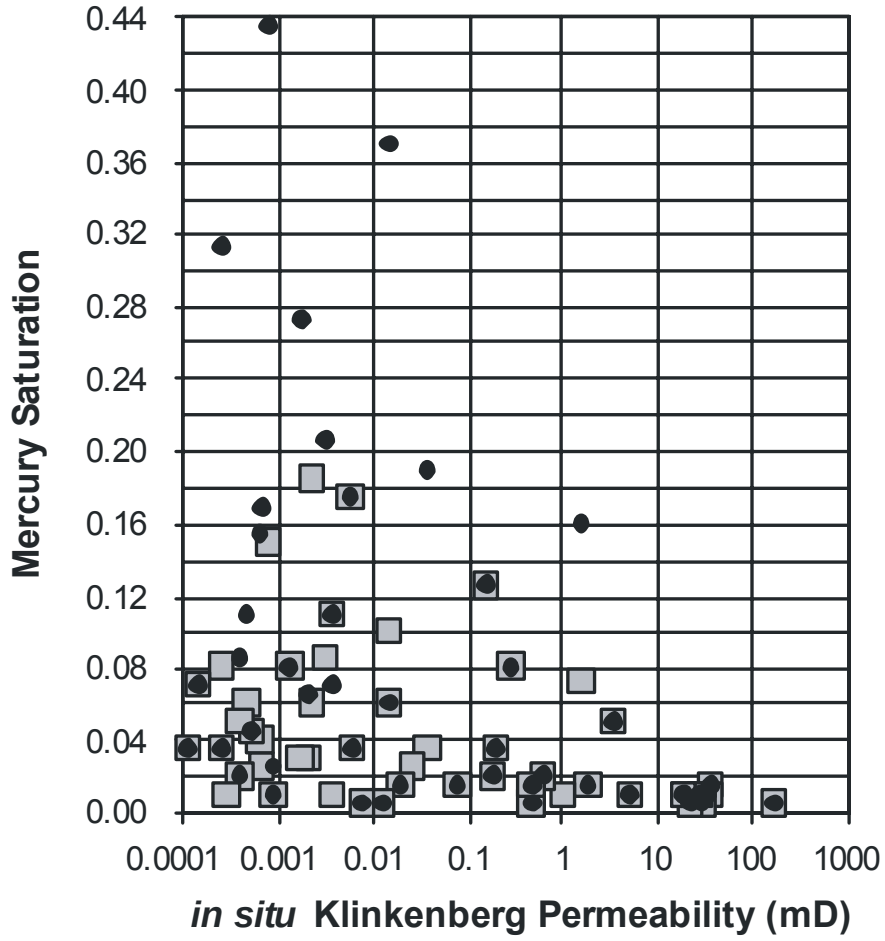

Figure 4.2.9. Crossplot of confined S_{nwc}, interpreted from the inflection in the capillary-pressure curves (gray squares), and the mercury saturations at which electrical resistance across the sample decreased by greater than 20% and for 52% of samples by more than several orders of magnitude (black circles). Inflection and resistance measures of S_{nwc} agree for 71% of samples. For remaining 29%, the inflection S_{nwc} is interpreted to represent "pretender" clusters in series network and resistance-S_{nwc} provides an accurate measure of the sample-spanning S_{nwc}.

4.2.3.5 Critical Gas Saturation

Table 4.2.1 summarizes results for air-brine critical gas saturations measurements. Figure 4.2.10 shows the distribution histogram of *in situ* air-brine critical gas saturations (S_{gc}) measured on 150 core plugs from a wide range of lithofacies of varied porosity and permeability.

Approximately 66% of the samples exhibit critical gas saturations less than $S_{gc} < 0.06$ and 84% of the samples exhibit $S_{gc} < 0.10$. These results are similar to the air-mercury critical nonwetting phase saturation values.

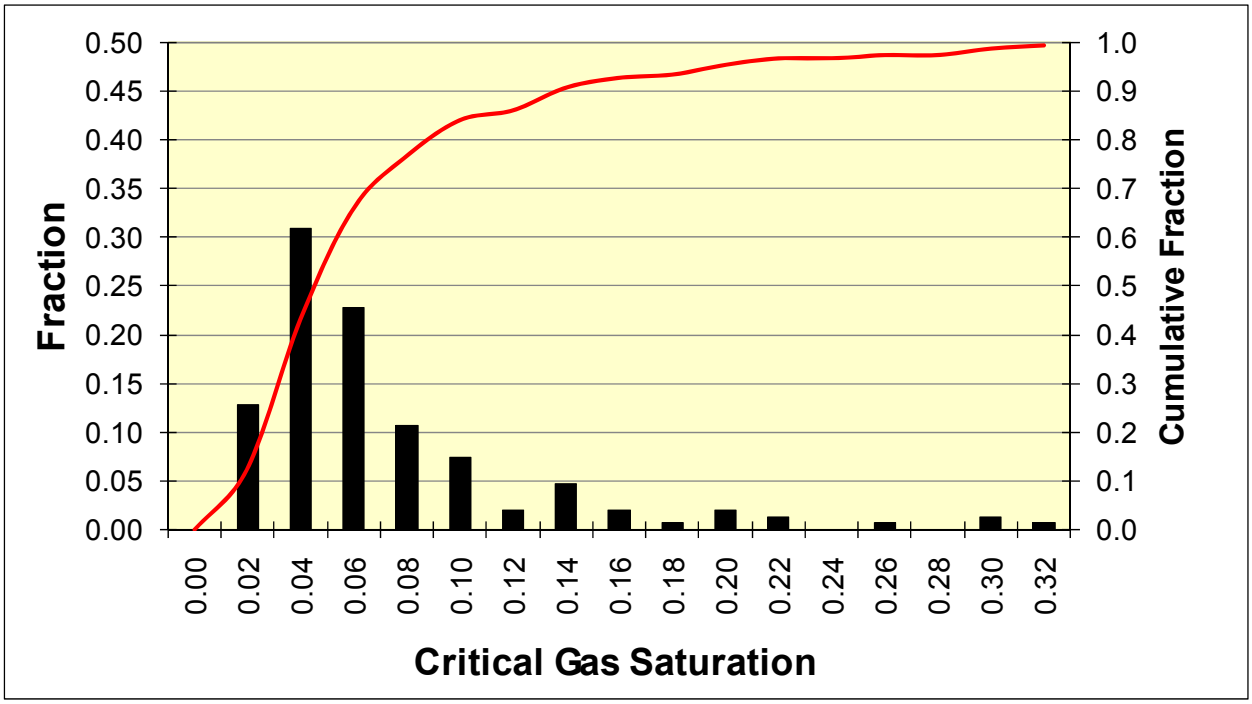

Figure 4.2.10. Distribution histogram of air-brine critical gas saturation for 150 Mesaverde core samples of widely varied lithofacies, porosity, and permeability.

Although the majority of samples exhibit low S_{gc} values, Figure 4.2.11 illustrates the relationship between S_{gc} and both permeability and primary sedimentary structure (PSS, as represented by the lithologic classification digit number 4). This figure shows that the distribution of S_{gc} values is not the same among rocks of different primary sedimentary structure and permeability.

The digital rock classification system used is discussed in more detail in Section 4.6. To represent primary sedimentary structure, the cores and plugs were classified using the following values for the fourth digit in the classification scheme:

FOURTH DIGIT: Primary sedimentary structures

1xx0x Vertical perm barriers, shale dikes, cemented vert. fractures
1xx1x Churned/bioturbated to burrow mottled (small scale)
1xx2x Convolute, slumped, large burrow mottled bedding (large scale)
1xx3x Lenticular bedded, discontinuous sand/silt lenses
1xx4x Wavy bedded, continuous sand/silt and mud layers
1xx5x Flaser bedded, discontinuous mud layers
1xx6x Small scale (< 4 cm) x-laminated, ripple x-lam, small scale hummocky x-bd
1xx7x Large scale (> 4 cm) trough or planar x-bedded
1xx8x Planar laminated or very low angle x-beds, large scale hummocky x-bd
1xx9x Massive, structureless

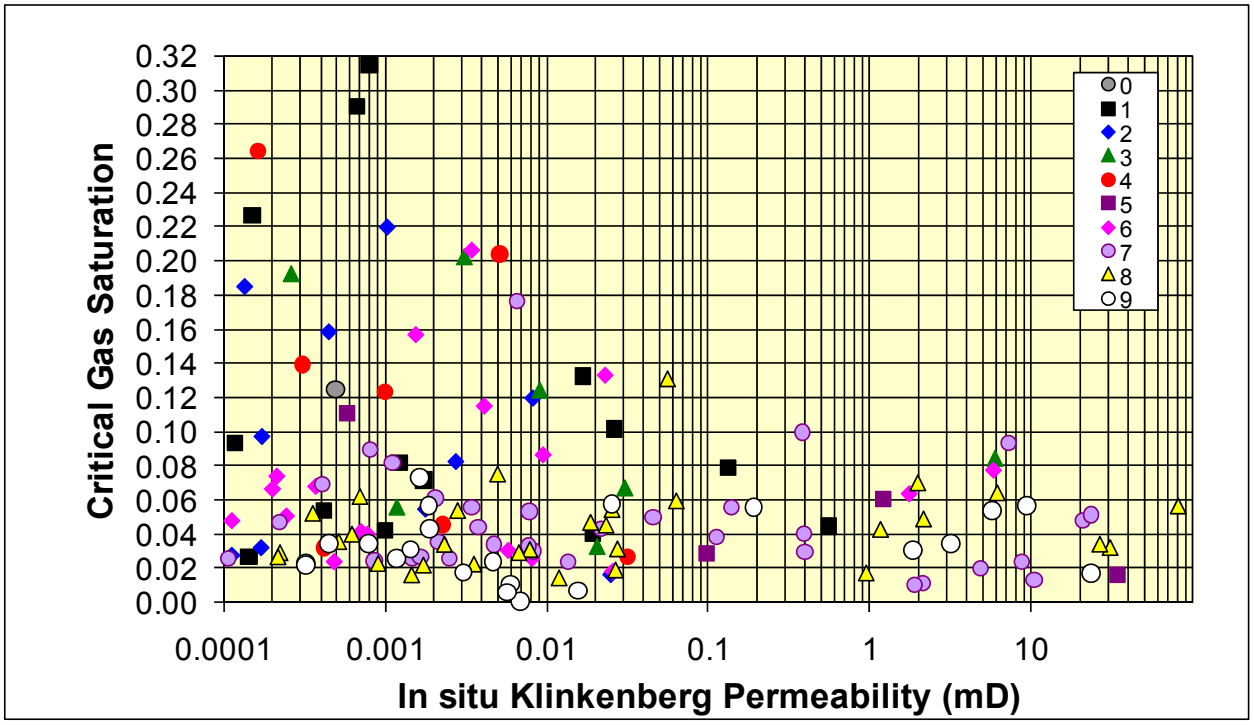

Figure 4.2.11. Crossplot of air-brine critical gas saturation versus *in situ* Klinkenberg permeability for 150 Mesaverde core samples shown parametrically with primary sedimentary structure.

Figure 4.2.11 shows that Sgc is influenced by both primary sedimentary structure and permeability. Because permeability is also dependent on primary sedimentary structure the relative influence of these two variables requires principal component analysis (PCA) . However, given the small sample population, PCA would not be quantitatively useful and the analysis here is more semi-quantitative. Although it is highly dependent on the distribution of permeabilities of

the samples measured in each PSS class, in general, average S_{gc} increases with decreasing PSS RC4 value (e.g., RC4 = 9 decreasing to RC4 = 0): $S_{gc9} = 0.032$, $S_{gc8} = 0.043$, $S_{gc7} = 0.047$, $S_{gc6} = 0.070$, $S_{gc5} = 0.055$, $S_{gc4} = 0.119$, $S_{gc3} = 0.109$, $S_{gc2} = 0.100$, $S_{gc1} = 0.1150$, $S_{gc0} = 0.125$. Over 90% of all large-scale trough and planar crossbedded, planar laminated, and massive bedded sandstones and siltstones (1xx7x $\leq$ RC4 $\leq$ 1xx9x) of any permeability exhibit $S_{gc} < 0.06$. Sandstones with small-scale cross-laminated and ripple-cross-laminated bedding exhibit both low S_{gc} (i.e. $S_{gc} < 0.08$) but exhibit $0.08 < S_{gc} < 0.22$ for rocks with $k_{ik} < 0.01$ mD. With increasing complexity of sedimentary structures that lead to baffles or restriction to flow along the axis of the core (and in the direction of gas movement for breakthrough), rocks with primary sedimentary structure digital classification values less than 5 (i.e., 1xx0x $\leq$ RC4 $\leq$ 1xx5x) each exhibit a general pattern of increasing S_{gc} with decreasing permeability. Critical gas saturation values for all the rocks with 1xx0x $\leq$ RC4 $\leq$ 1xx5x range widely from low to high values. This wide range is interpreted to be the result of the highly variable nature of the exact structure of the bedding perpendicular to flow. Rock with a PSS that is very highly churned and bioturbated can exhibit properties similar to massive-bedded rock or can have convolute but continuous beds that span the sample length. Both of these rock types would exhibit low S_{gc}.

Summary of Critical Gas Saturation Results
Analysis of Critical Permeability, Capillary Pressure, and Electrical Properties for Mesaverde Tight Gas Sandstones from Western U.S. Basins
US DOE # DE-FC26-05NT42660
Alan P. Byrnes, Robert M. Cluff, John C. Webb, Daniel A. Krygowski, Stefani D. Whittaker
website: http://www.kgs.ku.edu/mesaverde

USGS Library Number	Basin	API Number	Well Name	Operator	State	Township	Range	Sec	Quarter Section	Plug Depth ft	A/ B/ C	Routine Porosity %	*in situ* Klinkenberg Gas Permeability mD	*in situ* Porosity %	*in situ* Critical Gas Saturation %	Threshold pressure at Sgc (psig)
B029	Green River	4903520088	A-1 WASP	INEXCO OIL COMPANY	WY	36N	112W	28	NWNESW	10573.1	B	3.1	0.000201	2.6	6.7	550
B029	Green River	4903520088	A-1 WASP	INEXCO OIL COMPANY	WY	36N	112W	28	NWNESW	11443.7	A	2.8	0.000322	2.4	2.3	380
B029	Green River	4903520088	A-1 WASP	INEXCO OIL COMPANY	WY	36N	112W	28	NWNESW	11447.8	A	4.8	0.001634	4.2	7.3	200
B029	Green River	4903520088	A-1 WASP	INEXCO OIL COMPANY	WY	36N	112W	28	NWNESW	11457.8	A	4.4	0.002707	3.7	8.3	220
B029	Green River	4903520088	A-1 WASP	INEXCO OIL COMPANY	WY	36N	112W	28	NWNESW	11457.9	A	5.5	0.000110	4.8	2.8	600
B029	Green River	4903520088	A-1 WASP	INEXCO OIL COMPANY	WY	36N	112W	28	NWNESW	11459.2	A	4.5	0.001844	3.8	5.7	150
B029	Green River	4903520088	A-1 WASP	INEXCO OIL COMPANY	WY	36N	112W	28	NWNESW	11460.6	A	4.3	0.015529	3.6	0.7	70
B029	Green River	4903520088	A-1 WASP	INEXCO OIL COMPANY	WY	36N	112W	28	NWNESW	11609.1	A	5.8	0.007724	5.2	5.3	140
B029	Green River	4903520088	A-1 WASP	INEXCO OIL COMPANY	WY	36N	112W	28	NWNESW	11706.9	A	3.8	0.000405	3.2	6.9	340
B029	Green River	4903520088	A-1 WASP	INEXCO OIL COMPANY	WY	36N	112W	28	NWNESW	11721.9	A	4.3	0.000320	3.7	2.3	340
B029	Green River	4903520088	A-1 WASP	INEXCO OIL COMPANY	WY	36N	112W	28	NWNESW	11722.0	A	4.3	0.000447	3.7	3.5	340
E712	Green River	4903506020	B-54 BIG PINEY	BELCO PETROLEUM	WY	29N	113W	26	SESENE	3403.9	A	16.7	1.198236	15.9	6.1	40
E712	Green River	4903506020	B-54 BIG PINEY	BELCO PETROLEUM	WY	29N	113W	26	SESENE	3462.0	A	18.8	26.795410	18.1	3.4	4
E712	Green River	4903506020	B-54 BIG PINEY	BELCO PETROLEUM	WY	29N	113W	26	SESENE	3480.8	A	8.8	0.005797	8.0	3.1	110
E712	Green River	4903506020	B-54 BIG PINEY	BELCO PETROLEUM	WY	29N	113W	26	SESENE	3503.7	B	8.8	0.000792	8.0	31.5	220
E712	Green River	4903506020	B-54 BIG PINEY	BELCO PETROLEUM	WY	29N	113W	26	SESENE	3519.3	B	16.1	6.019506	15.2	8.5	10
E894	Green River	4903520822	1 OLD ROAD	AMERICAN HUNTER EXPL	WY	27N	108W	27	SENWSE	11897.3	A	5.2	0.000995	4.4	12.3	260
E894	Green River	4903520822	1 OLD ROAD	AMERICAN HUNTER EXPL	WY	27N	108W	27	SENWSE	11956.1	A	8.5	0.007916	7.7	3.1	80
R780	Green River	4903505742	C-47 TIP TOP SHALLOW	BELCO PETROLEUM	WY	28N	113W	22	SWNE	2754.7	A	21.3	1.900607	20.5	1.0	15
R780	Green River	4903505742	C-47 TIP TOP SHALLOW	BELCO PETROLEUM	WY	28N	113W	22	SWNE	2783.3	A	22.3	23.284897	21.5	1.8	4
R780	Green River	4903505742	C-47 TIP TOP SHALLOW	BELCO PETROLEUM	WY	28N	113W	22	SWNE	2817.7	A	20.1	2.123074	19.3	1.1	10
R780	Green River	4903505742	C-47 TIP TOP SHALLOW	BELCO PETROLEUM	WY	28N	113W	22	SWNE	2845.5	A	22.6	8.693646	22.0	2.4	10
S873	Green River	4903506200	K-2 MASON	BELCO PETROLEUM	WY	31N	113W	13	SESE	6989.8	A	10.7	0.138347	9.8	5.6	30
S873	Green River	4903506200	K-2 MASON	BELCO PETROLEUM	WY	31N	113W	13	SESE	9397.3	A	8.4	0.000358	7.6	5.2	340
SHV	Green River	4903523799	VIBLE 1D-11D	SHELL E&P	WY	31N	109W	11	SENE	12507.1	A	5.1	0.000627	4.4	4.0	300
SHV	Green River	4903523799	VIBLE 1D-11D	SHELL E&P	WY	31N	109W	11	SENE	12508.7	A	3.0	0.000219	2.5	4.7	460
SHV	Green River	4903523799	VIBLE 1D-11D	SHELL E&P	WY	31N	109W	11	SENE	12518.5	A	5.9	0.001720	5.2	7.2	280
T195	Green River	4903508024	5 PINEDALE	EL PASO NATURAL GAS	WY	30N	108W	5		12158.5	A	11.0	0.016716	10.2	13.3	60
T195	Green River	4903508024	5 PINEDALE	EL PASO NATURAL GAS	WY	30N	108W	5		12162.0	A	7.2	0.000796	6.4	8.9	260
T203	Green River	4903705405	1 CHIMNEY ROCK	MOUNTAIN FUEL SUPPLY	WY	18N	102W	12	SESW	6741.0	A	14.3	81.918992	13.5	5.7	4
T204	Green River	4903705349	B-2A SPIDER CREEK	HUMBLE OIL & REF	WY	18N	110W	27	NESW	9041.1	A	11.6	1.820888	10.7	3.1	10
T204	Green River	4903705349	B-2A SPIDER CREEK	HUMBLE OIL & REF	WY	18N	110W	27	NESW	9063.0	A	15.2	206.013238	14.3	1.9	2
T204	Green River	4903705349	B-2A SPIDER CREEK	HUMBLE OIL & REF	WY	18N	110W	27	NESW	9098.0	A	6.6	0.018831	5.9	4.7	60
E437	Piceance	0504506578	MV 24-20 CHEVRON	BARRETT ENERGY	CO	6S	96W	20	SENW	6579.5	A	7.5	0.000441	6.7	15.9	440
E437	Piceance	0504506578	MV 24-20 CHEVRON	BARRETT ENERGY	CO	6S	96W	20	SENW	6591.9	A	2.4	0.000711	2.0	4.2	380
E437	Piceance	0504506578	MV 24-20 CHEVRON	BARRETT ENERGY	CO	6S	96W	20	SENW	6592.5	A	2.6	0.000163	2.0	26.4	340
B43C	Piceance	0504511402	LAST DANCE 43C-3-792	BILL BARRETT CORP.	CO	7S	92W	3	NESE	3544.8	C	10.5	0.392302	9.6	4.0	24
B43C	Piceance	0504511402	LAST DANCE 43C-3-792	BILL BARRETT CORP.	CO	7S	92W	3	NESE	3992.5	C	2.9	0.000576	2.4	11.1	320
B43C	Piceance	0504511402	LAST DANCE 43C-3-792	BILL BARRETT CORP.	CO	7S	92W	3	NESE	4013.3	B	12.9	0.189783	12.0	5.6	18
B43C	Piceance	0504511402	LAST DANCE 43C-3-792	BILL BARRETT CORP.	CO	7S	92W	3	NESE	4393.6	A	8.7	0.006524	7.9	17.6	120
E458	Piceance	0510309406	M-30-2-96W /D-037934	FUEL RESOURCES DEV	CO	2N	96W	30	SWSW	6379.5	A	3.8	0.000303	3.3	13.9	429
E458	Piceance	0510309406	M-30-2-96W /D-037934	FUEL RESOURCES DEV	CO	2N	96W	30	SWSW	6509.4	A	10.7	0.026856	9.9	1.9	70
PA424	Piceance	0504510927	Williams PA-424-34	WILLIAMS E&P	CO	6S	95W	34	NWSWSE	4600.3	A	12.2	0.001876	11.3	4.3	200
PA424	Piceance	0504510927	Williams PA-424-34	WILLIAMS E&P	CO	6S	95W	34	NWSWSE	4651.6	A	6.7	0.013426	6.0	2.4	80
PA424	Piceance	0504510927	Williams PA-424-34	WILLIAMS E&P	CO	6S	95W	34	NWSWSE	4660.4	A	7.0	0.003568	6.1	2.3	150
PA424	Piceance	0504510927	Williams PA-424-34	WILLIAMS E&P	CO	6S	95W	34	NWSWSE	4691.5	A	13.3	0.006865	12.5	0.1	100
PA424	Piceance	0504510927	Williams PA-424-34	WILLIAMS E&P	CO	6S	95W	34	NWSWSE	5140.5	A	11.6	0.025086	10.8	5.8	60
PA424	Piceance	0504510927	Williams PA-424-34	WILLIAMS E&P	CO	6S	95W	34	NWSWSE	6148.6	A	9.9	0.007606	9.1	3.3	110
PA424	Piceance	0504510927	Williams PA-424-34	WILLIAMS E&P	CO	6S	95W	34	NWSWSE	6599.5	A	7.8	0.001551	7.0	15.7	300
PA424	Piceance	0504510927	Williams PA-424-34	WILLIAMS E&P	CO	6S	95W	34	NWSWSE	6632.8	A	3.5	0.005072	2.9	20.4	220
R091	Piceance	05045XXXX4	BOOK CLIFFS 1	USGS-CG	CO	7S	104W	17	NESW	255.8	A	24.9	112.214149	24.3	0.9	2
R091	Piceance	05045XXXX4	BOOK CLIFFS 1	USGS-CG	CO	7S	104W	17	NESW	296.9	A	4.9	0.000168	4.2	3.3	340
R091	Piceance	05045XXXX4	BOOK CLIFFS 1	USGS-CG	CO	7S	104W	17	NESW	387.3	A	9.8	0.000985	8.8	4.3	300
R091	Piceance	05045XXXX4	BOOK CLIFFS 1	USGS-CG	CO	7S	104W	17	NESW	512.2	A	10.6	0.009037	9.7	12.4	90
S905	Piceance	05103XXXX3	21011-5 MOON LAKE	WESTERN FUELS ASSOC	CO	2N	101W	1	NESW	812.9	A	17.0	20.889012	16.2	4.8	6
S905	Piceance	05103XXXX3	21011-5 MOON LAKE	WESTERN FUELS ASSOC	CO	2N	101W	1	NESW	816.5	A	10.6	0.020497	9.8	3.3	50
S905	Piceance	05103XXXX3	21011-5 MOON LAKE	WESTERN FUELS ASSOC	CO	2N	101W	1	NESW	817.8	A	8.7	0.001175	7.9	5.6	200
T63X-2G	Piceance	0510310391	T63X-2G	EXXON-MOBIL	CO	3S	97W	2	NESWNE	10572.9	B	4.3	0.000214	3.7	7.4	480
T63X-2G	Piceance	0510310391	T63X-2G	EXXON-MOBIL	CO	3S	97W	2	NESWNE	10615.6	A	6.1	0.001754	5.3	5.5	340
T63X-2G	Piceance	0510310391	T63X-2G	EXXON-MOBIL	CO	3S	97W	2	NESWNE	10619.7	A	7.3	0.002467	6.5	2.6	180
T649	Piceance	0504560011	MWX-2	CER CORPORATION	CO	6S	94W	34	SESWNW	5734.1	A	8.7	0.004707	7.9	3.4	130
T649	Piceance	0504560011	MWX-2	CER CORPORATION	CO	6S	94W	34	SESWNW	5838.7	A	6.6	0.001456	5.8	2.6	260
T649	Piceance	0504560011	MWX-2	CER CORPORATION	CO	6S	94W	34	SESWNW	7124.7	A	11.1	0.003447	10.2	20.6	130
T649	Piceance	0504560011	MWX-2	CER CORPORATION	CO	6S	94W	34	SESWNW	7272.8	A	8.9	0.002340	8.1	3.4	150
T649	Piceance	0504560011	MWX-2	CER CORPORATION	CO	6S	94W	34	SESWNW	7276.2	A	8.4	0.001734	7.5	2.2	130
T649	Piceance	0504560011	MWX-2	CER CORPORATION	CO	6S	94W	34	SESWNW	7340.4	A	2.1	0.000106	1.7	2.6	600
T649	Piceance	0504560011	MWX-2	CER CORPORATION	CO	6S	94W	34	SESWNW	7350.4	A	4.5	0.000372	3.8	6.8	420
T649	Piceance	0504560011	MWX-2	CER CORPORATION	CO	6S	94W	34	SESWNW	7877.5	A	7.6	0.000910	6.9	2.3	200
T649	Piceance	0504560011	MWX-2	CER CORPORATION	CO	6S	94W	34	SESWNW	8117.9	A	6.5	0.002272	5.8	4.6	160
E393	Powder River	4900525627	1 BARLOW 21-20	LOUISIANA LAND & EXP	WY	48N	75W	20	NENW	6969.7	B	20.7	1.175542	20.0	4.3	15
E393	Powder River	4900525627	1 BARLOW 21-20	LOUISIANA LAND & EXP	WY	48N	75W	20	NENW	6996.0	A	5.9	0.001431	5.3	3.2	220
E393	Powder River	4900525627	1 BARLOW 21-20	LOUISIANA LAND & EXP	WY	48N	75W	20	NENW	7000.9	B	17.3	31.026357	16.6	3.2	3
E393	Powder River	4900525627	1 BARLOW 21-20	LOUISIANA LAND & EXP	WY	48N	75W	20	NENW	7039.2	B	17.1	6.208784	16.2	6.4	10
E393	Powder River	4900525627	1 BARLOW 21-20	LOUISIANA LAND & EXP	WY	48N	75W	20	NENW	7060.4	A	14.5	0.056370	13.7	13.1	40
E932	Powder River	4900921513	2 FRED STATE	DAVIS OIL COMPANY	WY	35N	70W	36	NESESW	7544.3	A	16.4	3.133322	15.6	3.5	8
E932	Powder River	4900921513	2 FRED STATE	DAVIS OIL COMPANY	WY	35N	70W	36	NESESW	7546.9	A	10.5	0.019167	9.7	4.1	140
E932	Powder River	4900921513	2 FRED STATE	DAVIS OIL COMPANY	WY	35N	70W	36	NESESW	7579.1	B	16.9	0.005629	16.2	0.7	130
S835	Powder River	4900906335	2 SHAWNEE	BELCO PETROLEUM	WY	33N	69W	23	NENW	6979.0	A	16.6	0.958439	15.7	1.7	18
S838	Powder River	4900905481	3 SHAWNEE	BELCO PETROLEUM	WY	33N	69W	23	C SENE	6946.2	A	14.3	2.170747	13.4	4.9	10
S838	Powder River	4900905481	3 SHAWNEE	BELCO PETROLEUM	WY	33N	69W	23	C SENE	6956.2	B	15.3	0.557633	14.5	4.5	20
S838	Powder River	4900905481	3 SHAWNEE	BELCO PETROLEUM	WY	33N	69W	23	C SENE	6998.5	A	5.8	0.001210	5.1	8.2	260
T715	Sand Wash	0508106724	1-791-0513 Craig Dome	COCKRELL OIL CORP	CO	7N	91W	28	NESESW	3487.4	A	17.5	23.375258	16.6	5.1	3
T717	Sand Wash	0508106718	1-691-0513 West Craig	COCKRELL OIL CORP	CO	6N	91W	5	SESWSW	1733.0	A	5.8	0.024733	5.1	1.7	40
T717	Sand Wash	0508106718	1-691-0513 West Craig	COCKRELL OIL CORP	CO	6N	91W	5	SESWSW	1733.0	B	17.9	0.001016	17.1	22.0	260
B646	Uinta	4304730584	11-17F RIVER BEND UNIT	MAPCO INCOPORATED	UT	10S	20E	17	SENENW	8233.0	B	5.8	0.004637	5.1	2.4	150
B646	Uinta	4304730584	11-17F RIVER BEND UNIT	MAPCO INCOPORATED	UT	10S	20E	17	SENENW	8245.1	A	2.6	0.000781	2.1	3.5	280
B646	Uinta	4304730584	11-17F RIVER BEND UNIT	MAPCO INCOPORATED	UT	10S	20E	17	SENENW	8287.4	B	7.5	0.021744	6.8	4.3	50
B646	Uinta	4304730584	11-17F RIVER BEND UNIT	MAPCO INCOPORATED	UT	10S	20E	17	SENENW	8302.5	A	1.0	0.000112	0.6	4.8	600
E946	Uinta	4304730545	2-7 FLAT MESA	ENSERCH EXPLORATION	UT	10S	23E	7	NESENW	6352.1	A	7.3	0.001099	6.5	6.2	240
E946	Uinta	4304730545	2-7 FLAT MESA	ENSERCH EXPLORATION	UT	10S	23E	7	NESENW	6468.5	A	11.9	0.381945	11.1	10.0	20
E946	Uinta	4304730545	2-7 FLAT MESA	ENSERCH EXPLORATION	UT	10S	23E	7	NESENW	6472.7	A	9.0	0.045374	8.2	5.0	50
E946	Uinta	4304730545	2-7 FLAT MESA	ENSERCH EXPLORATION	UT	10S	23E	7	NESENW	6508.2	A	3.1	0.000484	2.6	2.4	340
E946	Uinta	4304730545	2-7 FLAT MESA	ENSERCH EXPLORATION	UT	10S	23E	7	NESENW	6515.5	A	16.3	1.997454	15.5	7.0	10
E946	Uinta	4304730545	2-7 FLAT MESA	ENSERCH EXPLORATION	UT	10S	23E	7	NESENW	6530.2	A	9.8	0.023465	8.9	4.5	50
E946	Uinta	4304730545	2-7 FLAT MESA	ENSERCH EXPLORATION	UT	10S	23E	7	NESENW	6530.4	A	9.9	0.063938	9.1	6.0	40
E946	Uinta	4304730545	2-7 FLAT MESA	ENSERCH EXPLORATION	UT	10S	23E	7	NESENW	6709.8	A	2.2	0.000117	1.7	9.4	600
E946	Uinta	4304730545	2-7 FLAT MESA	ENSERCH EXPLORATION	UT	10S	23E	7	NESENW	7287.1	A	5.6	0.001467	4.9	1.6	240
E946	Uinta	4304730545	2-7 FLAT MESA	ENSERCH EXPLORATION	UT	10S	23E	7	NESENW	7293.5	A	3.8	0.000490	3.3	12.5	500
E946	Uinta	4304730545	2-7 FLAT MESA	ENSERCH EXPLORATION	UT	10S	23E	7	NESENW	7312.7	A	7.8	0.003034	7.0	1.8	150
E946	Uinta	4304730545	2-7 FLAT MESA	ENSERCH EXPLORATION	UT	10S	23E	7	NESENW	7314.3	A	5.8	0.004122	5.0	11.5	140
E946	Uinta	4304730545	2-7 FLAT MESA	ENSERCH EXPLORATION	UT	10S	23E	7	NESENW	7671.1	A	4.8	0.097314	4.2	2.9	24
E946	Uinta	4304730545	2-7 FLAT MESA	ENSERCH EXPLORATION	UT	10S	23E	7	NESENW	7689.7	A	7.4	0.003743	6.5	4.4	120
E946	Uinta	4304730545	2-7 FLAT MESA	ENSERCH EXPLORATION	UT	10S	23E	7	NESENW	7885.4	A	9.8	0.025778	9.0	1.9	60
KM36O	Uinta	4304735788	NBU 9-20-36O State	KERR-MCGEE OIL&GAS ONSHORE	UT	9S	20E	36	SESE	8218.5	A	5.8	0.001167	5.0	2.6	320
KM36O	Uinta	4304735788	NBU 9-20-36O State	KERR-MCGEE OIL&GAS ONSHORE	UT	9S	20E	36	SESE	8234.4	A	8.7	0.003403	7.9	5.6	150
KM36O	Uinta	4304735788	NBU 9-20-36O State	KERR-MCGEE OIL&GAS ONSHORE	UT	9S	20E	36	SESE	8234.6	B	9.1	0.098252	8.4	3.0	90
R829	Uinta	4304730852	4-5 US LAMCO	ENSERCH EXPLORATION	UT	13S	20E	5	C SW	5621.2	A	10.4	0.393697	9.5	2.9	24
R829	Uinta	4304730852	4-5 US LAMCO	ENSERCH EXPLORATION	UT	13S	20E	5	C SW	5626.2	A	12.5	7.192303	11.7	9.3	8
R999	Uinta	4304730860	3-24 US LAMCO	CHAMPLIN PETROLEUM	UT	13S	20E	24	NESE	7158.9	B	2.7	0.000149	2.2	22.7	480
S172	Uinta	43019XXXX1	3 BOOK CLIFFS	USGS-CG	UT	17S	24E	3	SE	174.0	A	7.0	0.000416	6.3	5.4	380
S172	Uinta	43019XXXX1	3 BOOK CLIFFS	USGS-CG	UT	17S	24E	3	SE	175.2	A	19.9	33.989674	19.2	1.7	5
S172	Uinta	43019XXXX1	3 BOOK CLIFFS	USGS-CG	UT	17S	24E	3	SE	252.1	A	14.9	0.132551	14.1	7.9	40
S172	Uinta	43019XXXX1	3 BOOK CLIFFS	USGS-CG	UT	17S	24E	3	SE	334.5	A	3.6	0.000142	3.1	2.8	550
S174	Uinta	43019XXXX2	4 BOOK CLIFFS	USGS-CG	UT	17S	24E	31	NWSW	161.7	A	12.1	0.031330	11.3	2.7	24
S174	Uinta	43019XXXX2	4 BOOK CLIFFS	USGS-CG	UT	17S	24E	31	NWSW	183.4	A	9.8	0.111533	9.0	3.8	30
S174	Uinta	43019XXXX2	4 BOOK CLIFFS	USGS-CG	UT	17S	24E	31	NWSW	189.2	A	21.0	5.654409	20.3	5.4	6
S174	Uinta	43019XXXX2	4 BOOK CLIFFS	USGS-CG	UT	17S	24E	31	NWSW	189.2	B	22.2	9.305694	21.5	5.7	8
DR3	Washakie	4903722304	3 DRIPPING ROCK	CELSIUS	WY	14N	94W	8	SESWNW	12415.1	A	14.1	0.027608	13.3	3.2	60
DR3	Washakie	4903722304	3 DRIPPING ROCK	CELSIUS	WY	14N	94W	8	SESWNW	12420.2	A	7.5	0.000418	6.8	3.2	300
DR3	Washakie	4903722304	3 DRIPPING ROCK	CELSIUS	WY	14N	94W	8	SESWNW	12428.1	A	12.0	0.004999	11.2	7.5	80
DR5	Washakie	4903722355	5 DRIPPING ROCK	CELSIUS	WY	14N	94W	19	SESWNE	12686.7	A	12.8	0.012012	11.9	1.4	70
DR5	Washakie	4903722355	5 DRIPPING ROCK	CELSIUS	WY	14N	94W	19	SESWNE	12704.2	B	10.6	0.002825	9.8	5.4	160
E489	Washakie	4903721053	3 UNIT FIVE MILE GULCH	AMOCO PRODUCTION	WY	21N	93W	35	C SW	10615.6	A	11.0	0.008138	10.2	12.0	140
E489	Washakie	4903721053	3 UNIT FIVE MILE GULCH	AMOCO PRODUCTION	WY	21N	93W	35	C SW	10668.9	A	6.7	0.002028	6.0	6.1	180
E489	Washakie	4903721053	3 UNIT FIVE MILE GULCH	AMOCO PRODUCTION	WY	21N	93W	35	C SW	10675.8	A	10.1	0.025526	9.2	5.5	70
S231	Washakie	4903721075	1 CHAMPLIN 237 AMOCO C	AMOCO PRODUCTION	WY	17N	94W	5	SWNESW	11110.1	A	4.3	0.000170	3.6	9.8	360
S231	Washakie	4903721075	1 CHAMPLIN 237 AMOCO C	AMOCO PRODUCTION	WY	17N	94W	5	SWNESW	11202.6	B	4.0	0.000846	3.4	2.4	260
S265	Washakie	4903720033	102-7-10 ARCH UNIT	ANADARKO E&P CO. LP	WY	19N	98W	7	SWSW	4889.0	C	17.7	10.448296	16.9	1.3	5
S265	Washakie	4903720033	102-7-10 ARCH UNIT	ANADARKO E&P CO. LP	WY	19N	98W	7	SWSW	4890.0	B	8.9	0.008143	8.0	2.6	90
S276	Washakie	4903705683	65-1-7 ARCH UNIT	FOREST OIL CORP	WY	19N	99W	1	NWSE	4729.0	A	12.2	0.026052	11.3	10.2	70
S276	Washakie	4903705683	65-1-7 ARCH UNIT	FOREST OIL CORP	WY	19N	99W	1	NWSE	4736.2	A	17.3	4.874144	16.5	2.0	15
S276	Washakie	4903705683	65-1-7 ARCH UNIT	FOREST OIL CORP	WY	19N	99W	1	NWSE	4756.9	A	8.5	0.003079	7.8	20.2	240
S276	Washakie	4903705683	65-1-7 ARCH UNIT	FOREST OIL CORP	WY	19N	99W	1	NWSE	4761.0	A	7.6	0.000260	6.8	19.2	460
T592	Washakie	4900721170	C-1T FEE	FUEL RESOURCES DEV	WY	12N	90W	11	NENW	2340.7	A	13.5	0.030472	12.7	6.7	80
T595	Washakie	4903723956	5-2 SIBERIA RIDGE	AMOCO PRODUCTION	WY	21N	94W	5	SW	10651.9	A	10.1	0.006773	9.2	2.9	110
WLDR	Washakie	9999999999	WILD ROSE 1	N/A	WY	N/A	N/A	N/A	N/A	10015.6	A	5.3	0.000779	4.7	4.0	340
WLDR	Washakie	9999999999	WILD ROSE 1	N/A	WY	N/A	N/A	N/A	N/A	10204.8	A	6.8	0.023128	8.0	13.3	50
B049	Wind River	4901320724	31-22 TRIBAL PHILLIPS	BROWN TOM INC	WY	4N	3E	31	NWSENW	9072.2	A	12.4	5.885782	11.5	7.4	9
B049	Wind River	4901320724	31-22 TRIBAL PHILLIPS	BROWN TOM INC	WY	4N	3E	31	NWSENW	9081.0	A	11.4	1.770554	10.6	6.4	8
B049	Wind River	4901320724	31-22 TRIBAL PHILLIPS	BROWN TOM INC	WY	4N	3E	31	NWSENW	11698.9	A	1.0	0.000133	0.7	18.5	600
C233	Wind River	4901320786	1-9 LYSITE	MICH WISC PIPELINE	WY	38N	91W	9	SWNE	8183.5	B	5.1	0.000245	4.4	5.1	460
C233	Wind River	4901320786	1-9 LYSITE	MICH WISC PIPELINE	WY	38N	91W	9	SWNE	8616.1	A	12.9	0.009541	12.1	5.7	90
C233	Wind River	4901320786	1-9 LYSITE	MICH WISC PIPELINE	WY	38N	91W	9	SWNE	8619.2	B	6.9	0.001643	6.1	2.7	160
C233	Wind River	4901320786	1-9 LYSITE	MICH WISC PIPELINE	WY	38N	91W	9	SWNE	11927.2	A	9.9	0.005937	9.1	1.1	100
C899	Wind River	4901320836	1-27 LOOKOUT	MONSANTO OIL	WY	39N	91W	27	CSWNE	16565.1	A	2.8	0.000224	2.2	2.9	420
C899	Wind River	4901320966	1-27 LOOKOUT	MONSANTO OIL	WY	39N	91W	27	CSWNE	16706.8	A	5.6	0.000518	4.8	3.6	260
C899	Wind River	4901320836	1-27 LOOKOUT	MONSANTO OIL	WY	39N	91W	27	CSWNE	16723.9	A	5.2	0.000702	4.5	6.2	260
D031	Wind River	4901320966	CHEVRON 2-1	MONSANTO OIL	WY	38N	91W	1	SWNENW	15681.1	A	9.9	0.002119	9.1	3.5	200
D031	Wind River	4901320966	CHEVRON 2-1	MONSANTO OIL	WY	38N	91W	1	SWNENW	15702.1	A	6.9	0.000669	6.1	29.0	320
D031	Wind River	4901320966	CHEVRON 2-1	MONSANTO OIL	WY	38N	91W	1	SWNENW	15750.1	A	4.1	0.000218	3.6	2.7	380

Table 4.2.2. Summary of air-brine critical gas saturation measurements.

4.2.3.6 Discussion

With the exception of the six high S_{nwc} values, the low S_{nwc} values measured for confined and unconfined conditions, and the low S_{gc} values for rocks with 1xx7x ≤ RC4 ≤ 1xx9x, are consistent with published, low-permeability sandstone, gas S_{gc} values (Chowdiah, 1987; Kamath and Boyer, 1993). Unconfined S_{nwc} values may be slightly higher than confined because mercury is allowed to enter the sample from all sides, representing a larger surface area and consequently more surface pores, allowing more invasion prior to establishment of the sample-spanning cluster. The effect of sample size and surface area on capillary pressure was investigated by Larson and Morrow (1981). Thompson et al. (1987) referred to these invaded paths that do not ultimately lead to a sample-spanning cluster as "pretender" paths. Higher S_{gc} values are also consistent with the larger surface area supporting multiple nucleation sites, which is associated with higher S_{gc} (Li and Yortsos, 1993, 1995a; Du and Yortsos, 1999).

Given that average grain size for these rocks ranged from 50 to 200 μm (microns), and assuming that pore throats are distributed between each grain, then a 2.5-cm cube of rock (approximately a core plug) contains a network of pores with a lattice size dimension of L = ~500 to 125 for grain sizes of 50 μm and 200 μm, respectively. Inserting these dimensions into Equation 4.2.7, the theoretical, critical-percolation saturation for the core plug networks, assuming they comprise a random percolating network, is S_{gc} = 0.033 (L = 500) and S_{gc} = 0.064 (L = 125). These values are in reasonable agreement with the values measured by mercury intrusion analysis. If scaled up to bed-scale or reservoir-thickness scales that can exceed 1 meter in thickness, Equation 4.2.7 would indicate that S_{gc} approaches < 0.01–0.02.

The above analysis supports the commonly applied assumption that S_{gc}<0.05. However, the six mercury samples exhibiting higher S_{nwc} and complex sedimentary structure, the 14 samples exhibiting higher S_{Hg} before resistance decreased, and the association of increasing air-brine S_{gc} with decreasing RC4 value, indicate that critical saturation can be greater for certain sedimentary structures, pore architectures, or boundary conditions. Percolation theory and averaging of capillary pressure as it applies to S_{gc} for different bed architectures provide a conceptual framework for understanding S_{gc} and models for predicting limits on S_{gc}.

4.2.3.6.1 Pore Networks and k_{rg}, S_{gc}

Pore networks can be broadly classified as exhibiting three end-member architectures and an important intermediate architecture: 1) Percolation network (N_p)—random orientation of pore sizes within the network, 2) Parallel network ($N_{//}$)—preferential orientation of pore sizes or beds of different N_p networks parallel to the invasion direction, 3) Series network ($N_{\perp}$)—preferential sample-spanning orientation of pore sizes or beds of different N_p networks perpendicular to the invasion direction, and 4) Discontinuous series network ($N_{\perp d}$)—preferential non-sample-spanning orientation of pore sizes or beds of different N_p networks perpendicular to the invasion direction (Figure 4.2.10). Different sandstone lithologies and the four pore-networks and their relationship to S_{gc} and k_{rg} is discussed. Gas is used as the invading phase for the following discussion.

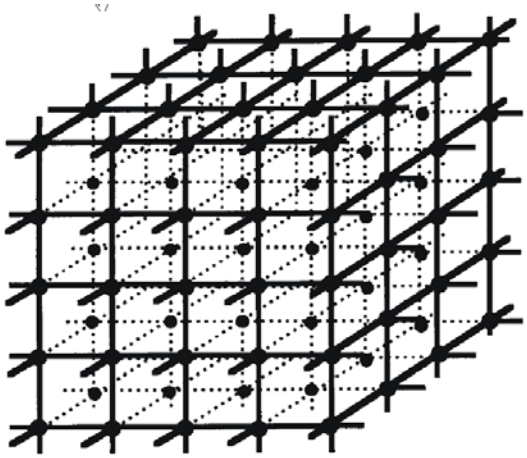

1) Percolation Network (N_p)—macroscopically homogeneous, random distribution of bond sizes, e.g., Simple Cubic Network (z=6)

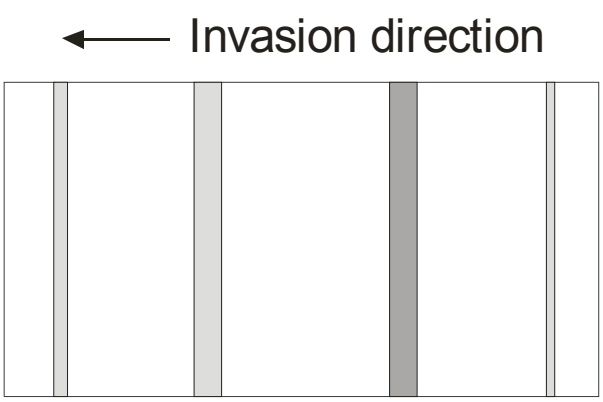

3) Series network ($N_{\perp}$)—preferential sample-spanning orientation of pore sizes or beds of different N_p networks perpendicular to the invasion direction.

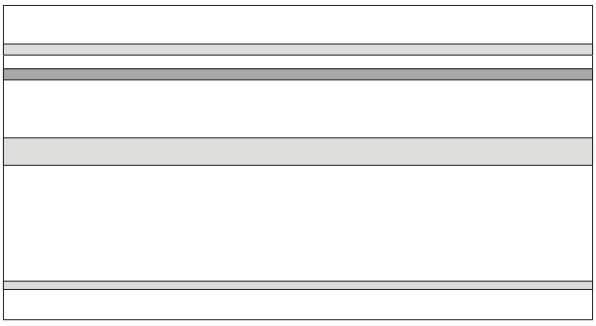

2) Parallel Network ($N_{\parallel}$)—preferential orientation of pore sizes or beds of different N_p networks parallel to the invasion direction.

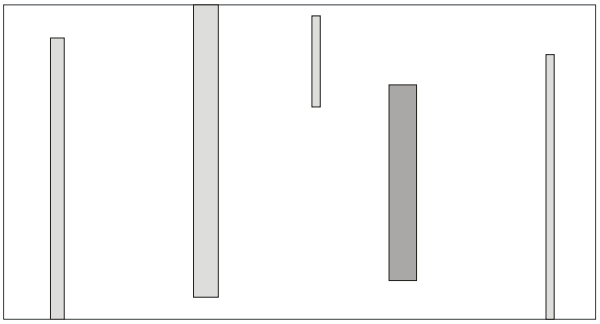

4) Discontinuous series network ($N_{\perp d}$)—preferential non-sample-spanning orientation of pore sizes or beds of different N_p networks perpendicular to the invasion direction. Represents continuum between $N_{\perp}$ and N_p.

Figure 4.2.10. Conceptual pore network models: 1) percolation (N_p), 2) parallel ($N_{//}$), 3) series ($N_{\perp}$), and 4) discontinuous series ($N_{\perp d}$).

Percolation Network (N_p)

A massive-bedded or uniformly bioturbated sandstone, siltstone, or shale might exhibit a pore network that can be represented by a percolation network. As discussed above, for this network, formation of the percolation cluster would occur at $S_g < 0.03–0.07$ at the core-plug scale and would approach $S_{gc} < 0.01–0.02$ at large scales following Equation 4.2.7. Massive-bedded sandstone and siltstone is a common lithology in low-permeability sandstones and therefore low S_{gc} is likely to be common in many reservoir systems.

Parallel Network ($N_{//}$)

Planar- and horizontally laminated bedding is common in marine and tidal flat environments. In addition, many sedimentary structures that might be Series Networks on a large scale can exhibit $N_{//}$ properties at smaller scales including core scale. Parallel networks perform similarly to percolation networks except that portions of the network are not involved in the invasive flow associated with establishing S_{gc}. The critical-gas saturation of this system is the critical saturation of the lowest threshold-entry pressure layer ($S_{gc,low}$; generally the highest-permeability layer) within the system, volumetrically normalized to the total system volume to express the critical saturation relative to the total system volume (S_{gc}). Because the volume of the layer is less than the volume of the total system, the network dimension is smaller and $S_{gc,low}$, from Equation 4.2.7, is greater than if the entire system exhibited the percolating layer properties. However, renormalization of the layer $S_{gc,low}$ to the total system volume results in a lower S_{gc}. Since S_{gc} approaches $S_{gc} < 0.02$ at large scales in percolating systems, it approaches similar or lower values in parallel systems. It is important to note that many rocks exhibit microscopic- to millimeter-scale lamination. The presence of a single, sample-spanning, 1-millimeter-thick lamina in a core, even with high $S_{gc,low}$, can result in a very low S_{gc} value for the core (e.g., a lamina with $S_{gc,low} = 0.5$, representing 1% of the total core volume, results in a core $S_{gc} = 0.005$). Frequently, core sampling procedures avoid sampling series flow architecture by orienting plugs parallel to bedding, thereby creating a sample with $N_{//}$ properties. Following establishment of S_{gc}, the total system gas relative permeability represents the vector solution of the various layer relative permeabilities both parallel to flow and between layers (cross flow).

Series Network ($N_{\perp}$)

Sedimentary bedding structures that represent series networks in one or more dimensions at one or more scales are abundant in nature (e.g., trough crossbedding, large- and small-scale planar crossbedding, low-angle planar bedding, hummocky bedding, flaser bedding). Within these structures scales of series networks range from millimeter-scale laminae to decameter scale crossbedding. If the continuity of the beds is broken such that the beds are not sample-spanning, then the series network is discontinuous as discussed below.

In a $N_{\perp}$ network, percolation across the system does not occur until the invading gas pressure equals or exceeds the threshold pressure ($Pc_{Sgc,high}$) required to achieve critical

saturation in the single barrier-bed with the highest pressure needed to allow percolation through that barrier-bed ($S_{gc,high}$). If invasion occurs under equilibrium-capillary pressure conditions, then S_{gc} for the entire system is a function of the capillary-pressure properties of the barrier beds in the system and is the average of the individual bed saturations at $Pc_{Sgc,high}$ ($S_{g,Pc\text{-}Sgc,high}$) normalized for bed pore volumes :

$$S_{gc} = [\Sigma(S_{g,Pc\text{-}Sgc,high})_i \phi_i V_i] / [\Sigma \phi_i V_i] \qquad [4.2.9]$$

Figure 4.2.11 illustrates a simple crossbedded system consisting of two lithologies that exhibits very high S_{gc} as a result of the significant difference in the capillary pressure properties of the beds (e.g., siltstone laminae within sandstone). Corey and Rathjens (1956) observed critical-gas saturations of 0.60 in a crossbedded sandstone with flow perpendicular to bedding.

$S_{gc,high}$ for the most-restrictive barrier-bed can be considered to follow Equation 7 and approaches zero at infinite size. However, the system S_{gc} does not approach zero but approaches a constant since the adjacent beds are all at the saturations associated with the threshold pressure of the restrictive barrier bed. Equilibrium capillary-pressure conditions result in the maximum S_{gc} for a system. For systems with a pressure gradient across the system (e.g., flowing core test), S_{gc} is reduced as a result of the lower capillary pressures, and consequent lower gas saturations, in the downgradient portion of the system. Given the time frames available, reservoirs are likely to be charged under capillary pressure equilibrium conditions.

Average absolute permeability in series flow has been shown to be the harmonic average of the bed permeabilities. Weber (1982) presented equations for calculating directional permeability in common crossbedding structures. Directional, gas-relative permeability can be calculated using similar methodology. It is important to note that most reservoir-, flow-simulation software treat capillary pressure and relative permeability as scalars and do not provide directional components (e.g., krg_x, krg_y, Pc_x, etc.) as they do for permeability (e.g., k_x, k_y, k_z)

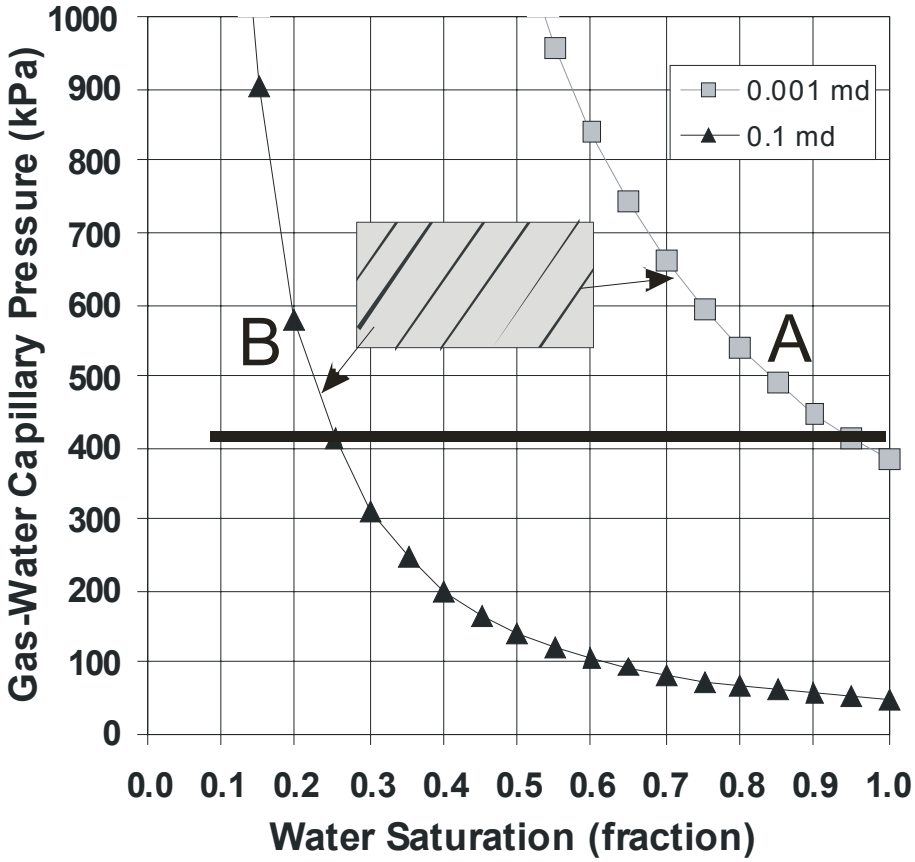

Figure 4.2.11. Example for a crossbedded sandstone, consisting of higher-permeability/low-capillary-pressure sandstone (B) interbedded with low-permeability/high-capillary-pressure siltstone laminae (A), showing how S_{gc} can reach high values for invasion in a series network. For gas to flow across this system it must exceed the capillary pressure for the S_{gc} of the 0.001 mD fine beds ($Pc_{Sgc,high}$ on curve A). At $Pc_{Sgc,high}$ the 0.1 mD sandstone is desaturated to $S_{g,Pc\text{-}Sgc,high} = 0.75$. Assuming that the pore volume of the shale is negligible, the volume of this rock is largely the 0.1 mD facies and $S_{gc} = 0.75$.

Discontinuous Series Network ($N_{\perp d}$)

The $N_{\perp}$ network discussed above requires that the barrier beds be sample-spanning perpendicular to the direction of invasion. Beds may not be sample-spanning or may have holes. These represent discontinuous series networks ($N_{\perp d}$) and represent a continuum between a Percolation, N_p, and a Series, $N_{\perp}$, network. Critical saturations in a $N_{\perp d}$ network range between N_p and $N_{\perp}$ critical saturations as a function of the network size, and the frequency, length, and property differences among the discontinuous barriers and the "host" sample-spanning network.

Fundamentally, since a continuous path across the system exists through the "host" network, S_{gc} in a $N_{\perp d}$ network follows Equation 4.2.7. However, because some potential paths for the sample-spanning cluster are blocked, at any given network dimension, more "pretender" paths (Thompson et al., 1987) are formed and S_{gc} is greater than for a N_p network of the same dimension. Though a formal mathematical analysis is not known, it can be estimated that S_{gc} in a $N_{\perp d}$ network follows Equation 7 but exhibits a decrease in slope as barrier-beds approach sample-spanning dimensions.

4.2.3.7 Conclusions

Mercury intrusion capillary pressure and associated resistance data, and air-brine critical gas saturation measurements presented for low-permeability sandstones exhibiting a wide range in lithology, support the commonly applied assumption that $S_{gc} < 0.05$. However, the association of increasing S_{gc} with decreasing primary sedimentary structure rock classification digit 4,and higher S_{nwc} with rocks exhibiting complex sedimentary structure, indicate the dependence of S_{gc} on pore network architecture. Percolation theory for random networks indicates that S_{gc} asymptotically approaches zero as the network dimension approaches infinity. Analysis of pore-network dimensions appropriate for cores and reservoir beds indicates that S_{gc} approaches < 0.01–0.02. Percolation theory and averaging of capillary pressure as it applies to S_{gc} for different primary sedimentary structures and bed architectures provide a conceptual framework for understanding S_{gc} and models for predicting limits on S_{gc}. Three end-member network architectures and an important intermediate architecture are appropriate: 1) Percolation network, N_p; 2) Parallel network, $N_{//}$; 3) Series network, $N_{\perp}$; and 4) Discontinuous series network, $N_{\perp d}$.

Applying these models to sedimentary structures, the models suggest that critical-gas saturation is likely to be low (e.g., $S_{gc} < 0.03$–0.07 at core scale and $S_{gc} < 0.02$ at reservoir scale) in massive-bedded or homogeneous sandstones of any permeability representing N_p networks. In lithologies representing parallel networks, $N_{//}$, such as sandstone cores with laminae and reservoirs with planar and horizontal bedding, S_{gc} is likely to be lower than massive-bedded sandstones. In lithologies exhibiting series network, $N_{\perp}$ properties, such as sandstones with trough crossbedding, large- and small-scale planar crossbedding, low-angle planar bedding, hummocky bedding, and flaser bedding, S_{gc} does not asymptotically approach zero with increasing network dimension but approaches a constant reflecting the capillary pressure

property differences and relative pore volumes among the beds in series and the "tightest" bed limiting percolation. For these networks S_{gc} values range widely and have been observed to reach $S_{gc} = 0.6$. Discontinuous series networks, $N_{\perp d}$, representing lithologies exhibiting series network properties but for which the restrictive beds are not sample-spanning, exhibit S_{gc} values intermediate between N_p and $N_\perp$ networks.

The analysis and data presented in this study indicate that gas relative permeability can be effectively modeled in low-permeability gas sandstones using the modified Corey (1954) equation. The limited data support two different Corey-type models: 1) constant k_{rg} exponents ($p = 1.7$, $q = 2$) with variable S_{gc}, and 2) near-constant, low S_{gc} with a varied p exponent. Results from this study can be interpreted to indicate that in heterolithic lithologies with complex sedimentary structures the (p=C; $S_{gc}(k)$) model may be more appropriate, whereas in massive-bedded and laminated lithologies the ($p(k)$; $S_{gc}<0.05$) may apply.

Consideration of the four network architectures lends insight into the complications of heterogeneous lithologies at differing spatial scales and underscores the difficulty of upscaling laboratory-derived relative permeabilities for reservoir simulation. Though anisotropy is well recognized and dealt with for absolute permeability, the analysis here suggests that consideration of capillary pressure and relative permeability anisotropy may be warranted. Finally, given the limited amount of air-brine S_{gc} data for low-permeability sandstones, further work is needed but this study would indicate that this work should be closely integrated with rock lithology.

Subtask 4.3. Measure *In Situ* and Routine Capillary Pressure

4.3.1 Task Statement

Relationships between "irreducible" water saturation and permeability (Byrnes, 1997; Byrnes and Castle, 2000) and between threshold entry pressure or principal pore throat diameter (PPTD) and permeability (Byrnes and Keighin, 1993; Keighin, 1995; Byrnes, 1997; Byrnes, 2003) have been published. The relationship between threshold entry pressure (P_{te}) and permeability and between permeability and lithofacies at any given porosity requires that capillary pressure change with lithofacies at any given porosity. With change in both the threshold entry pressure, the critical or percolating pore throat size capillary pressure (P_{pc}) and pore throat size distribution with decreasing permeability, Byrnes (2003, 2005) illustrated generalized capillary pressure shapes for western tight gas sandstones. Byrnes and Keighin

(1993) and Keighin (1995) showed that the *in situ* P_{pc} values range from 15 to 84% of unconfined P_{te} values illustrating the change in capillary pressure with confining stress.

Though general capillary pressure relationships for low-permeability sandstones have been published, very few publications thoroughly characterize the lithologic properties of the samples. In addition, with the exception of Byrnes and Keighin (1993) and Keighin (1995), no published studies have investigated the stress dependence of Mesaverde capillary pressure properties. To fully characterize both the basic capillary pressure relationships of Mesaverde rocks ranging widely in lithology, porosity, permeability, and basin, capillary pressure analysis was performed on pairs of representative samples. Mercury intrusion analysis from 2 to 9,300 psi (14–64,124 kPa) injection pressure was used. Paired samples, exhibiting similar porosity, permeability, and lithology were used for the unconfined analysis and the confined analysis.

All the capillary pressure published work cited above investigates drainage capillary pressure properties. These, in fact, represent the principal capillary pressure property of interest for many low-permeability sandstones because they have remained on a primary drainage cycle throughout geologic time. There are, however, regions where reservoirs have leaked and undergone water imbibition and areas where portions of the gas column have undergone cyclic drainage-imbibition in response to burial and resulting pore volume change from compaction and diagenesis and saturation change from pore pressure increases and decrease. For these areas an understanding of the drainage and imbibition capillary pressure properties is required. To address the need for this information samples were selected for cyclic drainage-imbibition capillary pressure analysis.

4.3.2 Methods

4.3.2.1 Unconfined Capillary Pressure

Subsequent to lithologic description, and paired-plugs porosity and permeability analysis core pairs were selected for unconfined, confined, and unconfined imbibition-drainage analysis. Samples were selected to represent each basin, range in lithofacies, and range in porosity and permeability. The selected cores were transferred to a vacuum desiccator and maintained at vacuum conditions for a period of not less than 8 hours until ready for analysis. Each sample was transferred from the vacuum desiccator to the capillary pressure instrument and evacuated to a pressure of less than 0.01 torr for a period of 15 minutes. The sample was then subjected to

increasing incremental mercury injection pressures ranging from 2 to 9,300 psia (14–64,124 kPa). At each pressure, saturation equilibrium was assumed to have been established when the volume of mercury injected was less than 0.1% of the pore volume for a three-minute period. Injected mercury volumes were corrected for system and mercury compressibility effects. Pore volume was corrected for sample compressibility to the threshold entry pressure. Accuracy and precision vary with sample pore volume and outer pore sizes and surface roughness. Pump injection volumes are readable to 0.001cc. Based on pore volumes from 1 to 3 cc, estimated precision for the measurement is 0.5% for pore sizes less than 107μm. A simple flow schematic of the unconfined and confined mercury intrusion apparatuses is shown in Figure 4.3.1.

4.3.2.2 Confined Capillary Pressure

For confined samples each matching plug was transferred from the vacuum desiccator to a Hassler type confining pressure cell and subjected to a hydrostatic confining stress and evacuated to a pressure of less than 0.01 torr for a period of 30 minutes. The first 20 analyses were performed at a hydrostatic confining pressure of 34.5 MPa (5,000 psi) greater than the mercury injection pressure, maintaining a net effective stress of 34.5 MPa (5,000 psi). All subsequent samples were measured at a hydrostatic confining pressure of 27.6 MPa (4,000 psi) greater than the mercury injection pressure, maintaining a net effective stress of 27.6 MPa (4,000 psi). Resistance across the core was measured using stainless steel electrodes on each end of the core. A schematic of the apparatus is shown in Figure 4.2.4. Confining pressures ranged from 4,000 psi (27.6 MPa) up to 11,300 psi (77.2 MPa). Because of the small pressure steps taken during the analysis, the application of a new, higher, confining stress before increasing mercury pressure did not result in a significant additional stress although issues arise for stress on uninvaded pores as discussed below.

Incremental pore pressure ranged from 2 to 7,200 psi (0.01–49.6 MPa). At each pressure, equilibrium was assumed to have been established when the volume of mercury injected was less than 0.1% of the pore volume for a three-minute period. Injected mercury volumes were corrected for system and mercury compressibility effects. Pore volume was corrected for sample compressibility. Accuracy and precision vary with sample pore volume and outer pore sizes and surface roughness and uncertainty in the precise sample pore volume compressibility. Pump injection volumes are readable to 0.001cc. Based on pore volumes from 1 to 3 cc, estimated precision for the measurement is 0.5% for pore sizes less than 107μm.

It is important to note that the equilibration times of the confined samples were significantly greater than the unconfined samples. Equilibration times for pressures below the threshold entry pressure were similar to unconfined samples but at injection pressures where mercury was entering the pore space, and particularly at the pressures associated with initial saturation changes, equilibration times for a single pressure step could reach as long as 0.5–3 hours, with time dependent on the pore size (and associated permeability). These equilibration times resulted in most of the confined mercury intrusion analyses requiring 2–3 days to perform.

Because the confined analysis required more than a standard work day to complete, analyses were stopped at the end of a work day to be resumed the following day. To test equilibrium criteria for some samples, injection at the end of a work day was stopped following achieving equilibrium at a given injection pressure step and the sample was left overnight with the confining stress left constant and the mercury injection system left shut-in at the last equilibrium pressure. If mercury continued to enter the sample during the night as a result of the sample having not been at complete equilibrium, the injection pressure would decrease. For over 80% of the samples tested, the volume of mercury required to return the mercury injection pressure to the equilibrium pressure of the previous day, when the analysis was halted, was less than 0.2% of the pore volume. This is greater than the defined equilibrium criteria but was insufficient to significantly change the capillary pressure curve and was considered acceptable for an 8–12 hour equilibration time period. These results are interpreted to confirm that the equilibrium criteria used met acceptable standards for obtaining equilibrium saturation. For the remaining ~20% of samples that required greater than 0.2% of the pore volume to re-establish the previous day's injection pressure, most of these were very low permeability samples ($k_{ik} < 0.001$ mD), were stopped at a saturation early in the capillary pressure transition interval, and were stopped at a point that met equilibrium criteria but, unlike other samples, exhibited continued injection at near the equilibrium criteria.

4.3.2.3 Unconfined, Cyclic Drainage-Imbibition Capillary Pressure

Unconfined, cyclic drainage-imbibition capillary pressure analyses were performed similar to the unconfined (drainage) capillary pressure analyses described above. The sample began on a primary drainage cycle with the goal of trying to achieve a mercury saturation near approximately $S_{Hg} = 33 \pm 10\%$. At any equilibrium saturation of $S_{Hg} < 25\%$ another pressure injection step was performed. If $25\% < S_{Hg} < 33\%$ the primary drainage cycle was terminated. If

S_{Hg} < 25% and the next pressure injection step resulted in S_{Hg} > 33%, the primary drainage cycle was terminated only when saturation reached equilibrium and not at S_{Hg} = 33%. The exact saturation at which a given injection pressure would reach equilibrium was not known and, as such, the saturation at the termination of the primary drainage curve was not known until equilibrium saturation for the pressure applied was achieved.

Once the sample had reached the saturation at which the primary drainage cycle was to be stopped, injection pressures were incrementally reduced in the same increments at which they were increased for the primary drainage cycle. Equilibrium on this primary imbibition cycle was assumed to have been established when the volume of mercury injected was less than 0.1% of the pore volume for a three-minute period. Pressure was reduced incrementally until the pressure was returned to initial vacuum conditions. The mercury level was dropped below the sample and the sample allowed to equilibrate with the atmosphere. The sample was then removed from the apparatus, weighed to confirm the residual saturation, and immediately returned to the apparatus. In the apparatus the sample was again confined and evacuated to a pressure of less than 0.01 torr for a period of 30 minutes.

To measure the secondary drainage cycle, the sample was then subjected to increasing incremental mercury injection pressures the same as the primary drainage pressure steps and then continuing to incrementally increase injection pressures with the goal of trying to achieve a mercury saturation near approximately $S_{Hg} = 60 \pm 10\%$. At any equilibrium saturation of S_{Hg} < 50% another pressure injection step was performed. If S_{Hg} > 50% the secondary drainage cycle was terminated. If S_{Hg} < 50% and the next pressure injection step resulted in S_{Hg} > 60%, the secondary drainage cycle was terminated only when saturation reached equilibrium and not at S_{Hg} = 60%. The exact saturation at which a given injection pressure would reach equilibrium was not known and, as such, the saturation at the termination of the secondary drainage curve was not known until equilibrium saturation for the pressure applied was achieved.

Following the secondary drainage cycle, the sample was subjected to a secondary imbibitions cycle following a procedure similar to the primary imbibitions cycle. A third drainage and imbibitions cycle were also performed. The third drainage cycle was stopped at the maximum injection pressure of 9,300 psi (64.1 MPa).

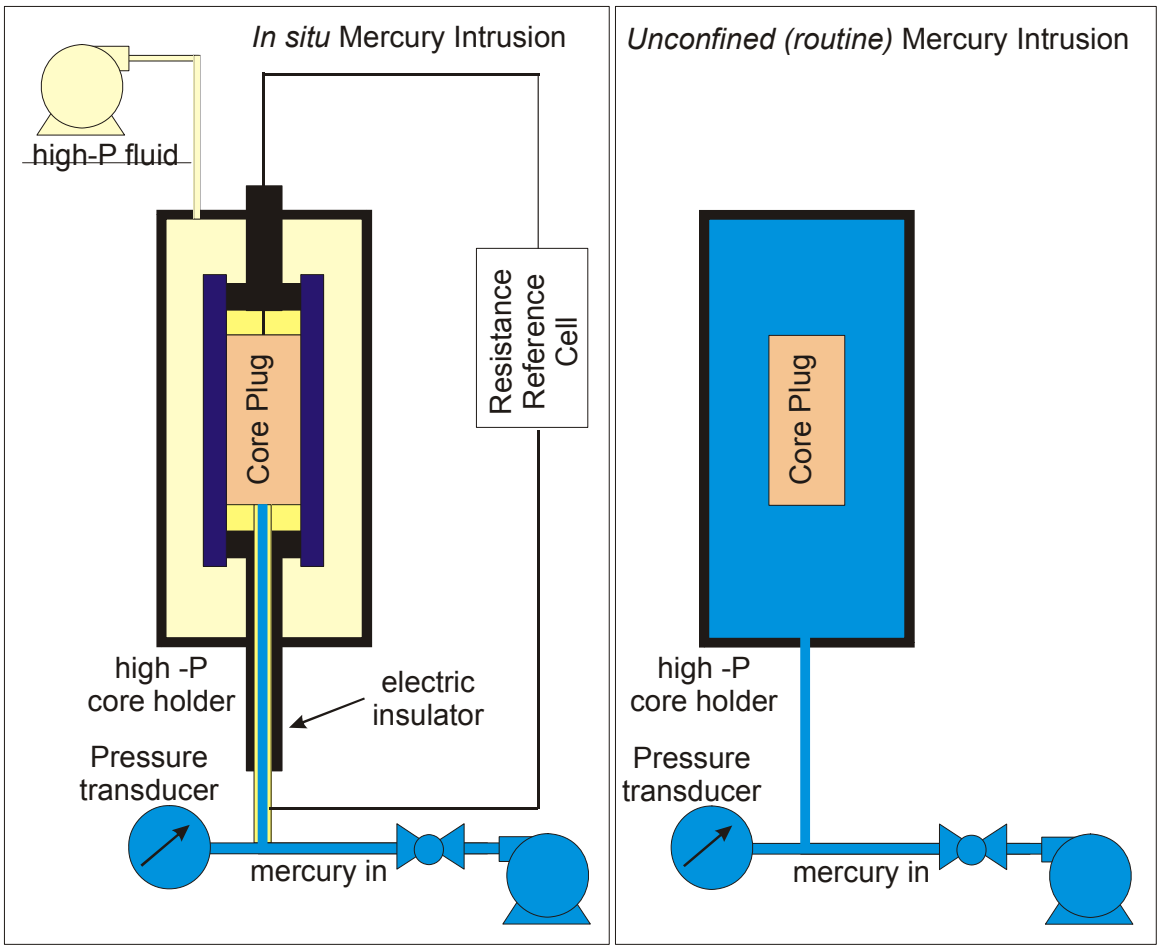

Figure 4.3.1 Flow schematic of unconfined and confined mercury intrusion apparatuses.

4.3.3 Results

Standard unconfined mercury intrusion analysis for injection pressures ranging from 2 to 9,300 psi (14-64,124 kPa) provided drainage capillary pressure curves for 121 advanced properties samples. Confined (at a net effective stress of 4,000 psi (27.6 MPa)) mercury capillary pressure curves were measured on 81 cores. For 33 cores unconfined imbibition-drainage capillary pressure curves were measured for three (3) drainage and three (3) imbibitions cycles, representing a total of 99 capillary pressure curves. Capillary pressure data were obtained for samples from 38 wells in all basins, representing the range of lithofacies, and a range of routine porosity from 1.3% to 23.8% and in situ Klinkenberg permeability from 0.000005 mD to 171 mD.

Figure 4.3.2 illustrates that capillary pressure ranges widely for all Mesaverde rock samples. Selected representative drainage capillary pressure curves are shown in Figure 4.3.3.

These curves exhibit the trend that threshold entry pressure (P_{te}, the minimum pressure at which the nonwetting phase can invade the sample pore space excluding minor surface pores) measured by extrapolation of the Pc curve in the transition zone to Sw = 100% (avoiding surface pore influence on the Pc curve), increases with decreasing permeability. This trend is the direct result of the association between decreasing pore throat size and permeability. They also show that at any given capillary pressure wetting-phase saturation increases with decreasing permeability.

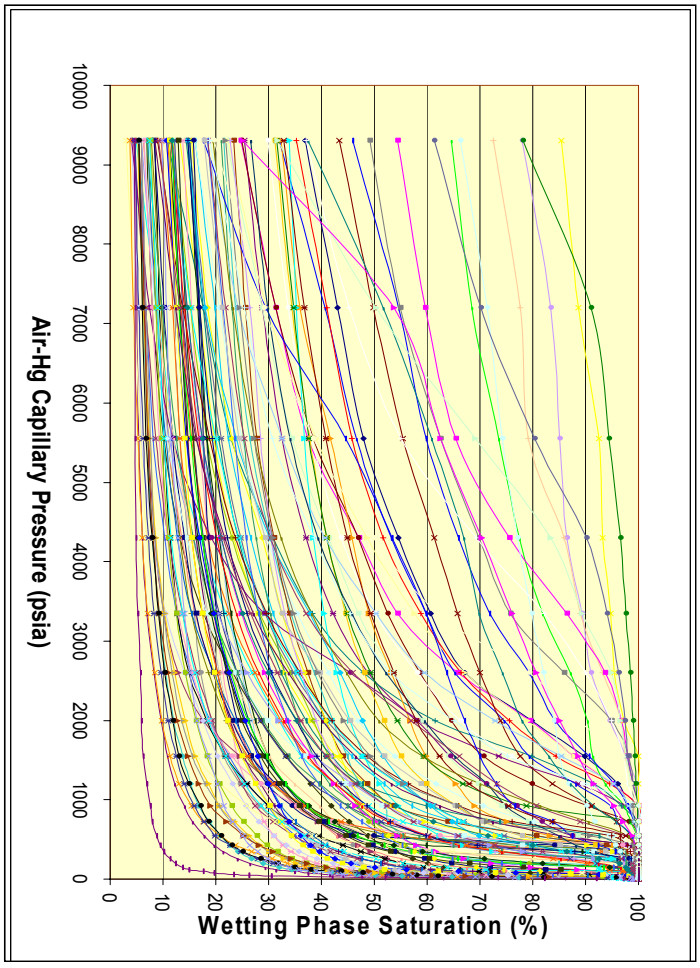

Figure 4.3.2. Air-mercury capillary pressure curves for selected samples ranging in *in situ* Klinkenberg permeability from 0.000005 mD to 171 mD. These curves exhibit increasing threshold entry pressure and increasing "irreducible" water saturation with decreasing permeability.

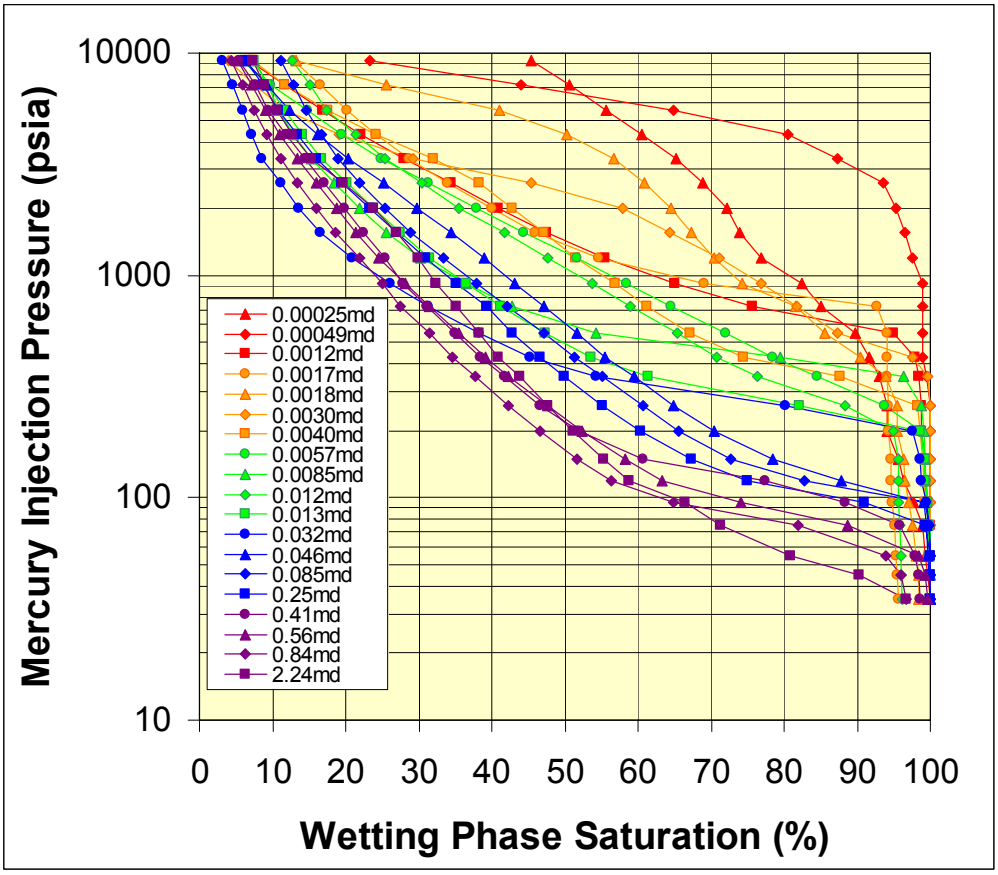

Figure 4.3.3. Air-mercury capillary pressure curves for selected samples ranging in *in situ* Klinkenberg permeability from 0.00025 mD to 2.24 mD. These curves exhibit increasing threshold entry pressure and increasing "irreducible" wetting-phase saturation with decreasing permeability.

4.3.3.1 Capillary Pressure Drainage-Imbibition Hysteresis

Thirty three (33) samples were tested for capillary pressure drainage-imbibition hysteresis involving three drainage-imbibition cycles for each sample (99 capillary pressure curves in total). These three cycles represent drainage saturations reaching successively non-wetting phase saturations (S_{nw}) of $S_{nw} = 0.33\pm0.15$, $S_{nw} = 0.57\pm0.10$, and $S_{nw} = 0.87\pm0.10$. Figure 4.3.4 illustrates the hysteresis curves for a single sample, while Figure 4.3.5 illustrates eight sandstones spanning a range of permeabilities. A significant fraction of the trapped non-wetting phase saturation (Snw) results from the early intrusion at low S_{nw} values.

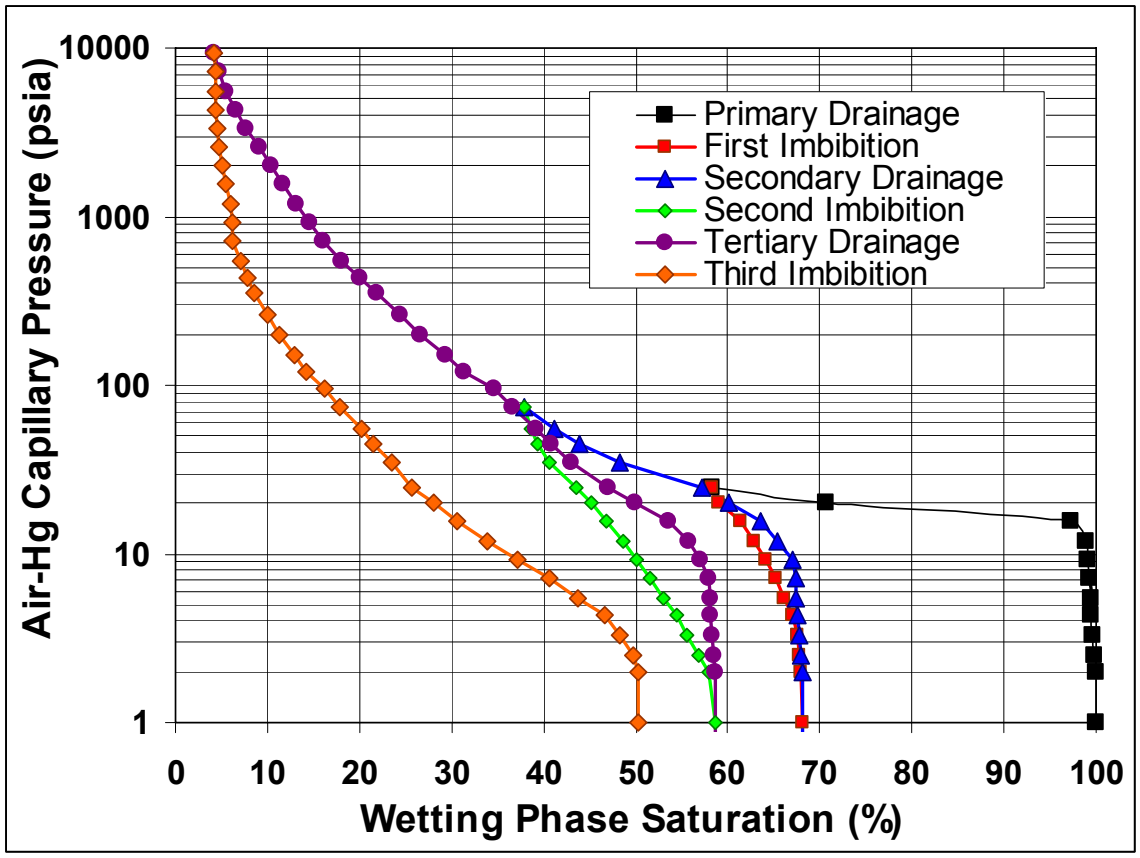

Figure 4.3.4. Air-mercury successive drainage and imbibition capillary pressure curves for one sample exhibiting hysteresis with successively increasing residual nonwetting phase saturation (S_{nwr}) with increasing initial nonwetting phase saturation (S_{nwi}).

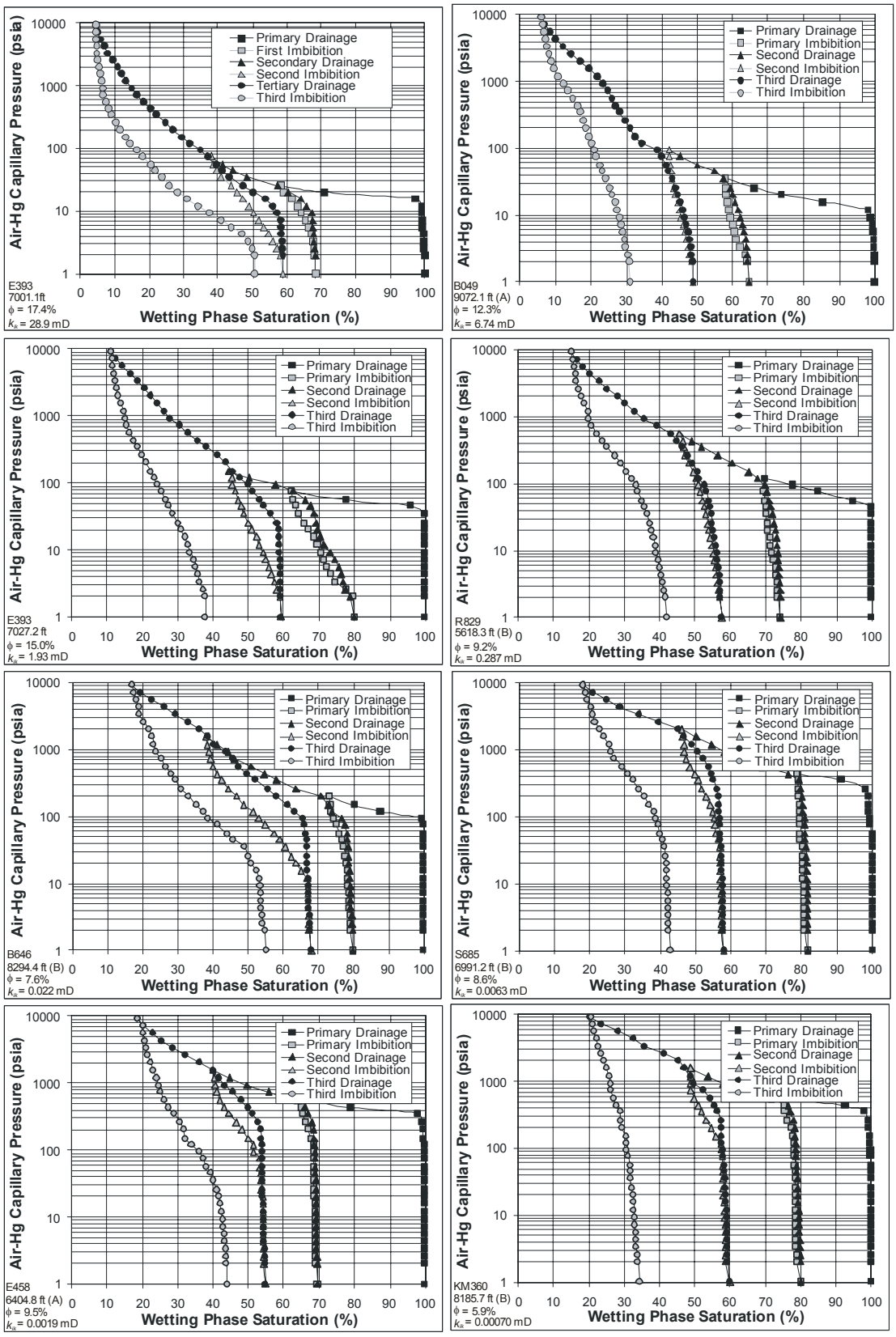

Figure 4.3.5. Example air-mercury successive drainage and imbibition capillary pressure curves.

Figure 4.3.6 illustrates the relationship between the residual saturation to imbibition and the initial drainage saturation for each cycle. In addition to residual saturation measurements on the 33 hysteresis samples, all MICP samples were weighed following analysis. Residual mercury trapped in the core was determined gravimetrically and residual nonwetting phase saturation calculated. For these samples the initial mercury (nonwetting phase) saturation represented the mercury saturation achieved at 9,300 psi (64.1 MPa) intrusion pressure. This saturation is near, or represents a wetting phase saturation less than, "irreducible" saturation. Figure 4.3.5 illustrates the relationship between residual nonwetting phase saturation and the initial nonwetting phase saturation for the hysteresis and the single-cycle unconfined MICP samples. The relationship between initial and residual nonwetting phase saturation was characterized by Land (1971) for strongly wet samples:

$$1/S_{nwr}^* - 1/S_{nwi}^* = C \qquad [4.3.1]$$

where $S_{nwr}^* = S_{nwr}/(1-S_{wirr})$ and $S_{nwi}^* = S_{nwi}/(1-S_{wirr})$.

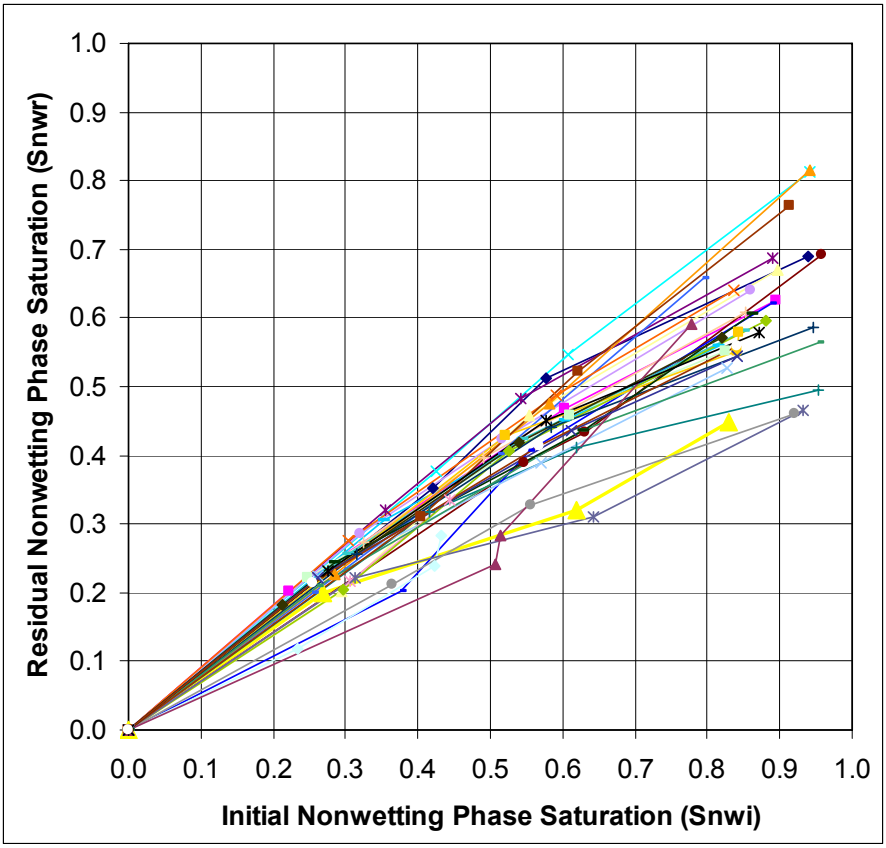

Figure 4.3.6. Crossplot of residual versus initial mercury (nonwetting) saturation for 33 Mesaverde sandstone samples.

Three different measurement populations are compared; unconfined, unconfined with hysteresis, and confined. Unconfined with hysteresis are separated from the unconfined because the hysteresis samples have data for measurements at $S_w < S_{wirr}$ except for the third and last hysteresis drainage-imbibition cycle. Confined samples are samples for which capillary pressure analysis was performed with the sample under a net confining stress of 4,000 psi (27.6 MPa) as described below. Table 4.3.1 compares Land C values for the different sample populations with S_{wirr} defined as either equal to the minimum saturation achieved in the MICP analysis ($S_{wirr} = 1-S_{nwmax}$) or S_{wirr} equal to zero ($S_{wirr} = 0$). The average Land C values represent the average of individual C values calculated for each sample using equation 4.3.1. The Land C Minimum Error values represent the C values that provide a minimum error for all samples in a given population using a single C value.

Sample Condition	Swirr definition	Land C Average	C Standard Error	Land C Minimum Error	Snwr Standard Error	Snwr Std Error C=0.55
all	$S_{wirr} = 1-S_{nwmax}$	0.57	0.329	0.53	0.077	0.077
unconfined	$S_{wirr} = 1-S_{nwmax}$	0.61	0.294	0.59	0.087	0.088
hysteresis	$S_{wirr} = 1-S_{nwmax}$	0.61	0.383	0.51	0.056	0.057
confined	$S_{wirr} = 1-S_{nwmax}$	0.44	0.249	0.45	0.088	0.085
all	$S_{wirr} = 0$	0.73	0.443	0.63	0.073	0.073
unconfined	$S_{wirr} = 0$	0.78	0.360	0.71	0.080	0.081
hysteresis	$S_{wirr} = 0$	0.75	0.562	0.59	0.057	0.057
confined	$S_{wirr} = 0$	0.61	0.316	0.54	0.078	0.078
all	$S_{wirr} = 0$, Snwi<70%			0.70	0.054	0.053
unconfined	$S_{wirr} = 0$, Snwi<70%			0.83	0.062	0.061
hysteresis	$S_{wirr} = 0$, Snwi<70%			0.70	0.052	0.051
confined	$S_{wirr} = 0$, Snwi<70%			0.50	0.038	0.039

Table 4.3.1. Comparison of average Land C values for different sample populations calculated from averaging individual sample C values and from solution of the minimum error for each a single C value for each population.

Average C values, calculated from the average of the individual sample C values using equation 4.3.1 (with $S_{wirr} = 1$-Swmin and $S_{wirr} = 0$) average 0.07 greater than minimum error C values. Variance of the individually determined C values is significant, averaging 0.37. Land C values that result in the minimum error for a given population average 0.61 ± 0.20 for all populations and 0.65 ± 0.20 for the populations where $S_{wirr} = 0$. Standard error is greater for $S_{wirr} = 1 - S_{nwmax}$ than for $S_{wirr} = 0$ even with input of individual known sample S_{wirr} values. This argues that optimum prediction of S_{wnr} is obtained using $S_{wirr} = 0$.

Although the Land C values appear to vary widely, resulting predicted residual saturation values are not highly sensitive for the range of C values exhibited. Iterative solution indicates that C = 0.55 results in the minimum error in residual saturation for all populations with $S_{wirr} = 0$. Using C = 0.55 the resulting error in S_{nwr} prediction is only 0.001±0.0015 different from the standard error values obtained using C value that provide the minimum error for each population (Table 4.3.1). Figure 4.3.7 illustrates initial (S_{nwi}) and residual nonwetting phase saturations (S_{nwr}) for the unconfined MICP samples, for which $S_{nwi} = 1 - S_{nwmax}$, and the unconfined hysteresis samples, for which 2 of 3 $S_{nwi} < 1 - S_{nwmax}$. Trapping is slightly greater in the hysteresis samples.

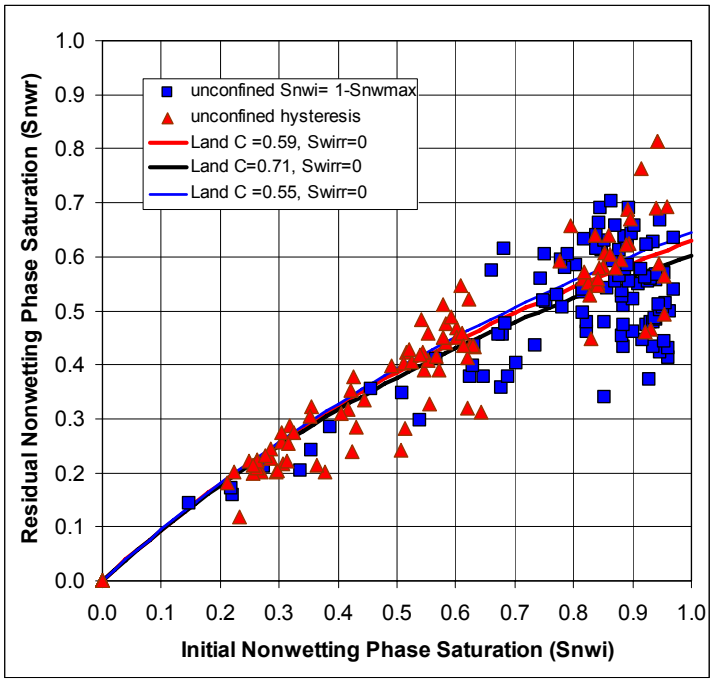

Figure 4.3.7. Crossplot of residual and initial nonwetting phase saturation for unconfined samples including samples where $S_{nwi} = 1\ S_{nwmax}$ (blue squares) and hysteresis/imbibition samples where two of three measurements were obtained at $S_{nwi} < 1 - S_{nwmax}$ (red triangle).

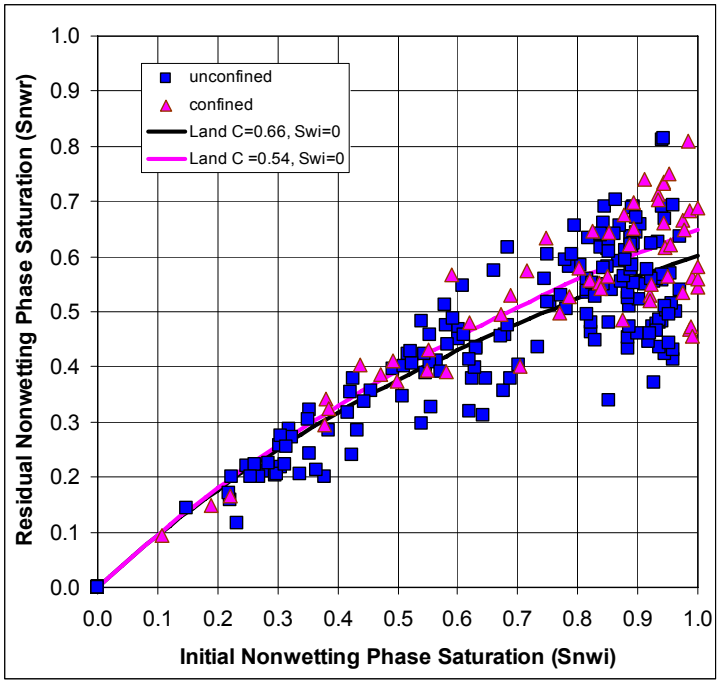

Figure 4.3.8. Crossplot of residual and initial nonwetting phase saturation for unconfined samples (blue squares) and confined samples (magenta triangles). Higher S_{nwr} values in confined samples result in slightly greater Land C value. Whether increased trapping is due to confining stress effects or boundary conditions is still being investigated.

Comparing the residual and initial saturations for unconfined and confined samples (Figure 4.3.8) shows that confined samples exhibit slightly greater residual saturation than unconfined with C = 0.54 and C = 0.66 for confined and unconfined (including unconfined and unconfined hysteresis samples), respectively. Greater trapping in confined samples may be the result of a change in the pore body:pore throat relationship due to confining stress or it may be the result of the limit placed on exit boundary conditions. Unconfined samples allow mercury to exit the sample from all sides whereas confined samples only allow mercury to exit from one entry face. Assuming a constant number of exit paths in any given direction and the same snap-off conditions, a decrease in the number of exit paths is likely to increase the nonwetting phase volume behind junctions undergoing snap-off in one direction. This change in boundary conditions would likely result in some additional trapping. Whether the increase in residual non-wetting phase saturation is the result of confining stress effects or the difference in boundary conditions is being investigated. Assuming that pore bodies are not strongly affected by

confining stress and that confined samples have smaller pore throats than unconfined samples, then greater pore body:pore throat ratios in confined samples compared with unconfined samples would also result in higher residual nonwetting phase saturations.

Based on analysis of prediction error for the confined and unconfined sample populations, prediction of S_{nwr} using C = 0.55 and S_{wirr} = 0 appears to provide minimum error for the range of possible measurement condition populations. Utilization of C values specific for a population results in improvement in prediction that is generally less than 2% of S_{nwr}.

4.3.3.2 Unconfined and Confined Capillary Pressure

Unconfined and *in situ* (confined) mercury intrusion capillary pressure (MICP) analyses are compared for 81 pairs of twinned sandstones core plugs. Two matched core plugs were obtained by cutting a single long core plug into two plugs of 3-5 cm in length. On both plugs porosity and permeability were measured. Statistics for the 652 adjacent core plug pairs have been discussed in Section 4.12 and 4.13. From the total population of 652 core plug pairs, the 81 pairs were selected to represent the range of basins, lithofacies, porosity, and permeability for unconfined and *in situ* (confined) MICP analysis. Pairs represent all basins, 27 wells, and range in porosity from 1.3% to 24.3% and *in situ* Klinkenberg permeability from 0.000036 mD to 171 mD ($3.6x10^{-8}$ to $1.7x10^{-1}$ μm^2).

Figure 4.3.9 illustrates example unconfined and *in situ* MICP curves for pairs of high- to low-permeability from different wells and basins. Comparison among pairs shows that threshold entry pressures increase with decreasing permeability. Between core plugs in a pair set several trends are evident. *In situ* and unconfined curves for high-permeability cores (k_{ik} > 1 mD) are nearly identical. With decreasing permeability the difference between unconfined and *in situ* threshold entry pressure increases. For all pairs this difference is greatest at the threshold entry pressure and decreases with decreasing wetting-phase saturation. At wetting phase saturations of 30-50% the *in situ* MICP curve crosses the unconfined curve and exhibits 0-5% lower wetting phase saturation with increasing capillary pressure. It can be interpreted that confining stress exerts principal influence on the largest pore throats and that pore throats accessed at non-wetting phase saturations below approximately 50% are not significantly affected by confining stress. This is consistent with these smaller pores comprising pore space within pore bodies or in regions of the rocks where stress is not concentrated.

Laboratory air-mercury capillary pressure data were converted to reservoir gas-brine capillary pressure data using the standard equation (Purcell, 1949):

$$Pc_{res} = Pc_{lab} (\sigma\cos\theta_{res}/\sigma\cos\theta_{lab}) \quad [4.3.2]$$

where Pc_{res} is the gas-brine capillary pressure (psia) at reservoir conditions, Pc_{lab} is the laboratory-measured capillary pressure (psia), $\sigma\cos\theta_{res}$ is the interfacial tension (σ, dyne/cm) times the cosine of the contact angle (θ, degrees) at reservoir conditions, and $\sigma\cos\theta_{lab}$ is the interfacial tension times the cosine of the contact angle at laboratory conditions. For air-mercury capillary pressure measurements, an air-mercury interfacial tension of 484 dyne/cm and a contact angle of 140 degrees was assumed.

To determine the water saturation in any given rock as a function of height above the free-water level, it is necessary to convert the capillary pressure data to height above free-water level. This conversion was performed using the standard relation (Hubbert, 1953):

$$H = Pc_{res}/(E(\rho_{brine}-\rho_{gas})) \quad [4.3.3]$$

where H is the height (ft) above free-water level, Pc_{res} is the capillary pressure (psia) at reservoir conditions, ρ_{brine} and ρ_{gas} are the density of brine and gas at reservoir conditions and E is a constant (0.433(psia/ft)/(g/cc)) for converting density to pressure gradient.

From the air-mercury capillary pressure data, pore-throat diameter was calculated using the modified Washburn (1921) relation:

$$D = 4F\sigma\cos\theta/Pc \quad [4.3.4]$$

where Pc = capillary pressure (psia), F = 0.145 ((psia·cm·μm)/dyne), θ = contact angle (140 degrees), σ = interfacial tension (484 dyne/cm), and D = pore-throat diameter (μm, microns). This relation assumes that the nonwetting phase (i.e., gas) enters the pores through circular pore throats.

Variables in equations 4.3.2 to 4.3.4 that change with reservoir pressure, temperature, gas chemistry, and brine chemistry include σ, ρ_{brine}, and ρ_{gas}. To convert laboratory properties to reservoir properties for use in the equations above the range of Mesaverde reservoir conditions were defined as 1) reservoir pressures – 2,500-13,000 psia (17.2-89.6 MPa); 2) temperatures – 90-260 ^{o}F (32.2-126.7 ^{o}C), 3) gas gravity – 0.55-0.70, and 4) brine density – 1.00-1.11 grams/cubic

centimeter (g/cc). For the range in temperature, methane-water interfacial tension (σ) ranges from 33-58 dyne/cm (Jennings and Newman, 1971). To provide a common reference frame for all capillary pressure curves the following values were assigned: $\sigma\cos\theta_{res}$ = 40 dyne/cm, $\sigma\cos\theta_{lab}$ = 370.8 dyne/cm, ρ_{gas} = 0.216 g/cc (0.935 psi/ft, 2.115 kPa/m), and ρ_{brine} = 1 g/cc (0.430 psi/ft, 9.727 kPa/m), MICP pressures can be transformed into equivalent height above free water using Equation 4.3.3.

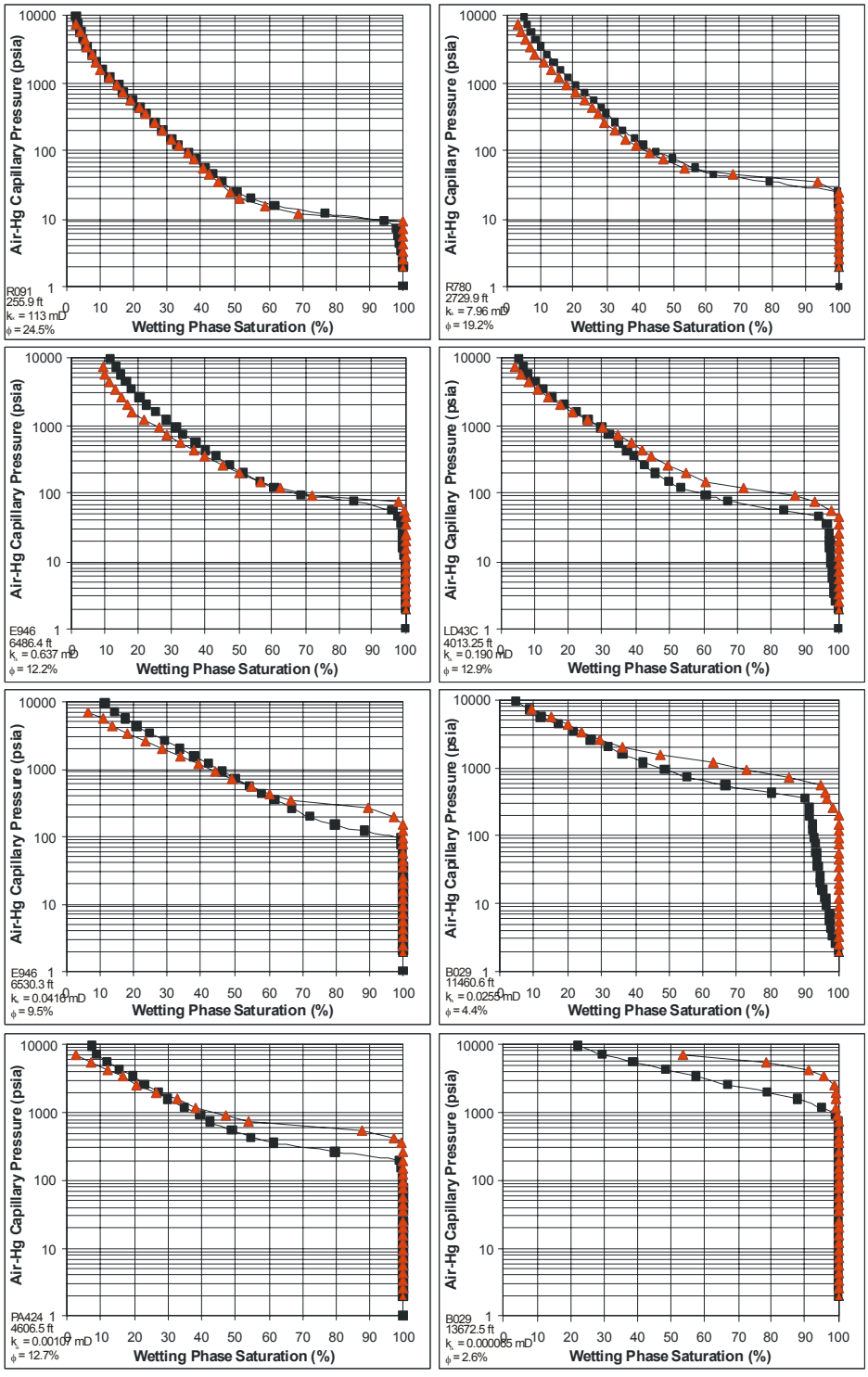

Figure 4.3.9. Examples of *in situ* (red triangles) and unconfined (black squares) air-mercury capillary pressure curves. Threshold entry pressure for samples under *in situ* conditions are greater than for unconfined conditions with the difference in pressure increasing with decreasing permeability. At higher pressures, curves frequently cross. Trends are similar to those reported by Byrnes and Keighin (1993).

Figure 4.3.10 illustrates the relationship between MICP-measured threshold entry pressure and the ratio of Klinkenberg permeability/porosity. It also shows the equivalent relationships for threshold entry-pore diameter and threshold entry-gas column height calculated using equations 4.3.2 through 4.3.4.

Data are presented for both unconfined and *in situ* MICP measurements. Several details concerning the variables plotted are important to note. The abscissa in Figure 4.3.10 represents two different ratios: the unconfined and *in situ* data. For the *in situ* data the abscissa represents k_{ik}/ϕ_i, the ratio of the *in situ* Klinkenberg permeability and the *in situ* porosity (calculated from the routine helium porosity corrected for compression to *in situ* conditions using equations presented in Section 4.1.2). The MICP equipment used does not provide direct measurement of the sample pore volume under confining stress; thus, empirical correction of unconfined measured pore volume using helium to confined stress conditions is required. This empirical correction introduces uncertainty of approximately $\pm$0-3.5% (1 std. dev.) into the *in situ* pore volume, varying with saturation, that translates to a possible error in wetting phase saturation of up to $\pm$0-3.5% (1 std dev). Error increases with decreasing wetting phase saturation and "irreducible" saturation is the most affected.

The compressible nature and the threshold entry pressure of these rocks also results in uncertainty for standard unconfined MICP. Up to the threshold entry pressure, mercury has not entered the sample and mercury both surrounds the sample and compresses the sample hydrostatically. For sandstones with permeability greater than 0.2 mD ($2x10^{-4}$ μm^2), the threshold entry pressure of mercury is less than 100 psi (700 kPa) and corresponding pore volume compression is less than 1%. However, with decreasing permeability the threshold entry pressure and resulting confining stress increases (Figure 4.3.10) and pore volume decreases. For low-permeability sandstones with $k_{ik} < 0.001$ mD ($1x10^{-6}$ μm^2), confining stress exceeds 1,000 psi (6.9 MPa) and pore volume is correspondingly an average of 3.5% less than unconfined conditions. As mercury enters the sample pore volume, it increases the pore pressure of the fraction of the pore volume occupied and decreases the net effective stress for portions of the sample while uninvaded portions of the rock sample remain compressed. With step-wise increase in injection pressure and confining stress for uninvaded rock volume, the net effective stress on the uninvaded rock continually changes while invaded portions are decompressed. Comparison

of saturations calculated using the unconfined pore volume and pore volume corrected for mercury-induced confining stress are being analyzed.

For the unconfined data the abscissa represents k_{mk}/ϕ_a, the ratio of the geometric mean of the routine Klinkenberg permeability, measured under "routine" conditions of 600 psi (4.1 MPa) confining stress, and the *in situ* Klinkenberg permeability, measured under 4,000 psi (27.6 MPa) confining stress, divided by the unconfined routine helium porosity, ϕ_a. The mean permeability and not the routine Klinkenberg permeability is used because 1) the lower-permeability rocks are under confining stress by surrounding mercury at the threshold entry pressure, and 2) for all samples routine and *in situ* permeabilities were measured prior to MICP resulting in permeability hysteresis. *In situ* permeability was measured at 4,000 psi (27.6 MPa) confining stress. When this confining stress was released, the permeability of most samples does not return immediately to the routine permeability but instead exhibits permeability hysteresis and time-dependent change of routine permeability. The permeability that most closely corresponds to the stress conditions of the unconfined MICP is a Klinkenberg permeability measured at the threshold entry pressure (P_{te}) measured immediately prior to MICP analysis. This permeability is intermediate between the initially measured routine and *in situ* Klinkenberg permeabilities. Klinkenberg permeability at this precise stress condition was not measured and the mean Klinkenberg permeability represents a value that is closer to this condition than either the routine or *in situ* values. Figure 4.3.11 illustrates the relationship between unconfined P_{te} and routine *in situ* and mean permeabilities, and shows that the mean permeability exhibits the same relationship as the *in situ* MICP for which these stress issues do not exist.

Figure 4.3.10 illustrates the good correlation between the threshold entry pore size (and corresponding pressure or gas column height) and permeability. The slope of this relationship is statistically identical for both unconfined and confined conditions because the abscissa represents each set of conditions. Unconfined samples exhibited higher permeabilities and larger threshold entry pore diameters. With application of confining stress the permeability decreased due to the decrease in pore throat diameter. The slope of the relationship between pore size and permeability, 0.5, is the same as the scaling parameter proposed by Leverett (1941) who proposed normalizing capillary pressure using $(k/\phi)^{0.5}$. Because permeability is well correlated with threshold pore throat size, it can be used to correct unconfined capillary pressure curves to *in situ* conditions.

Permeability shows little dependence on confining stress for high-permeability rocks (k > 1 mD, $1x10^{-3}$ μm^2) because confining stress induces little change in pore throat size. The influence of confining stress on permeability increases with decreasing permeability. Figures 4.3.9 through 11 show that confining stress has little influence on pore size or capillary pressure in the higher-permeability rocks and the influence increases with decreasing rock permeability. Although permeability is treated as the independent variable because it is a convenient variable to measure and is the abscissa in Figures 4.3.9-11, permeability is actually the dependent variable and pore size, and its change with confining stress is the independent variable.

The results presented here indicate that capillary pressure measurements on low-permeability sandstones are significantly influenced by confining stress, consistent with observed permeability changes.

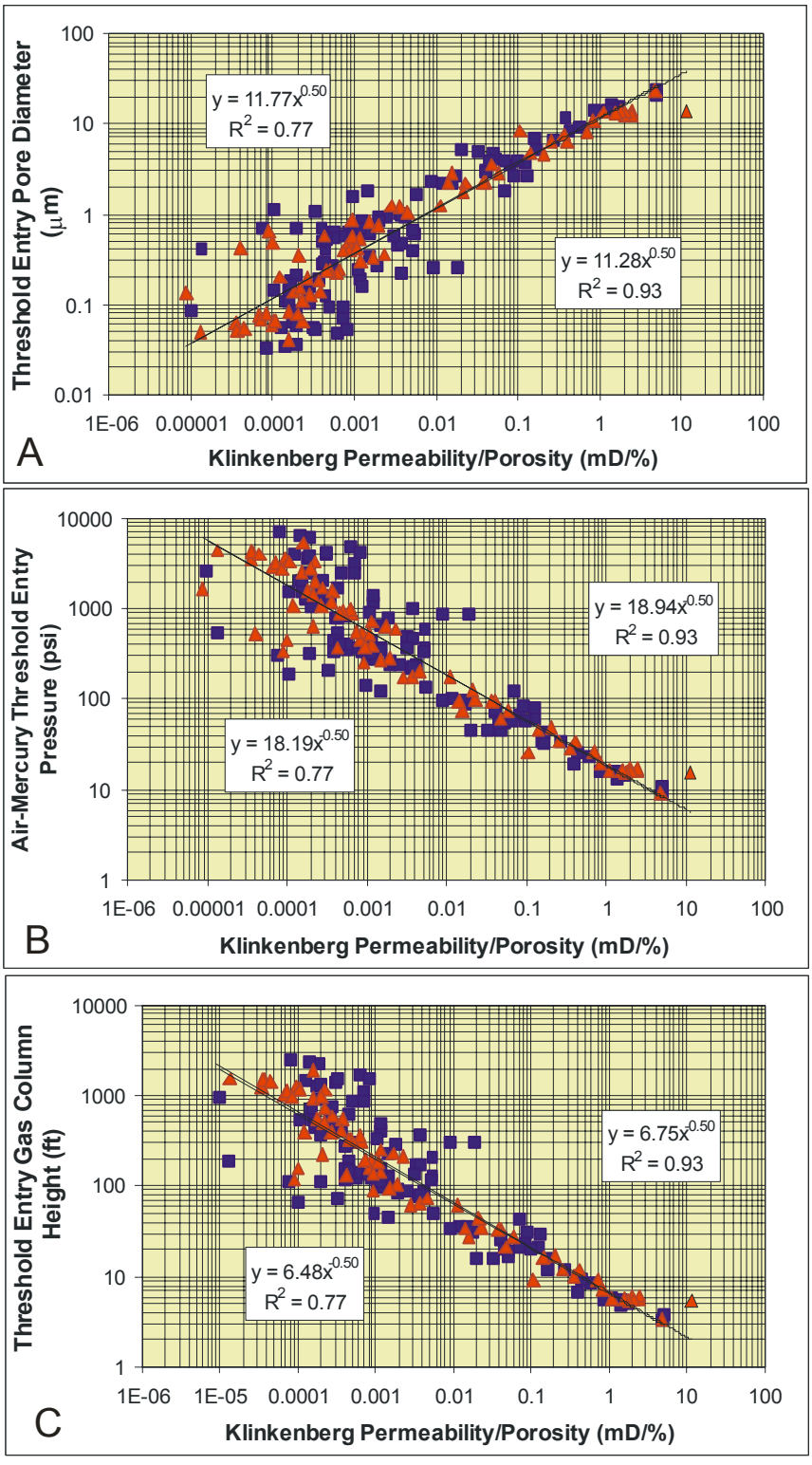

Figure 4.3.10. Crossplot of threshold entry pore diameter (A), air-Hg pressure (B), and gas column height (C), measured by MICP and calculated using equations 4.3.1-4.3.3 in text, versus the ratio of k_{ik}/ϕ_i for *in situ* data (red triangles), and k_{mk}/ϕ_a for unconfined data (blue squares). Variables and stress conditions are discussed in the text.

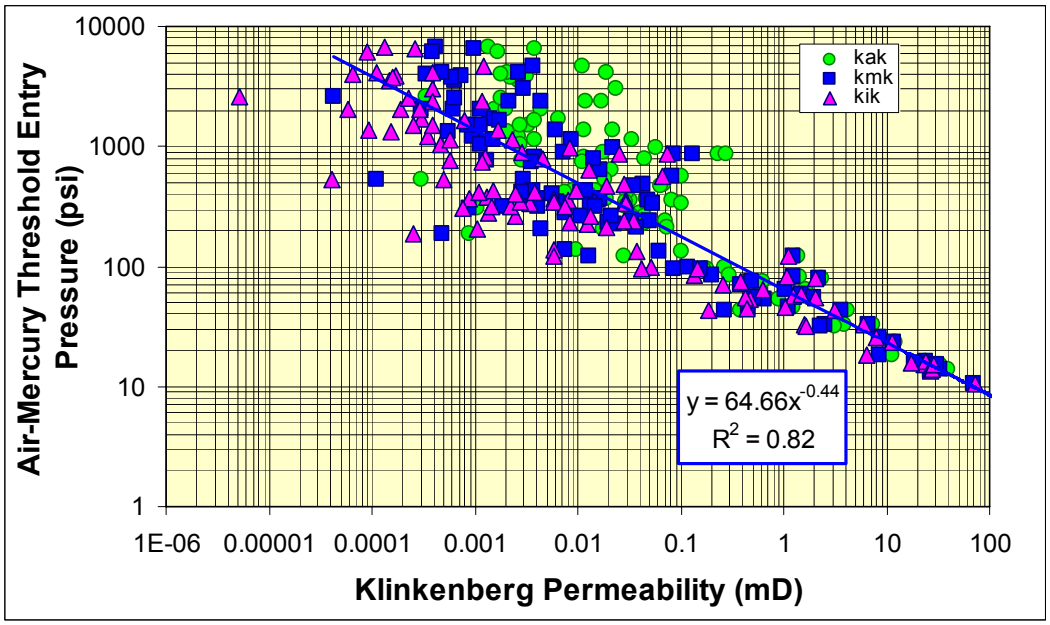

Figure 4.3.11. Crossplot of air-mercury threshold entry pressure versus the routine Klinkenberg permeability (green circles), measured at 600 psi (4.1 MPa) confining stress, *in situ* Klinkenberg permeability (magenta triangles), measured at 4,000 psi (27.6 MPa) confining stress, and the geometric mean of these permeabilities (blue squares).

Subtask 4.4. Measure Electrical Properties

4.4.1 Task Statement

Wireline log determination of water saturation and identification of pay in tight gas sandstones is complicated by the low porosity, argillaceousness, and, in some rocks, the high cation exchange capacity (CEC) of the clays in the sandstones and the low salinity of the formation brines (Kukal et al., 1983). The problems of wireline log analysis in shaly sands is well recognized (Fertl, 1987; Worthington, 1985) and numerous algorithms have been proposed for calculating water saturations in shaly sands including the empirical Simandoux (1963) or Indonesia and Fertl equations and the more theoretical Dual Water and Waxman-Smits models (Waxman and Smits, 1969; Waxman and Thomas, 1974; Clavier, Coats, and Dumanoir, 1984). To calculate water saturation, accurate values of water salinity, porosity exponent, saturation exponent, and cation exchange capacity (if present) are needed. Isolated CEC data are available for Mesaverde (Volk et al., 1979; Gall et al., 1981), but no comprehensive study has been published.

To supplement the published electrical resistivity data and provide data for rocks that are well characterized lithologically, the goal of this task was to measure the electrical resistivity of 150 cores at multiple salinities to be able to determine the cation exchange capacity of the rocks and provide a basis for estimating the Archie porosity exponent at a specified brine salinity. These data would provide a basis on which water saturation can be more accurately calculated from electric wireline log response.

4.4.2 Methods

To measure the Archie exponent from brine-saturated resistivity, the cleaned cores were evacuated for a period of eight (8) hours and then saturated with a deaerated sodium chloride brine solution. The brine concentrations used and the sequence of concentrations are discussed below. After vacuum saturation, complete saturation was obtained by applying a pressure of 1,000 psi (7 MPa) for a period of 24 hours to the saturating brine and samples. Complete saturation was confirmed by agreement between helium-measured porosity and gravimetric-saturation porosity values within 0.1 porosity percent. The cores were left immersed in deaerated brine for a period of 2-8 weeks.

After the cores had reached equilibrium with the brine, each was placed in a biaxial Hassler-type core holder and subjected to a hydrostatic confining stress of 200 psi (1.38 MPa) and a micropipette for effluent fluid set to zero. A schematic of the resistivity apparatus is shown in Figure 4.4.1. The confining stress was then increased to 4,000 psi (27.6 MPa) approximating reservoir stress conditions. Pore volume decrease was determined by measuring the brine displaced from the core by compression using the micropipette, correcting for system compressibility and estimating pore volume change from the sleeve set pressure of 50 psi (0.35 MPa) to 200 psi (1.38 MPa). Pore pressure was at atmospheric pressure. Porosity calculations were performed assuming that the grains of the rock were incompressible, and hence the bulk volume decreased by the same amount as the pore volume. Porosity was referenced to an assumed condition that at 50 psi (0.35 MPa) the pore volume equaled the routine helium pore volume.

Electrical resistivity was measured using a two-electrode configuration with gold-plated end electrodes. Brine-saturated core resistivity at 10 kHz (R_o) was recorded only after the core had achieved equilibrium with the electrical resistivity of the core remaining constant within 0.1% for a three (3) minute period. In general, resistivity equilibrium, including reaching a near constant pore volume compression on the time scale of the resistivity measurement, required 10 ± 5 minutes but approached periods for some cores of one hour. Values were referenced to a temperature of 20°C (68°F). Archie porosity exponents, ***m***, representing the ratio of the logarithm of measured formation resistivity factor ($\log(R_o/R_w)$) and the logarithm of porosity ($\log\phi$) are presented in Table 4.4.1. These porosity exponent values assume an Archie intercept, a = 1, with $R_o/R_w = 1$ at $\phi = 100\%$.

Electrical resistivity measurements were performed on core plugs selected to range widely in geographic location, lithology, porosity, and permeability. To evaluate possible Waxman-Smits cation exchange effects, analyses were performed at 20,000 ppm NaCl (n = 138), 40,000 ppm NaCl (n = 310), 80,000 ppm NaCl (n = 198), and 200,000 ppm NaCl (n = 265). In comparison to high-permeability rocks, achieving a known salinity in low-permeability rocks is experimentally difficult. Low brine permeability does not easily allow flow-through displacement, especially for large numbers of samples. To change sample-pore water salinities, samples were dried at 70°C for several hours and then immersed in a methyl alcohol bath for 24-48 hours. The samples were then soxhlet extracted with methyl alcohol for 3 days, dried, and vacuum/pressure saturated with methyl alcohol and again immersed in the methyl alcohol bath for a minimum of 3 days. The samples were then dried at 70°C in a convection oven for not less

than 24 hours and weighed to confirm that sample weights returned to original pre-saturation weights for clean, dry samples. The samples were then vacuum/pressure saturated, as described above, with the next brine of different salinity and left immersed for 2-8 weeks. For each salinity change this process was repeated.

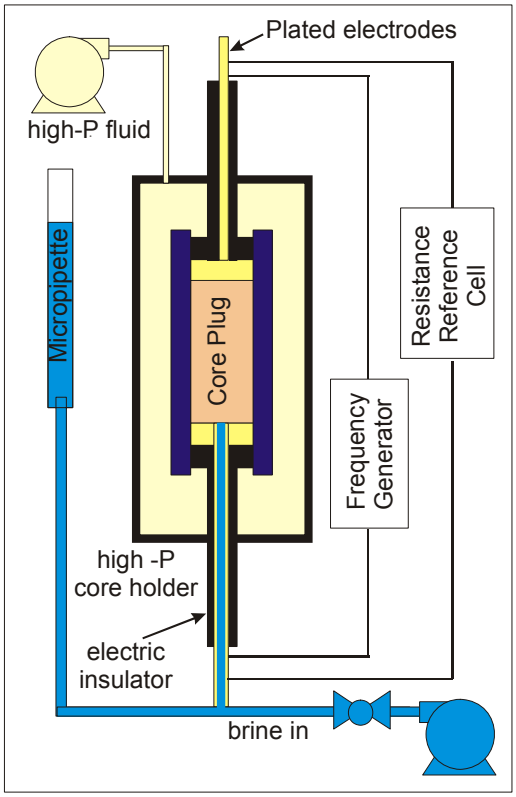

Figure 4.4.1. Schematic of resistivity apparatus.

The sequence of measurements at different salinities varied with each sample due to the long time period over which sample selection and measurements were performed. Early in the program 108 samples were selected and saturated with 200,000 ppmw NaCl to measure a resistivity similar to, though not precisely the same as, a multisalinity-measured, salinity-independent resistivity. A complete suite of 150 samples (as defined by the project design) was not selected because at the time it was known more industry cores would be added to the study. Although equilibrium was established for the 200,000 ppmw NaCl brine, subsequent measurements for two lower-salinity brines did not result in linear core conductivity-brine conductivity relationships indicating that the salinity of the brine in the pores was not as designed or the cores had not reached equilibrium with the lower-salinity brine(s). It was interpreted that removing salt left by high salinity brines was not sufficiently effective for

subsequent constant, known, low-salinity resistivity measurements. For these samples, data are reported for the equilibrium 200,000 ppmw NaCl but subsequent non-equilibrium, low-salinity data are not reported.

To avoid having to remove high concentration of salt for subsequent salinity measurements, new, clean cores were selected and saturated, measured, cleaned, and resaturated, as described above, with brines in the sequence 40,000 ppmw NaCl, 80,000 ppmw NaCl, and 200,000 ppmw NaCl brine. By sequentially increasing in brine salinity, minor remnant salt not removed by the cleaning process would increase the salinity of the subsequent brine but represented a negligible change in salinity of the higher-salinity brine.

Subsequent to the analysis of the cores above, it was decided that measurements should be conducted at lower salinities. A new set of cores were selected and were saturated, measured, cleaned, and resaturated, as described above with brines in the sequence 20,000 ppmw NaCl, 40,000 ppmw NaCl, and 80,000 ppmw NaCl brine.

4.4.3 Results

4.4.3.1 Archie Porosity Exponent versus Porosity

A total of 907 resistivity measurements were performed at various salinities (Table 4.4.1). These data provided a basis for examining in more depth the relationship between the Archie porosity exponent and porosity. The estimation of water saturation in sandstones is commonly performed using the empirical relation developed by Archie (1940), known as Archie's Law:

$$S_w = [(a*R_w)/(\phi^{\boldsymbol{m}} * R_t)]^{1/\boldsymbol{n}} \qquad [4.4.1]$$

Where; S_w = water saturation (fraction), a = Archie cementation intercept, R_w = water resistivity (ohm-m), R_t = formation resistivity (ohm-m), ϕ = porosity (fraction), ***m*** = Archie porosity exponent, and ***n*** = Archie saturation exponent.

This relation implicitly assumes that the rock matrix is nonconductive and that the brine with resistivity Rw, is the single electrical conductor within a nonconductive matrix. Guyod (1944) termed ***m*** the "cementation exponent" because it often increases with increased cementation. The more general term for ***m***, porosity exponent, is used here due to porosity exponent-porosity relations shown below. Models exist that account for multiple conducting

phases. The generalized model of Glover et al. (2000) models two conducting phases of any volume fraction and connection distribution. Waxman and Smits (1969) and others (Waxman and Thomas, 1974; Clavier, Coats, and Dumanoir, 1984) proposed modification of the Archie equation to model conductive solids, and excess conductivity related to elevated salinity near charged clay surfaces along pore walls resulting from the cation exchange capacity of the clay surfaces:

$$S_w = [(F^*R_w)/R_t(1+ R_wBQ_v/S_w)]1/n^* \qquad [4.4.2]$$

Where F* = salinity/clay conductivity independent formation factor, Qv = cation exchange capacity of the core (meq/cc), B = specific counter-ion activity [(equiv/l)/(ohm-m)], and ***n**** = saturation exponent free of excess conductivity. This equation is similar to the Archie equation but includes an additional term for the conductivity associated with the exchange cations. This can also be written as

$$S_w = \sqrt[n^*]{\frac{\frac{a^*}{\phi^{m^*}} R_w}{R_t\left(1+\frac{R_wBQ_v}{S_w}\right)}} \qquad [4.4.3]$$

Where the F* term (intrinsic formation factor; free of excess conductivity) has been replaced by a^*/ϕ^{m^*}.

Although the models presented in equations 4.4.2 and 4.43 work well for many rocks, it is important to note that these are empirical models and do not present a fundamental physical-chemical relationship.

Figure 4.4.2 shows the individual Archie porosity exponent values for all samples sorted by brine salinity. The data for all salinities exhibit a significant change in the m vs ϕ relationship for samples with porosity less than approximately 6-8% compared with those with porosity greater than 6-8%. Archie porosity exponents for rocks with $\phi > 8\%$ range from $1.7 < \boldsymbol{m} < 2.2$, which are values commonly reported for consolidated sandstones. Archie porosity exponents for rocks with $\phi < 8\%$ exhibit a strong correlation with ***m*** decreasing with decreasing porosity and approaching a value of $1.0 < \boldsymbol{m} < 1.2$ at $\phi = 0$.

Table 4.4.1.

Summary Multisalinity Archie Porosity Exponent Data
Analysis of Critical Permeability, Capillary Pressure and Electrical Properties for Mesaverde Tight Gas Sandstones from Western U.S. Basins
US DOE # DE-FC26-05NT42660
Alan P. Byrnes, Robert M. Cluff, John C. Webb, Danial A. Krygowski, Stefani D. Whittaker
website: http://www.kgs.ku.edu/mesaverde

											20K ppm brine salinity			40K ppm brine salinity			80K ppm brine salinity			200K ppm brine salinity		
										brine salinity (Kppm) >		20			40			80			200	
										Cw (mhos) >		3.02			5.73			10.50			20.4	
										Rw (ohmm) >		0.331			0.17452			0.09524			0.049	
USGS Library Number	Basin	API Number	Well Name	Operator	depth	A/B /C	Rock Type Code	Routine Porosity	In situ Porosity	In situ Klinkenberg Gas Perameability	Formation Resistivity Factor	Co	Archie Porosity Exponent, m in situ	Formation Resistivity Factor	Co	Archie Porosity Exponent, m in situ	Formation Resistivity Factor	Co	Archie Porosity Exponent, m in situ	Formation Resistivity Factor	Co	Archie Porosity Exponent, m in situ
					ft			%	%	mD	Ro/Rw	= 1 / Ro	m, A=1	Ro/Rw	= 1 / Ro	m, A=1	Ro/Rw	= 1 / Ro	m, A=1	Ro/Rw	= 1 / Ro	m, A=1
B029	Green River	4903520088	A-1 WASP	INEXCO OIL COMPANY	10537.2	A	13256	3.5	3.3	0.000190	186.9	0.0162	1.53	252.8	0.0227	1.62						
B029	Green River	4903520088	A-1 WASP	INEXCO OIL COMPANY	10573.1	B	13266	3.1	2.7	0.000201										445.4		1.69
B029	Green River	4903520088	A-1 WASP	INEXCO OIL COMPANY	11332.9	A	16286	3.5	3.2	0.000728				286.1	0.0200	1.65	453.8	0.0231	1.78	532.9		1.83
B029	Green River	4903520088	A-1 WASP	INEXCO OIL COMPANY	11332.9	C	16286	3.6	3.3	0.000832	258.4	0.0117	1.63	327.8	0.0175	1.70	443.5	0.0237	1.79			
B029	Green River	4903520088	A-1 WASP	INEXCO OIL COMPANY	11374.9	B	14296	0.5	0.3	0.000018	301.8	0.0100	0.99	490.1	0.0117	1.08	753.8	0.0139	1.15			
B029	Green River	4903520088	A-1 WASP	INEXCO OIL COMPANY	11443.7	A	15276	2.8	2.4	0.000322										637.8		1.74
B029	Green River	4903520088	A-1 WASP	INEXCO OIL COMPANY	11443.8	A	15276	3.1	2.9	0.000681				298.3	0.0192	1.61				638.6		1.83
B029	Green River	4903520088	A-1 WASP	INEXCO OIL COMPANY	11443.8	B	15276	6.6	6.2	0.00178	298.3	0.0101	2.05	329.2	0.0174	2.08	382.6	0.0274	2.14			
B029	Green River	4903520088	A-1 WASP	INEXCO OIL COMPANY	11447.8	A	19276	4.8	4.3	0.00163										275.2		1.79
B029	Green River	4903520088	A-1 WASP	INEXCO OIL COMPANY	11450.2	B	15226	4.7	4.3	0.00684	242.0	0.0125	1.75	272.6	0.0210	1.79						
B029	Green River	4903520088	A-1 WASP	INEXCO OIL COMPANY	11457.8	A	15226	4.4	3.9	0.00271										420.6		1.87
B029	Green River	4903520088	A-1 WASP	INEXCO OIL COMPANY	11457.9	A	15226	5.5	5.0	0.000110										465.8		2.05
B029	Green River	4903520088	A-1 WASP	INEXCO OIL COMPANY	11459.1	A	15296	5.4	4.8	0.000827				257.9	0.0222	1.83	360.9	0.0291	1.94	430.9		2.00
B029	Green River	4903520088	A-1 WASP	INEXCO OIL COMPANY	11459.2	A	15296	4.5	4.0	0.00184										433.1		1.89
B029	Green River	4903520088	A-1 WASP	INEXCO OIL COMPANY	11460.5	A	13286	4.4	3.5	0.1324				260.4	0.0220	1.66				395.3		1.79
B029	Green River	4903520088	A-1 WASP	INEXCO OIL COMPANY	11474.5	B	13276	2.6	2.3	0.000407				366.3	0.0156	1.56				981.1		1.82
B029	Green River	4903520088	A-1 WASP	INEXCO OIL COMPANY	11474.5	C	13276	2.8	2.5	0.00146	293.7	0.0103	1.55	418.5	0.0137	1.64						
B029	Green River	4903520088	A-1 WASP	INEXCO OIL COMPANY	11515.1	A	14296	0.7	0.5	0.0000001				505.4	0.0113	1.16						
B029	Green River	4903520088	A-1 WASP	INEXCO OIL COMPANY	11530.7	A	12296	0.6	0.4	0.000023										614.8		1.15
B029	Green River	4903520088	A-1 WASP	INEXCO OIL COMPANY	11534.0	B	14296	1.5	1.3	0.000137	195.2	0.0155	1.21	280.6	0.0204	1.29	351.0	0.0299	1.35			
B029	Green River	4903520088	A-1 WASP	INEXCO OIL COMPANY	11534.2	A	14296	1.7	1.3	0.000043				260.3	0.0220	1.29	338.0	0.0311	1.35	618.7		1.49
B029	Green River	4903520088	A-1 WASP	INEXCO OIL COMPANY	11548.0	C	13246	5.8	5.5	0.00100				169.0	0.0339	1.77	240.0	0.0438	1.89	321.5		1.99
B029	Green River	4903520088	A-1 WASP	INEXCO OIL COMPANY	11548.0	A	13246	5.1	4.8	0.00112				168.8	0.0339	1.69				275.6		1.85
B029	Green River	4903520088	A-1 WASP	INEXCO OIL COMPANY	11550.0	A	15226	5.3	5.2	0.000756				169.7	0.0338	1.73	207.4	0.0506	1.80	296.5		1.92
B029	Green River	4903520088	A-1 WASP	INEXCO OIL COMPANY	11550.2	A	15226	5.1	4.9	0.000389				178.8	0.0321	1.71	227.7	0.0461	1.79	286.3		1.87
B029	Green River	4903520088	A-1 WASP	INEXCO OIL COMPANY	11552.3	A	15276	3.9	3.6	0.000659				356.2	0.0161	1.77	600.6	0.0175	1.93	779.6		2.00
B029	Green River	4903520088	A-1 WASP	INEXCO OIL COMPANY	11578.2	C	13266	0.2	0.1	0.000002										1617.0		1.07
B029	Green River	4903520088	A-1 WASP	INEXCO OIL COMPANY	11587.2	A	13267	3.5	3.3	0.000902				223.2	0.0257	1.58	271.7	0.0386	1.64	330.0		1.69
B029	Green River	4903520088	A-1 WASP	INEXCO OIL COMPANY	11592.7	B	13257	4.7	4.5	0.000227				152.3	0.0376	1.62	199.5	0.0526	1.70	313.2		1.85
B029	Green River	4903520088	A-1 WASP	INEXCO OIL COMPANY	11609.1	A	15276	5.9	5.4	0.00772										365.2		2.02
B029	Green River	4903520088	A-1 WASP	INEXCO OIL COMPANY	11609.2	A	15276	5.3	4.6	0.00475				216.7	0.0264	1.75				405.0		1.95
B029	Green River	4903520088	A-1 WASP	INEXCO OIL COMPANY	11615.1	A	15276	4.6	4.0	0.00192				230.0	0.0249	1.68				485.8		1.92
B029	Green River	4903520088	A-1 WASP	INEXCO OIL COMPANY	11705.5	A	15276	3.2	2.8	0.000520				270.3	0.0212	1.57				417.6		1.69
B029	Green River	4903520088	A-1 WASP	INEXCO OIL COMPANY	11706.7	A	16276	4.0	3.8	0.000524				237.4	0.0241	1.67				496.5		1.89
B029	Green River	4903520088	A-1 WASP	INEXCO OIL COMPANY	11706.9	A	16276	3.8	3.4	0.000405										501.1		1.84
B029	Green River	4903520088	A-1 WASP	INEXCO OIL COMPANY	11716.1	B	16276	4.1	3.9	0.000431				300.4	0.0191	1.76				683.3		2.01
B029	Green River	4903520088	A-1 WASP	INEXCO OIL COMPANY	11716.1	A	16276	3.8	3.5	0.000562				307.0	0.0187	1.71				497.0		1.86
B029	Green River	4903520088	A-1 WASP	INEXCO OIL COMPANY	11721.9	A	16296	4.4	3.9	0.000320										481.3		1.91
B029	Green River	4903520088	A-1 WASP	INEXCO OIL COMPANY	11722.0	A	16296	4.3	3.9	0.000447										442.5		1.87
B029	Green River	4903520088	A-1 WASP	INEXCO OIL COMPANY	11724.2	A	16296	3.7	3.5	0.000863				289.4	0.0198	1.68	501.3	0.0209	1.85	631.8		1.92
B029	Green River	4903520088	A-1 WASP	INEXCO OIL COMPANY	11724.3	B	16296	4.1	3.7	0.000585	232.3	0.0130	1.65	296.6	0.0193	1.72						
B029	Green River	4903520088	A-1 WASP	INEXCO OIL COMPANY	11727.5	A	19296	2.6	2.4	0.000295				511.2	0.0112	1.67				928.2		1.83
B029	Green River	4903520088	A-1 WASP	INEXCO OIL COMPANY	11728.6	A	16296	1.3	1.0	0.000004										1365.9		1.58
B029	Green River	4903520088	A-1 WASP	INEXCO OIL COMPANY	11739.0	A	15276	4.5	3.9	0.00158				235.6	0.0243	1.69	397.9	0.0264	1.85	449.7		1.89
B029	Green River	4903520088	A-1 WASP	INEXCO OIL COMPANY	11758.3	A	15286	4.7	3.7	0.000470				351.8	0.0163	1.77	419.6	0.0250	1.83	512.3		1.89
B029	Green River	4903520088	A-1 WASP	INEXCO OIL COMPANY	11758.4	A	15296	4.6	3.6	0.00110				352.8	0.0162	1.77	395.4	0.0266	1.80	494.1		1.87
E712	Green River	4903506020	B-54 BIG PINEY	BELCO PETROLEUM	3403.9	A	13256	16.7	15.3	1.20	29.9	0.1010	1.81	36.8	0.1556	1.92						
E712	Green River	4903506020	B-54 BIG PINEY	BELCO PETROLEUM	3431.9	B		17.5	15.8	15.7	27.9	0.1083	1.80	30.6	0.1870	1.85	32.4	0.3244	1.88			
E712	Green River	4903506020	B-54 BIG PINEY	BELCO PETROLEUM	3433.9	A	15585	17.2	15.4	24.5	26.5	0.1139	1.75	29.6	0.1933	1.81						
E712	Green River	4903506020	B-54 BIG PINEY	BELCO PETROLEUM	3461.6	A	15585	18.3	16.6	27.5	24.9	0.1211	1.79	26.8	0.2136	1.83	28.5	0.3685	1.87			
E712	Green River	4903506020	B-54 BIG PINEY	BELCO PETROLEUM	3461.7	A	15585	17.9	16.5	2.42				29.3	0.1954	1.87	30.9	0.3395	1.90	32.3		1.93
E712	Green River	4903506020	B-54 BIG PINEY	BELCO PETROLEUM	3462.0	A	15585	18.8	17.5	26.8										27.9		1.91
E712	Green River	4903506020	B-54 BIG PINEY	BELCO PETROLEUM	3480.8	A	13265	8.9	8.3	0.00580	76.8	0.0393	1.75	106.6	0.0538	1.88	119.9	0.0876	1.92			
E712	Green River	4903506020	B-54 BIG PINEY	BELCO PETROLEUM	3503.7	B	12219	8.8	8.1	0.000792										117.8		1.89
E712	Green River	4903506020	B-54 BIG PINEY	BELCO PETROLEUM	3511.8	A	15575	13.1	12.1	0.7063				63.3	0.0905	1.96				66.5		1.99
E712	Green River	4903506020	B-54 BIG PINEY	BELCO PETROLEUM	3519.3	B		16.1	14.9	6.02										42.1		1.97
E712	Green River	4903506020	B-54 BIG PINEY	BELCO PETROLEUM	3519.3	A		16.3	15.2	6.81	36.3	0.0831	1.91	36.3	0.1578	1.90						
E894	Green River	4903520622	1 OLD ROAD	AMERICAN HUNTER EXPL	11897.3	A	12245	5.2	4.8	0.000995	152.6	0.0198	1.65	222.1	0.0258	1.78	292.4	0.0359	1.87			
E894	Green River	4903520622	1 OLD ROAD	AMERICAN HUNTER EXPL	11915.2	B	15295	8.4	8.0	0.00372	82.7	0.0365	1.75	122.3	0.0468	1.90						
E894	Green River	4903520622	1 OLD ROAD	AMERICAN HUNTER EXPL	11921.8	A	15218	5.0	4.6	0.000271				147.8	0.0388	1.62	229.7	0.0457	1.77	275.4		1.83
E894	Green River	4903520622	1 OLD ROAD	AMERICAN HUNTER EXPL	11923.3	A	13218	4.1	3.7	0.00644				479.8	0.0119	1.87				913.3		2.07
E894	Green River	4903520622	1 OLD ROAD	AMERICAN HUNTER EXPL	11927.8	A	15586	11.3	10.5	0.00925	70.0	0.0432	1.89	74.0	0.0775	1.91	93.7	0.1121	2.02			
E894	Green River	4903520622	1 OLD ROAD	AMERICAN HUNTER EXPL	11956.1	A	15586	8.5	7.8	0.00792										155.3		1.98
R780	Green River	4903505742	C-47 TIP TOP SHALLOW	BELCO PETROLEUM	2699.8	B	15596	21.2	19.7	28.2	19.7	0.1536	1.83	19.8	0.2896	1.84	20.6	0.5099	1.86			
R780	Green River	4903505742	C-47 TIP TOP SHALLOW	BELCO PETROLEUM	2754.7	B	16575	20.7	18.7	1.29	22.2	0.1362	1.85	22.3	0.2565	1.85	22.8	0.4597	1.87			
R780	Green River	4903505742	C-47 TIP TOP SHALLOW	BELCO PETROLEUM	2754.7	A	16575	21.3	19.8	1.90										23.9		1.96
R780	Green River	4903505742	C-47 TIP TOP SHALLOW	BELCO PETROLEUM	2759.9	A	15275	9.1	8.8	0.000708	87.3	0.0346	1.84	101.7	0.0563	1.91	142.1	0.0739	2.04			
R780	Green River	4903505742	C-47 TIP TOP SHALLOW	BELCO PETROLEUM	2783.3	A	15595	22.3	20.7	23.3										20.8		1.93
R780	Green River	4903505742	C-47 TIP TOP SHALLOW	BELCO PETROLEUM	2783.4	A	15595	22.3	20.7	21.5	17.2	0.1751	1.81	21.2	0.2704	1.94						
R780	Green River	4903505742	C-47 TIP TOP SHALLOW	BELCO PETROLEUM	2817.7	A	15575	20.1	18.7	2.12										25.8		1.94
R780	Green River	4903505742	C-47 TIP TOP SHALLOW	BELCO PETROLEUM	2831.8	A	15285	23.6	22.2	2.73				22.8	0.2513	2.08	22.2	0.4727	2.06	22.7		2.08
R780	Green River	4903505742	C-47 TIP TOP SHALLOW	BELCO PETROLEUM	2831.9	B	15285	20.4	19.0	3.22				21.6	0.2649	1.85	22.9	0.4583	1.89	23.4		1.90
R780	Green River	4903505742	C-47 TIP TOP SHALLOW	BELCO PETROLEUM	2845.5	B	15577	22.0	20.6	6.34	16.3	0.1859	1.76	17.1	0.3348	1.80	18.2	0.5771	1.83			
R780	Green River	4903505742	C-47 TIP TOP SHALLOW	BELCO PETROLEUM	2845.5	A	15577	22.6	21.0	8.69										18.8		1.88
S873	Green River	4903506200	K-2 MASON	BELCO PETROLEUM	6989.8	A	15275	10.7	9.9	0.1383										85.9		1.92
S873	Green River	4903506200	K-2 MASON	BELCO PETROLEUM	7703.8	A	16295	12.1	11.2	0.2386	60.2	0.0502	1.87	63.9	0.0897	1.90						
S873	Green River	4903506200	K-2 MASON	BELCO PETROLEUM	9393.3	A	12235	3.4	3.0	0.000024										506.5		1.78
S873	Green River	4903506200	K-2 MASON	BELCO PETROLEUM	9393.5	A	13265	2.7	2.6	0.000054	242.1	0.0125	1.51	402.1	0.0143	1.64	499.5	0.0210	1.70			
S873	Green River	4903506200	K-2 MASON	BELCO PETROLEUM	9397.3	A	15286	8.4	8.3	0.000358				169.4	0.0338	2.06						
SHELL Vible	Green River	4903523799	VIBLE 1D-11D	SHELL E&P	12507.1	A	15287	5.1	5.0	0.000627				378.8	0.0151	1.98						
SHELL Vible	Green River	4903523799	VIBLE 1D-11D	SHELL E&P	12508.7	A	15275	3.0	2.6	0.000219				708.0	0.0081	1.80	603.6	0.0174	1.75			
SHELL Vible	Green River	4903523799	VIBLE 1D-11D	SHELL E&P	12518.5	A	15217	5.9	5.5	0.00172	215.1	0.0140	1.85	270.3	0.0212	1.93	339.8	0.0309	2.00			
SHELL Vible	Green River	4903523799	VIBLE 1D-11D	SHELL E&P	12529.0	A	13266	1.4	1.2	0.000025				553.3	0.0104	1.42						
T195	Green River	4903508024	5 PINEDALE	EL PASO NATURAL GAS	12158.5	A	13276	11.0	10.1	0.0167										116.6		2.08
T195	Green River	4903508024	5 PINEDALE	EL PASO NATURAL GAS	12159.5	A	16295	9.3	8.5	0.000003										209.8		2.17
T195	Green River	4903508024	5 PINEDALE	EL PASO NATURAL GAS	12159.6	A	16295	9.0	7.8	0.0111	137.6	0.0220	1.93	167.0	0.0343	2.00	193.4	0.0543	2.06			
T195	Green River	4903508024	5 PINEDALE	EL PASO NATURAL GAS	12161.5	B	16275	6.5	6.3	0.000361	249.4	0.0121	1.99	298.2	0.0192	2.06	361.4	0.0291	2.13			
T195	Green River	4903508024	5 PINEDALE	EL PASO NATURAL GAS	12162.0	A	16275	7.2	6.6	0.000796										383.3		2.18
T204	Green River	4903705349	B-2A SPIDER CREEK	HUMBLE OIL & REF	9022.9	A	16295	12.1	11.0	10.2	56.3	0.0537	1.82	61.8	0.0928	1.86	62.4	0.1682	1.87			
T204	Green River	4903705349	B-2A SPIDER CREEK	HUMBLE OIL & REF	9041.1	A	16296	11.6	10.7	1.82										68.6		1.89
T204	Green River	4903705349	B-2A SPIDER CREEK	HUMBLE OIL & REF	9063.0	A	17596	15.2	13.0	206	36.9	0.0818	1.77	37.4	0.1531	1.77	36.4	0.2884	1.76			
T204	Green River	4903705349	B-2A SPIDER CREEK	HUMBLE OIL & REF	9098.0	A	13286	6.6	5.4	0.0188	94.5	0.0320	1.56	136.8	0.0419	1.68	163.8	0.0641	1.74			
B43C	Piceance	0504511402	LAST DANCE 43C-3-792	BILL BARRETT CORP.	3544.8	C		10.5	9.6	0.3923	61.2	0.0493	1.76	93.3	0.0614	1.94						
B43C	Piceance	0504511402	LAST DANCE 43C-3-792	BILL BARRETT CORP.	3577.6	A		1.8	1.7	0.000062	344.6	0.0088	1.43	481.6	0.0119	1.51	690.6	0.0152	1.60			
B43C	Piceance	0504511402	LAST DANCE 43C-3-792	BILL BARRETT CORP.	3970.0	B		0.9	0.8	0.000088	449.7	0.0067	1.27	519.7	0.0110	1.30	733.3	0.0143	1.38			
B43C	Piceance	0504511402	LAST DANCE 43C-3-792	BILL BARRETT CORP.	3992.5	C		3.0	2.7	0.000576	162.8	0.0186	1.41	184.5	0.0311	1.45						
B43C	Piceance	0504511402	LAST DANCE 43C-3-792	BILL BARRETT CORP.	4013.3	B		12.9	11.9	0.1898	61.9	0.0488	1.94	74.7	0.0767	2.02						
B43C	Piceance	0504511402	LAST DANCE 43C-3-792	BILL BARRETT CORP.	4393.6	A		8.7	7.8	0.00652	76.7	0.0394	1.70	87.1	0.0658	1.75						
B43C	Piceance	0504511402	LAST DANCE 43C-3-792	BILL BARRETT CORP.	5715.4	B		7.6	6.9	0.00334	74.0	0.0408	1.61	128.0	0.0447	1.81						
B43C	Piceance	0504511402	LAST DANCE 43C-3-792	BILL BARRETT CORP.	6042.4	A		5.4	5.1	0.000854	109.8	0.0275	1.58	137.4	0.0417	1.65						
B43C	Piceance	0504511402	LAST DANCE 43C-3-792	BILL BARRETT CORP.	6337.1	C		3.8	3.4	0.000212	140.6	0.0215	1.46	227.0	0.0252	1.60						
E436	Piceance	0504506571	MV 33-34	BARRETT ENERGY	6579.5	B	13226	5.8	5.5	0.000363	114.6	0.0264	1.63	155.0	0.0370	1.73						
E436	Piceance	0504506571	MV 33-34	BARRETT ENERGY	6579.5	A	13226	7.5	7.3	0.00044				112.5	0.0509	1.80	180.7	0.0581	1.99	229.8		2.08
E436	Piceance	0504506571	MV 33-34	BARRETT ENERGY	6579.8	A	13268	5.3	4.7	0.000247	118.9	0.0254	1.57	157.0	0.0365	1.66	198.1	0.0530	1.73			
E436	Piceance	0504506571	MV 33-34	BARRETT ENERGY	6579.8	B	13268	5.6	5.4	0.000742				159.7	0.0359	1.74	184.4	0.0569	1.79	214.0		1.84
E436	Piceance	0504506571	MV 33-34	BARRETT ENERGY	6580.1	A	13268	5.3	4.8	0.000579				196.9	0.0291	1.74	207.1	0.0507	1.76	220.7		1.78
E436	Piceance	0504506571	MV 33-34	BARRETT ENERGY	6582.0	A	14266	3.8	3.6	0.000479	139.6	0.0216	1.48	183.2	0.0313	1.56	254.2	0.0413	1.66			
E436	Piceance	0504506571	MV 33-34	BARRETT ENERGY	6582.3	A	14266	5.2	5.0	0.000377				143.6	0.0399	1.66	204.7	0.0513	1.78	239.4		1.83
E436	Piceance	0504506571	MV 33-34	BARRETT ENERGY	6591.9	A	13266	2.4	2.3	0.000711				167.7	0.0342	1.36	203.7	0.0516	1.41	370.4		1.57
E436	Piceance	0504506571	MV 33-34	BARRETT ENERGY	6592.5	A	12246	2.6	2.2	0.000163	128.6	0.0235	1.28	186.4	0.0307	1.38	264.5	0.0397	1.47			
E458	Piceance	0510309406	M-30-2-96W /D-037934	FUEL RESOURCES DEV	6379.5	A	13246	3.8	3.6	0.000303	170.1	0.0178	1.54	214.7	0.0267	1.61	279.6	0.0376	1.69			
E458	Piceance	0510309406	M-30-2-96W /D-037934	FUEL RESOURCES DEV	6508.3	A	13286	9.1	8.2	0.0180	97.5	0.0310	1.83	111.4	0.0514	1.88	120.4	0.0872	1.91			
E458	Piceance	0510309406	M-30-2-96W /D-037934	FUEL RESOURCES DEV	6509.4	A	14286	10.8	10.2	0.0269	87.2	0.0347	1.96	93.4	0.0614	1.99	114.0	0.0921	2.08			
PA424	Piceance	0504510927	Williams PA-424-34	WILLIAMS E&P	4574.6	A		4.7	4.4	0.00279	154.9	0.0195	1.61	181.4	0.0316	1.66	203.2	0.0517	1.70			
PA424	Piceance	0504510927	Williams PA-424-34	WILLIAMS E&P	4600.3	A	15297	12.2	11.3	0.00188										146.6		2.28
PA424	Piceance	0504510927	Williams PA-424-35	WILLIAMS E&P	4635.4	A		2.4	2.1	0.000771	110.9	0.0272	1.22	156.2	0.0367	1.31	228.2	0.0460	1.41			
PA424	Piceance	0504510927	Williams PA-424-36	WILLIAMS E&P	4651.6	A		6.7	6.2	0.0134	83.5	0.0362	1.59	124.4	0.0461	1.73	158.4	0.0663	1.82			
PA424	Piceance	0504510927	Williams PA-424-37	WILLIAMS E&P	4660.4	A	16286	7.0	6.4	0.00357										278.9		2.05
PA424	Piceance	0504510927	Williams PA-424-38	WILLIAMS E&P	4686.4	A	15286	7.9	7.1	0.00311				126.4	0.0453	1.83	202.7	0.0518	2.01	227.5		2.05
PA424	Piceance	0504510927	Williams PA-424-39	WILLIAMS E&P	4691.5	A	16296	13.3	12.3	0.00687										117.2		2.27
PA424	Piceance	0504510927	Williams PA-424-40	WILLIAMS E&P	4696.5	A		10.8	10.2	0.00307	54.1	0.0559	1.75	72.9	0.0786	1.88	84.7	0.1240	1.94			
PA424	Piceance	0504510927	Williams PA-424-41	WILLIAMS E&P	5140.5	A	16296	11.6	10.7	0.0251										133.2		2.19
PA424	Piceance	0504510927	Williams PA-424-42	WILLIAMS E&P	5142.5	A	16286	8.3	7.6	0.00844	81.2	0.0372	1.71	100.6	0.0570	1.79	133.7	0.0785	1.90			
PA424	Piceance	0504510927	Williams PA-424-43	WILLIAMS E&P	5185.6	A	15286	6.6	6.0					121.4	0.0472	1.70	179.5	0.0585	1.84	188.5		1.86
PA424	Piceance	0504510927	Williams PA-424-44	WILLIAMS E&P	5192.7	A		7.9	7.1	0.00936	104.9	0.0288	1.76	137.9	0.0416	1.86	156.1	0.0673	1.91			
PA424	Piceance	0504510927	Williams PA-424-45	WILLIAMS E&P	6146.5	A	16276	9.4	8.9	0.00580	64.1	0.0471	1.72	81.0	0.0707	1.81	106.3	0.0988	1.93			
PA424	Piceance	0504510927	Williams PA-424-46	WILLIAMS E&P	6148.6	A	15276	9.9	9.3	0.00761				97.0	0.0591	1.93				130.7		2.05
PA424	Piceance	0504510927	Williams PA-424-47	WILLIAMS E&P	6152.5	A	13278	9.5	8.9	0.00567				85.8	0.0668	1.84	99.8	0.1052	1.90	137.7		2.03
PA424	Piceance	0504510927	Williams PA-424-48	WILLIAMS E&P	6599.5	A	13266	7.8	7.5	0.00155				94.1	0.0609	1.75	137.1	0.0766	1.90	182.6		2.01
PA424	Piceance	0504510927	Williams PA-424-49	WILLIAMS E&P	6632.8	A		3.5	3.3	0

Table 4.4.1.

Summary Multisalinity Archie Porosity Exponent Data
Analysis of Critical Permeability, Capillary Pressure and Electrical Properties for Mesaverde Tight Gas Sandstones from Western U.S. Basins
US DOE # DE-FC26-05NT42660
Alan P. Byrnes, Robert M. Cluff, John C. Webb, Danial A. Krygowski, Stefani D. Whittaker
website: http://www.kgs.ku.edu/mesaverde

											20K ppm brine salinity			40K ppm brine salinity			80K ppm brine salinity			200K ppm brine salinity		
										brine salinity (Kppm) >	20			40			80			200		
										Cw (mhos) >	3.02			5.73			10.50			20.4		
										Rw (ohmm) >	0.331			0.17452			0.09524			0.049		
USGS Library Number	Basin	API Number	Well Name	Operator	depth	A/B /C	Rock Type Code	Routine Porosity	In situ Porosity	In situ Klinkenberg Gas Peremeability	Formation Resistivity Factor	Co	Archie Porosity Exponent, m in situ	Formation Resistivity Factor	Co	Archie Porosity Exponent, m in situ	Formation Resistivity Factor	Co	Archie Porosity Exponent, m in situ	Formation Resistivity Factor	Co	Archie Porosity Exponent, m in situ
					ft			%	%	mD	Ro/Rw	= 1 / Ro	m, A=1	Ro/Rw	= 1 / Ro	m, A=1	Ro/Rw	= 1 / Ro	m, A=1	Ro/Rw	= 1 / Ro	m, A=1
R091	Piceance	05045XXXX4	BOOK CLIFFS 1	USGS-CG	213.0	A	12293	6.4	4.9	0.000225	67.3	0.0449	1.40	92.9	0.0617	1.50						
R091	Piceance	05045XXXX4	BOOK CLIFFS 1	USGS-CG	242.4	A	13219	6.7	6.4	0.000164				74.0	0.0775	1.57				83.6		1.61
R091	Piceance	05045XXXX4	BOOK CLIFFS 1	USGS-CG	255.8	A	15567	24.9	23.4	112	14.1	0.2150	1.82	14.6	0.3922	1.85	14.8	0.7078	1.86			
R091	Piceance	05045XXXX4	BOOK CLIFFS 1	USGS-CG	256.5	A	13258	11.0	10.0	0.000082	60.3	0.0501	1.78	72.8	0.0787	1.86	77.3	0.1358	1.89			
R091	Piceance	05045XXXX4	BOOK CLIFFS 1	USGS-CG	257.3	A	11219	6.9	6.3	* 0.000167										75.3		1.56
R091	Piceance	05045XXXX4	BOOK CLIFFS 1	USGS-CG	387.3	A	12219	9.6	8.8	* 0.000985										51.7		1.62
R091	Piceance	05045XXXX4	BOOK CLIFFS 1	USGS-CG	512.2	A	12236	10.6	9.8	* 0.00904										61.8		1.77
S905	Piceance	05103XXXX3	21011-5 MOON LAKE	WESTERN FUELS ASSOC	788.0	A	13225	1.9	1.6	* 0.000067							228.9	0.0459	1.31	367.1		1.43
S905	Piceance	05103XXXX3	21011-5 MOON LAKE	WESTERN FUELS ASSOC	790.3	A	12239	5.0	4.5	* 0.000209										158.4		1.63
S905	Piceance	05103XXXX3	21011-5 MOON LAKE	WESTERN FUELS ASSOC	812.6	B	13236	18.4	17.5	17.2	22.6	0.1337	1.79	21.8	0.2630	1.77						
S905	Piceance	05103XXXX3	21011-5 MOON LAKE	WESTERN FUELS ASSOC	812.7	A	13276	18.1	17.2	22.0				22.3	0.2569	1.76	22.8	0.4607	1.78	21.9		1.75
S905	Piceance	05103XXXX3	21011-5 MOON LAKE	WESTERN FUELS ASSOC	812.9	A	14577	17.0	15.8	* 20.9										22.7		1.69
S905	Piceance	05103XXXX3	21011-5 MOON LAKE	WESTERN FUELS ASSOC	816.5	A	12239	10.6	9.1	0.0205				50.2	0.1142	1.64	52.4	0.2003	1.65	58.8		1.70
S905	Piceance	05103XXXX3	21011-5 MOON LAKE	WESTERN FUELS ASSOC	817.6	B	11239	2.7	1.3	0.000441	32.9	0.0918		38.4	0.1491							
S905	Piceance	05103XXXX3	21011-5 MOON LAKE	WESTERN FUELS ASSOC	817.8	A	11239	8.7	7.7	0.00118				59.8	0.0958	1.59				61.8		1.61
T63X2G	Piceance	0510310391	T63X-2G	EXXON-MOBIL	10555.6	B	15286	7.1	6.8	0.00159	108.6	0.0278	1.74	138.7	0.0413	1.83						
T63X2G	Piceance	0510310391	T63X-2G	EXXON-MOBIL	10572.9	B	15265	4.3	4.1	0.000214				207.6	0.0276	1.67						
T63X2G	Piceance	0510310391	T63X-2G	EXXON-MOBIL	10615.6	B	15225	6.1	5.8	0.00175	115.8	0.0261	1.67	183.0	0.0313	1.83	215.3	0.0488	1.89			
T63X2G	Piceance	0510310391	T63X-2G	EXXON-MOBIL	10615.6	B	15225	6.3	5.9	0.00178				244.6	0.0234	1.94						
T63X2G	Piceance	0510310391	T63X-2G	EXXON-MOBIL	10619.7	A	15276	7.3	6.8	0.00247				192.7	0.0297	1.96	176.5	0.0595	1.93			
T63X2G	Piceance	0510310391	T63X-2G	EXXON-MOBIL	10636.3	A	13265	2.5	2.4	0.000038				402.1	0.0142	1.61						
T649	Piceance	0504560011	MWX-2	CER CORPORATION	4885.4	B		4.3	4.1	0.000427	131.6	0.0230	1.52	181.0	0.0317	1.62	299.0	0.0351	1.78			
T649	Piceance	0504560011	MWX-2	CER CORPORATION	4939.8	A		9.0	8.6	0.00426	65.4	0.0462	1.70	91.2	0.0628	1.84						
T649	Piceance	0504560011	MWX-2	CER CORPORATION	4945.1	B		10.1	9.6	0.00750	64.8	0.0466	1.78	88.8	0.0645	1.91	112.3	0.0935	2.01			
T649	Piceance	0504560011	MWX-2	CER CORPORATION	5734.1	A	16276	8.7	8.0	* 0.00471										157.9		2.00
T649	Piceance	0504560011	MWX-2	CER CORPORATION	5737.3	A	16276	9.4	8.7	0.00220				89.9	0.0637	1.84	102.7	0.1022	1.90	132.6		2.00
T649	Piceance	0504560011	MWX-2	CER CORPORATION	5757.0	A	13225	0.8	0.6	* 0.000014										1623.5		1.43
T649	Piceance	0504560011	MWX-2	CER CORPORATION	5838.6	B		7.1	6.7	0.00160	78.0	0.0388	1.61	128.1	0.0447	1.79	177.5	0.0591	1.91			
T649	Piceance	0504560011	MWX-2	CER CORPORATION	5838.7	A		6.6	6.0	* 0.00146										255.2		1.97
T649	Piceance	0504560011	MWX-2	CER CORPORATION	6536.3	A		8.2	7.8	0.00318				136.5	0.0420	1.93	162.2	0.0647	1.99	190.0		2.05
T649	Piceance	0504560011	MWX-2	CER CORPORATION	6550.3	A		7.2	6.3	0.000870				132.8	0.0431	1.76	125.5	0.0837	1.74	155.3		1.82
T649	Piceance	0504560011	MWX-2	CER CORPORATION	6554.3	B		6.3	5.8	0.00227	97.8	0.0309	1.61	116.2	0.0493	1.67	176.4	0.0595	1.82			
T649	Piceance	0504560011	MWX-2	CER CORPORATION	7082.5	A		0.9	0.8	0.000024				168.7	0.0340	1.07				527.4		1.31
T649	Piceance	0504560011	MWX-2	CER CORPORATION	7124.7	A		11.1	10.2	* 0.00345										130.5		2.14
T649	Piceance	0504560011	MWX-2	CER CORPORATION	7133.5	A		10.2	9.7	0.00670				87.3	0.0656	1.92	119.8	0.0876	2.05	144.5		2.13
T649	Piceance	0504560011	MWX-2	CER CORPORATION	7136.8	A		6.9	6.1	0.00219				102.1	0.0561	1.65	113.6	0.0924	1.69	114.6		1.69
T649	Piceance	0504560011	MWX-2	CER CORPORATION	7141.9	A		3.9	3.8	0.000065				139.8	0.0410	1.51				324.2		1.76
T649	Piceance	0504560011	MWX-2	CER CORPORATION	7218.7	B		3.6	3.3	0.000385	214.7	0.0141	1.57	279.5	0.0205	1.65	372.9	0.0282	1.73			
T649	Piceance	0504560011	MWX-2	CER CORPORATION	7272.8	A	13285	8.9	8.2	* 0.00234										154.1		2.01
T649	Piceance	0504560011	MWX-2	CER CORPORATION	7276.2	A	15295	8.4	8.1	0.00173				129.7	0.0442	1.94	157.0	0.0669	2.01	218.3		2.14
T649	Piceance	0504560011	MWX-2	CER CORPORATION	7319.7	A	13257	5.7	5.4	0.000183				145.0	0.0395	1.71				284.8		1.94
T649	Piceance	0504560011	MWX-2	CER CORPORATION	7340.4	A	15275	2.1	1.8	* 0.000106										625.5		1.60
T649	Piceance	0504560011	MWX-2	CER CORPORATION	7350.4	A	15265	4.5	4.0	* 0.000372										340.5		1.82
T649	Piceance	0504560011	MWX-2	CER CORPORATION	7851.3	A		3.8	3.7	0.000244				174.8	0.0328	1.57	226.8	0.0463	1.64			
T649	Piceance	0504560011	MWX-2	CER CORPORATION	7865.6	B		7.6	7.3	0.000505	113.9	0.0265	1.81	107.0	0.0535	1.78						
T649	Piceance	0504560011	MWX-2	CER CORPORATION	7877.5	A		7.6	7.4	0.000910				168.8	0.0339	1.97	166.3	0.0632	1.96	183.6		2.00
T649	Piceance	0504560011	MWX-2	CER CORPORATION	7880.1	A		7.6	7.0	0.00179				114.2	0.0502	1.79	129.4	0.0812	1.83			
T649	Piceance	0504560011	MWX-2	CER CORPORATION	8117.9	A		6.5	5.9	* 0.00227										291.8		2.01
E393	Powder River	4900525627	1 BARLOW 21-20	LOUISIANA LAND & EXP	6969.7	B	15287	20.7	19.6	1.18	25.6	0.1179	1.99	27.8	0.2064	2.04	30.3	0.3465	2.09			
E393	Powder River	4900525627	1 BARLOW 21-20	LOUISIANA LAND & EXP	6969.9	A	15287	20.2	19.1	1.20				29.4	0.1952	2.04	30.7	0.3420	2.07	31.3		2.08
E393	Powder River	4900525627	1 BARLOW 21-20	LOUISIANA LAND & EXP	6995.8	B	15295	5.4	5.0	0.00111				199.0	0.0288	1.76				343.1		1.94
E393	Powder River	4900525627	1 BARLOW 21-20	LOUISIANA LAND & EXP	6995.8	A	15295	5.1	4.6	0.00115	189.5	0.0159	1.70	227.9	0.0251	1.76	337.9	0.0311	1.89			
E393	Powder River	4900525627	1 BARLOW 21-20	LOUISIANA LAND & EXP	6996.0	A	15295	5.9	5.4	* 0.00143										324.3		1.97
E393	Powder River	4900525627	1 BARLOW 21-20	LOUISIANA LAND & EXP	6996.2	A	15295	7.1	6.2	0.00473	104.2	0.0290	1.68	140.6	0.0408	1.78	191.5	0.0548	1.89			
E393	Powder River	4900525627	1 BARLOW 21-20	LOUISIANA LAND & EXP	7000.9	B	15587	17.4	16.3	31.0	29.0	0.1041	1.86	29.6	0.1934	1.87	32.1	0.3271	1.91			
E393	Powder River	4900525627	1 BARLOW 21-20	LOUISIANA LAND & EXP	7012.0	A	14276	6.2	6.1	0.000068				99.3	0.0577	1.64	139.5	0.0753	1.76	266.7		2.00
E393	Powder River	4900525627	1 BARLOW 21-20	LOUISIANA LAND & EXP	7039.2	B	14286	17.1	15.9	* 6.21										35.0		1.93
E393	Powder River	4900525627	1 BARLOW 21-20	LOUISIANA LAND & EXP	7039.4	A	14286	16.6	15.7	6.29	24.9	0.1211	1.74	31.1	0.1842	1.86	33.2	0.3165	1.89			
E393	Powder River	4900525627	1 BARLOW 21-20	LOUISIANA LAND & EXP	7053.0	A	14597	23.7	22.4	7.37				19.4	0.2947	1.99	20.4	0.5139	2.02	20.6		2.02
E393	Powder River	4900525627	1 BARLOW 21-20	LOUISIANA LAND & EXP	7060.4	A	13285	14.5	13.4	* 0.0564										47.4		1.92
E393	Powder River	4900525627	1 BARLOW 21-20	LOUISIANA LAND & EXP	7060.6	A	13285	16.1	15.1	2.74	25.4	0.1188	1.71	34.1	0.1682	1.86						
E393	Powder River	4900525627	1 BARLOW 21-20	LOUISIANA LAND & EXP	7076.6	A	14297	22.4	21.3	1.03				25.3	0.2264	2.09	26.2	0.4012	2.11	26.1		2.11
E932	Powder River	4900921513	2 FRED STATE	DAVIS OIL COMPANY	7538.0	A	13517	15.9	14.9	0.9404				41.4	0.1385	1.96				51.0		2.07
E932	Powder River	4900921513	2 FRED STATE	DAVIS OIL COMPANY	7544.3	A	15597	16.4	15.2	3.13	38.5	0.0785	1.94	42.4	0.1353	1.99	44.0	0.2387	2.01			
E932	Powder River	4900921513	2 FRED STATE	DAVIS OIL COMPANY	7546.9	A	13217	10.5	9.5	0.0192				100.6	0.0569	1.96	101.8	0.1032	1.96	120.5		2.03
E932	Powder River	4900921513	2 FRED STATE	DAVIS OIL COMPANY	7549.9	B	15295	3.3	2.9	0.000051	438.3	0.0069	1.72	666.5	0.0086	1.84						
E932	Powder River	4900921513	2 FRED STATE	DAVIS OIL COMPANY	7557.1	A	13217	12.4	11.5	* 0.00259	47.4	0.0638	1.78				84.8	0.1238	2.05			
E932	Powder River	4900921513	2 FRED STATE	DAVIS OIL COMPANY	7557.4	B	13217	12.8	11.9	0.00647				61.6	0.0931	1.94	79.5	0.1321	2.06	89.0		2.11
E932	Powder River	4900921513	2 FRED STATE	DAVIS OIL COMPANY	7568.1	B	15587	16.7	15.9	0.00635				46.4	0.1235	2.09	55.0	0.1911	2.18	65.7		2.27
E932	Powder River	4900921513	2 FRED STATE	DAVIS OIL COMPANY	7568.5	B	15597	16.0	15.3	0.00539	40.9	0.0738	1.97	48.6	0.1178	2.07	60.7	0.1729	2.18			
E932	Powder River	4900921513	2 FRED STATE	DAVIS OIL COMPANY	7579.1	B	15597	16.9	15.8	0.00563				54.2	0.1057	2.16	67.4	0.1557	2.28	69.2		2.29
S835	Powder River	4900906335	2 SHAWNEE	BELCO PETROLEUM	6946.1	A	14286	15.6	14.5	* 2.59										41.4		1.92
S835	Powder River	4900906335	2 SHAWNEE	BELCO PETROLEUM	6946.2	A	14286	14.3	13.2	* 2.17										54.8		1.98
S835	Powder River	4900906336	2 SHAWNEE	BELCO PETROLEUM	6956.2	B	13216	15.3	14.2	* 0.5576										53.0		2.03
S835	Powder River	4900906335	2 SHAWNEE	BELCO PETROLEUM	6979.0	A		16.6	15.4	* 0.9584										39.8		1.97
S838	Powder River	4900905481	3 SHAWNEE	BELCO PETROLEUM	6985.7	A	13286	7.8	7.6	0.000798				53.3	0.1075	1.55	73.3	0.1432	1.67	119.8		1.86
S838	Powder River	4900905481	3 SHAWNEE	BELCO PETROLEUM	6985.8	A	13286	5.5	5.2	0.000378	35.1	0.0861	1.20	49.6	0.1154	1.32	72.6	0.1447	1.45			
S838	Powder River	4900905481	3 SHAWNEE	BELCO PETROLEUM	6998.5	A	15216	5.8	5.3	* 0.00121										144.6		1.69
B646	Uinta	4304730584	11-17F RIVER BEND UNIT	MAPCO INCOPORATED	7287.7	B		4.7	3.7	0.0151	166.0	0.0182	1.55	185.5	0.0309	1.58	186.0	0.0564	1.59			
B646	Uinta	4304730584	11-17F RIVER BEND UNIT	MAPCO INCOPORATED	8233.0	B	16296	5.8	5.3	* 0.00464										246.7		1.87
B646	Uinta	4304730584	11-17F RIVER BEND UNIT	MAPCO INCOPORATED	8245.1	A	13296	2.6	2.3	* 0.000781										386.2		1.57
B646	Uinta	4304730584	11-17F RIVER BEND UNIT	MAPCO INCOPORATED	8287.4	B	16277	7.5	6.9	* 0.0217										177.0		1.93
B646	Uinta	4304730584	11-17F RIVER BEND UNIT	MAPCO INCOPORATED	8294.4	A	16277	7.7	6.6	0.0252	116.1	0.0260	1.75	127.6	0.0449	1.78	137.3	0.0765	1.81			
B646	Uinta	4304730584	11-17F RIVER BEND UNIT	MAPCO INCOPORATED	8302.5	A	13265	1.0	0.8	* 0.000112										535.0		1.28
B646	Uinta	4304730584	11-17F RIVER BEND UNIT	MAPCO INCOPORATED	8362.3	B	16296	8.9	7.8	0.0143	132.4	0.0228	1.91	145.7	0.0393	1.95	165.8	0.0633	2.00			
B646	Uinta	4304730584	11-17F RIVER BEND UNIT	MAPCO INCOPORATED	8448.3	A	15266	5.6	5.2	0.00159	114.2	0.0265	1.60	149.9	0.0382	1.70	235.9	0.0445	1.85			
E946	Uinta	4304730545	2-7 FLAT MESA	ENSERCH EXPLORATION	6344.9	C	13216	2.5	1.8	0.000664				153.0	0.0375	1.26				249.4		1.38
E946	Uinta	4304730545	2-7 FLAT MESA	ENSERCH EXPLORATION	6351.5	A	14266	9.5	8.4	0.00649				128.3	0.0447	1.95	127.4	0.0824	1.95	132.9		1.97
E946	Uinta	4304730545	2-7 FLAT MESA	ENSERCH EXPLORATION	6351.5	C	14266	10.1	8.5	0.00923	94.9	0.0318	1.84	103.3	0.0555	1.88	127.8	0.0821	1.96			
E946	Uinta	4304730545	2-7 FLAT MESA	ENSERCH EXPLORATION	6351.7	A	13266	8.3	7.6	0.00165				100.3	0.0571	1.79				164.5		1.98
E946	Uinta	4304730545	2-7 FLAT MESA	ENSERCH EXPLORATION	6352.1	A	13276	7.3	6.7	* 0.00110										219.9		1.99
E946	Uinta	4304730545	2-7 FLAT MESA	ENSERCH EXPLORATION	6357.5	B	13266	0.6	0.3	0.00127	303.6	0.0100	0.96	460.6	0.0124	1.03						
E946	Uinta	4304730545	2-7 FLAT MESA	ENSERCH EXPLORATION	6362.5	A	13246	2.8	2.4	0.000170				138.1	0.0415	1.32				274.0		1.50
E946	Uinta	4304730545	2-7 FLAT MESA	ENSERCH EXPLORATION	6468.4	A	16576	12.1	11.0	0.4345				71.1	0.0806	1.93	71.4	0.1470	1.93	73.1		1.94
E946	Uinta	4304730545	2-7 FLAT MESA	ENSERCH EXPLORATION	6468.5	A	16576	11.9	11.0	* 0.3819										75.9		1.96
E946	Uinta	4304730545	2-7 FLAT MESA	ENSERCH EXPLORATION	6468.6	A	16576	12.1	10.9	0.2572				68.3	0.0839	1.90	76.1	0.1380	1.95	79.4		1.97
E946	Uinta	4304730545	2-7 FLAT MESA	ENSERCH EXPLORATION	6472.7	A	16276	9.0	8.3	* 0.0454										128.4		1.95
E946	Uinta	4304730545	2-7 FLAT MESA	ENSERCH EXPLORATION	6475.2	A	16576	13.0	11.7	0.3895				61.7	0.0928	1.92	67.9	0.1546	1.96	70.2		1.98
E946	Uinta	4304730545	2-7 FLAT MESA	ENSERCH EXPLORATION	6475.2	B	16576	12.4	11.2	0.4442	66.2	0.0457	1.91	67.2	0.0853	1.92						
E946	Uinta	4304730545	2-7 FLAT MESA	ENSERCH EXPLORATION	6475.3	C	16576	12.5	11.5	* 0.2655										70.8		1.97
E946	Uinta	4304730545	2-7 FLAT MESA	ENSERCH EXPLORATION	6475.3	A	16576	12.4	11.1	0.5834				62.1	0.0922	1.88	66.0	0.1590	1.90	69.1		1.92
E946	Uinta	4304730545	2-7 FLAT MESA	ENSERCH EXPLORATION	6475.4	A	16576	11.9	10.7	0.3072				68.0	0.0843	1.89	74.3	0.1413	1.93	77.2		1.95
E946	Uinta	4304730545	2-7 FLAT MESA	ENSERCH EXPLORATION	6482.0	C	16286	3.0	2.8	0.000027				218.1	0.0263	1.50	362.0	0.0290	1.64	538.7		1.76
E946	Uinta	4304730545	2-7 FLAT MESA	ENSERCH EXPLORATION	6482.0	A	16286	2.7	2.2	0.000095				206.7	0.0277	1.39	327.1	0.0321	1.51	511.7		1.63
E946	Uinta	4304730545	2-7 FLAT MESA	ENSERCH EXPLORATION	6486.4	A	16576	12.5	11.8	0.6580				53.4	0.1073	1.86				58.2		1.90
E946	Uinta	4304730545	2-7 FLAT MESA	ENSERCH EXPLORATION	6486.5	A	16576	10.9	9.6	0.2455				70.0	0.0819	1.81	75.0	0.1399	1.84	78.9		1.87
E946	Uinta	4304730545	2-7 FLAT MESA	ENSERCH EXPLORATION	6486.5	B	16576	11.3	10.0	0.2857	66.4	0.0455	1.82	69.4	0.0826	1.84	73.5	0.1429	1.87			
E946	Uinta	4304730545	2-7 FLAT MESA	ENSERCH EXPLORATION	6486.6	A	16576	8.7	7.6	0.0532				92.4	0.0620	1.76				106.7		1.81
E946	Uinta	4304730545	2-7 FLAT MESA	ENSERCH EXPLORATION	6486.7	A	16576	9.9	8.3	0.1457				81.3	0.0704	1.77				89.7		1.81
E946	Uinta	4304730545	2-7 FLAT MESA	ENSERCH EXPLORATION	6489.6	A	16576	11.3	9.9	0.1855				71.6	0.0800	1.85	77.9	0.1347	1.88	78.7		1.89
E946	Uinta	4304730545	2-7 FLAT MESA	ENSERCH EXPLORATION	6489.6	C	16576	11.2	10.2	0.2165	57.1	0.0529	1.77	80.2	0.0715	1.92	81.9	0.1282	1.93			
E946	Uinta	4304730545	2-7 FLAT MESA	ENSERCH EXPLORATION	6489.7	A	16576	11.8	10.7	0.2690				69.2	0.0828	1.90				76.7		1.94
E946	Uinta	4304730545	2-7 FLAT MESA	ENSERCH EXPLORATION	6492.5	A	15286	9.8	8.9	0.0314				99.5	0.0576	1.90	110.2	0.0953	1.94	117.6		1.97
E946	Uinta	4304730545	2-7 FLAT MESA	ENSERCH EXPLORATION	6492.6	A	15286	10.2	9.1	0.0166				96.5	0.0594	1.91				114.0		1.98
E946	Uinta	4304730545	2-7 FLAT MESA	ENSERCH EXPLORATION	6508.2	A	13266	3.1	2.7	* 0.000484										275.1		1.56
E946	Uinta	4304730545	2-7 FLAT MESA	ENSERCH EXPLORATION	6511.4	A	15276	8.4	7.5	* 0.0244				106.9	0.0536	1.80	115.8	0.0907	1.83	124.3		1.86
E946	Uinta	4304730545	2-7 FLAT MESA	ENSERCH EXPLORATION	6511.5	A	15276	8.7	7.8	0.0367				109.3	0.0524	1.84	110.4	0.0951	1.85	122.6		1.89
E946	Uinta	4304730545	2-7 FLAT MESA	ENSERCH EXPLORATION	6515.5	C	16586	13.3	11.3	* 1.31	40.5	0.0746	1.70	44.2	0.1295	1.74	46.1	0.2276	1.76			
E946	Uinta	4304730545	2-7 FLAT MESA	ENSERCH EXPLORATION	6515.5	A	16586	16.3	15.1	* 2.00										43.3		1.99
E946	Uinta	4304730545	2-7 FLAT MESA	ENSERCH EXPLORATION	6516.6	A	16586	15.1	13.0	* 1.94				43.1	0.1329	1.84	45.2	0.2322		43.4		1.85
E946	Uinta	4304730545	2-7 FLAT MESA	ENSERCH EXPLORATION	6518.1	A	13266	5.2	4.6	0.00125				166.3	0.0344	1.66				221.2		1.76
E946	Uinta	4304730545	2-7 FLAT MESA	ENSERCH EXPLORATION	6527.6	A	16596	10.4	8.7	0.0643				89.0	0.0644	1.84	90.6	0.1159	1.85	91.6		1.85
E946	Uinta	4304730545	2-7 FLAT MESA	ENSERCH EXPLORATION	6527.7	A	16596	9.6	8.8	* 0.0567										99.1		1.89
E946	Uinta	4304730545	2-7 FLAT MESA	ENSERCH EXPLORATION	6530.2	A	16586	9.8	9.0	* 0.0235										111.8		1.96
E946	Uinta	4304730545	2-7 FLAT MESA	ENSERCH EXPLORATION	6530.2	C	16586	9.5	8.5	0.0609	88.4	0.0342	1.82	102.0	0.0562	1.87	111.4	0.0942	1.91			
E946	Uinta	4304730545	2-7 FLAT MESA	ENSERCH EXPLORATION	6530.3	A	16586	8.9	7.9	0.0701				103.3	0.0555	1.82	115.6	0.0908	1.87	121.1		1.89
E946	Uinta	4304730545	2-7 FLAT MESA	ENSERCH EXPLORATION	6530.4	A	16586	9.9	9.1	* 0.0639										103.0		1.93
E946	Uinta	4304730545	2-7 FLAT MESA	ENSERCH EXPLORATION	6686.8	A	14276	8.1	7.3	0.00235				136.6	0.0419	1.88	142.2	0.0738	1.90	169.4		1.96
E946	Uinta	4304730545	2-7 FLAT MESA	ENSERCH EXPLORATION	6688.2	A	15276	7.0	6.0	0.00474				148.4	0.0386	1.78	182.9	0.0574	1.85	193.3		1.87
E946	U

Table 4.4.1.

Summary Multisalinity Archie Porosity Exponent Data
Analysis of Critical Permeability, Capillary Pressure and Electrical Properties for Mesaverde Tight Gas Sandstones from Western U.S. Basins
US DOE # DE-FC26-05NT42660
Alan P. Byrnes, Robert M. Cluff, John C. Webb, Danial A. Krygowski, Stefani D. Whittaker
website: http://www.kgs.ku.edu/mesaverde

											20K ppm brine salinity			40K ppm brine salinity			80K ppm brine salinity			200K ppm brine salinity		
										brine salinity (Kppm) >	20			40			80			200		
										Cw (mhos) >	3.02			5.73			10.50			20.4		
										Rw (ohmm) >	0.331			0.17452			0.09524			0.049		
USGS Library Number	Basin	API Number	Well Name	Operator	depth	A/B /C	Rock Type Code	Routine Porosity	In situ Porosity	In situ Klinkenberg Gas Peremeability	Formation Resistivity Factor	Co	Archie Porosity Exponent, m in situ	Formation Resistivity Factor	Co	Archie Porosity Exponent, m in situ	Formation Resistivity Factor	Co	Archie Porosity Exponent, m in situ	Formation Resistivity Factor	Co	Archie Porosity Exponent, m in situ
					ft			%	%	mD	Ro/Rw	= 1 / Ro	m, A=1	Ro/Rw	= 1 / Ro	m, A=1	Ro/Rw	= 1 / Ro	m, A=1	Ro/Rw	= 1 / Ro	m, A=1
E946	Uinta	4304730545	2-7 FLAT MESA	ENSERCH EXPLORATION	6695.8	A	13276	4.0	3.2	0.000606				179.2	0.0320	1.51				246.8		1.60
E946	Uinta	4304730545	2-7 FLAT MESA	ENSERCH EXPLORATION	6702.8	A	13266	7.8	6.5	0.00250				104.2	0.0550	1.70				153.6		1.84
E946	Uinta	4304730545	2-7 FLAT MESA	ENSERCH EXPLORATION	6709.8	A	13216	2.2	1.9	0.000117										569.2		1.60
E946	Uinta	4304730545	2-7 FLAT MESA	ENSERCH EXPLORATION	7272.3	A	13276	9.0	7.7	0.00638				96.5	0.0594	1.79	118.6	0.0885	1.87	131.3		1.91
E946	Uinta	4304730545	2-7 FLAT MESA	ENSERCH EXPLORATION	7272.3	C	13276	9.0	7.5	0.00751	93.4	0.0323	1.75	100.1	0.0572	1.78						
E946	Uinta	4304730545	2-7 FLAT MESA	ENSERCH EXPLORATION	7276.2	A	14266	7.3	6.3	0.00653				113.5	0.0505	1.71	125.4	0.0837	1.74	133.8		1.77
E946	Uinta	4304730545	2-7 FLAT MESA	ENSERCH EXPLORATION	7278.8	A	13266	7.0	6.5	0.00133				101.1	0.0567	1.69				141.9		1.81
E946	Uinta	4304730545	2-7 FLAT MESA	ENSERCH EXPLORATION	7279.2	A	13286	6.2	5.7	0.000356				112.5	0.0509	1.65				176.6		1.80
E946	Uinta	4304730545	2-7 FLAT MESA	ENSERCH EXPLORATION	7279.4	A	13286	7.0	6.5	0.00146				103.9	0.0551	1.70	154.3	0.0680	1.84	174.7		1.89
E946	Uinta	4304730545	2-7 FLAT MESA	ENSERCH EXPLORATION	7279.9	A	13296	6.3	5.6	0.000735				151.5	0.0378	1.74	173.2	0.0606	1.78	203.1		1.84
E946	Uinta	4304730545	2-7 FLAT MESA	ENSERCH EXPLORATION	7284.3	B	14296	7.8	6.9	0.00310	97.0	0.0312	1.71	109.2	0.0524	1.76						
E946	Uinta	4304730545	2-7 FLAT MESA	ENSERCH EXPLORATION	7284.3	A	14296	7.7	6.7	0.00323				98.9	0.0579	1.70				167.4		1.89
E946	Uinta	4304730545	2-7 FLAT MESA	ENSERCH EXPLORATION	7284.4	A	14296	8.0	7.0	0.00266				120.2	0.0477	1.80	139.3	0.0754	1.86	162.7		1.91
E946	Uinta	4304730545	2-7 FLAT MESA	ENSERCH EXPLORATION	7284.5	A	14296	6.9	6.2	0.00505				95.5	0.0600	1.70				160.6		1.90
E946	Uinta	4304730545	2-7 FLAT MESA	ENSERCH EXPLORATION	7287.1	A	13286	5.6	5.1	0.00147										213.9		1.80
E946	Uinta	4304730545	2-7 FLAT MESA	ENSERCH EXPLORATION	7289.9	A	13266	4.9	4.3	0.00139				141.5	0.0405	1.58				181.7		1.65
E946	Uinta	4304730545	2-7 FLAT MESA	ENSERCH EXPLORATION	7293.4	C	13206	3.7	3.4	0.000584	152.2	0.0199	1.48	191.3	0.0300	1.55						
E946	Uinta	4304730545	2-7 FLAT MESA	ENSERCH EXPLORATION	7293.5	A	13206	3.9	3.5	0.000490										264.4		1.66
E946	Uinta	4304730545	2-7 FLAT MESA	ENSERCH EXPLORATION	7299.3	A	13256	6.9	5.7	0.00170				114.0	0.0503	1.65	137.0	0.0766	1.71	148.9		1.74
E946	Uinta	4304730545	2-7 FLAT MESA	ENSERCH EXPLORATION	7300.1	A	13256	5.5	4.5	0.00244				132.7	0.0432	1.58				187.2		1.69
E946	Uinta	4304730545	2-7 FLAT MESA	ENSERCH EXPLORATION	7300.6	A	13256	5.8	4.8	0.00156				159.9	0.0358	1.67	179.1	0.0586	1.70	195.3		1.73
E946	Uinta	4304730545	2-7 FLAT MESA	ENSERCH EXPLORATION	7301.4	A	13266	2.5	1.7	0.000209				208.8	0.0274	1.32	363.0	0.0289	1.45	461.8		1.51
E946	Uinta	4304730545	2-7 FLAT MESA	ENSERCH EXPLORATION	7301.4	B	13266	2.6	1.9	0.000282	166.7	0.0181	1.30	235.6	0.0243	1.39						
E946	Uinta	4304730545	2-7 FLAT MESA	ENSERCH EXPLORATION	7311.7	C	12216	2.0	1.7	0.00100										487.0		1.52
E946	Uinta	4304730545	2-7 FLAT MESA	ENSERCH EXPLORATION	7311.9	A	13266	5.3	4.6	0.000665				160.6	0.0357	1.65				250.4		1.79
E946	Uinta	4304730545	2-7 FLAT MESA	ENSERCH EXPLORATION	7312.7	A	14296	7.8	7.1	0.00303										163.0		1.93
E946	Uinta	4304730545	2-7 FLAT MESA	ENSERCH EXPLORATION	7313.4	A	13256	5.7	4.8	0.0748				146.1	0.0392	1.64	177.5	0.0591	1.70	192.8		1.73
E946	Uinta	4304730545	2-7 FLAT MESA	ENSERCH EXPLORATION	7313.8	A	13266	5.9	5.0	0.00386				140.6	0.0407	1.65	197.1	0.0533	1.76	218.9		1.80
E946	Uinta	4304730545	2-7 FLAT MESA	ENSERCH EXPLORATION	7313.8	C	13266	6.7	5.6	0.0151	131.3	0.0230	1.70	139.3	0.0411	1.72	187.3	0.0561	1.82			
E946	Uinta	4304730545	2-7 FLAT MESA	ENSERCH EXPLORATION	7314.3	A	13266	5.8	5.3	0.00412										198.0		1.80
E946	Uinta	4304730545	2-7 FLAT MESA	ENSERCH EXPLORATION	7671.1	B	13256	4.3	3.7	0.0658	207.7	0.0145	1.62	274.2	0.0209	1.70						
E946	Uinta	4304730545	2-7 FLAT MESA	ENSERCH EXPLORATION	7671.1	A	13256	4.8	4.3	0.0973										333.8		1.85
E946	Uinta	4304730545	2-7 FLAT MESA	ENSERCH EXPLORATION	7686.4	A	13266	3.8	3.0	0.3151				252.0	0.0227	1.57				382.6		1.69
E946	Uinta	4304730545	2-7 FLAT MESA	ENSERCH EXPLORATION	7689.7	A	14276	7.4	6.8	0.00374										189.1		1.95
E946	Uinta	4304730545	2-7 FLAT MESA	ENSERCH EXPLORATION	7701.1	A	13216	0.9	0.8	0.000097				273.4	0.0210	1.17				979.8		1.44
E946	Uinta	4304730545	2-7 FLAT MESA	ENSERCH EXPLORATION	7704.4	B	12226	3.2	2.8	0.000200				193.8	0.0296	1.48	335.2	0.0313	1.63	470.9		1.73
E946	Uinta	4304730545	2-7 FLAT MESA	ENSERCH EXPLORATION	7707.5	A	13256	2.9	2.2	0.0364				253.2	0.0226	1.45	328.9	0.0319	1.52	348.6		1.53
E946	Uinta	4304730545	2-7 FLAT MESA	ENSERCH EXPLORATION	7885.4	A	14266	9.8	9.0	0.0258										127.2		2.01
E946	Uinta	4304730545	2-7 FLAT MESA	ENSERCH EXPLORATION	7887.1	A	14266	11.9	11.2	0.0284				88.3	0.0649	2.04	91.7	0.1144	2.06	96.0		2.08
E946	Uinta	4304730545	2-7 FLAT MESA	ENSERCH EXPLORATION	7887.8	A	13266	6.9	6.3	0.00423										245.7		1.99
E946	Uinta	4304730545	2-7 FLAT MESA	ENSERCH EXPLORATION	7887.8	C	13266	7.0	6.1	0.00462	159.3	0.0190	1.81	152.3	0.0376	1.79						
KM36O	Uinta	4304735788	NBU 9-20-360 State	KERR-MCGEE OIL&GAS	8187.2	A		4.5	4.2	0.00136	235.8	0.0128	1.72	361.0	0.0159	1.86	381.3	0.0275	1.88			
KM36O	Uinta	4304735788	NBU 9-20-360 State	KERR-MCGEE OIL&GAS	8218.5	A		5.8	5.4	0.00117				197.6	0.0290	1.81	188.8	0.0556	1.80			
KM36O	Uinta	4304735788	NBU 9-20-360 State	KERR-MCGEE OIL&GAS	8225.6	B		1.6	1.4	0.000133	325.5	0.0093	1.36	525.8	0.0109	1.48						
KM36O	Uinta	4304735788	NBU 9-20-360 State	KERR-MCGEE OIL&GAS	8234.4	A		8.7	8.1	0.00340	103.0	0.0293	1.85	129.1	0.0444	1.94	176.8	0.0594	2.06			
KM36O	Uinta	4304735788	NBU 9-20-360 State	KERR-MCGEE OIL&GAS	8234.6	B		9.2	8.2	0.00825	116.8	0.0259	1.90	126.4	0.0453	1.93	169.9	0.0618	2.05			
KM36O	Uinta	4304735788	NBU 9-20-360 State	KERR-MCGEE OIL&GAS	8277.4	A		4.2	3.8	0.00335	162.6	0.0186	1.56	219.3	0.0261	1.65	255.3	0.0411	1.70			
KM36O	Uinta	4304735788	NBU 9-20-360 State	KERR-MCGEE OIL&GAS	8317.5	A		7.7	7.5	0.000149	87.6	0.0345	1.72	127.4	0.0450	1.87						
R829	Uinta	4304730852	4-5 US LAMCO	CHAMPLIN PETROLEUM	5621.2	A	16276	10.4	9.5	0.3937	91.8	0.0329	1.92	93.5	0.0613	1.93	95.6	0.1099	1.94			
R829	Uinta	4304730852	4-5 US LAMCO	CHAMPLIN PETROLEUM	5626.2	A	16275	12.6	11.6	7.19	44.2	0.0683	1.76	56.5	0.1015	1.87	57.6	0.1824	1.88			
R829	Uinta	4304730852	4-5 US LAMCO	CHAMPLIN PETROLEUM	5702.2	A	12245	2.3	2.0	0.000035										438.1		1.55
R829	Uinta	4304730852	4-5 US LAMCO	CHAMPLIN PETROLEUM	5812.1	B	13266	3.8	3.7	0.000101	233.3	0.0129	1.65	299.2	0.0191	1.72	316.6	0.0332	1.74			
R999	Uinta	4304730860	3-24 LAMCO	CHAMPLIN PETROLEUM	7156.0	B	11219	2.8	2.7	0.000003				154.4	0.0371	1.39	250.1	0.0420	1.53			
R999	Uinta	4304730860	3-24 LAMCO	CHAMPLIN PETROLEUM	7156.0	A	11219	2.7	2.4	0.000105										533.5		1.67
R999	Uinta	4304730860	3-24 LAMCO	CHAMPLIN PETROLEUM	7158.9	B	13215	2.7	2.4	0.000149										463.1		1.64
R999	Uinta	4304730860	3-24 LAMCO	CHAMPLIN PETROLEUM	7158.9	A	13215	2.3	2.0	0.000171										556.4		1.61
R999	Uinta	4304730860	3-24 LAMCO	CHAMPLIN PETROLEUM	7169.6	A	14295	1.9	1.7	0.000110	265.2	0.0114	1.38	388.6	0.0147	1.47						
S172	Uinta	43019XXXX1	3 BOOK CLIFFS	USGS-CG	124.1	A	13219	15.2	13.8	0.1027	27.3	0.1105	1.67	28.5	0.2012	1.69	30.4	0.3456	1.72			
S172	Uinta	43019XXXX1	3 BOOK CLIFFS	USGS-CG	174.0	A	12217	7.0	6.4	0.000416										88.2		1.63
S172	Uinta	43019XXXX1	3 BOOK CLIFFS	USGS-CG	175.2	A	13257	19.9	18.5	34.0										22.3		1.84
S172	Uinta	43019XXXX1	3 BOOK CLIFFS	USGS-CG	206.0	A	11219	10.6	9.8	0.00488										58.1		1.75
S172	Uinta	43019XXXX1	3 BOOK CLIFFS	USGS-CG	252.1	A	12217	14.9	13.8	0.1326										39.5		1.86
S172	Uinta	43019XXXX1	3 BOOK CLIFFS	USGS-CG	334.5	A	11219	3.6	3.2	0.000142										146.7		1.45
S172	Uinta	43019XXXX1	3 BOOK CLIFFS	USGS-CG	398.8	A	12239	10.9	9.5	0.0463				47.0	0.1219	1.64	54.5	0.1927	1.70	62.3		1.76
S174	Uinta	43019XXXX2	4 BOOK CLIFFS	USGS-CG	161.7	A		12.1	11.2	0.0313										54.8		1.83
S174	Uinta	43019XXXX2	4 BOOK CLIFFS	USGS-CG	183.4	A		9.8	9.0	0.1115										87.7		1.86
S174	Uinta	43019XXXX2	4 BOOK CLIFFS	USGS-CG	184.5	A		14.2	13.5	0.2104	36.3	0.0832	1.79	40.4	0.1418	1.84	43.1	0.2436	1.88			
S174	Uinta	43019XXXX2	4 BOOK CLIFFS	USGS-CG	189.2	A		21.0	19.5	5.65										18.6		1.79
S174	Uinta	43019XXXX2	4 BOOK CLIFFS	USGS-CG	189.2	B		22.2	20.9	9.31	18.2	0.1658	1.86	22.5	0.2541	1.99						
S174	Uinta	43019XXXX2	4 BOOK CLIFFS	USGS-CG	189.3	A		21.9	20.6	6.12				18.1	0.3173	1.83				18.0		1.83
DR3	Washakie	4903722304	3 DRIPPING ROCK	CELSIUS	12415.1	A		14.1	13.0	0.0276										99.6		2.26
DR3	Washakie	4903722304	3 DRIPPING ROCK	CELSIUS	12416.8	A		13.7	12.7	0.0271	62.3	0.0485	2.00	78.4	0.0731	2.11						
DR3	Washakie	4903722304	3 DRIPPING ROCK	CELSIUS	12420.2	A		7.5	6.9	0.000418										194.6		1.97
DR3	Washakie	4903722304	3 DRIPPING ROCK	CELSIUS	12428.1	A		12.0	11.1	0.00500										133.9		2.23
DR3	Washakie	4903722304	3 DRIPPING ROCK	CELSIUS	12439.1	A		10.8	10.3	0.00386	77.2	0.0391	1.91	100.4	0.0570	2.03	118.8	0.0884	2.10			
DR3	Washakie	4903722304	3 DRIPPING ROCK	CELSIUS	12441.8	A		10.3	9.2	0.00791				109.4	0.0524	1.97	138.7	0.0757	2.07	169.5		2.15
DR3	Washakie	4903722304	3 DRIPPING ROCK	CELSIUS	12448.3	A		9.4	9.2	0.00107				85.0	0.0674	1.86				159.5		2.12
DR3	Washakie	4903722304	3 DRIPPING ROCK	CELSIUS	12452.8	A		7.6	7.3	0.000002	119.0	0.0254	1.83	151.0	0.0379	1.92	194.9	0.0539	2.02			
DR3	Washakie	4903722304	3 DRIPPING ROCK	CELSIUS	12453.7	A		5.5	5.3	0.000107	99.2	0.0305	1.57	146.0	0.0393	1.70						
DR5	Washakie	4903722355	5 DRIPPING ROCK	CELSIUS	12686.7	A		12.8	11.8	0.0120										110.5		2.20
DR5	Washakie	4903722355	5 DRIPPING ROCK	CELSIUS	12693.3	B		13.2	12.4	0.0151	64.7	0.0467	2.00	77.5	0.0740	2.08						
DR5	Washakie	4903722355	5 DRIPPING ROCK	CELSIUS	12704.2	B		10.6	10.1	0.00283	56.5	0.0534	1.76	78.8	0.0727	1.91	92.9	0.1130	1.98			
DR5	Washakie	4903722355	5 DRIPPING ROCK	CELSIUS	12704.2	A		11.4	11.1	0.00348				68.9	0.0832	1.92				122.5		2.18
DR5	Washakie	4903722355	5 DRIPPING ROCK	CELSIUS	12713.7	A		8.7	8.2	0.00191	84.1	0.0359	1.77	121.2	0.0473	1.92	126.3	0.0831	1.94			
E489	Washakie	4903721053	3 UNIT FIVE MILE GULCH	AMOCO PRODUCTION	10608.7	A		4.3	3.9	0.000079										363.0		1.81
E489	Washakie	4903721053	3 UNIT FIVE MILE GULCH	AMOCO PRODUCTION	10612.0	A		6.6	6.4	0.000011										263.3		2.03
E489	Washakie	4903721053	3 UNIT FIVE MILE GULCH	AMOCO PRODUCTION	10612.0	B		6.3	6.1	0.000719	99.0	0.0305	1.64	140.2	0.0409	1.77						
E489	Washakie	4903721053	3 UNIT FIVE MILE GULCH	AMOCO PRODUCTION	10612.3	A		5.6	5.5	0.000145				161.9	0.0354	1.75	177.5	0.0591	1.78	268.0		1.92
E489	Washakie	4903721053	3 UNIT FIVE MILE GULCH	AMOCO PRODUCTION	10613.8	A		9.5	9.1	0.00140				106.3	0.0539	1.95	148.5	0.0707	2.09	164.8		2.13
E489	Washakie	4903721053	3 UNIT FIVE MILE GULCH	AMOCO PRODUCTION	10615.6	A		11.0	10.0	0.00814				119.2	0.0481	2.08	132.1	0.0795	2.12	144.0		2.16
E489	Washakie	4903721053	3 UNIT FIVE MILE GULCH	AMOCO PRODUCTION	10615.6	B		10.1	9.1	0.0117	106.5	0.0284	1.95	131.0	0.0437	2.03						
E489	Washakie	4903721053	3 UNIT FIVE MILE GULCH	AMOCO PRODUCTION	10615.8	A		10.4	9.4	0.0159				106.9	0.0536	1.98				146.5		2.11
E489	Washakie	4903721053	3 UNIT FIVE MILE GULCH	AMOCO PRODUCTION	10627.0	A		2.3	2.0	0.000069				201.5	0.0284	1.35	296.8	0.0354	1.45	489.1		1.58
E489	Washakie	4903721053	3 UNIT FIVE MILE GULCH	AMOCO PRODUCTION	10634.0	A		3.3	3.1	0.000139				253.4	0.0226	1.59	383.2	0.0274	1.71	677.3		1.87
E489	Washakie	4903721053	3 UNIT FIVE MILE GULCH	AMOCO PRODUCTION	10634.0	B		2.2	2.0	0.000184	236.4	0.0128	1.40	319.1	0.0180	1.48	401.3	0.0262	1.54			
E489	Washakie	4903721053	3 UNIT FIVE MILE GULCH	AMOCO PRODUCTION	10636.2	A		5.4	5.2	0.00145				229.4	0.0250	1.84	275.3	0.0381	1.90	303.3		1.93
E489	Washakie	4903721053	3 UNIT FIVE MILE GULCH	AMOCO PRODUCTION	10650.0	A		6.2	6.0	0.000309				154.8	0.0370	1.80	252.6	0.0416	1.97	293.3		2.02
E489	Washakie	4903721053	3 UNIT FIVE MILE GULCH	AMOCO PRODUCTION	10651.0	A		4.3	4.0	0.000187				176.8	0.0324	1.61	226.4	0.0464	1.68	327.9		1.80
E489	Washakie	4903721053	3 UNIT FIVE MILE GULCH	AMOCO PRODUCTION	10658.1	A		8.4	7.7	0.00541				185.6	0.0309	2.03	221.6	0.0474	2.10	231.5		2.12
E489	Washakie	4903721053	3 UNIT FIVE MILE GULCH	AMOCO PRODUCTION	10662.1	A		6.2	5.9	0.00147				173.6	0.0330	1.82	258.2	0.0407	1.96	278.7		1.99
E489	Washakie	4903721053	3 UNIT FIVE MILE GULCH	AMOCO PRODUCTION	10662.5	A		4.7	4.4	0.000234				208.7	0.0275	1.71	230.9	0.0455	1.75	349.2		1.88
E489	Washakie	4903721053	3 UNIT FIVE MILE GULCH	AMOCO PRODUCTION	10666.3	A		8.4	8.2	0.000785				127.0	0.0451	1.94				225.9		2.17
E489	Washakie	4903721053	3 UNIT FIVE MILE GULCH	AMOCO PRODUCTION	10668.2	A		7.9	7.5	0.00215				128.1	0.0447	1.87	138.9	0.0756	1.90	205.8		2.06
E489	Washakie	4903721053	3 UNIT FIVE MILE GULCH	AMOCO PRODUCTION	10668.2	B		7.9	7.4	0.00232	125.3	0.0241	1.85	146.6	0.0391	1.91	171.6	0.0612	1.97			
E489	Washakie	4903721053	3 UNIT FIVE MILE GULCH	AMOCO PRODUCTION	10669.0	A		6.7	6.1	0.00261				226.0	0.0254	1.94	263.8	0.0398	2.00	358.1		2.10
E489	Washakie	4903721053	3 UNIT FIVE MILE GULCH	AMOCO PRODUCTION	10670.9	A		8.7	7.6	0.0309				168.0	0.0341	1.99	178.1	0.0589	2.02	182.1		2.02
E489	Washakie	4903721053	3 UNIT FIVE MILE GULCH	AMOCO PRODUCTION	10675.3	A		10.4	9.6	0.0299				107.5	0.0533	2.00				155.0		2.15
E489	Washakie	4903721053	3 UNIT FIVE MILE GULCH	AMOCO PRODUCTION	10675.4	A		10.1	9.1	0.0327				115.3	0.0497	1.98				154.5		2.10
E489	Washakie	4903721053	3 UNIT FIVE MILE GULCH	AMOCO PRODUCTION	10675.7	A		10.2	9.2	0.0208				133.7	0.0429	2.05	174.6	0.0601	2.16	187.5		2.19
E489	Washakie	4903721053	3 UNIT FIVE MILE GULCH	AMOCO PRODUCTION	10675.8	A		10.1	9.4	0.0255				133.9	0.0428	2.07	137.5	0.0764	2.08	152.9		2.13
E489	Washakie	4903721053	3 UNIT FIVE MILE GULCH	AMOCO PRODUCTION	10682.0	A		10.2	9.8	0.00243				93.6	0.0612	1.95	142.6	0.0736	2.13	162.5		2.19
E489	Washakie	4903721053	3 UNIT FIVE MILE GULCH	AMOCO PRODUCTION	10682.3	A		9.2	8.9	0.00420				106.7	0.0537	1.93	140.8	0.0746	2.04	168.8		2.12
E489	Washakie	4903721053	3 UNIT FIVE MILE GULCH	AMOCO PRODUCTION	10693.4	A		2.6	2.5	0.000140				345.1	0.0166	1.59				1002.0		1.88
E489	Washakie	4903721053	3 UNIT FIVE MILE GULCH	AMOCO PRODUCTION	10706.9	A		5.0	4.7	0.000830				268.8	0.0213	1.83	486.1	0.0216	2.03	525.4		2.05
E489	Washakie	4903721053	3 UNIT FIVE MILE GULCH	AMOCO PRODUCTION	10709.7	A		6.1	5.8	0.000376				190.4	0.0301	1.84	310.6	0.0338	2.01	376.8		2.08
E489	Washakie	4903721053	3 UNIT FIVE MILE GULCH	AMOCO PRODUCTION	10710.3	A		6.2	5.8	0.00310				249.4	0.0230	1.93	330.5	0.0318	2.03	376.6		2.08
E489	Washakie	4903721053	3 UNIT FIVE MILE GULCH	AMOCO PRODUCTION	10715.8	A		5.3	4.9	0.000920				326.2	0.0176	1.92	295.2	0.0356	1.89	524.5		2.08
E489	Washakie	4903721053	3 UNIT FIVE MILE GULCH	AMOCO PRODUCTION	10717.0	A		11.9	11.3	0.00120				215.7	0.0266	2.47	270.8	0.0388	2.57	330.2		2.66
E489	Washakie	4903721053	3 UNIT FIVE MILE GULCH	AMOCO PRODUCTION	10723.7	A		1.6	1.3					1377.3	0.0042	1.66				3372.3		1.87
S265	Washakie	4903720033	102-7-10 ARCH UNIT	ANADARKO E&P CO. LP	4728.0	A	12219	7.4	7.1	0.000322				79.0	0.0725	1.65				88.5		1.69
S265	Washakie	4903720033	102-7-10 ARCH UNIT	ANADARKO E&P CO. LP	4729.0	A	12219	12.2	10.7	0.0261				50.0	0.1146	1.75	53.8	0.1953	1.78	55.9		1.80
S265	Washakie	4903720033	102-7-10 ARCH UNIT	ANADARKO E&P CO. LP	4731.0	B	12236	10.0	8.2	0.00406				60.3	0.0950	1.64	70.0	0.1500	1.70	83.8		1.77
S265	Washakie	4903720033	102-7-10 ARCH UNIT	ANADARKO E&P CO. LP	4736.2	A	15275	17.3	16.2	4.87	28.6	0.1056	1.84	29.8	0.1925	1.86	30.1	0.3486	1.87			
S265	Washakie	4903720033	102-7-10 ARCH UNIT	ANADARKO E&P CO. LP	4756.9	A	12239	8.6	7.9	0.00308										80.2		1.73
S265	Washakie	4903720033	102-7-10 ARCH UNIT	ANADARKO E&P CO. LP	4761.0	B	11235	8.4	8.1	0.000118	54.9	0.0550	1.59	59.6	0.0962	1.63						
S265	Washakie	4903720033	102-7-10 ARCH UNIT	ANADARKO E&P CO. LP	4761.0	A	11235	7.6	6.9	0.000260										116.6		1.78
S265	Washakie	4903720033	102-7-10 ARCH UNIT	ANADARKO E&P CO. LP	4889.0	C	16576	17.7	15.6	10.4	25.

Table 4.4.1.

Summary Multisalinity Archie Porosity Exponent Data
Analysis of Critical Permeability, Capillary Pressure and Electrical Properties for Mesaverde Tight Gas Sandstones from Western U.S. Basins
US DOE # DE-FC26-05NT42660
Alan P. Byrnes, Robert M. Cluff, John C. Webb, Danial A. Krygowski, Stefani D. Whittaker
website: http://www.kgs.ku.edu/mesaverde

													20K ppm brine salinity			40K ppm brine salinity			80K ppm brine salinity			200K ppm brine salinity		
												brine salinity (Kppm) >	20			40			80			200		
												Cw (mhos) >	3.02			5.73			10.50			20.4		
												Rw (ohmm) >	0.331			0.17452			0.09524			0.049		
USGS Library Number	**Basin**	**API Number**	**Well Name**	**Operator**	**depth**	**A/B /C**	**Rock Type Code**	**Routine Porosity**	**In situ Porosity**		**In situ Klinkenberg Gas Peremeability**		Formation Resistivity Factor	Co	Archie Porosity Exponent, m in situ	Formation Resistivity Factor	Co	Archie Porosity Exponent, m in situ	Formation Resistivity Factor	Co	Archie Porosity Exponent, m in situ	Formation Resistivity Factor	Co	Archie Porosity Exponent, m in situ
					ft			%	%		mD		Ro/Rw	= 1 / Ro	m, A=1	Ro/Rw	= 1 / Ro	m, A=1	Ro/Rw	= 1 / Ro	m, A=1	Ro/Rw	= 1 / Ro	m, A=1
T695	Washakie	4903723956	5-2 SIBERIA RIDGE	AMOCO PRODUCTION	10669.4	A	12217	3.0	2.6	*	0.000070											507.5		1.71
T715	Washakie	0508106724	1-791-2613 Craig Dome	COCKRELL OIL CORP	3467.4	A	15577	17.5	16.2	*	23.4											27.5		1.82
T715	Washakie	0508106724	1-791-2613 Craig Dome	COCKRELL OIL CORP	3467.6	A	15577	17.3	16.7		30.1		25.4	0.1189	1.81	25.8	0.2220	1.82	26.6	0.3946	1.83			
T717	Washakie	0508106724	1-791-2613 Craig Dome	COCKRELL OIL CORP	1733.0	B	12226	17.9	16.6	*	0.00102											98.9		2.56
T717	Washakie	0508106724	1-791-2613 Craig Dome	COCKRELL OIL CORP	1733.0	A	12226	5.8	4.8		0.0247		60.3	0.0501	1.35	99.0	0.0579	1.52	161.4	0.0651	1.68			
T717	Washakie	0508106724	1-791-2613 Craig Dome	COCKRELL OIL CORP	1733.8	A	12216	3.9	3.2		0.000172		58.4	0.0517	1.18	80.1	0.0715	1.28						
WLDR	Washakie	9999999999	WILD ROSE 1	N/A	10015.6	A		5.4	5.1		0.000779					301.2	0.0190	1.91	273.3	0.0384	1.88			
WLDR	Washakie	9999999999	WILD ROSE 1	N/A	10204.8	A		8.8	7.6		0.0231					183.0	0.0313	2.02	194.6	0.0539	2.04			
B049	Wind River	4901320724	31-22 TRIBAL PHILLIPS	BROWN TOM INC	9072.2	A		12.4	11.2		5.89		54.9	0.0550	1.83	58.5	0.0980	1.86	63.0	0.1667	1.90			
B049	Wind River	4901320724	31-22 TRIBAL PHILLIPS	BROWN TOM INC	9081.0	A		11.4	10.5	*	1.77											76.7		1.93
B049	Wind River	4901320724	31-22 TRIBAL PHILLIPS	BROWN TOM INC	11698.9	A	13226	1.0	0.8	*	0.000133											2276.3		1.58
B049	Wind River	4901320724	31-22 TRIBAL PHILLIPS	BROWN TOM INC	11770.2	A	15276	2.8	2.6		0.000211		141.2	0.0214	1.35	242.5	0.0236	1.50						
B049	Wind River	4901320724	31-22 TRIBAL PHILLIPS	BROWN TOM INC	11801.8	A	13246	1.4	1.3		0.000163					719.9	0.0080	1.51				2324.7		1.78
C899	Wind River	4901320836	1-27 LOOKOUT	MONSANTO OIL	16565.1	A	15286	2.8	2.4	*	0.000224											721.2		1.77
C899	Wind River	4901320836	1-27 LOOKOUT	MONSANTO OIL	16616.5	A	12249	0.9	0.7	*	0.000014											1315.3		1.43
C899	Wind River	4901320836	1-27 LOOKOUT	MONSANTO OIL	16626.0	A	11299	1.9	1.6		0.000077		383.1	0.0079	1.45	709.5	0.0081	1.59						
C899	Wind River	4901320836	1-27 LOOKOUT	MONSANTO OIL	16653.8	A	12246	1.4	0.8		0.000158					439.0	0.0131	1.25				1130.7		1.44
C899	Wind River	4901320836	1-27 LOOKOUT	MONSANTO OIL	16706.8	A	15286	5.6	5.1	*	0.000518											343.0		1.96
C899	Wind River	4901320836	1-27 LOOKOUT	MONSANTO OIL	16709.9	A	15216	5.6	5.4		0.000616		135.2	0.0223	1.68	180.8	0.0317	1.78						
C899	Wind River	4901320836	1-27 LOOKOUT	MONSANTO OIL	16723.9	A	15286	5.2	4.7	*	0.000702											348.8		1.91
D031	Wind River	4901320966	CHEVRON 2-1	MONSANTO OIL	15647.1	A	11239	0.9	0.6	*	0.000024					378.9	0.0151	1.16				946.2		1.34
D031	Wind River	4901320966	CHEVRON 2-1	MONSANTO OIL	15663.2	A	15276	7.3	6.7		0.000768		87.6	0.0345	1.65	117.0	0.0490	1.76						
D031	Wind River	4901320966	CHEVRON 2-1	MONSANTO OIL	15681.1	A	15276	9.9	9.2	*	0.00212		73.5	0.0411	1.80	82.6	0.0694	1.85	111.8	0.0939	1.98			
D031	Wind River	4901320966	CHEVRON 2-1	MONSANTO OIL	15702.1	A	13216	6.9	6.3	*	0.000669											174.8		1.87
D031	Wind River	4901320966	CHEVRON 2-1	MONSANTO OIL	15750.1	A	14286	4.1	4.0		0.000218		143.5	0.0210	1.54	172.4	0.0332	1.60						

* - inidcates in situ porosity value is estimated from compressibility trends
All Formation Resistivity Factor data were measured at a hydrostatic confining pressure of 4,000 psi (27.6 Mpa)
All Formation Resistivity Factor data were corrected to a temperature of 20 degrees Centigrade.

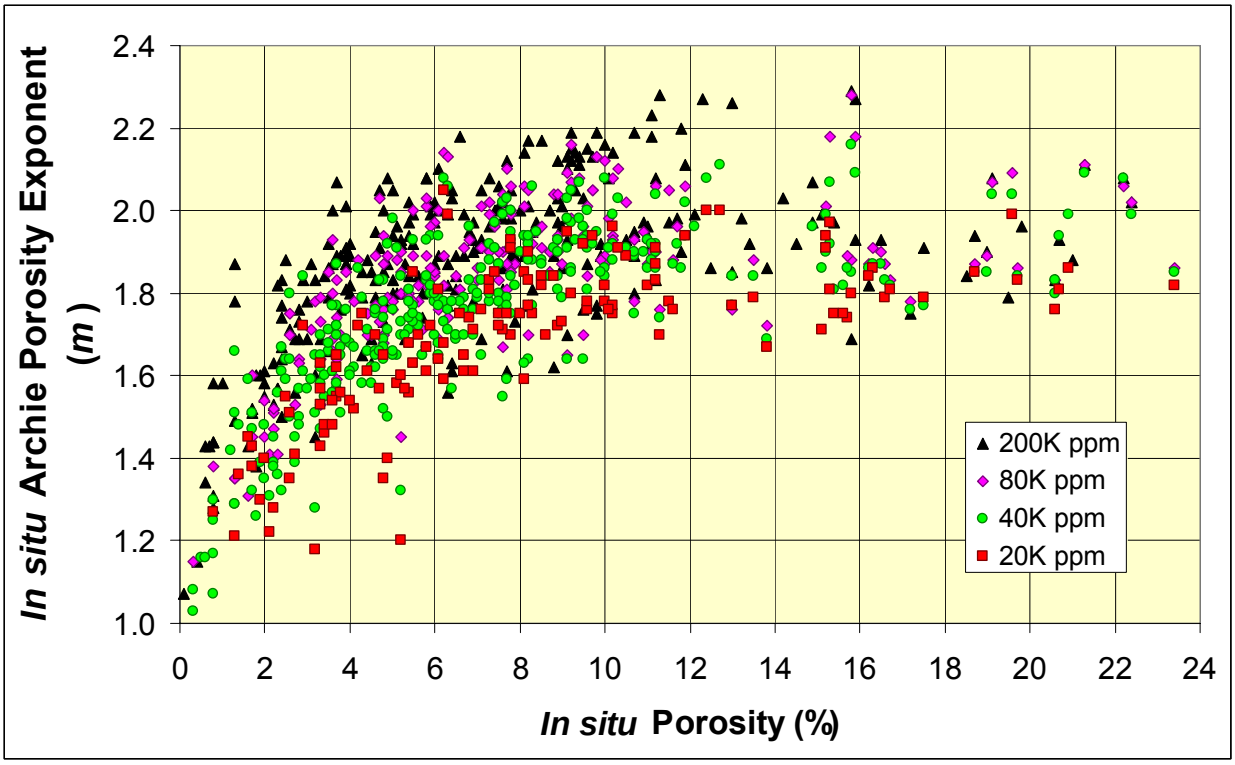

Figure 4.4.2. Archie porosity exponent, ***m***, versus *in situ* porosity for Mesaverde sandstone samples at various salinities. Trends for all salinities indicate ***m*** decreases with decreasing porosity.

Utilizing the largest set of data at 40,000 ppm NaCl, which also represents a salinity similar to those commonly found in the Mesaverde, the Archie porosity exponent can be modeled either empirically or with a dual porosity model (Serra, 1989).

The dual porosity model for a fractured reservoir or a reservoir with touching vugs represents the conductivity as two circuits in parallel and can be represented by

$$\boldsymbol{m} = \log[(\phi-\phi_2)^{m1} + \phi_2^{m2}]/\log\phi \qquad [4.4.4]$$

where ϕ = bulk porosity (fraction), ϕ_2 = fracture or touching vug porosity, m_1 = matrix porosity exponent, and m_2 = fracture or touching vug porosity exponent.

In Figure 4.4.3 the porosity exponent data are approximately bracketed by for the following conditions:

High: $m_1 = 2.15$, $\phi_2 = 0.0015$, $m_2 = 1$

Intermediate: $m_1 = 2.0$, $\phi_2 = 0.0035$, $m_2 = 1$

Low: $m_1 = 1.8$, $\phi_2 = 0.007$, $m_2 = 1$

The intermediate solution parameters were estimated by trial-and-error solution for the parameters that provided the minimum average error between the dual-porosity model and the measured data.

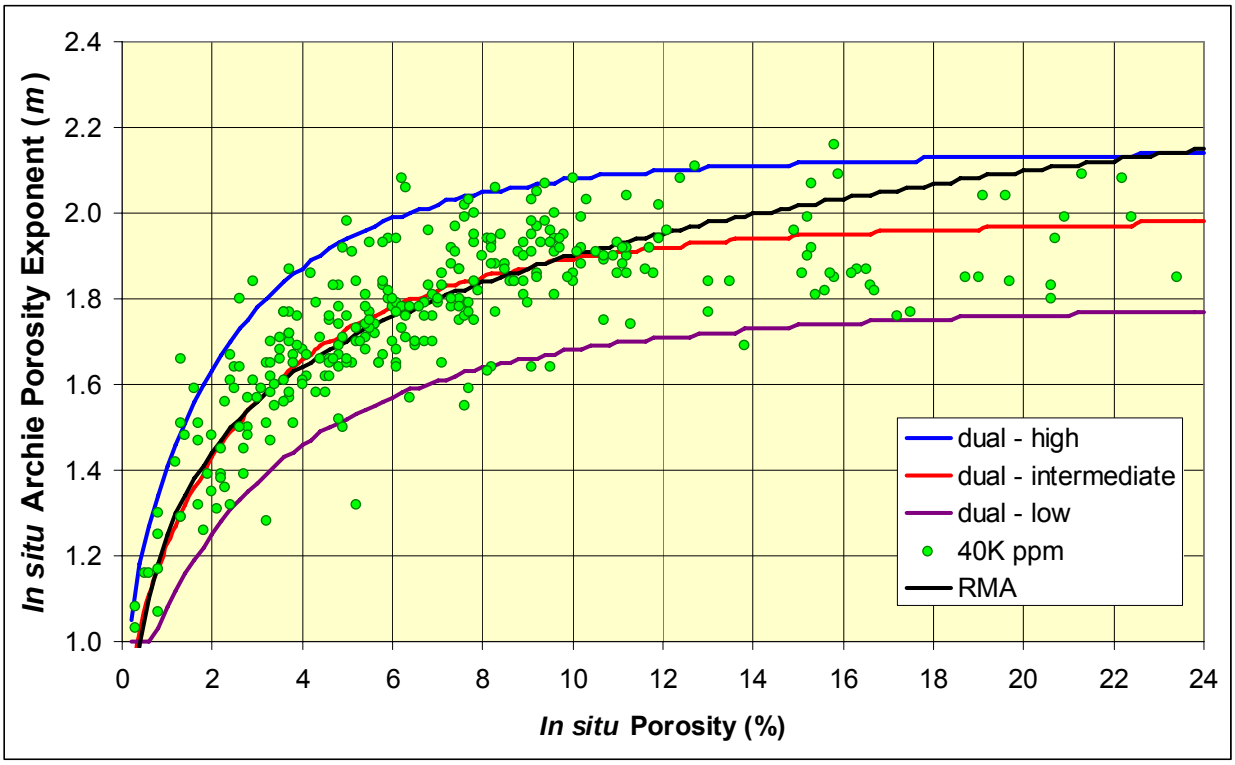

Figure 4.4.3. Crossplot of *in situ* Archie porosity exponent, ***m*** (assuming a = 1) versus *in situ* porosity showing decreasing ***m*** with decreasing porosity and both RMA empirical model (black curve) and high (blue), low (purple), and intermediate (red) dual-porosity models.

Also shown in Figure 4.4.3 is the empirical reduced major axis (RMA) analysis solution of the relationship between $\log_{10}\boldsymbol{m}$ and porosity. This relationship can be expressed

$$\boldsymbol{m}_{40k} = 0.653 \log\phi + 1.248 \qquad [4.4.5]$$

where $\boldsymbol{m}_{40k}$ = Archie porosity exponent at 40,000 ppm NaCl, ϕ = porosity in percent.

The RMA analysis provides a more accurate solution for minimum error at the low and high end porosities and appropriately handles the uncertainty in the porosity variable. A linear regression analysis (LRA) provides an estimation of ***m*** using

$$\boldsymbol{m}_{40k} = 0.530 \log\phi + 1.344 \qquad [4.4.6]$$

The contrast between the RMA and linear regression analysis (LRA) solutions are shown in Figure 4.4.4.

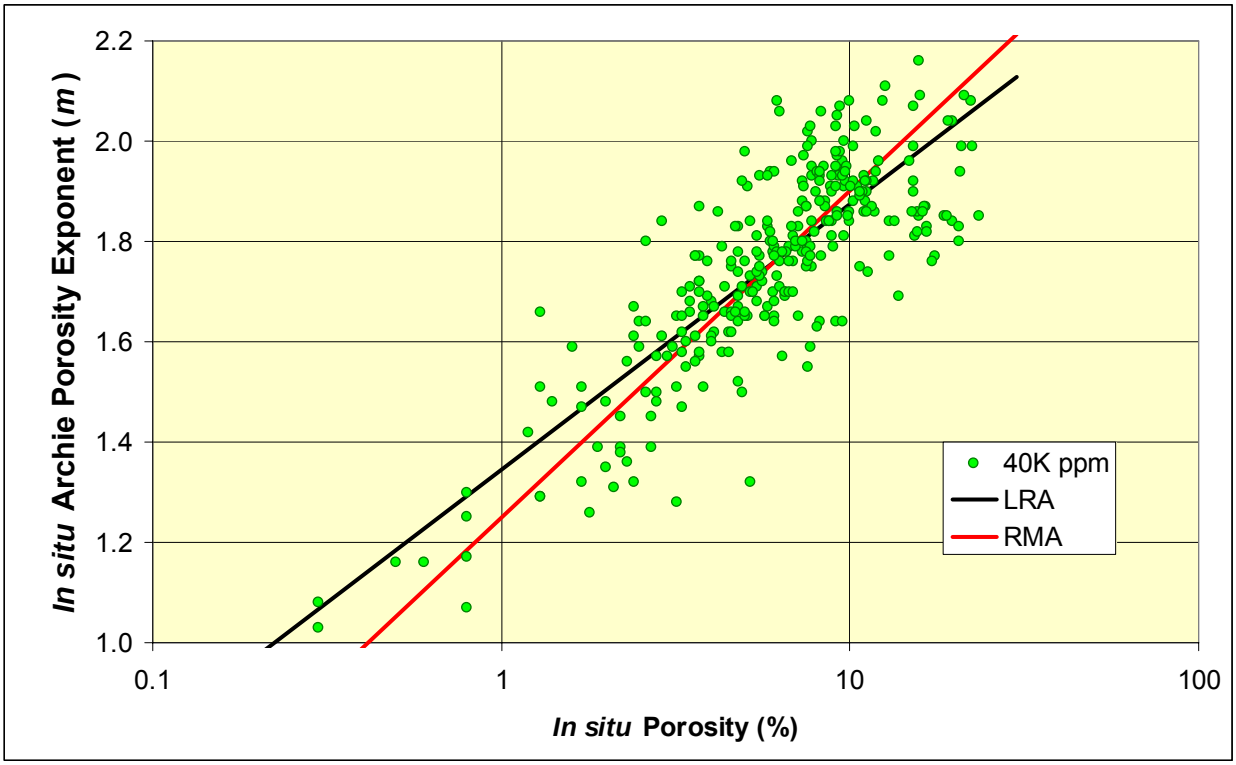

Figure 4.4.4. Crossplot of *in situ* Archie porosity exponent, ***m*** (assuming A=1), versus $\log_{10}$ *in situ* porosity. Correlations can be interpreted using eith LRA (black line) or RMA (red line).

It is important to note that although the dual porosity model is capable of matching the pattern of Archie ***m*** data in Figure 4.4.6, this alone does not validate the implicit pore architecture of the model for the tight gas sandstones studied. This model assumes that there is present in these sandstones a microfracture(s) that carry current parallel to the matrix. This has not been directly observed. Alternate interpretations of the results are that as porosity decreases,

1) Electrical efficiency increases,
2) Remaining pores may become progressively more sheet-like or fracture-like with diminishing tortuosity,
3) Conductivity of a few larger pores increases disproportionately to their relative volume,
4) Remaining pores may exhibit decreased ***m***.

The empirical RMA log-linear equation predicts very similar ***m*** values to the dual porosity model up to approximately 14% porosity. At greater porosity each dual-porosity model approaches a constant that remains constant for all greater porosity; however, the RMA model predicts increasing ***m*** values with increasing porosity, which is incorrect. Therefore this equation is limited to $\phi < 14\%$. For $\phi > 14\%$ a constant ***m*** = 1.95 is the average of all values.

These results and models cannot be robustly extrapolated to porosity values greater than 24%. Both modeling approaches predict constant porosity exponent values with increasing porosity, which cannot hold true for all higher porosity values.

A porosity exponent approaching ***m*** = 1 is consistent with a simple model that as porosity approaches zero the pore system must approach a very limited number of sample-spanning pores, and ultimately for electrical current to flow at all across a system at very low porosity the remaining pore must have limited tortuosity. The porosity exponent of both a capillary and a sheet-like crack or slot is ***m*** = 1. With this simple model it would be predicted that $\boldsymbol{m} \rightarrow 1$ as $\phi \rightarrow 0$ %.

The models for ***m*** above all predict increasing or constant ***m*** with increasing porosity. However, because ***m*** = 1 at $\phi = 100\%$ (the system is 100% brine therefore $R_o = R_w$ and FRF = $R_o/R_w = 1$), ***m*** must decrease at some high porosity and with increasing porosity $\boldsymbol{m} \rightarrow 1$ as $\phi \rightarrow 100\%$. Mesaverde rocks do not approach these porosity values, and the nature of ***m*** at the high porosities where this may occur is not an issue for these reservoir rocks.

4.4.3.2 Salinity Dependence of Archie Porosity Exponent and Cation Exchange Capacity

Figure 4.4.5 illustrates the basic Waxman-Smits model for excess conductivity and how BQv can be determined from multiple salinity measurements of core and brine conductivity. The relationship can be expressed

$$Co = (1/F^*)\,(Cw + BQv) \qquad [4.4.7]$$

Where Co = core conductivity at Sw = 100% (mho/m), Cw = water conductivity (mho/m), F* = salinity/clay conductivity independent formation factor, Qv = cation exchange capacity of the core (meq/cc), B = specific counter-ion activity [(equiv/l)/(ohm-m)], F*/F = (1 + BQv/Cw).

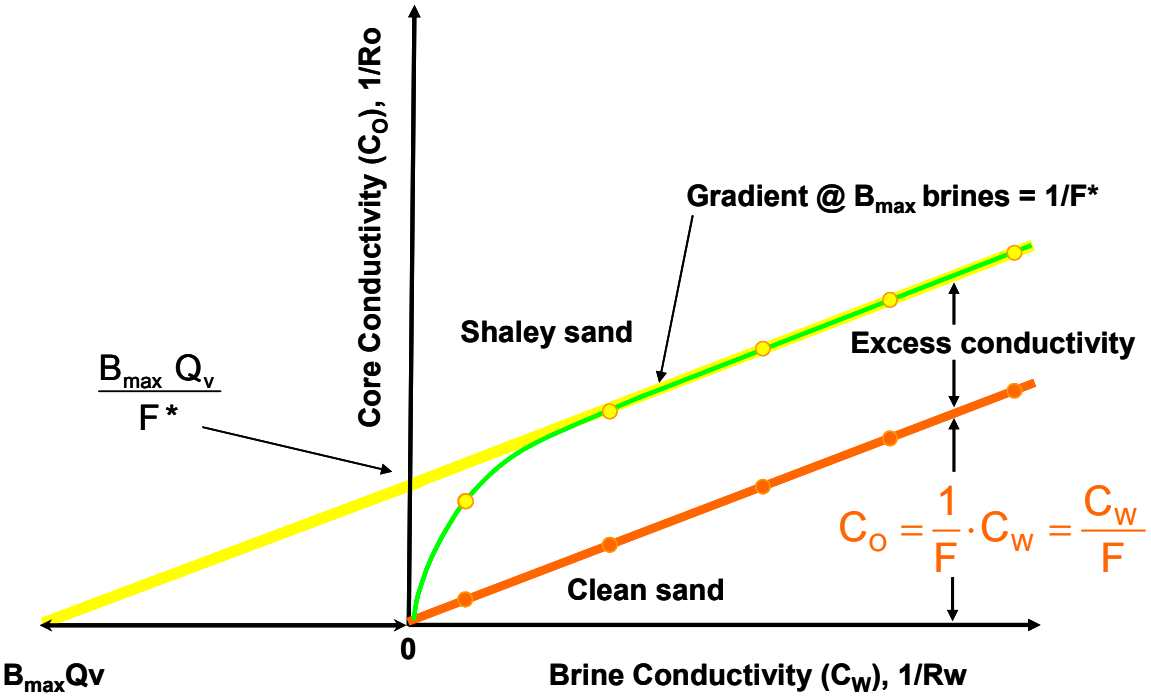

Figure 4.4.5. Relationship of Waxman-Smits model parameters illustrating their determination from multi-salinity measurements of core and brine conductivity.

Comparing measured core conductivities versus the saturating brine conductivity (Figure 4.4.6), nearly all cores exhibit some salinity dependence and the dependence is highly linear with a mean correlation coefficient $r^2 = 0.97 \pm 0.05$ for 308 samples (Figure 4.4.6). This dependence can be modeled using the Waxman-Smits equations or using empirical relationships.

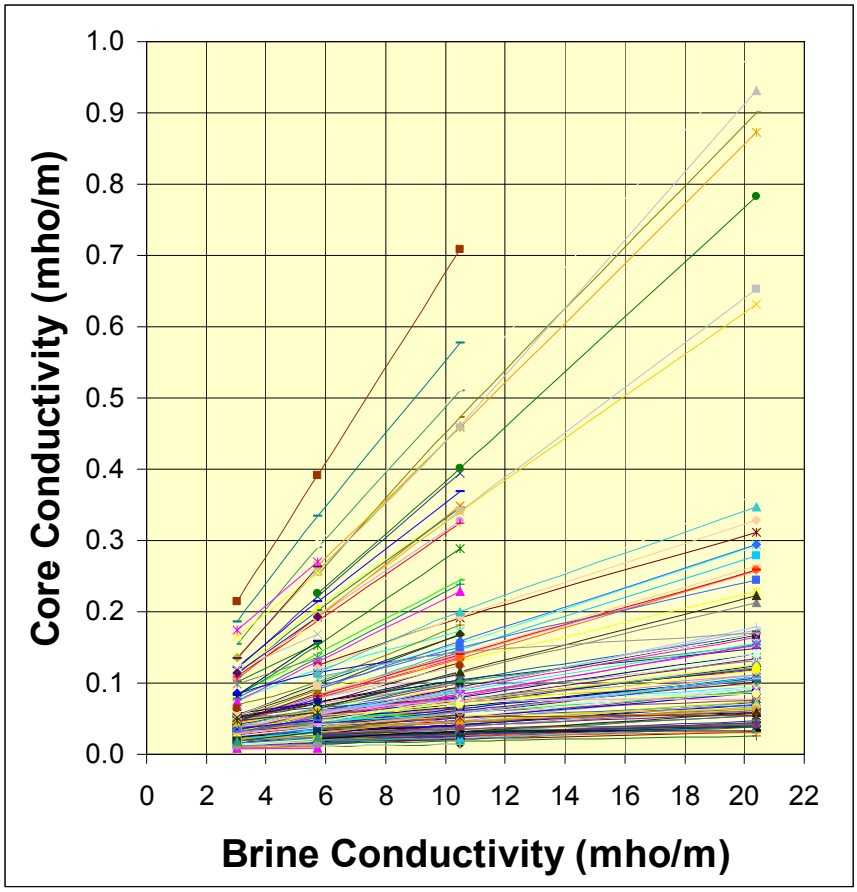

Figure 4.4.6. Core conductivity versus saturating brine conductivity for 308 samples.

Although Waxman-Smits parameters can be effectively applied in many wireline log analysis applications, simple empirical models provide an easy method to predict the Archie porosity exponents. The data provided in Table 4.4.1 can be used to determine appropriate Waxman-Smits parameters for those interested in this approach. The following discussion provides a simple model for predicting the Archie porosity exponent from empirical equations.

The salinity dependence shown in Figure 4.4.6 can be translated to a relationship between porosity exponent and salinity as shown in Figure 4.4.7. The log-linear relationship between ***m*** and logarithm of brine resistivity (R_w) allows the correction of predicted ***m*** values obtained using Equation 4.4.5 to any salinity.

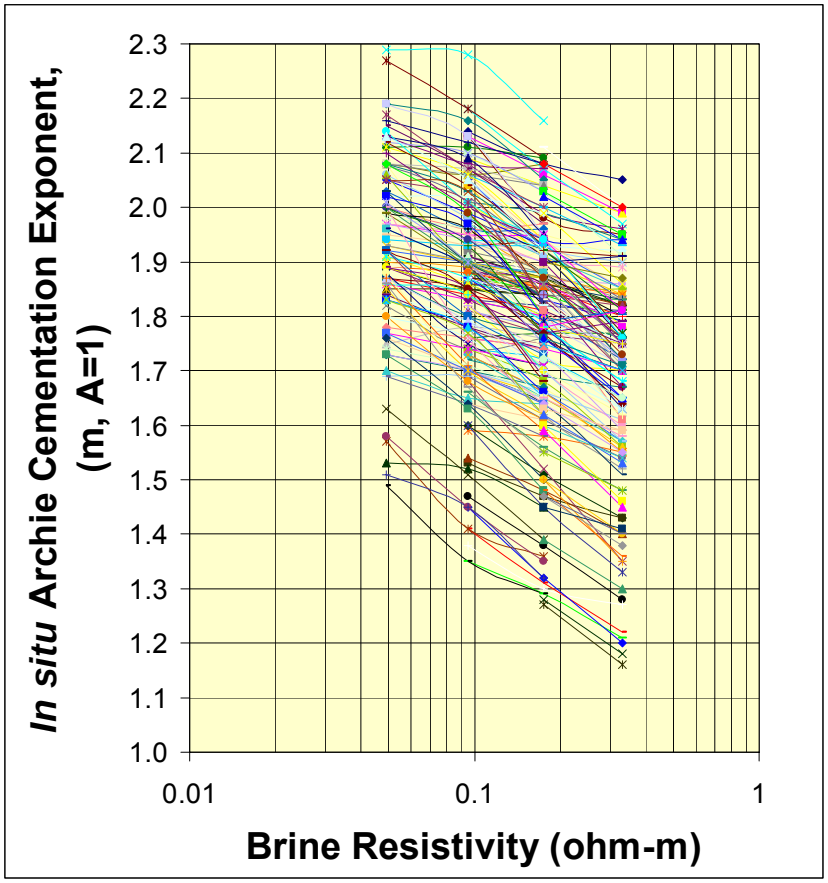

Figure 4.4.7. Crossplot of Archie porosity exponent versus saturating brine resistivity for 308 samples. All samples exhibit a highly linear relationship.

Although each core exhibits a highly linear relationship between ***m*** and $\log R_w$, the exact slope of each core varies with a mean value for all cores of;

$$\text{Average Slope}_{m\text{-}Rw} = -0.27 \pm 0.32 \text{ (2 standard deviations)} \quad [4.4.8]$$

Where $\text{Slope}_{m\text{-}Rw}$ = slope of m_{Rw} versus logRw.

The slopes exhibit a weak correlation with salinity (Figure 4.4.8). This correlation can be used to improve the prediction of ***m*** at any salinity:

$$\text{Slope}_{m\text{-}Rw} = 0.00118\ \phi - 0.355 \quad [4.4.9]$$

where ϕ is porosity in percent.

Combining equations 4.4.5 and 4.4.9, the Archie porosity exponent at any given porosity and reservoir brine salinity can be predicted using

$$\boldsymbol{m}_X = \boldsymbol{m}_{40} + \text{Slope}_{m\text{-}Rw} (\log Rw_X + \log Rw_{40K}) \quad [4.4.10]$$

replacing all terms:

$$\boldsymbol{m}_X = (0.653 \log\phi + 1.248) + (0.0118\ \phi\text{-}0.355) \times (\log Rw_X + 0.758); \quad 0\% \leq \phi < 14\% \quad [4.4.11]$$

$$\boldsymbol{m}_X = 1.95 + (0.0118\ \phi\text{-}0.355) \times (\log Rw_X + 0.758); \quad \phi \geq 14\% \quad [4.4.12]$$

where $\boldsymbol{m}_x$ = m at salinity X, $\boldsymbol{m}_{40}$ = $\boldsymbol{m}$ at 40K ppm NaCl, log Rw_X = $\log_{10}$ of resistivity of brine at salinity X, $\log Rw_{40K}$ = $\log_{10}$ of resistivity of 40K ppm NaCl = 0.758 (at 20 ^oC).

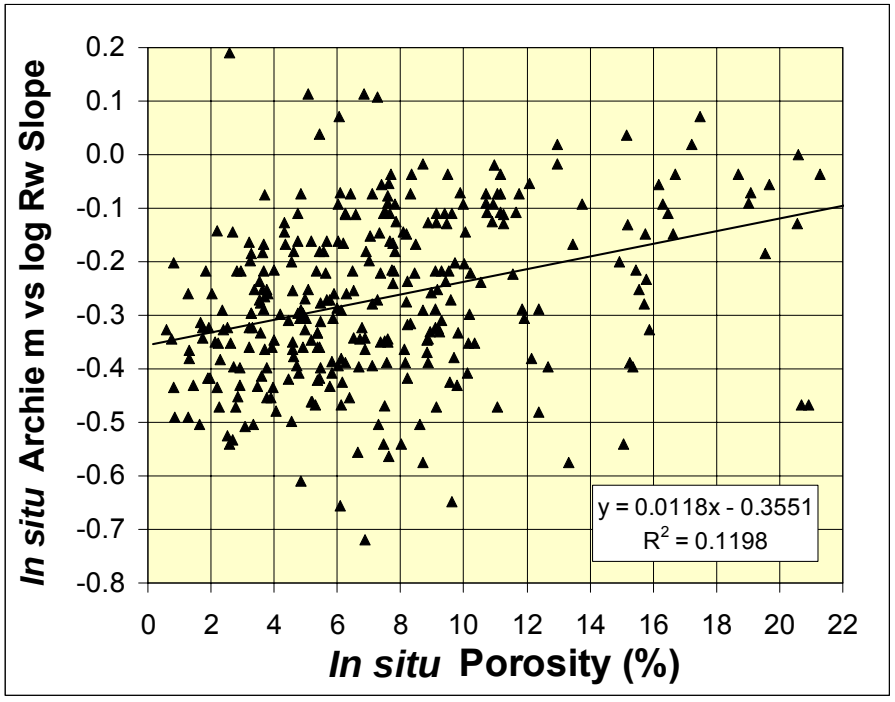

Figure 4.4.8. Crossplot of slope of Archie $\boldsymbol{m}$ versus [logR_w versus porosity].

Subtask 4.5. Measure Geologic and Petrologic Properties

4.5.1 Task Statement

Most published studies of TGS properties are tied to location but are rarely distinguished by lithofacies. This places potential, and sometimes unknown, limits on application or results. Though non-lithofacies specific petrophysical relationships can be developed, because rock mineralogy and texture exert control on pore architecture, petrophysical properties are lithofacies dependent. Lithofacies can be estimated from wireline log signatures. This calibration requires that the lithofacies be characterized using a digital system. To address this need all cores were described to provide an understanding of pay and nonpay rock types, their log signatures, lithofacies, stratigraphy, depositional sequences, and flow-unit continuity. The cores were graphically logged with emphasis on lithology, including bedform-type argillaceousness, small-scale (i.e., centimeters to meter-scale) heterogeneities, porosity type and distribution, and macro-scale diagenetic products. Based on the lithofacies present, representative core samples were obtained from all wells sampled. From the population of core plugs representing all lithofacies observed in all basins, a select set of samples were selected from the cores for which advanced properties analysis was performed. For these samples thin-section point count analysis (300 counts) was performed to assist in characterization of rock composition and rock and pore architecture. Core photos and thin-section photomicrographs illustrated observations and interpretations.

4.5.2 Methods

Core descriptions were prepared by examining slabbed and unslabbed core material at various core storage facilities, including the USGS Core Research Center and Triple O Slabbing (both of Denver, Colorado), and Shell Oil Bellaire Technology Center and PTS Laboratories, Inc. (both of Houston, Texas). Core material is permanently stored at these facilities, as well as the facilities of Core Laboratories, Inc., and ExxonMobil (both of Houston, Texas). Table 4.5.1 lists the wells from which cores were described. In all, a total of 6,447 feet of core are included in this study, from seven Rocky Mountain tight gas sand basins.

API STATE CODE	API COUNTY CODE	API WELL #	BASIN	FIELD	WELL	OPERATOR	Twn		Rng		Sec
49	035	20622	GREEN RIVER	WILDCAT	1 OLD ROAD	AMERICAN HUNTER EXPL	27	N	108	W	27
49	013	08024	GREEN RIVER	PINEDALE	5 PINEDALE	EL PASO NATURAL GAS	30	N	108	W	5
49	035	20088	GREEN RIVER	MERNA	A-1 WASP	INEXCO OIL COMPANY	36	N	112	W	28
49	035	06020	GREEN RIVER	BIG PINEY	B-54 BIG PINEY	BELCO PETROLEUM	29	N	113	W	26
49	035	05742	GREEN RIVER	TIP TOP SHALLOW	C-47 TIP TOP SHALLOW	BELCO PETROLEUM	28	N	113	W	22
49	035	06200	GREEN RIVER	MASON	K-2 MASON	BELCO PETROLEUM	31	N	113	W	13
49	035	24198	GREEN RIVER	PINEDALE	Vible 1B-11D	SHELL E&P	31	N	109	W	11
05	045		PICEANCE		1 BOOK CLIFFS-DRILL HOLE	USGS-CG	7	S	104	W	17
05	103		PICEANCE	LOWER WHITE RIVER	21011-5 MOON LAKE	WESTERN FUELS ASSOC	2	N	101	W	1
05	103	10391	PICEANCE	WILLOW RIDGE	EM T63X-2G	EXXON-MOBIL	3	S	97	W	2
05	045	11402	PICEANCE	MAMM CREEK	LAST DANCE 43C-3-792	BILL BARRETT CORP.	S	7	92	W	3
05	103	09406	PICEANCE	WHITE RIVER DOME	M-30-2-96W /D-037934	FUEL RESOURCES DEV	2	N	96	W	30
05	045	06578	PICEANCE	GRAND VALLEY	MV 24-20 CHEVRON	BARRETT ENERGY	6	S	96	W	20
05	045	06001	PICEANCE	RULISON	MWX-2 SUPERIOR	CER CORPORATION	6	S	94	W	34
05	045	10927	PICEANCE	PARACHUTE	PUCKETT/TOSCO PA 424-34	WILLIAMS E&P	6	S	95	W	34
49	005	25627	POWDER RIVER	BRIDGE DRAW	1 BARLOW 21-20	LOUISIANA LAND & EXP	48	N	75	W	20
49	009	21513	POWDER RIVER	MIKES DRAW	2 FRED STATE	DAVIS OIL COMPANY	35	N	70	W	36
49	009	06335	POWDER RIVER	FLAT TOP	2 SHAWNEE	BELCO PETROLEUM	33	N	69	W	2
49	009	05481	POWDER RIVER	FLAT TOP	3 SHAWNEE	BELCO PETROLEUM	33	N	69	W	23
05	081	06718	SAND WASH	WEST CRAIG	1-691-0513	COCKRELL OIL CORP	6	N	91	W	5
05	081	06724	SAND WASH	CRAIG DOME	1-791-2613	COCKRELL OIL CORP	7	N	91	W	26
43	047	30584	UINTA	NATURAL BUTTES	11-17F RIVER BEND UNIT	MAPCO INCOPORATED	10	S	20	E	17
43	047	30545	UINTA	BONANZA	2-7 FLAT MESA FEDERAL	ENSERCH EXPLORATION	10	S	23	E	7
43	019		UINTA		3 BOOK CLIFFS	USGS-CG	17	S	24	E	3
43	047	30860	UINTA	WILDCAT	3-24 US LAMCO	CHAMPLIN PETROLEUM	13	S	20	E	24
43	019		UINTA		4 BOOK CLIFFS	USGS-CG	17	S	24	E	31
43	047	30584	UINTA	AGENCY DRAW	4-5 US LAMCO	ENSERCH EXPLORATION	13	S	20	E	5
43	047	36565	UINTA	NATURAL BUTTES	NBU 1022-1A	KERR-MCGEE OIL&GAS ONSHORE	10	S	22	E	1
46	047	36401	UINTA	NATURAL BUTTES	NBU 920-36O	KERR-MCGEE OIL&GAS ONSHORE	9	S	22	E	36
49	037	21075	WASHAKIE		WILD ROSE 1	AMOCO PRODUCTION	17	N	94	W	5
49	037	05405	WASHAKIE	CHIMNEY ROCK	1 CHIMNEY ROCK	MOUNTAIN FUEL SUPPLY	18	N	102	W	12
49	037	21053	WASHAKIE	FIVE MILE GULCH	3 UNIT	AMOCO PRODUCTION	21	N	93	W	35
49	037	23956	WASHAKIE	SIBERIA RIDGE	5-2 SIBERIA RIDGE UNIT	AMOCO PRODUCTION	21	N	94	W	5
49	037	05683	WASHAKIE	PATRICK DRAW	65-1-7 ARCH UNIT	FOREST OIL CORP	19	N	99	W	1
49	037	05577	WASHAKIE	ARCH	ARCH UNIT UPRR #102-7-10	ANADARKO E&P CO. LP	19	N	98	W	7
49	037	05349	WASHAKIE		B-2A SPIDER CREEK	HUMBLE OIL & REF	18	N	110	W	27
49	007	21170	WASHAKIE	SAVERY	C-11 /FEE	FUEL RESOURCES DEV	12	N	90	W	11
49	037	22304	WASHAKIE	DRIPPING ROCK	DRIPPING ROCK #3	CELSIUS	14	N	94	W	8
49	037	22355	WASHAKIE	DRIPPING ROCK	DRIPPING ROCK #5	CELSIUS	14	N	94	W	19
49	037	99999	WASHAKIE		WILD ROSE	BP AMERICA PRODUCTION, INC.	18	N	94	W	33
49	013	20836	WIND RIVER	MADDEN	1-27 LOOKOUT	MONSANTO OIL	39	N	91	W	27
49	013	20786	WIND RIVER	LYSITE	1-9 LYSITE	MICH WISC PIPELINE	38	N	91	W	9
49	013	20966	WIND RIVER	MADDEN	2-1 CHEVRON	MONSANTO OIL	38	N	91	W	1
49	013	20724	WIND RIVER		31-22 TRIBAL PHILLIPS	BROWN TOM INC	4	N	3	E	31

Table 4.5.1 List of wells for which cores were described.

4.5.2.1 Core and Sample Description

Core and core plug samples were examined using a stereo binocular microscope or hand lens. Grain size and sorting of sediment was determined by using grain-size comparators standardized for geologic investigation. In addition, lithology, composition, bed thickness, bedding contacts, sedimentary structures, and details of visible porosity, fractures, and cementation were recorded. A key feature of this investigation is the use of a rock-typing classification system that characterizes lithology, composition, grain size, sorting, sedimentary structure, and cementation in a simple five digit code (Table 4.5.2) previously reported by Cluff, Byrnes, and Webb (1994). This digital classification system has allowed us to closely correlate core analysis data with wire-line log data, allowing direct comparison of measured and calculated petrophysical data. Results of core descriptions, digital rock-type data, and interpreted depositional environments were presented on graphic charts for each core interval that was described. These core charts are available as PDF images on the Project website. Digital rock-type data for all cores examined during this study were also recorded in Excel spreadsheets which are included on the Project website.

The fine-grained intervals of the Mesaverde Group are dominated by mudstones and silty shales (rock types 10x19 and 11x29), lenticular and wavy-bedded very shaly sandstones (12x3x and 12x4x), and wavy-bedded to ripple cross-laminated shaly sandstones (13x4x and 13x6x). The sandstone intervals of the Mesaverde Group are dominated by ripple cross-laminated and crossbedded, very fine to fine-grained sandstones (rock types 14x6x, 14x7x), low angle cross-laminated to planar laminated sandstones (14x8x), and massive sandstones (14x9x). Medium-grained sandstones are mostly restricted to the Upper Almond (15x7x and 15x9x). The rock classification system used is objective and independent of any interpretations of depositional environments or stratigraphic position.

Table 4.5.2 Digital rock number scheme for siliciclastic core description.

FIRST DIGIT: Basic Lithology

0xxxx Organic rocks (coals, etc.)
1xxxx Siliciclastic rocks

SECOND DIGIT: Grain size, sorting, texture

10xxx Shales
11xxx Silty shales (60-90% clay)
12xxx Siltstones or very shaly sandstones (40-65% clay and silt)
13xxx Moderately shaly sandstones (10-40% clay and silt)
14xxx Sandstones, fine to very fine
15xxx Sandstones, medium
16xxx Sandstones, coarse

THIRD DIGIT: Degree of consolidation or cementation

1x0xx Totally cemented, dense, hard, unfractured
1x1xx Dense, fractured
1x2xx Well indurated, mod-low porosity (3-10%), unfractured
1x3xx Well indurated, mod-low porosity (3-10%), fractured
1x4xx Well indurated, mod-low porosity (3-10%), highly fractured
1x5xx Indurated, mod-high porosity (>10%), unfractured
1x6xx Indurated, mod-high porosity (>10%), fractured
1x7xx Indurated, mod-high porosity (>10%), highly fractured
1x8xx Poorly indurated, high-very high porosity, soft
1x9xx Unconsolidated sediment

FOURTH DIGIT: Primary sedimentary structures

1xx0x Vertical perm barriers, shale dikes, cemented vertical fractures
1xx1x Churned/bioturbated to burrow mottled (small scale)
1xx2x Convolute, slumped, large burrow mottled bedding (large scale)
1xx3x Lenticular bedded, discontinuous sand/silt lenses
1xx4x Wavy bedded, continuous sand/silt and mud layers
1xx5x Flaser bedded, discontinuous mud layers
1xx6x Small scale (< 4 cm) x-laminated, ripple x-lam, small scale hummocky crossbed
1xx7x Large scale (> 4 cm) trough or planar crossbedded
1xx8x Planar laminated or very low angle crossbeds, large scale hummocky crossbed
1xx9x Massive, structureless

FIFTH DIGIT: Dominant cementation or pore-filling mineral

1xxx0 Sulfide pore filling (RhoG = 3.85-5.0)
1xxx1 Siderite (RhoG = 3.89)
1xxx2 Phosphate (RhoG = 3.13-3.21)
1xxx3 Anhydrite or gypsum (RhoG = 2.98 or 2.35)
1xxx4 Dolomite (RhoG = 2.89)
1xxx5 Calcite (RhoG = 2.71)
1xxx6 Quartz (RhoG = 2.65)
1xxx7 Authigenic clay (RhoG = 2.12-2.76)
1xxx8 Carbonaceous debris (RhoG = 2.0)
1xxx9 No pore-filling material or detrital clay-filled intergranular voids

4.5.2.2 Thin Section Petrography

Thin section preparation of low-permeability sandstones has always been hampered by the inability to efficiently impregnate sandstone samples with blue-dye epoxy because of the low permeability and the consequent inability to flow epoxy deeply enough into the sample. Most commercial epoxies have an approximate viscosity of 100 centipoise (cp) and a pot life (the time for which the epoxy is liquid before viscosity increases by orders of magnitude) of approximately 30 minutes. To maximize impregnation many techniques have been developed, most notably high-pressure impregnation. The depth of penetration is a function of the driving pressure, the pressure in the pores of the sample, the permeability, epoxy viscosity, and capillary forces if epoxy wets the surface. Table 4.5.4 illustrates the theoretical depth of penetration of a 100-cp viscosity epoxy into billets of 12.5-mm thickness with application of standard atmospheric pressure into a sample initially evacuated by vacuum. These calculations indicate that for the standard pot life of 30 minutes (1800 seconds), epoxy penetrates less than 0.27 mm into rocks of less than 0.1 mD. This would indicate that for most low-permeability sandstones, the standard impregnation technique does not provide thin sections with blue-dye epoxy in the pore space. Even with high-pressure impregnation, where conventionally the samples are placed in a gas-pressure vessel and exposed to a gas pressure over the epoxy covering the sample of approximately 1,500 psi (10.3 MPa), impregnation is less than 1 mm for samples with permeability less than 0.01 mD (Table 4.5.3).

To improve impregnation efficiency and depth, experiments using long-pot-life epoxy and pressure were conducted with Zach Wenz of the University of Kansas, Department of Geology. Experiments on Mesaverde sandstone samples found that good impregnation was achieved using an extended pot-life viscosity with moderate pressure. The optimum methodology involved the following steps: 1) cut sandstone billets not greater than 1 cm in thickness to allow efficient evacuation prior to epoxy immersion, 2) grind billet face flat prior to impregnation, 3) evacuate sample to $< 10^{-3}$ torr vacuum, 4) pour extended pot-life epoxy over sample while still under vacuum insuring that sample is completely immersed under epoxy, 5) release vacuum, 6) place samples in high pressure vessel, 7) pressure vessel to approximately 100-150 psi (700-1000 kPa), 8) leave samples under pressure until epoxy sets or becomes very viscous (e.g., 8-16 hours). An effective 10-hour pot-life viscosity that worked well for the Mesaverde sandstones studied is EPO-TEK 301-2FL®, which is similar to EPO-TEK 301 ®

epoxy that is commonly used in thin-section preparation. Table 4.5.3 illustrates the approximate depth of penetration for a 100-cp extended-pot-life epoxy.

Applied Pressure psi	Capillary force psi	Total pressure psi	Permeablility mD	Epoxy Impregnation Depth (mm) time (min) 2	time (min) 4	time (min) 8	time (min) 10	time (min) 20	time (min) 30	time (min) 300	time (min) 600
14.7	0.3	15	1000	1.25E+01	1.25E+01	1.25E+01	1.25E+01	1.25E+01	1.25E+01	1.25E+01	1.25E+01
14.7	0.7	15	100	1.01E+01	1.25E+01	1.25E+01	1.25E+01	1.25E+01	1.25E+01	1.25E+01	1.25E+01
14.7	1.9	17	10	1.08E+00	2.17E+00	4.33E+00	5.41E+00	1.08E+01	1.25E+01	1.25E+01	1.25E+01
14.7	4.9	20	1	1.28E-01	2.57E-01	5.13E-01	6.41E-01	1.28E+00	1.92E+00	1.25E+01	1.25E+01
14.7	13.0	28	0.1	1.81E-02	3.62E-02	7.23E-02	9.04E-02	1.81E-01	2.71E-01	2.71E+00	5.43E+00
14.7	17.4	32	0.05	1.05E-02	2.10E-02	4.19E-02	5.24E-02	1.05E-01	1.57E-01	1.57E+00	3.14E+00
14.7	34.2	49	0.01	3.19E-03	6.38E-03	1.28E-02	1.60E-02	3.19E-02	4.79E-02	4.79E-01	9.58E-01
14.7	45.7	60	0.005	1.97E-03	3.95E-03	7.89E-03	9.87E-03	1.97E-02	2.96E-02	2.96E-01	5.92E-01
14.7	89.9	105	0.001	6.83E-04	1.37E-03	2.73E-03	3.42E-03	6.83E-03	1.02E-02	1.02E-01	2.05E-01
14.7	120.3	135	0.0005	4.41E-04	8.81E-04	1.76E-03	2.20E-03	4.41E-03	6.61E-03	6.61E-02	1.32E-01
147	0.3	147	1000	1.25E+01	1.25E+01	1.25E+01	1.25E+01	1.25E+01	1.25E+01	1.25E+01	1.25E+01
147	0.7	148	100	1.25E+01	1.25E+01	1.25E+01	1.25E+01	1.25E+01	1.25E+01	1.25E+01	1.25E+01
147	1.9	149	10	9.72E+00	1.25E+01	1.25E+01	1.25E+01	1.25E+01	1.25E+01	1.25E+01	1.25E+01
147	4.9	152	1	9.92E-01	1.98E+00	3.97E+00	4.96E+00	9.92E+00	1.25E+01	1.25E+01	1.25E+01
147	13.0	160	0.1	1.04E-01	2.09E-01	4.18E-01	5.22E-01	1.04E+00	1.57E+00	1.25E+01	1.25E+01
147	17.4	164	0.05	5.37E-02	1.07E-01	2.15E-01	2.68E-01	5.37E-01	8.05E-01	8.05E+00	1.61E+01
147	34.2	181	0.01	1.18E-02	2.37E-02	4.73E-02	5.92E-02	1.18E-01	1.77E-01	1.77E+00	3.55E+00
147	45.7	193	0.005	6.29E-03	1.26E-02	2.52E-02	3.15E-02	6.29E-02	9.44E-02	9.44E-01	1.89E+00
147	89.9	237	0.001	1.55E-03	3.09E-03	6.19E-03	7.74E-03	1.55E-02	2.32E-02	2.32E-01	4.64E-01
147	120.3	267	0.0005	8.73E-04	1.75E-03	3.49E-03	4.36E-03	8.73E-03	1.31E-02	1.31E-01	2.62E-01
1470	0.3	1470	1000	1.25E+01	1.25E+01	1.25E+01	1.25E+01	1.25E+01	1.25E+01	1.25E+01	1.25E+01
1470	0.7	1471	100	1.25E+01	1.25E+01	1.25E+01	1.25E+01	1.25E+01	1.25E+01	1.25E+01	1.25E+01
1470	1.9	1472	10	1.25E+01	1.25E+01	1.25E+01	1.25E+01	1.25E+01	1.25E+01	1.25E+01	1.25E+01
1470	4.9	1475	1	9.63E+00	1.25E+01	1.25E+01	1.25E+01	1.25E+01	1.25E+01	1.25E+01	1.25E+01
1470	13.0	1483	0.1	9.68E-01	1.94E+00	3.87E+00	4.84E+00	9.68E+00	1.25E+01	1.25E+01	1.25E+01
1470	17.4	1487	0.05	4.86E-01	9.71E-01	1.94E+00	2.43E+00	4.86E+00	7.29E+00	1.25E+01	1.25E+01
1470	34.2	1504	0.01	9.82E-02	1.96E-01	3.93E-01	4.91E-01	9.82E-01	1.47E+00	1.25E+01	1.25E+01
1470	45.7	1516	0.005	4.95E-02	9.90E-02	1.98E-01	2.47E-01	4.95E-01	7.42E-01	7.42E+00	1.48E+01
1470	89.9	1560	0.001	1.02E-02	2.04E-02	4.07E-02	5.09E-02	1.02E-01	1.53E-01	1.53E+00	3.06E+00
1470	120.3	1590	0.0005	5.19E-03	1.04E-02	2.08E-02	2.60E-02	5.19E-02	7.79E-02	7.79E-01	1.56E+00
				Standard Pot-life						Extended Pot-life	

Table 4.5.3. Epoxy impregnation into 12.5-mm-thick sample, ϕ = 10%, with 100-cp viscosity epoxy for various impregnation pressures, sample permeabilities, and time of impregnation. Note that standard pot-life epoxies have pot-life of 30 minutes and impregnation effectively stops at this time and corresponding depth. Extended pot-life epoxies remain viscous for periods up to 300-600 minutes and are capable of effective to complete penetration at moderate to high injection pressures. Depth of penetration for a given pressure, permeability, and time is color coded for convenience: Orange < 0.1 mm, tan 0.1-1mm, white 1-10mm, blue >10mm.

End cuts from core plug samples selected for advanced-properties analysis were impregnated with blue-dye epoxy in a heated, laboratory vacuum oven. Following evacuation, nitrogen from a compressed gas cylinder was used to force the blue epoxy into porous samples. After curing, the epoxy-impregnated sample was sliced, polished and mounted on a glass slide. The sample was then trimmed with a fine diamond saw, and ground to near 30 microns on a lapidary wheel, with final polishing accomplished by hand on a lap wheel. Each thin section was stained with a mixture of Alizarin red-S and potassium ferricyanide for identification of calcite

and ferroan carbonates and stained for identification of potassium feldspar by sequential etching over HF acid, and staining in barium chloride and sodium cobaltinitrate. A cover slip was applied using an easily removable, synthetic, heat-sensitive adhesive.

Thin sections were examined using Nikon Optiphot and E. Leitz Orthoplan petrographic microscopes. Photomicrographs of representative textural and diagenetic features were taken with an Olympus E410 Digital camera. Additional photomicrographs for illustration of detailed features of diagenesis and porosity evolution were taken with a trinocular mounted Nikon FM2 data-back camera and Nikon AFX auto-exposure unit. Photograph magnifications have been calibrated by an E. Leitz micrometer, with a 0.01-mm graduated scale. Photomicrographs for each thin section sample at multiple magnifications are posted on the Project website.

Point counting of thin sections for composition and porosity distribution was accomplished using a Swift Instruments Automatic Point Count stage, which is designed to move the sample through a predetermined grid, while the analyst identifies constituents of the sample at each point on the grid. Three hundred points were counted for each sample. Details of grain size, sorting, nature and distribution of cements, porosity, and clay distribution are noted during point count analysis. All data were recorded in Microsoft Excel spreadsheets. Percentage and compositional ratios are calculated in Microsoft Excel spreadsheets, graphic plots are generated in Excel and Corel Quattro spreadsheets.

4.5.3 Results

Core descriptions, core slab images, thin section photomicrographs, and graphic presentation of core descriptions are too large for presentation in this report. These data and images are available on the ***Project Website (http://www.kgs.ku.edu/mesaverde/)***. It is beyond the scope of this study to provide a comprehensive analysis of the lithologic and petrologic properties of the cores studied. The goal of this task in the study was to provide the needed lithologic characterization of the core.

The Project Website presents graphic images of digitally described cores listed in Table 4.5.1. Figures 4.5.1 and 4.5.2 provide examples of representative core descriptions. Digital classification for each 0.5-ft interval are presented both on the core description and in separate Excel files.

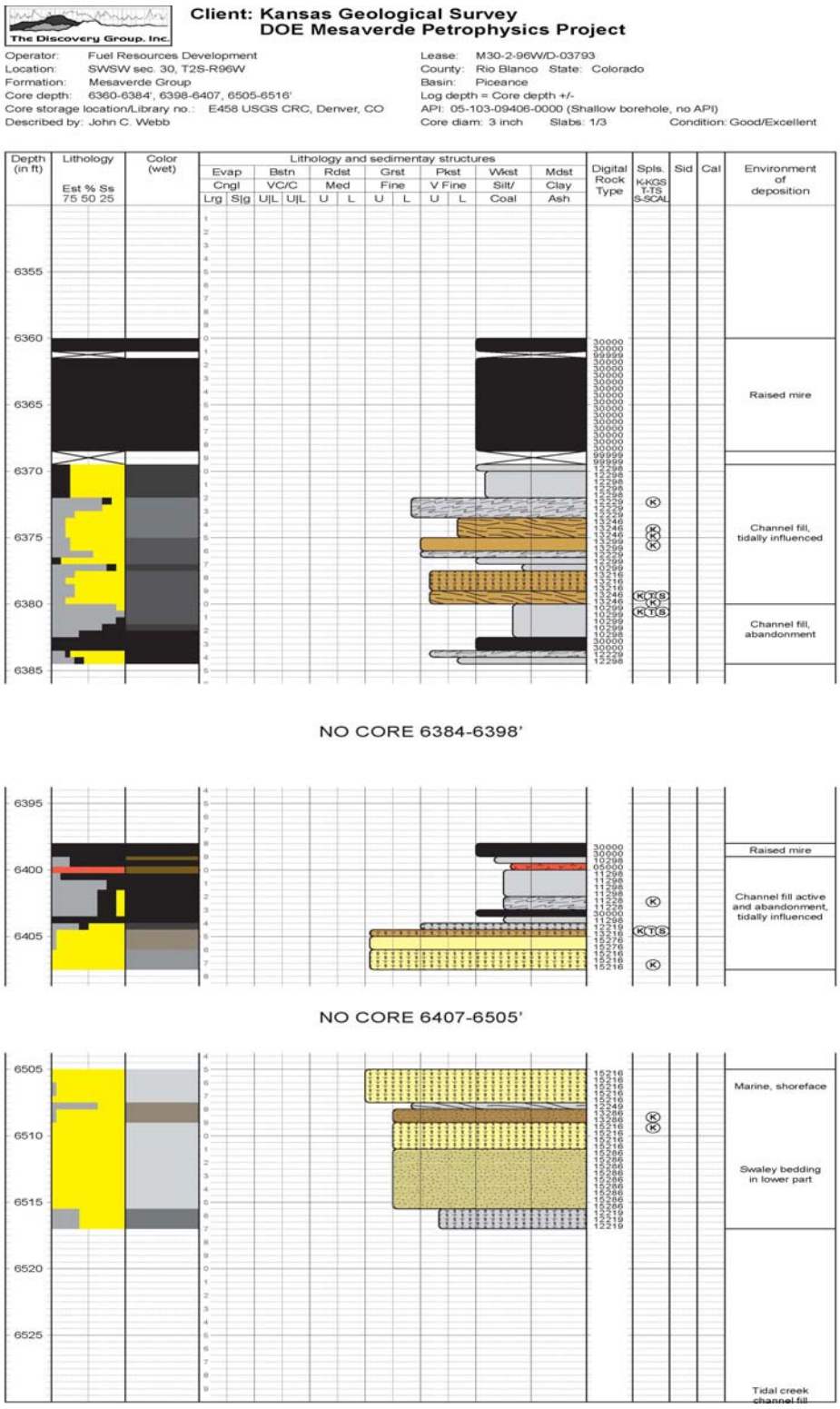

Figure 4.5.1. Example of core description.

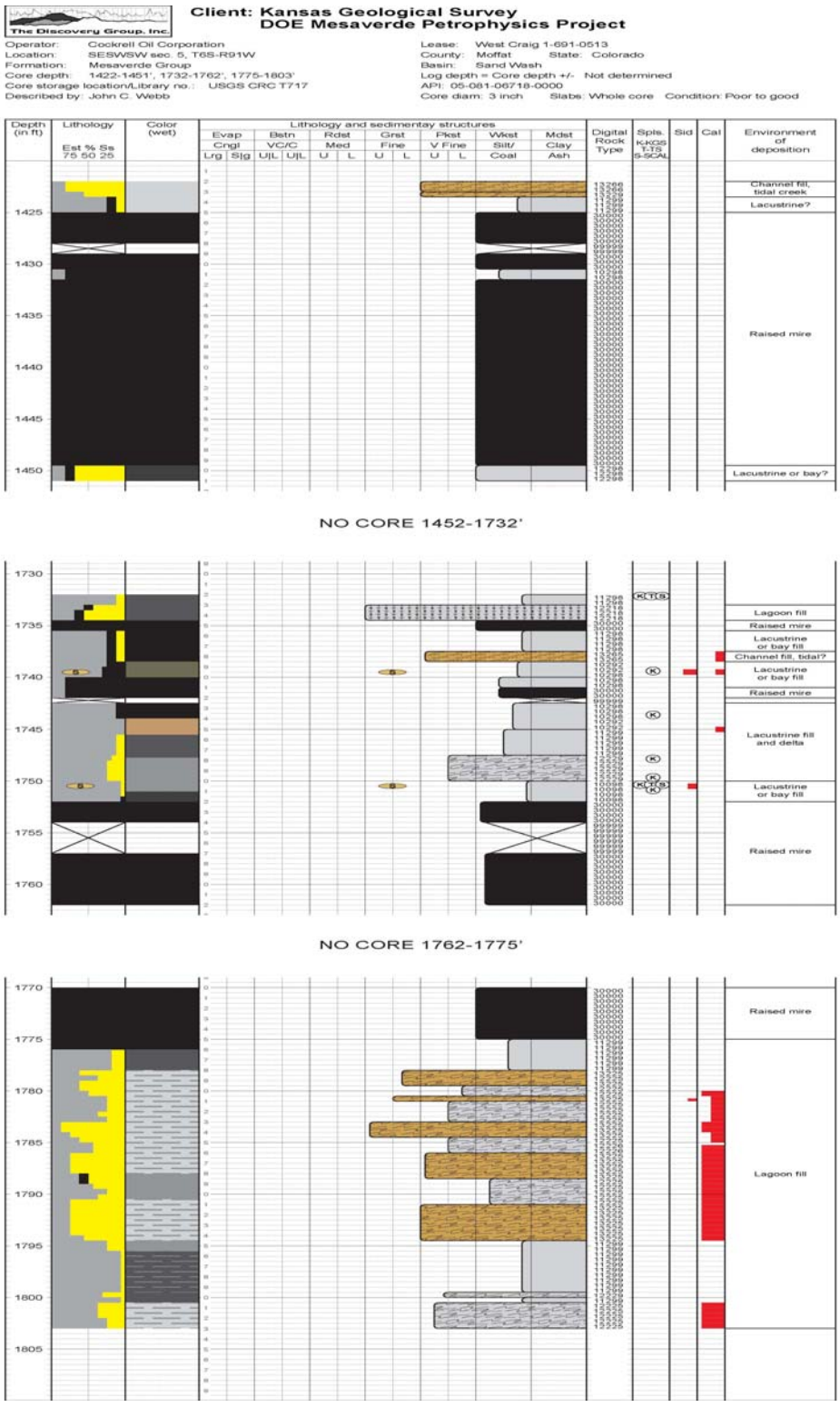

Figure 4.5.2. Example of core desciption.

The Project Website contains over 550 core slab photos of slabs from which core plugs were obtained. These images represent a comprehensive image library of the lithofacies present in the Mesaverde in the basins studied. Figure 4.5.3 illustrates some of the lithofacies present in the Mesaverde sampled.

For 150 samples thin-section images at various magnification are presented. Figures 4.5.4. through 4.5.8 illustrate thin-section photomicrographs for different pore types in the Mesaverde in the Piceance Basin.

These data provide a tool for users to analyze. The following discussion does not try to provide a comprehensive analysis of the Measverde but, rather, briefly summarizes some of the lithologic properties exhibited by the Measverde.

4.5.3.1 Lithofacies and Sedimentary Structures

Sedimentary lithofacies in the Mesaverde Group range from coal and carbonaceous shale to shale and silty shale, very fine to medium, and locally coarse-grained sandstone. Figure 4.5.3 illustrates some of the lithofacies present in the Mesaverde sampled. Argillaceous rock types of the Mesaverde Group are dominated by laminated, bioturbated to massive shale, silty shale, and shaly siltstone. Very shaly and shaly sandstones include burrowed, planar- and ripple-laminated, wavy- and lenticular-bedded, and massive lithologies. Sandstone intervals are dominated by very fine to medium-grained sandstone, exhibiting burrowed, ripple cross-laminated, trough cross-bedded, low-angle cross-laminated and planar-laminated sedimentary structures, and massive to contorted bedding. Shale lithoclast conglomerates with clast and sandy matrix supported textures are also locally present.

4.5.3.2 Depositional Environment

Depositional environments range from near shore marine to continental, and include shoreface, foreshore, prodeltaic and deltaic, lagoonal and bay-fill, tidal inlet, tidal channel and mudflat, swamp and raised mire, active and abandoned fluvial channel fill, overbank, and levee. Rooted and texturally disturbed lithologies indicate the intermittent to prolonged presence of vegetation, subaerial exposure, and weathering in some cored intervals. Tidal influence is recognized in channel and bay fill environments by the presence of clay and carbonaceous drapes on ripple, planar, and trough cross laminations, inclined heterolithic bedding (typically consisting

of thinly bedded, closely alternating, horizontal to low-angle beds of shale, mudstone, shaly sandstone, or sandstone). In addition, some active channel-fill sandstones exhibit cryptobioturbation (a blotchy pattern of highly concentrated, indistinct burrowing), which may indicate the presence of brackish to saline environments and the possibility of tidal influence.

4.5.3.3 Mineralogy

Sandstones consist of quartz arenite, litharenite, and feldspathic litharenite. Feldspar is predominantly plagioclase, much of which has been altered to albite. Potassium feldspar is locally prominent, especially where associated rock fragments indicate a contribution from volcanic terrains. Rock fragments include those derived from sedimentary (chert, mudstone, carbonate), metamorphic (phylite, schist, micaceous/quartzose) and volcanic (silicified, argillitic, porphyritic, microlitic) rocks, and even plutonic (quartz/feldspathic) terrains are locally present. Cements include quartz, ferroan calcite and ferroan dolomite, clay minerals, siderite, and pyrite. For most samples, sediment deposited in marine shoreline environments exhibits a more quartzose composition than coeval sediment deposited in fluvial and coastal-plain environments. Sandstone deposited in intertidal or coastal-plain environments typically contain clay drapes, clay pellets, or burrowing indicative of brackish to marine environments, and are therefore shalier than coeval fluvial or shoreface environments.Figure 4.5.9 and 4.5.11 illustrate Folk compositional plots that can be constructed from the data.

4.5.3.4 Diagenesis

Detrital composition influences the type and degree of diagenesis. Porosity reduction in quartzose sandstones occurs by pervasive cementation by quartz, while feldspathic and lithic-rich sandstones exhibit little cementation by quartz. Instead, these lithologies exhibit strong to severe compaction, and may contain small to moderate amounts of clay mineral cement. Clay cements are also locally present in quartzose sandstones, and where abundant, may inhibit the precipitation of quartz cement. Secondary intergranular and moldic porosity have developed in some sandstones, and typically comprise the bulk of mesoporosity. Typical dissolution targets include carbonate and chert rock fragments, precursor calcite cements, detrital feldspars, and rarely, volcanic rock fragments. Microporosity within clay cement typically exceeds mesoporosity.

4.5.3.5 Lithologic Influence on Permeability

For most lithofacies, average porosity increases with increasing grain size (including decreasing shaliness; example Figure 4.5.12). Permeability at any given porosity increases with increasing grain size and increasing sorting, though this relationship is further influenced by the nature of cementation, and to a much lower degree, sedimentary structure. A visual assessment of the partitioning of porosity (microporosity vs. mesoporosity) and the abundance and distribution of clay mineral cement helps to explain the variation of permeability within rock types of similar grain size. Pore type, resulting from mechanical and chemical compaction and diagenesis also influences permeability-porosity relationships (Figure 4.5.13).

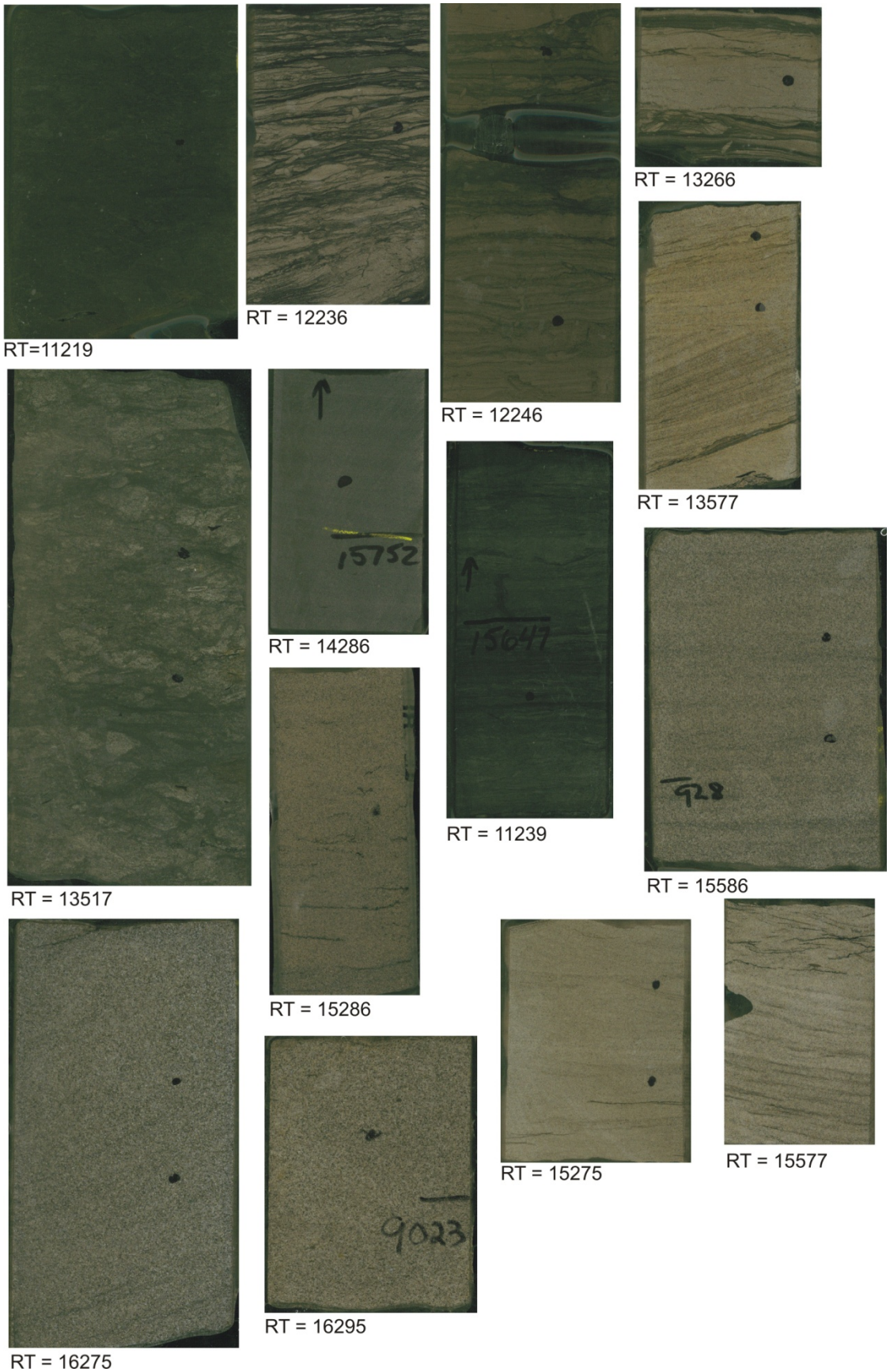

Figure 4.5.3. Example Mesaverde lithofacies with rock-type digital classification.

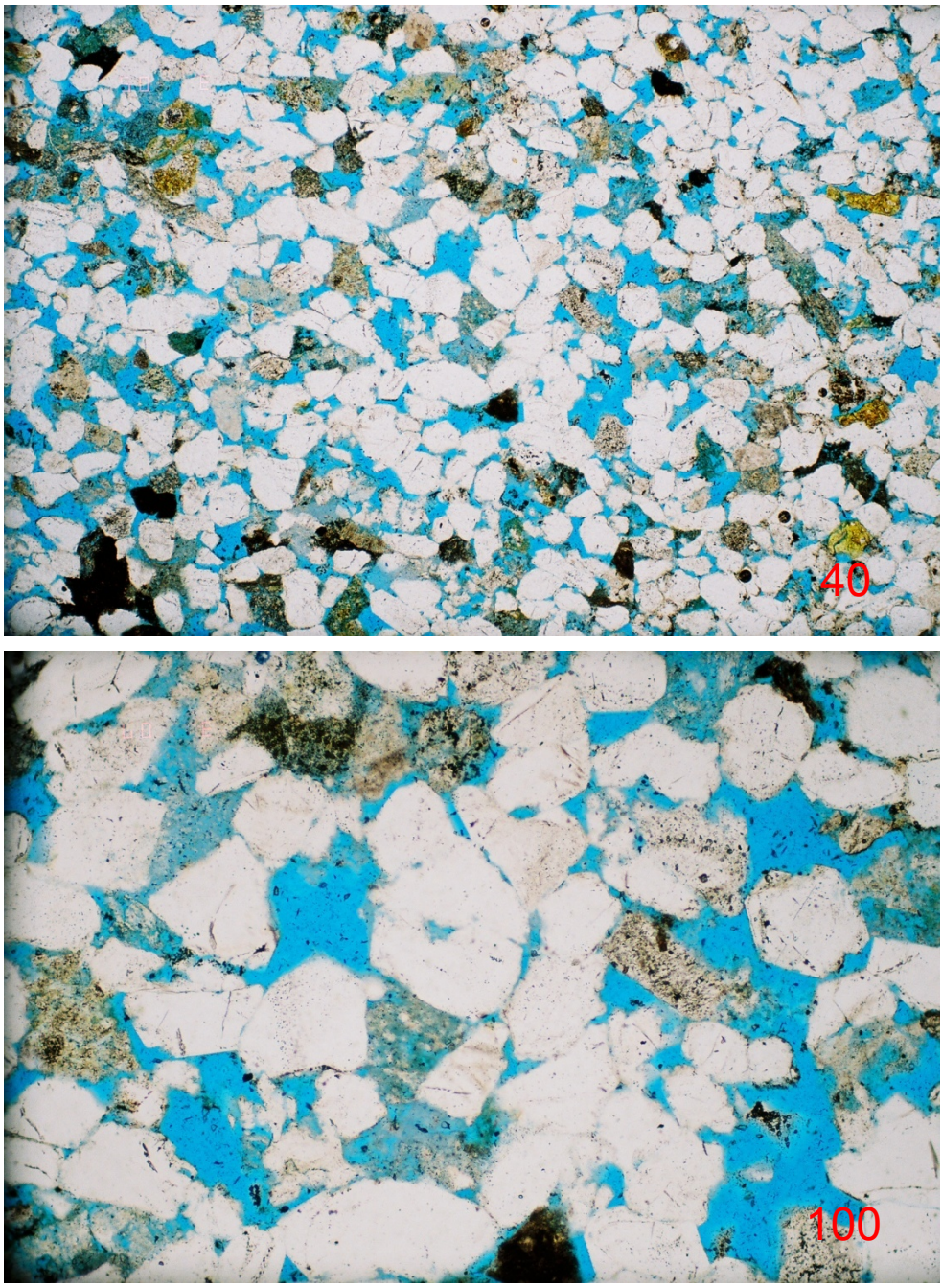

Figure 4.5.4. Example Mesaverde thin section for Type I porosity(shallow burial). Porosity consists of well-connected primary and secondary intergranular mesopores, sparse moldic pores, quartz overgrowth cement. Quartz cement is sparse. Lack of pore-lining clay cement reduces Swi and improves relative permeability. USGS CB #1 Book Cliffs, 255.8', Rock type 15567, ϕ = 24.8%, GD = 2.64 g/cc, Ka = 137.62 mD.

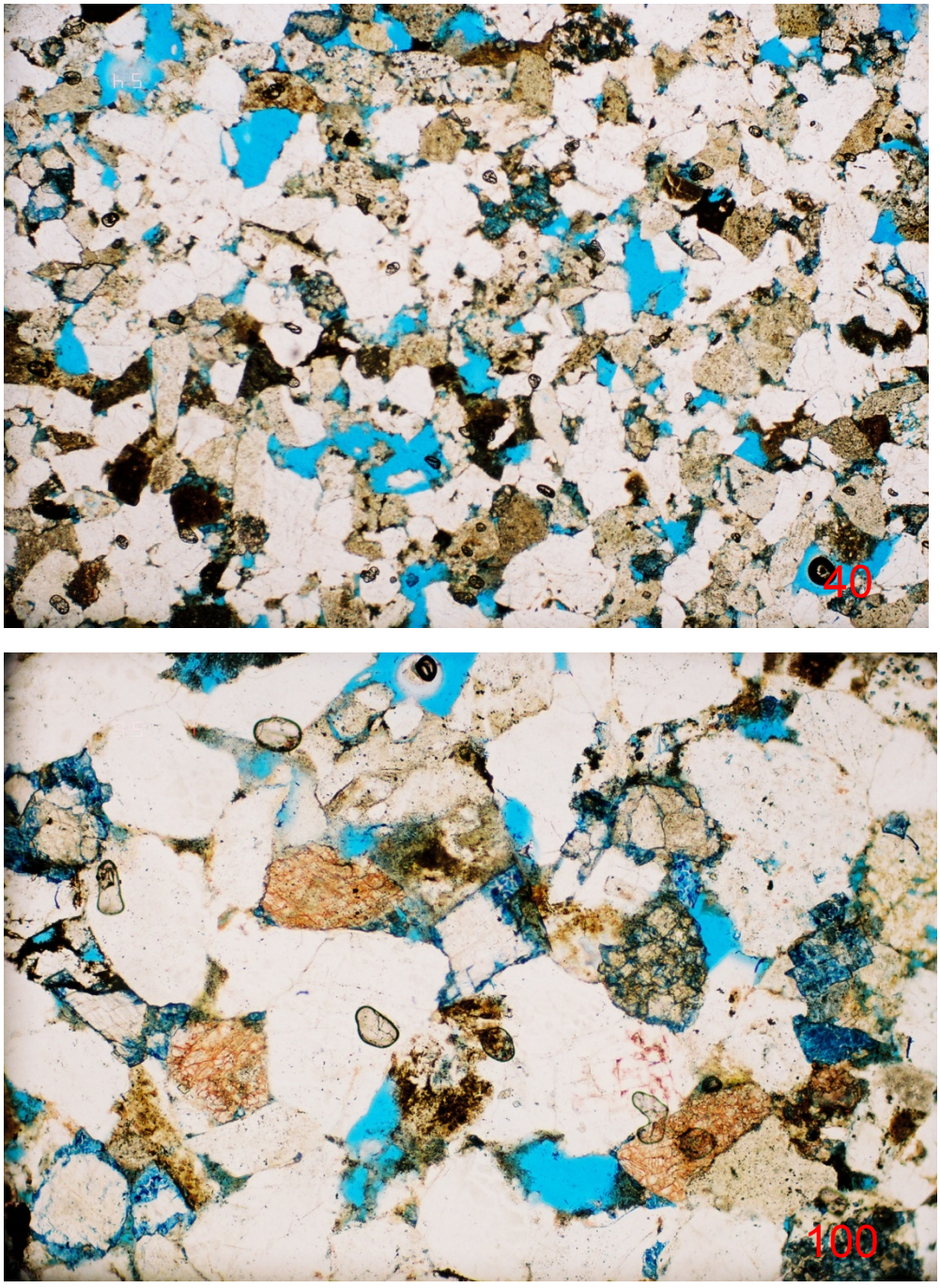

Figure 4.5.5. Example Mesaverde thin section for Type II porosity. Porosity consists of poorly to moderately connected moldic and secondary intergranular mesopores with traces of pore-lining ML/IS(?) clay, containing microporosity. Quartz cement is prominent, ferroan calcite is sparse. Pore-lining clay cement causes elevated Swi and reduced relative permeability. Williams PA 424, 6148.8', Rock Type 15276, ϕ = 9.9%, GD = 2.66 g/cc, Ka=0.0237 mD.

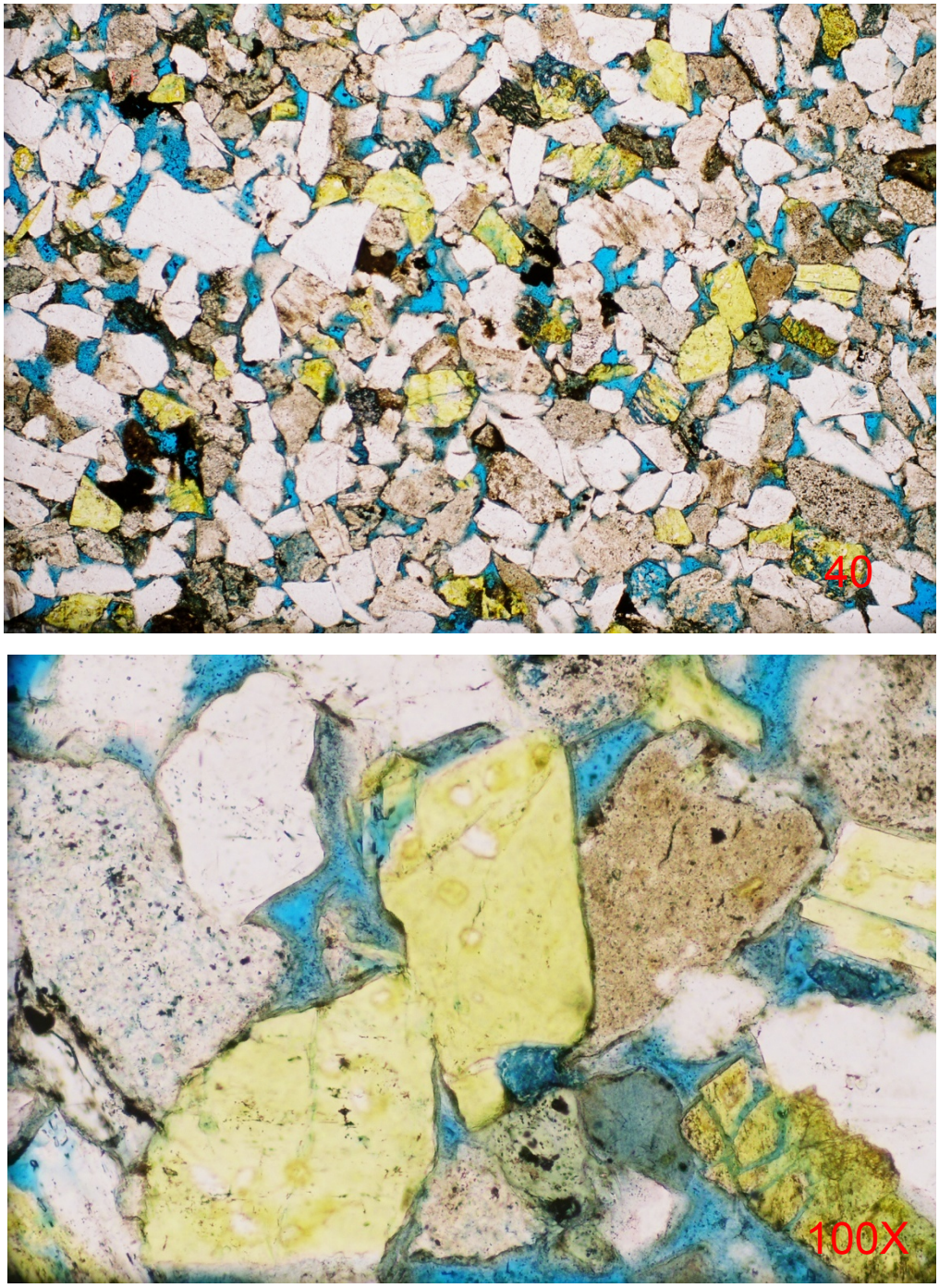

Figure 4.5.6. Example Mesaverde thin section for Type III porosity. Porosity consists of clay-lined intergranular pores; pore throats are occluded by clay cement, which causes elevated Swi, reduced relative permeability, and increased Pc entry pressure. Cements include chlorite or ML-IS clay, traces of nonferroan or ferroan calcite, traces of quartz overgrowths. Inhomogeneous packing and over-sized intergranular pores indicate the development of secondary intergranular porosity. Williams PA424, 4600.3', Rock Type 15297, ϕ = 12.2%, GD = 2.65g/cc, Ka = 0.0178 mD.

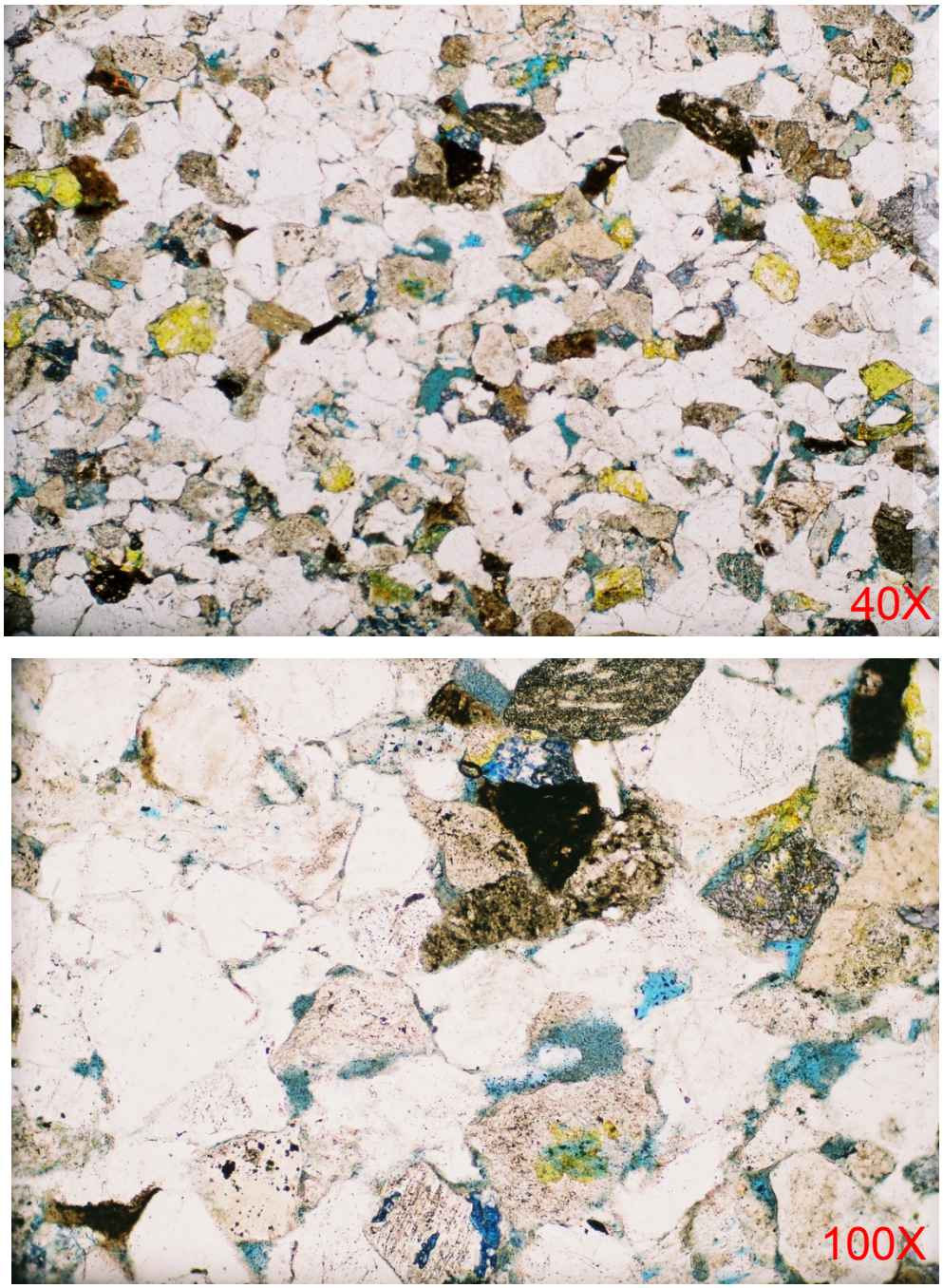

Figure 4.5.7. Example Mesaverde thin-section for Type IV porosity. Porosity consists almost entirely of sparse, poorly connected, clay-filled intergranular microporosity. Quartz cement is prominent, ferroan calcite is sparse. Pore-filling clay cement causes elevated Swi, reduced relative permeability, and increased Pc entry pressure. Williams PA 424, 4686.4', Rock type 15286, ϕ = 7.9%, GD = 2.65 g/cc, Ka = 0.211 mD.

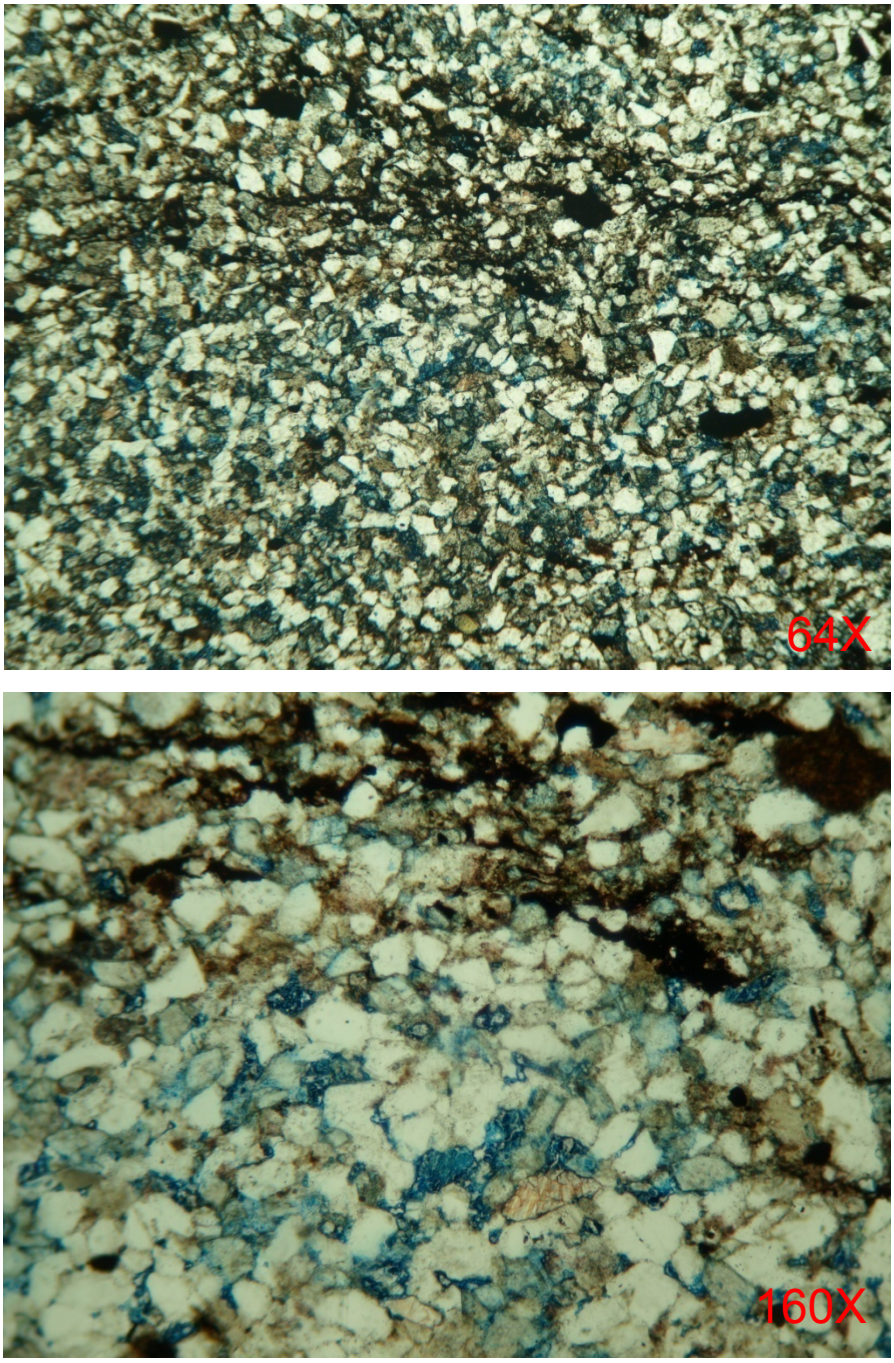

Figure 4.5.8. Example Mesaverde thin section for Type V porosity. Porosity consists entirely of sparse, poorly connected microporosity within interparticle voids of mudstone and shale matrix. Cements include siderite, ferroan calcite, and pyrite. Organic matter is locally common. Abundant clay causes highly elevated Swi, severely reduced permeability, and elevated Pc entry pressure. CER MWX-2, 7085.5', Rock type 11299, ϕ = 2.4%, GD = 2.70 g/cc, Ka = 0.0020 mD.

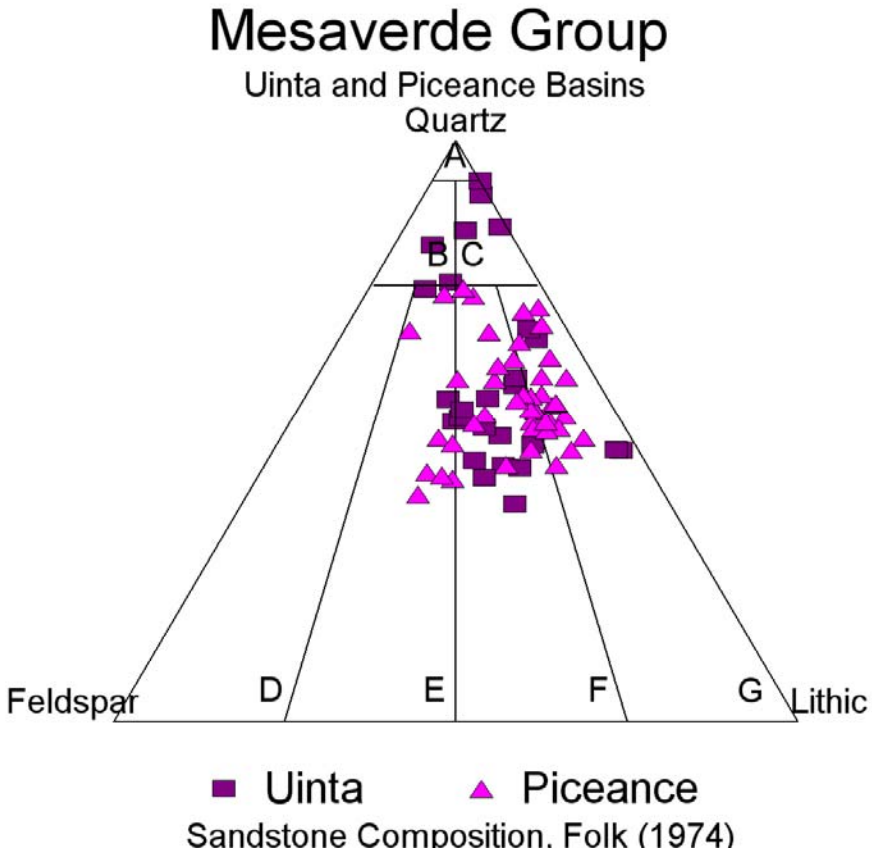

Figure 4.5.9. Example Quartz-Feldspar-Lithics (QFL) ternary plot comparing sandstone composition between the Unita and Piceance basins.

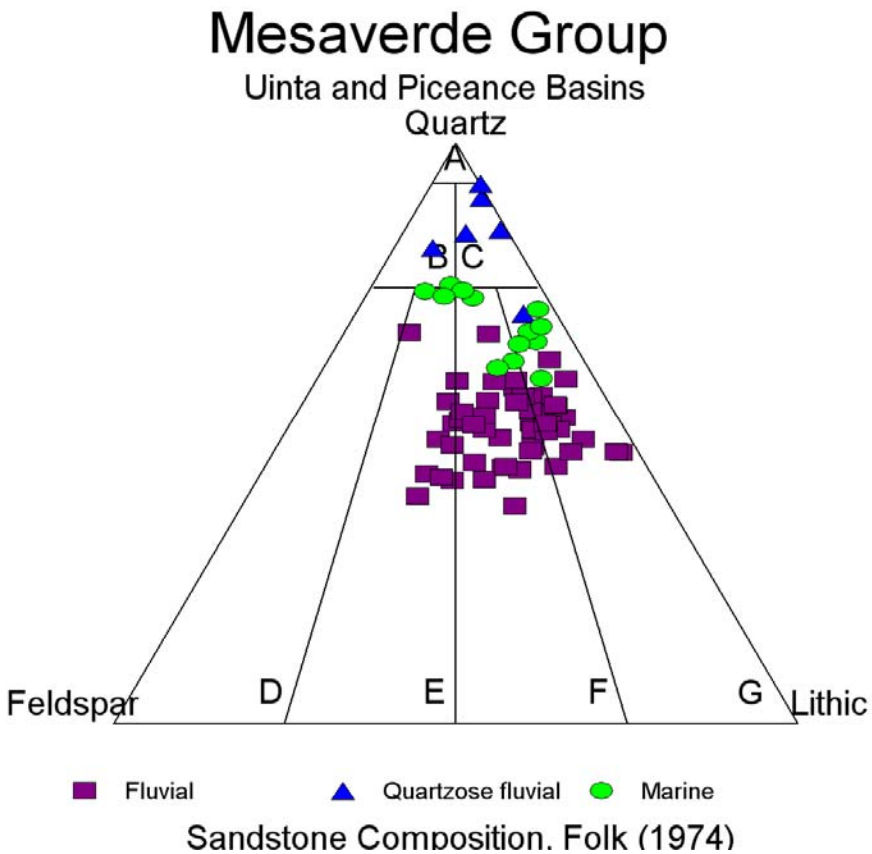

Figure 4.5.10. Example Quartz-Feldspar-Lithics (QFL) ternary plot comparing sandstone composition among different depositional environments in the Piceance basins.

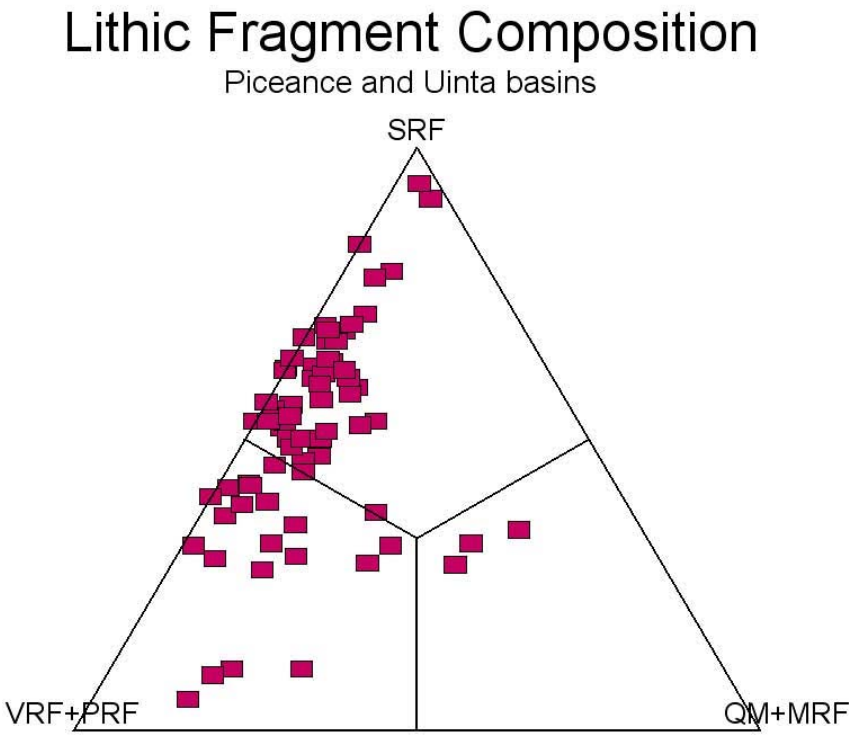

Figure 4.5.11. Example ternary plot of lithic fragment provenance for sandstones in the Uinta and Piceance basins.

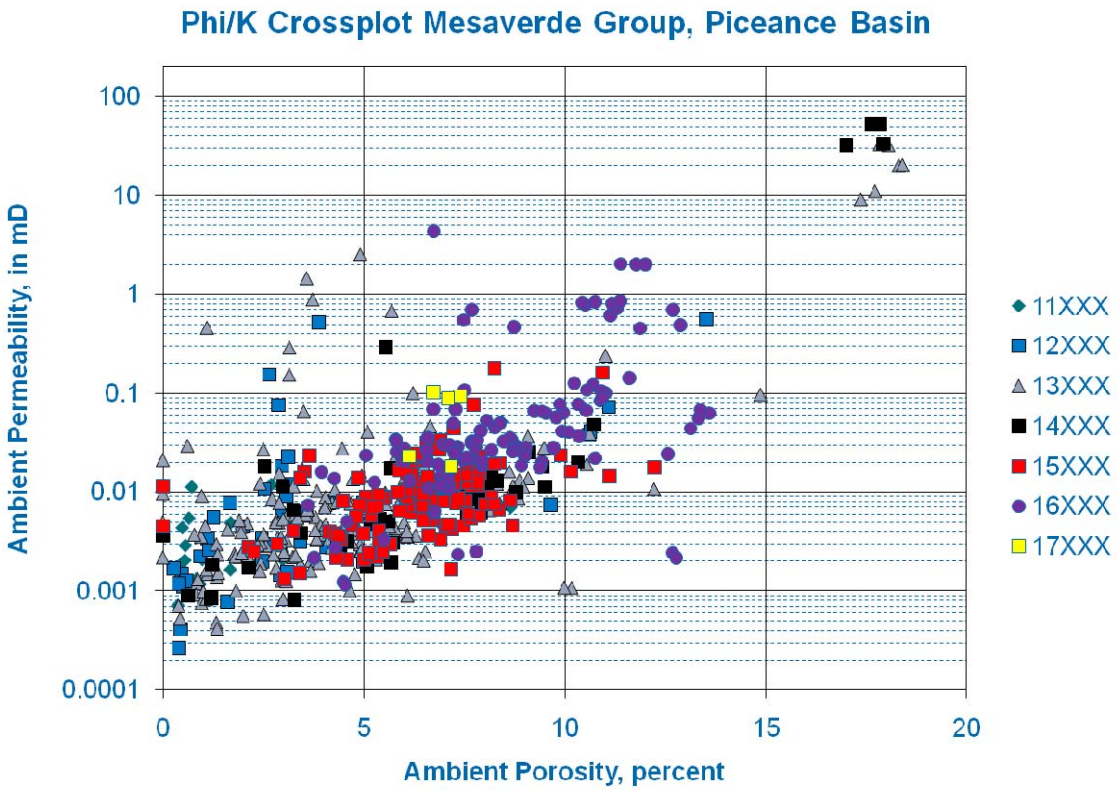

Figure 4.5.12. Example from Piceance Basin illustrating the influence of grain size on permeability in the Piceance Basin.

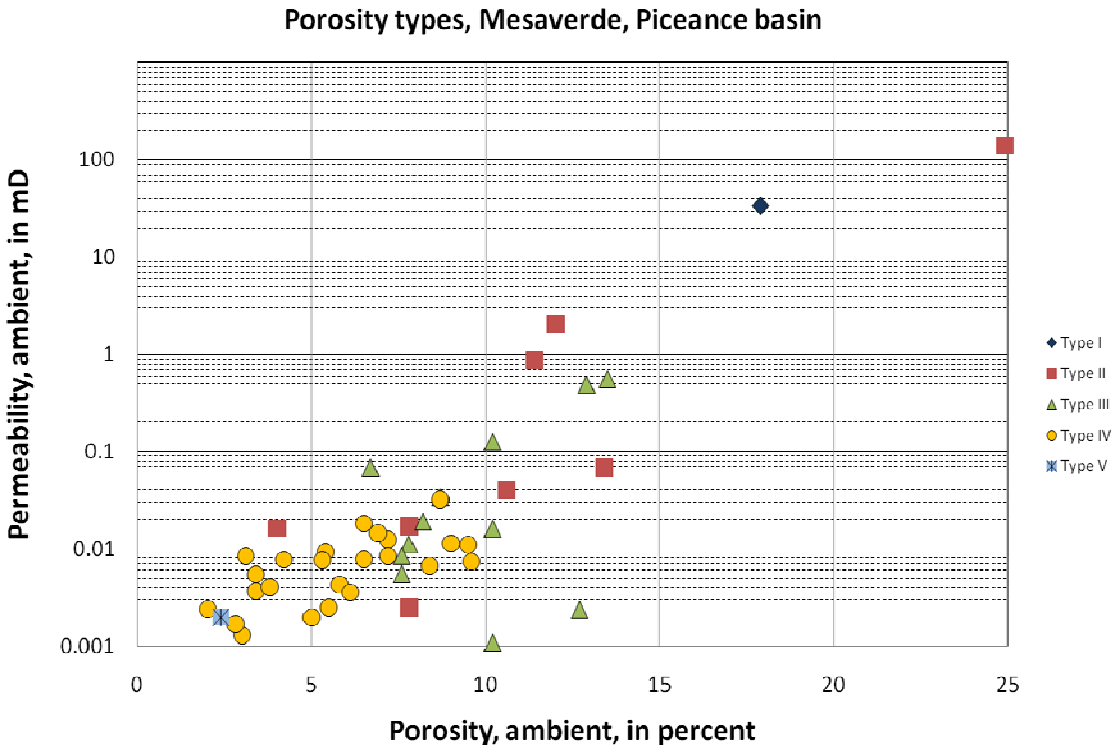

Figure 4.5.13. Example from Piceance Basin of the influence of pore type on porosity and permeability in the Piceance Basin.

Subtask 4.6. Perform standard log analysis

4.6.1 Task Statement

Standard log analysis is the benchmark against which to measure whether newly developed algorithms improve predictive accuracy. The goal of this subtask is to obtain standard wireline log interpretation of the wells using industry standard practices.

4.6.2 Methods

The basic log model employed in this project is a generic, Rocky Mountain tight gas petrophysical model similar to that used by several large companies and service vendors active in the Mesaverde plays. The model begins with a volume of shale computation based on the gamma ray log, computes a total porosity and effective porosity from the neutron and density logs, an Archie water saturation using locally determined formation water resistivity, and a permeability estimate using a Timur-equation approach (Timur, 1968).

Basic log-analysis parameters

The log-analysis parameters were initially set as follows:

- Volume of shale model: linear using GR log
- GR clean and GR shale endpoints: set by zone, individually picked for each well log
- Density matrix: 2.65 g/c3
- Fluid density: 1.0 g/c3
- Neutron matrix: neutron porosity input in LS units, output in SS units
- Porosity used: density-neutron cross-plot porosity corrected for shale effect ("effective" porosity)
- Water saturation model: Archie
- Archie constants: a = 1, m = 1.85, n = 2
- Permeability model: Timur equation with porosity exponent set by zone, BVWirr set by zone, and Swi exponent of 2

Shale volume.

Shale volume was estimated from the gamma ray with a linear relationship:

$$Vsh = \frac{GR_{\log} - GR_{clean}}{GR_{shale} - GR_{clean}} \qquad [4.6.1]$$

a. The clean gamma ray value was set at or near the lowest gamma ray value in the zone.

b. The shale gamma ray value was set at an average gamma ray value of the shales in the zone, ignoring any organic rich or black shale intervals.

Total porosity

Total porosity was determined from the neutron-density crossplot where the density input was bulk density (g/cm3) and the neutron porosity input was in limestone units (v/v or decimal).

a. Density porosity output was labeled PHID and is in sandstone units with a matrix of 2.65 g/c3 (initially).

b. Neutron porosity output was labeled PHIN and is in sandstone units.

c. Crossplot total porosity is labeled PHIDN and is in decimal units. A copy of this curve is also labeled PHIX.

Effective porosity

We use effective porosity in the sense of a clay-bound water corrected porosity. In sandstone reservoirs, this is assumed to be close to the connected pore volume available to store hydrocarbons. It was determined from the neutron and density by the following procedure:

a. For each zone and each well, a locally determined shale porosity was determined from a graphic density-neutron crossplot color coded by Vshale as the Z value. The shale porosity value was set at the center of the high Vshale cluster.

b. From the selected shale point, three values are determined--the density porosity of shale (PHIDsh), neutron porosity of shale (PHINsh), and the total porosity of shale (PHIDNsh).

c. Each of the individual porosity values, PHID, PHIN, and PHIDN are then corrected to effective porosity by the following equation

$$PhiE = PhiT - Vsh * PhiSh \qquad [4.6.2]$$

where PhiE is the shale corrected effective porosity, PhiT is the log determined total porosity (density, neutron, or crossplot), and PhiSh is the matching shale total porosity. Vsh is the linear estimate of shale volume from the gamma ray (equation 4.6.1).

d. The effective density-neutron crossplot porosity (PHIDNE) was used in this study as the main porosity. A copy of this curve is also saved as PHIE.

e. PHIE was compared to the *in situ* corrected core porosities and the input variables for either grain density or the shale point was adjusted as necessary to calibrate the porosity model to core. The final PHID therefore often has a zoned grain density that varied from the starting value of 2.65.

Water saturation computation

The basic log analysis model used the Archie saturation equation with constant electrical parameters, variable formation water salinity, and deep resistivity as an approximation of Rt.

a. The deep resistivity curve was copied to RT. For most wells with array induction logs, the deep curve is a good approximation of RT. For older wells with induction logs this assumption is not valid, but the tornado chart solutions for formation resistivity rarely changed the answer significantly except in shallow, water-bearing intervals of the Mesaverde.

b. The neutron-density crossplot porosity (PHIX) was used for the saturation calculation.

c. Rw was estimated from a Pickett plot for each zone in each well.

d. The Archie exponents were set to a = 1, m = 1.85, n = 2 based on prior experience and general Rocky Mountain guidelines. Sw is therefore

$$Sw = [(a*Rw)/(PhiX^{m} * Rt)]^{1/n} \quad [4.6.3]$$

$$Sw = [Rw/(PhiX^{1.85} * Rt)]^{0.5} \quad [4.6.4]$$

e. Bulk Volume Water was computed from the effective porosity:

$$BVW = PHIE * SW \quad [4.6.5]$$

Permeability

a. Bulk volume water irreducible (BVWI) was estimated from one of two methods:

   i. On a depth plot, intervals where the value of BVW is approximately constant over several sandstones was assumed to indicate zones at or near irreducible saturation; or

   ii. On a Pickett plot, we looked for vertical trends in the data at the right side of the data set, which also represent a constant value of BVW. Generally this is more difficult.

b. Calculated Swi from the bulk volume irreducible and total porosity:

$$SWI = BVWI / PHIX \qquad [4.6.6]$$

   By using total porosity instead of effective the Swi estimate includes clay-bound water.

c. Estimated permeability from the generalized Timur (1988, eq. 8) equation

$$K\log = KCOEF \frac{PHIX^{KPHIEXP}}{SWI^{KSWIEXP}} \qquad [4.6.7]$$

   Where the permeability exponents KPHIEXP and KSWIEXP were set by zone to best approximate the *in situ* core permeabilities. Nominal values of 6 and 2 were used initially, then iteratively adjusted to match core. KCOEF was set to 62,500. Total porosity was used in this formula instead of effective by convention; consequently, the porosity coefficients determined are lower than they would be if PhiE were substituted in the formula.

Filter results for coals and bad hole.

Two filters were run to clean up the results for graphical output.

a. Coals were flagged as clean intervals (Vsh < 0.3) with low bulk density (< 2.1 g/c3)

b. Bad hole was flagged by intervals with excessive borehole size (>3" above bit size) or excessive density correction (drho > 0.2 g/c3). The calculated porosity and saturations in the bad hole intervals were nulled.

4.6.3 Results

Standard log analysis was performed on all the primary wells. These analyses incorporate wireline quality control, depth correction for core to log depth, calculation of porosity from density log response using matrix densities appropriate to basin, and water saturations calculated using a standard Archie equation with constant porosity exponent. Figure 4.6.1 illustrates a portion of an example log interpretation available on the website. Figure 4.6.2 illustrates the various porosity computations compared to core data.

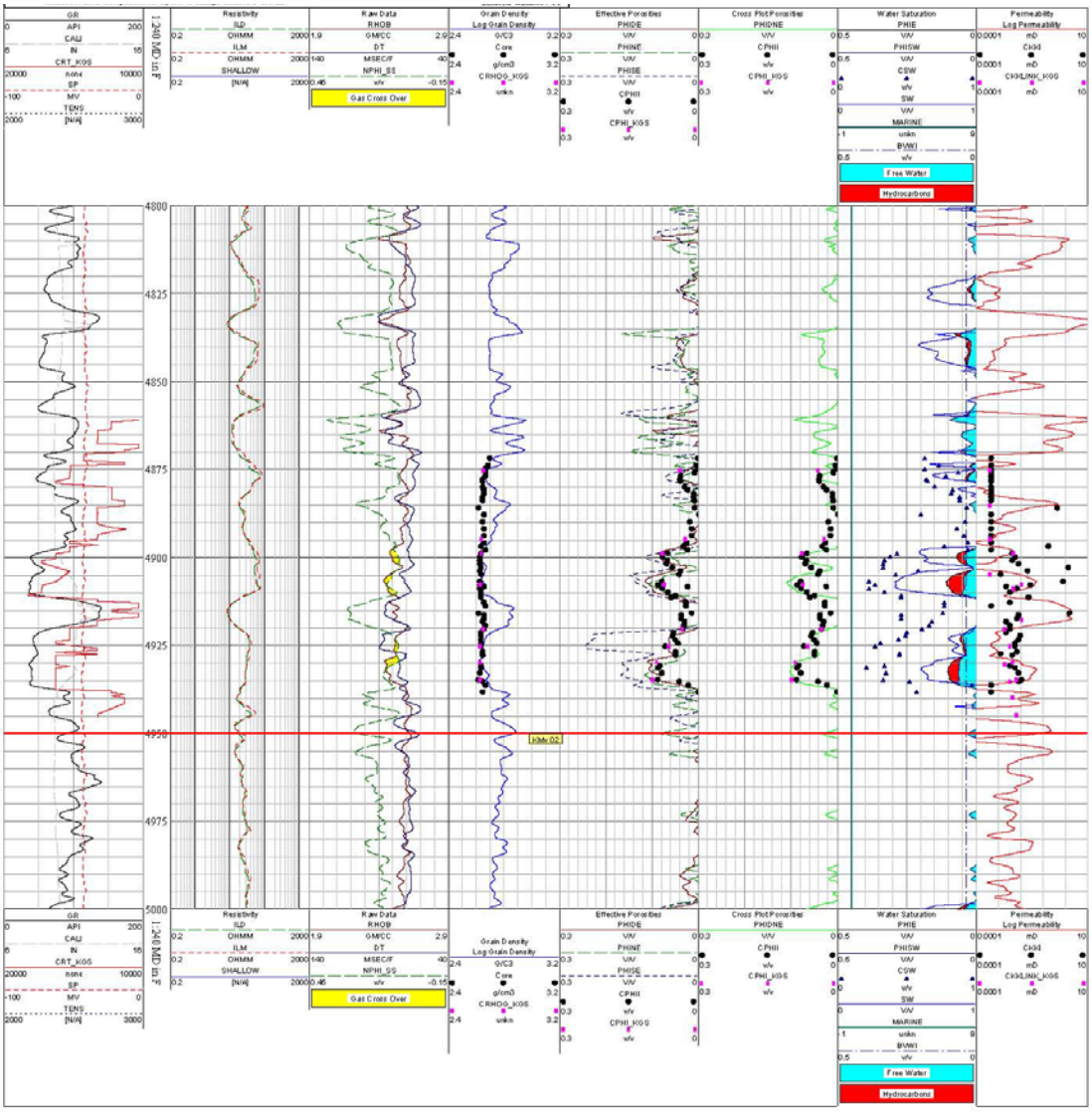

Figure 4.6.1. Example of wireline log presenting standard log analysis interpretation. Logs for other wells are available on the project website: http://www.kgs.ku.edu/mesaverde/reports.html

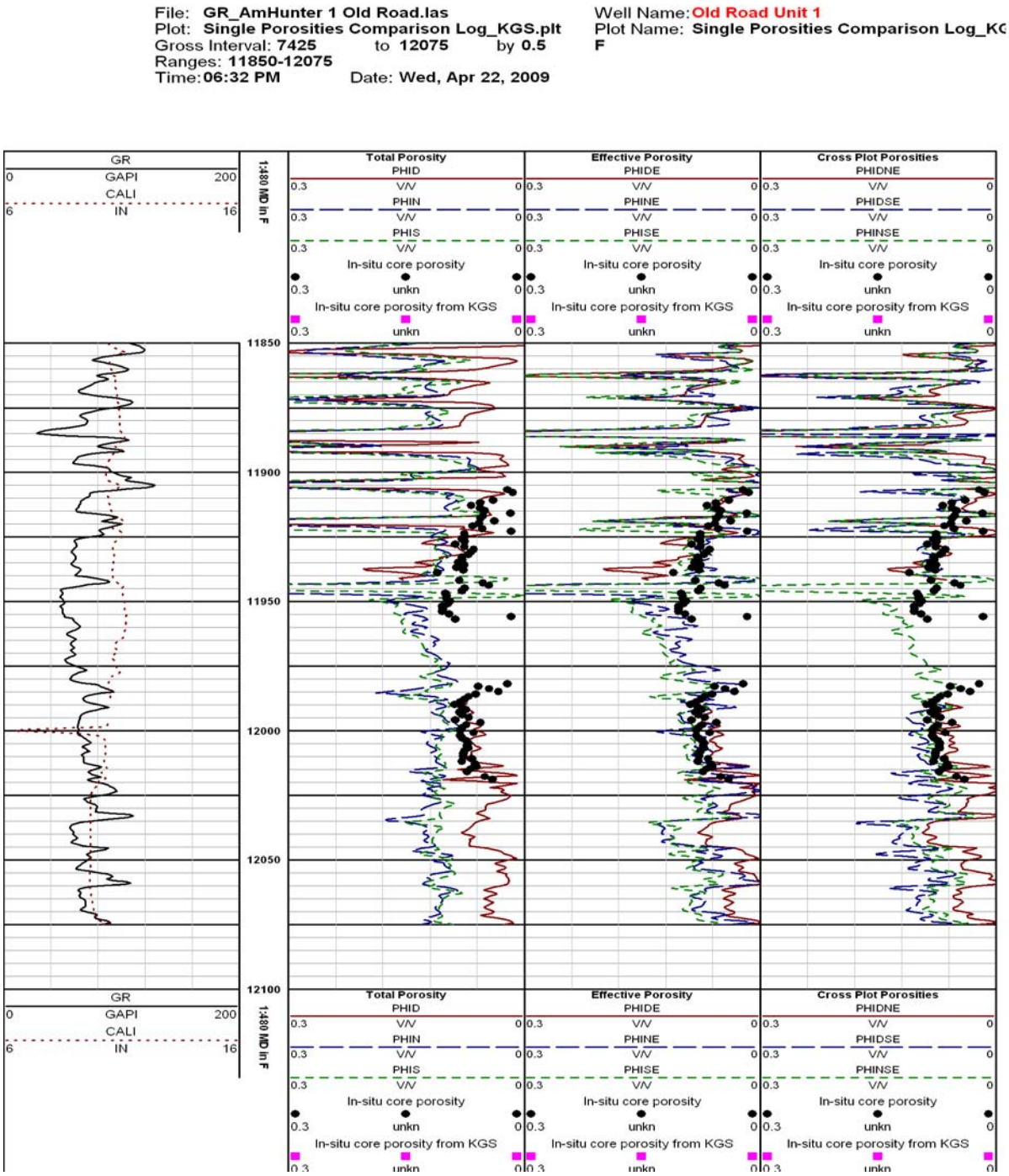

Figure 4.6.2. Example of porosity comparison plot from the standard log analysis interpretation. Track 2 presents Total Porosity comparisons as described above; Track 3 compares the Effective Porosity calculations (shale corrected), and Track 4 the Crossplot Effective Porosities.

Task 5. Build Database and Web-based Rock Catalog

Subtask 5.1. Compile Published and Measured Data into Database

5.1.1 Task Description

Many previous studies have been publsihed reporting Mesaverde petrophysical properties, but the data are in print form and not digital. To make these previoulsy published data accessible, the data were digitized in Task 3. The goal of this task was to develop code for providing the data on the web. Code was to be written that would provide web-based access to the data and all data were to be available as a complete database.

5.1.2 Methods

Original plans were to present data in a single database format. However, it was found that the nature of publication reporting format and the diverse nature of the data was not conducive to the use of a single database. Such a format would have resulted in the data being in what would have been subsections of a master database that would have effectively been individual tables. At two public technical presentations at technical society meetings the audience was polled as to whether they preferred a simple Excel-style workbook format or an Oracle-style database. The response at both surveys was greater than 90% preferred the Excel-style format. An Excel format for data presentation was used.

5.1.3 Results

Over 9 gigabytes of data are available for download from the Project Website. In brief these data comprise:

1. Excel workbooks containing tables of data from previous studies
2. Excel workbooks containing data for all petrophysical measurements performed in this study including;
    a. 2,102 helium porosity
    b. 2, 075 routine air permeability
    c. 2,062 *in situ* Klinkenberg permeability
    d. 2,101 grain density measurements
    e. 907 electrical resistivity measurements

f. 301 mercury-intrusion capillary pressure analyses
g. 150 air-brine critical gas saturation measurements
h. 113 pore volume compressibility analyses
i. 310 air-brine *in situ* porosity measurements

3. 550 core slab images representing the range of lithofacies exhibited by the Mesaverde in the six basins studied
4. 750 thin-section photomicrographs from 41 wells
5. 6,447 feet (2,054 m) of digital core descriptions presented both in Excel workbook format and in graphical core descriptions for 42 wells from 6 basins
6. graphical core descriptions of core from 42 wells
7. 21 standard wireline log analyses
8. 21 advanced wireline log analyses
9. pdf files of all technical slide and poster presentations
10. pdf files of all technical quarterly reports

Subtask 5.2. Modify Existing Web-Based Software to Provide Data Access

5.2.1 Task Description

The goal of this task was to provide data in a user-friendly format. It was originally planned that users would be able to investigate relational properties on the Project Website. However, in polling of users at national technical meetings, including two presentation sessions where 50 to 150 people were polled following a technical presentation on the project, users unanimously voted for the site to provide facile download of data and that they preferred to analyze the data on their own computers rather than using a link to the data.

5.2.2 Methods

User friendly web pages were constructed that provide easy selection and downloading of project reports, data, and images. The Project Website was designed to provide what is believed to be the easiest format for data selection and download. The total amount of data exceeds 9 gigabytes precluding a single selection and download option.

5.2.3 Results

A Project Website was constructed that has been in operation since the projection inception. All products of the study are available on the website. Rapid download is provided by packaging of the large datasets in Zip file format. Data are organized by basin, well, and labeled by data type.

Task 6. Analyze Wireline-Log Signature and Analysis Algorithms

Subtask 6.1: Compare Log and Core Properties

6.1.1 Task Statement

Wireline log-calculated properties, including porosity, water saturation, and lithofacies, will be integrated and compared with core-derived properties including porosity, permeability, lithofacies, and capillary pressure-derived water saturation. Possible unique log signatures for lithofacies will be evaluated and differences between standard log-calculated parameters and core properties will be analyzed.

6.1.2 Methods

Comparisons between wireline log-calculated properties and core data were conducted using the basic model calculations described in Subtask 4.6. The log-calculated properties included volume of shale from the gamma ray curve, porosity, absolute permeability, water saturation, and apparent grain density.

The core data used for comparison were the measured *in situ* porosity or permeability for core plug samples collected in this study, as documented in Subtask 4.1, or the calculated *in situ* porosity and permeability based on available routine core analyses after application of the equations given in Subtask 4.1. The five-digit lithofacies descriptor (Subtask 4.5) was also imported, and correlation between the rock-type data curve and the open-hole gamma ray was used to depth shift the core data into alignment with the wireline logs. Depth corrections are all linear shifts, without interpolation of values between core sample depths, and any breaks in the depth shifting were placed as physical gaps in the core coverage. The depth corrections were recorded in the well data spreadsheets posted on the project website. Examples of depth shifted core data are shown in Figures 4.6.1, 4.7.1, 4.7.2, and 4.7.3.

Crossplots between various wireline log-determined properties and the corresponding core-determined properties (e.g. log porosity vs. core porosity) were constructed in Excel using the depth-shifted core data and the log properties at those depths. All crossplots are listed in

Table 6.1.1 below, and are included in the Excel files "ConstantM_xplots.xls" which are posted on the project website under each well. These plots were used with the automatic trend-fitting functions in Excel to evaluate the strength of correlations between the core-determined properties vs. various log-derived estimations of the corresponding properties.

Table 6.1.1 – Core to Log comparison plots included in Excel ConstantM_xplots.xls.

Density porosity vs. Core porosity
Effective density porosity vs. Core porosity
Effective density-neutron crossplot porosity vs. Core porosity
Log-determined permeability vs. *In situ* core permeability
Core porosity vs. Core permeability
Log-determined water saturation vs. Log porosity
Log porosity vs. Log permeability

6.1.3 Results

Petrophysical log models in Rocky Mountain tight gas sandstone reservoirs generally follow the following four-step sequence:

1. Compute shale volume (Vshale) from the gamma ray, neutron-density separation, or spontaneous potential logs. Due to gas suppression of the SP and variable formation water salinities, the SP is rarely used as a Vshale indicator in the Mesaverde. Neutron-density separation can be an accurate measure of shaliness, but because proper tool standoff procedures are not often followed this method is not widely used. Most analysts use the gamma ray with some form of a Vshale equation. We used a linear model as described in Subtask 4.6; in areas with lithic sandstones and high potassium feldspar contents the sands become radioactive and an alternate model such as the Steiber or Clavier equations may be more appropriate (Ransom, 1977). Because we do not have a direct quantitative measure of shaliness from cores, the only comparisons between our log Vshale measure and cores was comparison to the visual core-description rock numbers.

2. Compute total and effective porosity from the density, neutron, and sonic logs. Total porosity is calculated in the conventional manner with appropriate matrix and

fluid assumptions. Our total porosity computations (Subtask 4.6) assumed a constant sandstone matrix, 2.65 g/c3 grain density, 51 μsec/f matrix transit time, and freshwater in the formation. These are typical Rocky Mountain values. Many companies prefer to stop at this point and use the density log-determined total porosity for all subsequent calculations.

The main problems with the total porosity computations involve variable matrix properties, especially the matrix density, and the presence of gas in the near wellbore environment. Uncorrected environmental effects on the neutron log plague log evaluations in many areas, particularly when incomplete information was recorded about the tool configuration and corrections applied in the field. Additionally, both the sonic and the neutron logs show a strong shale- or clay-bound water effect, such that they read porosities that are significantly higher than measured core porosities in shaly intervals. When the total porosity is corrected for clay-bound water this is usually called the "effective porosity," which in sandstone reservoirs is close to the engineering definition of the connected pore volume available for hydrocarbon storage. Both total and effective porosities can be cross-plotted to determine variable matrix property-independent porosities, including density-neutron crossplot porosity and a sonic-neutron crossplot porosity. The density-sonic crossplot was also calculated, but was found to be of limited value and usually yields a value similar to the density log alone.

The crossplots between the various total and effective porosity measures and core porosity were used to evaluate which log measure of porosity is closest to the core-determined value, and if the corrections used to calculate effective porosity are appropriate.

3. Compute water saturation by the Archie equation or a shaly sandstone derivative thereof. In this project, we used the Archie method as outlined in Subtask 4.6. Comparisons to routine core-analysis water saturations are directionally useful, with the core saturations often validating the magnitude of the changes in the log saturations, but quantitatively are of limited use due to flushing during the coring process. No native state core data were available for comparisons. Some

comparisons to theoretical Swi from capillary-pressure data were made, but this was not investigated exhaustively due to time limitations.

4. Compute permeability from either porosity or porosity and estimated irreducible water saturation. Our preliminary estimate of permeability from logs used a modified Timur equation as described in Subtask 4.6, which was compared to core data using both depth plots and crossplots. These plots were useful to evaluate the appropriate coefficients for the Timur equation and the approximate expected range in those coefficients.

6.1.3.1 Log-Core Porosity Comparisons

Log porosity-core porosity comparison plots were created in Excel for all wells with *in situ* core-porosity data. Depth plots showing the depth-shifted core data and the log-calculated porosities were also printed for each well. The log-calculated porosities that were compared to the cores included

- Single porosity comparisons
  - Total density porosity, effective density porosity
  - Total neutron porosity, effective neutron porosity
  - Total sonic porosity, effective sonic porosity
- Crossplot porosity comparisons
  - Total density-neutron porosity, effective density-neutron porosity
  - Total sonic-neutron porosity, effective sonic-neutron porosity

The total density porosity vs. core and effective density porosity vs. core crossplots are included in the Excel workbooks for each well described above. Also, the effective density-neutron cross-plot porosity vs. core is included for each well. Examples of these plots are shown below in Figures 6.1.1 through 6.1.3.

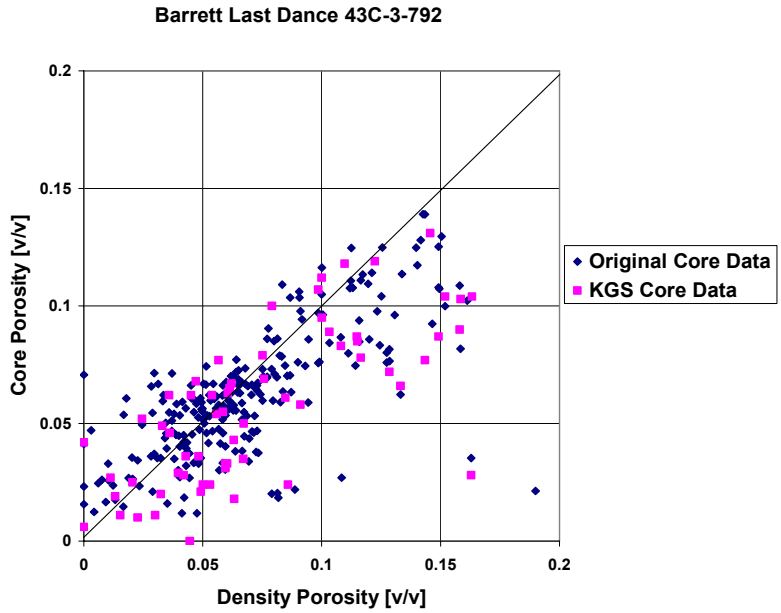

Figure 6.1.1. Total density porosity vs. core porosity, Barrett Last Dance 43C-3-792 well, Piceance Basin.

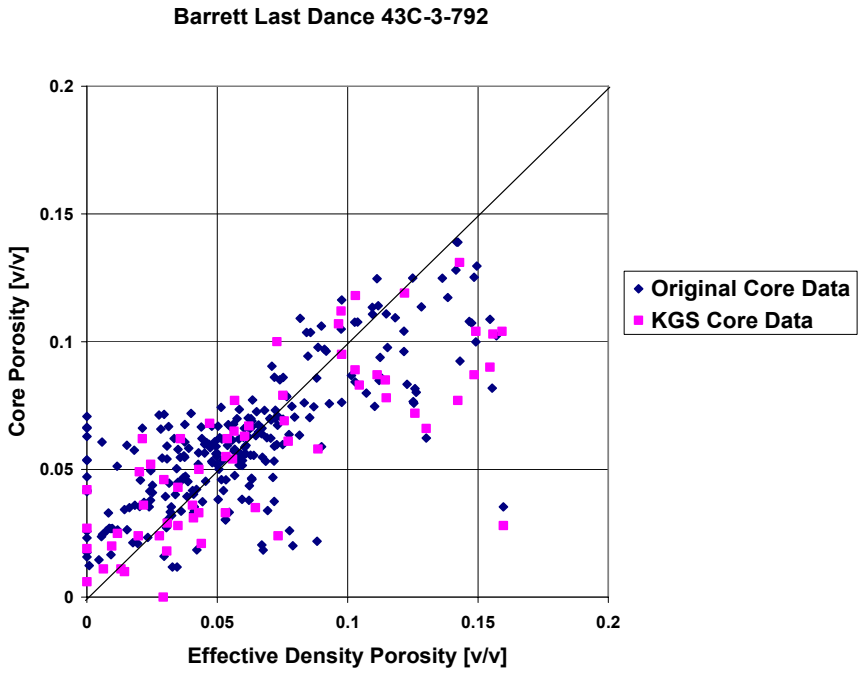

Figure 6.1.2. Effective (shale-corrected) density porosity vs. core porosity, Barrett Last Dance 43C-3-792 well, Piceance Basin.

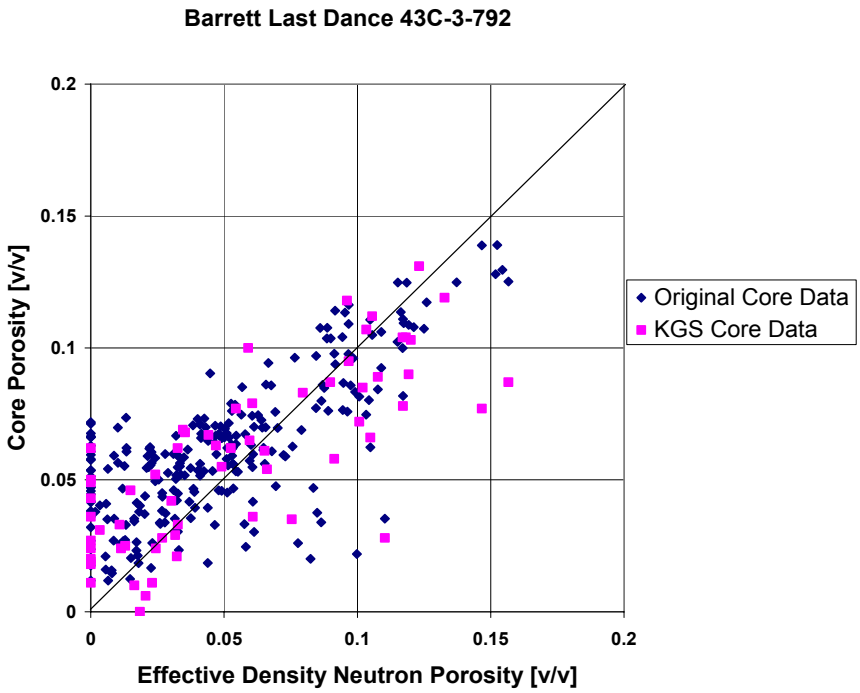

Figure 6.1.3 Effective (shale-corrected) density-neutron porosity vs. core porosity, Barrett Last Dance 43C-3-792 well, Piceance Basin.

6.1.3.2 Core Permeability vs. Log Permeability Comparisons

Log-derived permeability was calculated using several alternative models and several parameters in each model equations were varied. Comparisons to core permeability were made to validate the approach and assess which methods have the broadest application.

Commonly used permeability estimators from logs are based on the empirical Carman-Kozeny model (c.f. discussion in Dullien, 1992):

$$K = A * \phi^{3} / S^{2} \qquad [6.1.1]$$

where K is permeability in millidarcies, A is an empirical constant ("the Kozeny constant"), ϕ is porosity, and S is the surface area per unit bulk volume. Because S is not directly measured with any logging device, irreducible or residual water saturation of the formation has been considered a proxy for internal surface area, leading to various empirical equations of the general form:

$$K = A * \phi^{B} / Swi^{C} \qquad [6.1.2]$$

where *A, B,* and *C* are rock-type or formation-specific variables determined from core data. Timur (1968) summarized the development of these models and proposed a specific model based on 155 sandstone cores we refer to as the "Timur equation." The particular form of this equation we use in modified form was first published by Schlumberger as a chart in August 1955:

$$K = 250^2 * \phi^6 / Swi^2 \qquad [6.1.3]$$

This chart was printed in the1957 through 1979 editions of the Schlumberger chartbooks as Chart E-4 or later as Chart K-2(1). The chart was not cited to any source other than prior general work by Wyllie and Rose (1950), but the specific empirical equation presented has been attributed to Tixier in many texts and secondary references. Chart K-2 was dropped from the 1984 and later chartbooks and replaced by a similar empirical relationship (Chart K-3) with different values for *A* and *B*.

We adjusted the values for the exponent *B* in equation 6.1.2 to achieve the best possible match between the core data and the log-estimated permeability. We generally leave the leading constant at 250 and also maintain the value of *C* as 2. Swi is calculated at every depth step by comparing the calculated water saturation to the theoretical minimum water saturation determined from an assumed bulk-volume irreducible divided by porosity, taking the lesser of the two. The calculated permeability turns out to be relatively insensitive to the choice of bulk-volume irreducible, which we set between 0.03 and 0.06 by inspection of each log on a zone by zone basis.

Finding the best value for the exponent *B* was accomplished visually in a depth-plot view (e.g. Figure 6.1.4) without resorting to detailed statistical analysis. For rocks with microdarcy permeability, the appropriate value for *B* was often close to the nominal value of 6 in equation 6.1.3, with higher values driving the calculated permeability towards lower values. Generally speaking the log estimates of permeability are within an order of magnitude of the core results, but commonly show greater spread than the core data as illustrated below. The log model is highly sensitive to very small changes in effective porosity which are magnified by the exponent in the model.

(1) Historical Logging Interpretation Chartbooks from the period 1947-1999, now long out of print, have been compiled in electronic format by the Denver Well Logging Society and are available from the American Association of Petroleum Geologists bookstore and other professional societies.

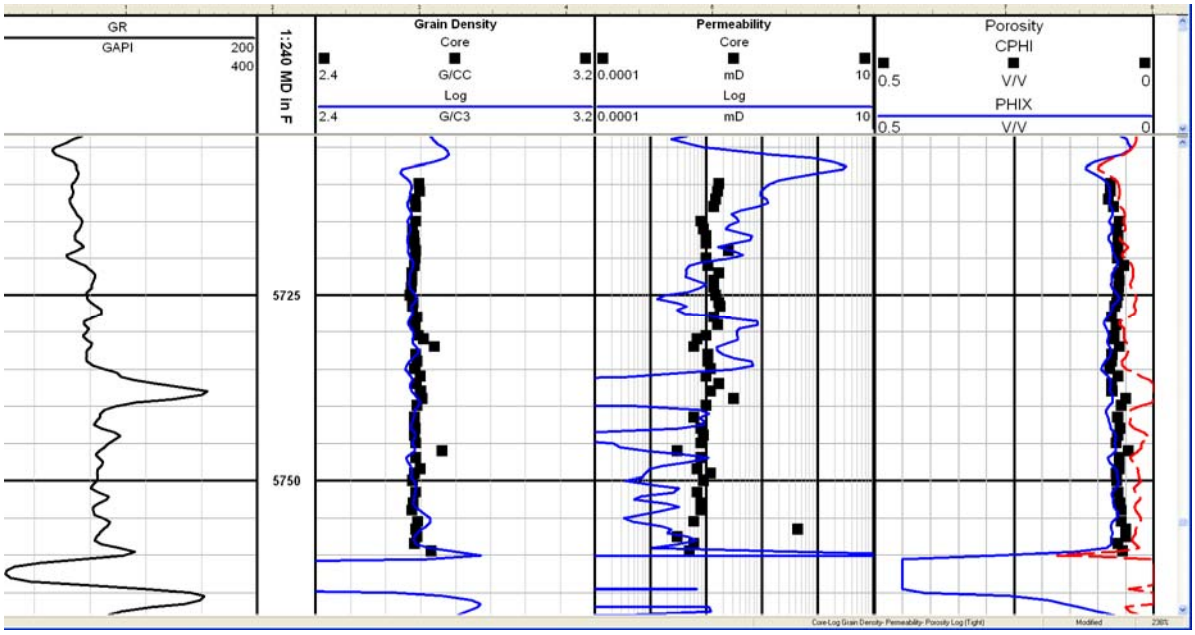

Figure 6.1.4 Depth-plot comparison of log-determined grain density, permeability, and porosity to core data; Barrett Last Dance 43C-3-792 well, Piceance Basin.

Alternative log models, using basin specific porosity-permeability equations derived from the core analyses in this study, are described in Subtask 6.2 below.

6.1.3.3 Permeability from NMR Logs

An alternative approach to determining permeability from conventional porosity and saturation is to use a nuclear magnetic resonance (NMR) log to directly measure total porosity and bulk-volume irreducible. To the extent the NMR porosity is lithology independent (that is, it is relatively insensitive to the matrix density and mineralogy as compared to nuclear porosity tools) and the bulk-volume irreducible is measured in some fashion as opposed to estimated, the resulting permeability from a Timur-like equation should be considerably improved.

The two primary equations used to calculate permeability from NMR tools are the Coates equation (Coates et al., 1991):

$$K = C * (FFI/BVI)^2 \phi^4 \qquad [6.1.4]$$

and the SDR (Schlumberger Doll Research) equation (Kenyon et al., 1988):

$$Ksdr = C * T_{2gm}^{\ 2} \phi^4 \qquad [6.1.5]$$

where the FFI/BVI is based on a T_2 cutoff dividing the NMR spectra into a bound fluid and a free fluid region, T_{2gm} is the geometric mean of the T_2 spectra, and C is a locally determined constant (not the same between equations). In both cases these are functionally equivalent to the general form proposed by Timur (Eqn. 6.1.2), where FFI/BVI and T_{2gm} serve at the proxy for internal surface area of the rock instead of 1/Swi. Furthermore, if the porosity exponent is allowed to vary, these equations become sufficiently flexible that they can match a very wide range in rock types and formation permeability.

In this study, only two wells had NMR logs in the public domain. These were the Amoco Siberia Ridge 5-2 in the Washakie Basin, and the Williams PA 424-34 in the Piceance Basin. NMR logs have not gained wide acceptance in tight gas sandstones and consequently are infrequently run, and the data are not always released to State agencies.

In the case of the Siberia Ridge 5-2, NMR data from an older version Schlumberger CMR tool (1998 CMRT) and core data were available over one reservoir zone, an Upper Almond marine bar sandstone. These data are shown in Figure 6.1.5 below. The PA 424-34 was logged with a 2005 Halliburton MRIL tool over several thousand feet, with three intervals extensively cored. The middle of these intervals is shown in Figure 6.1.6 below. In both wells, permeability was calculated by the Coates and SDR models, the vendor-calculated permeability is shown, and the conventional-log Timur equation permeability is shown. The correspondence between the NMR permeability and core permeability is excellent.

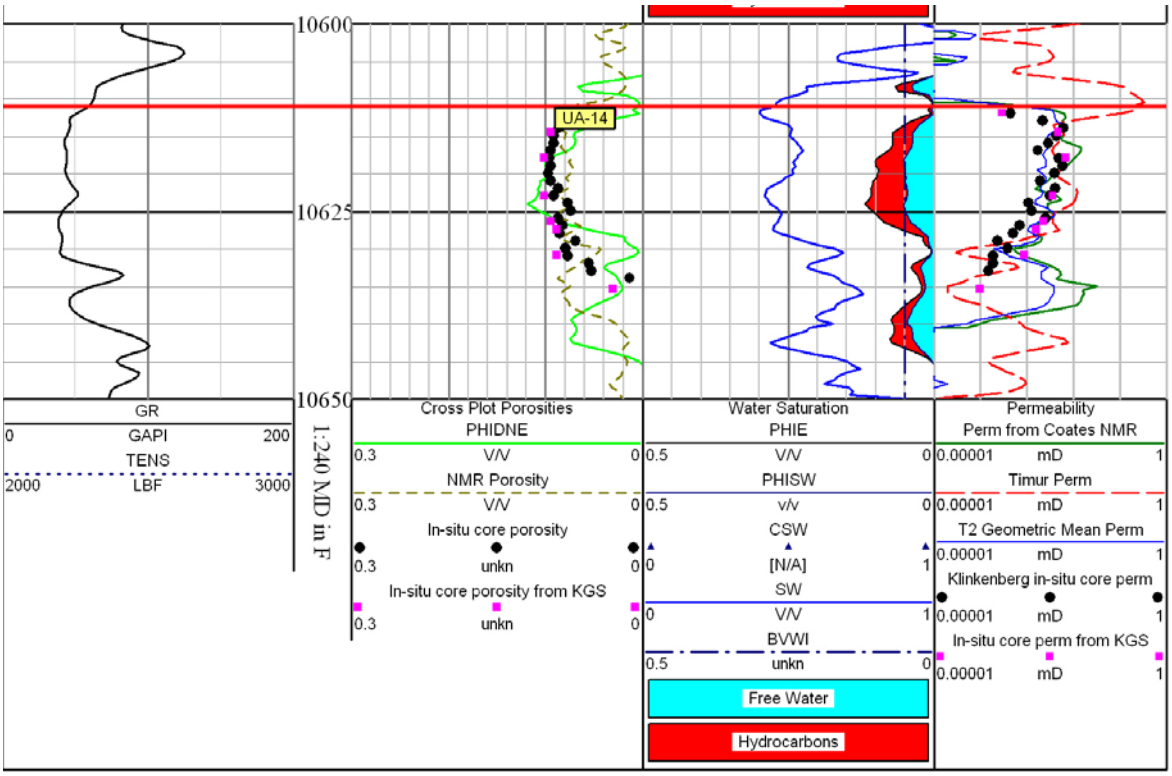

Figure 6.1.5. CMR porosity and permeability comparison to standard density-neutron derived effective porosity (PHIDNE), standard log-based permeability (Timur perm), and core data. In this well, all methods compare favorably with all log measures and cores agreeing within less than an order of magnitude of permeability.

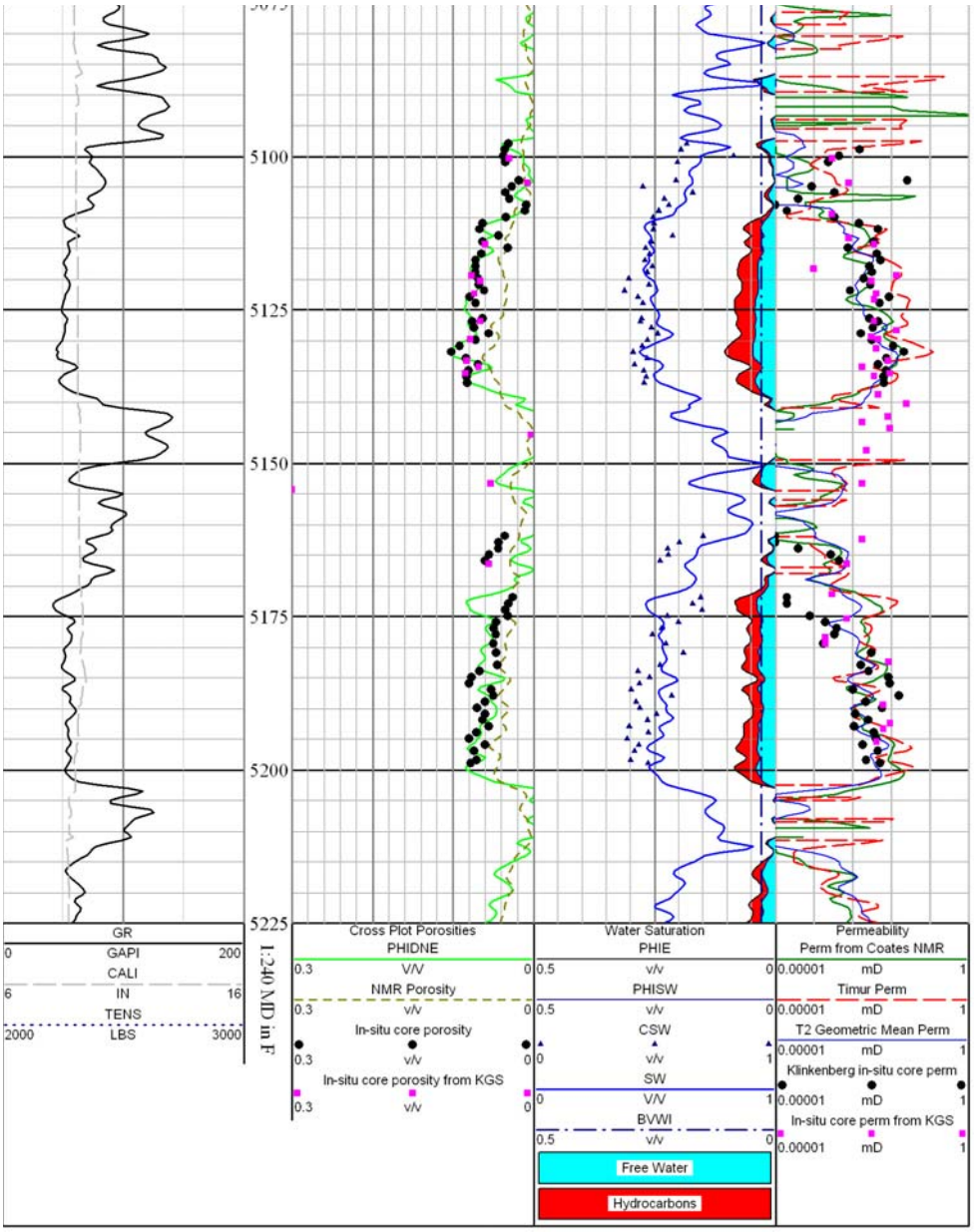

Figure 6.1.6. CMR porosity and permeability comparison to standard density-neutron derived effective porosity (PHIDNE), standard log-based permeability (Timur perm), and core data. Again all methods compare favorably with all log measures and cores agreeing within less than an order of magnitude of permeability, although the Timur equation permeability tends to drift above the core data cloud while the NMR estimates by both the Coats and T2GM (SDR) methods track closely. Note the correspondence in this well between log-calculated water

saturation and routine core-analysis saturation. In this well the NMR porosity undershoots both core and the conventional PHIDNE calculations.

6.1.3.4 Water Saturation

Ground truth data for the log water saturation model was limited. Routine core analysis saturations as reported by the operators are of limited value and only provide directional information about saturation trends. The reasons for this include the fact that all of the wells were drilled with water-based muds and, although the rocks are very tight and do not invade deeply, they are invaded within the diameter of a standard core. Proprietary special core studies using radioactive tracers at Wamsutter, Jonah, and Pinedale fields have all demonstrated contamination of the cores by mud filtrate. Also, as a high-pressured gas reservoir core is slowly retrieved, the gas expansion will try to blow out some of the native fluids that could drive routine water saturations towards lower values. The net result is the as-received saturations are of very limited utility for calibrating a log model.

Without special coring procedures, the only other methods for independently verifying log model calculated saturations are 1) comparison to capillary pressure-derived saturations, based on a saturation-height model; or 2) comparison to an independent wireline measurement of saturation such as NMR bulk-volume irreducible. Capillary Sw-h models are seriously limited because the actual hydrocarbon-column heights are generally unknown, appear to be greater than appears reasonable when calculated assuming the rocks are in drainage equilibrium, and do not agree with reservoir pressure-elevation plots. Most formation-evaluation specialists in the Rockies no longer attempt to fit capillary-height models to observed saturation trends, given very limited insight from attempts in the past. One possibility is most of these fields are no longer in primary drainage equilibrium, but instead are on imbibition curves or secondary (or higher) drainage curves as a result of basin uplift, structural tilting, and breeching of the original reservoir seals (Shanley et al., 2007).

Figure 6.1.7 below, taken from the deep Piceance Basin, illustrates the problem very well. On a saturation-porosity crossplot ("Buckles plot") most of the points in the well lie along a iso-BVW line close to 0.03. This suggests the entire section is at or near an irreducible water saturation, which would imply a very substantial hydrocarbon-column height in this well assuming the reservoirs are all connected and in primary drainage equilibrium. Although most,

if not all, of these sandstones are gas charged as evidenced by shows and production testing, the pressure data in this basin do not support continuous gas columns thousands of feet thick. If that were the case, the deviation from a hydrostatic pressure gradient would be greatest at the top of the section and would steadily diminish downwards along a gas-density gradient to intersect the hydrostatic line at the free water level, which presumably is close to or below the TD of the well. In fact the observed pressure gradients in this basin, as documented by Nelson (2003a; 2003b; Figure 6.1.8), are generally the opposite, with the deviation increasing downwards and then abruptly returning to hydrostatic if the well were drilled deep enough. If mud weights are taken as an approximate indicator of pore pressure at depth, there are hundreds of well profiles to support this observation.

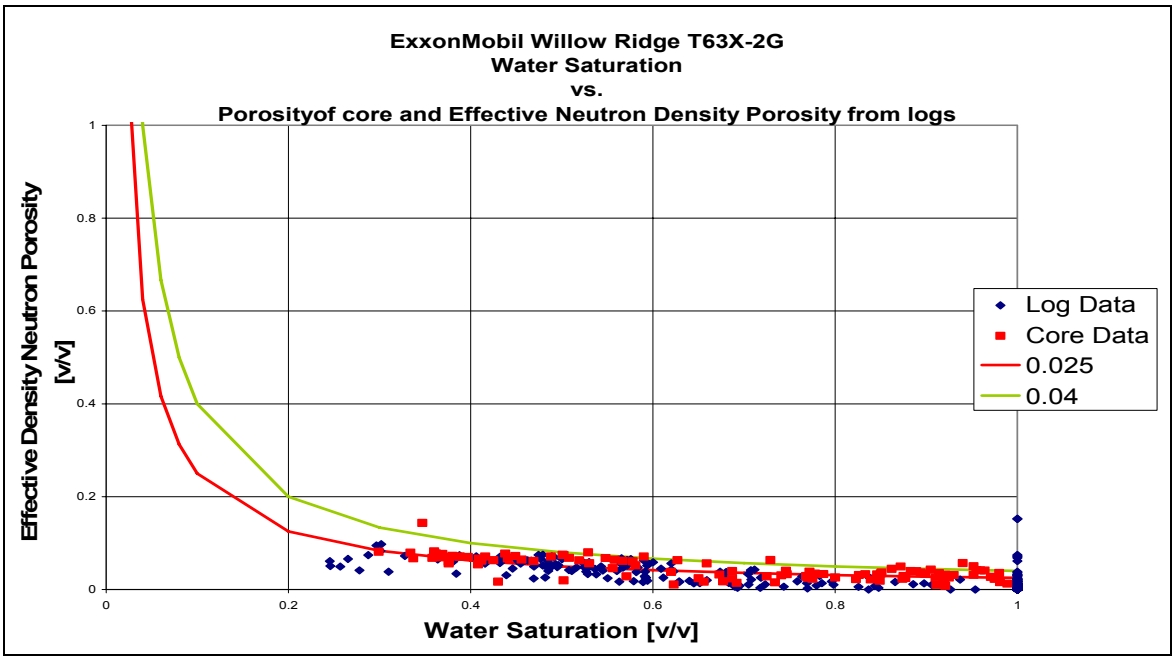

Figure 6.1.7 Water saturation-porosity crossplot with iso-bulk volume water lines at 2.5% and 4%. Note the close correspondence between log and core data, and both follow a low and roughly constant BVW near bulk-volume irreducible.

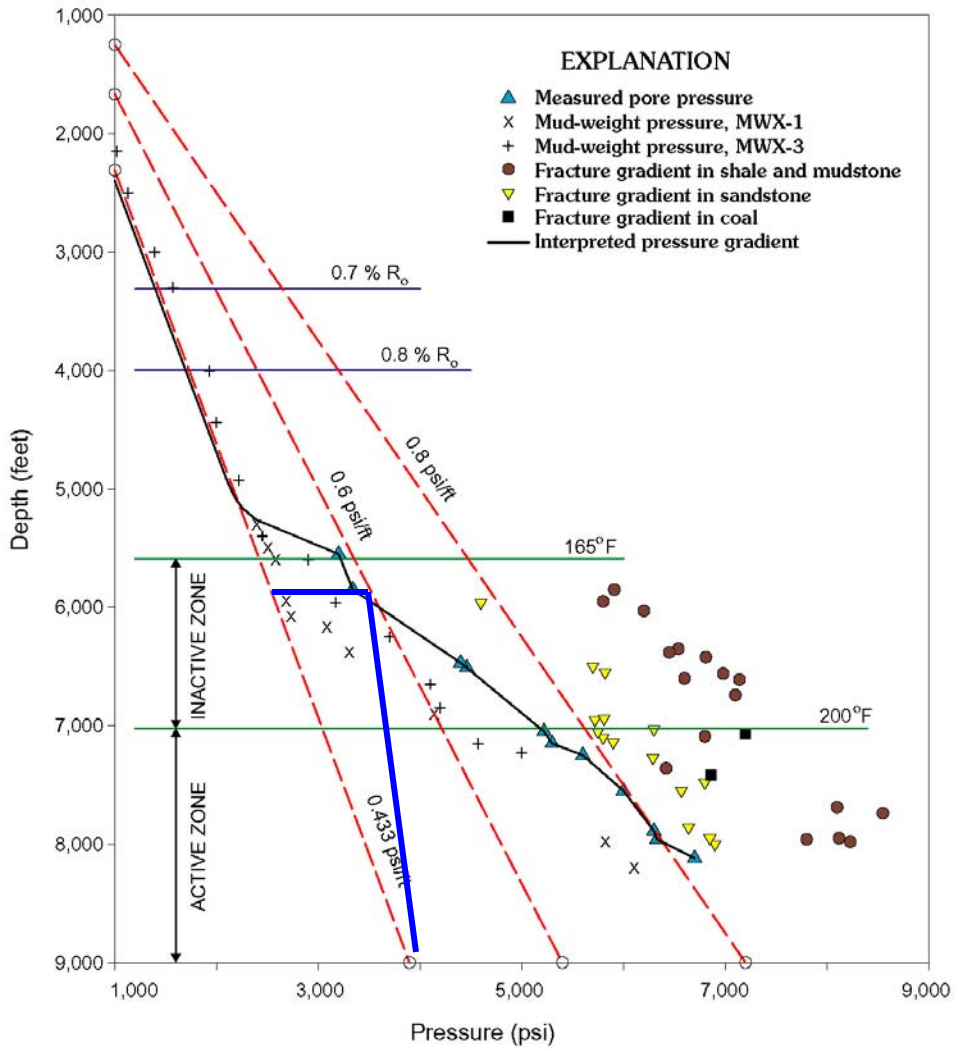

Figure 6.1.8 Pressure-depth plot for the MWX site in Rulison field, Piceance Basin, Colorado (from Nelson, 2003b, Fig 8). Assuming top of a continuous gas column lies at or near 6,000 ft, and a free water level exists near 9,000 ft (~3,000 ft column height), the measured pressure profile should look something like the blue line shown here, with a gas column rising off the water line at the free water level at a slope of 0.1-0.2 psi/ft (depending on exact gas density) and then abruptly returning to the hydrostatic gradient at the top of the gas column. The observed pressure trend in these wells, and all others in the basin, increases downwards towards a value approaching the lithostatic gradient.

6.1.3.5 Rock-Type Identification from Log Data

One of the most vexing problems in log analysis of sand-shale sequences is detailed rock type identification given a limited suite of measurements. A broad variety of crossplots were constructed to investigate relationships between raw and calculated log data and the rock-type codes from core descriptions in an attempt to derive algorithms to predict rock types from log data in the absence of core. These included crossplots of the data against selected digits extracted from the rock-type code (e.g. the second digit or the grain-size term) and aggregates of rock types. Based on inspection of the more promising plots, select multivariate plots were constructed to determine if a more detailed multivariate analysis, for example cluster analysis, might improve the predictability. Generally speaking, multivariate methods sometimes work well if broad trends are visible in the single variable comparisons, but if no significant trends are visible in any of the variables considered then combining variables rarely improves the situation.

Due to limited time and the very large size of the database, we were not able to perform a comprehensive data mining that compares all possible combinations of variables. Consequently we used our general knowledge of the system and tool responses to guide the comparisons we investigated. The raw data needed to explore rock-typing relationships are available in the individual LAS files on the project website, which include both the depth-shifted full five-digit rock numbers and the individual digits parsed apart as separate curves.

6.1.3.5.1 Gamma Ray and Vshale - Crossplots of raw gamma ray values and calculated Vshale values, which substitute for rigorously normalized gamma ray logs in this study, were made against the entire rock numbers and against the 2nd digit (grain-size term) of the rock number. Depth plots of the rock number in the gamma ray track proved extremely useful for depth shifting the core descriptions and also for general rock-type interpretation. However, in a more rigorous quantitative application of attempts to predict the actual rock number or grain size of the sandstones from the gamma ray log, the rock type classes proved to have too much overlap (Figure 6.1.9). Although the gamma ray (Vshale) generally decreases with increasing average grain size, a specific value of the gamma ray is of little use in predicting what the grain-size term would be. R2 values of regressions were not significant.

Depth plots illustrating the rock type-gamma ray correlation are included in the well files on the project website.

6.1.3.5.2 Deep Resistivity - As with the gamma ray log, plots of deep resistivity against rock number and the 2nd digit of the rock number were made for several wells where by visual inspection we felt correlations were likely. Again a trend of increasing resistivity with increasing grain size is apparent (e.g. Figure 6.1.10), but in all cases the overlap between rock types limits the utility of the relationship.

6.1.3.5.3 Bulk Density, Neutron Porosity, and Photoelectric Factor- The bulk density, neutron porosity, PEF, and combinations thereof were investigated as the most lithology-sensitive measurements available in a common logging suite. There were too few sonic logs available in our dataset to add this additional curve. Conventional crossplots of density-neutron, sonic-neutron, sonic-density, and density-PEF proved to be of little value other than to distinguish clean sandstone from shaly sandstone, shale, and carbonate-cemented sandstone. Crossplots were constructed coding for the rock-type number, 2nd and 3rd rock-type digits, and comparing the density-neutron separation against lithology (Figure 6.1.11). All proved to be hopelessly overlapping and the results were considered inconclusive. No further effort was expended on this task.

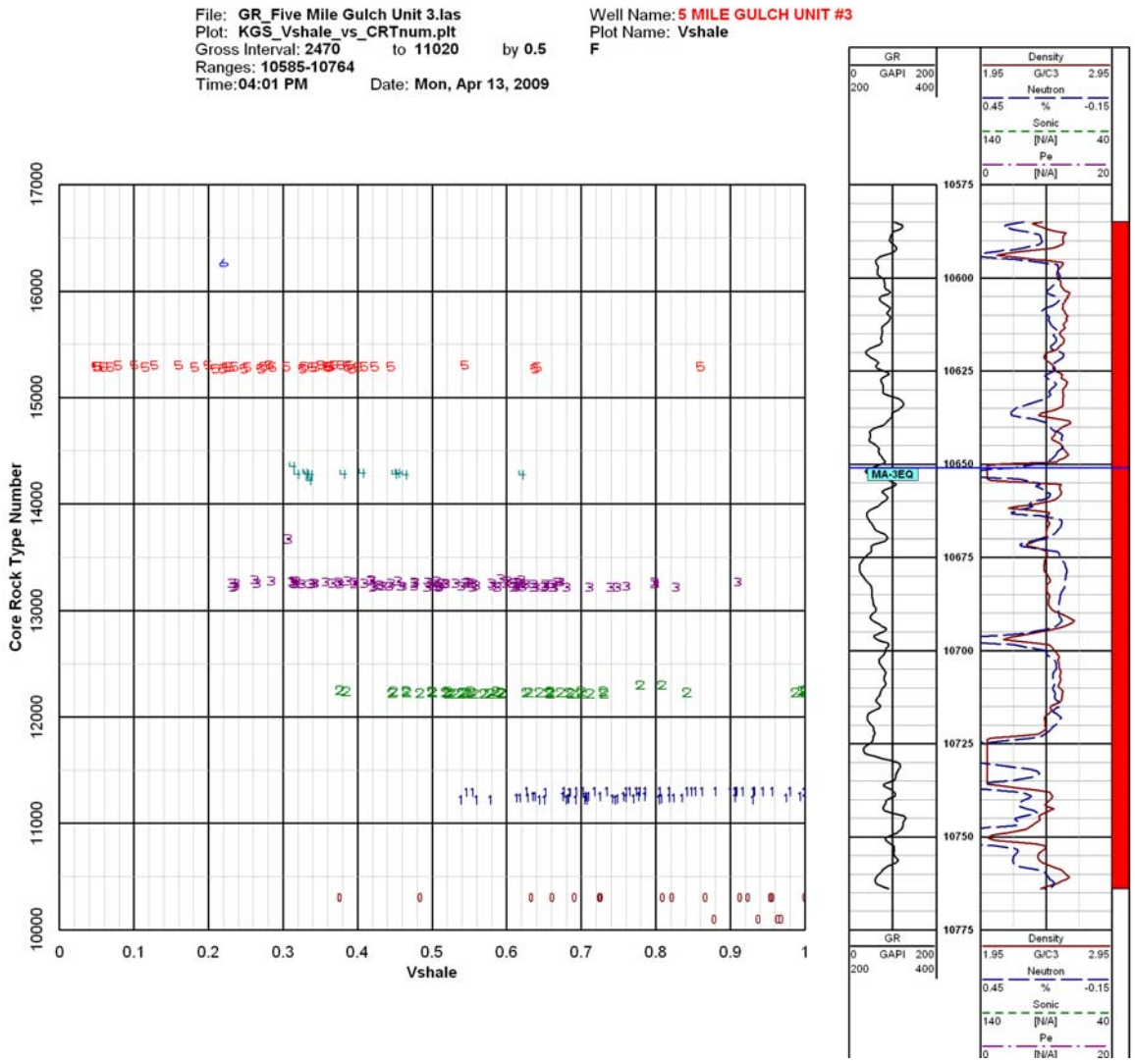

Figure 6.1.9 Volume of shale vs. rock-type number. This plot shows the relative progression of rock-type number increasing with decreasing Vshale. The trend is largely a function of grain size. The broad overlap between rock-type numbers at any given Vshale largely negates the utility of this log indicator for quantitative log analysis (e.g., at Vsh = 0.6, the rock numbers range from 12000 to 15200's).

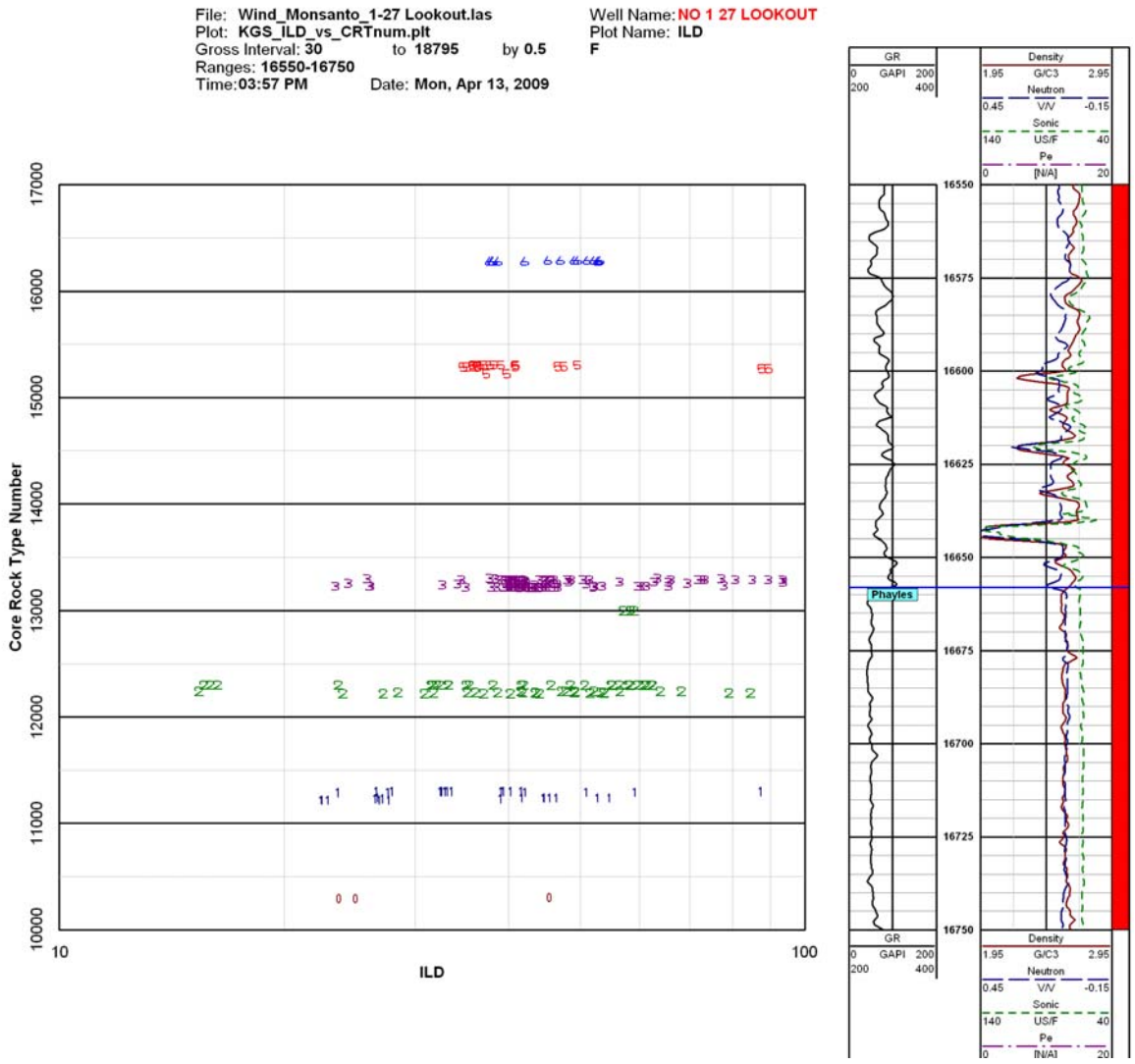

Figure 6.1.10 Log of deep resistivity vs. rock-type number. In this case the shalier sands (rock types <13300) dominate the low-resistivity (<30 ohmm) sandstones, but at over 30 ohmm all rock types are represented at any resistivity.

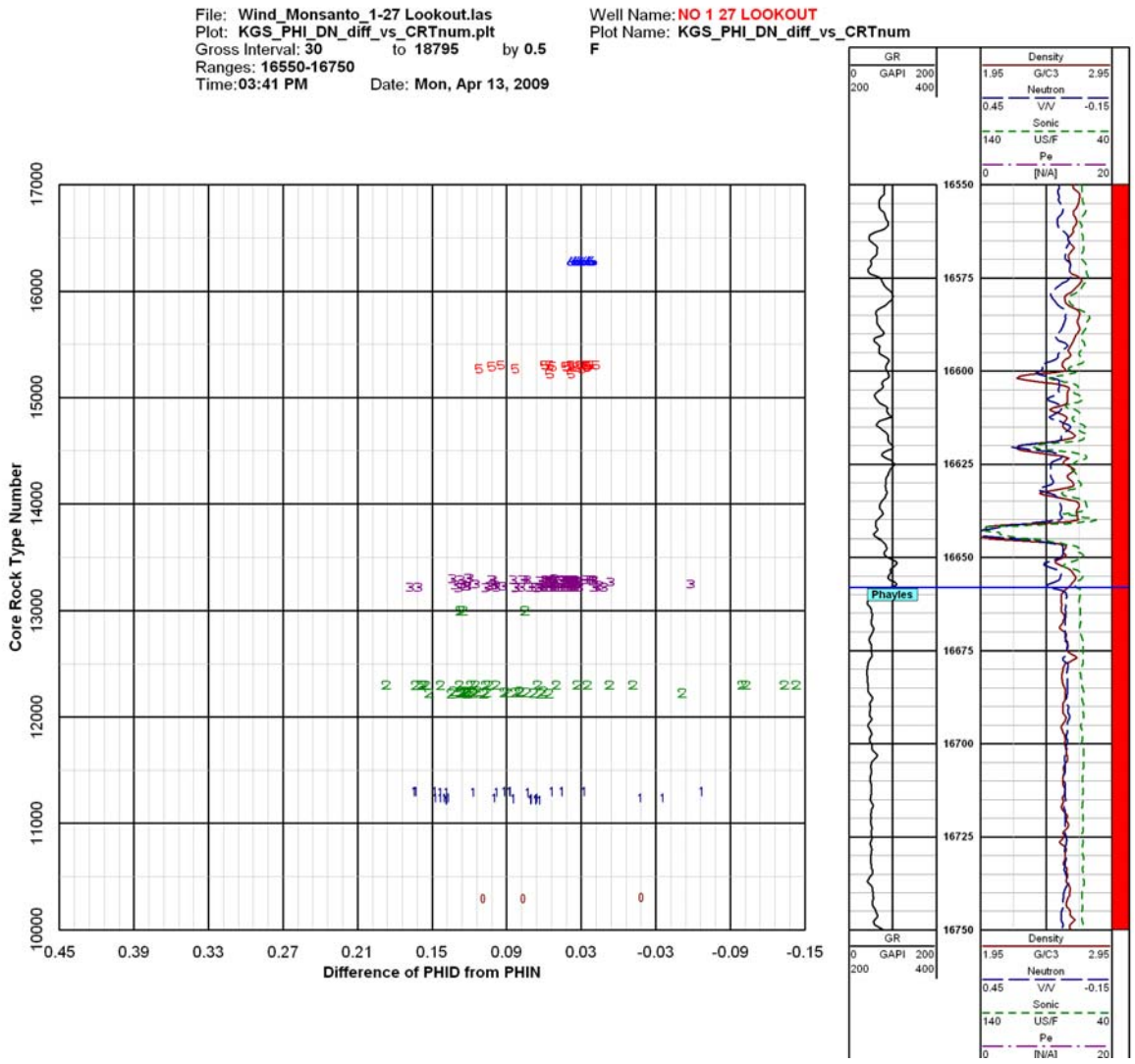

Figure 6.1.11 NPHI - DPHI separation vs. rock-type number. Clean sandstones (rock-type 14000 and higher) tend to track or show slight gas cross-over effect, but the shalier rock types show a broad range in separation. This is partly due to shale effect on the neutron log, but also to mismatched vertical resolution of the neutron and density tools. Again the utility of this measurement for quantitative rock typing is very limited.

Subtask 6.2: Evaluate Results and Determine Log-Analysis Algorithm Inputs

6.2.1 Methods

The advanced log analysis procedure builds on the basic analysis methodology outlined under Task 2.6.2, with changes to the saturation and permeability calculations as described below.

6.2.1.1 Porosity Models

We were unable to improve significantly on the porosity models described in Subtasks 4.6 and 6.1. Although a variable grain density vs. rock-type model could be a significant improvement over other methods, our inability to find a means to perform detailed rock typing from log data alone precludes this approach. Using a zoned grain-density model based on geologic knowledge of the section, tied to core-grain densities, offers the best approach for single log porosity determination. For example, in the Washakie Basin the upper Almond marine sandstones exhibit grain densities clustered around 2.68 g/c3, while the main Almond fluvial sandstones cluster near 2.65 g/c3. The main problem lies in determining where to draw a boundary between the dominantly fluvial and dominantly marine section, because the uppermost part of the main Almond exhibits transitional characteristics. Most workers in the area draw the break near the top of the uppermost significant coal seam. Similar approaches work in the Mesaverde sections of the Uinta and Piceance basins, separating dominantly marine sandstones with some carbonate cement and higher average grain densities from nonmarine sandstone sections.

Overall, the shale-corrected density-neutron crossplot porosity was the best predictor of *in situ* porosity; however, this method only works with good neutron log data. The sonic-neutron effective porosity was the second best predictor, and it tends to be more robust in areas with poor hole conditions.

6.2.1.2 Permeability Modeling Using Basin-Specific Phi-K Relations

For this analysis each basin was evaluated individually and basin-specific porosity-permeability regression coefficients were determined as described in Subtask 4.1 of this report.

The individual y on x linear regressions are located on the spreadsheet DOE_k-phi_REG_080721.xls on the project website and are summarized in the following table:

Table 6.2.1 Porosity-permeability regression parameters determined by basin.

Basin	*β0*	*β1*
Green River Basin	-4.417	28.102
Piceance Basin	-4.437	26.724
Powder River Basin	-4.515	29.319
Uinta Basin	-4.295	29.905
Wind River Basin	-4.361	17.874
Washakie Basin	-5.027	31.751

Permeability was calculated as a function of effective porosity using the basin specific values for β0 and β1 given above:

$$\log_{10}K\_DOE = \beta0 + \beta1*PhiE \qquad [6.2.1]$$

where β1 is the slope of the linear regression, β0 is the y intercept, and PhiE is porosity in %. This permutation of the permeability was labeled K_DOE in the LAS files.

Alternate methods to estimate permeability from logs include the Timur equation approach that was previously described in Subtask 6.1. This was calculated using two different estimates of water saturation: the first using a basic Archie water-saturation equation with constant ***m*** = 1.85 and n = 2; and the second using a variable ***m*** in the Archie saturation equation as described below. The change from a constant porosity exponent to a variable exponent based on porosity and water salinity in Archie's equation changes the resultant water saturation. This in turn changes the computed bulk volume water, but because BVW = porosity X Sw, the change tends to be quite small. We found the estimate of bulk-volume irreducible is so similar, the permeability from the modified Timur equation was nearly the same as from the constant porosity exponent case.

Comparing the three calculated permeabilities, in the majority of wells the match to core permeability was best using the basin-specific regression equation. Generally speaking the match is better at high porosities (>9%) than at low porosity. In general, our estimates of permeability

using the Timur equation tend to overshoot the core-measured permeability values at porosities <9%. This was true for both the constant ***m*** and variable ***m*** approaches. Nonetheless, the Timur equation approach is better than using a single equation for the entire Mesaverde such as Eqn. 4.1.4.

6.2.1.4 Advanced Water Saturation Model

Under Subtask 6.1 our basic approach to water saturation calculations was described. We also described the results of our core determined electrical resistivity properties in Subtask 4.4, including the variation in Archie porosity exponent as a function of porosity and water salinity. These observations lead to an improved water-saturation methodology that we believe corrects for excess surface conductivity effects that are normally accounted for using some variation of a shaly sand equation, oftentimes requiring estimates of bound-water conductivity or cation-exchange capacity of the rock that may not be available.

The data described in Subtask 4.4 are broadly summarized as follows:

1. The Archie porosity exponent "m" decreases with decreasing porosity with a general trend of :

   $$\boldsymbol{m} = 0.676 \log \phi + 1.22 \qquad [6.2.2]$$

   where ϕ is the *in situ* porosity in %. This equation was determined using the 40k ppm salinity dataset, which is the largest single dataset.
2. At any given porosity, the porosity exponent increases with increasing water salinity.
3. At porosity >14% ***m*** is capped at a constant value of 1.95. The regression equation above predicts a continuously increasing value for ***m*** as porosity increases, but the dataset at high porosities, if analyzed independently, does not support an ever-increasing porosity exponent.

Subtask 4.4 discusses several explanations for this behavior, including a dual-porosity model where a small fraction of the porosity (<1% porosity) consists of microfractures or sheet-like pores that carry current in a parallel circuit to the matrix porosity. The apparent ***m*** of this circuit is quite low, approaching 1, whereas the matrix porosity has an ***m*** close to the conventional value of 2 for sandstone porosity. An alternative view is there is a small but very electrically efficient

surface conductivity effect that is in parallel to the matrix. Because the grain surfaces are extremely highly connected, there is no dead space and electrical efficiency of the surfaces approach unity. Matrix conductivity, on the other hand, is entirely through brine-filled pores and their connecting pore throats and is dominated by the geometry of the pore throats (Herrick and Kennedy, 1993).

Brine occupying those parts of pore bodies off the shortest conductive paths through the rock carry small eddy currents or are electrical dead space, reducing the efficiency of the rock in terms of how much of the porosity actually participates in electrical conduction. The average apparent ***m*** of a conventional sandstone reservoir is ~2, which is approximately the value we observed in high-porosity Mesaverde samples. The total conductivity of the rock is the sum of the surface conductance and the matrix conductance. Because the surface-conductivity effect is ubiquitous yet dominates the conductivity at low porosity, whereas it is a relatively minor percentage contributor at high porosity, the net effect is the trend of ***m*** vs. porosity illustrated by Figure 4.4.13.

The considerable scatter in Figure 4.4.13 represents natural variability of the pore geometry from one sample to the next, with attendant differences in electrical efficiency. Differences in surface conductivity, because it is a small part of the total conductivity, are secondary. The salinity dependence illustrated by Figures 4.4.14 and 4.4.15 is porosity independent, since the slopes of the log Rw vs. ***m*** are highly linear and are generally parallel. If Figure 4.4.11 is broken apart by brine-salinity range, the entire data cloud is observed to rise as the salinity increases, rather than one end rising faster than the other. These data suggest the impact of the surface conductance on the overall conductance decreases as salinity increases, which is consistent with a roughly constant surface conductance combined with increasing matrix conductivity with increasing brine conductivity.

Stepwise Log Analysis Procedure

Fundamentally, this process computes a variable Archie porosity (cementation) exponent "m" using the analytical data described in Subtask 4.4, using the 40,000 ppm salinity dataset as the base equation. The procedure begins by computing the formation water resistivity at laboratory conditions, to take it back to the conditions under which the electrical properties were measured. The Archie porosity exponent is then calculated as a function of porosity and water

resistivity. This value of ***m*** is substituted into Archie's equation in the usual manner with an a=1 to compute water saturation.

No resistivity index data were collected as part of this project and we continue to use n = 2 for the saturation exponent.

a. Follow steps a, b, and c as described in section 2.6.2.5.
b. Correct the formation water resistivity (Rw) at formation conditions, from Pickett plot or produced water analysis, to the equivalent resistivity at laboratory temperature of 75 degF using the Arps equation:

$$Rw\_75 = \frac{RWTf\,(RESTEMP + 6.77)}{81.77} \qquad [6.2.3]$$

RWTf = Rw at formation temperature, in ohmm

RESTEMP = reservoir temperature in degF

c. Compute the variable Archie porosity exponent "m" as a function of porosity as follows:

ArchieM = (0.676*log PHIX + 1.22) + (0.0118*PHIX – 0.355)

* (log RWTf + 0.758) [6.2.4]

This is identical to Eqn 4.4.8. At high porosity (>14%), Eqn 4.4.9 should be substituted.

d. Compute water saturation by the Archie equation (Subtask 2.6.2.5d) as before, except with the variable m, which we labeled as KLOG_VARM.
e. Recalculate BVW, BVWI, and SWI from the new Sw.
f. Using the new Sw and SWI, the Timur equation was re-run.

6.2.2 Results

Comparisons of the basic log model and the advanced saturation model are illustrated in Figures 6.2.1 and 6.2.2 below. Depth plots for all wells illustrating both models are included on the project website.

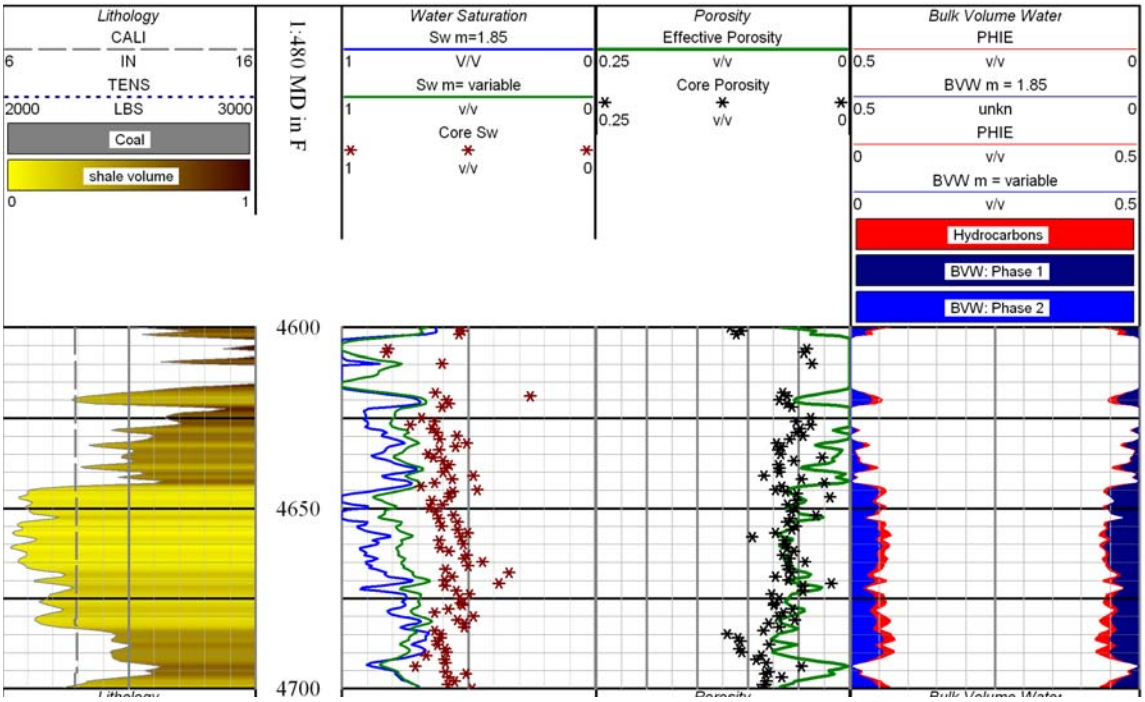

Figure 6.2.1. Example of water saturation computed using the constant ***m*** = 1.85 model (blue line) and variable ***m*** model (green line) in a low-porosity, generally wet zone. The separation is greatest in the clean sandstone interval around 4650 ft. The variable ***m*** model generally calculates lower water saturations, closer to the routine core Sw's, because the ***m*** value is lower than 1.85 at these porosities and formation water salinity.

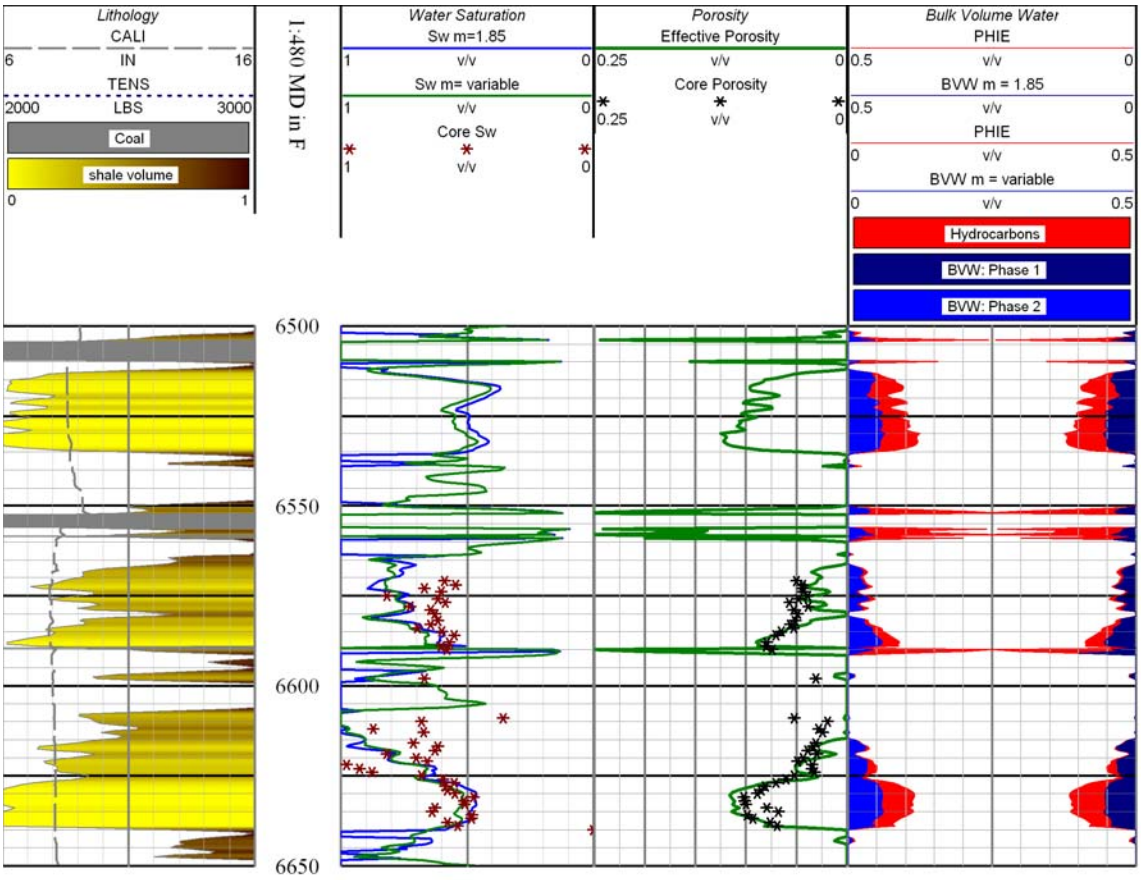

Figure 6.2.2. Example of water saturation computed using the constant ***m*** = 1.85 model (blue line) and variable ***m*** model (green line) in a higher-porosity gas zone. The separation is generally small because at these porosities the calculated ***m*** is close to the base case value of 1.85. Where the variable ***m*** model computes an ***m*** > 1.85, the calculated water saturation curves cross and the base-case model computes a lower saturation than the variable ***m*** model.

Overall, the impact of using the variable ***m*** model can be summarized as follows:

1. In low-porosity rocks, less than 8%, the calculated water saturations are significantly lower and there is more gas in place;
2. The calculated bulk-volume water irreducible is reduced slightly;
3. At porosities below bulk-volume irreducible, typically 3-5%, there is no difference between the models.
4. At high porosities, over ~9%, the variable ***m*** model calculates slightly higher water saturations than the base-case model. This is because our base model uses an average ***m*** of 1.85, which is centered on 8.5% porosity. Companies that use a conventional value of

2.0 will see an improvement in calculated water saturation at all porosities using our model.

5. This is a simpler approach than most shaly sand models that have been applied to the Mesaverde, and probably yields a more accurate estimate of *in situ* saturations.

Task 7. Simulate Scale-Dependence of Relative Permeability

Subtask 7.1. Construct Basic Bedform-Architecture Simulation Models

Initial results of critical gas saturation (S_{gc}) measurements and interpretation were presented at the AAPG Hedberg Conference at Vail in 2005. This early research led to this study of critical gas saturation. The results of the earlier work and the results found to date in this study were combined and presented in a publication for the Hedberg Conference Proceedings that will be published by the AAPG in 2007. A more complete analysis of the critical gas saturation results is presented in the paper: Byrnes, A. P., 2007, Issues with gas and water relative permeability in low-permeability sandstones, Am. Assoc. Petroleum Geologists, Hedberg Conference series volume 3, "Understanding, Exploring and Developing Tight Gas Sands," April 24-29, 2005, Vail, Colorado, Chapter 5, p 1-14.

Most of the S_{gc} data support the commonly applied assumption that $S_{gc} < 0.05$. However, a few heterolithic samples exhibiting higher S_{gc} indicate the dependence of S_{gc} on pore-network architecture and scale. Concepts from percolation theory and upscaling indicate that S_{gc} varies among four pore-network architecture models: 1) percolation (N_p), 2) parallel ($N_{//}$), 3) series ($N_{\perp}$), and 4) discontinuous series ($N_{\perp d}$). Analysis suggests that S_{gc} is scale- and bedding-architecture dependent in cores and in the field.

The models suggest that S_{gc} is likely to be very low in cores with laminae and laminated reservoirs and low (e.g., $S_{gc} < 0.03$-0.07 at core scale and $S_{gc} < 0.02$ at reservoir scale) in massive-bedded sandstones of any permeability. In crossbedded lithologies exhibiting series network properties, S_{gc} approaches a constant reflecting the capillary-pressure property differences and relative pore volumes among the beds in series. For these networks S_{gc} can range widely but can reach high values (e.g., $S_{gc} < 0.6$). Discontinuous series networks, representing lithologies exhibiting series network properties but for which the restrictive beds are not sample-spanning, exhibit S_{gc} intermediate between N_p and $N_{\perp}$ networks. Figure 7.1.1, presented previously, illustrates the possible bedform models. Equations presented in Section 4.2 provide the basis for predicting critical gas saturation.

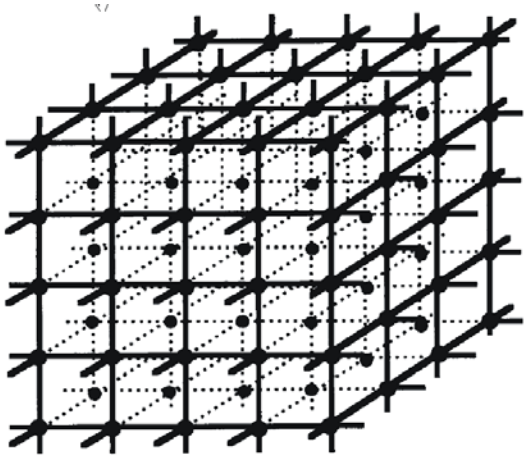

1) Percolation Network (N_p) - macroscopically homogeneous, random distribution of bond sizes, e.g., Simple Cubic Network (z = 6).

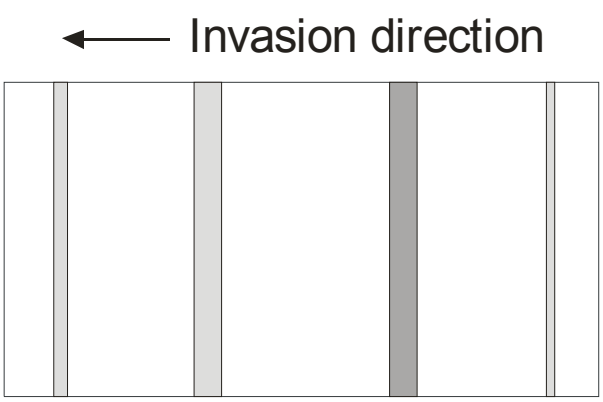

3) Series network ($N_\perp$) - preferential sample-spanning orientation of pore sizes or beds of different N_p networks perpendicular to the invasion direction.

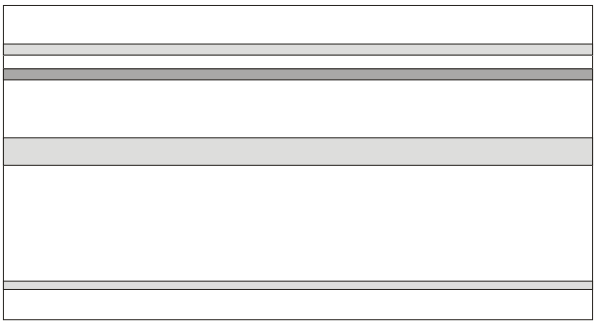

2) Parallel Network ($N_{||}$) - preferential orientation of pore sizes or beds of different N_p networks parallel to the invasion direction.

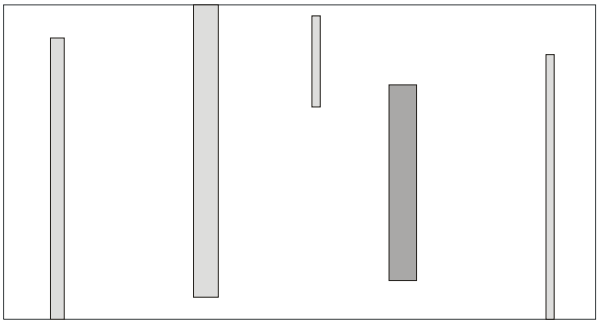

4) Discontinuous series network ($N_{\perp d}$) - preferential non-sample-spanning orientation of pore sizes or beds of different Np networks perpendicular to the invasion direction. Represents continuum between N *and* N_p.

Figure 7.1.1. Conceptual pore network models: 1) percolation (N_p), 2) parallel ($N_{//}$), 3) series ($N_\perp$), and 4) discontinuous series ($N_{\perp d}$).

Subtask 7.2. Perform Numerical Simulation of Flow for Basic Bedform Architectures

The analysis above indicates that critical gas saturation can vary widely as a function of bedform architecture. At the well scale the influence of critical gas saturation on relative permeability approaches the simple flow end members (Figure 7.2.1). Massive-bedded sandstones are appropriate represented by the matrix-scale relative permeability with $S_{gc} = 0$ and can be solved numerically. For sandstones with laminae or parallel bedding, the numerical

solution at the wellbore scale can be represented by the parallel flow solution. Based on the observed vertical change in porosity and permeability in the wells in this study, the relative contribution to flow changes on a vertical scale of as small as 0.5 feet (0.2 m).

A key question in assessing low-permeability reservoirs is the distribution of permeability. Assumptions or models of permeability architecture are fundamental to how permeability is modeled and is upscaled from finer-scale measurements. Frequently, in low-permeability rocks, core and log-analysis derived permeabilities are averaged geometrically to obtain an effective average *k*. Use of the geometric mean k assumes a random distribution of the permeabilities measured. Given that the drainage radius of many low-permeability reservoirs may range from 20 to 40 acres, assumption of a random permeability distribution may not be consistent with the depositional environments. Rather it is possible these reservoirs are likely to exhibit lateral continuity of lithofacies over many hundreds of feet. On this basis, average permeability should be calculated using the arithmetic average equation consistent with a parallel flow model with each bed contributing to total flow as a function of their permeability, saturation, and relative permeability curves. Using this approach, thin, high-permeability beds result in a significant increase in average permeability.

The number of combinations of parallel-bedded permeability architecture is infinite. To provide insight on the relative role of horizontal permeability vertical heterogeneity, a series of models were analyzed that parametrically investigate the role of total bed thickness, thin high-permeability bed permeability, and vertical permeability. For the parallel-flow model the differences in relative permeability result simply in different effective gas-permeability values. A simple layer model was constructed using the Computer Modeling Group (CMG) *IMEX* reservoir simulator. The model comprises 13 layers with total thickness varying from 50 ft to 300 ft (15-91 m) and measured 2 miles (3.2 km) on a side with a single well in the center (Fig. 7.2.2). The models comprised 1,125 total gridcells. In all models a single laterally extensive 1-foot (0.3-m)-thick bed exists in the vertical center of the model. Porosity was assigned a uniform value of 8.25% corresponding to Mesaverde rocks with *in situ* Klinkenberg permeability of ~0.01 mD ($1x10^{-4}$ μm^2). Water saturation was assigned a value of Sw = 0.5 which, using the gas relative-permeability equations described above, results in a gas relative permeability of k_{rg} = 0.14 and an effective gas permeability, $k_{eg,Sw}$ = 0.0014 mD ($1.4x10^{-6}$ μm^2). Vertical effective gas permeability was assigned a value of 10% of horizontal permeability or $k_{eg,Swv}$ = 0.00014 mD

($1.4x10^{-7}$ μm^2) except where otherwise analyzed. The simulations therefore represented the conditions of a base effective *in situ* Klinkenberg horizontal gas permeability of 0.0014 mD ($1.4x10^{-6}$ μm^2). Alternate models were also investigated with a base absolute permeability of 0.001 mD ($1x10^{-6}$ μm^2) corresponding to an in situ effective gas permeability of 0.00014 mD ($1.4x10^{-7}$ μm^2). Vertical permeabilities varied from 10% of horizontal to 0.0001% of horizontal, as noted. Gas properties were consistent with a 0.55 gravity gas. All models were assigned a reservoir pressure of 4,000 psi (27.6 MPa) and a well-bottomhole flowing pressure of 1,000 psi (6.9 MPa).

Figure 7.2.3 illustrates cumulative recovery from reservoirs with horizontal absolute permeabilities ranging from 0.001mD to 10 mD ($1x10^{-6}$ - $1x10^{-2}\mu m^2$; corresponding to *in situ* effective gas permeabilities of 0.00014 mD to 1.4 mD; $1.4x10^{-7}$ – $1.4x10^{-3}\mu m^2$) and thicknesses ranging from 50 ft to 300 ft (15-91 m). For all models with permeability less than ~10 mD ($1x10^{-2}$ μm^2), flow is still transient (i.e., pressure transient has not reached the reservoir boundary). Recovery from the 10 mD ($1x10^{-2}$ μm^2) reservoir begins to decline after 10 years due to the pressure decline reaching the model boundary (i.e., semi-steady state flow). Reservoirs with permeability equal to 100 mD ($1x10^{-1}$ μm^2) begin semi-steady state flow within two years.

The influence of a single 1-foot (0.3-m)-thick higher-permeability bed on cumulative gas production and gas rate from a reservoir with horizontal permeability of 0.01 mD ($1x10^{-5}$ μm^2) and vertical permeability of 0.001 mD is shown in Figure 7.2.4. Though the gas produced by the 100 mD ($1x10^{-1}$ μm^2), 10 mD ($1x10^{-2}$ μm^2), and 1 mD ($1x10^{-3}$ μm^2), 1-ft (0.3-m) intervals is significant (720 MMcf (20 MMm^3), 640 MMcf (18 MMm^3), and 204 MMcf (5.8 MMm^3), respectively at 50 yrs; Fig. 7.2.5), the role that a single high-permeability bed plays in draining vertically adjacent low-permeability beds is evident by comparing Figures 7.2.4A and 7.2.4B. Both of these figures show the enhanced recovery due to the presence of a high-permeability thin bed expressed as the ratio of gas produced when a 1-ft (0.3-m)-thick high-permeability is present to the gas produced when there is no high-permeability thin bed (shown in 0.01 mD ($1x10^{-5}$ μm^2) red curves in Fig. 7.2.4). Figure 7.2.4A shows the ratio including the recovery from the thin bed, and Figure 7.2.4B shows the ratio of incremental gas excluding the recovery from the thin bed and thus shows only the increased recovery from the vertically adjacent reservoir.

For the case where the thin bed has the same permeability as the adjacent reservoir (0.01 mD), the ratio is 1.0. If the thin bed has a permeability of 0.1 mD ($1x10^{-5}$ μm^2), the increased recovery ratio including the thin-bed contribution is 1.16 for a 50-ft (15.2-m)-thick reservoir, but the incremental ratio is only 1.01-1.02. Gas recovery progressively increases with increase in the horizontal permeability of the single, 1-ft (0.3-m)-thick high-permeability bed when the bed permeability exceeds ~1 mD ($1x10^{-3}$ μm^2). Increase in recovery increases with increasing permeability of the thin bed and decreasing thickness of the reservoir. Increase with increasing thin-bed permeability is due to an increase in the ability of the bed to drain vertically adjacent reservoir and carry the gas to the wellbore. Comparison of pressures in the upper- and lower-most beds with the central, thin, high-permeability bed shows that pressure differences are generally less than 5 psi (34.52 kPa) and are not greater than 20 psi (138 MPa) at any given time during production for thin-bed permeabilities from 0.01 mD to 100 mD ($1x10^{-4}$ -$1x10^{-1}\mu m^{2;}$). The relative increase with decreasing reservoir thickness is therefore not due to inability to drain beds that are vertically farther from the thin bed, but rather is due to the limited flow capacity of the bed. Gas flow into the high-permeability bed and the ability of the bed to flow that gas to the wellbore control what the pressure is in the thin bed, which in turn controls total flow. Where the thin bed only has to drain up and down 25 ft (7.6 m) in comparison to 150 ft (45.7 m), gas flow and pressure decrease are greater and the thin bed is able to effectively drain the vertical beds and in so doing decrease in pressure and thereby reach out laterally to a greater distance from the wellbore.

For the vertical permeabilities present in the models shown (k_v = 0.001 mD; $1x10^{-6}\mu m^2$), the primary rate limiting constraint is the thin-bed permeability. But the ability of gas to flow vertically to the high-permeability thin bed is controlled by vertical permeability (k_v). Figure 7.2.5 shows the dependence of incremental cumulative gas (cumulative gas less gas from thin bed) on the vertical permeability for a reservoir with 0.01 mD ($1x10^{-4}$ μm^2) and a 1-ft (0.3-m)-thick bed of 10 mD ($1x10^{-2}$ μm^2). The ratio of incremental cumulative gas decreases with increasing reservoir thickness; however, the ratio for each reservoir thickness is relative to the recovery at that thickness without the thin bed. Ratios are lower for the 300-ft (91-m)-thick than the 50-ft (15.2-m)-thick reservoir, but recovery from the 300-ft (91-m)-thick reservoir is six times greater. For all reservoir thicknesses, increase in k_v greater than $1x10^{-5}$ mD ($1x10^{-8}$ μm^2) does not significantly increase recovery over that obtained at k_v =$1x10^{-5}$ mD ($1x10^{-8}$ μm^2). With k_v

decrease below $1x10^{-5}$ mD ($1x10^{-8}$ μm^2) recovery decreases with decreasing vertical permeability down to $1x10^{-8}$ mD ($1x10^{-11}$ μm^2). For k_v below approximately $1x10^{-8}$ mD ($1x10^{-11}$ μm^2), recovery is similar to recovery for vertical permeability equal to zero, that is, there is no cross-flow and no vertical drainage to the high-permeability thin bed.

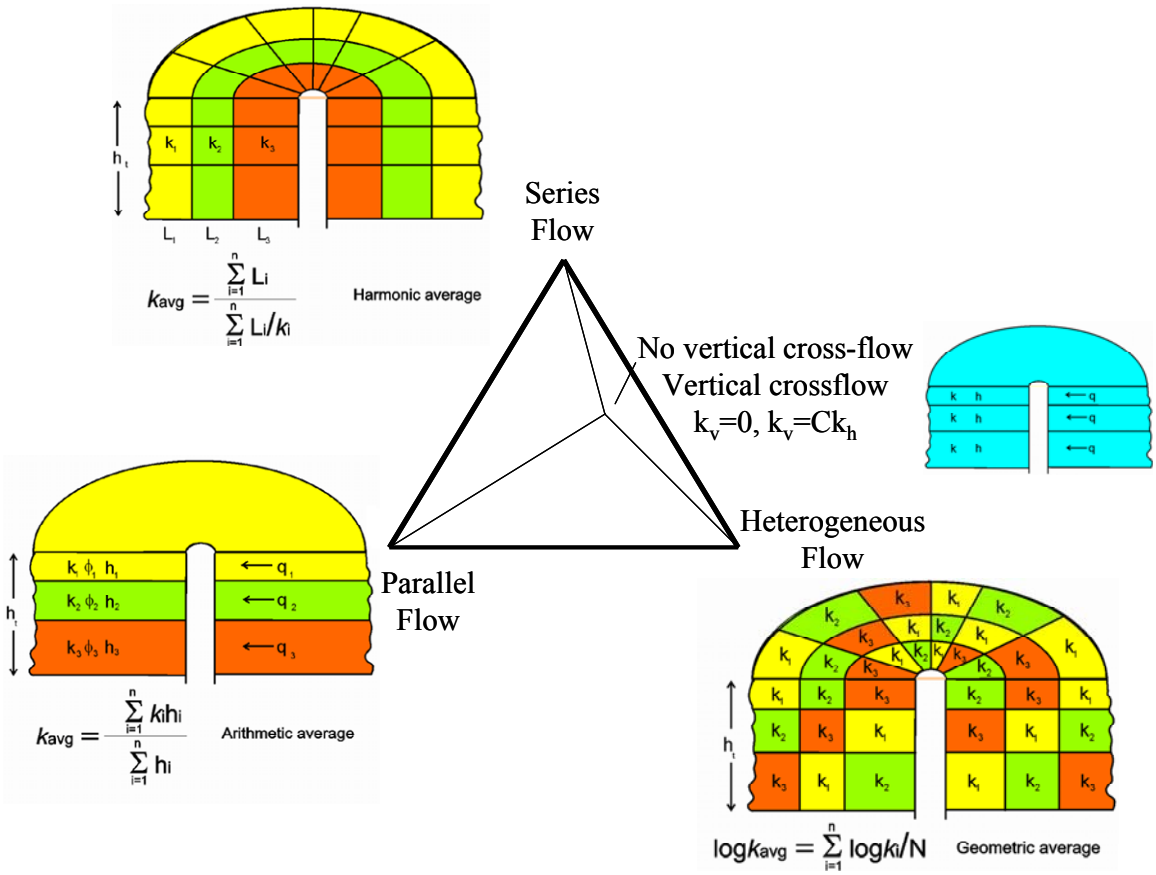

Figure 7.2.1 Flow end members upscaling (averaging) equations.

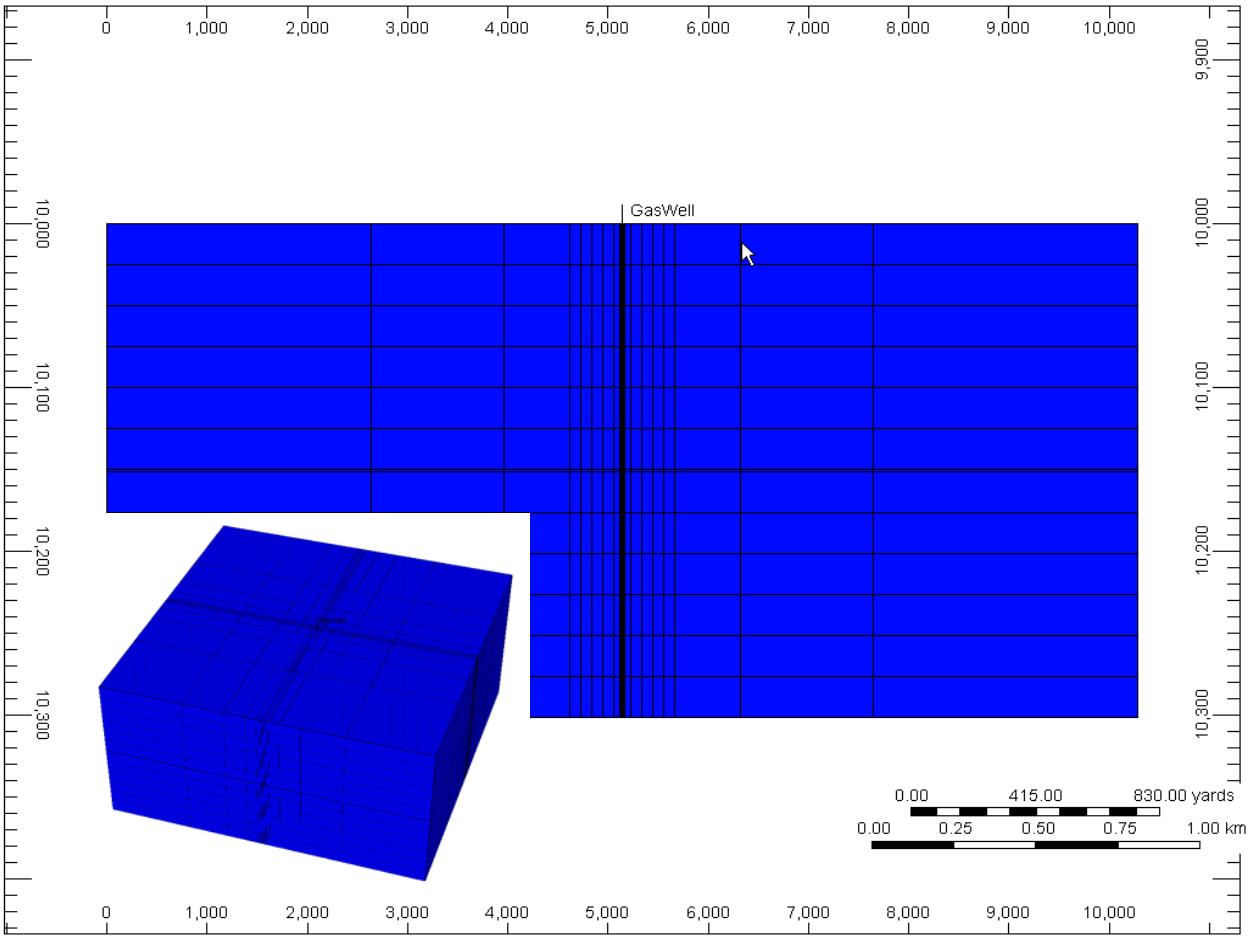

Figure 7.2.2. Computer Modeling Group (CMG) *IMEX* simulation model used to examine influence of reservoir properties. Large cross section shows cut-away to vertical layer with gas well. Inset 3-D figures shows the central locations of the gas well.

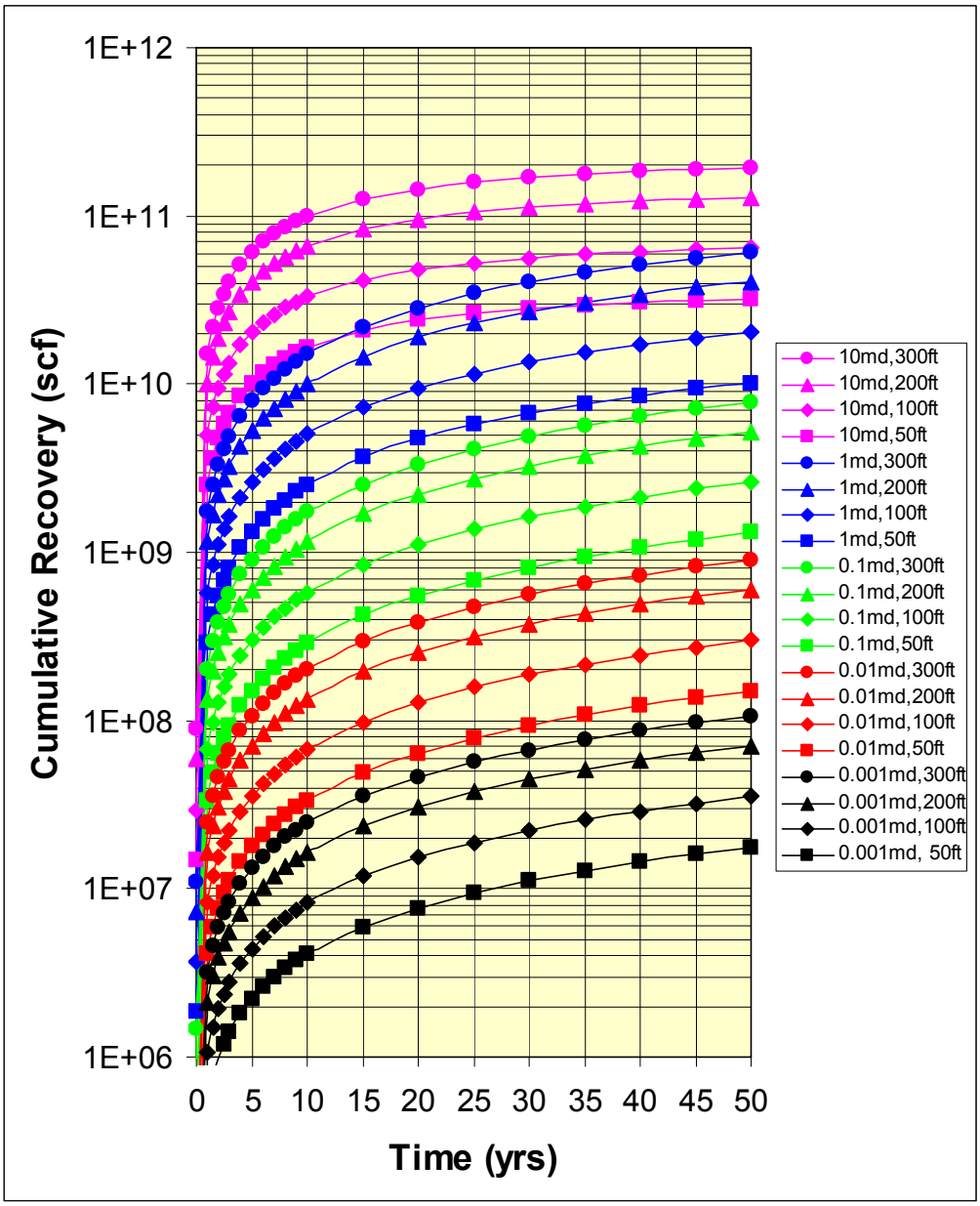

Figure 7.2.3. Cumulative gas recovery versus time for models with varying absolute permeability and thickness. Legend lists absolute permeability values but model results reflect recovery from reservoirs at S_w = 50% and k_{rg} = 0.14. Recovery also reflects assumed initial pressure of 4,000 psi, flowing bottom-hole pressure of 1,000 psi, and gas properties consistent with a 0.55 gravity gas.

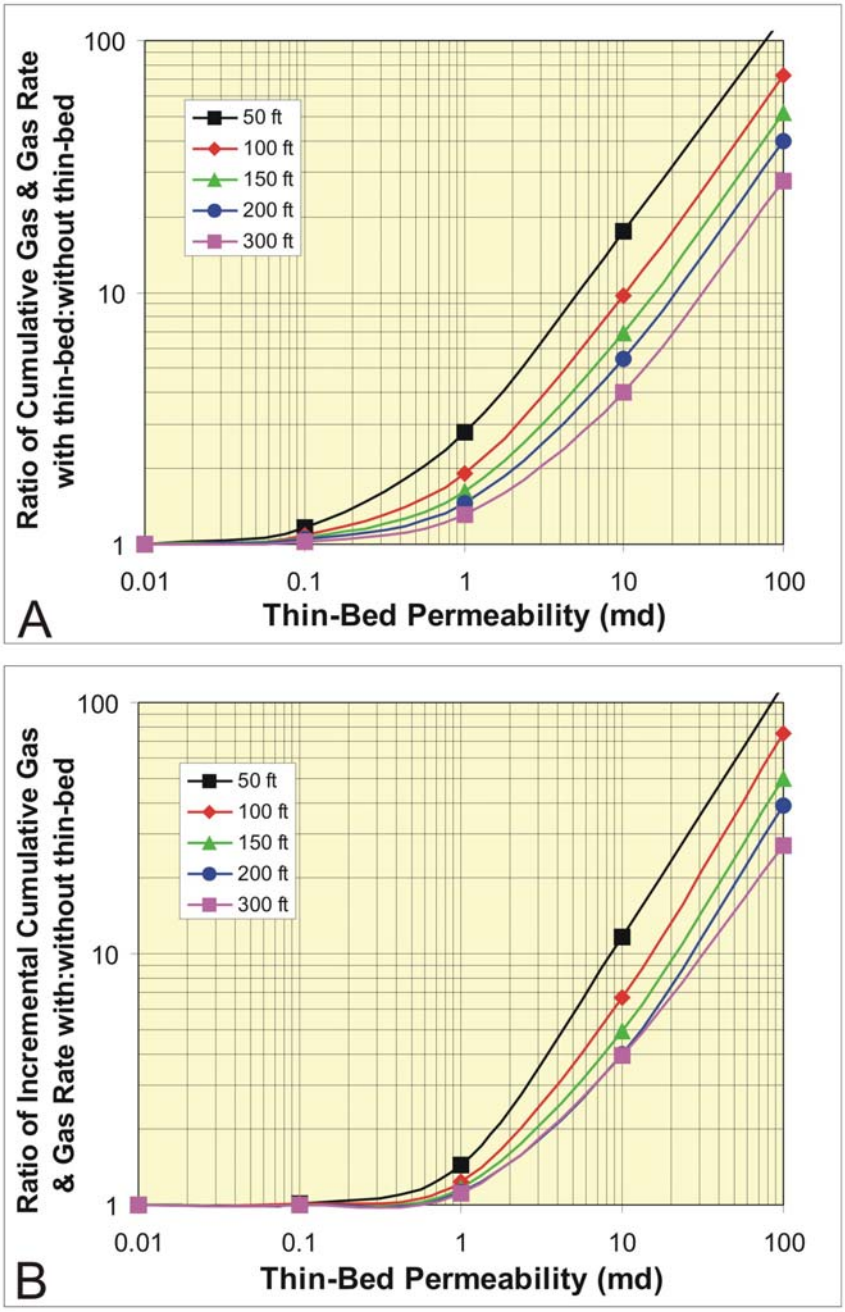

Figure 7.2.4. Crossplot of the ratio of the cumulative gas and gas production rate with a 10-mD thin bed (1-ft thick) to the cumulative gas or gas rate without the thin-bed including the gas recovered from the thin bed (A) and excluding the gas recovered from the thin bed representing only the additional gas produced from beds vertically adjacent to the high-permeability thin bed (B). Cumulative recovery increases significantly with increasing thin-bed permeability above ~1 mD and with decreasing total reservoir thickness.

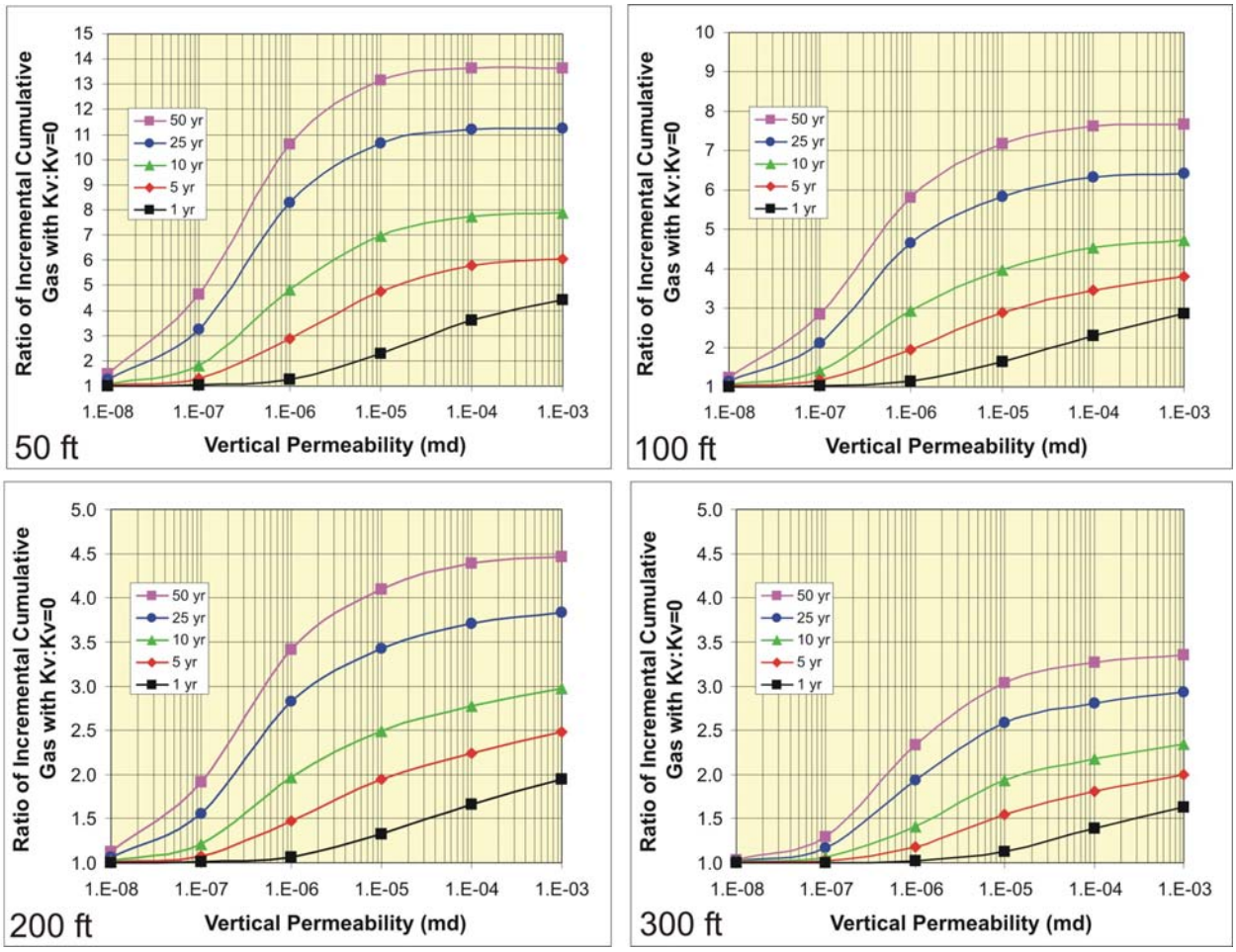

Figure 7.2.5. Crossplot showing the dependence of incremental cumulative gas (cumulative gas less gas from thin bed) on the vertical permeability (k_v) for a reservoir with 0.01 mD and a 1-ft thick bed of 10 mD. Ratio increases with increasing time with expansion of drainage radius. The ratio decreases with increasing reservoir thickness, however, the ratio for each reservoir thickness is relative to the recovery at that thickness without the thin bed. For all reservoir thicknesses increase in k_v greater than $1x10^{-5}$ mD does not significantly increase recovery over that obtained at $k_v = 1x10^{-5}$ mD. With k_v decrease below $1x10^{-5}$ mD recovery decreases with decreasing vertical permeability down to $1x10^{-8}$ mD. For k_v below approximately $1x10^{-8}$ mD recovery is similar to recovery for vertical permeability equal to zero, that is, no cross-flow and no vertical drainage to the high-permeability thin bed.

Task 8. Technology Transfer

Subtask 8.1 Technology Transfer

8.1.1 Early Project Presentations

A Powerpoint presentation was created at the start of the project to present to companies to inform them of the project and request participation through contribution of newly obtained fresh core. Presentations were made to major and independent gas industry companies to solicit participation directly through contribution of core and indirectly through review of activities and methods and results. Presentations were made in both Denver, CO, and Houston, TX. Examples of companies for whom presentations were made include: Exxon-Mobil, BP Exploration and Production, Inc., Shell Exploration and Production, Encana, Williams Gas, and Bill Barrett Corp.

Companies that contributed core to the study as a result of these solicitations and in-house presentations included Kerr-McGee, Bill Barrett Corp., Williams Rocky Mountain Production Company, Exxon-Mobil, Shell Exploration and Production, and Encana. Many other companies expressed interest in the project but were unable to contribute cores due to logistical constraints.

8.1.2 Project Website

The Mesaverde Project website was initiated at the project inception. All reports, including technical quarterly reports were posted on the website, and available for download, when they were submitted. The Mesaverde project website (http://www.kgs.ku.edu/mesaverde) includes all project findings, copies of project reports and presentations in PDF format.

8.1.2 Technical Presentations

Technical presentations at professional society meetings were an integral part of the project. The following lists the technical presentations followed by abstracts. Beyond technical society meeting presentations, technical talks were presented at several society lunches but are not reviewed here.

A technical paper was prepared as part of the proceedings of the American Association of Petroleum Geologists Hedberg Conference on "Understanding, Exploring, and Developing Tight Gas Sands" held in Vail, Colorado. The paper explores models for critical gas saturation. Aspects

of the paper are presented in Section 4.2. An abstract of the paper follows. A publication resulting from this presentation is included in the AAPG Hedberg Conference volume #3 published in May 2008.

A combined oral and poster presentation was presented at the Rocky Mountain Section meeting of the American Association of Petroleum Geologists at Snowbird, UT, in October 6-9, 2007. The presentations covered results of Mesaverde properties measured as of mid-2007. In addition, residual saturation measurements sand trends were used to interpret properties of the Ericson and a talk was presented on this subject. The talk and poster are posted on the project website.

A technical talk was presented at the American Association of Petroleum Geologists Annual Meeting in San Antonio, TX, April 20-23, 2008. This was the last overview presentation that attempted to cover all aspects of the project.

Three technical presentations were given at the American Association of Petroleum Geologists Rocky Mountain Section/Colorado Oil & Gas Association Regional Meeting in Denver, CO, July 7-10, 2008. Each of these were in-depth analyses of particular tasks that were of special interest to the E&P community. All presentations are on the project website and abstracts are presented below.

A one-day workshop is scheduled for the AAPG Annual Meeting in Denver, CO in June 2009. This workshop will complete the technology transfer phase of the project.

Abstracts of technical presentations and posters

Issues with gas relative permeability in low-permeability sandstones

Alan P. Byrnes

Review of gas relative permeability (k_{rg}) studies of low-permeability sandstones indicates they can be modeled using the Corey equation, but scarce data near the critical-gas saturation (S_{gc}) limit k_{rg} modeling at high water saturations. Confined mercury injection capillary pressure and coupled electrical resistance measurements on Mesaverde sandstones of varied lithology were used to measure critical nonwetting saturation. Most of these data support the commonly applied assumption that $S_{gc} < 0.05$. However, a few heterolithic samples exhibiting higher S_{gc} indicate the dependence of S_{gc} on pore network architecture. Concepts from percolation theory and upscaling indicate that S_{gc} varies among four pore network architecture models: 1) percolation (N_p), 2) parallel ($N_{//}$), 3) series ($N_{\perp}$), and 4) discontinuous series ($N_{\perp d}$). Analysis suggests that S_{gc} is scale- and bedding-architecture dependent in cores and in the field.

The models suggest that S_{gc} is likely to be very low in cores with laminae and laminated reservoirs and low (e.g., $S_{gc} < 0.03$-0.07 at core scale and $S_{gc} < 0.02$ at reservoir scale) in massive-bedded sandstones of any permeability. In crossbedded lithologies exhibiting series network properties, S_{gc} approaches a constant reflecting the capillary pressure property differences and relative pore volumes among the beds in series. For these networks S_{gc} can range widely but can reach high values (e.g., $S_{gc} < 0.6$). Discontinuous series networks, representing lithologies exhibiting series network properties but for which the restrictive beds are not sample-spanning, exhibit S_{gc} intermediate between N_p and $N_{\perp}$ networks.

Consideration of the four network architectures lends insight into the complications of heterogeneous lithologies at differing spatial scales and underscores the difficulty of upscaling laboratory-derived relative permeabilities for reservoir simulation. Analysis also indicates that for some architectures capillary pressure and relative permeability anisotropy may need to be considered.

Reference: A. P. Byrnes, 2007, Issues with gas relative permeability in low-permeability sandstones; in K. Shanley, W. Camp, and S. Cumella (eds.), Understanding, exploring, and developing tight-gas sands – 2005 Vail Hedberg Conference, Chapter 5, p. 1-14.

Regional petrophysical properties of Mesaverde low-permeability sandstones

Alan P. Byrnes, John C. Webb, and Robert M. Cluff

Petrophysical properties of Mesaverde Group tight gas sandstones for the range of lithofacies present in the Washakie, Uinta, Piceance, Upper Greater Green River, Wind River, and Powder River basins exhibit consistent trends among lithofacies. Grain density for 2400 samples averages 2.654±0.033 g/cc (±1sd) with grain-density distributions differing slightly among basins. The Klinkenberg gas slip proportionality constant, b, can be approximated using the relation: $b(atm) = 0.851\ k_{ik}^{-0.34}$. Regression provides a relation for *in situ* Klinkenberg permeability (k_{ik}): $\log k_{ik} = 0.282\ \phi_i + 0.18\ RC2 - 5.13$ (±4.5X,1 sd), where ϕ_i = *in situ* porosity, and RC2 = a size-sorting index. Artificial neural network analysis provides prediction within ±3.3X. Analysis of 700 paired samples indicates 90% of all samples exhibit porosity within 10%-20%. Permeability exhibits up to 40% variance from a mean value for 80% of samples.

Capillary pressure (Pc) exhibits an air-mercury threshold entry pressure (P_{te}) versus k_{ik} trend of $P_{te} = 30.27\ k_{ik}^{-0.44}$ and wetting-phase saturation at any given Pc (for 350< Pc < 3350 psia air-Hg) and k_{ik} of $S_w = A\ k_{ik}^{-0.138}$ where $A = -13.1*\ln(Pc_{air\text{-}Hg})+117$. Accuracy of the Leverett J function is poorer. Hysteresis Pc analysis indicates that residual nonwetting-phase saturation to imbibition (*Srnw*) increases with increasing initial nonwetting phase saturation (*Snwi*) consistent with the Land-type relation: 1/Snwr-1/Snwi = 0.8±0.2. Electrical resistivity measurements show that the Archie cementation exponent (*m*) decreases with decreasing porosity (ϕ) below approximately 6% and can be generally described by the empirical relationship: $m = 0.95\text{-}0.092\ \phi + 0.635\ \phi^{0.5}$. These relationships are still being investigated. The Mesaverde Project website is (http://www.kgs.ku.edu/mesaverde).

Presented at AAPG Rocky Mountain section meeting, Snowbird, UT, October 2007

What's the matter with the Ericson?

Robert M. Cluff, Keith W. Shanley, and John W. Robinson

The Cretaceous Ericson Formation is a clean, quartzose, blanket-like sandstone that underlies the prolific gas productive Almond Formation across the entire Washakie Basin. The top several tens of feet of the Ericson are penetrated by most wells drilled to the Almond in order to obtain sufficient rathole for logging the entire Almond. Thus there are thousands of Ericson tests, most of which show one or more indications of gas pay in the Ericson. These include 6-11% porosity, resistivity >50 ohm-m, neutron-density gas cross-over, and mudlog shows. Archie saturation calculations using appropriate R*w* values almost universally indicate "gas pay" comparable to overlying Almond sands. And yet, nearly all attempts at completions in the Ericson result in extremely high water volumes with minor amounts of gas, typically <250 MCFD. Commercial production has only been found over large structural closures, such as Canyon Creek field, or in very small areas of a few wells on regional dip.

Our interpretation is the Ericson displays all the characteristics of a watered out gas reservoir. Log and mudlog gas shows are probably real, and calculated Archie saturations are approximately correct. Completion attempts demonstrate the Ericson is at or near residual gas saturation (S*gr*), with high relative permeability to water and low relative permeability to gas. Consequently the Ericson appears to have formerly been a widespread gas reservoir, perhaps filled over most of the central Washakie Basin in the early Tertiary, but with late Tertiary uplift and structural re-adjustment of the Wamsutter Arch gas spilled laterally to the east and west leaving a residual gas column behind. The stratigraphic continuity of the Ericson and high net:gross offers little in the way of internal trapping opportunities, so producible gas only occurs in local stratigraphic traps and over structural closures. The remaining enigma was the very high S*gr*, by our calculations 40 to 60% in most wells, which we find to be fully consistent with recently determined imbibition capillary pressure behavior in tight sandstones.

What's the matter with the Ericson is that it has leaked its gas charge, and what was left behind is not producible. Clearly gas charge is widespread and there is sufficient reservoir quality for the sands to produce, so exploration efforts should focus on structural closures, subtle fault traps, or large stratigraphic pinchouts. Minor producible accumulations will continue to be

found by serendipity, but they will be difficult to recognize because S*gr* is so high and is close to initial saturation conditions.

Presented at AAPG Rocky Mountain section meeting, Snowbird, UT, October 2007

Lithofacies and Petrophysical Properties of Mesaverde Tight-Gas Sandstones in Western U.S. Basins

Alan P. Byrnes, John C. Webb, Robert M. Cluff, Daniel A. Krygowski, and Stefani D. Whittaker

The relationship between core and log petrophysical properties and lithofacies sedimentary characteristics is examined in Mesaverde Group tight gas sandstones from 40 cores in the Washakie, Uinta, Piceance, Greater Green River, Wind River, and Powder River basins.

Shaly intervals of the Mesaverde Group are dominated by mudstones and silty shales; burrowed, lenticular and wavy-bedded very shaly sandstones; and wavy-bedded to ripple cross-laminated shaly sandstones. Sandstone intervals are dominated by ripple cross-laminated , crossbedded, planar laminated, and massive, very-fine to fine-grained sandstones.

For 2200 core plugs measured, grain density averages 2.654+0.033 g/cc (error of 1 std dev) with distributions differing slightly among basins. Core porosity ranges from 0 to 25%, averaging 7.2%. In situ Klinkenberg permeability ranges from 0.0000001 to 200 millidarcies, averaging 0.002 millidarcies. Characteristic of most sandstones, permeability at any given porosity increases with increasing grain size and improved sorting, with secondary influences including sedimentary structure and the nature of cementation. Multivariate and neural network permeability prediction methods exhibit a standard error of 4.5X and 3.3X respectively. Capillary threshold entry pressure and pore characteristric length are well correlated with permeability. Archie cementation exponent (m) can be modeled with a dual porosity matrix-fracture model with m approaching one as porosity approaches zero. Critical gas saturation is generally less than 5% but increases with increasing bedform complexity. Integration of wireline log analysis and core petrophyscial relationships provides guidelines and equations for predicting reservoir properties.

The Mesaverde Project website is (http://www.kgs.ku.edu/mesaverde).

Presented at AAPG Annual Meeting, San Antonio, TX, April 2008

Evidence for a Variable Archie Porosity Exponent "m" and Impact on Saturation Calculations for Mesaverde Tight Gas Sandstones; Piceance, Uinta, Green River, Wind River, and Powder River Basins

Robert M. Cluff and Alan P. Byrnes

We have measured formation resistivity factors (FRF = Ro/Rw) on a suite of over 300 Mesaverde core plugs at four brine salinities. The samples range from 0.2 to 23.4% porosity at 4000 psi NCS (ϕi); *in situ* permeability from 2 nD to 206 mD; and brine salinities of 20K, 40K, 80K, and 200K ppm NaCl. The Archie porosity (cementation) exponent "m" was calculated from the measured FRF assuming a = 1. Our prior unpublished work in the Washakie Basin focused on sample sets with porosity > 6% and found only a weak correlation between m and porosity. Present data show strong curvature where m decreases as a function of porosity below approximately 8% porosity. The relationship can be described by the dual porosity model or equally well by a family of logarithmic equations: $m = a\ ln(\phi i) + b$ (m standard deviation = 0.13). The zero porosity intercept *b* increases with salinity from 1.25 (20K ppm) to 1.57 (200K ppm). The coefficient "*a*" decreases (0.23 to 0.16) with increasing salinity.

The impact of these relationships is that m decreases with decreasing porosity and salinity. At low porosity (<6%) m is significantly less than the nominal constant value of 1.85 commonly assumed for tight gas sandstones. Above 12% porosity, m is best characterized by a constant value of 1.9 ± 0.05. Therefore there is more gas in these rocks at low porosities than a constant m model predicts, but there is little impact on saturation calculations at high porosity.

Presented at AAPG Rocky Mountain Section meeting, Denver, CO, July 2008

Lithofacies and Petrophysical Properties of Mesaverde Tight-Gas Sandstones in Western U.S. Basins

John C. Webb, Alan P. Byrnes, Robert M. Cluff, Dan A. Krygowski, and Stefani D. Whittaker

The relationship between core and log petrophysical properties and lithofacies are examined in Mesaverde Group tight gas sandstones from 40 cores in the Washakie, Uinta, Piceance, Greater Green River, Wind River, and Powder River basins. Fine-grained intervals of the Mesaverde Group include mudstones and silty shales; burrowed, lenticular and wavy-bedded very shaly sandstones; and wavy-bedded to ripple cross-laminated shaly sandstones. Sandstone intervals include ripple cross-laminated and cross-bedded, very fine to fine-grained sandstones, low-angle cross-laminated to planar laminated sandstones, and massive sandstones. Lithofacies were deposited in nonmarine, paludal, marginal marine, and marine environments. For all lithofacies undifferentiated in the cores sampled, grain density averages 2.654+0.033 g/cc (error of 1 std dev) with grain-density distributions differing slightly among basins. Core porosity ranges from 0 to 25%, averaging 7.2% (n = 2200). In situ Klinkenberg permeability ranges from 0.0000001 to 200 millidarcies, averaging 0.002 millidarcies. Characteristic of most sandstones, permeability at any given porosity increases with increasing grain size, and increasing sorting though this relationship is further influenced by the nature of cementation. Cements include chlorite, ML-IS and illitic clays, quartz, calcite, and ferroan calcite. Capillary threshold entry pressure and pore characteristric length are well correlated with permeability. Archie cementation exponent, m, can be modeled with a dual-porosity matrix-fracture model with m approaching one as porosity approaches zero. Critical gas saturation is generally less than 5% but increases with increasing bedform complexity. Integration of wireline log analysis and core petrophysical relationships provides guidelines and equations for predicting reservoir properties. The Mesaverde Project website is (http://www.kgs.ku.edu/mesaverde).

Presented at AAPG Rocky Mountain section meeting, Denver, CO, July 2008

Capillary Pressure Properties of Mesaverde Group Low-Permeability Sandstones in Six Basins, Western U.S

Alan P. Byrnes, D. Osborn, A. Knoderer, O. Metheny, T. Hommertzheim, J. Byrnes, R. Cluff, J. Webb

Drainage and imbibition air-mercury capillary-pressure properties were measured for over 100 Mesaverde Group low-permeability sandstones from six basins in the Western U.S. For all samples pore-throat diameters associated with the threshold-entry pressure (P_e) decrease with decreasing permeability. Stressed (4,000 psi NCS) and unstressed curve pairs for high-permeability cores (k>1 mD) are nearly identical; however, with decreasing permeability the unstressed and stressed threshold-entry pressures diverge. For all sample pairs this difference is greatest at P_e and the curves converge with decreasing wetting phase saturation (S_w) down to 30-50%, where the stressed curve crosses the unstressed curve and thereafter exhibits 0-5% lower S_w with increasing capillary pressure.

The data imply that confining stress exerts principal influence on the largest pore throats and that pore throats accessed at nonwetting phase saturations below approximately 50% are not significantly affected by confining stress. This is consistent with these smaller pores comprising pore space within pore bodies or in regions of the rocks where stress is not concentrated.

Hysteresis analysis involving three drainage-imbibition cycles for each sample were performed on 32 samples and residual mercury saturation was measured for over 200 samples where initial mercury nonwetting phase saturation (S_{nwi}) corresponds to conditions near "irreducible" wetting-phase saturation (S_{wirr}). The relationship between S_{nwi} and residual non-wetting (S_{nwr}) saturations following imbibition is well characterized by a Land-type relationship: $1/S_{nwr}^* - 1/S_{nwi}^* = C$, where $S_{nwr}^* = S_{nwr}/(1-S_{wirr})$, $S_{nwi}^* = S_{nwi}/(1-S_{wirr})$, and $C = 0.55$ at $S_{wirr} = 0$. Results indicate that residual nonwetting phase saturations (e.g., gas) are high following imbibition.

Presented at AAPG Rocky Mountain Section meeting, Denver, CO, July 2008

Subtask 8.2. Reporting Requirements

A project overview including project objectives and improvements to be achieved, project schedule, and budget was presented at a project kickoff meeting at the National Energy Technology Laboratory in Morgantown, WV, on December 12, 2005.

All project quarterly reports and technical presentations are posted on the Mesaverde Project website.

REFERENCES

Archie, G., 1942, The electrical resistivity log as an aid in determining some reservoir characteristics: Transactions of AIME.

Berkowitz, B., and R. P. Ewing, 1998, Percolation theory and network modeling applications in soil physics: Surveys in Geophysics, v. 19, p. 23-72.

Broadbent, S. R., and J. M. Hammersley, 1957, Percolation processes I. Crystals and mazes: Proceedings of the Cambridge Philosophical Society, v. 53, p. 629-641.

Brooks, R. H., and A. T. Corey, 1966, Properties of porous media affecting fluid flow: J. Irrig. Drainage Div., v. 6 (June 1966), p. 61-88.

Burdine, N. T., 1953, Relative permeability calculations from pore-size distribution data: Petroleum Transactions Am. Inst. Mechanical Engineers, v. 198, p. 71-77, paper SPE 225-G.

Byrnes, A. P., 1997, Reservoir characteristics of low-permeability sandstones in the Rocky Mountains: The Mountain Geologist v. 43, no. 1, p. 39-51.

Byrnes, A. P., 2007, Issues with gas relative permeability in low-permeability sandstones; in, K. Shanley, W. Camp, and S. Cumella (eds.), Understanding, Exploring, and Developing Tight-Gas Sands: 2005 Vail Hedberg Conference, Chapter 5, p. 1-14.

Byrnes, A. P., J. C. Webb, and R. C. Cluff, 2007, Regional petrophysical properties of Mesaverde low-permeability sandstones: Am. Assoc. Petroleum Geologists, Rocky Mountain Section, Meeting Abstracts, October 6-9, 2007, Snowbird, UT.

Byrnes, A. P., K. Sampath, and P. L. Randolph, 1979, Effect of pressure and water saturation on the permeability of western tight sandstones: Proceedings of the 5th Annual U.S. Dept. Energy Symposium on Enhanced Oil and Gas Recovery, Tulsa, Oklahoma, August 22-26, 1979, p. 247-263.

Byrnes, A. P., 2003, Aspects of permeability, capillary pressure, and relative permeability properties and distribution in low-permeability rocks important to evaluation, damage, and stimulation: Proceedings Rocky Mountain Association of Geologists - Petroleum Systems and Reservoirs of Southwest Wyoming Symposium, Denver, Colorado, September 19, 2003, 12 p.

Byrnes, A. P., 2005, Permeability, capillary pressure, and relative permeability properties in low-permeability reservoirs and the influence of thin, high-permeability beds on production; in, Gas in Low Permeability Reservoirs of the Rocky Mountain Region, M. G. Bishop, S. P. Cumella, J. W. Robinson, and M. R. Silverman eds.: Rocky Mountain Assoc. of Geologists, 2005 Guidebook CD, p. 69-108.

Byrnes, A. P., and C. W. Keighin, 1993, Effect of confining stress on pore throats and capillary pressure measurements, selected sandstone reservoir rocks: American Association of Petroleum Geologists Annual Convention Program Abstracts, April 25-28, New Orleans, p. 82.

Byrnes, A. P., and J. W. Castle, 2000, Comparison of core petrophysical properties between low-permeability sandstone reservoirs--Eastern U.S. Medina Group and Western U.S. Mesaverde Group and Frontier Formation: SPE 60304 proceedings of the 2000 SPE Rocky Mountain Regional/Low Permeability Reservoirs Symposium, Denver, CO, March 12-15, 2000, p. 10.

Byrnes, A. P., J. C. Webb, R. M. Cluff, D. A. Krygowski, and S. D. Whittaker, 2008, Lithofacies and petrophysical properties of Mesaverde tight-gas sandstones in Western U.S. basins; American Association of Petroleum Geologists Annual Convention Program Abstracts, San Antonio, TX.

Byrnes, A. P., D. Osborn, A. Knoderer, O. Metheny, T. Hommertzheim, J. P. Byrnes, R.C.Cluff, J. C. Webb, 2008, Capillary Pressure Properties of Mesaverde Group Low-Permeability Sandstones in Six Basins, Western U.S: Am. Assoc. Petroleum Geologists Rocky Mountain Section Meeting Abstracts, July 2008, Denver, CO.

Cafiero, R., G. Caldarelli, and A. Gabrielli, 1997, Surface effects in invasion percolation: Phys. Rev. E, v. 56, no. 2, p. 1291-1294.

Caruso, G. F., 2008, Outlook for U.S. natural gas markets: Presentation given at LNG 2008 , April 22, San Antonio, Texas, http://www.eia.doe.gov/neic/speeches/caruso042208.pdf

Castle, J. W., and A. P. Byrnes, 1997, Petrophysics of low-permeability Medina Sandstone, northwestern Pennsylvania, Appalachian Basin: The Log Analyst, v. 39, no. 4, p. 36-46.

Castle, J. W., and A. P. Byrnes, 2005, Petrophysics of Lower Silurian sandstones and integration with the tectonic-stratigraphic framework, Appalachian basin, United States: AAPG Bulletin, v. 89, no. 1 (January 2005), p. 41-60.

Castle, J. W., and A. P. Byrnes, 1998, Petrophysics of low-permeability Medina Sandstone, northwestern Pennsylvania, Appalachian Basin: The Log Analyst, v. 39, no. 4, p. 36-46.

Chandler, R., J. Koplik, K. Lerman, and J. F. Willemsen, 1982, Capillary displacement and percolation in porous media: J. Fluid Mech., v. 119, p. 249-267.

Chowdiah, P., 1987, Laboratory measurements relevant to two-phase flow in a tight gas sand matrix: Proceedings of the 62nd Annual Technical Conference and Exhibition of the Society of Petroleum Engineers, Dallas, Texas, September 27-30, Paper SPE 16945, 12 p.

Closmann, P. J., 1987, Studies of critical gas saturation during gas injection: Soc Pet. Engineers Reservoir Engineering, Aug. (1987), Paper SPE 12335-PA, p. 387-393.

Cluff, R. M., A. P. Byrnes, and J. C. Webb, 1995, Rock-petrophysics-log correlation in the Mesaverde group, Washakie basin: American Association of Petroleum Geologists, Annual Convention Program Abstracts, June 12-15, Denver, CO, p. 122.

Cluff, R. M., K. W. Shanley, and J. W. Robinson, 2007, What's the matter with the Ericson?: Am. Assoc. Petroleum Geologists, Rocky Mountain Section, Meeting Abstracts, October 6-9, 2007, Snowbird, UT.

Cluff, R. M., and A. P. Byrnes, 2008, Evidence for a variable Archie porosity exponent "m" and impact on saturation calculations for Mesaverde tight gas sandstones--Piceance, Uinta, Green River, Wind River, and Powder River basins: Am. Assoc. Petroleum Geologists, Rocky Mountain Section, Meeting Abstracts, July 2008, Denver, CO.

Corey, A. T., 1954, The interrelations between gas and oil relative permeabilities: Producers Monthly, v. 19 (Nov 1954), p. 38-41.

Corey, A. T., and C. H. Rathjens, 1956, Effect of stratification on relative permeability: Journal of Petroleum Technology, v. 8, no. 12 (Dec. 1956), Paper SPE 744-G, p. 69-71.

Desbarats, A. J., 1987, Numerical simulation of effective permeability in sand-shale formation: Water Resources Research, v. 23, no. 2, p. 273-286.

Du, C., and Y. C. Yortsos, 1999, A numerical study of the critical gas saturation in a porous medium: Transport in Porous Media, v. 35, p. 205-225.

Dutton, S. P., et al., 1993, Major low-permeability sandstone gas reservoirs in the continental United States: Texas Bureau of Economic Geology, Report of Investigations no. 211, 221 p.

EIA, 2005, Annual Energy Outlook 2005: Energy Information Administration, DOE/EIA-0383(2005), http:/www.eia.doe.gov/, 249 p.

Feder, J., 1988, Fractals: Plenum Press, New York, 283 p.

Ferer, M., G. S. Bromhal, and D. H. Smith, 2003, Pore-level modeling of drainage--Crossover from invasion percolation fingering to compact flow: Physical Review E, v. 67, 051601-1-12,

Firoozabadi, A., B. Ottesen, and M. Mikklesen, 1989, Measurement and modeling of supersaturation and critical gas saturation: Part 1. Measurements: Proceedings of the 1989 Soc. Petroleum Engineers Fall Meeting, San Antonio, Texas, Oct. 8-11, Paper SPE 19694.

Glover, P. W., M. J. Hole, and J. Pous, 2000, A modified Archie's law for two conducting phases: Earth and Planetary Science Letters, v. 180, no. 3-4, p. 369-383.

Guyod, H, 1944, Fundamental data for the interpretation of electric logs: The Oil Weekly, v. 115, no. 38 (October 30, 1944), p. 21-27.

Haldorsen, H. H., 1986, Simulator parameter assignment and the problem of scale in reservoir engineering; in, Reservoir Characterization, L. W. Lake and H. B. Carrol ,Jr., eds.: Academic Press, London, p. 293-340.

Handy, L. L., 1958, A laboratory study of oil recovery by solution gas drive: Petroleum Transactions AIME, v. 213, p. 310-315.

Honarpour, M. M., A. S. Cullick, N. Saad, and N. V. Humphreys, 1995, Effect of rock heterogeneity on relative permeability--Implications for scaleup: J. Pet. Tech., Nov., p. 980-986.

Honarpour, M. M., L. F. Koederitz, and A. H. Harvey, 1982, Empirical equations for estimating two-phase relative permeability in consolidated rock: Transactions of American Institute of Mechanical Engineers, v. 273, p. 2905-2923.

Hunt, E. B., Jr. and V. J. Berry, Jr., 1956, Evolution of gas from liquids flowing through porous media: Am. Inst.Chem. Eng. J., v. 2, p. 560-567.

Jones, F. O., and W. W. Owens, 1980, A laboratory study of low-permeability gas sands: Journal of Petroleum Technology, v. 32, no. 9, Paper SPE 7551-PA, p.1631-1640.

Kamath, J. and R. E. Boyer, 1993, Critical gas saturation and supersaturation in low permeability rocks: Presented at the 1993 Society of Petroleum Engineers Fall Meeting, Houston, TX, Oct. p. 3-6, Paper SPE 26663.

Katz, A. J., and A. H. Thompson, 1986, Quantitative prediction of permeability in porous rock: Physical Review B, v. 34, p. 8179-8181.

King, P. R., 1989, The use of renormalization for calculating effective permeability: Transport in Porous Media, v. 4, p. 37-58.

Koplik, J., and T. J. Lasseter, 1982, Two-phase flow in random network models of porous media: Proc. Annual Meeting of Soc. Pet. Eng., New Orleans, LA, Paper SPE 11014, 12 p.

Koplik, J., C. Lin, and M. Vermette, 1984, Conductivity and permeability from microgeometry: J. Appl. Phys., v. 56, p. 3127-3131.

Kortekaas, T. F. M., and F. V. Poelgeest, 1989, Liberation of solution gas during pressure depletion of virgin and watered-out reservoirs: Presented at the 1989 Fall Meeting of the Soc. Petroleum Engineers, San Antonio, TX, Oct. 8-11, paper SPE 19693.

Kukal, G. C., C. L. Biddison, R. E. Hill, E. R. Monson, and K. E. Simons, 1983, Critical problems hindering accurate log interpretation of tight gas sand reservoirs: Proceedings of the SPE, AIME/U.S. DOE 1983 Symposium on low permeability reservoirs, Denver, CO, March 14-16 (1983), Paper SPE 11620, p. 181.

Larson, R. G., and N. R. Morrow, 1981, Effects of sample size on capillary pressure in porous media: Powder Technology, v. 30, no. 2, p. 123-139.

Larson, R. G., L. E. Scriven, and H. T. Davis, 1977, Percolation theory of residual phases in porous media: Nature, v. 268, p. 409-413.
Larson, R. G., L. E. Scriven, and H. T. Davis, 1981, Percolation theory of two phase flow in porous media: Chemical Engineering Science, v. 36, p. 57-73.
Lenormand, R., and C. Zarcone, 1985, Invasion percolation in an etched network--Measurement of a fractal dimension: Phys. Rev. Lett., v. 54, p. 2226-2229.
Lenormand, R., and M. R. Thiele, 1997, Calculation of large scale relative permeabilities from stochastic properties of the permeability filed and fluid properties: Proc. Fourth International Reservoir Characterization Technical Conference, Houston, TX, March 2-4, p. 137-139.
Lenormand, R., C. Zarcone, and A. Sarr, 1983, Mechanisms of the displacement of one fluid by another in a network of capillary ducts: J. Fluid Mech., v. 135, p. 337-353.
Li, X., and Y. C. Yortsos, 1991, Visualization and numerical studies of bubble growth during pressure depletion: Presented at the 64th Annual Technical and Exhibition of the Soc. Petroleum Engineers, Dallas, TX, Oct. 6-9, Paper SPE 22589.
Li, X., and Y. C. Yortsos, 1993, Critical gas saturation--Modeling and sensitivity studies: Proceedings of the 68th Annual Technical Conference of the Soc. Petroleum Engineers, Houston, TX, Oct. 3-6, Paper SPE 26662, p. 589-604.
Li, X., and Y. C. Yortsos, 1995a, Theory of multiple bubble growth in porous media by solute diffusion: Chem. Engineering Science, v. 50, p. 1247-1271.
Li, X., and Y. C. Yortsos, 1995b, Visualization and simulation of bubble growth in pore networks: Am Inst.Chem. Eng. J., v. 41, p. 214-222.
Lin, C., and M. H. Cohenm, 1982, Quantitative methods for microgeometric modeling: Journal of Applied Physics, v. 53, p. 4152-4165.
Moulu, J. C., and D. Longeron, 1989, Solution-gas drive--Experiments and simulation: Paper presented at the Fifth European Symp. on Improved Oil Recovery, Budapest, Hungary.
Ostensen, R. W., 1983, Microcrack permeability in tight gas sandstone: Society of Petroleum Engineering Journal, v. 23, no. 6, p. 919-927.
Randolph, P. L., 1983, Porosity and permeability of Mesaverde sandstone core from the U.S. DOE Multiwell Experiment, Garfield County, Colorado: Proceedings 1983 SPE/DOE Joint Symposium on low permeability gas reservoirs, March 13-16, 1983, Denver, CO, Paper SPE/DOE 11765, p. 449-460.
Sahimi, M., 1993, Flow phenomena in rocks--From continuum models to fractals, percolation, cellular automata, and simulated annealing: Reviews of Modern Physics, v. 65, no. 4, p. 1393-1534.
Sahimi, M., 1994, Applications of percolation theory: Taylor and Francis, London, 258 p.
Sampath, K., and C. W. Keighin, 1981, Factors affecting gas slippage in tight sandstones: Proceedings of the 1981 SPE/DOE Symposium on Low Permeability Gas Reservoirs, Denver, CO, May 27-29 (1981), Paper SPE 9872, p. 409-416.
Schowalter, T. T., 1979, Mechanics of secondary hydrocarbon migration and entrapment: AAPG Bull., v. 63, no. 5, p. 723-760.
Shanley, K. W., R. M. Cluff, and J. W. Robinson, 1984, Factors controlling prolific gas production from low-permeability sandstone reservoirs--Implications for resource assessment, prospect development, and risk analysis: AAPG Bulletin, v. 88, no. 8, p. 1083-1121.
Soeder, D. J., 1988, Porosity and permeability of eastern Devonian gas shale: SPE, Inst. of Gas Technology, SPE Formation Evaluation, Paper SPE 15213, p. 116-124.

Thomas, R. D., and D. C. Ward, 1972, Effect of overburden pressure and water saturation on gas permeability of tight sandstone cores: Journal of Petroleum Technology, Paper SPE 3634-PA, v. 25, no. 2, p. 120-124.
Thompson, A. H., A. J. Katz, and R. A. Raschke, 1987, Mercury injection in porous media--A resistance Devil's staircase with percolation geometry: Physical Review Letters, v. 58, no. 1, p. 29-32.
Timur, A., 1968, An investigation of permeability, porosity, and residual water saturation relationship for sandstone reservoirs: The Log Analyst, v. 9, no. 4, p. 8.
Vairogs, J., C. L. Hearn, D. W. Dareing, and V. W. Rhoades, 1971, Effect of rock stress on gas production for low-permeability rocks: Journal of Petroleum Technology, v. 24, no. 9, p. 1161-1167.
Wall, G. C., and R. J. C. Brown, 1981, The determination of pore-size distributions from sorption isotherms and mercury penetration in interconnected pores--The application of percolation theory: J. Colloid Interface Sci., v. 82, p. 141-149.
Walls, J. D., 1981, Tight gas sands--Permeability, pore structure and clay: Proceedings of the 1981 SPE/DOE Symposium on Low Permeability Gas Reservoirs, Denver, CO, May 27-29 (1981), Paper SPE 9871, p. 399-409.
Walls, J. D., A. M. Nur, and T. Bourbie, 1982, Effects of pressure and partial water saturation on gas permeability in tight sands--Experimental results: Journal of Petroleum Technology, April 1982, Paper SPE 9378-PA, p. 930-936.
Walls, J. D., A. M. Nur, and T. Bourbie, 1982, Effects of pressure and partial water saturation on gas permeability in tight sands--Experimental results: Journal of Petroleum Technology, April 1982, p. 930-936.
Ward, J. S., and N. R. Morrow, 1987, Capillary pressure and gas relative permeabilities of low permeability sandstone: Society of Petroleum Engineers, Formation Evaluation, Sept. 1987, Paper SPE 13882, p. 345-356.
Waxman, M. H., and L. J. M. Smits, 1968, Electrical conductivities in oil-bearing shaly sands: Journal of Society of Petroleum Engineers, v. 8, p. 107-122.
Waxman, M. H., and E. C. Thomas, 1974, Electrical conductivities in shaly sands-I. The relation between hydrocarbon saturation and resistivity index; II. The temperature coefficient of electrical conductivity: Journal Petroleum Technology, February, p. 213-225.
Webb, J. C., R. M. Cluff, D. A. Krygowski, S. D. Whittaker, and A. P. Byrnes, 2008, Lithofacies and petrophysical properties of Mesaverde tight-gas sandstones in western U.S. basins: Am. Assoc. Petroleum Geologists, Rocky Mountain Section Meeting, Abstracts, July 2008, Denver, CO.
Weber, K. J., 1982, Influence of common sedimentary structures on fluid flow in reservoir models: Journal of Petroleum Technology, v. 34, p. 665-672.
Wei, K. K., N. R. Morrow, and K. R. Brower, 1986, Effect of fluid, confining pressure, and temperature on absolute permeabilities of low permeability sandstones: Society of Petroleum Engineers, Formation Evaluation, Aug. 1986, p. 413-423.
Wilkinson, D., 1984, Percolation model of immiscible displacement in the presence of buoyancy forces: Phys. Rev. A, v. 30, p. 520-531.
Wilkinson, D., and J. F. Willemsen, 1983, Invasion percolation--A new form of percolation theory: J. Phys. Rev. A 16, p. 3365-3376.
Wilkinson, D., 1986, Percolation effects in immiscible displacement: Physical Review A, v. 34, p. 1380-1391.
Wyllie, M. R. J., 1962, Relative permeability; in, Petroleum Production Handbook, T. Frick (ed.):

McGraw Hill, 2 vols.
Yanuka, M., and I. Balberg, 1991, Invasion percolation in a continuum model: J. Phys. A, Math. Gen., v. 24, p. 2565-2568.
Yanuka, M., F. Dullien, and D. Elrick, 1986, Percolation processes and porous media: I. geometrical and topological model of porous media using a three dimensional joint pore size distribution: Journal of Colloid and Interface Science, v. 112, p. 24-36.
Yortsos, Y. C. and M. Parlar, 1989, Phase change in binary systems in porous media--Application to solution gas drive: Presented at the 1989 Society of Petroleum Engineers Fall Meeting, San Antonio, TX, Oct. 8-9, Paper SPE 19697.

National Energy Technology Laboratory

626 Cochrans Mill Road
P.O. Box 10940
Pittsburgh, PA 15236-0940

3610 Collins Ferry Road
P.O. Box 880
Morgantown, WV 26507-0880

One West Third Street, Suite 1400
Tulsa, OK 74103-3519

1450 Queen Avenue SW
Albany, OR 97321-2198

2175 University Ave. South
Suite 201
Fairbanks, AK 99709

Visit the NETL website at:
www.netl.doe.gov

Customer Service:
1-800-553-7681